「鋪面評估與維修」
補充講義

授課教師：李英豪

淡江大學土木工程學系
民國八十五年三月

「鋪面評估與維修」補充講義

目錄

資料來源：

1. 李英豪、李英明，“剛性路面損壞與維修：損壞型態與原因、損壞維修，”道路工程設計與維修實務班講義，台灣省建築師公會建築研修中心，民國八十四年一月十四日。
2. 陳建桓、李英豪，“由面層撓度值回算鋪面彈性模數的初步研究”，中華民國第八屆鋪面工程學術研討會論文輯(已接受)，台北國際會議中心，中原大學，中華民國八十四年十二月六日至八日。
3. 林炳森、李泰明、吳元廷、鄒譽名，“路面評審儀應用於剛性路面之回算法”，中華民國第八屆鋪面工程學術研討會論文輯，台北國際會議中心，中原大學，中華民國八十四年十二月六日至八日。
4. Hall, K. T., “Performance, Evaluation, and Rehabilitation of Asphalt-Overlaid Concrete Pavements,” Ph.D. Thesis, University of Illinois, Urbana, Illinois, 1991, pp. 88-104.
5. Korovesis, G. T., “Analysis of Slab-on-Grade Pavement Systems Subjected to Wheel and Temperature Loadings,” Ph.D. Thesis, University of Illinois, Urbana, Illinois, 1990, pp. 305-334.
6. Ioannides, A. M., “Analysis of Slab-on-Grade for a Variety of Loading and Support Conditions,” Ph.D. Thesis, University of Illinois, Urbana, Illinois, 1984, pp. 187-188.
7. 交通部台灣區國道新建工程局，“北二高剛性路面建造講習”，第50-63頁，中華民國七十九年。
8. Lee, Y. H., and M. I. Darter, "Loading and Curling Stress Models for Concrete Pavement Design," Transportation Research Record 1449, Transportation Research Board, National Research Council, Washington, D.C., 1994, pp. 101-113.
9. Lee, Y. H., and M. I. Darter, "New Predictive Modeling Techniques for Pavements," Transportation Research Record 1449, Transportation Research Board, National Research Council, Washington, D.C., 1994, pp. 234-245.
10. Portland Cement Association, “Thickness Design for Concrete Highway and Street Pavements,” Skokie, Illinois, 1984.
11. 周義華，運殊工程，鼎漢國際工程顧問股份有限公司，第二版，中華民國八十二年八月。
12. Federal Aviation Administration, “Airport Pavement Design and Evaluation,” FAA Advisory Circular AC 150/5320-6C, 1978.

13. American Concrete Pavement Association, "Pavement Analysis Software" (PAS), Arlington Heights, Illinois, U.S.A., 1993.
14. Portland Cement Association, "PCAPAV -Thickness Design of Highway and Street Pavements," Skokie, Illinois, U.S.A., 1990.
15. Lee, Y. H., J.. H. Bair, C. T. Lee, S. T. Yen, Y. M. Lee, "Modified PCA Stress Analysis and Thickness Design Procedures," Presented at the 76th Annual Meeting of the Transportation Research Board and Accepted for Publication in the Future Transportation Research Record, 1997.
16. AASHTO, "AASHTO Guide for Design of Pavement Structures," Volume I, 1993.
17. Hall, K. T., and M. I. Darter, " Structural Overlay Strategies for Jointed Concrete Pavements," Volume VI, Appendix A - User's Manual for the EXPEAR Computer Program", ERES Consultants, Inc., Federal Highway Administration, 1990.
18. Darter, M. I., and K. T. Hall, "Case Studies in Rehabilitation Strategy Development," *Concrete International*, Magazine of the American Concrete Institute, December 1993.

A 鋪面評估與維修簡介

A.1 剛性路面損壞與維修

資料來源：

李英豪、李英明，“剛性路面損壞與維修：損壞型態與原因、損壞維修，” 道路工程設計與維修實務班講義，台灣省建築師公會建築研修中心，民國八十四年一月十四日。

道路工程設計施工與維修實務班
講義 —

『剛性路面損壞與維修：損壞型態與原因、損壞維修』

主講人：淡江大學土木系李英豪副教授

時間：民國八十四年一月十四日

委訓單位：行政院勞委會職訓局公訓組

承辦單位：台灣省建築師公會建築研修中心

剛性路面損壞與維修：剛性鋪面損壞型態與原因、損壞維修

波特蘭水泥混凝土鋪面又稱爲剛性鋪面，主要可以分成三大類型：接縫式無筋混凝土鋪面（JPCP）、接縫式鋼筋混凝土鋪面（JRCP）與連續式鋼筋混凝土鋪面（CRCP）。接縫式無筋混凝土鋪面與接縫式鋼筋混凝土鋪面之破壞種類相近似，因此本講義將破壞之類型分成接縫式混凝土鋪面（JCP）與連續式鋼筋混凝土鋪面兩大類型來加以討論。

本講義取材自國內外之相關研究資料彙編而成，各種破壞程度的定義、分類與說明示意圖則是依據美國正進行的長期鋪面績效研究（SHRP/LTPP）「鋪面調查手冊」。在損壞維修部份主要參考美國聯邦公路總署（FHWA)之「鋪面維修技術」訓練教材與國內交通技術標準規範之「公路養護手冊」。

1.0 接縫式混凝土鋪面損壞型態與原因

接縫式混凝土鋪面損壞形態的種類主要可分類爲以下四大類型：

a. 裂縫：包含角隅斷裂、縱向裂縫、橫向裂縫與耐久性("D")裂縫。
b. 接縫破壞：包含接縫填充料破壞、縱向接縫剝落與橫向接縫剝落。
c. 表面破壞：包含龜裂、表面剝落與鬆散、粒料磨損與脫落。
d. 其它：包含隆起(或擠破)、接縫斷層(或高差)、車道與路肩高差、車道與路肩分離、修補/修補損壞與唧水或噴泥現象等。

以下即針對接縫式混凝土鋪面損壞型態與原因分別加以介紹：

1.1 角隅斷裂(Corner Break)

角隅斷裂是剛性鋪面版在角隅部份產生了貫穿鄰近橫向與縱向接縫的斷裂，此斷裂與行車方向約呈45度的交角，可能發生在版的任一角隅。角隅 斷裂在角隅兩邊的長度一般從0.3公尺至版寬的一半，產生的原因主要是由於交通重覆荷重結合路基承載力喪失（loss of support）與溫度應力（curling stresses）等因素而引起。（如圖一所示）

角隅斷裂若不及時維修，會因交通載重重覆作用而產生鬆散，水分亦會經裂縫滲入基底層使損害範圍擴大。

角隅斷裂與角隅剝落（corner spalling）是兩種不同的破壞型態，其主要的差異在於角隅斷裂的破壞垂直貫穿整個剛性鋪面版，而角隅剝落則是因爲鄰近接縫邊緣部份的鋪面混凝土分離而引起。

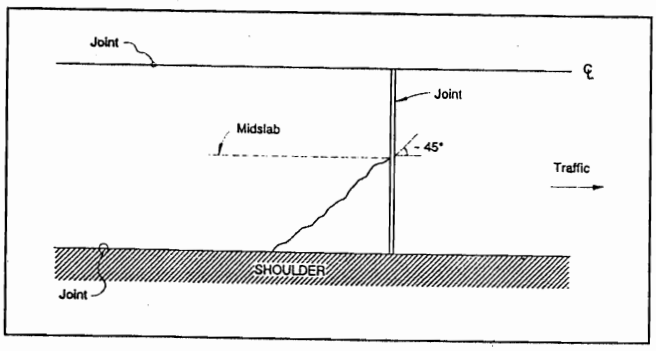

圖一　角隅斷裂之示意圖

角隅斷裂的破壞程度可區分爲輕度（low）、中度（moderate）與重度（high）三種，量測的方式是記錄各破壞程度下的角隅裂縫數量。其破壞程度爲：1.輕度：斷裂發生剝落的長度在10％以下，無可量測的斷層發生，且角隅未斷裂爲兩塊或兩塊以上。2.中度：斷裂發生輕度剝落的長度在10％以上，接縫或裂縫斷層在13公釐以下，且角隅未斷裂爲兩塊或兩塊以上。3.重度：斷裂發生中度或重度剝落的長度在10％以上，接縫或裂縫斷層大於13公釐，且角隅斷裂爲兩塊或兩塊以上。

1.2a 縱向裂縫(Longitudinal Cracking)

縱向裂縫大部份與鋪面中心線平行，產生的原因通常是因爲重載交通荷重重覆作用結合基層承載力喪失或版中溫、濕度應力所引起，縱向接縫施工不良亦是產生縱向裂縫的原因之一。（如圖二所示）

縱向裂縫的破壞程度可區分爲輕度、中度與重度三種，量測的方式是記錄各破壞程度下的縱向裂縫長度，並記錄各破壞程度經填充完整後的縱向裂縫長度。其破壞程度爲：1.輕度：裂縫寬度小於3公釐，無剝落與無可量測之斷層者；有裂縫但填充良好者亦屬輕度。2.中度：裂縫寬度在大於等於3公釐、小於13公釐，剝落小於75公釐或斷層者小於13公釐以下者屬之。3.重度：裂縫寬度大於等於13公釐，剝落大於等於75公釐或斷層者大於等於13公釐以下者屬之。

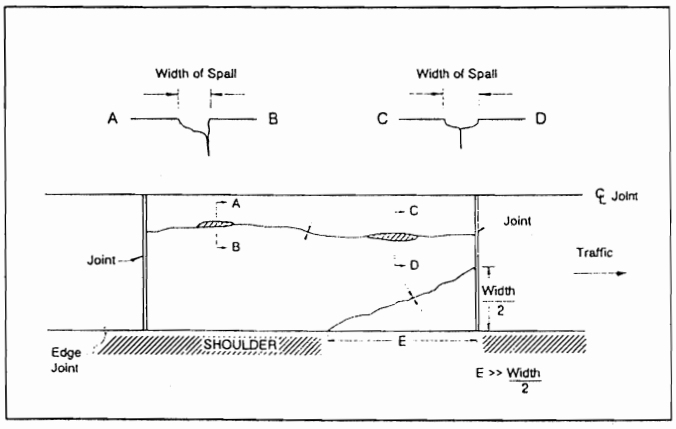

圖二　縱向裂縫之示意圖

1.2b 橫向裂縫(Transverse Cracking)

橫向裂縫大部份與鋪面中心線垂直，產生的原因通常是因爲重載交通荷重重覆作用結合基層承載力喪失或溫、濕度應力而引起。（如圖三所示）

橫向裂縫的破壞程度可區分爲輕度、中度與重度三種，量測的方式是記錄各破壞程度下的橫向裂縫數量與長度，並記錄各破壞程度經填充完整後的橫向裂縫數量與長度。其破壞程度爲：1.輕度：裂縫寬度小於3公釐，無剝落與無可量測之斷層者；有裂縫但填充良好者亦屬輕度。2.中度：裂縫寬度在大於等於3公釐、小於6公釐，剝落小於75公釐或斷層者小於6公釐以下者屬之。3.重度：裂縫寬度大於6公釐，剝落大於等於75公釐或斷層者大於等於6公釐者屬之。

對於縱向與橫向裂縫而言，將剛性鋪面版分割爲2~3塊者，通常是由於交通荷重、溫度應力與收縮應力而起；而輕度的裂縫破壞一般由版內含水量變化或摩擦因素而起，對JRCP而言輕度的裂縫破壞並不認定爲主要的結構破壞；但中度與重度裂縫破壞則認定爲主要的結構破壞。

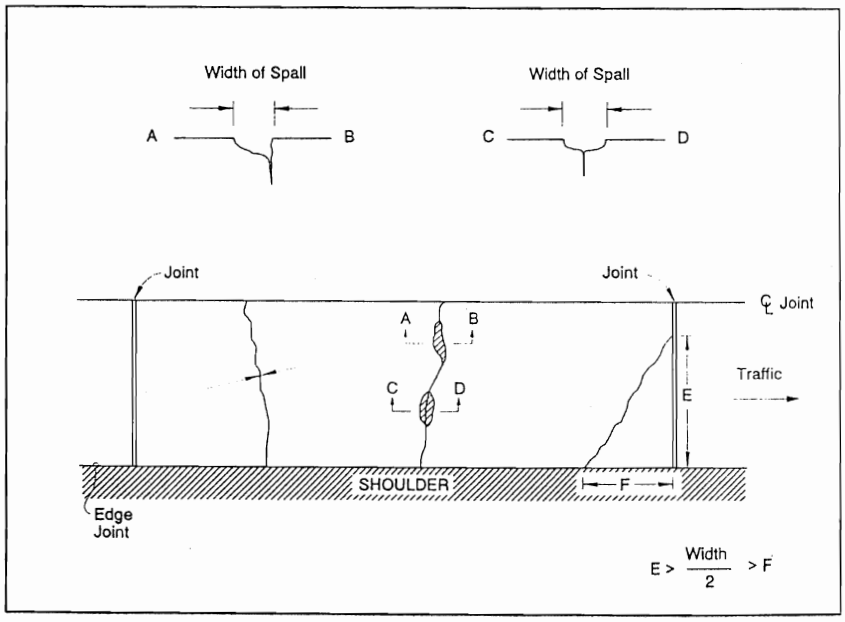

圖三　橫向裂縫之示意圖

1.3 耐久性("D")裂縫(Durability or "D" Cracking)

耐久性裂縫產生的原因是因爲鋪面混凝土無法承受環境因素（如：凍融作用）的反覆作用而由角隅開始向接縫或裂縫處延伸形

成密集的新月形細微裂縫。耐久性裂縫一般與接縫或裂縫呈平行，通常在裂縫周圍附近顏色較深。（如圖四所示）

其破壞程度可區分爲輕度、中度與重度三種，量測的方式是記錄產生耐久性裂縫之版的數量，並記錄各破壞程度下的面積。其破壞程度爲：1.輕度：耐久性裂縫輕微，沒有碎裂塊產生，且在耐久性裂縫區域內未曾修補。2.中度：耐久性裂縫區域內有一些小碎塊產生。3.重度：耐久性裂縫十分明顯，區域內有大量小碎塊產生。

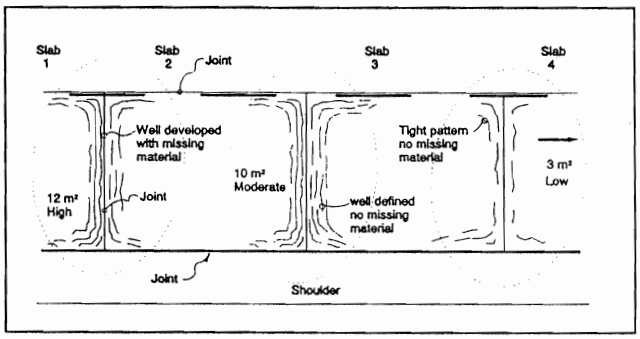

圖四　耐久性("D")裂縫之示意圖

1.4 接縫填充料破壞(Joint Seal Damage)

接縫填充料破壞是指不可壓縮物質（如：石子、土壤）或水可從表面滲入接縫之中。常見的接縫填充料破壞有以下幾種類型：接縫填充料被擠出接縫、接縫填充料硬化、斷裂或分離、或接縫填充料完全喪失等。接縫填充料破壞通常可由接縫處有外物填積或接縫處雜草衍生判斷。

橫向接縫填充料破壞的破壞程度可區分爲輕度、中度與重度三種，量測的方式是判斷橫向接縫是否曾經用填充料填充。若是曾經用填充料填充，記錄其各破壞程度下橫向接縫填充料破壞的數量。其破壞程度爲：1.輕度：小於10％長度之接縫產生破壞。2.中度：10~50％長度之接縫產生破壞。3.重度：大於50％長度之接縫產生破壞。

縱向接縫填充料破壞不須判斷其破壞程度。量測時記錄曾經用填充料填充者的縱向裂縫數量，並記錄其總長度。若單獨之縱向接縫填充料破壞長度在1公尺者以上可另外標註。接縫或裂縫被石子或土壤填塞可能會導致版無膨脹的空間而產生翹屈、鬆散或剝落等現象。此外，接縫或裂縫填充不良，亦會讓水滲入，使得基底層軟化而降低承載力。

1.5 接縫剝落（Joints Spalling）

接縫剝落是指接縫0.6公尺內之鋪面版產生裂縫、斷裂或碎裂成小塊狀之情況。 又分成縱向接縫剝落與 橫向接縫剝落二種。

接縫剝落是由於接縫或裂縫處因爲累積不可壓縮物質（如：石子或土壤等）使鋪面版伸縮時產生超額應力結合交通載重作用；或是接縫處混凝土因工作過度使得混凝土強度降低結合交通載重作用均是引起剝落的因素。接縫剝落通常不會垂直貫穿整個鋪面版。（如圖五所示）

接縫剝落的破壞程度可區分爲輕度、中度與重度三種，量測的方式是記錄其各破壞程度下接縫剝落的長度。其破壞程度爲：1.輕度：剝落的區域的寬度（從接縫中心線算起）在7.5公釐以內，且未曾修補者。2.中度：剝落的區域的寬度（從接縫中心線算起）在7.5公釐至15公釐以內，其鋪面材質有散失。3.重度：剝落的區域的寬度（從接縫中心線算起）在15公釐以上，其鋪面材質有散失。

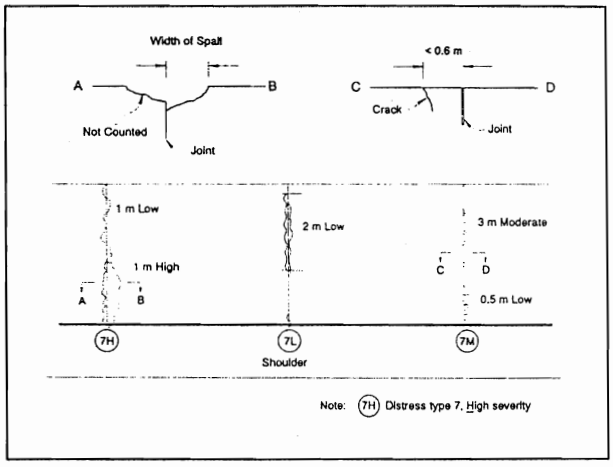

圖五　橫向接縫剝落之示意圖

1.6 龜裂(Map Cracking)、表面剝落(Scaling)與鬆散（Raveling）

龜裂是鋪面版表面產生一系列淺而細如毛髮狀、網狀的裂縫，且這些裂縫只裂至鋪面版表面。一般較大的裂縫產生於縱向，而橫向裂縫則將縱向的裂縫加以連結。 其引起的原因是鋪面版表面整飾

過度，龜裂可能進而引起表面剝落。龜裂量測時不需判定其破壞程度，記錄發生龜裂區域的數量與受影響的面積。

表面剝落是鋪面版面層細如毛髮狀的裂縫損壞，面層損壞通常產生於0.3公分至1.3公分深的面層。版的各處皆可能發生表面剝落。表面剝落引起的原因是建造不良、級配不良或凍融作用。冬季鋪面撒鹽，鹽水結冰後融解亦是原因之一。表面剝落量測時不需判定其破壞程度，記錄發生表面剝落區域的面積即可。

鬆散爲細粒料自組織中移失，與表面剝落是不同的破壞形式。其分辨的方法是表面剝落一般爲點狀，而鬆散則爲連續發生於受影響的鋪面上，在輪跡位置最爲嚴重。鬆散發生的原因可能爲細粒料品質不良、粗骨材雨水泥砂漿間結合不良或因車輪（如：釘輪）所造成。

1.7 粒料磨損(Polished Aggregate)

粒料磨損是鋪面版表面水泥砂漿或紋路磨損使得粒料暴露，使車輪與與鋪面間抗滑力降低。粒料磨損量測時不需判定其破壞程度（但表面磨損也反應了表面摩擦力的降低），記錄發生粒料磨損區域的面積即可。

1.8 脫落（Popouts）

脫落是因爲凍融作用與骨材的膨脹而使鋪面表面破碎成小碎塊而鬆脫。脫出的小碎塊大小一般爲2.5~10公分，發生的深度一般爲1.3~5公分。脫落量測時不需判定其破壞程度，記錄每平方公尺內發生脫落的數量。（如圖六所示）

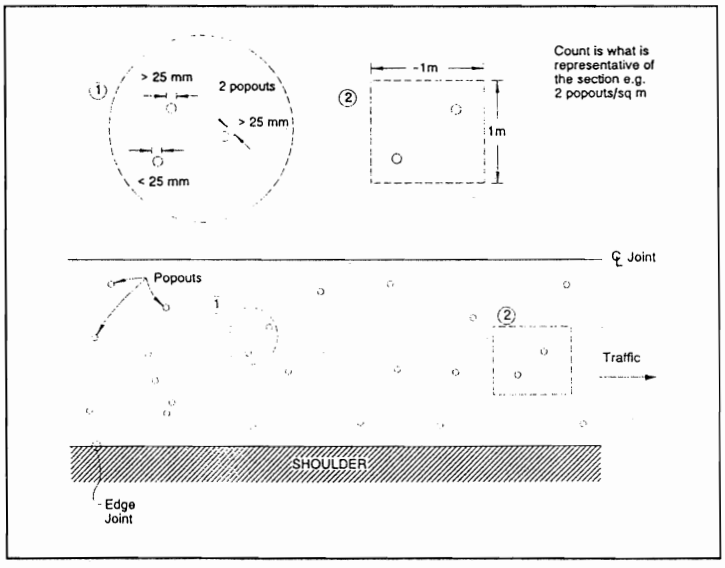

圖六　脫落之示意圖

1.9 隆起(或擠破) (Blowups)

隆起是鋪面版在接縫或裂縫處產生局部性的翹起，在隆起的區域一般皆會伴隨著混凝土碎塊。隆起一般發生於氣溫較高時，產生的原因是橫向接縫或橫向裂縫處因爲石子或土壤填積而沒有足夠的空間吸納混凝土版的擴張，由於內在應力產生了翹屈現象，於是在接縫或裂縫附近產生隆起。在公用管線切割後之修補處與排水入水口處亦容易產生隆起。（如圖七所示）

隆起量測時不需判定其破壞程度（但隆起的程度可由行車舒適性與安全性來定義），記錄隆起的數量即可。

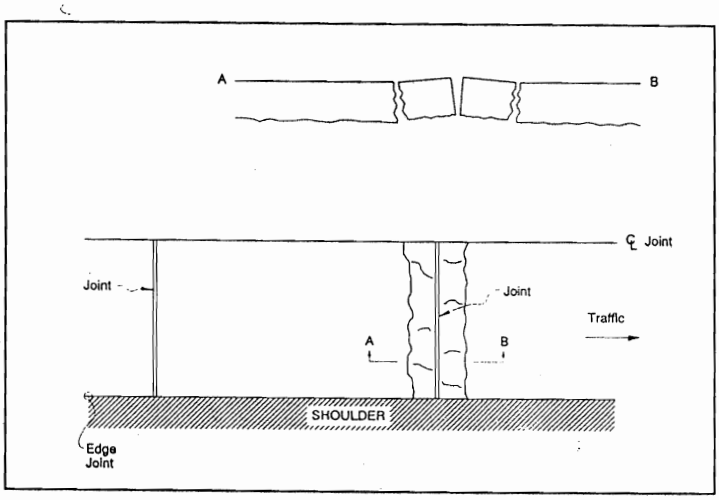

圖七　隆起(或擠破)之示意圖

1.10 接縫斷層(或高差)(Joint Faulting)

接縫斷層是接縫或裂縫兩側鋪面版產生不同高程的現象。在量測時不需判定其破壞程度，記錄時以公釐爲單位，量測的位置位於從版外側邊緣算起各0.3與0.75公尺處，其值的正負判斷方式如圖八所示。

接縫斷層高差大於1~2公釐時，即可察覺因車胎衝擊所產生的噪音，大於3公釐時行車所產生的震動便會使乘車者感覺不適。

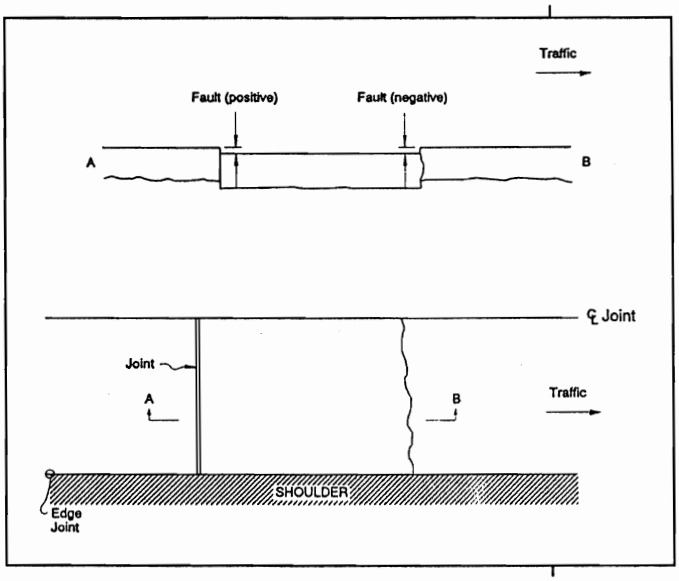

圖八　接縫斷層(或高差)之示意圖

1.11 車道與路肩高差(Lane-to-Shoulder Dropoff)

車道與路肩高差是版的邊緣與路肩產生不同高程的現象，典型的情況爲路肩發生沉降（settlement）。其量測時不需判定其破壞程度，記錄時以公釐爲單位，記錄的位置爲版與路肩之接縫處，每隔15公尺量測一次，其值的正負判斷方式爲路肩低於車道爲正，反之爲負。（如圖九所示）

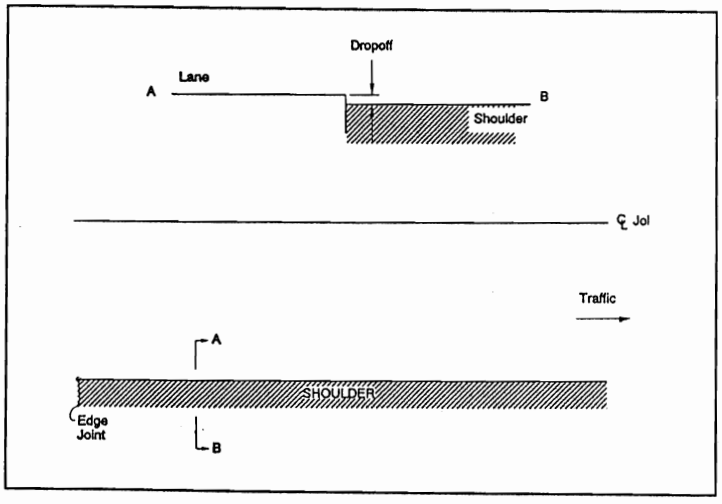

圖九　車道與路肩高差之示意圖

1.12 車道與路肩分離(Lane-to-Shoulder Separation)

車道與路肩分離是車道與路肩間的接縫變寬而分離的現象，量測時不需判定其破壞程度，記錄時以公釐爲單位，記錄的位置爲版與路肩之接縫處，記錄接縫分離的寬度，每隔15公尺量測一次，並標註每個接縫處是否曾經填充過。（如圖十所示）

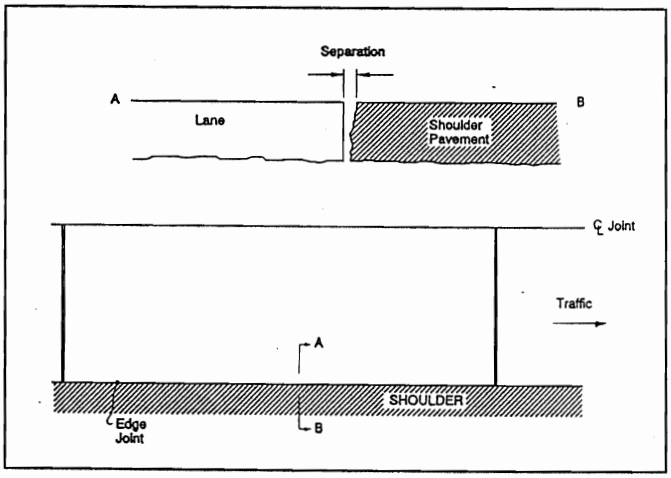

圖十　車道與路肩分離之示意圖

車道與路肩分離的產生主要是因爲鄰近路肩的土壤壓實不良、土壤中含水量過高或排水不良等因素所引起。若車道與路肩分離產生而不加以維修，則水分會經由分離處滲入使得路基加速侵蝕。

1.13 修補/修補損壞(Patching / Patch Deterioration)

修補即是將原始之混凝土移除、置換，並以新的材料填補，而其面積大於0.1平方公尺者。修補損壞則爲修補發生如剝落、裂縫等損壞。（如圖十一所示）

修補或修補損壞的破壞程度可區分爲輕度、中度與重度三種，量測的方式是依修補的材料分別記錄其各破壞程度下修補或修補損壞的數量與面積。其破壞程度爲：1.輕度：修補區域只有很輕微的破壞，沒有斷層或沉降。2.中度：修補區域有中度的破壞，斷層或沉降小於6公釐。3.重度：修補區域有重度的破壞，斷層或沉降大於等於6公釐。

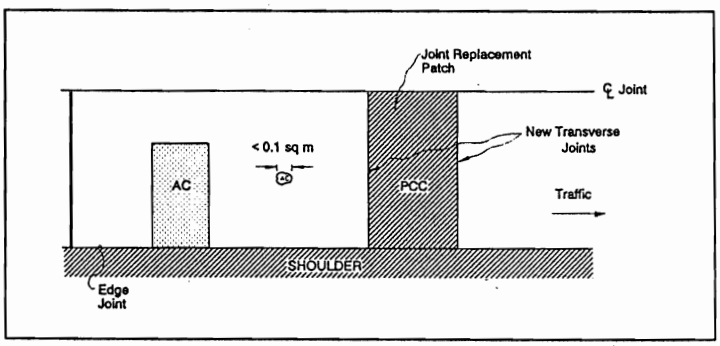

圖十一　修補/修補損壞之示意圖

1.14 唧水或噴泥現象(Water Bleeding and Pumping)

唧水或噴泥現象爲版在交通載重作用下變形，使基底層中水份挾帶細粒料經由接縫或裂縫而噴出。唧水或噴泥現象可由鋪面接縫或裂縫附近累積著細粒料或接縫斷層（或高差）而偵測得知，這些細粒料是從基底層滲出而累積在鋪面表面。唧水或噴泥現象亦表示接縫填充不良，會進而導致路基承載力喪失，並在交通載重重複作用下使鋪面版損壞。唧水或噴泥現象量測時不需判定其破壞程度，記錄其發生的數量與長度。

2.0 連續式鋼筋混凝土鋪面

連續式鋼筋混凝土鋪面損壞形態的種類主要可分爲以下三大類：

a. 裂縫：縱向裂縫、橫向裂縫與耐久性("D")裂縫。

b. 表面破壞：包含龜裂、表面剝落與鬆散、粒料磨損與脫落。

c. 其它：包含隆起(或擠破)、車道與路肩高差、車道與路肩分離、修補/修補損壞、唧水或噴泥現象、縱向接縫填充料破壞、縱向接縫剝落、橫向建造接縫破壞與貫穿等。

由於連續式鋼筋混凝土鋪面損壞形態與接縫式無筋剛性鋪面損壞形態有許多類似相通之處，以下僅就其不同之破壞形態加以介紹：

2.1 橫向建造接縫破壞（Transverse Construction Joint Deterioration）

連續式鋼筋混凝土鋪面是連續鋪築的，但每階段工作結束後（如每日收工時）仍會有建造接縫。橫向建造接縫破壞是指在橫向建造接縫附近產生許多密集相間的橫向裂縫或許多交錯的裂縫，其破壞程度可區分爲輕度、中度與重度三種，量測的方式是記錄其各破壞程度下橫向建造接縫破壞的數量。其破壞程度爲：1.輕度：在橫向建造接縫0.6公尺內，無剝落或斷層發生。2.中度：在橫向建造接縫0.6公尺內，有剝落發生，但剝落小於75公釐。3.重度：在橫向建造接縫0.6公尺內，有剝落發生，且剝落大於等於75公釐並產生分離者。（如圖十二所示）

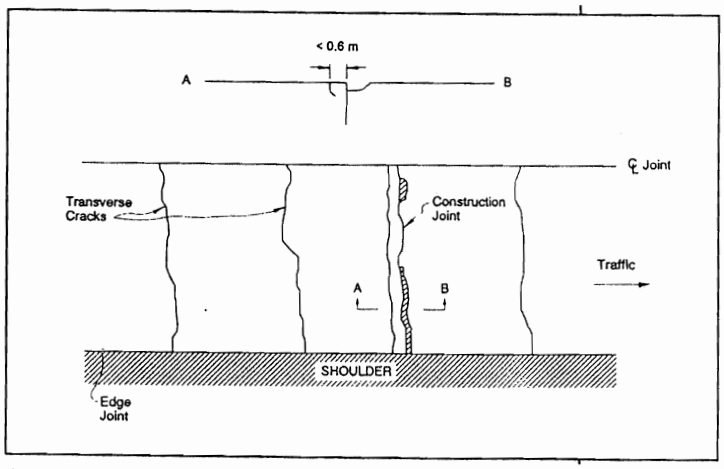

圖十二　CRCP橫向建造接縫破壞之示意圖

2.2 貫穿（Punchout）

貫穿之形成爲兩相近（通常在0.6公尺以內）之橫向裂縫、一條較短縱向裂縫與鋪面邊緣或縱向接縫包圍成一區域，此一區域會因爲交通載重的作用而與鋪面版分離或產生剝落、斷層等現象。（如圖十三所示）

其破壞程度可區分爲輕度、中度與重度三種，量測的方式是記錄其各破壞程度下貫穿破壞的數量。裂縫仍須記錄於橫向裂縫與縱向裂縫之中。破壞程度爲：1.輕度：在橫向裂縫與縱向裂縫情況輕微，剝落小於75公釐或斷層小於6公釐。但不包含"Y"型的裂縫貫穿型式。2.中度：剝落大於等於75公釐但小於150公釐或斷層大於等於6公釐但小於13公釐。3.重度：剝落大於等於15公釐或斷層大於等於13公釐或在交通作用下已與鋪面版產生移動或分離者。

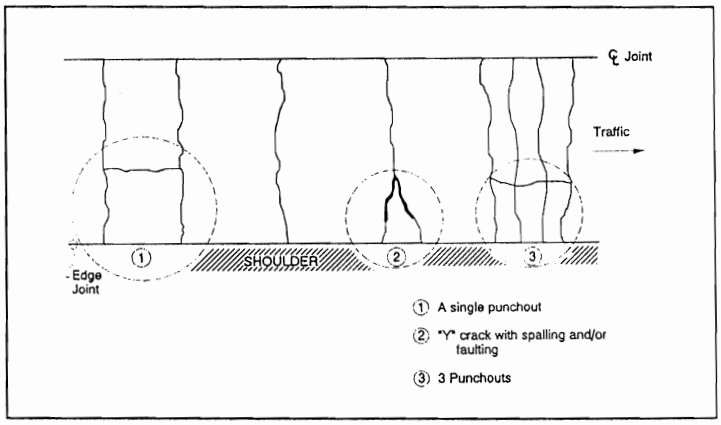

圖十三　CRCP貫穿之示意圖

其他連續式鋼筋混凝土鋪面損壞形態之示意圖如下：

1. CRCP橫向裂縫

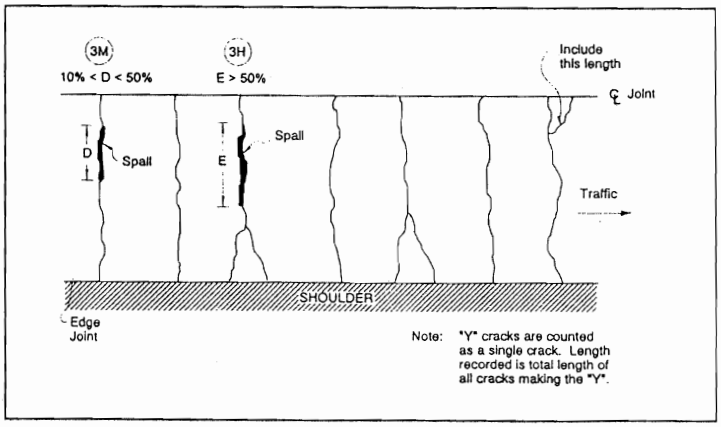

圖十四　CRCP橫向裂縫之示意圖

2. CRCP縱向裂縫

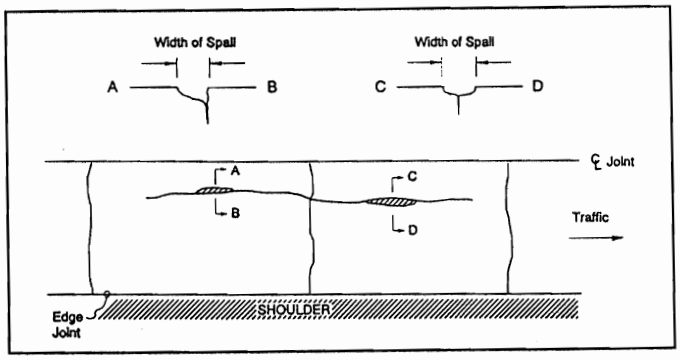

圖十五　CRCP縱向裂縫之示意圖

3. CRCP隆起（或擠破）

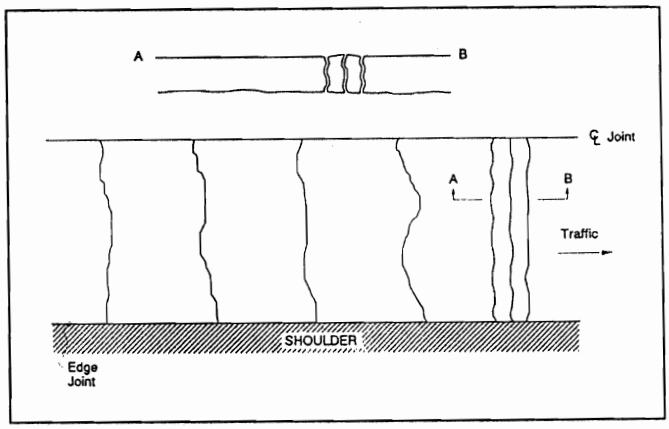

圖十六　CRCP隆起(或擠破)之示意圖

4. CRCP耐久性（"D"）裂縫

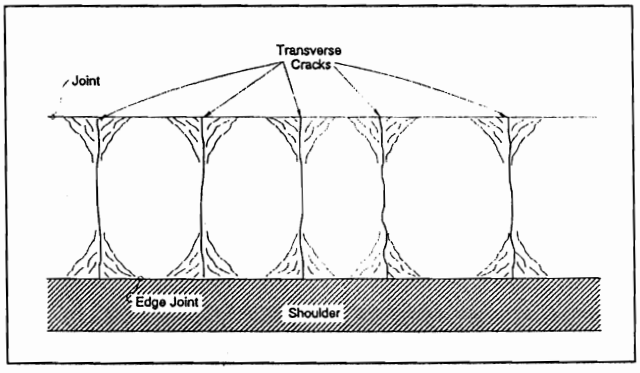

圖十七　CRCP耐久性("D")裂縫之示意圖

3.0 剛性鋪面損壞維修

剛性鋪面若發生損壞時，其維修方式一般以下列基本步驟決定：

1. 損壞狀況的調查。
2. 推斷引起破壞的原因。
3. 決定判斷是否維修，若需維修並訂定維修時間。
4. 維修方式與施工法的訂定與交通管制措施的擬定。
5. 實施維修。
6. 維修效果評估與追蹤調查。

維修方式可分爲預防性與矯治破壞式的維修方式。在進行鋪面維修的工作時，許多的維修方法可被採用，端賴工程師的經驗與經費等相關因素來決定。本講義包含若干不同的維修方法與技術可供工程人員參考。其主要的養護的方式一般有：

1. 全厚度接縫式混凝土鋪面修補（Full-Depth Repair of JCP）
2. 全厚度連續式混凝土鋪面修補（Full-Depth Repair of CRCP）
3. 瀝青混凝土修補（Patching with Bituminous Mixture）
4. 部分厚度的剝落修補（Partial-Depth Spall Repair）
5. 版基底層的穩定與版的升高方法（Slab stabilization and Slab Jacking）
6. 鋪面的打磨方法（Diamond Grinding, Grooving, and Cold Milling）
7. 應力傳遞設施的修補（Load transfer Restoration）
8. 接縫與裂縫的填封（Joint and Crack Sealing）
9. 路肩改善方法（Shoulder Improvement）等。

對於維修的方法若能妥善加以選擇將可得到經濟而有效的結果。

3.1 全厚度接縫式混凝土鋪面修補

全厚度接縫式混凝土鋪面修補時所採用的材料爲波特蘭混凝土，瀝青混凝土不建議採用，因爲會使鋪面糙度值惡化且其維修成本並不見得較經濟。

可以採用全厚度接縫式混凝土鋪面修補方式的破壞形態有隆起、角隅斷裂、耐久性裂縫、剝落與曾經修補而再次破壞的鋪面等。在進行全厚度接縫式混凝土鋪面修補時主要考慮的要項如下：

1.接縫的設計

接縫的設計對全厚度接縫式混凝土鋪面修補而言是十分重要的，因爲全厚度修補可以想像爲置換成一個新的剛性鋪面版，而版與版之間的應力傳遞應予維持，若應力傳遞不良會導致更嚴重的剝落、唧水作用、高差與角隅斷裂等破壞。

一般對剛性鋪面版的橫向接縫而言，可採用粗糙面與平滑面兩種切割方式。粗糙面是切割30％以下的深度，以骨材互鎖作用提供應力傳遞的效果；而平滑面則是切割深度在30％以上，但須提供應力傳遞的設施（如綴縫筋，dowel bar）。對於高載重交通量的鋪面建議採用平滑面的切割方式。綴縫筋的設計主要須考慮綴縫筋的直徑、數量和擺置間距、未來重車交通量與允許之鋪面高差等因素。

2.修補位置與區域的訂定及修補區域的準備

鋪面表面完好並不代表鋪面內部無破壞產生，所以就鋪面版的結構狀況劃定修補的區域時，除依據經驗外，尚可利用鑽心試體得知鋪面的狀況，利用非破壞性檢測亦可。

修補區域訂定應該注意要能防止潛在性破壞發生，修補時最好能做鋪面車道全寬度的修補。修補區域的邊界應離現有的橫向接縫1.8公尺以上，否則將使臨接版產生額外的應力造成破壞。

修補區域劃定以後即進行版的切割，建議採用全厚度的切割方式。切割之後的剛性鋪面版可以打除或直接拉起，直接拉起的方式可以避免渣碎殘留而較易於清理。清理之後並修補基底層並安放綴縫筋。

3.混凝土的澆置

澆置混凝土時應注意需充分搗實，使修補區域邊緣能與原有剛性鋪面版相互接合。加水增加工作度的做法應當避免，以免使混凝土強度降低或產生潛縮（shrinkage）。若爲增加工作度可以考慮添加減水劑。

4.接縫的填封

混凝土的澆置之後需儘早對接縫重新填封，如此可防止剝落與水份入滲的產生。

5.養治與開放交通

鋪面能否開放交通可依下列方式考慮：

a.混凝土抗壓強度與破裂模數是否已達要求？

b.以混凝土的性質來考慮，是否混凝土已達最短養治時間。

若達上述要求且鋪面經掃紋且檢視合格則鋪面可重新開放交通。

3.2 全厚度連續式混凝土鋪面修補

可以採用全厚度連續式混凝土鋪面修補方式的破壞形態有隆起、貫穿、耐久性裂縫、建造接縫破壞、剝落與曾經修補而再次破壞的鋪面等，若是小區域輕度的坡壞可以考慮部分厚度的修補方式。在進行全厚度連續式混凝土鋪面修補時主要考慮的要項如同上節所述：

1.接縫的設計
2.修補位置與區域的訂定及修補區域的準備
3.混凝土的澆置
4.接縫的填封
5.養治與開放交通

3.3 瀝青混凝土修補

瀝青混凝土修補之施工方式是將鋪面破壞打除至健全混凝土後，清潔渣碎。塗撒黏結材料，以每層不超過4英吋的方式逐層壓實修補。

3.4 部分厚度的剝落修補

以部分厚度的剝落修補方式處理的破壞形態有輕度剝落、表面剝落與輕度的耐久性裂縫等。其主要處理鋪面表層的損壞，對於剝落超過1/3版厚的破壞就不適宜了。對於損壞是否超過1/3版厚，可以鑽心採樣以決定是採用全厚度或部分厚度的修補方式。

修補時可依交通條件選擇普通水泥、早強水泥或超早強水泥使用，若修補的厚度太淺，其最大粗骨材粒徑不可超出施工厚度的1/3。其施工方式是將修補損壞部分打除至健全混凝土處，清潔渣碎並使版保持溼潤。修補範圍附近作好防護以免澆注混凝土時污染附近正常鋪面，之後澆灑水泥砂漿，澆注混凝土、搗實並鏝平。待初凝之後掃紋，並進行養治，養治應至少72小時始能開放交通。若修補部分有接縫，則必須先將原有的填縫移除約1英吋深，先作暫時的填縫以防外物進入接縫，待鋪面修補最後移去暫時填縫料，重新進行接縫的填封。

3.5 版基底層的穩定與版的升高方法

版基底層支承力的喪失是引起剛性鋪面版加速破壞（如：唧水作用、高差與破裂等）的主要原因。版基底層的穩定即是將波特蘭混凝土材料或瀝青混凝土材料利用機具以壓力注入版與基底層的空隙之中；版的升高即是將版提高以保持鋪面版之間的平整。

版基底層的穩定在使用波特蘭混凝土材料方面須注意其坍度（須能使材料完全填充孔隙）及強度，一般使用水泥飛灰砂漿。瀝青混凝土材料方面則需採用低針入度（15-30）與高軟化點（204-232℃）的材料。

版基底層的穩定僅應用於接縫或裂縫有支承力喪失的情況，若唧水作用產生但基底層仍有支承能力時，採用版基底層的穩定的方式反而會使版產生破裂並產生浪費。

版的升高進行時須量測其上升的高度，一般以鋼絲線配合測量儀器來進行以保持鋪面版之間的平整。

3.6 鋪面的打磨方法

鋪面的打磨方法即是利用機具將鋪面打磨以維持其平整度。其主要是能磨平高差或使鋪面保持良好的抗滑能力。

鋪面的打磨方法須將引起高差的原因加以考慮，以減輕未來的破壞程度，必要時須先對其產生之原因加以處理。

3.7 應力傳遞設施的修補

應力傳遞設施的修補是將傳遞效率降低之應力傳遞設施加以修補，可以防範接縫剝落、唧水作用、高差與裂縫的加劇破壞。

無應力傳遞設施的接縫式無筋混凝土鋪面其應力傳遞效率通常較差，因此無法承受較高的載重重複作用。因此在修補時需將交通載重列入考慮，必要時可加入應力傳遞設施。

3.8 接縫與裂縫的填封

接縫與裂縫的填封若保持良好狀況，可以防止水或異物侵入以避免破壞狀況的加劇。

裂縫的修補應先查明引起裂縫的原因，原因排除之後再進行裂縫的填縫。其修補與填縫的方法是沿著裂縫切割3/8英吋寬、3/4英吋深的溝槽，並清潔溝槽之後使溝槽具備良好的黏結性，之後以填封劑填入溝槽。

接縫填充料破壞需先清除舊接縫材料至少1英吋深並以空壓機施以高壓空氣清除舊接縫縫隙中之泥沙與雜物，最好能清除至鋪面底

版。清除完畢之後重新施做填縫料，施做時接縫處需保持乾燥，若潮濕可以瓦斯火焰烘乾。

3.9 路肩改善方法

路肩可以提供鋪面的側向支撐，亦可作爲緊急救護等用途。爲提供路肩與主車道間的應力傳遞效率，可以施作連繫鋼筋（tie bar，間距18-24英吋），以防止車道與路肩分離、高差與裂縫等破壞。

4.0 結語

就實際的情況而言，剛性鋪面損壞原因的判定與維修方式的選擇並無固定的模式可循，可謂是一門“決定的藝術”。本講義所提供的方式旨在提供一通用的觀點，提供工程師在鋪面維修時的參考。實際作業時，工程師仍需以其逐漸累積的經驗與知識檢視鋪面現實狀況，並參酌現有資源以做出維修方式最有效而經濟的選擇。

最後，淡江大學土木工程研究所研究生李英明在本講義編寫期間協助資料彙整與打字，使本講義能夠如期完成，謹此致上最深謝意。

5.0 參考文獻

1. 顏聰、林炳森、蕭伯聰，"剛性路面實用設計本土化研究期末報告"，交通部台灣區國道新建工程局，書籍編號026。
2. 賴森榮，"北二高剛性路面建造講習", 交通部台灣區國道新建工程局，訓練教材001，民國七十九年。
3. 交通部，"交通技術標準規範公路類公路工程部--公路養護手册"，幼獅出版社，民國七十八年六月。
4. 侯羿、賴森榮，"臺灣區高速公路路面養護管理系統"，臺灣營建研究中心，民國七十八年。
5. 周家蓓，"市區道路鋪面養護管理系統建立之研究"，交通部運輸研究所，民國八十一年十一月。
6. 周家蓓，"臺灣地區一般公路鋪面養護管理系統建立之研究"，交通部運輸研究所，民國八十二年十月。
7. 林志棟，"本省路面工程整修標準芻議"，鋪面管理維護系統研討會專集(一)，中央大學，民國八十年。
8. ASTM, "1993 Annual Book of ASTM Standards," Volume 04.03: "Road and Paving Materials; Pavement Management Technologies," 1993.
9. SHRP, "Distress Identification Manual for the Long-Term Pavement Performance Project," SHRP-P-338, Strategic Highway Research Program, National Research Council, Washington, D.C., 1993.
10. Darter, M. I., and S. H. Carpenter, "Techniques for Pavement Rehabilitation, " Participant's Notebook, U.S. Department of Transportation, Federal Highway Administration, National Highway Institute, Third Revision, October, 1987.
11. Yoder, E. J., and M. W. Witczak, "Principles of Pavement Design," John Wiley & Sons Inc., Second Edition, 1975.
12. Huang, Y. H., "Pavement Analysis and Design," Prentice Hall, Englewood Cliffs, New Jersey, 1993.
13. Sargious M., "Pavement and Surfacings for Highways and Airports," 虹橋書局, 1975.

B 柔性鋪面之回算與結構評估

B.1 柔性鋪面之回算
(含BISDEF程式之使用介紹)

B.2 柔性鋪面之結構評估

B.3 由面層撓度值回算鋪面彈性模數的初步研究

資料來源：

陳建桓、李英豪，“由面層撓度值回算鋪面彈性模數的初步研究”，中華民國第八屆鋪面工程學術研討會論文輯(已接受)，台北國際會議中心，中原大學，中華民國八十四年十二月六日至八日。

B.4 BISAR程式之使用介紹

B.1 柔性鋪面之回算
(含BISDEF程式之使用介紹)

STRUCTURAL CHARACTERIZATION OF PAVEMENT LAYERS AND DETERMINATION OF ALLOWABLE AIRCRAFT LOADS

1. BASIC APPROACH

The determination of the load-carrying capacity or the maximum allowable load for a given pavement requires the following major steps:

1. Measure pavement deflection basins at selected points throughout the pavement feature.

2. Backcalculate the elastic or resilient modulus of each pavement layer and the subgrade. Determine Moduli for different seasons.

3. Use the elastic moduli and layer thicknesses in a structural model (such as the elastic layer program) to compute critical stresses and strains in the pavement under actual aircraft loadings for different seasons.

4. Use fatigue cracking and permanent deformation (rutting) prediction models to estimate the number of load applications to structural failure of the pavement for each aircraft type and varying gross aircraft loads. Use values for the load-carrying capacity for individual aircraft such as those shown in Figure 1. → Pass Damage

5. If several critical aircraft will regularly use the pavement, an analysis of the combined effect of all aircraft must be conducted using either the equivalent aircraft approach or a cumulative damage method, such as Miner's.

Prof. M. Darter
Civil Aviation Training
Jeddah, Saudi Arabia
1984

Module 2.8B

Structural Evaluation By NDT (Deflections)

CHAPTER 1 *

INTRODUCTION

1.1 General

Providing a quantitative basis for evaluating the pavement structural condition at any stage of its service life is one of the main objectives of flexible pavement Nondestructive Testing (NDT). A structural pavement evaluation is needed to:

1) Determine if a pavement structure is adequate to accomodate an anticipated change in mission (traffic),

2) Provide material properties for overlay design when the pavement is reaching its final serviceability, and

3) Develop rehabilitation recommendations and optimal maintenance strategies based on routine structural evaluation.

There is general agreement among pavement engineers and researchers that the measurement of the surface deflection basin provides valuable information for the structural evaluation of

* Ph.D. Thesis, Mario Hoffman, 1980. U. Illinois.

flexible pavements. To quantitatively interpret surface deflection measurements made during the load testing of pavements, the actual structure and its subgrade must be replaced by a mechanistic model(s).

The structural evaluation of a flexible pavement is, to an extent, an inverted design process. If the cross section and properties of the paving materials and support system are known, it is possible to compute the pavement response (stresses, strains, and displacements) for given loading conditions. In the evaluation process, the response of the pavement is observed and the material properties are backcalculated.

Among the different load responses, only surface deflections are easily measurable. Deflection is a basic response of the whole system to the applied load. It is frequently used as an indicator of the load carrying capacity of the pavement. Also, surface deflection measurements are rapid, relatively cheap, and nondestructive. All these factors make NDT attractive and useful.

The problem of evaluating a pavement is a complex one. The pavement structure is composed of various materials. The behavior of these materials under load is far from the ideal materials assumed in classical mechanics. Their properties vary diurnally, seasonally, and with repetitions of loading. In addition, the load-response characteristics of flexible pavements are stress and rate of loading dependent. All these factors must be fully understood and accounted for in the

development of a methodology for structural evaluation.

1.2 Surface Deflections in Pavement Evaluation

Surface deflections have been used for many years as pavement performance indicators. In 1955, results from the WASHO Road Test established the values of 45 and 35 mils as limiting values of allowable maximum deflection under an 18 kip axle for flexible pavements in spring and fall respectively (1). Following the concept developed in the WASHO Road Test, many other investigators and agencies adopted and established their own limiting deflection criteria (2,3,4).

Subsequently, researchers related the limiting deflection criteria to traffic (5,6), and to combined traffic and thickness of the asphalt concrete layer (7,8). Limiting deflection criteria for different types of structures and traffic for both airport and highway pavements were developed (9,10,11,12). Correlations between surface deflections and the Present Serviceability Index derived from the AASHO Road Test were modified and incorporated into a pavement design method (14,15). Table 1.1 summarizes some typical limiting deflection criteria reported in the literature.

In the early 1950's, while developing light vibrators for wave propagation analysis of pavements, Shell investigators in Holland proposed a limited stiffness value of 1,100 kips/in to prevent cracking of the asphalt concrete pavement surface (16). The stiffness value, defined as the load required to produce a

unit deflection, became especially popular in the field of airport pavement evaluation (12,17,18).

Parallel to the development of limiting deflection and stiffness criteria, researchers considered the curvature of the deflection basin, but few limiting curvature criteria were developed. Furthermore, there is no unique definition of curvature nor any established method for its measurement. Different geometric functions are used to describe the deflected shape of the pavement's surface: a circle (19), a sine curve (15), and a parabola (20). Criteria are reported for radius of curvature (19), the ratio between the size of the deflection basin and the maximum deflection (21), the "slope" of the deflection basin (22), and the product between the radius of curvature and the maximun deflection (20). Table 1.2 summarizes limiting stiffness and curvature criteria for pavement evaluation.

Once a limiting deflection criterion is established and adopted, the evaluation scheme is generally complemented by a method for the determination of the overlay required to reduce the measured deflections below a desired limit. The Asphalt Institute (5), the TRRL (10), and others have developed such methods that are widely used.

The limiting deflection and curvature criteria, developed over long years of observations, experience, and empirical correlations with performance indicators, proved to be unsatisfactory for pavements, materials, and environmental

conditions different from those considered in the correlations. In the last 15 years, parallel to the development of mechanistic methods of pavement design, more emphasis has been placed on the development of more fundamental methods of pavement evaluation. Measured deflection basin parameters are used as input into a mechanistic pavement model and the model parameters are backcalculated. This is the main topic of this dissertation.

1.3 Statement of the Problem

A mechanistic method of pavement design generally starts with a component analysis of the different materials (laboratory testing of material specimens). The different components are then incorporated into a system (layered model), and the behavior of the whole system under load is analyzed (stresses, strains, deflections). In a mechanistic pavement evaluation method the system response is measured (surface deflections), the response is analyzed with the use of a layered model, and the material properties are backcalculated. The analogies and differences between a component and system analyses are illustrated in Figure 1.1.

The laboratory determination of the resilient modulus requires the interpretation of a "nondestructive test": a) The specimen is axially loaded, b) its deformation is measured, and c) the resilient modulus is calculated as the ratio between the deviator stress and the recoverable strain.

The backcalculation of material properties based on NDT interpretation is a "full-scale test": a) The specimen (the pavement) is loaded, b) its deflection basin is measured, and c) the material properties are backcalculated using a selected layered model. The analogies of both methods of test are evident.

The same concern excercised in laboratory procedures to simulate the repetitive nature and magnitude of traffic loadings applies to the load testing of pavements. The interpretation of a full-scale test imposes complications and difficulties compared with the relatively simple component testing at the laboratory. The obvious advantages of pavement NDT are:

1) Realistic loading simulating actual traffic loadings can be applied,

2) The complex interactions among different layers in the pavement are incorporated into the pavement "sample,"

3) The specimens (the layers) are loaded in a realistic three dimensional fashion (very difficult to reproduce in the lab),

4) The backcalculated parameters represent the "layer material" rather than the "specimen material" at the lab,

5) The layer materials can be tested under different seasonal and environmental conditions and at any time during the life of the pavement,

TABLE 1.1 Limiting Deflection Criteria for Pavement Evaluation

Reference	Deflection Criteria	Remarks
WAASHO (1)	Spring Δ_{max} = 45 mils Fall Δ_{max} = 35 mils	Conventional flexible pavements. Deflections measured under 18 kip axle.
Hveem (4)	$\Delta_{all} \leq$ 50 mils (1) $\Delta_{all} \leq$ 17 mils (2)	(1) Surface treatment; (2) AC layer thickness = 4 in. Deflections measured under 15 kip axle. Δ_{all} = allowable maximum deflection
Carneiro (3)	20 mils $\leq \Delta_{max} \leq$ 35 mils	Conventional flexible pavements. Benkelman beam deflections under 18 kip. axle, 80 psi tire pressure.
Whiffin et al (6)	20 mils $\leq \Delta_{max} \leq$ 30 mils (1) 5 mils $\leq \Delta_{max} \leq$ 15 mils (2)	(1) Asphalt concrete over granular base. (2) Asphalt concrete over cement treated base. Traffic volume considered. Benkelman beam deflections under 14 kip axle, 85 psi tire pressure.
State of California (8)	Δ_{all} = f(Tac,N)	Δ_{all} = Allowable maximum deflection Tac = Thickness of AC layer N = Number of repetitions of a 5 kip EWL Examples: Δ_{all} = 80 mils for Tac = 1.5 in. and N = 10,000 Δ_{all} = 37 mils for Tac = 1.5 in. and N = 10^6 Δ_{all} = 46 mils for Tac = 6 in. and N = 10,000 Δ_{all} = 22 mils for Tac = 6 in. and N = 10^6
Asphalt Institute (5)	Δ_{all} = f(DTN, Temp)	DTN = Design traffic number = average daily 18 kip axle loads Δ_{all} = Allowable maximum deflection (plus two standard deviations) Examples: Δ_{all} = 22 mils for DTN = 1000 Δ_{all} = 100 mils for DTN = 2 Benkelman Beam Deflections
Lister (7)	N = f($\Delta_{in.}$, pavement type)	N = Cumulative number of 18 kip axle repetitions $\Delta_{in.}$ = Initial Benkelman beam deflection (14 kip axle) Graphical relations between N and $\Delta_{in.}$ for different pavement types. For AC pavement with granular base layer: $\Delta_{in.}$ = 20 mils; N = 4.5×10^6 $\Delta_{in.}$ = 40 mils; N = 0.5×10^6
Nagumo et al (13)	$\log N = 0.179\Delta^2 - 1.117\Delta + 6.772$	N = Number of repetitions to failure of heavy loads (over 18 kip) Δ = Benkelman beam deflections
Joseph and Hall (11)	$\Delta = 1.1315/N^{0.233}$	Δ = Initial deflection (mils) under a given load N = Repetitions to failure of that load

Laboratory Testing of a Specimen

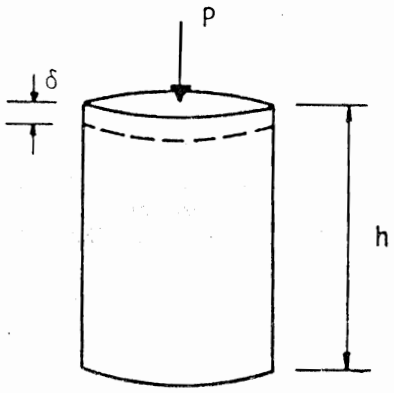

1. Apply axial load;
2. Measure axial deformation;
3. Compute "E" based on the ratio:

$$E = \frac{\text{Deviator Stress}}{\text{Recoverable Strain}}$$

Component Characterization → System Response

Full-Scale Testing of a Pavement

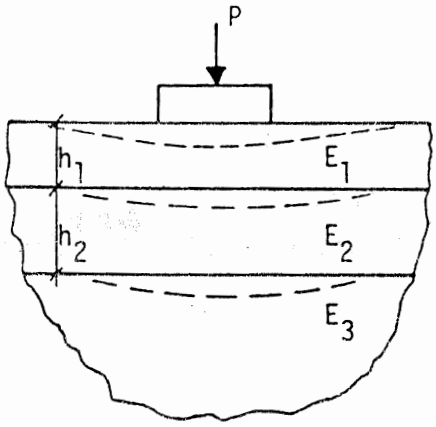

1. Apply NDT load;
2. Measure surface deflections;
3. Compute "E's" based on a Layered Model

System Response → Component Characterization

Figure 1.1 Component versus System Analysis of Pavement Structures

Figure 1. Allowable Gross Aircraft Loads for Outer Portion of Taxiway on B-727 Aircraft**

[A particular pavement. presentation

Pass Intensity Level	Passes	Coverages *	Allowable Loads, kips			
			Rutting Subgrade 0.5 in.	% Fatigue Cracking		
				50	25	10
I	50,000	15,385	120	134 x	130	120
II	15,000	4,615	150	170	165	155
III	3,000	923	> 190.5	> 190.5	> 190.5	> 190.5
IV	500	154	> 190.5	> 190.5	> 190.5	> 190.5

* P/C = 3.25

** Maximum loads acceptable for interior portion of taxiway for all Levels.

x Interpretation: This pavement section can handle about 50,000 passes of a B727 aircraft load at 134 kips before 50% fatigue cracking would develop.

2. BASIC CONCEPTS FOR FLEXIBLE PAVEMENTS

Pavement Characterization

One-layer pavements can be characterized using Boussinesq theory:

$$DEF = 1.5\ p\ a\ /\ E$$

where: DEF = measured deflection, ins. or cm
p = pressure on loading plate, psi or kg/sq.cm
a = radius of load plate, ins. or cm
E = modulus of elasticity of layer, psi or kg/sq.cm

Example-- A Falling Weight Deflectometer was used to measure the deflection directly on top of a compacted silty clay subgrade. The load and other information are as follows:

Load = 2000 pounds or 908 kg
Radius of plate = 5.9 ins or 15 cm.
Measured maximum deflection beneath plate = 0.025 ins. or 63.5 mm

Compute the E of the silty clay subgrade (Answer: 6474 psi or 455 kg/sq.cm).

Two-layer pavements can be characterized using two-layer elastic layer theory and a simple chart such as the one shown in Figure 2. The backcalculation of the elastic moduli of the two layers requires the measurement of the deflection basin at four uniformly spaced intervals of 0, 12, 24, and 36 in. (0, 30, 61, and 91 cm). The thickness of the upper layer must also be known. The curvature of the deflection basin is therefore measured, and can then be used to compute the E1 and E2. The "area" of the deflection basin is first computed according to the following formula:

$$AREA = 6 \left(1 + 2D1/D0 + 2D2/D0 + D3/D0 \right)$$

where: AREA = A value representing the stiffness of the pavement relative to the subgrade (ranges from 36 for a perfectly stiff pavement that does not bend, to 11.1 for a pavement which is as stiff as the subgrade).

D0,D1,D2,D3 = Measured deflections at 0, 12, 24 and 36 in. (0, 30, 61 and 91 cm) from the center of the loading plate.

Typical values of AREA for different pavements placed over a soft subgrade are as follows:

Pavement/Soft Subgrade	AREA
Surface Treatment	11 - 15
Weak Flexible Pavement	16 - 20
Stiff Flexible Pavement	21 - 25
Concrete Slab	29 - 32

Other factors which must be known are the maximum deflection (MDEF), the total load on the plate (P), and the thickness of the pavement layer (t). The chart shown in Figure 2 is then entered as illustrated and the E1/E2 ratio determined, followed by the determination of the following ratio:

$$MDEF\ E2\ /\ P\ (x\ 10^{-2})$$

Once this is known, E2 and E1 are computed.

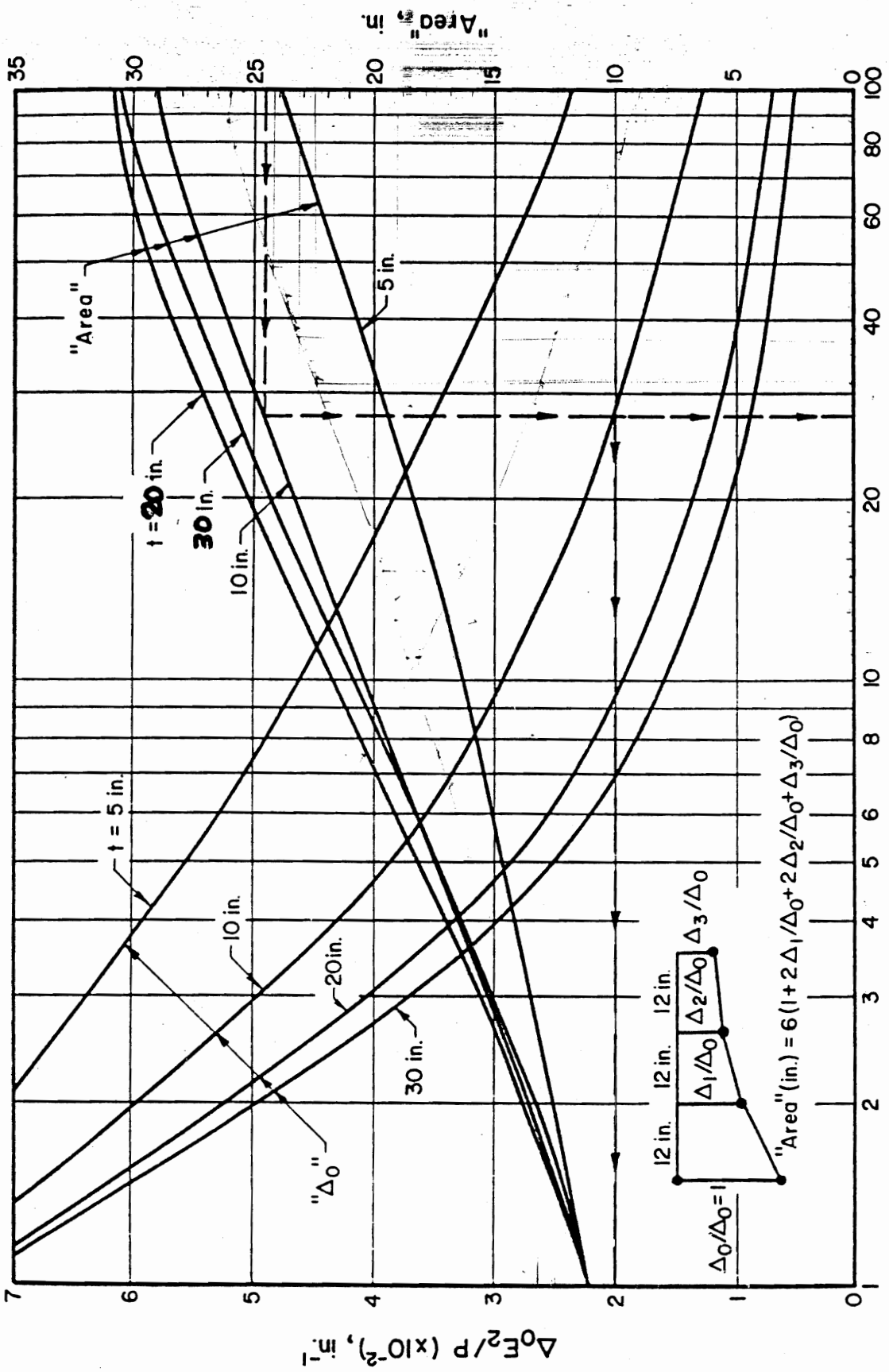

Figure 12. Variation of the "Area" and the Maximum Deflection Factor in a Two-Layer Linear Elastic Model.

FWD EXAMPLE OUTPUT

Date: 10071982 Temp: 78 F
Roadway: PARKING LOT
Time: 2:00 PM

Load Radius [a] =6 in
r's=0 12 24 36 48 60 72

SHUNTVAL in VOLTS: 7.18336
STEP: 6

BURRELL St.

Station FIRST TEST DEMO FOR PROF.		DARTER		
Ld (lbs) →	6231	5854	8907	9020
Df1(mil)	21.2	20.2	31.3	31.5
Df2(mil)	13.4	12.9	20.2	20.4
Df3(mil)	7.8	7.6	12.0	12.1
Df4(mil)	4.8	4.8	7.6	7.6
Df5(mil)	3.1	3.1	5.0	5.0
Df6(mil)	2.3	2.3	3.6	3.7
Df7(mil)	1.8	1.7	2.8	2.8
Area(in)	19.4	19.6	19.8	19.8
dsm(kpi)	294	289	285	286
DSM(kpi)	281			

Station FIRST TEST DEMO FOR PROF.		DARTER		
Ld.(lbs)	12648	12696	15964	15934
Df1(mil)	44.2	44.5	55.9	56.4
Df2(mil)	28.8	29.0	36.4	36.9
Df3(mil)	17.2	17.2	21.8	22.0
Df4(mil)	10.9	11.0	13.8	13.8
Df5(mil)	7.1	7.2	8.9	9.0
Df6(mil)	5.1	5.1	6.3	6.3
Df7(mil)	3.8	3.9	4.8	4.8
Area(in)	20.0	19.9	20.6	20.0
dsm(kpi)	286	285	286	282
DSM(kpi)	270			

SHUNTVAL in VOLTS: 7.18092
STEP: 6

PARKING LOT

Station FIRST TEST DEMO FOR PROF.		DARTER		
Ld.(lbs)	6515	6634	9718	9119
Df1(mil)	23.4	21.8	33.0	31.8
Df2(mil)	9.0	8.7	13.3	13.1
Df3(mil)	4.3	4.3	6.0	6.1
Df4(mil)	2.6	2.7	3.8	3.8
Df5(mil)	2.0	2.1	2.9	2.9
Df6(mil)	1.9	1.8	2.5	2.5
Df7(mil)	1.4	1.4	2.0	2.3
Area(in)	13.5	13.9	13.7	14.0
dsm(kpi)	278	305	294	296
DSM(kpi)	247			

Station FIRST TEST DEMO FOR PROF.		DARTER		
Ld.(lbs)	12371	12359	15376	15478
Df1(mil)	44.3	44.3	57.4	51.0
Df2(mil)	18.8	18.9	24.5	24.9
Df3(mil)	8.7	8.8	11.1	11.3
Df4(mil)	5.3	5.3	6.6	6.7
Df5(mil)	3.9	4.0	4.9	5.0
Df6(mil)	3.5	3.5	4.3	4.5
Df7(mil)	3.0	2.9	3.6	3.7
Area(in)	14.2	14.2	14.1	15.3
dsm(kpi)	279	279	268	303
DSM(kpi)	462			

EXAMPLE RESULTS - TWO LAYER ANALYSIS

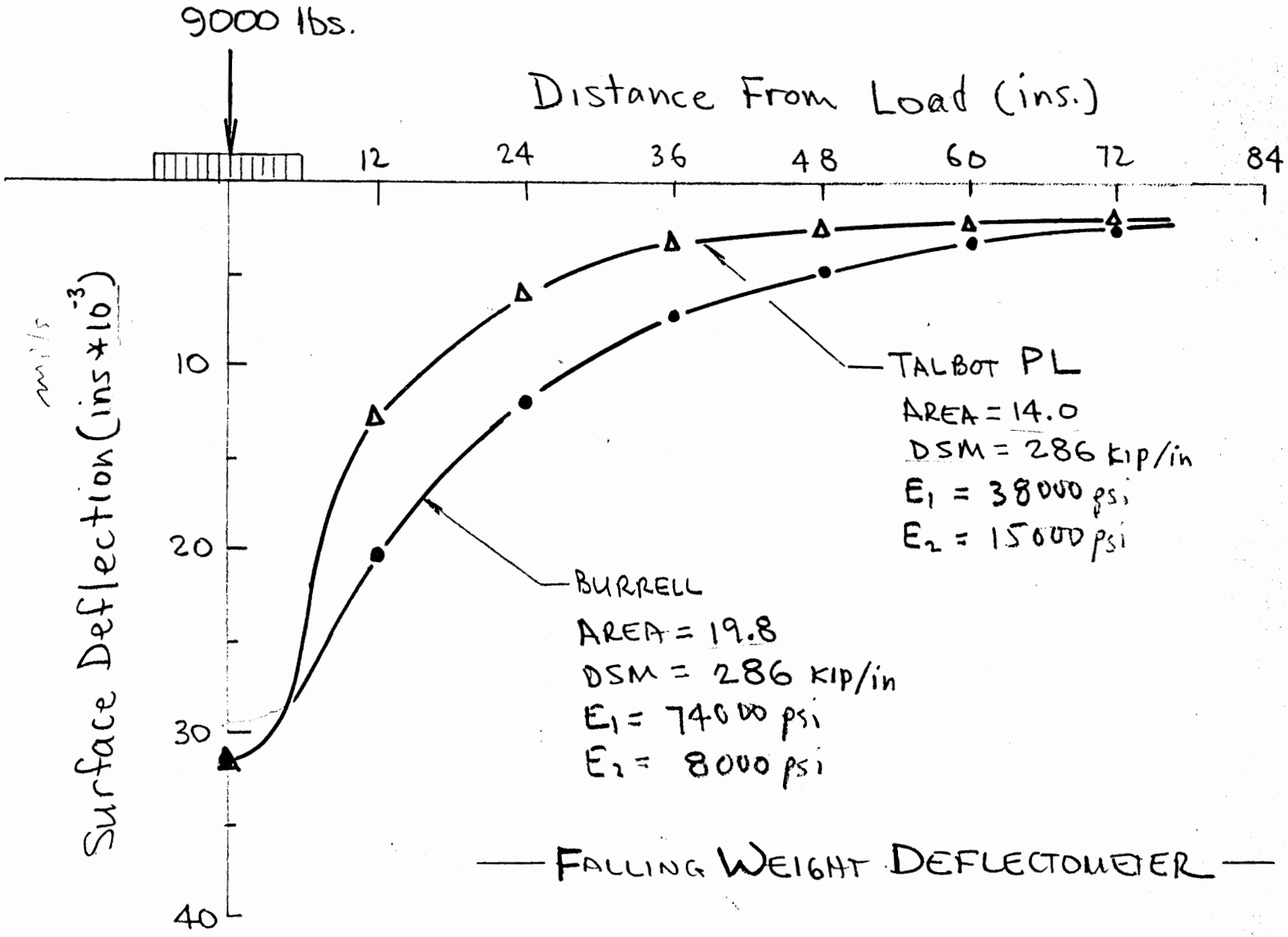

Example-- A two-layer pavement consisting of an asphalt concrete layer over a silty clay subgrade was tested with the Falling Weight Deflectometer and the following results obtained:

Asphalt concrete layer = 7.5 in. (19 cm)
Load = 9216 pounds or 4184 kg
Radius of plate = 5.9 ins. or 15 cm.
Measured deflection basin

Distance from Plate Center			Deflection	
0 ins.	(0 cms.)	D0	0.0278 ins.	0.7061 mm
12	(30)	D1	0.0186	0.4724
24	(61)	D2	0.0104	0.2642
36	(91)	D3	0.0058	0.1473

Compute the E1 of the asphalt concrete and the E2 of the subgrade using the AREA concept and Figure 2. (Answer: E1 = 116,150 psi or 8165 kg/sq.cm, and E2 = 10,100 psi or 710 kg/sq.cm.

Three- and four-layer pavements can be analyzed using an elastic layer computer program that begins with an assumed E for each layer and then iterates the E's of each layer until the measured deflection basin matches well with the computed deflection basin. The program developed by the Corps of Engineers will be demonstrated herein. This program can be used with good results as long as the engineer has a basic knowledge of the typical stiffnesses of different materials and can apply judgement in the analysis process.

All of the assumptions inherent in elastic layer theory are involved in this backcalculation procedure. Inputs required to backcalculate the moduli are as follows:

1. Layer thicknesses
2. Estimated E values for each layer and allowable upper and lower limits
3. Poisson's ratios for each layer (they have very little effect)
4. Deflection basin measurements at four locations

The computer program will then go through an iteration process by changing the moduli of the layers until the error between measured deflections and computed deflections is within a few percent. Three to five iterations are normally adequate, with a typical CPU time between 3 and 15 seconds.

Example-- A three-layer runway pavement has been tested with a Falling Weight Deflectometer and the following data obtained for a test site:

Pavement structure: 3 in (7.6 cm) asphalt concrete
12 in (30.4 cm) granular base
Silty clay subgrade
FWD Load = 16,182 pounds (7347 kg)
Radius of load plate = 5.9 in (15 cm)
Measured deflection basin:

Distance	Deflection	
0 ins. (0 cms.)	0.074 ins.	(188 mm)
12 ins. (30)	0.044	(112)
24 ins. (61)	0.024	(61)
36 ins. (91)	0.015	(38)

Starting values assumed for E's:
Asphalt concrete = 200,000 psi (14,060 kg/sq.cm)
Granular base = 15,000 psi (1,055 kg/sq.cm)
Silty clay subgrade = 10,000 psi (703 kg/sq.cm)
Allowable range of E's:
Asphalt concrete = 100,000 to 1,000,000 psi (7,030 to 70,300 kg/sq.cm)
Granular base = 10,000 to 60,000 psi (703 to 4,218 kg/sq.cm)
Subgrade = 5,000 to 30,000 psi (352 to 2,109 kg/sq.cm)

Results by iteration using the elastic layer theory backcalculation program for this problem are as follows:

Iteration	E Modulus (psi)	Deflection Basin -- ins. D0	D1	D2	D3
	Measured =	0.074	0.044	0.024	0.015
1 ASSUMED VALUES	200,000 AC 15,000 Base 10,000 Subgrade	0.075	0.036	0.018	0.012
2	496,277 AC 13,785 Base 8,202 Subgrade	0.071	0.042	0.023	0.015
3 FINAL	529,162 AC 12,261 Base 7,949 Subgrade	0.074	0.044	0.024	0.015

The resulting E values are very well within typical resilient repeated load laboratory tests for these materials and the final computed deflection basin matches the measured basin very closely.

BISDEF OUTPUT

An example run using the BISDEF PC program is given on the next page. This batch program uses BINPUT for entering data into a fixed format file that is then run by BISDEF. This program was developed by the CORPS of Engrs.

```
* # ** # ** # ** # ** # ** # ** # ** # ** # ** # *
        P R O B L E M   N U M B E R  =   1
* # ** # ** # ** # ** # ** # ** # ** # ** # ** # *
```

3-Layer Runway Pavement

DEFLECTION READINGS IN MILS
****

POSITION NUMBER	1	2	3	4
DEFLECTIONS	74.00	44.00	24.00	15.00
WEIGHTING FACTOR:	0.0135	0.0227	0.0417	0.0667

NUMBER OF VARIABLE LAYERS AND TARGET DEFLECTIONS = 3

VARIABLE LAYER NO	SYSTEM LAYER NO	VALUE OF MAXMUM MODULUS	VALUE OF MINIMUM MODULUS
1	1	1000000.0	100000.0
2	2	60000.0	10000.0
3	3	30000.0	5000.0

INITIAL PAVEMENT PARAMETERS
****

LAYER NUMBER	CALCULATION METHOD	YOUNG'S MODULUS	POISSON'S RATIO	THICKNESS	INTERFACE SPRINGCOMPL
1	ROUGH	0.2000E+06	0.3500E+00	0.3000E+01	0.0000E+00
2	ROUGH	0.1500E+05	0.4000E+00	0.1200E+02	0.0000E+00
3		0.1000E+05	0.4500E+00		

LOAD INFORMATION
****

LOAD NUMBER	NORMAL STRESS	SHEAR STRESS	RADIUS OF LOADED AREA	LOAD - POSITION X	Y	SHEAR DIRECTION
1	0.1479E+03	0.0000E+00	0.5900E+01	0.0000E+00	0.0000E+00	0.0000E+00

DEFLECTIONS COMPUTED FOR INITIAL MODULUS VALUES

POSITION	OFFSET	DEFLECTION	MEASURED	DIFFERENCE	% DIFF.
1	0.00	75.2409	74.0000	-1.2409	-1.7
2	12.00	35.8979	44.0000	8.1021	18.4
3	24.00	18.1959	24.0000	5.8041	24.2
4	36.00	11.9746	15.0000	3.0254	20.2
			ABSOLUTE SUM:	18.1725	64.4437
			ARITHMETIC SUM:		61.0899
			AVERAGE:	4.5431	16.1109

**********BISDEF OUTPUT SUMMARY**********

PREDICTED E'S FOR ITERATION NO.: 2

PREDICTED E DISREGARDING BOUNDRY CONDITIONS

LAYER NO.	MODULUS
1	526905.
2	12253.
3	7945.

DEFLECTIONS COMPUTED FOR FINAL MODULUS VALUES

POSITION	OFFSET	DEFLECTION	MEASURED	DIFFERENCE	% DIFF.
1	0.00	73.8465	74.0000	0.1535	0.2
2	12.00	44.1808	44.0000	-0.1808	-0.4
3	24.00	23.5897	24.0000	0.4103	1.7
4	36.00	15.2249	15.0000	-0.2249	-1.5
			ABSOLUTE SUM:	0.9696	3.8275
			ARITHMETIC SUM:		0.0067
			AVERAGE:	0.2424	0.9569

FINAL MODULUS VALUES

LAYER NO.:	1	2	3
MODULUS:	526905.	12253.	7945.

ABSOLUTE SUM OF % DIFF. WITHIN TOLERANCE

CHANGE IN MODULUS VALUES NOT WITHIN TOLERANCE

TYPICAL ELASTIC MODULUS VALUES

MATERIAL	TYPICAL VALUE-psi	TYPICAL RANGE-psi
Fine Grain Soil	8000	3000 - 15000
Coarse Grain Soil	20,000	15000 - ~~30000~~ 60,000
Granular Base	30,000	20,000 - 60,000
Cement Stab. Base	1,000,000	500,000 - 2,000,000
Asphalt Concrete	500,000 (70°F) 1,500,000 (40°F) 100,000 (100°F)	200,000 - 800,000
Portland Cement Concrete	5 million	3-10 Million

B.2 柔性鋪面之結構評估

CE 421
FLEXIBLE PAVEMENT STRUCTURAL EVALUATON
USING BACKCALCULATED MODULI

1. Measure deflection basins at representative locations along the project (e.g., 100 ft. intervals or less for projects less than one mile, and 300 to 500 ft. intervals for longer projects). Set FWD loading as close as possible to wheel load of design or critical vehicle. For highways, use 9-kips. For airports use maximum (normally 24-kips). Also, run lighter and heavier loads (if possible) so that the extent of load or stress sensitivity can be determined.

Do not normally place the load plate on cracks. However, it may be desirable to obtain some deflections on alligator cracks or other prominent cracks to later determine the extent of deterioration at those locations.

2. Measure AC surface temperature hourly throughout the testing period by drilling a 2 inch deep hole, filling with oil or water, and inserting a thermometer. Measure deflections at one or more points each hour for use as reference points to adjust other deflections if temperature changes significantly.

3. Plot a maximum deflection profile along the project and examine the profile for uniformity (adjust the maximum deflection for uniform temperature). If there exists obvious variation along the project, it may be desirable to divide the project length into different design or evaluation sections. The reason for differences in deflections for the different sections should be determined (e.g., change in pavement thickness or soil type).

4. Back-calculate modulus of layers and subgrade for each test location using an elastic layered based computer program (ELSDEF OR BISDEF).

Do not average deflection basins back-calculate for the average basin. Look for a few points of erronous data where something may of happened to the deflection reading and delete if too far out (bad data always exists for some reason).

Determine the mean AC stiffness modulus for each design section at the field measurement temperature.

5. Estimate each pavement layer modulus value for each season (or month) under consideration.

AC stiffness varies greatly with temperature and must be adjusted for each seasonal period. Adjust the mean backcalculated AC stiffness modulus (at the field temperature) to the estimated pavement temperature for each major season (or month) over the year. Mean monthly air temperatures for the Champaign area are given in Figure 1 and an approximate relationship between mean monthly air temperature and AC layer temperature is given in Figure 2. Use the general shape of the graph in Figure 3 to adjust the stiffness modulus measured in the field at a given temperature to the mean pavement layer temperature for each month obtained from Figure 2. Assume that the slope of the stiffness modulus versus temperature is constant to make this adjustment.

Unstabilized granular base and subbase and fine grained subgrade soil modului may also need to be adjusted for seasonal conditions based upon expected frost and moisture conditions. An example of this is shown in Figure 4 for the central Illinois area.

FIGURE 1.--TEMPERATURE AND PRECIPITATION

[Data were recorded in the period 1951-73 at Urbana, Illinois]

Month	Temperature						Precipitation				
	Average daily maximum	Average daily minimum	Average daily	2 years in 10 will have-- Maximum temperature higher than--	2 years in 10 will have-- Minimum temperature lower than--	Average number of growing degree days*	Average	2 years in 10 will have-- Less than--	2 years in 10 will have-- More than--	Average number of days with 0.10 inch or more	Average snowfall
	°F	°F	°F	°F	°F	Units	In	In	In		In
January	33.2	18.0	25.6	60	-11	18	1.56	.63	2.35	4	5.3
February	37.4	21.0	29.3	62	-8	18	1.87	.89	2.70	5	5.7
March	47.9	30.5	39.2	78	9	172	3.24	1.43	4.78	7	5.2
April	62.2	41.7	52.0	84	25	364	3.79	2.00	5.34	8	.8
May	73.0	51.6	62.3	91	35	691	3.57	2.07	4.90	7	.0
June	82.7	61.0	71.8	97	46	954	4.40	2.42	6.14	7	.0
July	85.0	64.8	74.9	96	51	1,082	4.81	2.72	6.65	6	.0
August	83.8	62.7	73.2	94	47	1,029	3.06	1.44	4.44	4	.0
September	78.7	55.7	67.2	95	38	816	2.99	.87	4.70	5	.0
October	66.4	44.6	55.6	87	26	484	2.79	.93	4.31	5	.0
November	50.1	33.3	41.7	74	10	125	2.45	1.27	3.48	5	1.9
December	38.4	24.3	31.4	65	-3	33	2.40	.73	3.76	5	3.8
Yearly:											
Average	61.6	42.4	52.0	---	---	---	---	---	---	---	---
Extreme	---	---	---	100	-12	---	---	---	---	---	---
Total	---	---	---	---	---	5,786	36.93	30.76	44.37	68	22.7

* A growing degree day is a unit of heat available for plant growth. It can be calculated by adding the maximum and minimum daily temperatures, dividing the sum by 2, and subtracting the temperature below which growth is minimal for the principal crops in the area (40° F).

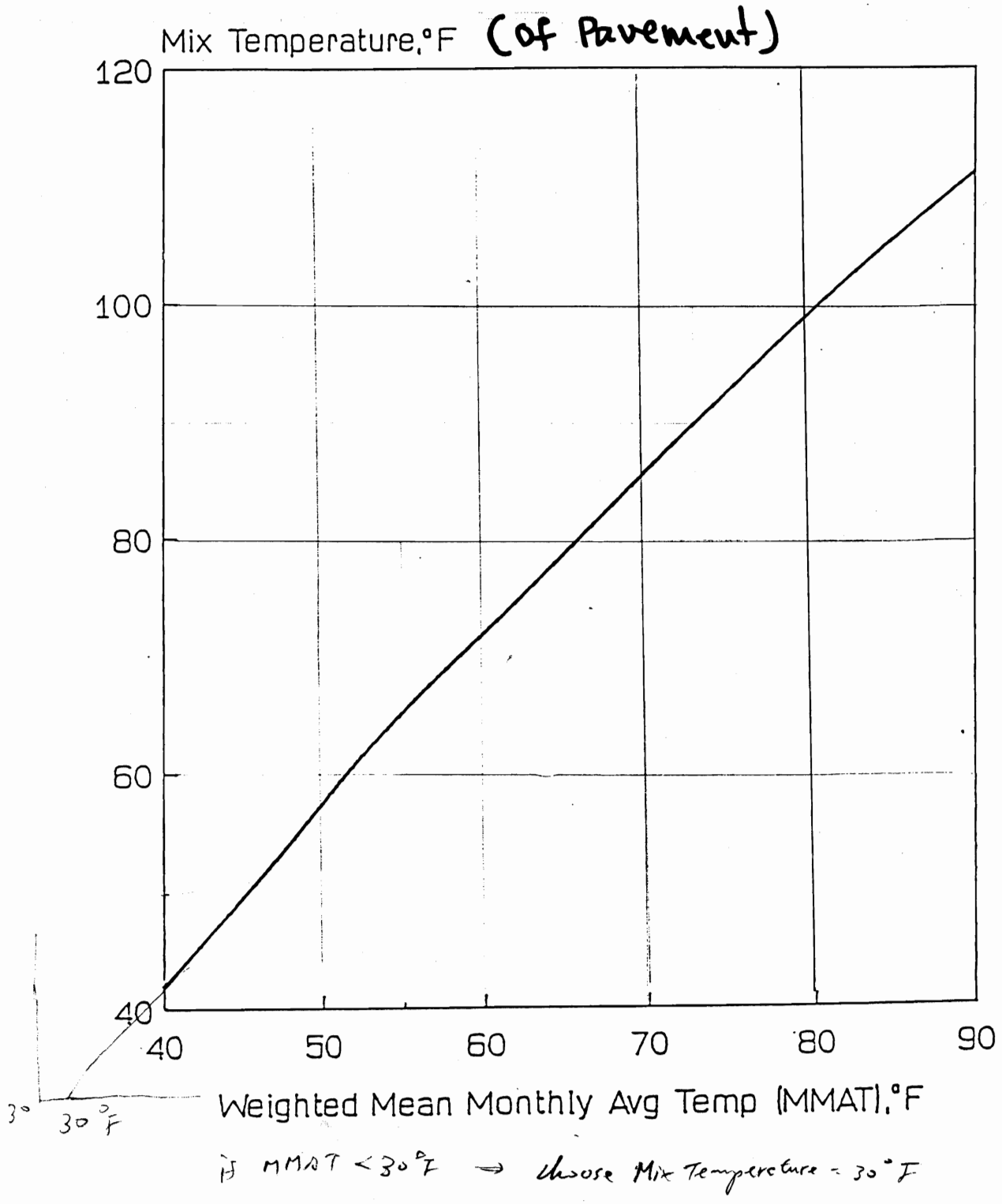

Figure 2. Determination of Seasonal Pavement Temperature.

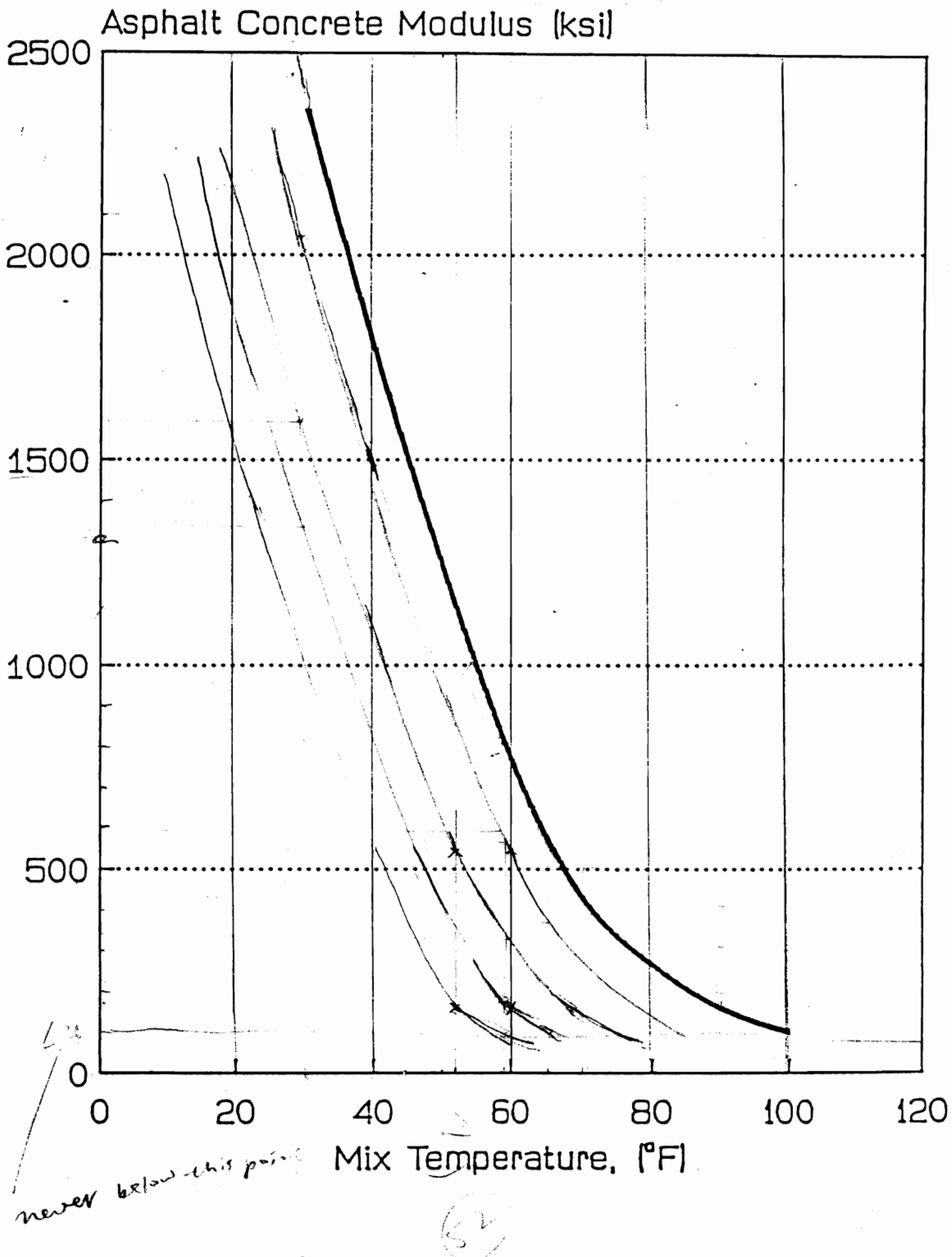

Figure 3. AC Modulus/Temperature Relationship.

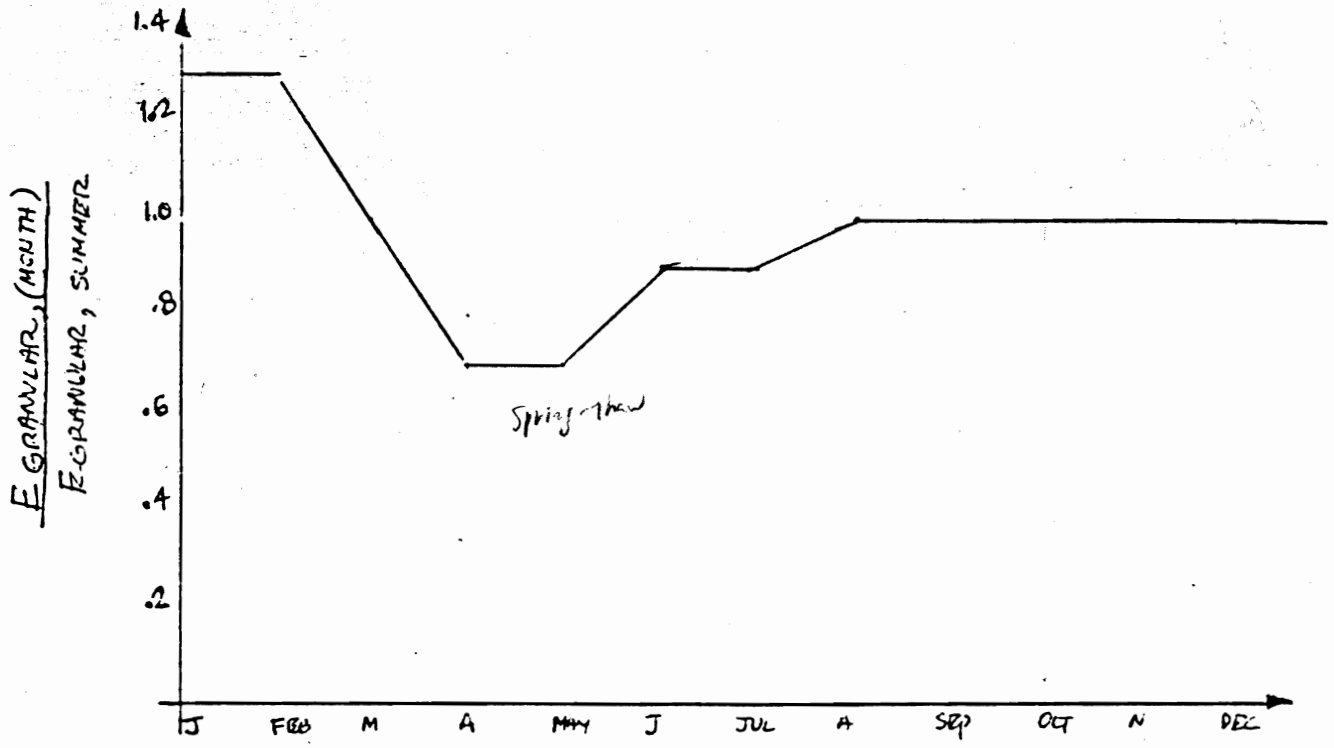

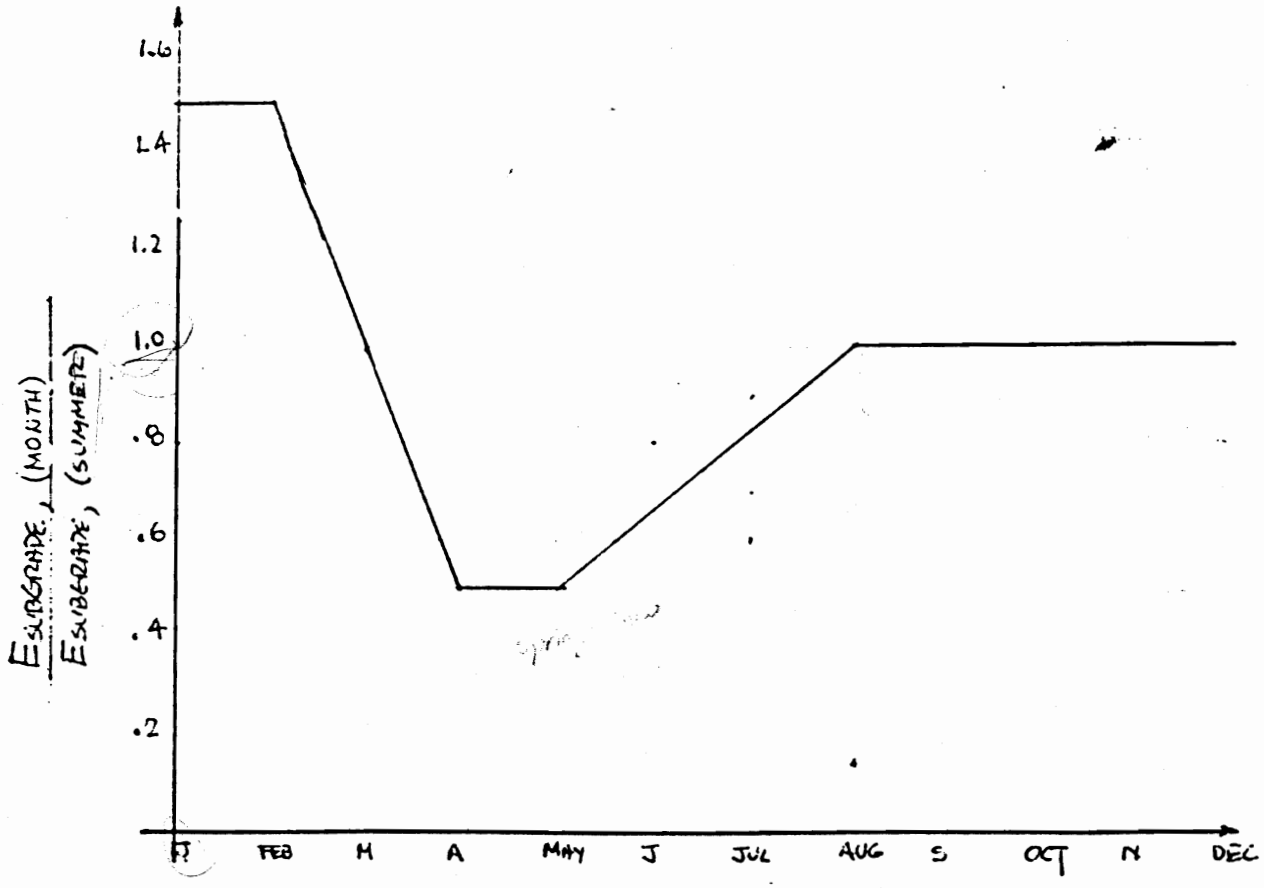

MONTH

Fig. 4. Estimated variation of granular and subgrade moduli values for the champaign area

6. Compute critical strains in pavement layers for each month over a year for each aircraft or truck under consideration using the elastic layered program. For highway evaluation, the 18-kip equivalent single axle load is normally used as the standard. However, the entire range of axle weights could be used, but this may require adjustment of subgrade and granular base moduli for lighter and heaver axle loads due to stress sensitivity.

7. Compute the expected or "allowable" number of load applications to "failure" using an AC fatigue model and a subgrade permanent deformation model for each month (denoted by N_i). Two reasonable models are given that were developed by the Corps of Engineers, and have been used successfully for consulting work.

Asphalt Concrete:

$$\log_{10}(COV) = - (5.0 \log_{10}TSTRAIN + 2.665 \log_{10}(Eac/14.22) + 0.392)$$

Where: COV = number of coverages to unknown amount of fatigue cracking
TSTRAIN = tensile strain in the AC layer
Eac = stiffness modulus of the AC layer, psi

Fine Grained Subgrade

$$COV = (0.005511 / VSTRAIN)^{6.527}$$

where: COV = number of coverages to 0.5 ins. of rutting
VSTRAIN = vertical strain on fine grained subgrade

8. Compute past damage (and future damage if desired to determine if pavement can withstand future loadings over some time period) using Miner's accumulated hypothesis:

$$DAMAGE = \sum n_i / N_i$$

where: n_i = no. of axle or gear loads for the ith month actually applied to the pavement at a given load magnitude.

N_i = no. of axle or gear loads for the ith month allowable to "failure" computed from fatigue or permanent deformation models.

If more than one axle or gear load is used, this summation must be repeated for each and the total damage summed for all axle or gear loads.

9. Develop a table of results (using a spreadsheet) for both past and future traffic such as shown below for the pavement.

Spreadsheet To Compute Past Fatigue Damage For A Given Pavement Section, Given Axle Type And Load Level.

MONTH	E1	E2	E3	10E-6 TSTRAIN	Nallow	Since Opening To Traffic n applied	DAMAGE n/N
JAN	2,000,000	50,000	25,000	150	10,000,000	100,000	0.10
FEB	ETC.						
MAR							
APR	700,000	20,000	5,000	400	350,000	100,000	0.29
MAY							
ETC.							
DEC							
						TOTAL FATIGUE DAMAGE =	0.85

10. Experience has shown that the DAMAGE values computed normally agrees with visable pavement fatigue cracking. Figure 5 shows some results for a group of highway pavements. A very general correlation between past computed Miner's Damage and field fatigue cracking is as follows:

Computed Past DAMAGE	Expected Pavement Condition
0.0 to 0.25	Fatigue cracking may not be visable, or only a small amount should be visable. Substantial life remains.
0.26 to 0.50	Fatigue cracking should definitely exist along the pavement. About half the pavements fatigue life remains. Extensive patching of fatigued areas would restore fatigue life to those areas.
0.50 to 1.50	From 25 to 75 percent of the length of the wheel path or length of the pavement should show fatigue cracking. No fatigue life exists unless extensive patching is done in the areas of fatigue cracking.
> 1.50	Fatigue cracking should be prevalent over most of the pavement length. No fatigue life exists.

When the computed DAMAGE results do not agree roughly with the visible fatigue cracking, the evaluation should be re-checked and modified. Potential problems include errors in estimating past traffic loadings, unrealistic back-calculation values for moduli, unreasistic adjustment of moduli over the year, and an inadequate fatigue curve used in the computation.

11. These evaluation results can be then used to assess remaining life of the existing pavement and also its ability to handle future traffic. The results are also very important for overlay design purposes. The greater the past damage, the thicker the overlay must be to support future traffic.

MID 7OCT88

由面層撓度值回算鋪面彈性模數的初步研究

陳建桓
淡江大學
土木工程研究所
碩士

李英豪
淡江大學
土木工程系
副教授

摘要

本文主要的目的乃是針對傳統回算程式的一些明顯缺點，如：彈性模數值的回算解可能不唯一，輸入模數值範圍的選擇仍沒有可依循之準則、而且回算過程不僅耗費時間甚至有時可能會有不收斂的問題等，做理論的研究改進。本文首先以Burmister與Scrivner的二層彈性理論之撓度方程式爲基礎，利用因次分析的原理推導出影響該函數的主要無因次參數。然後，再確立面層撓度值與回算彈性模數值的一對一函數關係，並依此建立資料庫與預估方程式組，以便於各層彈性模數值的快速運算。最後再以實例作初步的驗證，並提出未來應用與改進的具體建議。

一、前言

在鋪面管理系統中，對於道路鋪面的養護維修工作，有賴於定期對於現有道路鋪面的結構進行評估，以瞭解鋪面狀況。爲表示鋪面結構的強度，以往必須在鋪面上直接鑽心取樣，再於實驗室中求得應力與應變關係，以決定鋪面各層材料的彈性模數(Elastic Modulus)。這種方法不僅費時費事，而且鑽心取樣會對鋪面的結構造成直接的破壞，影響其結構強度。

近年來，利用非破壞性試驗(Non-Destructive Testing)量測鋪面表面撓度值以反映鋪面結構狀況，既不會破壞現有鋪面結構而且量測速度快，因此已被廣泛地應用。目前較常用的非破壞性試驗儀器有動力撓度儀(Dynaflect)、路面評審儀(Road Rater)、和衝擊荷重撓度儀(Falling Weight Deflectometer)等。然而，由於用以表示鋪面結構強度的彈性模數值，無法由非破壞性試驗量測的表面撓度值直接計算而得，因此，一般是以回算的方式回算出鋪面各層材料的彈性模數。

1.1 研究目的

目前回算程式所使用的回算法大致可分爲兩大類：反覆計算法和資料庫處理法。反覆計算法是利用一系列反覆計算與重複修正的步驟，以假設一組彈性模數值所計算出的撓度值與實測撓度值比較，使其誤差在指定可接受的誤差範圍內。資料庫處理法則是以鋪面與路基的彈性模數所計算出的表面撓度值，建立成一個大型的資料庫。使用時，將實際量測的撓度值與資料庫中的撓度值比較，找出一組合適的彈性模數值。

本研究主要目的乃針對傳統回算程式的一些明顯缺點，做理論的研究改進 [1]。由於傳統回算法過程複雜，若僅從多層線性彈性系統爲考量，目前仍存在一些問題尚待解決，如：

(1) 從量測之撓度值估算出彈性模數值的解可能不唯一。

(2) 回算程式中輸入資料範圍的選擇，將影響回算結果的正確性甚巨，然目前仍沒有可依循之準則。

(3) 反覆運算的過程不僅耗費時間，甚至有時可能會有不收斂的問題。

本文除了針對上述問題研究改進的方法，並擬融合資料庫回算法的理念與最新的統計迴歸方法，建立一個能由面層撓度值直接計算出各層彈性模數值的預估方程式組。該預估方程式組不僅可免除反覆運算的時間，在面層撓度量測與彈性模數值回算的過程亦有了及時性。如此，不僅可以在試驗現場立即計算出各層之彈性模數值，必要時亦可重複該非破壞性撓度試驗，以確保所量測資料與回算之彈性模數值的正確性。此外，若有必要運用傳統回算程式時，該預估方程式組的可能預估誤差範圍亦可做爲選定傳統回算程式中設定彈性模數值範圍的基本準則。

1.2 研究方法

當理論分析工具無法產生封閉型解，或是在研究涉及許多數值和經驗性的一些工程問題上時，因次分析(dimensional analysis)原理的應用顯然有其必要性。因次分析的方法考慮理論方程式的無因次形式，由一組與資料相關的無因次參數，代表多項有因次的變數間的繁複組合的最簡化關係。所以，在資料的分析上，可以減少相關參數的數目，並可節省相當多的時間與成本。此分析方法目前亦已受到工程界相當的肯定。

本文首先以Burmister與Scrivner的二層彈性理論之撓度方程式爲基礎[2, 3]，利用因次分析的原理推導出影響該函數的主要無因次參數，並反覆驗證之。然後，再將該無因次參數的撓度函數關係式轉換成彈性模數回算的函數關係式，並確立面層撓度值與該函數的一對一關係。其次，再以此無因次參數，選定可能的範圍並建立資料庫。並根據此資料庫與最新的統計迴歸方法（投影追逐迴歸法，Projection Pursuit Regression, PPR）[4, 5] 建立預估方程式組，以便於各層彈性模數值的快速運算。

二、二層彈性理論之發展

大家熟知的Boussinesq方程式是以一個集中荷重作用在單一的均勻土層，以解出應力和變位的問題。Burmister藉由荷重函數之貝索函數(Bessel Function)展開，對於一個相當於集中荷重作用在第一層表面之分佈力的任意疊加荷重，得到二層彈性系統中第一層表面的撓度方程式[2]。此系統是一垂直集中荷重P，作用在鋪面表面O點處，該點爲圓柱座標r及z之原點，z座標向下爲正（如圖一所示）。兩層均假設爲均值、等向性的線彈性材料，上層之彈性模數爲E_1、厚度爲h，下層之彈性模數爲E_2、厚度則爲無限，並假設兩層的柏松比皆爲0.5。該撓度方程式爲：

$$w = \frac{1.5P}{2\pi E_1}\int_0^\infty \left[\frac{e^{2mh} + 4Nmh - N^2 e^{-2mh}}{e^{2mh} - 2N(1+2m^2h^2) + N^2 e^{-2mh}}\right] J_0(mr)dm \qquad \text{(E. 1)}$$

$$N = \frac{E_1 - E_2}{E_1 + E_2} = \frac{1 - E_2/E_1}{1 + E_2/E_1}$$

其中：

P = 作用於鋪面表面的垂直力，[F]。
h = 上層的厚度，[L]。
E_1 = 上層的彈性模數，[FL^{-2}]。
E_2 = 下層的彈性模數，[FL^{-2}]。
w = 鋪面表面的垂直撓度，[L]。
r、z = 圓柱座標（r = 水平方向，z = 垂直方向），[L]。
m = 參數。
$J_0(x)$ = 第一類的零階貝索函數。
N = E_1和E_2的函數。
其中 [F]、[L]代表力與長度之單位。

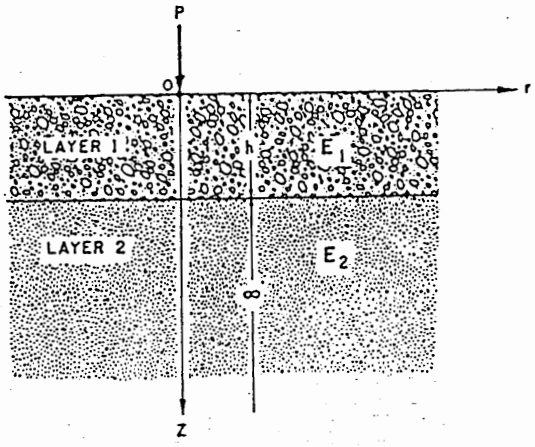

圖一　點荷重作用在二層彈性系統的表面上 [3]

Burmister再據此推導出二層彈性系統在圓形均佈荷重作用下中心點之撓度方程式。依因次分析的原理，該撓度方程式可簡化爲：

$$w_c = \frac{1.5pa}{E_2} F_w\left(\frac{a}{h}, \frac{E_2}{E_1}\right) = \frac{1.5pa}{E_2} F_w \qquad \text{(E. 2)}$$

其中：

w_c = 荷重中心點下方的垂直撓度，[L]。
p = 作用於鋪面表面的垂直均佈壓力，[FL^{-2}]。
a = 荷重半徑，[L]。
F_w = a/h 和 E_2/E_1 的函數。

Scrivner 於 1973 年再針對動力撓度儀作用在鋪面一路基的二層彈性系統上做進一步的研究[3]。爲了能由動力撓度儀所測得的表面撓度資料轉換成鋪面及路基的彈性模數，Scrivner 乃將路基以上的全部材料，假設統合成一種材料，而形成簡化的二層系統(如圖一）。由於荷重的面積小， Scrivner 乃以點集中荷重的型式模擬上述之均佈荷重，以簡化數學運算。在距離 O 點水平距離 r 處之表面撓度 w，其與 h 、 P 、 E_1 、 E_2 之關係如下式：

$$\frac{4\pi E_1}{3P}wr = \int_{x=0}^{\infty} V * J_0(x)dx = F\left(\frac{E_2}{E_1} \quad , \quad \frac{r}{h}\right)$$

$$x = \frac{mr}{h}$$

$$V = \frac{1+4Nme^{-2m} - N^2e^{-4m}}{1-2N(1+2m^2)e^{-2m} + N^2e^{-4m}} \qquad \text{(E. 3)}$$

其中，$V = m$和N的函數。

因此，若假設距動力撓度儀荷重中心r_1、r_3處之鋪面表面撓度各爲w_1、w_3，將之代入上述的表面撓度方程式，並將所得的二方程式相除可得：

$$\frac{w_1r_1}{w_3r_3} = \frac{F_1\left(\frac{E_2}{E_1} \quad , \quad \frac{r_1}{h}\right)}{F_3\left(\frac{E_2}{E_1} \quad , \quad \frac{r_3}{h}\right)} = G\left(\frac{E_2}{E_1} \quad , \quad \frac{r_1}{h} \quad , \quad \frac{r_3}{h}\right) \qquad \text{(E. 4)}$$

其中，F_1、F_3、G爲E_2/E_1、r_1/h和r_3/h的函數。若選定一非破壞撓度量測儀器(如動力撓度儀)，且r_1、r_3和面層厚度h爲已知，則由方程式(E. 4) 中可知，w_1r_1 / w_3r_3僅是彈性模數比E_2/E_1的函數。因此，配合ELASTIC MODULUS II程式之應用，通常在某一精確度的要求下，可利用試誤法的收斂過程得到一個滿足前述方程式的解。再將所得E_2/E_1的值代回式(E. 3) 中，可解得E_1值，而E_2之值可由$E_2 = E_1 * (E_2/E_1)$式中求得。

三、 回算程式之基本理論與限制

回算法的基本原理是利用鋪面理論（如多層彈性理論與版理論），由量測的面層撓度值回算鋪面各層材料的彈性模數。較常用的鋪面理論分析模式，是利用Odemark的等值厚度公式簡化的多層彈性理論[6]。鋪面材料模式基本上是假設均質、等向性、和線彈性，通常此與材料的眞實狀況並不盡符合。因此，選用分析模式時，需注意其基本假設與限制。

一般回算程式的基本假設爲：當鋪面受到動力載重作用時，經由鋪面理論計算之撓度值與實際量測的撓度值相同時，存在唯一的一組彈性模數組合。因此，在各層厚度、荷重大小、荷重面積和柏松比已知的情況下，可先假設一組彈性模數組合並代入鋪面理論中計算出一組理論撓度值，再比較此一理論撓度值與實際量測撓度值之差異。如果兩者之誤差不在設定之容許範圍內，則須改變另一彈性模數組合，再重複前述之計算步驟。直到有一組彈性模數組合的撓度誤差在限定範圍內，則將此組彈性模數值視爲該鋪面之各層結構強度。

由回算的基本原理亦可發現，對於一組實測撓度值會有無限多的彈性模數組合所計算的理論撓度值與實測撓度值的誤差在設定的誤差範圍內。以Scrivner的研究爲例，Scrivner針對動力撓度儀的配置，在荷重面積半徑a及感應器位置r_1、r_3固定的狀況下，建立彈性模數回算的資料庫與曲線圖。如圖二之 w_1r_1 / w_3r_3 對彈性模數比E_1/E_2的厚度曲線圖，Scrivner並以$w_1r_1 / w_3r_3 = 1$及 $h = 11.2$ in.爲分區，將該圖分成四個部份討論。圖中可知，厚度大於11.2 in.的兩個部份有唯一解；而厚度小於11.2 in.的部份則是有兩組解或無解[3]。因此，在回算的

基本理論考量下，從量測之撓度值回算出彈性模數值的解可能不唯一。而此項最基本的理論限制，卻往往被傳統的回算程式所忽略。(1 in. = 2.54 cm)

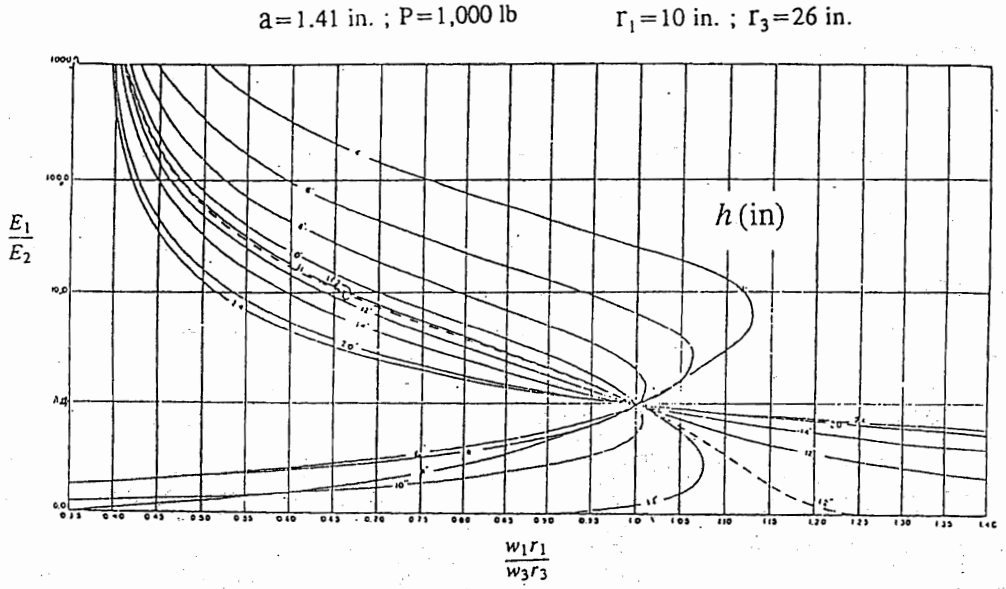

圖二　Scrivner 針對動力撓度儀所建立之鋪面厚度曲線圖 [3]

由於傳統的回算法，必須經由多次反覆運算使計算出之理論撓度值與實測撓度值的誤差在容許範圍內，以推估出各層材料之彈性模數值。然而，回算程式中各層彈性模數值範圍的輸入與誤差範圍的設定，對回算結果的正確性影響甚大。一般而言，若彈性模數值範圍設定過大，則回算結果較不理想，而且反覆運算次數可能會增加並使計算時間加長。另一方面，如果彈性模數值範圍設定過小，以致於眞正的解不在其中，則可能得到設定範圍的邊界值而非所求之正確值。此外，若再加上覆算次數之限制（或不足）以至無法收斂，則所得回算結果的正確性必然大受影響。因此，選擇適合的分析模式並減少對輸入值的猜測，將有助於得到較合理的回算結果。

四、無因次參數之選定及驗證

Scrivner只針對動力撓度儀的配置，在荷重面積半徑a及感應器位置r_1、r_3固定的狀況下，建立彈性模數回算的資料庫與曲線圖（如圖二）。若針對不同的撓度量測儀器，則荷重面積之半徑a及撓度量測位置r_1、r_3等參數均會變動，如道路評審儀之 a = 9 in.，r = 0、12、24、36、48 in.；衝擊荷重撓度儀之 a = 5.9 in.，r = 0、8、12、18、24、36、60 in.。因此，必須考慮加入a、r_1、r_3等參數於函數關係式中，以建立新的彈性模數回算曲線圖。因此，根據Burmister及Scrivner所提出的理論推導，可推估出如下之函數關係：(1 in. = 2.54 cm)

$$Y = \frac{4\pi E_1}{3P} w_1 r_1 = F'\left(\frac{E_2}{E_1}, \frac{r_1}{h}, \frac{h}{a}\right) \qquad \text{(E. 5)}$$

$$\frac{w_1 r_1}{w_3 r_3} = F\left(\frac{E_2}{E_1}, \frac{r_1}{h}, \frac{r_3}{h}, \frac{h}{a}\right) \qquad \text{(E. 6)}$$

由一系列的BISAR程式 [7] 運算結果，亦可印證出上式之關係：亦即僅有E_1 / E_2、r_1 / h、r_3 / h及 h / a四個無因次參數與 $w_1 r_1 / w_3 r_3$ 是相關的。簡而言之，當此四個無因次參數固定時，不管E_1、E_2、r_1、r_3、h、a之值如何變化，都不會影響 $w_1 r_1 / w_3 r_3$ 的值。較詳細的驗證結果，請參閱參考文獻 [1]。

五、回算資料庫之建立

設定式(E. 6) 中之無因次參數E_1 / E_2、r_1 / h、r_3 / h及 h / a之數值範圍，可建立一基本回算資料庫。因爲 $w_1 r_1 / w_3 r_3$ 只與上述四個參數相關，固定四個參數值， $w_1 r_1 / w_3 r_3$ 即不受影響。所以每一組參數只需取適當之E_1、E_2、r_1、r_3、h、及a之值（須滿足參數之值），代入BISAR程式 [7] 計算得該組之w_1及w_3，可得 $w_1 r_1 / w_3 r_3$ 之值。

此外，在有限的資源限制下，分析用之資料庫的規模不能太大，而且也必須兼顧廣泛的代表性。因此，本研究僅考慮鋪面和路基的彈性模數之可能大小，以決定E_1 / E_2的範圍。並考慮一般常用之非破壞性撓度量測儀器之荷重面積與感應器位置，以及第一層厚度，以建立r_1 / h、r_3 / h及 h / a之數值範圍。

在考慮一般E_1、E_2、h、a、r_1及r_3之可能大小範圍下，假設P = 2,400 lb 、E_2 = 1,000 psi 、h = 10 in.，選擇無因次參數E_1 / E_2、r_1 / h、r_3 / h及 h / a之數值範圍如下：（其中，並選定$r_1 > r_3$以減少不必要的重複運算，故總共可得1680組資料。1 lb=0.454 kg, 1 psi=0.07 kg/cm^2, 1 in.=2.54 cm）

E_1 / E_2 = 1, 2, 5, 10, 20, 50, 100, 200, 500, 1000, 2000, 5000
r_1 / h = 0.8 , 1.2 , 1.8 , 2.4 , 3.6 , 4.8 , 6.0
r_3 / h = 1.2 , 1.8 , 2.4 , 3.6 , 4.8 , 6.0, 7.2
h / a = 0.8 , 1.3 , 2.5 , 3.5 , 5.0

各無因次參數之值選定後，即以FORTRAN語言寫成資料整理及擷取的程式。自行撰寫之程式共分兩部份：第一部份是建立參數資料庫及BISAR程式之輸入檔；第二部份則是由BISAR程式之輸出檔擷取程式算出之撓度值，再與參數資料庫合併建立成資料庫。本研究利用程式來擷取所需資料及建立資料庫，除可避免人爲誤差外，也方便資料庫之修改與建立。

六、非線性預估模式組之建立

6.1 投影追逐迴歸分析法之介紹

Friedman和Stuetzle在1981年所發展的投影追逐迴歸法(Projection Pursuit Regression , PPR) [4, 8] 是利用小區域平均的技術，將回應表面(y's)模擬成一系列各項預估變數(x's)的非參數性變數的投影函數之和。假設存在如下之眞實模式：

$$y = \bar{y} + \sum_{m=1}^{M_0} \beta_m \phi_m \left(a_m^T x \right) + \varepsilon \qquad \text{(E. 7)}$$

其中，$x = (x_1、x_2、\cdots\cdots、x_p)^T$ 代表預估變數的向量。而$\bar{y}$是回應變數的期望值或平均值，β_m 是迴歸常數，ε是隨機誤差。在概念上，投影追逐迴歸法是將預估變數x投影到方向向量$a_1、a_2、\cdots、a_m$上，以得到其投影長度$a_m^T x$，其中$m = 1、\cdots\cdots、M_0$。並利用最佳化之技巧，以找到可以模擬多維回應表面的最佳非線性轉換函數 $\phi_1、\phi_2、\cdots、\phi_n$之組合。而 $\phi_m\left(a_m^T x\right)$ 係代表估計投影長度的未知非參數性的轉換函數。換言之，回應表面將被分成一系列平均投影項加在一起的總和。其中，第一投影項ϕ_1可代表參數空間上的主要趨勢，而其與回應表面值之差（或殘餘值）則成爲其他投影項的來源。

經由投影追逐迴歸分析法的輔助，可將多維空間上之回應表面轉換爲可以二維曲線圖形表示的平均投影曲線的和。此後，再利用傳統的線性迴歸方式，以求得符合投影曲線的方程式組。本研究採用如上所述之二階段迴歸分析方式[5]，以協助找尋較符合多維回應表面的正確的函數型式。在分析的過程中，亦能輕易地經由目視查證或與主題有關的工程知識，選擇合理的函數型式及適用的邊界條件，以模擬個別的投影曲線。

6.2 預估方程式組之建立

由前述二層彈性理論與因次分析的結果中可知，若欲藉由式(E. 6)推導出如公式(E. 8)中E_1 / E_2與無因次參數$w_1 r_1 / w_3 r_3、r_1 / h、r_3 / h$及$h / a$間之回算關係式，其解可能亦不唯一（亦即某些部份可能有唯一解、兩組解、或無解）。

$$\frac{E_2}{E_1} = G\left(\frac{w_1 r_1}{w_3 r_3} \quad , \quad \frac{r_1}{h} \quad , \quad \frac{r_3}{h} \quad , \quad \frac{h}{a}\right) \tag{E. 8}$$

因此，本文擬以$E_1 / E_2 = 1$和$w_1 r_1 / w_3 r_3 = 1$爲分區，並僅就『$E_1 / E_2 > 1$和$w_1 r_1 / w_3 r_3 \leqq 1$』的部份，提出較深入的研究（注意，此與Scrivner以往的分區圖不同）。本分區內曲線之一對一的關係，亦可由Scrivner的分區圖（如圖二）中很明顯地確立出來。並進而針對此部份的資料，利用S-PLUS統計軟體 [8] 及前述之二階段迴歸分析方式，將此五度空間的函數關係模擬成爲一非線性函數的預估方程式組。

由於變數E_1 / E_2的範圍甚大，故在統計迴歸的分析過程中必須取此變數的對數函數做爲回應變數，以減少迴歸分析上的困難。經由數十次詳細的投影追逐迴歸分析結果，最後選定如下之最佳預估方程式組，以模擬此五度空間的函數分區：

$$\log_{10}\left(\frac{E_1}{E_2}\right) = 2.283 + 0.948\,\Phi_1 + 0.514\,\Phi_2 + 0.253\,\Phi_3$$

$$\Phi_1 = \begin{cases} 0.864 + 16.373\,(A1) + 56.154\,(A1)^2 + 101.2\,(A1)^3 + 65.23\,(A1)^4 & \text{if } A1 \leq -0.05 \\ 1.637 + 72.73\,(A1) + 2056.2\,(A1)^2 + 35709.4\,(A1)^3 + 242630.6\,(A1)^4 & \text{if } -0.05 < A1 \end{cases}$$

$$\Phi_2 = \begin{cases} -2.006 + 1.388\,(A2) - 0.146\,(A2)^2 + 0.083\,(A2)^3 - 0.024\,(A2)^4 & \text{if } A2 \leq 3.0 \\ 10.388 - 9.964\,(A2) + 3.759\,(A2)^2 - 0.590\,(A2)^3 + 0.034\,(A2)^4 & \text{if } 3.0 < A2 \end{cases}$$

$$\Phi_3 = \begin{cases} 20.760 + 46.171\,(A3) + 40.127\,(A3)^2 + 15.617\,(A3)^3 + 2.224\,(A3)^4 & \text{if } A3 \leq -1.5 \\ 0.488 - 1.031\,(A3) - 0.563\,(A3)^2 + 0.206\,(A3)^3 + 0.053\,(A3)^4 & \text{if } -1.5 < A3 \leq 0 \\ 0.462 - 0.841\,(A3) - 5.209\,(A3)^2 + 4.505\,(A3)^3 - 1.552\,(A3)^4 & \text{if } 0 < A3 \end{cases}$$

$$A1 = -0.699x1 + 0.00046x2 - 0.00059x3 + 0.00151x4 + 0.715x5 - 0.00013x6 - 0.00003x7$$
$$A2 = -0.419x1 - 0.0864x2 + 0.813x3 + 0.167x4 - 0.355x5 - 0.0420x6 + 0.0298x7$$
$$A3 = 0.681x1 - 0.0998x2 + 0.383x3 - 0.307x4 + 0.534x5 + 0.0153x6 - 0.00084x7$$
$$X = [x1, x2, \ldots, x7] = \left[\frac{w_1 r_1}{w_3 r_3}, \frac{h}{a}, \frac{r_1}{h}, \frac{r_3}{h}, \frac{r_1}{h} * \frac{h}{r_3}, \frac{r_1}{h} * \frac{h}{a}, \frac{r_3}{h} * \frac{h}{a}\right] \quad \text{(E. 9)}$$

Statistics: N=1247，R^2=0.995，SEE=0.0645，CV=2.8%

Limits : $1 \leqq E_1/E_2 \leqq 5000$，$0.8 \leqq r_1/h \leqq 6$，$1.2 \leqq r_3/h \leqq 7.2$，
$0.8 \leqq h/a \leqq 5.0$，$w_1 r_1/w_3 r_3 \leqq 1$，$r_1 > r_3$

其中，N 代表資料數目，R^2值爲非線性預估方程式組之判定係數，SEE爲標準偏差，而CV爲變異係數。原回算資料庫之參數範圍亦是此預估方程式組的限制範圍。須注意的是投影的次數愈多，雖然可使判定係數(R^2)愈趨近於1並提高對資料的符合度，但同時也會增加方程式組的數目及複雜度。故預估方程式組的建立，必須在此中間取得一平衡點。
同理，爲求計算之方便，我們亦可利用前述建立預估模式的方法，將式(E. 5)模擬成如下之近似式，以計算出各層彈性模數值。

$$\log_{10}(Y) = \log_{10}\left(\frac{4\pi E_1}{3P} w_1 r_1\right) = 1.677 + 1.035\,\Phi_1 + 0.0788\,\Phi_2$$

$$\Phi_1 = \begin{cases} -1.625 + 0.801(A1) + 0.021(A1)^2 - 0.017(A1)^3 + 0.001(A1)^4 & \text{if } A1 \leq 2.5 \\ -2.654 + 2.017(A1) - 0.508(A1)^2 + 0.083(A1)^3 - 0.005(A1)^4 & \text{if } 2.5 < A1 \end{cases}$$

$$\Phi_2 = \begin{cases} 0.301 + 1.701(A2) - 0.023(A2)^2 - 0.014(A2)^3 - 0.003(A2)^4 & \text{if } A2 \leq 0 \\ 0.295 + 1.149(A2) - 0.225(A2)^2 - 0.262(A2)^3 + 0.078(A2)^4 & \text{if } 0 < A2 \leq 2.5 \\ 1.845 - 0.316(A2) - 0.079(A2)^2 + 0.012(A2)^3 - 0.001(A2)^4 & \text{if } 2.5 < A2 \end{cases}$$

$$A1 = 0.998x1 + 0.0130x2 - 0.0147x3 + 0.0633x4 - 0.00202x5$$
$$A2 = -0.827x1 - 0.107x2 + 0.472x3 + 0.284x4 + 0.0303x5$$
$$X = [x1, x2, \ldots, x5] = \left[\log_{10}\left(\frac{E_1}{E_2}\right), \frac{h}{a}, \frac{r_1}{h}, \log_{10}\left(\frac{E_1}{E_2}\right) * \frac{r_1}{h}, \frac{h}{a} * \frac{r_1}{h}\right] \quad \text{(E. 10)}$$

Statistics: N=420，R^2=0.9989，SEE=0.03266，CV=1.95%

Limits : $1 \leqq E_1/E_2 \leqq 5000$，$0.8 \leqq r_1/h \leqq 6$，$0.8 \leqq h/a \leqq 5.0$

如此，我們可以利用式(E. 9)的預估方程式組推估出彈性模數比E_1/E_2的近似值，再將所得之E_1/E_2值代入式(E. 10)中，以求得上層彈性模數值E_1，並計算出下層彈性模數值E_2。

七、預估模式組之驗證

本文所建立之預估方程式組，可由面層撓度值與其它相關資料直接計算二層彈性系統之彈性模數比，並進而計算出各層之彈性模數值。將運用此方式及BISDEF程式 [9] 回算所求得之彈性模數值與原假設已知之該組彈性模數值比較，以驗證其回算之精確度。茲將本文中初步建立的方程式組之應用實例及驗證過程敘述如下：

假設二層彈性系統的面層厚度 h=10 in.， 荷重 P=3,000 lb， 荷重盤半徑 a=7.69 in.， 撓度量測位置 r_1=36 in. 和 r_3=60 in.，若設上層及下層之彈性模數值 E_1=1,000,000 psi，E_2=5,000 psi 爲已知。由BISAR程式計算得其撓度值爲w_1=0.00386 in.， w_3=0.0028 in.。(1 lb=0.454 kg, 1 psi=0.07 kg/cm^2, 1 in.=2.54 cm)

現若假設上述之撓度值w_1，w_3爲已知，而E_1，E_2爲欲回算求得之未知彈性模數值。因此， h/a = 1.3，r_1/h = 3.6，r_3/h = 6.0， w_1r_1/w_3r_3 = 0.827。將上述參數代入前述之預估方程式組中，可得 $A1$ = -0.14267，$A2$ = 3.28976，$A3$ = 0.35660，ϕ_1 = -0.59584，ϕ_2 = 1.26694，ϕ_3 = -0.32111。最後將以上結果代入式(E. 9)中，可得$\log_{10}(E_1/E_2)$ = 2.28826，亦即E_1/E_2 = 194.20。

同理，將此 E_1/E_2 值代入前述之另一預估方程式組中，可得 $A1$ = 2.75956，$A2$ = 2.15223，ϕ_1 = 0.49000，ϕ_2 = 0.80058。再將以上結果代入式(E. 10)中，可得$\log_{10}(Y)$ = 2.2475，亦即是Y = 176.8068。因此，可計算出上層彈性模數值 E_1 = 911,259 psi，而下層之彈性模數值E_2 = 4,692 psi。此運算之結果不僅與原假設值甚爲相近，而且比傳統的回算程式(如BISDEF程式)更具有快速性與精確性。

八、結論與建議

一般回算程式必須輸入鋪面各層彈性模數值的範圍與起始值，而該彈性模數值範圍之設定，對於回算速度及回算結果之正確性有相當大的影響。此外，由回算的基本理論分析中得知，量測之面層撓度值所估算出之彈性模數值的解可能不唯一。此理論之嚴重限制在一般回算程式中均不予考慮，因此亦可能會影響回算結果之正確性甚巨。本文除了針對上述問題研究改進的方法，並融合資料庫回算法的理念與最新的統計迴歸方法，建立一個能由面層撓度值直接計算出各層彈性模數值的預估方程式組。

本文以無因次的參數及函數關係建立之資料庫及預估方程式組，比傳統的分析法更具代表性，所以適用範圍亦較廣。該預估方程式組不僅可免除反覆運算的時間，在面層撓度量測與彈性模數值回算的過程亦有了及時性。如此，不僅可免除反覆運算的時間，亦可在現場試驗中立即計算出各層之彈性模數值，必要時亦可重複該非破壞性撓度試驗，以確保所量測資料與回算之彈性模數值的正確性。此外，若有必要運用傳統回算程式時，該預估方程式組的可能預估誤差範圍亦可做爲選定傳統回算程式中設定彈性模數值範圍的基本準則。

在時間與經費的雙重限制下，本文僅提出二層彈性系統的回算問題之初步研究。對於參數範圍之選定、資料庫的規模大小、預估方程式組的精確度、溫度之校估、甚至三層或三層以上之系統等問題，仍須待未來作更深入的研究。茲將改進之建議簡述如下：

1. 本文所推導出之無因次參數，可做爲未來分析三層或三層以上系統之依據，並靈活擴展運用之。
2. 由於資料庫中之變數E_1/E_2的範圍甚大，故在前述的迴歸分析中必須取此變數的對數函數做爲回應變數，以減少分析上的困難。因此，各層彈性模數之估算誤差亦可能成對數增長。所建立之非線性方程式組的預估結果經初步驗證有相當之正確性，然爲提高預估方程式組的精確度，必要時可在迴歸分析時將資料庫做細部分區、愼選參數範圍、或增加非線性函數之投影項。但是，迴歸之投影項仍不宜增加過多，以免方程式組過於複雜，不利於計算。
3. 溫度校估在非破壞性撓度試驗分析鋪面結構強度的程序中，是非常重要的部份。尤其是國內最常用的瀝青材料，其材料性質受到溫度變化的影響極大。爲使回算彈性模數

之結果合理，量測撓度時必須同時記錄量測溫度，並配合當地之溫度校估模式，以便將撓度值校估爲設計時標準溫度下的撓度值，再回算得彈性模數值。

4. 若經由以上之深入研究改進，使所建立之預估方程式組更精確，且方程式更簡化，則有利於寫成程式以直接計算出各層之彈性模數值。此外，將該程式與非破壞性撓度量測儀器相結合，則可立即由現場量測撓度值得知鋪面之結構強度狀況。

致謝

本研究承蒙行政院國家科學委員會之經費贊助，特此致謝。研究期間蒙美國伊利諾大學Dr. K. T. Hall 與本所倪至寬博士提供許多寶貴意見與協助，在此並致上萬分之謝忱。

參考文獻

1. 陳建桓，「由鋪面撓度值回算鋪面彈性模數的理論研究」，淡江大學土木工程研究所運輸工程組碩士論文，淡水，台北，民國八十三年六月 (1994)。
2. Burmister, D. M., "The Theory of Stresses and Displacements in Layered Systems and Applications to the Design of Airport Runways", Proceedings, Highway Research Board, Vol. 23, pp. 126-144 (1943).
3. Scrivner, F. H., C. H. Michalak , and W. M. Moore, "Calculation of the Elastic Moduli of a Two-Layer Pavement System from Measured Surface Deflection", Highway Research Record No. 431, Highway Research Board, Washington, D.C. (1973).
4. Friedman, J. H. and W. Stuetzle, "Projection Pursuit Regression," Journal of the American Statistical Association, Vol. 76, pp. 817-823 (1981).
5. Lee, Y. H., and M. I. Darter, "New Predictive Modeling Techniques for Pavements," Transportation Research Record 1449, Transportation Research Board, Washington, D.C., pp. 234-245 (1994).
6. Odemark, N., "Investigations as to the Elastic Properties of Soils and Design of Pavements According to the Theory of Elasticity," (in Swedish), Bulletin 77, State Highway Commission, Stockholm, Sweden (1949). English Translated by M. A. Hibbs and J. Silfwerbrand and Edited by A. M. Ioannides (1989).
7. Shell Oil Co., "BISAR: Bitumen Structures Analysis in Roads, User's Manual," Koninklijke/Shell - Laboratorium, Shell-Research N.V., Amsterdam (1978).
8. STATISTICAL Sciences, Inc., "S-PLUS for Windows," User's Manuals and Reference Manuals, Seattle, Washington (1993).
9. Bush, A. J., III, "Computer Program BISDEF," U. S. Army Corps of Engineers Waterways Experiment Station (1985).

B.4 BISAR程式之使用介紹

Anastasios M. Ioannides
University of Illinois
2230C Newmark C. E. La
Urbana, IL 61801

PREPARATION OF A BISAR INPUT FILE, USING BISARIN


```
C:\CE320>bisarin

THIS PROGRAM CREATES A DATA FILE FOR THE ELASTIC
    LAYER PROGRAM "BISAR"

ENTER A NAME FOR YOUR DATA FILE (10 CHARACTERS OR LESS)
-example.in

 INPUT TITLE FOR BISAR RUN
- ce 320 example run for bisar demonstration

INPUT: NUMBER OF PROBLEMS- 3

****PAVEMENT INFORMATION****

TOTAL NUMBER OF LAYERS IN THE PAVEMENT SYSTEM --> 3

PAVEMENT TYPE:  R- RIGID (BISAR SET FOR SMOOTH
                         COMPUTATIONAL PROCEDURE)
                F- FLEXIBLE (BISAR SET FOR ROUGH
                         COMPUTATIONAL PROCEDURE)
                C- COMPOSITE [AC OVER PCC] (BISAR SET FOR
                         SMOOTH COMPUTATIONAL PROCEDURE)
               ............--> r
****ENTER THE FOLLOWING FOR EACH SYSTEM LAYER****
 LAYER NUMBER  1 :

        MODULUS OF ELASTICITY (PSI) --> 4000000

        POISSON'S RATIO..... --> 0.15

        LAYER THICKNESS (IN)..... --> 6

ENTER LAYER INTERFACE CONDITION RANGING FROM
 0 (COMPLETE ADHESION) TO 1000 (FRICTIONLESS SLIP) ......--> 1000

 LAYER NUMBER  2 :

        MODULUS OF ELASTICITY (PSI) --> 50000

        POISSON'S RATIO..... --> 0.15

        LAYER THICKNESS (IN)..... --> 12

ENTER LAYER INTERFACE CONDITION RANGING FROM
 0 (COMPLETE ADHESION) TO 1000 (FRICTIONLESS SLIP) ......--> 1000
```

LAYER NUMBER 3 :

MODULUS OF ELASTICITY (PSI) --> 3000

POISSON'S RATIO..... --> 0.5

******ENTER LOAD INFORMATION******

NUMBER OF LOADED AREAS.....--> 1

LOAD NUMBER 1 :

have to change !!!

VERTICAL LOAD (~~LB~~ (PSI)).....--> 100

RADIUS OF LOADED AREA (IN).....--> 5.641895

INPUT THE NUMBER OF EVALUATION POSITIONS
.....--> 4

POSITION NUMBER 1 :

LAYER NUMBER --> 1

X - CO-ORDINATE, (IN.) --> 0

Y - CO-ORDINATE, (IN.) --> 0

DEPTH, (IN.) --> 0

POSITION NUMBER 2 :

LAYER NUMBER --> 1

X - CO-ORDINATE, (IN.) --> 0

Y - CO-ORDINATE, (IN.) --> 0

DEPTH, (IN.) --> 6

POSITION NUMBER 3 :

LAYER NUMBER --> 2

X - CO-ORDINATE, (IN.) --> 0

Y - CO-ORDINATE, (IN.) --> 0

DEPTH, (IN.) --> 18

```
      POSITION NUMBER 4 :

      LAYER NUMBER --> 3

     -POSITION NUMBER 3 :

      LAYER NUMBER --> 2

      X - CO-ORDINATE, (IN.) --> 0

      Y - CO-ORDINATE, (IN.) --> 0

      DEPTH, (IN.) --> 18

****PAVEMENT INFORMATION****

TOTAL NUMBER OF LAYERS IN THE PAVEMENT SYSTEM --> 3

PAVEMENT TYPE:  R= RIGID (BISAR SET FOR SMOOTH
                         COMPUTATIONAL PROCEDURE)
                F= FLEXIBLE (BISAR SET FOR ROUGH
                         COMPUTATIONAL PROCEDURE)
                C= COMPOSITE [AC OVER PCC] (BISAR SET FOR
                         SMOOTH COMPUTATIONAL PROCEDURE)
               .............--> r

****ENTER THE FOLLOWING FOR EACH SYSTEM LAYER****

LAYER NUMBER  1 :

       MODULUS OF ELASTICITY (PSI) --> 4000000

                .....
```

Execution terminated : 0

SAMPLE INPUT FILE GENERATED

```
ce 320 example run for bisar demonstration
                  1
  3  1  1
 4000000.  0.15     6.00  1000.
   50000.  0.15    12.00  1000.
    3000.  0.50
  1
   100.00    5.642     0.00     0.00 0.  0.
  4
  1     0.00      0.00      0.00 0.
  1     0.00      0.00      6.00 0.
  2     0.00      0.00     18.00 0.
  3     0.00      0.00     18.00 0.
```

ATTENTION 'BISAR' USERS:

Line 3 of Input file generated by BISARIN must be adjusted as follows:

NLAYS ISMO IRED

- NLAYS ↑ number of layers (incl. soil)
- ISMO ↑ Use 1 for SMOOTH calculation, i.e. select "RIGID"
- IRED ↑ Use 0; BISARIN sometimes puts in 1, but that may cause errors in unbonded layers

HOW TO EXECUTE BISAR USING AN EXISTING INPUT FILE


```
C:\CE320>bisar

WELCOME TO BISAR ON MICRO-COMPUTER

TO RUN THIS PROGRAM YOU MUST ALREADY
HAVE A DATA FILE SET UP. TO SET UP THIS DATA
FILE SEE THE BISAR INPUT GUIDE OR RUN
THE BASIC COMPUTER PROGRAM -BISDATA-
                            BISARIN

NOTE: THE DATA FILE MUST ALREADY EXIST

ENTER BISAR DATA FILENAME  --->    example.in

NOTE: THE OUTPUT FILE MUST BE NEW

ENTER FILENAME FOR BISAR OUTPUT --->example.out


    e 320 example run for bisar demonstration

                    ****************
          DATE----->  1/13/1990

          TIME-----> 19  .68
                     ****  ****

     BEGIN CALCULATIONS FOR POSTION NUMBER-->  1
     TIME--> 19:16:44.95
     BEGIN CALCULATIONS FOR POSTION NUMBER-->  2
     TIME--> 19:16:54.83
     BEGIN CALCULATIONS FOR POSTION NUMBER-->  3
     TIME--> 19:17: 3.62
     BEGIN CALCULATIONS FOR POSTION NUMBER-->  4
     TIME--> 19:17:12.19
                    ****************
           DATE----->  1/13/1990

           TIME-----> 19:17:23. 7
                      **************

     TO TERMINATE THE RUN ENTER ------> <RETURN>
     FOR SCREEN OUTPUT ENTER --------->    <1>
     FOR PRINTED OUTPUT ENTER -------->    <2>
     FOR BOTH OUTPUTS ---------------->    <3>


     WHAT IS YOUR CHOICE ????--------->   1
```

ce 320 example run for bisar demonstration

****

DATE====> 1/13/1990

SAMPLE OUTPUT FILE PRODUCED

TIME====> 18:55:49.68

****

SYSTEM NUMBER 1

LAYER NUMBER	CALCULATION METHOD	YOUNG'S MODULUS	POISSON'S RATIO	THICKNESS	REDUCED SPRINGCOMPL
1	SMOOTH	4000000.	0.15	6.00	1000.00
2	SMOOTH	50000.	0.15	12.00	1000.00
3		3000.	0.50		

LOAD NUMBER	NORMAL STRESS	SHEAR STRESS	RADIUS OF LOADED AREA	LOAD - POSITION X	Y	SHEAR DIRECTION
1	0.1000E+03	0.0000E+00	0.5642E+01	0.0000E+00	0.0000E+00	0.0000E+00

****

POSTION NO. 1 LAYER NO. 1

X-COORDINATE==> 0.00

Y-COORDINATE==> 0.00

Z-DEPTH=======> 0.00

TOTAL STRESSES , STRAINS AND DISPLAEMENTS

	HORIZ IN X	HORIZ IN Y	VERITCAL	SHEAR YZ	SHEAR XZ	SHEAR XY
STRESS	-0.340E+03	-0.340E+03	-0.100E+03	0.000E+00	0.000E+00	0.000E+00
STRAIN	-0.685E-04	-0.685E-04	0.483E-06	0.000E+00	0.000E+00	0.000E+00
DISPLT	0.000E+00	0.000E+00	0.254E-01			

****

POSTION NO. 2 LAYER NO. 1

X-COORDINATE==> 0.00

Y-COORDINATE==> 0.00

Z-DEPTH=======> 6.00

TOTAL STRESSES , STRAINS AND DISPLAEMENTS

	HORIZ IN X	HORIZ IN Y	VERITCAL	SHEAR YZ	SHEAR XZ	SHEAR XY
STRESS	0.312E+03	0.312E+03	-0.578E+01	0.000E+00	0.000E+00	0.000E+00
STRAIN	0.665E-04	0.665E-04	-0.249E-04	0.000E+00	0.000E+00	0.000E+00
DISPLT	0.000E+00	0.000E+00	0.253E-01			

****

POSTION NO. 3 LAYER NO. 2
X-COORDINATE==> 0.00
Y-COORDINATE==> 0.00
Z-DEPTH=======> 18.00

TOTAL STRESSES , STRAINS AND DISPLAEMENTS

	HORIZ IN X	HORIZ IN Y	VERITCAL	SHEAR YZ	SHEAR XZ	SHEAR XY
STRESS	0.728E+01	0.728E+01	-0.117E+01	0.000E+00	0.000E+00	0.000E+00
STRAIN	0.127E-03	0.127E-03	-0.672E-04	0.000E+00	0.000E+00	0.000E+00
DISPLT	0.000E+00	0.000E+00	0.243E-01			

****

POSTION NO. 4 LAYER NO. 3
X-COORDINATE==> 0.00
Y-COORDINATE==> 0.00
Z-DEPTH=======> 18.00

TOTAL STRESSES , STRAINS AND DISPLAEMENTS

	HORIZ IN X	HORIZ IN Y	VERITCAL	SHEAR YZ	SHEAR XZ	SHEAR XY
STRESS	-0.943E+00	-0.943E+00	-0.117E+01	0.000E+00	0.000E+00	0.000E+00
STRAIN	0.386E-04	0.386E-04	-0.773E-04	0.000E+00	0.000E+00	0.000E+00
DISPLT	0.000E+00	0.000E+00	0.243E-01			

****

DATE====> 1/13/1990

TIME====> 18:56:25.60

****

***** T H E E N D *****

C 剛性鋪面之回算

C.1 剛性鋪面回算之介紹

資料來源：

林炳森、李泰明、吳元廷、鄒譽名，"路面評審儀應用於剛性路面之回算法"，中華民國第八屆鋪面工程學術研討會論文輯，台北國際會議中心，中原大學，中華民國八十四年十二月六日至八日。

C.2 剛性鋪面回算之封閉型解法

資料來源：

Hall, K. T., "Performance, Evaluation, and Rehabilitation of Asphalt-Overlaid Concrete Pavements," Ph.D. Thesis, University of Illinois, Urbana, Illinois, 1991, pp. 88-104.

C.3 ILLI-SLAB程式之使用手冊

資料來源：

Korovesis, G. T., "Analysis of Slab-on-Grade Pavement Systems Subjected to Wheel and Temperature Loadings," Ph.D. Thesis, University of Illinois, Urbana, Illinois, 1990, pp. 305-334.

C.4 對ILLI-SLAB使用者之建議

資料來源：

Ioannides, A. M., "Analysis of Slab-on-Grade for a Variety of Loading and Support Conditions," Ph.D. Thesis, University of Illinois, Urbana, Illinois, 1984, pp. 187-188.

C.1 剛性鋪面回算之介紹

路面評審儀應用於剛性路面之回算法

林炳森	李泰明	吳元廷	鄒譽名
國立中興大學	國道高速公路局	國立中興大學	國立中興大學
土木工程研究所	汐止五股段拓建工程處	土木工程研究所	土木工程研究所
教授	副處長	博士班研究生	碩士

摘要

本研究主要針對北二高（大溪龍潭段）之剛性路面爲研究對象，於現場以路面評審儀（Road Rater）進行非破壞性檢測，將所得之撓度值，以版理論發展之程式BACK進行回算，並與多層彈性理論的回算結果比較；其次以ILLISLAB程式模擬，將所得之撓度值與路面評審儀得到之撓度值相比較，以評估版理論回算程式之適用性。

研究結果顯示：多層彈性理論回算之混凝土彈性模數比版理論回算結果大，其值可能有高估的現象；以ILLISLAB程式模擬，所得到之撓度值與現場量測值接近，顯示BACK程式回算之混凝土彈性模數具可靠性，但路基反力模數稍有低估之虞。

一、前言

有鑑於目前國內應用於剛性路面之非破壞性撓度試驗，大多以撓度指標進行分析評估，此法係建立多項臨界值以評估路面強度，但指標值若未達臨界值時，則無法研判路面強度減弱位置及提供預警之功能。故本文採用回算法(Backcalculation)回算各層材料之強度性質以評估鋪面結構強度，希望對日後剛性路面的管理、養護及維修有所助益。

本文主要之研究目的有二：

1.以版理論爲基礎，配合路面評審儀之荷重模擬，發展回算程式，並與多層彈性理論之回算結果比較，以評估兩者之適用性。

2.將版理論之回算結果以ILLISLAB程式運算，所得到之撓度值與現場量測值比較，以評估回算結果之正確性。

二、文獻回顧

鋪面系統靜態之回算程序之處理方式有：

(一)迭代法

此法係先假設一組起始模數值，而後比較理論撓度值與量測之撓度值，若誤差在容許限度內，則該組模數值即爲所求，若誤差超出容許限度，則修正調整另一組模數值依前述方法重新計算，直至合理之模數值產生或依迭代次數限制後停止。而誤差之計算方式有平均絕對值(Average Absolute；AA)法或均方根(Root Mean Square；RMS)法。依本法發展之回算程式大多建立於靜態之多層彈性理論正算分析，如WESDEF、ELSDEF等程式。國內周家蓓與陳又菁即以ELSYM5程式配合修正係數法之迭代過程發展ELSBACK回算程式〔1〕。

(二)資料庫法

本法係先利用正算理論將各層可能之模數範圍建立成資料庫，且計算出理論撓度值，再與理論撓度值內插比較，並找出在容許誤差內，誤差最小之一組解，進而反算模數值。MODULUS即利用靜態之多層彈性理論BISAR建立資料庫，進行回算分析〔2〕。

(三)以版理論爲基礎之回算法

美國伊利諾大學以版理論爲基礎發展閉合解法(Close-Form Solution)之回算程式ILLIBACK，進行二層剛性路面之分析。所謂閉合解法，即利用統計迴歸分析方法，來建立面積指標AREA與相對勁度(Relative Stiffness)關係式，加上相對勁度與面層模數、路基反力模數或路基彈性模數等關係式，直接回算出彈性模數值之方法〔3,4,5〕。

(1)ILLIBACK回算程式：

此法(Ioannides et al.1989)可應用於緊密液態(Dense Liquid)或彈性固態(Elastic Solid)基礎上，混凝土版中央受到圓形荷重作用之情況，其回算過程〔6〕：

1.於現場進行非破壞性撓度試驗，並量測撓度值w_i。

2.由式一計算面積指標AREA。

$$AREA=6*(1+2*\frac{w_1}{w_0}+2*\frac{w_2}{w_0}+\frac{w_3}{w_0}) \quad \text{...式 一}$$

面積指標AREA(Hoffman & Thompson,1982)各撓度值均除以w_0使之標準化，主要爲除去不同荷重作用之影響與限制所得AREA的範圍〔7〕。

3.計算相對勁度半徑 l。

4.對於緊密液態基礎，可由圖1得到標準化撓度值 di,再由式二決定路基反力模數k值，可得四個k值，取其平均值。對於彈性固態基礎，可由圖2得到標準化撓度值d_i，再由式三決定路基彈性模數E_f，可得四個E_f值，取其平均值。

$$k = \frac{P \times d_i}{l_k^2 \times w_i} \quad \text{.....式 二}$$

式中 k：路基反力模式（pci），P：作用力（lb），d_i：標準化撓度值(由理論得到)，i=0,1,2,3，l_k：液態基礎之相對勁度半徑（in），w_i：實測撓度值（in）。

$$E_f = \frac{2 \times (1-\upsilon_f)^2 \times P \times d_i}{l_e \times w_i} \quad \text{....式 三}$$

式中 E_f：路基彈性模數（psi），υ_f：路基土壤之柏松比，l_e：固態基礎之相對勁度半徑（in）。

5.將k及E_f之平均值分別代入式四及五即可決定定混凝土版之彈性模數Ec。

對於緊密液態基礎：

$$E_c = \frac{12 \times (1-\upsilon_c^2) \times k \times l_k^4}{h^3} \quad \text{....式 四}$$

式中 E_c：混凝土版之彈性模數(psi)，υ_c：混凝土版之柏松比，h：混凝土版厚(in)。

對於彈性固態基礎：

$$E_c = \frac{6 \times (1-\upsilon_c^2) \times E_f \times l_e^3}{(1-\upsilon_f^2) \times h^3} \quad \text{.....式 五}$$

(2)閉合解(Closed-Form Solution)回算法：

1.由撓度試驗量測之撓度值，計算面積指標AREA(式一)。

2.將計算出之AREA值代入式六與式七可分別得緊密液態基礎與彈性固態基礎的相對勁度半徑。

$$l_k = \left[\frac{\ln\left(\frac{36-AREA}{1812.279}\right)}{-2.559} \right]^{\frac{1}{0.288}} \quad \text{....式 六}$$

$$l_e = \left[\frac{\ln\left(\frac{36-AREA}{4521.676}\right)}{-3.645} \right]^{\frac{1}{0.187}} \quad \text{....式 七}$$

式六與式七係由SAS統計分析軟體以漸近線模式迴歸而得。

3.路基反力模數k可由Westergaard's撓度方程式(式八)求得；路基彈性模數E_c可由Losberg's撓度方程式(式九)求得。

$$k=\left(\frac{P}{8\times d_0\times l_k^2}\right)\times\left\{1+\left(\frac{1}{2\pi}\right)\times\left[\ln\left(\frac{a}{2l_k}\right)+r-1.25\right]\times\left(\frac{a}{l_k}\right)^2\right\} \quad \text{.....式 八}$$

式中 d_0：荷重作用中心之撓度值(in)，a ：荷重半徑 (in)，r ：Euler's constant, 0.57721566490。

$$E_f=\left[\frac{2\times P\times\left(1-\upsilon_f^2\right)}{d_0\times l_e}\right]\times\left[0.19245+0.027\times\left(\frac{a}{l_e}\right)^2+0.0199\times\left(\frac{a}{l_e}\right)^2\times\ln\left(\frac{a}{l_e}\right)\right] \quad \text{..式 九}$$

4.由式四可得緊密液態基礎之混凝土彈性模數Ec；由式五可得彈性固態基礎之混凝土彈性模數E_c。

2.3 剛性路面之有限元素分析法

ILLISLAB與KENSLAB乃目前分析剛性路面應用最廣的兩個程式庫。ILLISLAB是由伊利諾大學發展出來的，可用於單層或雙層混凝土鋪面之結構分析，而基礎型式可爲溫氏基礎(Winkler Foundation)、回彈基礎型式(Stress Dependent Resilient Subgrade)、魏氏雙參數基礎模式(Vlasov Two-Parameter-Foundation)、布氏彈性固態(Boussinesq's Elastic Solid)基礎模式[8]。而KENSLAB則是由肯達基大學發展而成，其基礎型式有溫氏基礎、布氏彈性基礎、柏氏多層基礎(Burmister's Layer Foundation)[3,9]。

三、研究方法

3.1 試驗路段之結構型態及材料特性

北部第二高速公路主線在里程51k+500~60k+750採剛性路面鋪築，全長9.25公里。其中北上LT52k+166.2 ~54k+104.26和南下RT52k+157.6~54k+96.6路段不含低強度混凝土處理底層(LCB)，其餘路段均含低強度混凝土處理底層(LCB)。全部剛性路面均採用接縫式混凝土路面(Jointed Concrete Pavement,JCP)施工。本研究採用顏聰、林炳森(1994)「剛性路面實用設計本土化研究(二)」之剛性路面結構斷面與各層材料性質[10]。

3.2 路面評審儀之介紹 (ROAD RATER 2000型)

路面評審儀之儀器構造主要是由重817kg(1800lbs)質量塊之振動單元與一組(五個)速度感應器(Velocity Sensor)所組成。由質量塊之振動單元可產生正弦波形的動力載

重，當動力載重施加於路面時，可由速度感應器接收其反射波，經積分後可得撓度值。儀器詳細規格如表1所示。

3.3 BACK程式說明

本程式是以FORTRAN語言寫成，可用來回算液態基礎之路基反力模數k、混凝土彈性模數 E_{pcc} ，及彈性固態基礎之路基彈性模數 E_s 、混凝土彈性模數 E_{pcc} ；其操作程序如下：

1.程式啓動

BACK回算程式的啓動十分容易，只要在程式所在目錄下輸入指令BACK即可。

2.程式輸入

BACK回算所需的輸入資料包括量測之撓度值、施加荷重、混凝土的柏松比、混凝土版的厚度、路基土壤之柏松比(僅彈性固態基礎需輸入)。

3.程式輸出

BACK回算程式的輸出有螢幕和檔案兩種方式，當資料輸入完後，程式會詢問是否將回算結果存入檔案，而輸出結果如圖1。

四、結果與討論

有鑑於目前國內發展之回算程式，如AC、PCC、ELSBACK(AC、ELSBACK程式應用於柔性路面，PCC程式應用於剛性路面)，AC、PCC乃曾世明(1992)採用Vlasov和Leont'ev的層狀彈性理論、Odemark氏等值厚度觀念發展之回算程式〔11〕，而ELSBACK程式乃陳又菁(1993)利用ELSYM5並配合修正係數法發展而成〔1〕，此三者均以多層彈性理論爲基礎，但此理論較適合分析柔性路面，故本研究採用版理論之閉合解法，且配合荷重模擬發展一回算程式BACK，並與多層彈性理論之回算結果相比較，以探討程式之適用性。

4.1 程式之適用性

將BACK程式所得之回算結果分別與(一)、ILLISLAB程式原輸入模數值比較，(二)、ELSYM5程式回算結果比較，來說明BACK程式之適用性：

(一)、與ILLISLAB程式原輸入模數值比較：

分別討論混凝土版厚度爲8in(20cm),10in(25cm)，12in(30cm)三種情況；首先將各參數輸入ILLISLAB程式中，再將輸出得到之撓度值（D0,D12,D24,D36）以BACK程式回算，可求得混凝土彈性模數與路基反力模數；其回算結果與ILLISLAB程式原輸入模數值比較(如表2~4所示)，可顯示出:

1.BACK程式回算之路基反力模數絕大部份會低於ILLISLAB程式輸入之路基反力模數。

2.對於較軟弱之路基土壤（路基反力模數值小時），BACK程式回算結果與ILLISLAB程式之模數值有較大之誤差。

3.若混凝土版厚愈薄，BACK程式回算結果愈接近ILLISLAB程式原輸入之模數值。

(二)、與ELSYM5程式回算結果之比較：

將現場量測之撓度值分別以BACK程式(緊密液態、彈性固態基礎)、ELSYM5程式(配合荷重模擬與修正係數法)進行回算，並將BACK程式(緊密液態基礎)推求之混凝土彈性模數與較回算大些之路基反力模數輸入ILLISLAB程式中，所得到之撓度值與現場量測值、ELSYM5程式之計算值比較(如圖4、表5所示)，而回算結果如表5所示。

由表5可知：

1.多層彈性理論(ELSYM5程式)得到之撓度值(w_1 , w_2 , w_3 , w_4)，其 w_2 與量測值誤差較大。

2.ELSYM5程式回算之混凝土彈性模數較版理論（緊密液態基礎、彈性固態基礎）回算結果大(如圖6所示)。

3.對於版理論，不同基礎模式之回算結果差異頗大。

4.2 與PCC程式之回算結果作比較

由回算結果比較（如圖5、表6）顯示：

1.ILLISLAB程式所得之撓度值比PCC程式更接近現場量測值(由均方根誤差RMS知)。

2.BACK程式回算之混凝土彈性模數較PCC程式接近試驗值，顯示版理論更適合應用於剛性路面之回算。

3.PCC程式回算之混凝土彈性模數較BACK程式(緊密液態、彈性固態基礎）所得爲大(如圖7所示)。

4.3 以ILLISLAB程式發展之圖解法

由於版邊緣、接縫、角隅處受到鋼筋及邊界之影響，無法由BACK程式及多層彈性理論回算出彈性模數值。本研究利用ILLISLAB程式執行結果畫出面積指標AREA與荷重中點撓度W1之關係圖（如圖8~10所示），以提供回算時減少試誤之次數。

由現場量測之撓度值 w_1 、 w_2 、 w_3 、 w_4 ，可計算得面積指標AREA，即可由圖8~10概略求得混凝土彈性模數E值及路基反力模數k值。

五、結論與建議

5.1 結論

本研究係以版理論配合荷重模擬發展一回算程式BACK，對現場之撓度值進行回算，並以ILLISLAB程式評估其適用性，可獲得以下的結論：

1.由BACK程式知，緊密液態基礎回算之混凝土彈性模數比彈性固態基礎所得結果大，顯示不同的基礎型態對回算結果有很大的影響。

2.對於軟弱之路基土壤(k值小時)，接縫鋼筋對撓度值的影響不容忽視，故BACK程式之回算結果產生較大的誤差。

3.ELSYM5程式所得之撓度值，w_2與量測值有較大之誤差，且回算之混凝土彈性模數比BACK程式所得結果大。

4.由ILLISLAB程式得到之撓度值與現場量測之撓度值接近，顯示BACK程式回算之混凝土彈性模數具正確性，但路基反力模數稍有低估之虞。

5.ILLISLAB程式所得之撓度值比PCC程式更接近於現場量測值，且回算之混凝土彈性模數亦與試驗值接近，顯示版理論更適合應用於剛性路面之回算。

5.2 建議

1.路面評審儀於剛性路面所量測之撓度值很小，而撓度值之精確與否對回算結果影響甚大，因此，在進行撓度試驗時，需先校正量測之感應器，以減少對回算結果之誤差。

2.進行現場撓度值試驗時，對於同一點位需量測多次，取其平均值，以確保撓度值之精確性。

3.可於定點定期進行撓度試驗及量測溫度值，發展溫度修正模式，以作爲日後溫度校正之用。

4.未來回算程式可從動態回饋分析發展，使其更能反應出實際情況。

參考文獻

1.陳又菁,「鋪面撓度值在養護整修策略上之應用」，碩士論文，台灣大學研究所土木工程研究所，臺北（1993）。

2.Scullion,T.,Uzan,J.,Paredes,M.,"Modulus:A Microcmputer-Based Back-calculation System,"TRB,Transportation Research Record No.1260,pp.180~191（1990）。

3.Huang, Y.H.,Pavement Analysis and Design",Prentice Hall,Inc.,pp.446~460（1993）。

4.Darter,M.I.,Smith,K.,and Hall,K.T.," Concrete Pavement Backcalculation Results from Field Studies ",TRB, Transportation Research Record No.1337,pp.7-16（1993）。

5.Hall,K.T.,and Alaeddin M.," Back calulation of Asphalt Concrete Overlaid Portland Cement Concrete Pavement Layer Moduli ",Transportation Research

Record No.1293,pp.112~123（1992）。
6.Ioannides,A.M.,Barenberg,E.J.,and Lary,J.A.,"Interpretation of Falling Weight Deflectometer Results Using Principles of Dimensional Analysis."Proceeding,4th International Conference on Concrete Pavement Design and Rehabilitation, Purdue University,pp.231~247.（1989）。
7.Hoffman,M.S.,and Thompason,M.R.,"Comparative Study of Selected Nondestructive Testing Devices."TRB,Transportation Research Record No.852,pp.32~41（1982）。
8.Korovesis,G.T.," Analysis of Slab-on-Grade Pavement Systems Subjected to Wheel and Temper ature Loading.", Ph.D. Thesis, University of Illinois at Urbana Champaign.（1990）。
9.蘇子健,「接縫混凝土路面行爲之初步研究」，碩士論文，國立中興大學土木工程研究所，臺中（1992）。
10.顏聰、林炳森等,「剛性路面實用設計本土化研究(2)」，交通部台灣區國道新建工程局，書籍編號045,（1994）。
11.曾世明,「路面評審儀應用於鋪面的力學分析」，碩士論文，淡江大學土木工程研究所，台灣淡水（1992）。

表 1　路面評審儀之儀器規格

儀器規格	（英 制）	（公 制）
長	146 inches	370 cm
寬	82 inches	208 cm
高	57 inches	145 cm
最大靜態荷重	2400 lbs	1089 kg
最大動態荷重	200-3000 lbs	91-1362 kg
加壓承載版直徑	12 inches	30 cm
感應器間距	12 inches	30 cm
頻率	10-60 Hz	10-60 Hz

挽度單位 mil(=1/1000 inch)

註：本試驗使用頻率為15HZ。

表 2　BACK 程式回算結果與 ILLISLAB 程式原輸入值之比較(Hpcc=8 in)

ILLISLAB程式原輸入值				BACK程式回算之結果			
路基反力模數		混凝土彈性模數		路基反力模數		混凝土彈性模數	
kg/cm^3	pci	kg/cm^2	psi	kg/cm^3	pci	kg/cm^2	psi
2.77	100	70,373	1,000,000	2.96	107.00	65,560	931,609
		140,746	2,000,000	1.43	51.59	114,428	1,626,021
		211,119	3,000,000	1.46	52.62	229,052	3,254,832
		281,492	4,000,000	1.49	53.65	332,154	4,719,913
		351,865	5,000,000	1.66	60.00	382,282	5,432,232
		422,238	6,000,000	1.72	62.04	441,413	6,272,482
		492,611	7,000,000	1.75	63.03	499,875	7,103,223
		562,984	8,000,000	1.76	63.39	558,210	7,932,162
5.54	200	70,373	1,000,000	5.55	200.20	68,492	973,268
		140,746	2,000,000	5.17	186.51	141,923	2,016,723
		211,119	3,000,000	4.73	170.68	225,010	3,197,385
		281,492	4,000,000	4.74	170.96	294,042	4,178,332
		351,865	5,000,000	4.67	168.73	364,741	5,182,973
		422,238	6,000,000	4.62	166.71	432,819	6,150,355
		492,611	7,000,000	4.54	164.04	502,448	7,139,781
		562,984	8,000,000	4.53	163.58	562,818	7,997,644
8.31	300	70,373	1,000,000	8.10	292.48	70,035	995,194
		140,746	2,000,000	7.88	284.57	142,550	2,025,629
		211,119	3,000,000	7.81	282.01	213,941	3,040,099
		281,492	4,000,000	7.71	278.11	286,366	4,069,259
		351,865	5,000,000	7.62	275.05	357,071	5,073,976
		422,238	6,000,000	7.54	272.30	426,065	6,054,384
		492,611	7,000,000	7.46	269.25	494,782	7,030,847
		562,984	8,000,000	7.37	265.87	564,272	8,018,301
13.85	500	70,373	1,000,000	13.04	470.78	72,490	1,030,082
		140,746	2,000,000	13.41	483.99	139,963	1,988,879
		211,119	3,000,000	13.43	484.57	209,802	2,981,286
		281,492	4,000,000	13.38	483.08	279,935	3,977,878
		351,865	5,000,000	13.24	478.05	352,340	5,006,755
		422,238	6,000,000	13.19	475.92	421,907	5,995,304
		492,611	7,000,000	13.08	472.11	493,293	7,009,688

表 3　BACK 程式回算結果與 ILLISLAB 程式原輸入值之比較(Upcc=10 in)

ILLISLAB程式原輸入值				BACK程式回算之結果			
路基反力模數		混凝土彈性模數		路基反力模數		混凝土彈性模數	
kg/cm^3	pci	kg/cm^2	psi	kg/cm^3	pci	kg/cm^2	psi
2.77	100	70,373	1,000,000	3.69	133.30	58,757	834,942
		140,746	2,000,000	1.46	52.71	167,654	2,382,363
		211,119	3,000,000	1.71	61.86	221,694	3,150,266
		281,492	4,000,000	1.75	63.31	280,399	3,984,476
		351,865	5,000,000	1.76	63.62	337,360	4,793,890
		422,238	6,000,000	1.75	63.33	394,043	5,599,353
		492,611	7,000,000	1.74	62.87	450,306	6,398,843
		562,984	8,000,000	1.71	61.57	512,879	7,288,017
5.54	200	70,373	1,000,000	5.05	182.30	65,842	935,621
		140,746	2,000,000	4.74	171.03	147,297	2,093,093
		211,119	3,000,000	4.63	167.18	216,578	3,077,569
		281,492	4,000,000	4.50	162.49	284,814	4,047,213
		351,865	5,000,000	4.42	159.61	347,937	4,944,187
		422,238	6,000,000	4.32	155.86	413,533	5,876,310
		492,611	7,000,000	4.26	153.77	473,438	6,727,554
		562,984	8,000,000	4.17	150.59	537,111	7,632,348
8.31	300	70,373	1,000,000	7.90	285.00	71,154	1,011,095
		140,746	2,000,000	7.75	279.56	142,475	2,024,574
		211,119	3,000,000	7.52	271.30	214,428	3,047,018
		281,492	4,000,000	7.39	266.81	281,851	4,005,109
		351,865	5,000,000	7.27	262.49	347,439	4,937,106
		422,238	6,000,000	7.06	254.81	418,487	5,946,694
		492,611	7,000,000	7.03	253.62	476,502	6,771,092
		562,984	8,000,000	6.89	248.56	542,235	7,705,166
13.85	500	70,373	1,000,000	13.40	483.52	70,042	995,303
		140,746	2,000,000	13.37	482.57	140,223	1,992,569
		211,119	3,000,000	13.19	475.93	211,391	3,003,867
		281,492	4,000,000	13.08	472.24	279,766	3,975,480
		351,865	5,000,000	12.89	465.21	349,222	4,962,447
		422,238	6,000,000	12.64	456.37	420,208	5,971,161
		492,611	7,000,000	12.53	452.12	487,492	6,927,266

表 4　BACK 程式回算結果與 ILLISLAB 程式原輸入值之比較(Upcc=12 in)

ILLISLAB程式原輸入值				BACK程式回算之結果			
路基反力模數		混凝土彈性模數		路基反力模數		混凝土彈性模數	
kg/cm^3	pci	kg/cm^2	psi	kg/cm^3	pci	kg/cm^2	psi
2.77	100	70,373	1,000,000	1.22	44.20	95,043	1,350,565
		140,746	2,000,000	1.75	63.00	143,327	2,036,679
		211,119	3,000,000	1.75	63.20	202,694	2,880,284
		281,492	4,000,000	1.72	62.20	259,185	3,683,019
		351,865	5,000,000	1.70	61.40	316,422	4,496,352
		422,238	6,000,000	1.68	60.50	371,032	5,272,371
		492,611	7,000,000	1.65	59.50	425,759	6,050,033
		562,984	8,000,000	1.61	58.10	482,901	6,862,021
5.54	200	70,373	1,000,000	4.74	171.00	74,438	1,057,760
		140,746	2,000,000	4.57	165.00	143,452	2,038,457
		211,119	3,000,000	4.42	159.50	207,525	2,948,924
		281,492	4,000,000	4.25	153.30	272,055	3,865,897
		351,865	5,000,000	4.11	148.40	334,919	4,759,195
		422,238	6,000,000	4.00	144.30	396,814	5,638,722
		492,611	7,000,000	3.96	142.80	450,216	6,397,563
		562,984	8,000,000	3.84	138.70	514,277	7,307,872
8.31	300	70,373	1,000,000	7.79	281.00	71,302	1,013,204
		140,746	2,000,000	7.46	269.20	141,972	2,017,425
		211,119	3,000,000	7.20	259.70	209,884	2,982,445
		281,492	4,000,000	7.02	253.20	273,498	3,886,403
		351,865	5,000,000	6.75	243.80	341,155	4,847,817
		422,238	6,000,000	6.64	239.70	406,943	5,782,654
		492,611	7,000,000	6.44	232.50	466,434	6,628,022
		562,984	8,000,000	6.35	229.20	523,438	7,438,047
13.85	500	70,373	1,000,000	13.37	482.50	70,226	997,906
		140,746	2,000,000	13.19	475.90	139,792	1,986,446
		211,119	3,000,000	12.75	460.20	211,655	3,007,615
		281,492	4,000,000	12.56	453.20	277,684	3,945,889
		351,865	5,000,000	12.37	446.40	341,595	4,854,066
		422,238	6,000,000	11.98	432.50	413,108	5,870,259
		492,611	7,000,000	11.84	427.50	473,985	6,735,332

表 5　各程式回算結果之比較

作用點位	撓度值 (mils)				
* 12	W1	W2	W3	W4	RMS(%)
量測值	0.700	0.660	0.560	0.490	0
ILLISLAB計算值	0.702	0.658	0.572	0.475	0.485
ELSYM5計算值	0.707	0.621	0.560	0.492	0.992
回算結果					
	混凝土彈性模數		路基反力模數		
單位	kg/cm^2	psi	kg/cm^3	pci	
BACK(液態基礎)	262,041	3,723,596	6.07	219	
ILLISLAB輸入值	262,069	3,724,000	7.31	264	
	混凝土彈性模數 E1		級配層E2	底層E3	各層本意圖:
單位	kg/cm^2	psi	psi	psi	混凝土面層E1 / 級配層E2 / 底層E3
BACK(固態基礎)	216,076	3,070,433	33,660		
ELSYM5	335,128	4,762,162	43,213	24,999	

註: RMS Error(均方根誤差)$=\frac{1}{n}\left[\sum_{i=1}^{n} D_i^2\right]^{1/2}$　混凝土彈性模數=4.03 × 10^6 psi(試驗值)　路基反力模數=481 pci(平板載重試驗)

表 6　各程式回算結果之比較

作用點位	撓度值 (mils)				
中央點	W1	W2	W3	W4	RMS(%)
量測值	2.920	2.494	1.852	1.124	0
ILLISLAB計算值	2.921	2.500	1.794	1.149	1.586
PCC計算值	2.967	2.447	1.812	1.137	1.966
回算結果					
	混凝土彈性模數		路基反力模數		
單位	kg/cm^2	psi	kg/cm^3	pci	
BACK(液態基礎)	198,743	2,824,144	4.27	154	
ILLISLAB輸入值	198,733	2,824,000	4.35	157	各層本意圖:
	混凝土彈性模數 E1		級配層E2	底層E3	混凝土面層E1 / 級配層E2 / 底層E3
單位	kg/cm^2	psi	psi	psi	
PCC	240,552	3,418,244	59,963	33,000	

註: RMS Error(均方根誤差)$=\frac{1}{n}\left[\sum_{i=1}^{n} D_i^2\right]^{1/2}$　混凝土彈性模數=2.916*10^6 psi (試驗值)

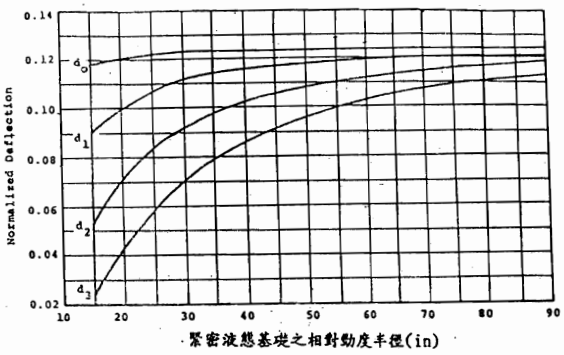

圖 1　標準化撓度值與相對勁度半徑之關係圖 (緊密液態基礎 Ioannides et al. 1989)

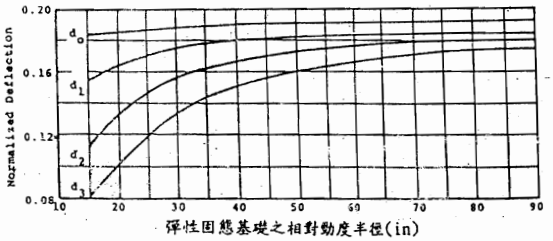

圖 2　標準化撓度值與相對勁度半徑之關係圖 (彈性固態基礎 Ioannides et al. 1989)

```
+++++++++++++++++++++++++++++++++++++++++++++++++
+                                               +
+          BACKCALCULATION RESULT               +
+          (  LIQUID  FOUNDATION  )             +
+                                               +
+       ---------- INPUT  DATA ----------        +
+                                               +
+         DEFLECTION D0  =  .000680 (in)        +
+         DEFLECTION D12 =  .000640 (in)        +
+         DEFLECTION D24 =  .000550 (in)        +
+         DEFLECTION D36 =  .000420 (in)        +
+         APPLIED LOAD P =  1910.0 (lb)         +
+       PCC POISSON RATIO Upcc= .20             +
+     PCC THICKNESS Dpcc =    12.00 (in)        +
+                                               +
+       ---------- OUTPUT DATA ----------       +
+                                               +
+         MODULUS OF SUBGRADE REACTION          +
+           K =  251.0  (psi/in)                +
+                                               +
+         CONCRETE ELASTIC MODULUS              +
+           Epcc =  3190008  (psi)              +
+                                               +
+++++++++++++++++++++++++++++++++++++++++++++++++
DO YOU WANT TO SOLVE ANOTHER PROBLEM ? (Y OR N) ---------->
```

圖 3　BACK 回算程式之輸出畫面

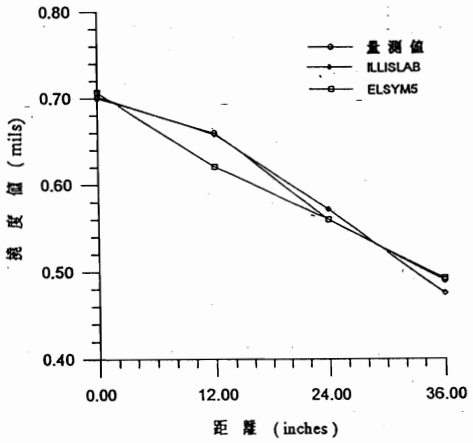

圖 4 各程式之撓度值與量測值之比較

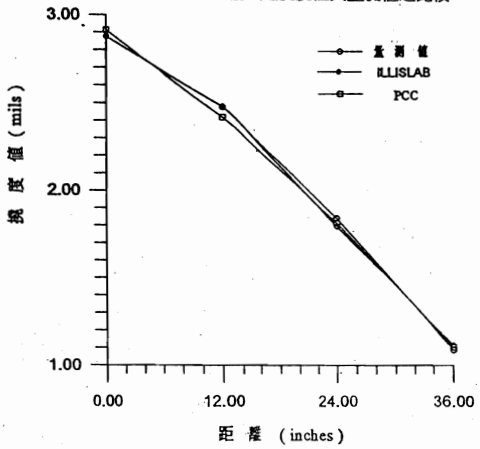

圖 5 各程式之撓度值與量測值之比較

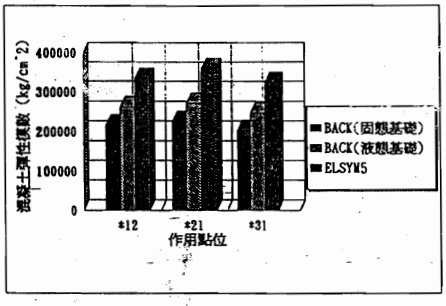

圖 6 各程式回算之混凝土彈性模數比較圖 (表 4.4-4.6)

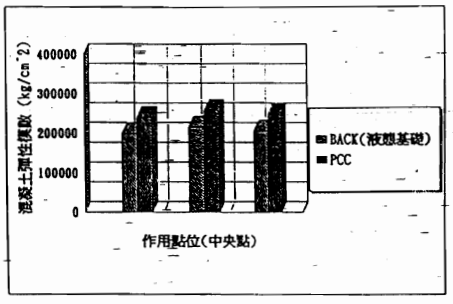

圖 7 各程式回算之混凝土彈性模數比較圖 (表 4.10-4.12)

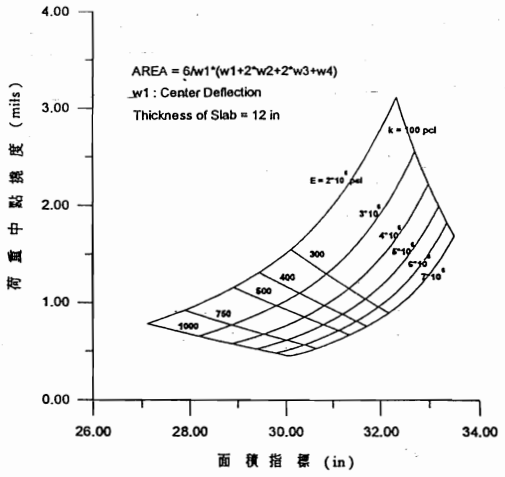

圖 8 ILLISLAB 程式發展之圖解法(版邊緣#11)

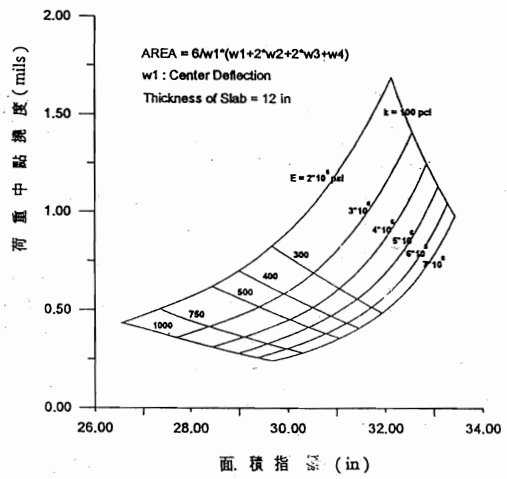

圖 9 ILLISLAB 程式發展之圖解法(版中央#12)

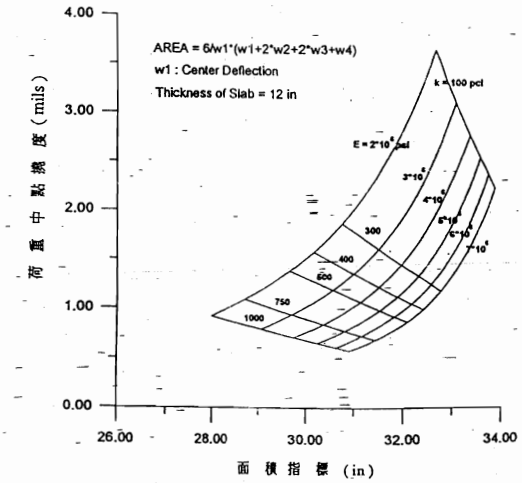

圖 10 ILLISLAB 程式發展之圖解法(版接縫#13)

C.2 剛性鋪面回算之封閉型解法

CHAPTER FOUR
BACKCALCULATION OF AC/PCC PAVEMENT LAYER MODULI

Backcalculation of pavement layer moduli is done for two purposes: structural evaluation and rehabilitation design. Several uses of backcalculation results in structural evaluation were described in Chapter Three. The use of backcalculated pavement and foundation moduli in rehabilitation design (specifically, overlay design) is addressed in Chapter Five. Both of these applications of backcalculation results are demonstrated in the case studies in Chapter Six.

Much of the distress seen in AC/PCC pavements is reflected from deterioration in the underlying PCC slab. The PCC distresses which are most responsible for AC overlay deterioration are slab cracking, punchouts, joint deterioration, localized deterioration resulting from poor durability ("D" cracking and reactive aggregate distress), and deterioration of PCC and AC patches. This deterioration will also reflect through a second AC overlay unless it is identified and repaired. This requires a coordinated effort of distress surveying, nondestructive deflection testing (NDT), and coring for materials samples. The information obtained is valuable in establishing a profile of condition along the length of the project, which may be used to identify areas requiring specific repair and to determine second rehabilitation options.

Analysis of deflections measured at locations where the underlying PCC is severely deteriorated, as in the case of "D" cracking, will produce low backcalculated *in situ* PCC modulus values. These low modulus values should not be interpreted as the true stress/strain response of the PCC as a homogeneous elastic layer, but rather as an indication of the extent to which its behavior departs from that of a sound slab, i.e., the extent of the PCC's deterioration. The ability to diagnose the condition of the PCC from analysis of deflection measurements is particularly valuable in evaluation of AC/PCC pavements, since the extent of the deterioration of the PCC is often not fully evident from visible distress. In some cases, the deterioration of the PCC may be so severe and so widespread that the only feasible rehabilitation alternatives are substantial structural improvements such as a very thick AC overlay, an unbonded PCC overlay, or reconstruction. A second AC overlay must be sufficiently thick to reduce stresses and deflections in the PCC slab to low levels.

Structural evaluation using NDT data is perhaps more difficult for AC/PCC pavements than for all other pavement types. The available computer programs for backcalculation of pavement layer moduli possess a variety of theoretical and practical limitations which hinder their usefulness in AC/PCC pavement analysis. Valid and repeatable results are typically only obtained from even the best of these tools by very knowledgeable pavement engineers with considerable experience in backcalculation.

Previous research [64, 65] has demonstrated that a closed-form solution exists for backcalculation of PCC and subgrade moduli for slab-on-grade systems. One of the advantages of this direct approach to determination of pavement layer properties is its efficiency in processing deflection data. However, the direct approach has been applied only to pavement structures with PCC surfaces. This approach is not directly applicable to analysis of AC-overlaid PCC pavements, unless the influence of the AC overlay can be accounted for in interpretation of deflection basins. The adaptations to the closed-form approach which are required in order to apply it to backcalculation of AC/PCC pavement layer moduli are described in this chapter.

4.1 LIMITATIONS OF AVAILABLE BACKCALCULATION TOOLS

Most of the tools currently used for backcalculation of pavement moduli are computer programs based on multilayer elastic theory. These programs determine the *in situ* elastic moduli of pavement layers by matching deflection basin measurements to deflections predicted by multilayer elastic theory, given the layer thicknesses and Poisson's ratios and the magnitude and area of the applied load. A few backcalculation programs exist which utilize the equivalent thickness concept, i.e., reduction of a multilayer elastic system to an equivalent system of fewer layers for which a solution is more easily obtainable. Backcalculation may also be done using plate theory, i.e., two-layer elastic theory for the special case of an upper layer which exhibits pure bending (without transverse shear deformation) in response to load. The use of plate theory permits the characterization of the subgrade as either a dense liquid or as an elastic solid.

In backcalculation programs based on multilayer elastic theory, actual deflections are matched to predicted deflections in one of two ways: by iterative numerical integration of elastic layer equations, or by searching a database of deflection basins which have been generated for ranges of layer thicknesses and moduli. Backcalculation by the equivalent thickness method may

also be done by iteration or by database search. Graphical procedures were used in the first backcalculation methods based on plate theory, but direct solutions may also be obtained from closed-form equations.

4.1.1 Iterative Backcalculation Programs

BISDEF [66], CHEVDEF [67], WESDEF [68], and ELSDEF are examples of iterative backcalculation programs which make repetitive calls to an elastic layer analysis subroutine (e.g., BISAR [69] for BISDEF) in order to match measured deflections to deflections predicted for program-selected layer moduli. The process stops when the measured and predicted deflections match within tolerance levels set by the user, or when the maximum number of iterations set by the user is reached. A detailed description of the solution algorithm used in these programs is given by Anderson. [70]

One limitation of iterative elastic layer backcalculation programs is that they require the user to enter starting values and ranges for the layer moduli. Unless appropriate starting values are selected, the program may never converge to a solution within the selected ranges. Some researchers have noted that there is no unique solution to the set of moduli which will produce a given deflection basin. Rather, there are as many solutions as there are layers in the pavement structure. [71, 72, 73] As a result, the solution toward which the program converges depends on the initial or "seed" modulus values selected. The boundary values must also be selected judiciously. Limits which are too narrow may prevent the program from converging to the correct solution. Limits which are too broad may allow the program to converge to an incorrect solution, particularly if inappropriate seed moduli are selected. Success with these programs thus requires not only a good knowledge of pavements and materials but also experience in backcalculation for the specific pavement type in question. It has even been suggested that iterative elastic layer backcalculation can never be truly automated until an expert system is developed to guide decisions such as selection of seed moduli. [71, 74] A second limitation of iterative elastic layer backcalculation is that it is time-consuming, increasingly so for increasing number of layers. Convergence to a solution may require several iterations for a pavement system of three or more layers.

In general, the iterative elastic layer backcalculation programs available do not perform well in analyzing AC/PCC pavements, for both of the reasons cited above. Frequently they are unable to match predicted and actual deflection basins well even when given carefully selected ranges of moduli and permitted to run several iterations. Their tendency is to underpredict the modulus of the AC surface, often going to the lower limit of the AC modulus range allowed by the user, and consequently overpredicting the modulus of the PCC slab. As a result, it is necessary to confine the AC modulus to a narrow range bracketing an appropriate value (determined by independent means, e.g., as a function of AC mix temperature), in order to obtain meaningful backcalculated modulus values for the PCC layer. The long execution time required for backcalculation of AC/PCC pavement layer moduli is also a significant limitation. Analysis of several dozen AC/PCC pavement deflection basins, such as might be measured on a highway section a few miles in length, may require several hours of program execution time even on a high-end personal computer. A considerable amount of additional time is required to code the input so that the program will execute successfully.

BOUSDEF [75] is an iterative backcalculation program similar to BISDEF, except that deflections for trial layer moduli combinations are computed not by an elastic layer subroutine but rather an equivalent thickness subroutine. This dramatically reduces execution time, which is BOUSDEF's major advantage over the BISDEF class of programs. However, the appropriateness of BOUSDEF for backcalculation of AC/PCC pavement layer moduli is questionable, owing to material behavior limitations which are inherent in the assumptions of the equivalent thickness method. These include the assumption that the pavement layers above the subgrade exhibit pure bending behavior, the assumption that all layers are fully bonded at their interfaces, the assumption that the layer moduli decrease with depth, and the assumption that the equivalent thickness of any layer (with respect to the layer below) is larger than the radius of the applied load.

4.1.2 Database Backcalculation Programs

Database backcalculation programs run much more quickly than iterative programs, but require a large amount of computer storage. Furthermore, a database backcalculation program can only be applied to situations comparable to those for which the database was generated, i.e.,

number of layers, material types, ranges of thicknesses and elastic moduli, interface bonding conditions, magnitude and geometry of loading, and number and spacing of sensors.

Of the backcalculation programs currently available, the database program COMDEF [76] is the only one developed specifically for AC/PCC pavements. COMDEF's database of deflection basins contains the results of more than 40,000 elastic layer program (BISAR) runs. As a result, the complete COMDEF database occupies more than 4 Megabytes of hard disk space on a personal computer. It is possible to load portions of the database corresponding to the specific cross-sections of interest to conserve hard disk space. A second and more serious limitation of COMDEF is that it requires deflections for 7 sensors at 12-inch spacings; it cannot accommodate fewer sensors or other spacings. COMDEF does not permit the user to choose whether to model the AC/PCC interface condition as bonded or unbonded, and the program's documentation does not indicate which interface condition (presumably bonded) was used in the development of the database.

MODULUS [77] is a database backcalculation program in which the deflection basin database is produced by a factorial of elastic layer program (CHEVRON) runs. MODULUS was developed for analysis of flexible pavements, but may be used to analyze AC/PCC pavements if a database of deflection basins is generated for the specific AC/PCC pavement cross-section to be analyzed. This process may take between 15 minutes and an hour depending on the complexity of the pavement structure and the capabilities of the computer used, and must be repeated for every cross-section of interest. At least 1 Megabyte of hard disk space must be available to store the generated database. Once the database is generated, analysis of deflection data proceeds fairly quickly.

4.1.3 Closed-Form Backcalculation

ILLI-BACK [65] is a backcalculation program based on closed-form solution of plate theory equations, intended for use in analysis of bare PCC pavements. ILLI-BACK executes more quickly than any other available backcalculation program, and could conceivably be used for real-time analysis of deflection data in the field. Another advantage of ILLI-BACK is that it determines a modulus of subgrade reaction (k-value, psi/inch) as well as an elastic modulus for the subgrade. Using the dense liquid (k-value) subgrade characterization, stresses at the slab

edge can be calculated for use in structural evaluation and rehabilitation design. However, the current version of ILLI-BACK can only be used for bare PCC pavements. Thus, ILLI-BACK is not an appropriate tool for analysis of AC/PCC pavements, since modelling the AC as a plate fails to account for the significant compression which occurs in an AC overlay of a PCC slab. Nonetheless, for the purposes of AC/PCC pavement backcalculation, the efficiency and repeatability of the closed-form approach make it the most appealing of the available backcalculation schemes, if it can be modified to account for the behavior of the AC surface.

4.2 CLOSED-FORM BACKCALCULATION FOR BARE PCC PAVEMENTS

A simple two-parameter approach to backcalculation of surface and foundation moduli for a two-layer pavement system was proposed by Hoffman and Thompson in 1981 for flexible pavements. [78] They proposed that the deflection basin could be characterized by its AREA as defined by the following equation:

$$AREA = 6 * \left[1 + 2\left(\frac{d_{12}}{d_0} \right) + 2\left(\frac{d_{24}}{d_0} \right) + \left(\frac{d_{36}}{d_0} \right) \right] \qquad 4.1$$

where d_0 = maximum deflection at the center of the load plate, inches

d_i = deflections at 12, 24, and 36 inches from plate center, inches

AREA has units of length, rather than area, since each of the deflections is normalized with respect to d_0 in order to remove the effect of different load levels and to restrict the range of values obtained. AREA and d_0 are thus independent parameters, from which the surface and foundation moduli in a two-layer pavement system may be determined. Hoffman and Thompson developed a nomograph for backcalculation of flexible pavement surface and subgrade moduli from d_0, AREA, and the pavement thickness. AREA may be defined for more sensors or other sensor spacings if desired. The term "AREA" as used here refers to AREA for four sensors at 12-inch spacing, according to Equation 4.1.

For a bare PCC pavement, the PCC slab's *in situ* elastic modulus (E_{pcc}) and the *in situ* subgrade k-value or elastic modulus (E_s) may be backcalculated from the maximum deflection d_0, the AREA of the deflection basin, and the slab thickness. A graphical approach for doing

this was developed by ERES Consultants in 1982. [79] The ILLI-SLAB finite element program was used to compute a matrix of deflection basins by varying the slab E and subgrade k for a given slab thickness. Intersecting k and E_{pcc} curves were plotted against AREA and d_0 axes, and the k and E_{pcc} for any deflection basin could then be interpolated by plotting its AREA and d_0 on the graph. In 1985, Foxworthy [49] improved the efficiency of this procedure by computerizing the interpolation process using a vectoring scheme. However, several ILLI-SLAB runs were still necessary to produce the matrix of k and E values for any given slab thickness.

Further investigation of this concept by Ioannides [64], and Ioannides, Barenberg, and Lary [65] has produced a closed-form solution procedure to replace the iterative and graphical procedures used previously, as well as the computer program ILLI-BACK for rapid analysis of deflection data for slab-on-grade pavement systems.

4.2.1 AREA versus ℓ

Research by Ioannides [64] has demonstrated that for a given load radius and sensor arrangement, a unique relationship exists between AREA and the dense liquid radius of relative stiffness of the pavement system, in which the subgrade is characterized by a k-value [80]:

$$\ell_k = \sqrt[4]{\frac{E_{pcc}\, D_{pcc}^{3}}{12\,(1 - \mu_{pcc}^{2})\, k}} \qquad 4.2$$

where ℓ_k = dense liquid radius of relative stiffness, inches
E_{pcc} = PCC elastic modulus, psi
D_{pcc} = PCC thickness, inches
μ_{pcc} = PCC Poisson's ratio
k = modulus of subgrade reaction, psi/inch

A different unique relationship exists between AREA and the elastic solid radius of relative stiffness of the pavement, in which the subgrade is characterized by an elastic modulus and a Poisson's ratio [81]:

$$\ell_e = \sqrt[3]{\frac{E_{pcc} D_{pcc}^3 (1 - \mu_s^2)}{6 (1 - \mu_{pcc}^2) E_s}} \quad 4.3$$

where ℓ_e = elastic solid radius of relative stiffness, inches

μ_s = subgrade Poisson's ratio

E_s = subgrade elastic modulus, psi

However, no equations for AREA versus ℓ_k or ℓ_e are provided in References 64 or 65. Therefore, equations for AREA versus ℓ were derived in this study, using the equations developed by Westergaard [80], Losberg [81], and Ioannides [64] for deflection of a plate on a dense liquid or elastic solid foundation at any distance from an applied load.

4.2.1.1 AREA versus ℓ_k

The equations for deflection of a PCC slab on a dense liquid foundation load are given by Losberg [81]:

If $0 < s < a/\ell_k$:

$$w(s) = \frac{P}{\pi \left(\frac{a}{\ell_k}\right)^2} \frac{\ell_k^2}{D} (1 - c_1 \, ber\, s - c_2 \, bei\, s) \quad 4.4$$

If $s > a/\ell_k$:

$$w(s) = \frac{P}{\pi \left(\frac{a}{\ell_k}\right)^2} \frac{\ell_k^2}{D} (c_3 \, ker\, s + c_4 \, kei\, s) \quad 4.5$$

where w(s) = deflection at s

r = distance from center of applied load

$s = r / \ell_k$

P = load

a = load radius

ber = Kelvin function of order 0, real (derivative is ber′)

bei = Kelvin function of order 0, imaginary (derivative is bei′)

ker = modified Kelvin function of order 0, real (derivative is ker′)

kei = modified Kelvin function of order 0, imaginary (derivative is kei′)

$$D = \frac{E_{pcc} D_{pcc}^{3}}{12 (1 - \mu_{pcc}^{2})} \tag{4.6}$$

Equations for the four constants c_1 through c_4 were developed by Ioannides [64]:

$$c_1 = 1 - \pi \left(\frac{a}{\ell_k}\right)^2 \frac{w_0 D}{P \ell_k^2} \tag{4.7}$$

$$w_0 = \left(\frac{P}{8 k \ell_k^2}\right) \left\{ 1 + \left(\frac{1}{2\pi}\right) \left[ln \left(\frac{a}{2 \ell_k}\right) + \gamma - 1.25 \right] \left(\frac{a}{\ell_k}\right)^2 \right\} \tag{4.8}$$

$$c_2 = \frac{\left(\frac{a}{\ell_k}\right)^2}{2} \left[\ln \left(\frac{2 \ell_k}{a}\right) + 0.5 - \gamma + \left(\frac{a}{\ell_k}\right)^2 \left(\frac{2\pi}{64}\right) \right] \tag{4.9}$$

γ = Euler's constant, 0.57721566490

$$c_3 = A - B\,c_4 \tag{4.10}$$

$$A = \frac{1 - c_1\, ber\left(\frac{a}{\ell_k}\right) - c_2\, bei\left(\frac{a}{\ell_k}\right)}{ker\left(\frac{a}{\ell_k}\right)} \tag{4.11}$$

$$B = \frac{kei\left(\frac{a}{\ell_k}\right)}{ker\left(\frac{a}{\ell_k}\right)} \tag{4.12}$$

$$c_4 = \frac{F - G\,A}{1 - G\,B} \tag{4.13}$$

$$F = \frac{-c_1\, ber'\left(\frac{a}{\ell_k}\right) - c_2\, bei'\left(\frac{a}{\ell_k}\right)}{kei'\left(\frac{a}{\ell_k}\right)} \tag{4.14}$$

$$G = \frac{ker'\left(\frac{a}{\ell_k}\right)}{kei'\left(\frac{a}{\ell_k}\right)} \tag{4.15}$$

These equations were solved for radial distances of 0, 12, 24, and 36 inches and for ℓ_k values from 15 to 80 using the IMSL [82, 83] library of functions available on the Apollo network of UNIX workstations at the University of Illinois. The deflections computed were used to obtain AREAs corresponding to each value of ℓ_k. The results are illustrated by the curve labelled "dense liquid" in Figure 4.1.

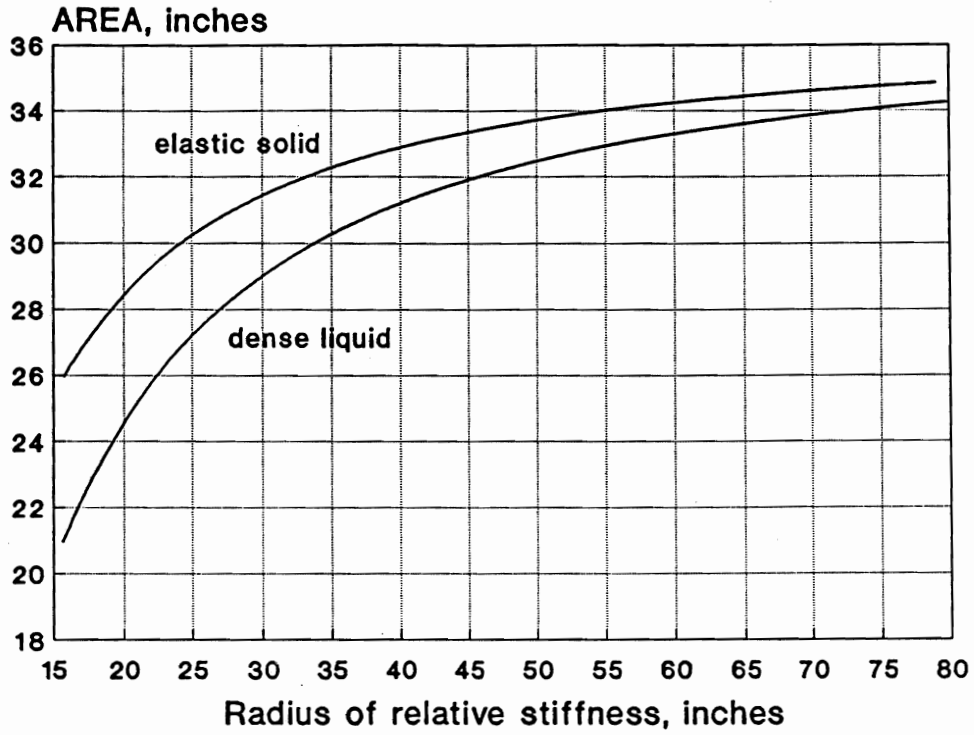

Figure 4.1 Deflection AREA versus radius of relative stiffness.

Since the curve asymptotically approaches an AREA value of 36 inches, an appropriate and meaningful equation form for modelling the relationship of AREA to ℓ is that of an asymptotic regression model, also called a monomolecular growth model. [84] Such a model has the following general form:

$$AREA = k_1 - k_2 e^{-k_3 \ell^{k_4}} \qquad 4.16$$

where k_1 is the asymptotic AREA value, k_2 is a parameter for the range of ℓ values, and k_3 and k_4 are scale parameters which govern the rate of growth. To predict ℓ as a function of AREA, the model may be rearranged to yield the following general form:

$$\ell = \left[\frac{\ln\left(\frac{k_1 - AREA}{k_2}\right)}{-k_3}\right]^{\frac{1}{k_4}} \qquad 4.17$$

The SAS statistical analysis software [33] was used to determine the parameters for each model by nonlinear regression. The model obtained for ℓ_k versus AREA is given by Equation 4.18. The fit of the model to the data is excellent, as illustrated by Figure 4.2. Values obtained from ILLI-BACK runs are also shown for comparison.

$$\ell_k = \left[\frac{\ln\left(\frac{36 - AREA}{1812.279133}\right)}{-2.559340}\right]^{4.387009} \qquad 4.18$$

R^2 = 99.99 percent (predicted versus actual values)

σ_Y = 0.097 inches (standard error of the estimate)

n = 63

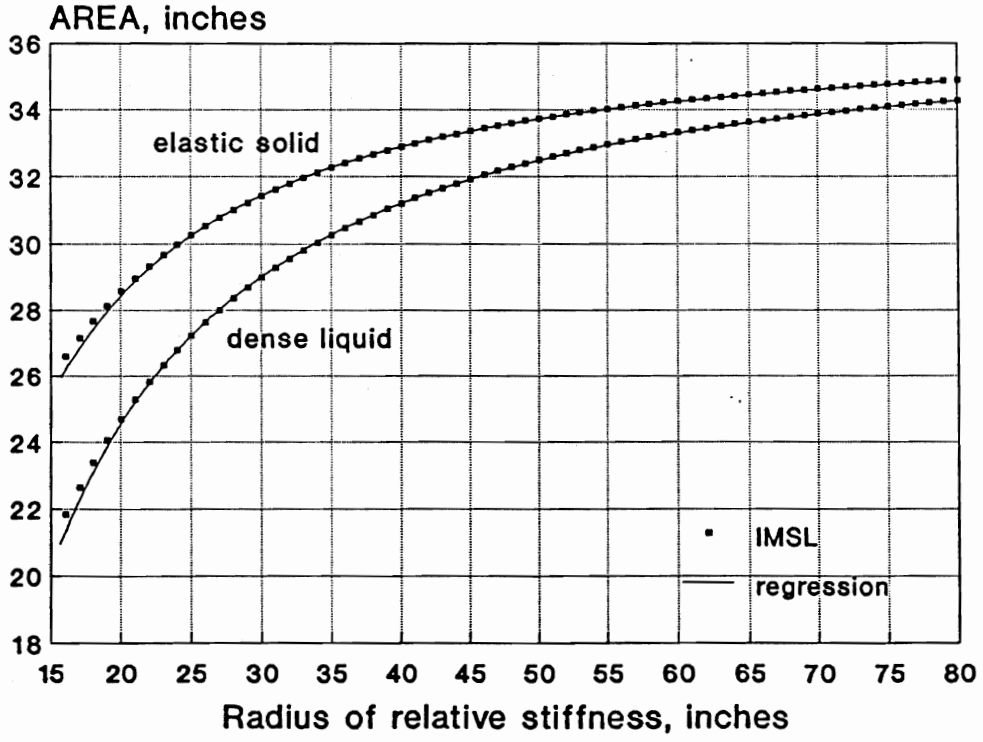

Figure 4.2 Comparison of AREA versus ℓ values and regression models.

4.2.1.2 AREA versus ℓ_e

For a PCC slab on an elastic solid foundation, the deflection at any distance from the applied load is given by the following equation from Losberg [81]:

$$w(r) = \frac{2\,P}{\pi\,a\,C}\int_0^{\infty}\frac{J_0\,(\alpha r)\,J_1(\alpha a)}{\alpha\,(1+\alpha^3\,\ell_e^3)}\,d\alpha \qquad 4.19$$

$$C = \frac{E_s}{(1-\mu_s^2)} \qquad 4.20$$

This integral was solved for radial distances of 0, 12, 24, and 36 inches and for ℓ_e values from 15 to 80 using the IMSL [82, 83] library on the Apollo network. The deflections computed were used to obtain an AREA corresponding to each value of ℓ_e. The results are illustrated by the curve labelled "elastic solid" in Figure 4.1.

The model obtained for ℓ_e versus AREA is given by Equation 4.21. The fit of the model to the data is excellent, as illustrated by Figure 4.2. Values obtained from ILLI-BACK runs are also shown for comparison.

$$\ell_e = \left[\frac{ln\left(\frac{36-AREA}{4521.676303}\right)}{-3.645555}\right]^{5.334281} \qquad 4.21$$

Residual R^2 = 99.99 percent

σ_Y = 0.118 inches

n = 83

4.2.2 Backcalculation of Subgrade k or E_s

With AREA calculated from measured deflections, ℓ_k or ℓ_e may be obtained from Equation 4.18 or 4.21. The k-value may be obtained by rearrangement of Westergaard's interior deflection equation [65, 80].

$$k = \left(\frac{P}{8\, d_0\, \ell_k^{\,2}}\right)\left\{1 + \left(\frac{1}{2\,\pi}\right)\left[ln\left(\frac{a}{2\,\ell_k}\right) + \gamma - 1.25\right]\left(\frac{a}{\ell_k}\right)^2\right\} \qquad 4.22$$

Figure 4.3 was developed from Equations 4.18 and 4.22 for load P = 9000 pounds and load radius a = 5.9055 inches. For loads within about 2000 pounds of this value, the deflections d_0, d_{12}, d_{24}, and d_{36} may be scaled linearly to 9000-pound deflections.

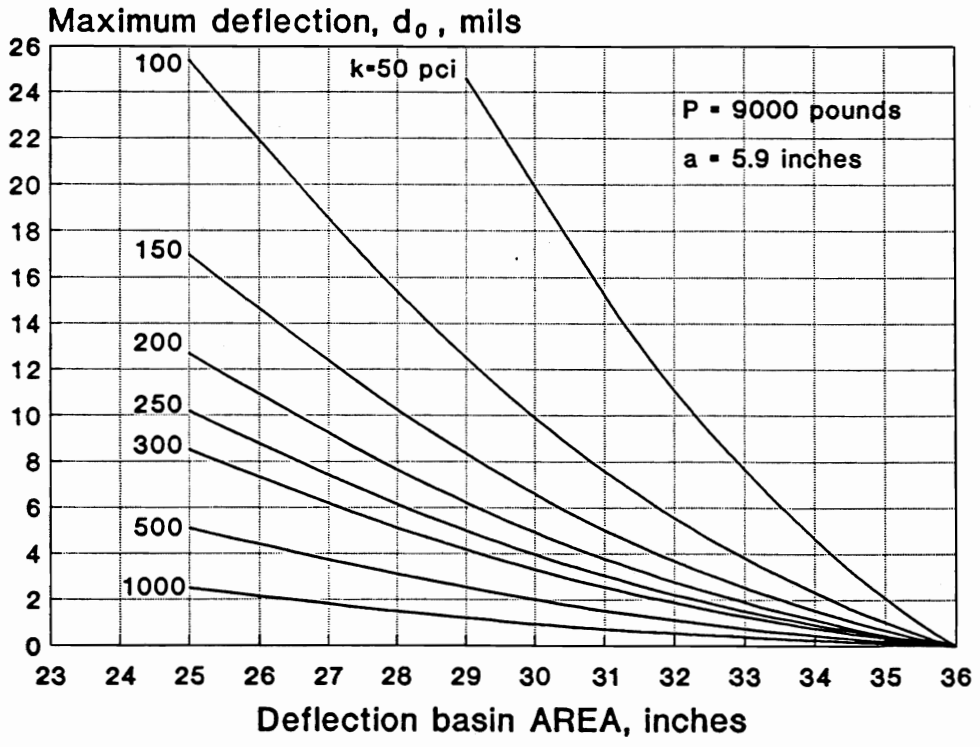

Figure 4.3 Determination of k-value from d_0 and AREA.

The elastic modulus of the subgrade E_s may be obtained by rearrangement of Losberg's deflection equation [81]:

$$E_s = \left[\frac{2\,P\,(1-\mu_s^2)}{d_0\,\ell_e}\right]\left[0.19245 - 0.0272\left(\frac{a}{\ell_e}\right)^2 + 0.0199\left(\frac{a}{\ell_e}\right)^2 ln\left(\frac{a}{\ell_e}\right)\right] \qquad 4.23$$

Figure 4.4 was developed from Equations 4.21 and 4.23 for load P = 9000 pounds, load radius a = 5.9055 inches, and subgrade Poisson's ratio μ_s = 0.50. Again, for loads within about 2000 pounds of this value, the deflections d_0, d_{12}, d_{24}, and d_{36} may be scaled linearly to 9000-pound deflections.

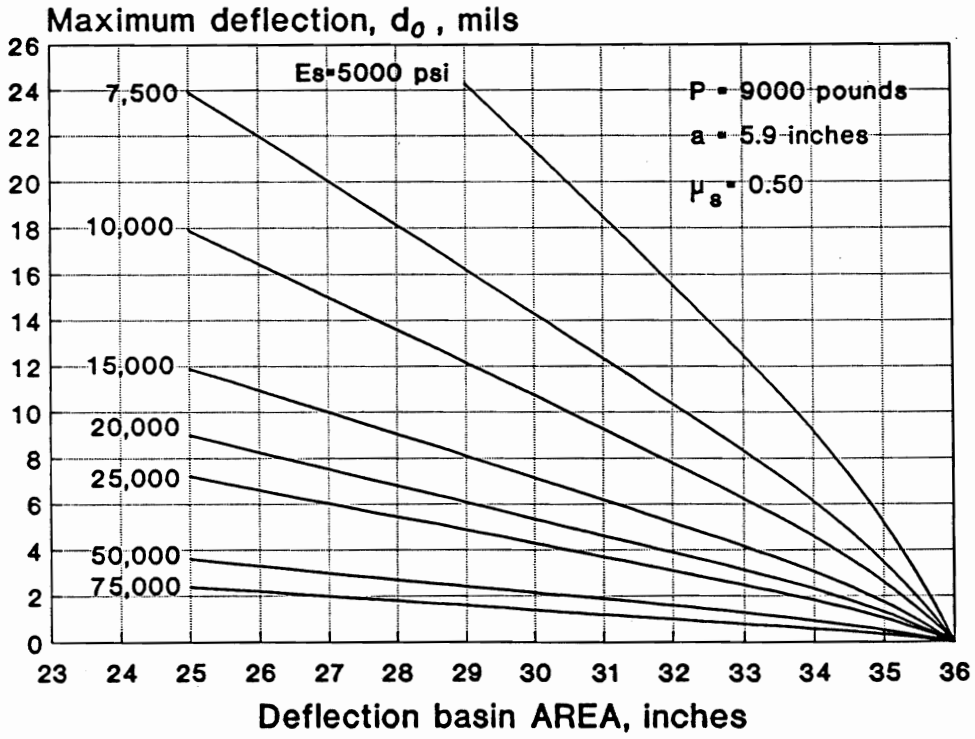

Figure 4.4 Determination of E_s from d_0 and AREA.

4.2.3 PCC Elastic Modulus

The elastic modulus of the PCC slab may be determined using the appropriate (dense liquid or elastic solid) definition of the radius of relative stiffness. Figure 4.5 was developed from Equations 4.2 and 4.18, assuming a PCC Poisson's ratio μ_{pcc} = 0.15 and load radius a = 5.9055 inches. Figure 4.6 was developed from Equations 4.3 and 4.21, assuming μ_{pcc} = 0.15, μ_s = 0.50, and a = 5.9055 inches. For either support characterization, the PCC elastic modulus E_{pcc} may be determined for a known value of slab thickness, D_{pcc}.

4.3 BACKCALCULATION FOR AC/PCC PAVEMENTS

In order to apply this closed-form backcalculation approach to AC/PCC pavements, deflections measured on the existing AC surface must be adjusted to account for the influence of the AC layer. The steps for doing this are described in this section.

4.3.1 AC Elastic Modulus

An existing AC/PCC pavement cannot be properly modelled as a slab on grade, since the AC overlay exhibits not only bending but also significant compression. To determine the amount of compression that occurs in the AC overlay, the elastic modulus of the AC layer must be determined. The recommended method for determining E_{ac} is to monitor the temperature of the AC mix during deflection testing, conduct diametral resilient modulus tests on cores obtained from the AC surface, and to establish a relationship between E_{ac} and temperature for use in assigning a modulus value to each deflection basin.

The AC mix temperature may be measured directly during deflection testing, as described in Chapter Three. If measured AC mix temperatures are not available, they may be approximately estimated from pavement surface and air temperatures using procedures developed by Southgate [85], Shell [86], the Asphalt Institute [87], or Hoffman and Thompson [78]. Pavement surface temperature may be monitored during deflection testing using a hand-held infrared sensing device which is aimed at the pavement. The mean air temperature for the five days prior to deflection testing, which is an input to some of the referenced methods for estimating mix temperature, may be obtained from a local weather station or other local sources.

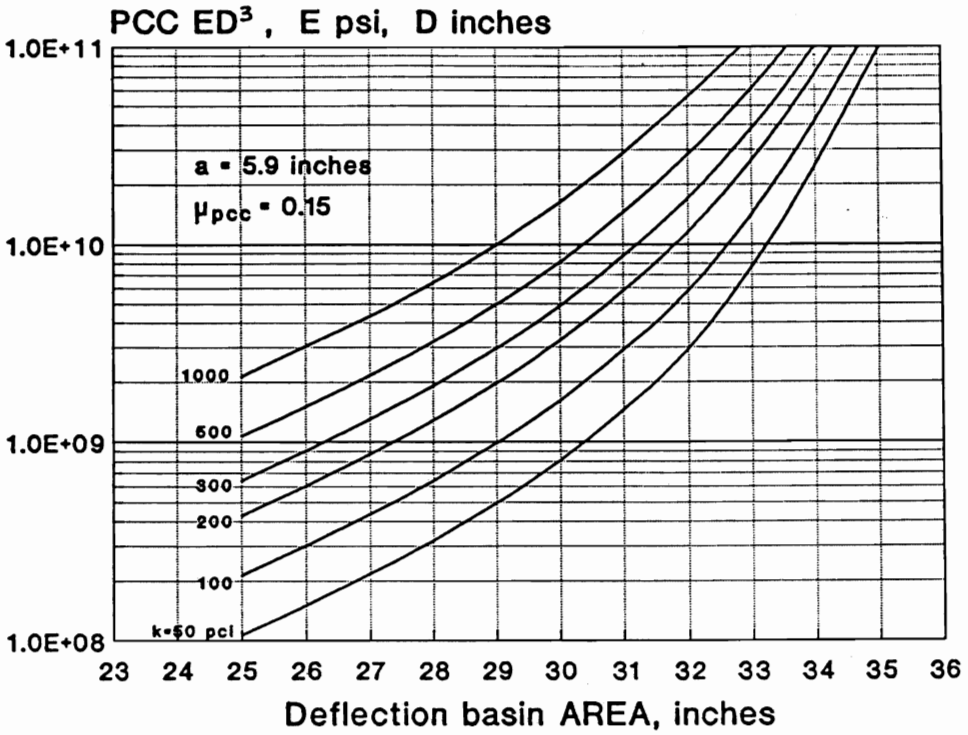

Figure 4.5 Determination of E_{pcc} from k-value, AREA, and slab thickness.

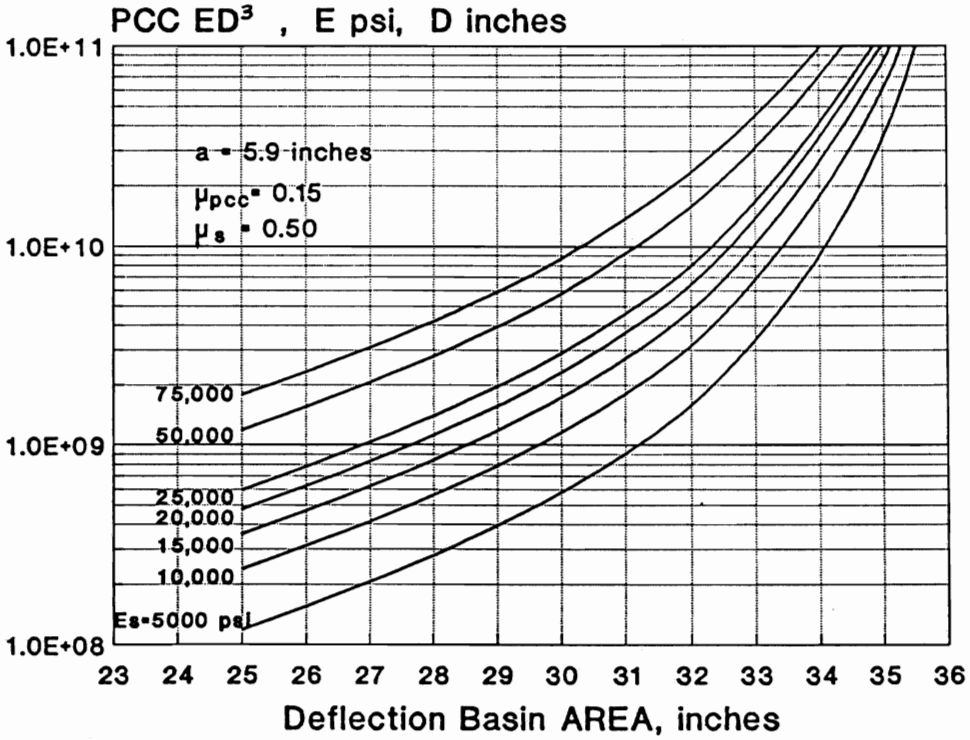

Figure 4.6 Determination of E_{pcc} from E_s, AREA, and slab thickness.

C.3 ILLI-SLAB程式之使用手冊

APPENDIX 1

INPUT GUIDE FOR ILLI-SLAB

(REVISED VERSION: MARCH 15, 1989)

ILLI-SLAB can be used to calculate deflections and stresses in jointed slab-on-grade pavements, with or without load transfer systems. The program can also accommodate a stabilized base or an overlay by assuming either perfect bond or no bond between the two layers.

The pavement system can consist of any number of slabs. The program is currently dimensioned to accept up to 10 slabs along each of the x- and y-axes. Elements and nodes are numbered consecutively from bottom to top along the y-axis, and from left to right along the x-axis. Joints are treated as rectangular elements having zero width.

The wheel loads may be applied to any of the slabs, and stresses and deflections at all nodes in the slab, stresses in the stabilized base or overlay, vertical stresses in the subgrade, and loads transferred by dowel bars or aggregate interlock are computed.

The program incorporates the two-parameter (VLASOV) and the elastic solid (BOUSSINESQ) subgrade models (IST=9 and IST=8, respectively), in addition to the more conventional WINKLER (IST=6) and SPRINGS (IST=7) idealization. When IST=8, only one slab is allowed. This slab must have a constant thickness and elastic modulus and must consist of only one layer. The symmetry capability is now operable with all options. The LINPACK routines, used with the BOUSSINESQ subgrade option, were developed at Argonne National Laboratories, and should be acknowledged as such in any resulting publications. The RESILIENT and VLASOV

subgrade options are intended for research purposes only. The relevant literature must be consulted before using these.

Versions after June 15, 1987 allow the computation of deflections and stresses due to a temperature gradient across the thickness of the slab. Wheel loads and gaps underneath the slab can also be accommodated when this option is used. Cards No. 3, No. 13, No. 32, No. 33 and No. 34 contain the pertinent inputs if deflections and stresses due to a temperature gradient and gaps are to be computed. In such cases, single slabs can be analyzed using the SPRINGS, WINKLER or BOUSSINESQ subgrade, while multiple slab systems can be analyzed using the SPRINGS or WINKLER subgrade models only. In this case dowel bars and/or aggregate interlock can be used as load transfer mechanisms. The self-weight of the slab should be taken into account in curling analysis (see Card No. 13). The subgrade modulus may vary at the nodes (see Cards No. 19 and 20).

When dowels are specified, loads may be transferred by shear, torsion or moment, or any combination of these. The default load transfer mechanism is by shear and moment. Dowel spacing need not be uniform and dowel bars may be specified at any node along an edge. For this purpose, Cards No. 9, No. 10, No. 22, No. 23, No. 26 and No. 27 need to be provided.

ILLI-SLAB can be used with any consistent system of units. The notation for the various fundamental quantities used in this write-up is:

Length	[L]
Force	[F]
Temperature	[Θ]

For example, using the American system of units the unit of length is the *inch* (in.), the unit of force is the *pound* (lb) and the unit of temperature is the degree Fahrenheit (°F).

The current version (March 15, 1989) accepts fixed-form input only, which is described below. It is implemented on the Apollo Network of the Civil Engineering Department at the University of Illinois. It uses up to 900,000 memory spaces and double precision arithmetic. To change the memory core so that it will fit on any given machine, the user should go into the Main Program and substitute the two occurrences of the number 900,000 by the appropriate word length that can be accommodated.

ILLI-SLAB is not currently available in a micro-computer version.

CARDS FOR FIXED FORM INPUT

FOR ILLI-SLAB

Card No. 1.

IFORM
I1

IFORM: A numeric flag indicating type of input data type used;

= 0, for free-form input;

= 1, for fixed-form input.

Card No. 2.

TITLE
20A4

TITLE : An 80-column label of alphanumeric characters used to identify the problem. This label will appear on the header part of the output.

Card No. 3.

NFOR	ISYM	ITEMP	IWESL
4I5			

NFOR: Number of loaded areas.

ISYM : Numeric flag indicating whether symmetry lines are used;

= 0, if no symmetry lines are used;

= 1, if x-axis is a line of symmetry;

= 2, if y-axis is a line of symmetry;

= 3, if x-axis and y-axis are lines of symmetry;

ITEMP : Numeric flag indicating whether temperature differentials or gaps exist;

= 0, if no temperature differentials nor gaps exist;

= 1, if otherwise.

IWESL : Numeric flag indicating whether the WESLIQID model is to be used in curling analysis (for single-slab, single-layer systems only).

=1, if the WESLIQID model will be used,

=0, if not.

Card No. 4.

NNODX(I), I= 1, MAXSLXY

10I5

NNODX(I): Number of nodes in slab(s), along the x-axis (MAXSLXY is set to 10; to change, alter the size of arrays NNODX and NNODY).

Card No. 5.

NNODY(I), I= 1, MAXSLXY

10I5

NNODY(I): Number of nodes in slab(s), along the y-axis (MAXSLXY is set to 10; to change, alter the size of arrays NNODX and NNODY).

Card No. 6.

NLAYER	COMP	CK	E0	PR0
I5	I5	F10.3	F10.3	F10.3

NLAYER: Number of layers above subgrade: 1 or 2.

COMP : Composite action factor;

= 0, for unbonded layers;

= 1, for fully bonded layers.

CK : Modulus of subgrade reaction, [FL^{-3}], if uniform;

= 0.0. if not uniform (see Card No. 19);

= -1.0, if elastic solid subgrade is used (IST=8).

E0 : Elastic Modulus of subgrade, [FL^{-2}] (leave blank if elastic solid subgrade is not used);

= GM, the Vlasov shear parameter when IST=9.

PR0 : Poisson's Ratio of subgrade (leave blank if elastic solid subgrade not used).

Card No. 7.

IST	ITMAX	TOL1	TOL2	IOT
I5	I5	F5.3	F5.3	I5

IST : A numeric flag for subgrade type:

= 0, if subgrade type varies (See Card No. 30);

= 1, for VERY SOFT subgrade;

= 2, for SOFT subgrade;

= 3, for MEDIUM subgrade;

= 4, for STIFF subgrade;

= 5, for OTHER subgrade (see Card No. 31);

= 6, for WINKLER energy consistent, uniform subgrade;

= 7, for SPRINGS subgrade;

= 8, for BOUSSINESQ subgrade;

= 9, for VLASOV subgrade.

Note that options IST = 1, 2, 3 and 4 are only operable using American units (i.e. lbs and in.). For these, recommended values for KR in first iteration are as follows:

VERY SOFT : KR = 300 psi/in.
SOFT : KR = 425 psi/in.
MEDIUM : KR = 725 psi/in.
STIFF : KR = 1000 psi/in.

ITMAX : Maximum number of iterations desired.

TOL1 : Tolerance for KR (Recommended value= 0.05, ie. 5%).

TOL2 : Tolerance for points exceeding TOL1 (Recommended value = 0.05, i.e. 5%).

IOT : Numeric flag for output type:

= 0, for partial output during intermediate iterations;

= 1, for full output during intermediate iterations.

Note: A new iteration is performed if the ratio of the number of nodes at which the updated KR is more than TOL1 (%) off the previous KR, to the total number of nodes, exceeds TOL2 (%).

Card No. 8.

ICON(I), I=1, 6	ISTEP
6I1	I4

ICON(I) = A numeric flag indicating which contour plots, if any, are desired:

ICON(1) = 1, if contours of deflection are wanted;
= 0, if not.

ICON(2) = 1, if contours of subgrade stress are wanted;
= 0, if not.

ICON(3) = 1, if contours of x-stress at bottom of Layer 1 are wanted;
= 0, if not.

ICON(4) = 1, if contours of y-stress at bottom of Layer 1 are wanted;
= 0, if not.

ICON(5) = 1, if contours of x-stress at bottom of Layer 2 are wanted;
= 0, if not.

ICON(6) = 1, if contours of y-stress at bottom of Layer 2 are wanted;
= 0, if not.

NB: ICON(5) and ICON(6) must be set to 0, if NLAYER=1 (see Card No. 6).

ISTEP : An integer specifying the density of the Virtual Grid in the contouring routines. The value of 40 produces pleasing contours. For coarser but quicker lower the value. For smoother but longer time raise the value. ISTEP should be less than 200.

Card No. 9 (Read only if there are more than one slabs along x-axis).

LTDX IBARXT IBARXS IBARXM

4I5

LTDX : Type of load transfer in x-direction;

= 0, if aggregate interlock;

= 1, if dowel bars;

= 2, if a combination of dowel bars and aggregate interlock.

IBARXT : Numeric flag for torsion on the dowel bars in x-direction;

= 0, if torsion is not to be considered (default);

= 1, if torsion is to be considered.

IBARXS : Numeric flag for shear on the dowel bars in x-direction;

= 0, if shear is not to be considered;

= 1, if shear is to be considered (default).

IBARXM: Numeric flag for moment on the dowel bars in x-direction;

= 0, if moment is not to be considered;

= 1, if moment is to be considered (default).

Card No. 10 (Read only if there are more than one slabs along y-axis).

LTDY IBARYT IBARYS IBARYM

4I5

See Card No. 9 for notations.

Card No. 11 (Use as many as needed).

XC(I), I=1, number of nodes along x-axis

8F10.3

XC(I) : x-coordinate of nodes along x-axis (read in ascending order), [L].

Card No. 12 (Use as many as needed).

YC(I), I=1,number of nodes along y-axis

8F10.3

YC(I) : y-coordinate of nodes along y-axis (read in ascending order), [L].

Card No. 13.

CT1	CE1	V(1)	CC1	DT1	ALPHA1
F10.3	E10.3	F10.3	F10.3	F10.3	E10.3

CT1 : Top layer thickness, if uniform, [L];
= 0.0, if not (see Card No. 14).

CE1 : Modulus of Elasticity for top layer, if uniform, $[FL^{-2}]$;
= 0.0, if not (see Card No. 15).

V(1) : Poisson's ratio of top layer.

CC1 : Unit weight of the top layer of the slab, $[FL^{-3}]$.

DT1 : Difference in temperature, $[\Theta]$ between the top and bottom surfaces of layer 1.

ALPHA1: Coefficient of thermal expansion for layer 1, $[LL^{-1}\Theta^{-1}]$.

Card No. 14 (Read only if CT1=0.0 in Card No. 13; use as many as needed).

T1(I), I=1, number of nodes
8F10.3

T1(I) : Thickness of the top layer at node I, [L].

Card No. 15 (Read only if CE1=0.0 in Card No. 13; use as many as needed).

E1(I), I=1, number of nodes
8F10.3

E1(I) : Modulus of Elasticity of the top layer at node I, [FL^{-2}].

Card No. 16 (Read only if NLAYER=2 in Card No. 6).

CT2	CE2	V(2)	CC2	DT2	ALPHA2
F10.3	E10.3	F10.3	F10.3	F10.3	E10.3

CT2 : Bottom layer thickness, if uniform, [L];
= 0.0, if not (see Card No. 17).

CE2 : Modulus of Elasticity for bottom layer, if uniform, [FL^{-2}];
= 0.0, if not (see Card No. 18)

V(2) : Poisson's ratio of bottom layer.

CC2 : Unit weight of the top layer of the slab, [FL^{-3}].

DT2 : Difference in temperature, [Θ] between the top and bottom surfaces of layer 2.

ALPHA2: Coefficient of thermal expansion for layer 2, [$L L^{-1}\Theta^{-1}$].

Card No. 17 (Read only if CT2=0.0 in Card No. 16; use as many as needed).

T2(I), I=1, number of nodes

8F10.3

T2(I) : Thickness of the bottom layer at node I, [L].

Card No. 18 (Read only if CE2=0.0 in Card No. 16; use as many as needed).

E2(I), I=1, number of nodes

8F10.3

E2(I) : Modulus of Elasticity of the bottom layer at node I, [FL^{-2}].

Card No. 19 (Read only if CK=0.0 in Card No. 6).

CK1 NNU

F10.3 I5

CK1 : Modulus of subgrade reaction for the majority of nodes, [FL^{-3}].

NNU : Number of nodes with different modulus of subgrade reaction.

Card No. 20 (Read only if NNU>0 in Card No. 19).

I, SUB(I), I = 1, NNU

I3 F10.3

I : Node number of node with different subgrade modulus than CK1.

SUB(I) : Modulus of subgrade reaction for node I, [FL^{-3}].

Card No. 21 (Read only if LTDX=1 or 2 in Card No. 9).

DIN	DOUT	DE	DS	DJW	DPR	DCI
F10.3	F10.3	E10.3	F10.3	F10.3	F10.3	E10.3

DIN : Inside diameter of dowel bars, [L];
= 0.0 for solid round bars.

DOUT : Outside diameter of dowel bars, [L].

DE : Modulus of elasticity of dowel bars, [FL^{-2}].

DS : Spacing of dowel bars, [L]. (Set DS=0.0, if spacing is non-uniform; see Card No. 22).

DJW : Joint width, [L].

DPR : Poisson's Ratio of dowel bars.

DCI : Dowel-Concrete Interaction, [FL^{-1}].

DCI for a round steel dowel bar may be determined using Friberg's dowel analysis, or from a relation developed on the basis of three-dimensional finite element results, as follows:

(a) Friberg's Analysis:

DCI={4*BETA**3*ES*I/(2+BETA*DJW)}

where:

BETA =[KD/(4*ES*I)]**0.25, [L^{-1}] ;

ES : Steel modulus of elasticity, [FL^{-2}];

I : Dowel moment of inertia, [L^4];
= {(D/2)**4}*3.14159/4;

K : Modulus of dowel support, [FL^{-3}];

D : Dowel diameter, [L]; and

DJW : Joint width, [L];

(b) Three-dimensional Analysis (valid for American units only):

DCI={E**0.75}/{(0.057-0.010*D)*(0.810+0.013*h)*(1+0.414*DJW)}

where:

E : Concrete modulus of elasticity, psi;

D : Dowel diameter, in.;

h: Slab thickness, in.; and

DJW: Joint width, in.;

Card No. 22 (Read only if DS=0.0 in Card No. 21).

NDNX

I5

NDNX : Number of nodes at which dowels will be explicitly specified, in x-direction.

Card No. 23 (Read only if DS=0.0 in Card No. 21).

NDX(I), I=1, NDNX

16I5

NDX(I): Node number of node at which a dowel is explicitly specified, in x-direction.

Card No. 24 (Read only if LTDX=0 or 2 in Card No. 9).

AGGX

E10.3

AGGX : Aggregate Interlock Factor in x-direction, $[FL^{-2}]$.

(For keyways use a large value, e.g. AGGX=1.0E+08 psi, if American units are used).

Card No. 25 (Read only if LTDY=1 or 2 in Card No. 10).

DIN	DOUT	DE	DS	DJW	DPR	DCI
F10.3	F10.3	E10.3	F10.3	F10.3	F10.3	E10.3

See Card No. 21 for notations.

Card No. 26 (Read only if DS=0.0 in Card No. 25).

NDNY
I5

NDNY : Number of nodes at which dowels will be explicitly specified, in y-direction.

Card No. 27 (Read only if DS=0.0 in Card No. 25).

NDY(I), I=1, NDNY
16I5

NDY(I): Node number of node at which a dowel is explicitly specified.

Card No. 28 (Read only if LTDY=0 or 2 in Card No. 10).

AGGY
E10.3

AGGY : Aggregate Interlock Factor in y-direction, [FL^{-2}].

(For keyways use a large value, e.g. AGGY=1.0E+08 psi, if American units are used).

Card No. 29 (Read NFOR times; see Card No. 3).

PRS	XX1	XX2	YY1	YY2
F10.3	F10.3	F10.3	F10.3	F10.3

PRS : Tire pressure, [FL^{-2}].

XX1, XX2 : Lower and upper limits of the loaded area in x-direction, in global coordinate system, [L].

YY1, YY2 : Lower and upper limits of the loaded area in y-direction, in global coordinate system, [L].

Card No. 30 (Read only if IST=0 in Card No. 7; use as many as needed).

NST(I), I=1, number of nodes
8I5

NST(I) : Subgrade Type (IST) under node I. See Card No. 7 for definition of various subgrade types. IST may take values between 1 and 7, here.

Card No. 31 (Read only if IST=5 in Card No. 7).

A1	A2	A3	A4	A5	DY
6F10.5					

A1, A2, A3, A4, A5, DY : Parameters for the regression equation defining KR as as function of deflection w. General form of the equation:

$KR = \{A1[1-\exp\{-A2(w/DY-A3)\}]+A4(w/DY-A3)+2\}/w$

KR = A5/DY, if w/DY<A3.

where:

w : deflection, [L];

KR : resilient subgrade modulus, [FL^{-3}].

Card No. 32 (Read only if ITEMP=1; see Card No. 3).

NOTC	IGAP	ICYCLE
I5	I5	I5

NOTC : Number of nodes at which reactive pressure is initially set to zero.

IGAP : Number of nodes where gaps exist underneath the slab.

ICYCLE : Maximum number of iterations requested.

Card No. 33 (Read only if NOTC>0 in Card No. 32; use as many as needed).

NODC(I), I=1, NOTC
16I5

NODC(I): Node number of node with zero initial reactive pressure.

Card No. 34 (Read only if IGAP>0 in Card No. 32; use as many as needed).

(NG(I), GAP(NG(I)), I=1, IGAP)
5(I5, F10.3)

NG(I): Node number of node with a gap.

GAP(NG(I)): Amount of gap at node NG(I), [L].

Card No. 35 (Read only if contours are to be plotted).

JCON(I), I=1, 6	RATIO
6I1	F10.7

JCON(I) : A numeric flag indicating over which slabs the contours requested in Card No. 8, are to be plotted (Contours can only be plotted over the first 6 slabs);

JCON(I) = 1, if contours over Slab I are to be plotted;

= 0, if not.

RATIO : A factor by which the y-scale is multiplied;

RATIO=1.0 specifies x- and y-scales are equal.

C.4 對ILLI-SLAB使用者之建議

5.6 RECOMMENDATIONS FOR ILLI-SLAB USERS

The following recommendations for future users of ILLI-SLAB can be formulated as a result of investigations presented in this Chapter:

1. The load(s) must be placed over the finite element mesh with at least one node at the anticipated location of maximum response. For example, in the case of interior loading, a central node must be provided. Otherwise, the results must be carefully interpreted. Any peaks in response missed by the finite element analysis because of node spacing, must be reconstructed;
2. The finest mesh practicable must be used. Accuracy of 99% can be expected if the element size, 2a, is about 0.8 times the thickness of the slab. There is no gain in making the mesh any finer than this, although correct answers will be obtained with finer meshes too. Computer resources are more efficiently utilized if element aspect ratios are improved, as per Recommendation 4, below, instead. A fine zone equal to twice the size of the loaded area(s) is recommended, with progressive decrease in fineness outside this area;

From: Ioannides, A.M., "Analysis of Slab-on-Grade for a Variety of Loading and Support Conditions," Ph.D. Thesis, University of Illinois, Urbana 1984.

3. The convergence characteristics of the work equivalent uniform subgrade `WINKLER' model (option IST=6 in modified ILLI-SLAB) are slightly better than those of the `SPRINGS' option (IST=7 in modified ILLI-SLAB). The latter option should only be used for research purposes;
4. Element aspect ratio should be kept close to unity, particularly in a region around the loaded area(s), extending to three times the radius of the loaded area. Within this region, this recommendation is a requirement. If at all possible, no element aspect ratio should be greater than 4 or 5, anywhere in the mesh.

These recommendations apply to all three fundamental loading conditions, viz. interior, edge and corner loading. Some of the meshes used in this study were designed before these guidelines were established, and illustrate that a compromise is often necessary.

D 剛性鋪面之應力分析

D.1 接縫式混凝土路面(JCP)應力分析

資料來源：

交通部台灣區國道新建工程局，“北二高剛性路面建造講習”，第50-63頁，中華民國七十九年。

D.2 接縫式混凝土鋪面邊界荷重與撓屈應力分析

資料來源：

Lee, Y. H., and M. I. Darter, "Loading and Curling Stress Models for Concrete Pavement Design," Transportation Research Record 1449, Transportation Research Board, National Research Council, Washington, D.C., 1994, pp. 101-113.

D.3 建立鋪面預估模式之新技術

資料來源：

Lee, Y. H., and M. I. Darter, "New Predictive Modeling Techniques for Pavements," Transportation Research Record 1449, Transportation Research Board, National Research Council, Washington, D.C., 1994, pp. 234-245.

D.1 接縫式混凝土路面(JCP)應力分析

7. 接縫式混凝土路面(JCP)應力分析

接縫式混凝土路面分析中，導致路面應力產生之因素如下：

(a)外加荷重

(b)溫度差異

(c)水份變化

(d)不均勻路基支承

上述各因素對路面之反應各有不同之影響，部份影響如圖 7.1 所示。

基於上述各種因素，臨界應力及撓度可能發生於混凝土路面中不同位置。如圖 7.2 所示，臨界應力可能發生於角隅(A)、橫向接縫(A′)或縱向接縫(B)，亦有可能發生於內部(C)。

在本節中，將介紹兩種最常用之應力分析方法。第一種方法主要將混凝土路面考慮爲一無限大之版塊，置於被視爲 Winkler 基礎之路基上，其荷重作用於角隅、邊緣或內部。因溫度差異而產生之翹曲(Warping)應力亦可用同一方法，以無限及有限大之版塊加以分析。 Westergaard ［11 - 13］最先使用此種方法決定波特蘭水泥混凝土之臨界應力，其結果爲 Pickett 及 Ray ［14］所引用而發展出影響圖，且被波特蘭水泥協會 PCA ［15］正式作爲公路及機場路面設計原始版本之依據。

第二種方法爲使用有限元素法，以決定波特蘭水泥混凝土版因荷重及溫差所產生之應力與撓度。此方法中，路面結構一般被模擬爲一長方形薄版置於 Winkler 基礎上，以有限元素法加以分析此剛性版之應力與應變。關於剛性路面有限元素分析法程式衆多，一般採用有限元素法分析時可在與路基爲全部或部份接觸之情況下，及橫向及縱向接縫之各種不同荷重傳遞設施下，決定波特蘭水泥混凝土版因荷重及溫度變化所產生之應力及撓度。

上述兩種方法將於 7.1 及 7.2 節中加以討論，路面因荷重及溫度變化所產生之應力，則將於其餘章節中敍述。

7.1 Westergaard 分析法

由於 Westergaard 分析非常複雜，因此其理論公式將予省略。以下將對較簡單之樑於彈性基礎上(Beam on Elastic Foundation)之分析法加以詳述，此法雖爲簡化之方法，惟與原 Westergaard 對版置於彈性基礎上(Plate on Elastic Foundation)之分析法類似，前者之結果可提供對後者之分析方法及結果某種程度上之了解。

7.1.1 Winkler 基礎上樑之應力分析

樑作用於 Winkler 基礎上之分析法，一如版作用於 Winkler 基礎上之 Westergaard 分析法，都基於下列假設：

(1)原爲平面之樑或版，彎曲後仍保持平面；

⑵樑或版爲均質、等向性及線性彈性；

⑶剪力對樑或版之撓度及撓曲應力之影響忽略不計；

⑷路基作用如 Winkler 基礎，即路基與樑或版之反力與該點之撓度成正比，如圖 7.3 。

基於上述⑴～⑶之假設，樑之力矩（M）、分佈荷重（P）、撓度（Z）、撓應力（Flexure Stress）（σ）及曲徑半徑（R）間之關係如下：

$$\frac{1}{R}=\frac{M}{EI} \qquad (7-1a)$$

$$\frac{1}{R}=\frac{d^2M}{dx^2} \qquad (7-1b)$$

$$P=\frac{d^2M}{dx^2} \qquad (7-1c)$$

$$M=EI\frac{d^2Z}{dx^2} \qquad (7-1d)$$

$$P=EI\frac{d^4Z}{dx^4} \qquad (7-1e)$$

$$\sigma=\frac{MC}{I} \qquad (7-1f)$$

E ：樑之彈性模數

I ：樑斷面之慣性矩，爲 $bh^3/12$ ， b 及 h 分別爲樑之寬及深度。

由上述方程式中，若荷重或彎矩爲已知，則可決定任一點之撓度；相同地，若彎矩已知，則可決定樑之撓應力。

對置於 Winkler 基礎上之樑（如圖 7.3 ），其分佈荷重包括外加荷重(P)及路基反力(q)，路基反力爲與撓度成正比，可表示爲 $q=-kz$ ； k 爲路基反力係數，故方程式 7 － 1e 可改爲

$$EI\frac{d^4Z}{dx^4}=P-KZ$$

或

$$\frac{d^4Z}{dx^4}+\frac{Z}{\ell^4}=\frac{P}{EI} \qquad (7-2)$$

其中 $\ell=\sqrt[4]{\frac{EI}{K}}$ $\qquad$ $\lambda=\sqrt[4]{\frac{K}{4EI}}$

上述爲一四階微分方程式，其表示撓度與外加荷重(P)之關係。而（7 - 2）式之解答與所定義之參數 ℓ 有關，例如：一有限長之樑置於 Winkler 基礎上，並承受一點荷重（如圖 7.4 所示），則利用方程式（7 - 2）可解得撓度與荷重間之關係如（7 - 3a）式

$$Z=\frac{P\lambda}{2K}e^{-\lambda x}(\cos\lambda x+\sin\lambda x) \qquad (7-3a)$$

$$M=-EI\frac{d^2Z}{dx^2}=\frac{P}{4\lambda}e^{-\lambda x}(\cos\lambda x-\sin\lambda x) \qquad (7-3b)$$

$$\sigma=\frac{6M}{bh^2} \qquad (7-3c)$$

一旦求得撓度，可將（7 - 3a）式代入（7 - 1d）式以求得彎矩如（7 － 3b）式；（7 - 3b）式代

入(7-1f)式可求得撓應力之關係如(7-3c)式。此例於各不同位置之撓度及應力分佈如圖 7.4 所示。

如樑之上下面溫度不同，假設其溫差爲(△T)，則將形成樑之翹曲(Warping)。因翹曲而形成之曲率可表爲(△T)α/h，其中α爲熱膨脹係數。因此，由溫差(△T)與外加荷重壩(P)(見(7－1a)式)同時作用所造成之曲率爲：

$$\frac{1}{R}=\frac{M}{EI}+\frac{(\triangle T)\alpha}{h}$$

或

$$\frac{d^2Z}{dx^2}=\frac{M}{EI}+\frac{(\triangle T)\alpha}{h} \qquad (7-4)$$

方程式(7-4) 可用以分析因溫度改變而使樑所產生之應力。

7.1.2 Winkler 基礎上版之翹曲應力(Warping Stress)

方程式(7-1)雖用於樑之問題，亦可推廣而應用於版之類似問題，惟一不同之處，爲版之問題須考慮柏松比(如圖 7.5)，因此：

$$\frac{\partial^2Z}{\partial x^2}=\frac{1}{EI}(Mx-\mu My)+\frac{(\triangle T)\alpha}{h} \qquad (7-5)$$

$$\frac{\partial^2Z}{\partial y^2}=\frac{1}{EI}(My-\mu Mx)+\frac{(\triangle T)\alpha}{h} \qquad (7-6)$$

其中μ爲柏松比(Poisson's Ratio)

狀況Ⅰ：無限大版塊之情形(內部點)

由於是無限大版塊，所以沒有邊界之分，版塊內任何一點均爲對稱，因此不可能有明顯之扭曲，因而沒有明顯之撓度，因此：

$$\frac{\partial^2Z}{\partial x^2}=\frac{\partial^2Z}{\partial y^2}=0 \text{ 及 } Mx=My=M$$

(7-5)式及(7-6)式改爲

$$\frac{(1-\mu)}{EI}M+\frac{(\triangle T)\alpha}{h}=0,\quad M=-\frac{(\triangle T)\alpha}{h}\frac{EI}{(1-\mu)}$$

$$\sigma=\frac{Mh}{2I}$$

$$\sigma=-\frac{(\triangle T)\alpha E}{2(1-\mu)} \qquad (7-7)$$

例：一典型之混凝土版：

$E=6\times10^6$psi

$\alpha=5\times10^{-6}$in / in /°F

$\mu=0.3$

當△T = 35°F，於版之表面將產生 750psi 之張力，此應力較一般混凝土之抗張強度爲大。由於溫差將隨版厚而增加，故因熱而產生之翹曲應力將因版厚增加而增大。

狀況Ⅱ：有限大版塊，方程式(7-5)及(7-6)可用以求較複雜之邊界條件問題，諸如在有限尺

寸之混凝土版內部或邊緣之應力等變數。這些分析已由 Bradburg ［17］所求出，其所求得之結果可以下列方程式表示：

$$\sigma_x=\frac{E\alpha(\Delta T)}{2}Cx \qquad \text{邊緣應力}$$

$$\sigma_x=\frac{E\alpha(\Delta T)}{2}\left(\frac{Cx+\mu Cy}{1+\mu}\right)$$

$$\sigma_y=\frac{E\alpha(\Delta T)}{2}\left(\frac{Cy+\mu Cx}{1+\mu}\right) \qquad \text{內部應力(7-8)}$$

其中 Cx 及 Cy 爲版長修正因子(如圖 7.6)；圖 7.6 中之 Lx 及 Ly 分別爲 x 及 y 方向之版長；ℓ 稱爲版之相對勁度半徑(Radius of Relative Stiffness)，其定義將於談到(7-10)式時再加說明。

7.1.3 Winkler 基礎上荷重所產生之版應力

在考慮二度空間之版作用時，可將一度空間之(7-2)式就版之問題而擴充爲如下之方程式：

$$\frac{\partial^4 Z}{\partial x^4}+2\frac{\partial^4 Z}{\partial x^2\partial y^2}+\frac{\partial^4 Z}{\partial y^4}=\frac{P-KZ}{D} \qquad (7-9)$$

其中 D 爲版之撓曲勁度，ℓ 爲相對勁度半徑，

$$D=\frac{Eh^3}{12(1-\mu^2)}$$

$$\ell=\sqrt[4]{\frac{D}{K}}=\sqrt[4]{\frac{Eh^3}{12(1-\mu^2)K}} \qquad (7-10)$$

相對勁度半徑結合了 E 、h 、k 、μ 之效應而成爲單一參數，如(7-2)式與(7-10)式中之 ℓ 即爲類似之型式。(7-10)式中版之寬度爲單位寬度，且由於版之柏松比效應，(7-10)式中亦增加了柏松比(μ)。

狀況 I ：角隅荷重

波特蘭水泥混凝土版因荷重作用於角隅所產生之應力及撓度之分析解(如圖 7.7)如下：

(a) $k=0$ (角隅下方無支承)

由基本之梁理論可求得最大抗彎應力如下：

$$\sigma_{max}=\frac{3p}{h^2}$$

(b) $k\neq 0$ $\qquad \Delta(X)=\frac{P}{K\ell^2}\left(1.1\,e^{-X/\ell}-\frac{0.88\,a_1}{\ell}e^{-2X/\ell}\right)$ (7-10a)

其中 ℓ 同(7-10)式之定義，且最大應力發生於 $L=2\,a_1\ell$

每單位寬度之最大彎矩，在 $x=L$ 處可表示爲：

$$M=\left[P(L-a_1)+\int_0^L K\Delta(X)\cdot 2X\cdot(L-X)\,dx\right]/2L$$

$$=\frac{P}{2}\left[1-\left(\frac{a_1}{\ell}\right)^{0.6}\right]$$

其最大應力爲：

$$\sigma=\frac{6M}{h^2}=\frac{3P}{h^2}\left[1-\left(\frac{a_1}{\ell}\right)^{0.6}\right] \qquad (7-10b)$$

狀況II：邊緣荷重及內部荷重

以(7-9)式解一有限版於邊緣及內部之應力與撓度，因其解答過於複雜，故不在此詳述。傳統上，這些問題之應力與撓度都可以 Pickett 及 Ray ［14］所發展之影響圖解之；最近 Packard ［18］亦發展一電腦程式以解決這些問題。

混凝土版置於 Winkler 基礎上之彎矩及撓度之影響圖見圖 7.8 至 7.11 ，其解法爲將接觸輪荷重映繪於影響圖上，再計算映繪面積內部所包含之格數，再利用下列方程式計算其撓度、彎矩及應力。

$$\text{撓度}\quad \Delta=\frac{0.0005\,P\,\ell^4 N}{D}$$

$$\text{彎矩}\quad M=\frac{P\,\ell^2 N}{10{,}000} \qquad (7-11)$$

$$\text{應力}\quad \sigma=\frac{6M}{h^2}$$

其中 P 爲平均接觸壓力， N 爲映繪面積中之格數， h 爲版厚， ℓ 及 D 則分別如(7-10)式中之定義。

7.2 有限元素法

本節將敍述以有限元素法決定混凝土版塊之應力及撓度之原理。此法係基於薄版理論，其假設與 7.1 節中樑置於彈性基礎上之假設相同。薄版置於 Winkler 基礎上之有限元素法，其基本方程式係由 Zienkiewicz 及 Cheung ［19］所提出，元素之佈置如圖 7 － 12 所示，元素於有限數量之節點相互聯接。此法可求得一組對所有節點之力與位移關係之聯立方程式如(7.12)式，由此可解得版中每一元素之未知節點位移。

$$k\,〔A〕\,\{\delta'\}=\{F\}\,〔K〕\,\{\delta\} \qquad (7-12)$$

上式中 k 爲路基反力模數；〔A〕爲一對角矩陣，表示路基反力分佈之面積；$\{\delta'\}$ 爲一表示路基位移之向量；{F} 爲一向量，表示所有作用於版上之力；$\{\delta\}$ 爲一節點位移向量；〔K〕爲版之組合勁度矩陣。求得節點位移之後，則可據以求得節點彎矩及應力。由於以某一元素計算所得之節點應力可能有別於以相鄰元素所求得者，因此，節點應力須採用所有相鄰元素所求得之平均應力值。

一般採用有限元素法計算混凝土版塊所發展之電腦程式具有下列之功能：

(1)部份或全部通過縱向及橫向接縫之荷重傳遞可表示爲荷重傳遞效率(Load transfer efficiency)。

(2)版之溫度捲曲應力(Thermal curling stress)。

(3)部份或全部之路基支承。

有限元素法之精確度已經由邊緣荷重作用於無限大版之 Westergaard 理論解，及影響圖〔16〕之解法得到証實。

有限元素法之解答亦曾與 AASHO 道路試驗〔16,20,21〕中有限版塊之邊緣應力實驗結果相比較， AASHO 道路試驗所用之版爲 15 呎長、 12 呎寬，且於橫向及縱向接縫分別設置綴縫筋及繫筋。有限元素法之結果與所測得之路面邊緣應力值如圖 7.13 所示。版之有限元素法解答之基本參數爲：楊氏模數 6.25×10^6psi ，由道路試驗所測得波特蘭水泥混凝土之柏松比 0.28,k 值 300pci 。量測所得之邊緣應力係由在相同位置實際量測之應變值求得。

版因溫度差異而產生之捲曲應力(Curling stress)，其有限元素法解之精確度已由美國 Virginia 州 Arlington 之 Tellen 及 Southerland 之試驗結果〔22〕得到証實；其比較結果則由 Darter 發表，如圖 7.14 。

以有限元素法計算捲曲應力，提供了較 Bradbury 〔17〕分析更爲實用之分析方法，有限元素法容許版於無重量條件下捲曲，然後再加上版之束縛重量，因此，版爲受制於其本身之重量。 Bradbury 模式則假設全部版面均受限制，因此將產生更高之應力。版厚及基礎模數在某一範圍內時，茲將上述兩種方法計算所得之應力比較如下：

以 Bradury 法〔17〕及有限元素法計算溫度邊緣捲曲應力(Curling stress)之比較：

版厚(吋)	模式	基礎模數 (k) — pci		
		50	200	500
8	有限元素法	134 * psi	204	247
	Bradbury	144	246	294
10	有限元素法	105	178	204
	Bradbury	98	255	330
14	有限元素法	66	129	145
	Bradbury	100	210	341

(參考資料:〔21〕)

使用參數：版長 ： 15 呎

溫度梯度 ： 3°F/ in

彈性模數 ： 5×10^6psi

熱膨脹係數： 5×10^{-6}/°F

以 Bradbury 模式計算所得之溫度捲曲應力，平均比以有限元素計算所得之數值大 43%。由於大部份 Bradbury 法與量測值之比較結果，都顯示量測值較低，因此，有限元素法較 Bradbury 模式更接近量測值。

總而言之，以有限元素法預估波特蘭水泥混凝土之應力，其精確度與以 Westergaard 法及 Bradbury 法所預估者相當，甚至更佳。

7.3.2 路面因素對荷重產生應力之影響

不同版厚、k 值、版長及支承侵蝕力等對邊緣應力(沿縱向接縫)之影響，詳見參考資料〔21〕。其中所採用之路面性質與本節開端處所列者相同，部份結果如圖 7 － 18 所示。

7.4 翹曲(Warping)產生之應力

不同路面性質對於因溫度差異所產生之翹曲應力，亦曾由 Darter 〔21〕以有限元素法加以研究，其結果如圖 7 - 19 。此結果顯示翹曲應力在縱向邊緣上最爲明顯，當溫度梯度(Gradient)爲正(日間)，混凝土版底部所產生之邊緣應力爲張力。

7.5 摩擦力產生之應力

混凝土乾縮及溫度改變均會使混凝土版產生張應力。此兩種因素均會使版收縮，且因基層之摩擦阻力使版產生張應力，其均勻變化時，所產生之最大張應力可由下式加以推估：

$$\sigma_T = \frac{r \cdot f \cdot L}{288} \qquad (7-13)$$

其中 σ_T：混凝土張應力，〔psi〕
r ：混凝土單位重，〔pcf〕
f ：平均路基摩擦係數，由 1.0 至 2.0 間
L ：版長，〔ft〕

7.3 荷重所產生之應力

本節將敍述荷重作用下，混凝土版塊所產生之應力［21］，基本上爲應用上節所述，以有限元素法程式計算混凝土版塊在受外力作用時所產生之應力。計算版之應力時，所採用之數據如下：

版長(L)＝15ft
版寬　＝12ft
版厚　＝10in
波特蘭水泥混凝土彈性模數　＝ 5×10^6psi
波特蘭水泥混凝土熱膨脹係數＝ 5×10^{-6}/°F
路基反力模數(k)　＝200pci
荷重　＝18kip (單軸)

根據以上數據所求得之結果加以討論如下。

7.3.1 縱向與橫向接縫附近及角隅之應力

將縱向與橫向接縫附近之臨界張應力(如圖 7.2)加以濃縮，其結果如圖 7 - 15 及 7 - 16 所示。圖中顯示卡車側向移動(D)對版底部所產生之張應力的影響。當荷重作用於縱向接縫附近時(如圖 7.15)，此荷重作用在版邊緣會產生最大之應力，由此荷重條件所產生之最大張應力約爲 220psi ；當荷重作於橫向接縫時，於橫向接縫所產生之應力則相當小(如圖 7.16)。計算應力時，橫向接縫之荷重傳遞效率假設爲 50%。

荷重作用於角隅所產生之最大張應力如圖 7.7 所示，對相同之路面性質仍採用(7 - 10a)式計算。當 k ＝ 200pci 時，最大張應力爲 185psi ； k ＝ 0 時，最大張應力則爲 270psi 。

在計算角隅應力時，橫向接縫爲假設沒有荷重傳遞設施，若有荷重傳遞設施存在，則最大角隅應力可大幅度減小。

由此分析可知，最大應力發生於縱向接縫附近，此位置不僅受荷重時之應力最大，且受溫度作用所產生之應力亦較高，(溫度效應將於下一節中討論)。因此，橫向裂縫較可能由此位置開始發生及擴展，此亦大致可由現場觀察結果加以証實。在 AASHO 道路試驗中，橫向裂縫首先發生者，在 91 次之 JCP 及 JRCP 路段中即佔了 61 次。圖 7.17 所示爲一 8 吋混凝土版中，裂縫開始發生及擴展之情形。由 Michigan 試驗道路之結果亦顯示，橫向裂縫爲主要之破壞型式，每哩情況如下：

	接縫間距，(呎)		
	30	20	15
橫　向	296	139	50
對　角	7	6	0
縱　向	4	20	11

(a) 荷 重

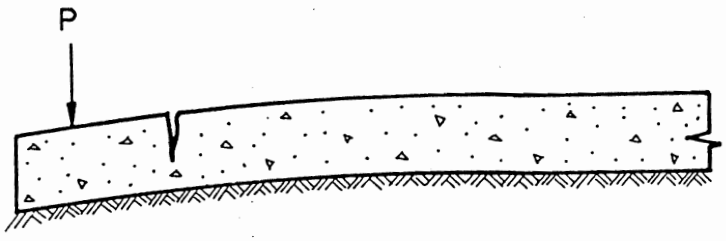

(b) 溫度及水份變化

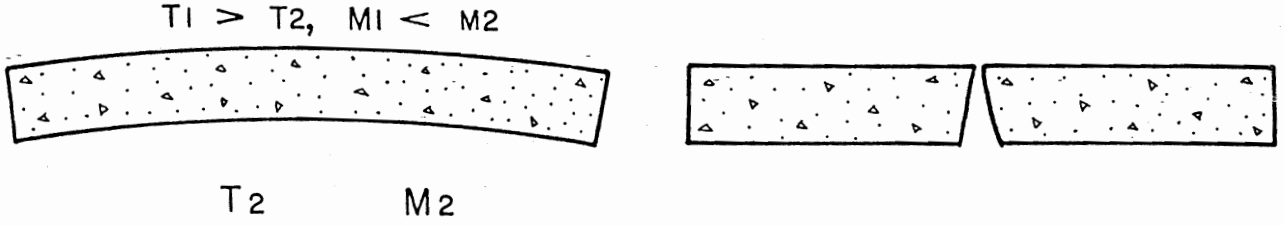

(c) 路基限制

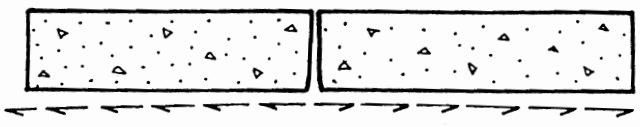

圖 7.1 PCC 路面之應力

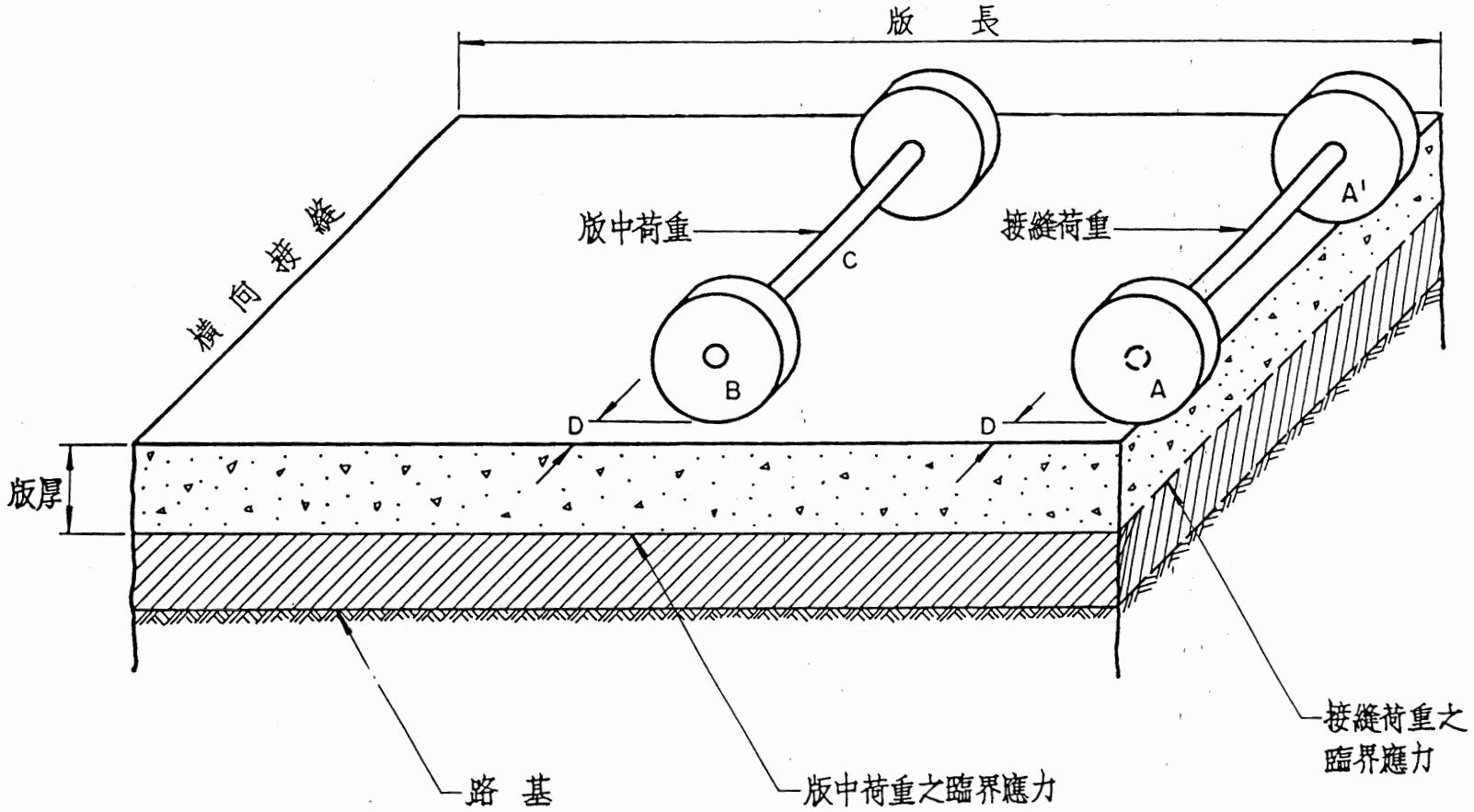

圖 7.2　　混凝土版之疲勞分析所考慮之荷重位置及應力

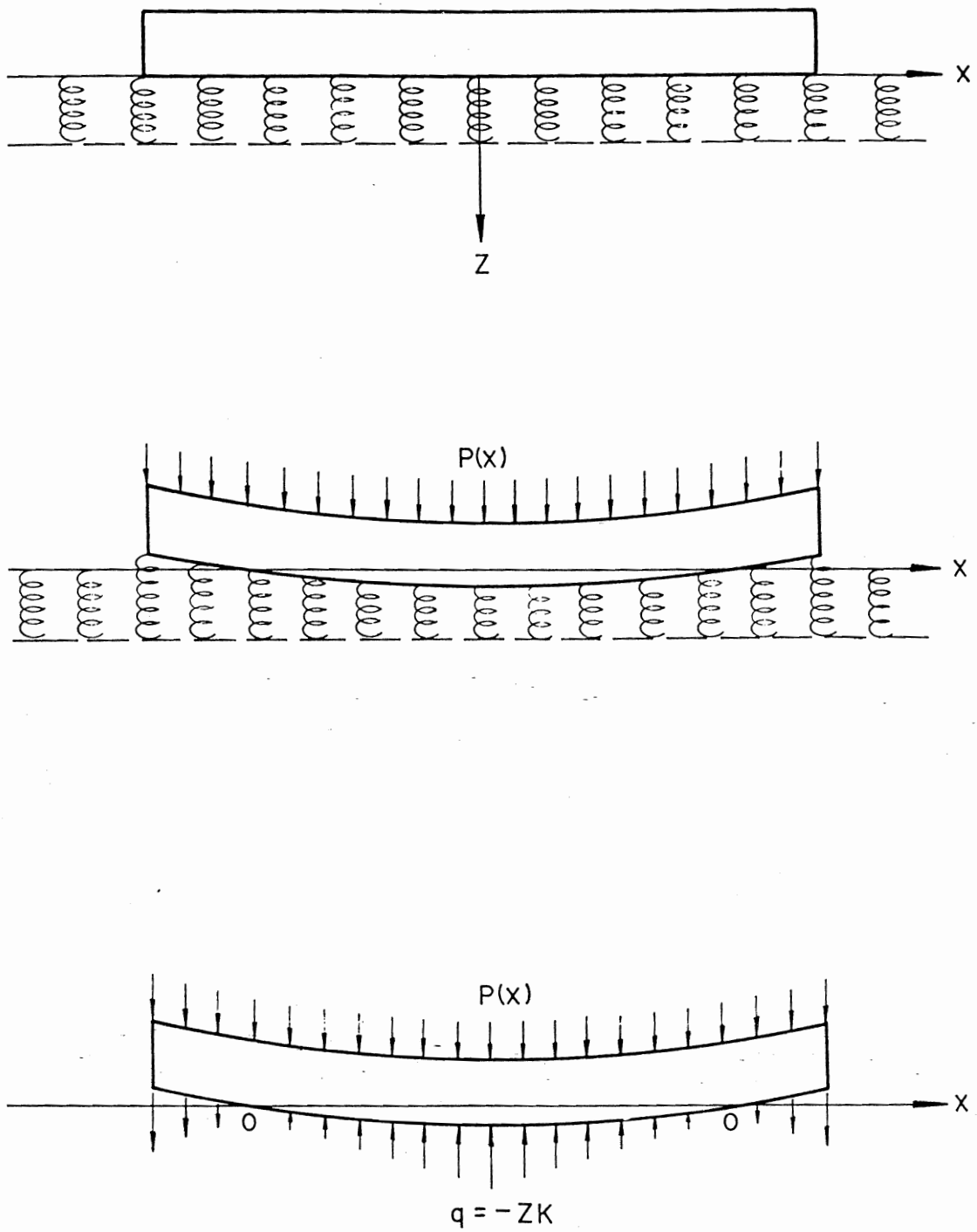

圖 7.3　　Winkler 基礎上之樑

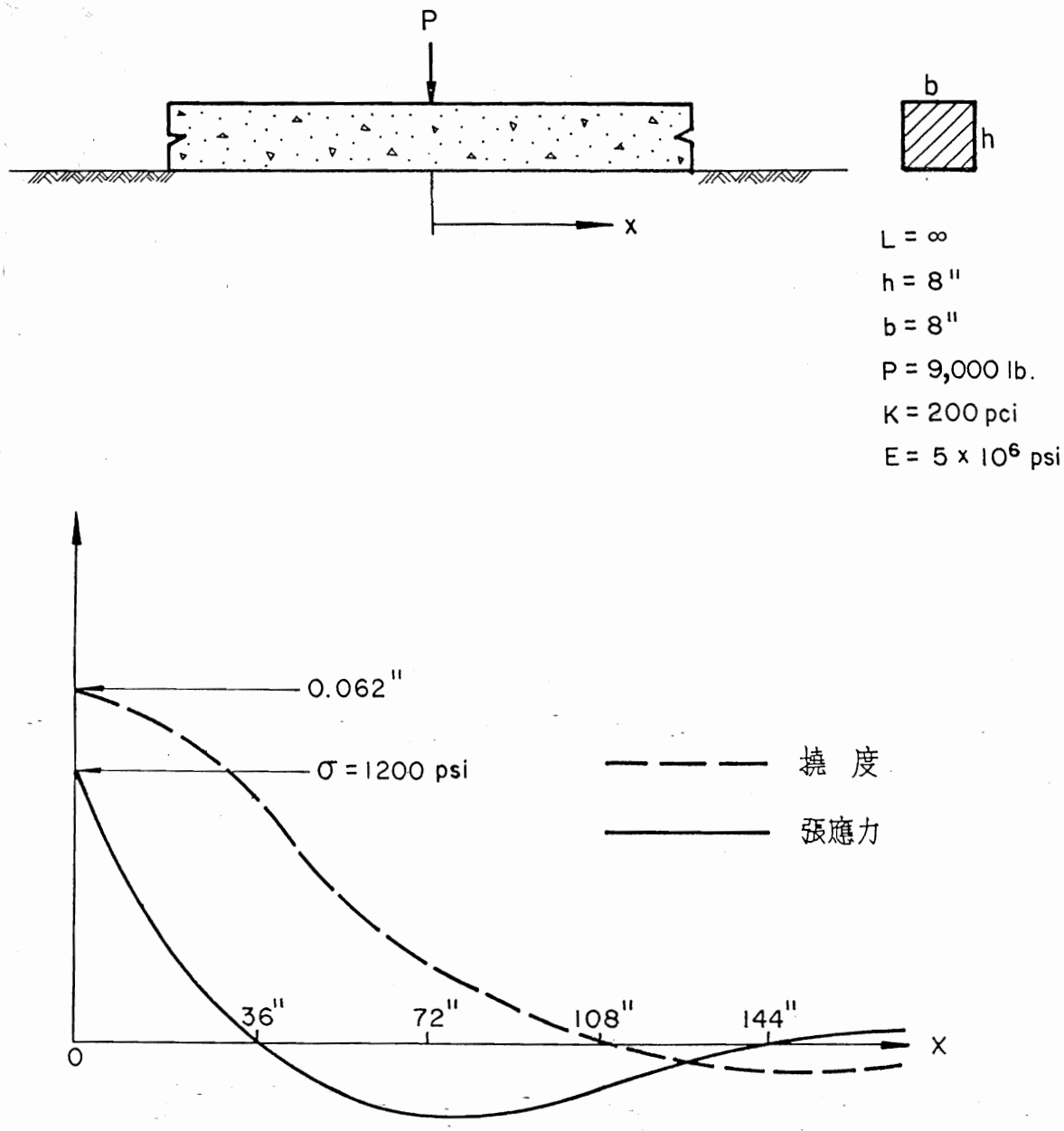

圖 7.4　　樑於 Winkler 基礎上之應力與撓度

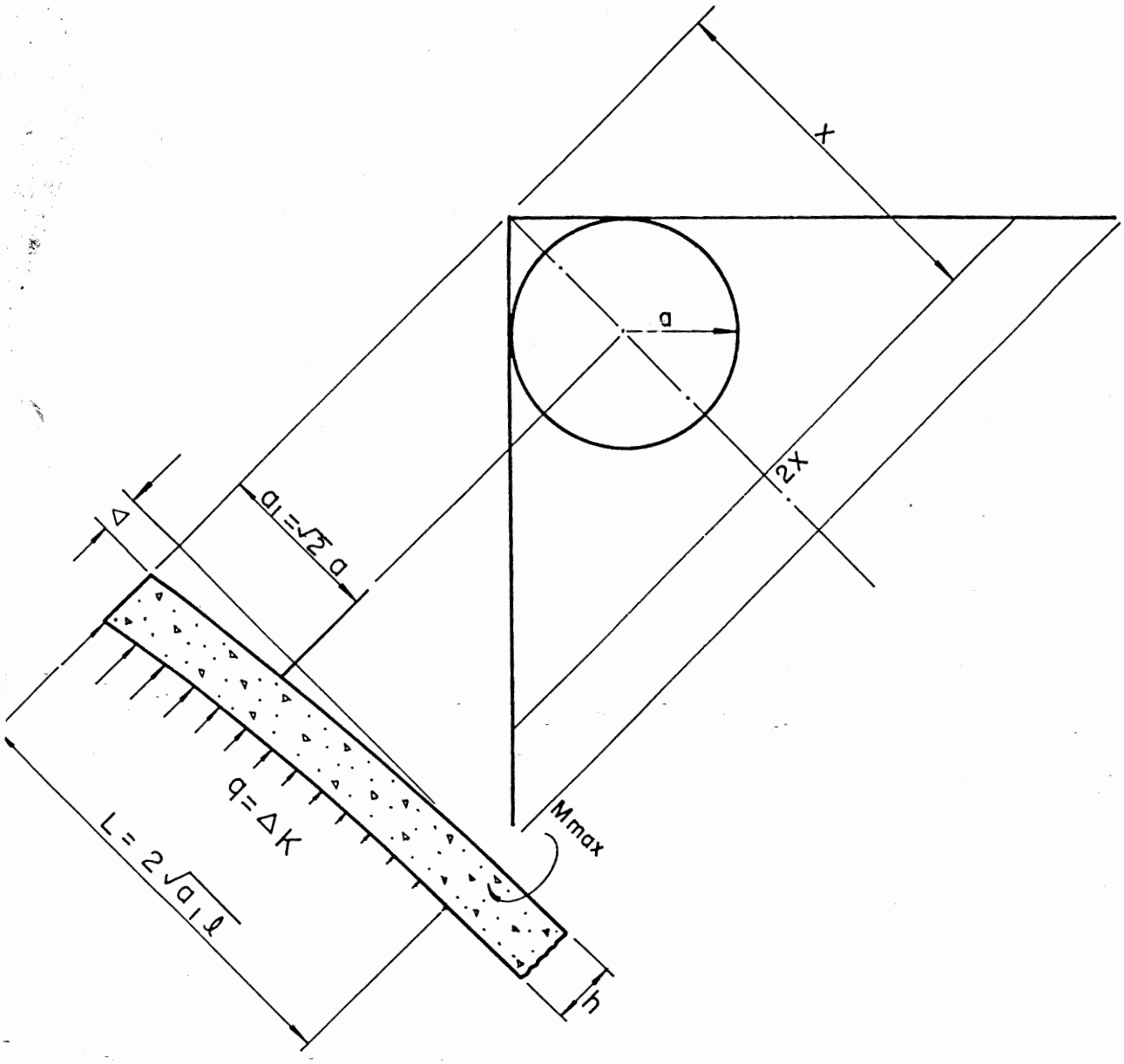

圖 7.7　　角隅荷重下之應力

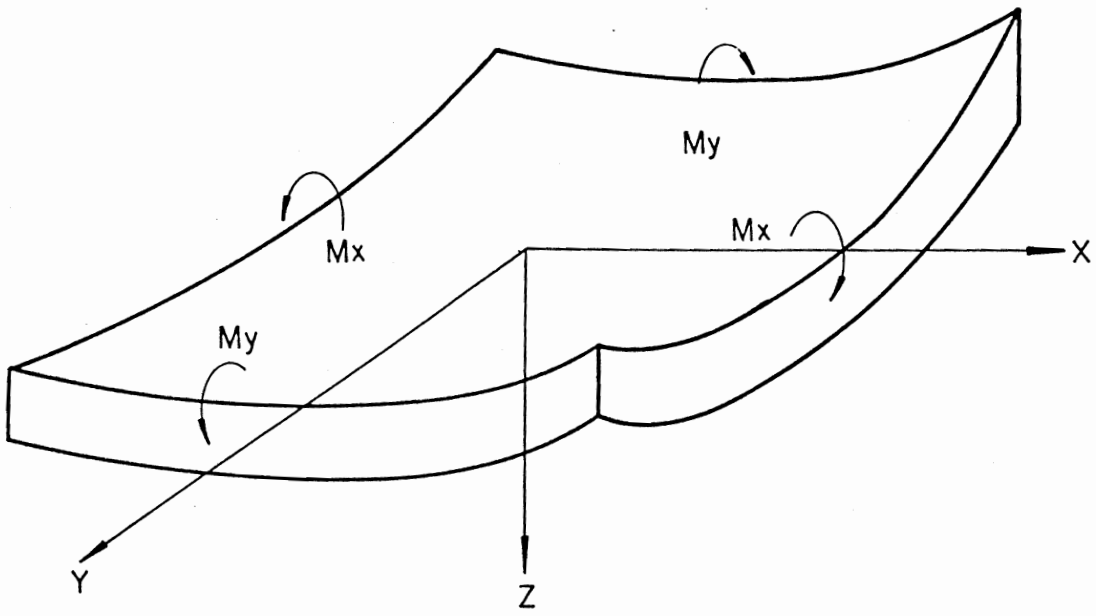

圖 7.5　　Winkler 基礎上之版

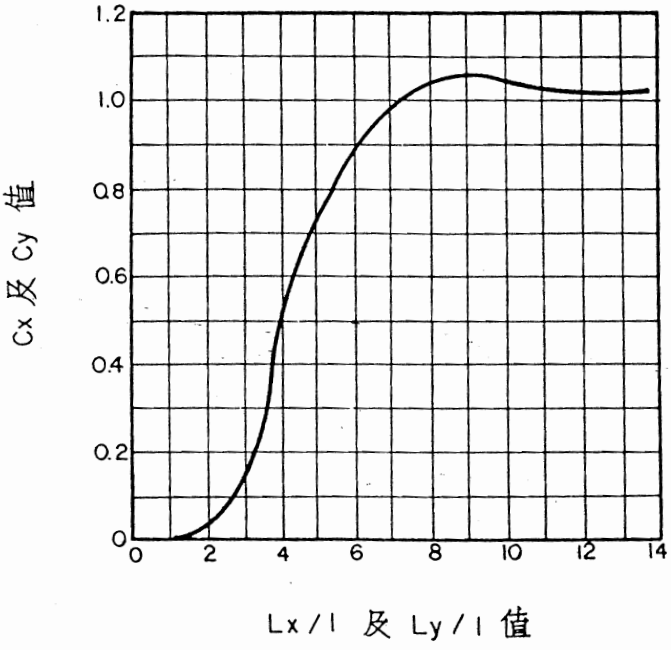

圖 7.6　　翹曲應力係數

Loading and Curling Stress Models for Concrete Pavement Design

YING-HAUR LEE AND MICHAEL I. DARTER

Determination of the edge loading tensile bending stress in a concrete slab due to individual and combination effects of wheel loading and thermal curling is important to a mechanistic-based design procedure. The recent discovery of two additional dimensionless mechanistic variables, such that the problems encountered in previous investigations that have used dimensional analysis for thermal-related curling problems are resolved, is described. A new regression technique (projection pursuit regression) together with traditional linear and nonlinear regressions are utilized to develop prediction models. These prediction models provide an accurate representation of the finite-element model. They are simple, easy to comprehend, dimensionally correct, may be extrapolated to wider ranges of other input parameters, and are ready for implementation in a spreadsheet or computer program. Examples of practical applications showing the use of the new models are also provided.

Cracking of slabs can be caused by three different repeated loading positions: transverse joint, longitudinal joint midway between transverse joints, and at the corner. Given certain design, construction, and loading conditions, any of these load positions could lead to fatigue cracking over time. This paper focuses on the longitudinal joint edge location, which could lead to transverse cracking. Determination of the maximum bending stress at the edge is important to a mechanistic-based design procedure (the other positions are also important and should be evaluated). The analysis of longitudinal edge stress due to the individual and combination effects of wheel loading and thermal curling is presented in this paper. Critical stresses from the corner loading is being pursued as part of continuing research at the University of Illinois.

Finite-element models have been successfully used to account for the effects of a finite slab size as well as the possible loss of support due to a linear temperature differential more realistically than theoretical solutions basded on infinite slab and full contact assumptions. However, because of the required run time and complexity of the finite-element model, finite-element analysis cannot easily be implemented as a part of a design procedure. Therefore, a series of finite-element runs were performed over a wide range of pavement designs. The resulting edge stresses were compared with theoretical Westergaard solutions, and adjustment factors were introduced to account for this discrepancy. Statistical regression techniques were utilized to develop predictive models for each adjustment factor. These predictive models were then used as an alternative to finite-element analysis to estimate stresses for pavement design with sufficient accuracy.

Previous predictive models (*1,2*) were based on a series of input parameters by using multiple regression and stepwise regression techniques. Thus, the resulting models contain only arbitrary linear combinations of variables, with few insights in describing their actual physical relationships. The results of the prediction are also limited to the ranges of the cases analyzed.

This paper presents a more mechanistic-based approach in developing such predictive models. Through the use of the principles of dimensional analysis, the dominating mechanistic variables were first identified on the basis of previous research. In addition, two newly discovered additional dimensionless mechanistic variables were necessary such that the problems encountered in previous investigations that used dimensional analysis for thermal-related curling problems are resolved. A new regression technique (projection pursuit regression) together with traditional linear and nonlinear regressions were used to develop prediction models.

Consequently, three closed-form mechanistic design models that have been carefully validated and that are ready for implementation in a spreadsheet or computer program are presented as a result of the present study. In contrast to those earlier predictive models, the new models not only used the dominating mechanistic variables identified herein but they were also properly formulated to satisfy applicable engineering boundary conditions. These stress models turned out to be accurate representations of the finite-element model. They are simple, easy to comprehend, and dimensionally correct and can be extrapolated to wider ranges of other input parameters. The parameter estimates of each model have their own physical meanings as well. Examples of practical applications showing the use of the new models are also provided.

This paper not only provides more complete coverage of the solutions to the cases analyzed but it also demonstrates the advantages of incorporating subject-related engineering knowledge and selecting proper functional forms for the predictive models. It will be of interest to those working on mechanistic pavement design and pavement prediction modeling.

IDENTIFICATION OF IMPORTANT MECHANISTIC VARIABLES

Primary Structural Responses Due to Loading

In the analysis of a slab-on-grade pavement system, Westergaard (*3*) and others (*4,5*) have presented closed-form solutions for three primary structural response variables, that is, slab bending stress, slab deflection, and subgrade stress, owing to a single wheel load. On the basis of the assumptions of an infinite or semi-infinite slab over a dense liquid foundation (Winkler foundation), three different loading conditions (interior, edge, and corner) were analyzed.

Y.-H. Lee, Department of Civil Engineering, Tamkang University, E725, #151, Ying-Chuan Road, Tamsui, Taipei, Taiwan 25137, Republic of China. M. I. Darter, Department of Civil Engineering, University of Illinois, NCEL #1212, 205 North Mathews Avenue, Urbana, Ill. 61801.

The Westergaard solutions for a circular edge loading based on medium-thick plate theory are given as follows:

$$\sigma_w = \frac{3(1+\mu)P}{\pi(3+\mu)h^2}\left[\log_e \frac{Eh^3}{100ka^4} + 1.84 - \frac{4\mu}{3} + \frac{1-\mu}{2} + 1.18(1+2\mu)\frac{a}{l}\right] \quad (1)$$

$$\delta_w = \frac{\sqrt{2+1.2\mu}\,P}{\sqrt{Eh^3k}}\left[1 - (0.76+0.4\mu)\frac{a}{l}\right] \quad (2)$$

$$l = \sqrt[4]{\frac{Eh^3}{12(1-\mu^2)k}} \quad (3)$$

where

σ_w = Westergaard's edge stress (FL^{-2}),
δ_w = Westergaard's edge deflection (L),
P = total applied wheel load (F),
a = radius of the applied circular load (L),
E = modulus of elasticity of the concrete slab (FL^{-2}),
h = thickness of the slab (L),
μ = Poisson's ratio of the concrete,
k = modulus of subgrade reaction (FL^{-3}), and
l = radius of relative stiffness of the slab subgrade system (L).

(Note that primary dimensions are represented by F for force and L for length.) The subgrade stress was not explicitly specified; however, it can easily be determined by multiplying the slab deflection by the modulus of subgrade reaction.

Through the use of the principles of dimensional analysis, earlier investigators (*4*) have demonstrated that theoretical Westergaard solutions for these three primary structural responses can be reduced to three dimensionless terms, shown as follows, which all depend on the normalized load radius alone for a constant Poisson's ratio (usually $\mu \approx 0.15$).

$$\frac{\sigma h^2}{P}, \frac{\delta k l^2}{P}, \frac{q l^2}{P} = f\left(\frac{a}{l}\right) \quad (4)$$

where σ and q are equal to slab bending stress and subgrade vertical stress (FL^{-2}), respectively, and δ is equal to slab deflection (L).

By doing so the relationships between the primary structural responses and the external wheel loading are concisely defined. The dependent variables are $\sigma h^2/P$, $\delta k l^2/P$, and $q l^2/P$, whereas the independent variable is the dominating factor a/l, rather than the other input parameters (E, h, μ, k, and a). These relationships are not only simple to understand but they also provide a dimensionally correct form for further analysis on a more complicated problem.

The analysis of finite slab length and width effect owing to an external wheel load is not possible until the introduction of finite-element models. According to previous research (*4,5*), the normalized slab length and width (L/l and W/l, respectively) are the dominating mechanistic variables for the finite extent of slab condition, where L and W are the finite slab length and width, respectively. In fact, theoretical treatments on the effect of thermal curling (rather than wheel loading), which can be traced back as early as Westergaard (*6*) and Bradbury (*7*), have already shown that the finite extent of slab condition is simply a function of these two dimensionless terms. Thus, the following expression can concisely describe the above relationships:

$$\frac{\sigma h^2}{P}, \frac{\delta k l^2}{P}, \frac{q l^2}{P} = f\left(\frac{a}{l}, \frac{L}{l}, \frac{W}{l}\right) \quad (5)$$

Primary Structural Responses Due to Thermal Curling

Considering the curling stresses caused by a linear temperature differential on a concrete slab over a dense liquid foundation, Westergaard (*6*) developed equations for three slab conditions (i.e., an infinite, a semi-infinite, and an infinitely long strip). For the case of an infinitely long strip that had a finite width W and an infinite length along the x-axis, the deflection and bending stress solutions along the y-axis are given as follows:

$$\sigma_y = \sigma_0\left\{1 - \frac{2\cos\lambda\cosh\lambda}{\sin 2\lambda + \sinh 2\lambda}\left[(\tan\lambda + \tanh\lambda)\cos\frac{y}{l\sqrt{2}}\cosh\frac{y}{l\sqrt{2}} + (\tan\lambda - \tanh\lambda)\sin\frac{y}{l\sqrt{2}}\sinh\frac{y}{l\sqrt{2}}\right]\right\} \quad (6)$$

$$\delta_y = -\delta_0\frac{2\cos\lambda\cosh\lambda}{\sin 2\lambda + \sinh 2\lambda}\left[(-\tan\lambda + \tanh\lambda)\cos\frac{y}{l\sqrt{2}}\cosh\frac{y}{l\sqrt{2}} + (\tan\lambda + \tanh\lambda)\sin\frac{y}{l\sqrt{2}}\sinh\frac{y}{l\sqrt{2}}\right] \quad (7)$$

$$\sigma_0 = \frac{E\alpha\Delta T}{2(1-\mu)},\ \delta_0 = \frac{(1+\mu)\,\alpha\,\Delta T\,l^2}{h},\ \lambda = \frac{W}{l\sqrt{8}} \quad (8)$$

where

σ_y = bending stress along the y-axis (y is equal to $\pm W/2$ at the slab edges) (FL^{-2}),
δ_y = deflection along the y-axis (L),
α = thermal expansion coefficient of the concrete slab (T^{-1}), and
ΔT = linear temperature differential through the thickness of the slab (T).

Bradbury (*7*) later expanded Westergaard's bending stress solutions for a slab with finite dimensions in both the x and the y directions. Thus, considering a narrow and long strip of slab, the curling stress along the edge of the slab could be determined by the following equation:

$$\sigma_c = \frac{CE\alpha\Delta T}{2} = \frac{E\alpha\Delta T}{2}\left[1 - \frac{2\cos\lambda\cosh\lambda}{\sin 2\lambda + \sinh 2\lambda}(\tan\lambda + \tanh\lambda)\right] \quad (9)$$

where σ_c is equal to bending stress at the edge of the slab due to thermal curling (FL^{-2}).

Similarly, the closed-form solutions derived for slab bending stress, slab deflection, and subgrade stress owing to a linear temperature differential can be summarized in the following expression by using dimensional analysis for a constant Poisson's ratio:

$$\frac{\sigma}{E}, \frac{\delta h}{l^2}, \frac{qh}{kl^2} = f\left(\alpha\Delta T, \frac{L}{l}, \frac{W}{l}\right) \quad (10)$$

Identification of Two Additional Dimensionless Parameters

For thermal-related curling problems, Westergaard's and Bradbury's analytical solutions are based on an assumption of full contact between the pavement slab and the subgrade. However, experimental data by Teller and Sutherland (*8*) have clearly shown that parts of the pavement slab were found without subgrade support when a temperature or moisture differential existed through the slab thickness. Thus, the effect of the loss of subgrade support owing to a temperature differential must be considered to account for the actual pavement condition more realistically. The ILLI-SLAB finite-element model (*9–11*), which has implemented this effect through an iterative procedure and which has been developed over the years at the Univesity of Illinois, was selected for this study.

Because of the above theoretical difference, attempts by earlier investigators (*12*) to relate the actual structural response due to the combination effect of a single wheel load and a temperature influence using only the aforementioned dimensionless parameters were not very successful. Thus, it was necessary to search for other possible mechanistic variables to describe this difference adequately. Particular attention was focused on the effect of the self-weight of the concrete slab on the thermal-induced curling stress. Westergaard (*6*) did not explicitly consider the self-weight effect in his deflection equation, since the center of the slab was assumed to be flat and the deflection was zero. On the other hand, the effect of self-weight is included in the ILLI-SLAB model. The deflection at the center is determined by

$$\delta_\gamma = \frac{\gamma h}{k} \quad (11)$$

where γ is equal to the unit weight of the concrete slab (FL^{-3}).

Considering Westergaard's analytical solution for deflection as shown in Equation 7, the deflection due to thermal curling alone may be described by normalized slab length and width (L/l and W/l, respectively), the dimensionless product of $\alpha\Delta T$, and the deflection factor (l^2/h). All these parameters are dimensionless except the last one, l^2/h, which has the same dimension as length and can be used as an indicator for the extent of loss of subgrade support. By taking the ratio of self-weight deflection versus l^2/h, the following dimensionless parameter, D_γ, was defined to represent the relative deflection stiffness due to the self-weight of the concrete slab and the possible loss of subgrade support:

$$D_\gamma = \frac{\gamma h^2}{kl^2} \quad (12)$$

It was hypothesized that the resulting ILLI-SLAB edge strain due to curling alone may be well characterized by L/l, W/l, $\alpha\Delta T$ as well as by this additional parameter (D_γ). To validate this hypothesis, 16 ILLI-SLAB runs were performed by keeping the above four parameters constant while changing any individual input variables. The resulting edge stress was numerically confirmed to be proportional to the elastic modulus of the concrete slab as summarized in Table 1. In other words the resulting edge strains are equal to each other.

By the same token this "deflection ratio" concept was applied again in searching for another dimensionless parameter for the effect of an applied wheel loading on a curled slab due to a linear temperature differential. On the basis of Westergaard's analytical solution for deflection shown in Equation 2, the edge deflection can be represented by two parameters, a/l and $P/(Eh^3k)^{1/2}$. The second one is a deflection factor that is analogous to P/kl^2 and that has the same dimension as length. By taking the ratio of this deflection factor versus l^2/h, the following dimensionless parameter, D_P, can be used as an indicator to represent the relative deflection stiffness due to the external wheel load and the loss of subgrade support:

$$D_P = \frac{Ph}{kl^4} = 12(1 - \mu^2)\frac{P}{Eh^2} \quad (13)$$

Thus, it was also hypothesized that six dimensionless parameters, a/l, L/l, W/l, $\alpha\Delta T$, D_γ, and D_P, would adequately describe the primary structural responses for the combination effect of loading plus thermal curling. To numerically validate this hypothesis, 16 ILLI-SLAB runs were performed and are summarized in Table 2. Keeping these six parameters constant and changing any individual input variables result in ILLI-SLAB edge stresses proportional to the elastic modulus of the concrete slab. Thus, a unique edge strain was obtained as well.

Equations 14 and 15 summarize the above relationships due to the effects of thermal curling alone and loading plus curling, respectively:

$$\frac{\sigma}{E}, \frac{\delta h}{l^2}, \frac{qh}{kl^2} = f\left(\alpha\Delta T, \frac{L}{l}, \frac{W}{l}, \frac{\gamma h^2}{kl^2}\right) \quad (14)$$

$$\frac{\sigma}{E}, \frac{\delta h}{l^2}, \frac{qh}{kl^2} = f\left(\frac{a}{l}, \alpha\Delta T, \frac{L}{l}, \frac{W}{l}, \frac{\gamma h^2}{kl^2}, \frac{Ph}{kl^4}\right) \quad (15)$$

Factorial Finite-Element Runs

A series of factorial finite-element runs were performed on the basis of the dominating variables identified previously. Small personal computer programs were written to generate the finite-element grids and input files to facilitate routine finite-element analyses. The finite-element mesh was designed according to the guidelines established in earlier studies (*10*). With the assistance of a file of batch commands, these factorial runs were performed as a background job on the HP/Apollo network. The desired results were automatically summarized to avoid untraced human errors.

NEW PREDICTIVE MODELING PROCEDURES

The proper selection of regression techniques is one of the most important factors to the success of prediction modeling. Tradi-

TABLE 1 ILLI-SLAB Runs: An Additional Parameter (D_γ) for Curling Only

ΔT °F	h in.	E Mpsi	k pci	L in.	W in.	α x10^{-6}	γ pci	σ_i psi
16	8.47	39.94	51	398.94	398.94	6.88	0.136	1156.576
16	21.18	2.56	51	398.94	398.94	6.88	0.022	74.405
40	8.47	39.94	51	398.94	398.94	2.75	0.136	1156.132
40	21.18	2.56	51	398.94	398.94	2.75	0.022	74.376
16	8.47	19.97	102	282.09	282.09	6.88	0.136	578.046
16	21.18	1.28	102	282.09	282.09	6.88	0.022	37.179
40	8.47	19.97	102	282.09	282.09	2.75	0.136	577.815
40	21.18	1.28	102	282.09	282.09	2.75	0.022	37.164
16	8.47	4.99	409	141.05	141.05	6.88	0.136	145.151
16	21.18	0.32	409	141.05	141.05	6.88	0.022	9.339
40	8.47	4.99	409	141.05	141.05	2.75	0.136	145.095
40	21.18	0.32	409	141.05	141.05	2.75	0.022	9.335
16	8.47	2.22	920	94.03	94.03	6.88	0.136	64.563
16	21.18	0.14	920	94.03	94.03	6.88	0.022	4.139
40	8.47	2.22	920	94.03	94.03	2.75	0.136	64.539
40	21.18	0.14	920	94.03	94.03	2.75	0.022	4.138

Note:

1. L/l = 5.0, W/l = 5.0, $\alpha\Delta T$ = 1.1E-04, D_γ = 3.0E-05, μ = 0.15.
2. 1 °F = (F - 32) / 1.8 °C, 1 inch = 2.54 cm, 1 psi = 6.89 kPa, 1 pci = 0.27 MN/m^3

tional "parametric" regression techniques such as linear and nonlinear regressions require the imposition of a parametric form on the functions, and then the parameter estimates are obtained afterward. With the multidimensional pavement engineering problems in mind, several unresolved deficiencies in the use of traditional stepwise regression and nonlinear regression were frequently identified. These include problems in the selection of correct functional form, violations of the embedded statistical assumptions, and failure to satisfy some engineering boundary conditions.

In situations in which little knowledge about the shape and the form of a function exists, several new "nonparametric" regression techniques developed over the past 10 years have gradually gained popularity. Without imposing an unjustified parametric assumption, nonparametric regression techniques strive to estimate the actual functional form that best fits the data through the use of scatter plot smoothers (*13*).

The projection pursuit regression (PPR or "projection") algorithm introduced by Friedman and Stuetzle (*14*) appears to have the most favorable features because of its capability of handling variable interactions when suggesting transformations to improve the fit. The projection algorithm strives to model a multidimensional response surface as a sum of several projected curves through the use of a local smoothing technique. The projected curves are essentially two-dimensional curves, which can be graphically displayed, easily visualized, and properly formulated. The relative importance of each projected curve can be determined by measuring the absolute value of each coefficient associated with them as well.

A new statistical package named S-PLUS that has been widely used by statisticians for data analysis (*15–18*) was selected because of the availability of this new regression technique. As a result the following two-step modeling procedure was adopted (*19*):

1. Use the projection algorithm to break down the multidimensional response surface into a sum of several smooth projected curves, and
2. Use traditional linear and nonlinear regression techniques to obtain the parameter estimates of each individual projected curves and the overall regression statistics.

PREDICTIVE MODELS FOR LOADING ONLY

The effects of an external wheel loading subjected to a finite slab length and a finite slab width were analyzed separately. Adjustment (multiplication) factors for each individual effect were developed. Their combination effects can be approximately represented by multiplying both adjustment factors together.

Effect of Finite Slab Length

An adjustment factor (R_L) for the finite slab length effect was developed on the basis of the following relationship:

$$R_L = \frac{\sigma_i}{\sigma_w} = f\left(\frac{a}{l}, \frac{L}{l}\right) \quad (16)$$

TABLE 2 ILLI-SLAB Runs: Two Additional Parameters (D_γ) and (D_P) for Loading Plus Curling

c in.	P lbs	ΔT °F	h in.	E Mpsi	k pci	L in.	W in.	α x10^{-6}	γ pci	σ_i psi
2.5*	1833	16	8.47	9.99	204.35	119.68	159.58	6.88	0.136	172.266
2.5*	733	16	21.18	0.64	204.35	119.68	159.58	6.88	0.022	11.039
2.5*	1833	40	8.47	9.99	204.35	119.68	159.58	2.75	0.136	172.239
2.5*	733	40	21.18	0.64	204.35	119.68	159.58	2.75	0.022	11.038
5.0	3666	16	8.47	19.97	102.17	169.26	225.68	6.88	0.136	344.294
5.0	1466	16	21.18	1.28	102.17	169.26	225.68	6.88	0.022	22.063
5.0	3666	40	8.47	19.97	102.17	169.26	225.68	2.75	0.136	344.239
5.0	1466	40	21.18	1.28	102.17	169.26	225.68	2.75	0.022	22.060
7.5	8248	16	8.47	44.93	45.41	253.89	338.51	6.88	0.136	773.457
7.5	3299	16	21.18	2.88	45.41	253.89	338.51	6.88	0.022	49.565
7.5	8248	40	8.47	44.93	45.41	253.89	338.51	2.75	0.136	773.335
7.5	3299	40	21.18	2.88	45.41	253.89	338.51	2.75	0.022	49.557
10.0	14663	16	8.47	79.88	25.54	338.51	451.35	6.88	0.136	1360.855
10.0	5865	16	21.18	5.11	25.54	338.51	451.35	6.88	0.022	87.211
10.0	14663	40	8.47	79.88	25.54	338.51	451.35	2.75	0.136	1360.642
10.0	5865	40	21.18	5.11	25.54	338.51	451.35	2.75	0.022	87.197

Note:

1. Load dimensions are c x c, except those starred cases use 2c x c. L/l = 3.0, W/l = 4.0, $\alpha\Delta T$ = 1.1E-04, D_γ = 3.0E-05, D_P = 3.0E-05, μ = 0.15.
2. 1 °F = (F - 32) / 1.8 °C, 1 lb = 4.45 N, 1 inch = 2.54 cm, 1 psi = 6.89 kPa, 1 pci = 0.27 MN/m^3.

where σ_w is Westergaard's edge stress solution given in Equation 1 (FL^{-2}), and σ_i is the edge stress determined by the finite-element model (FL^{-2}). On the basis of a previous investigation (*7*), the maximum edge stress condition or Westergaard's infinite slab assumption may be achieved by selecting a value of 5.0 or more for the normalized slab length term (L/l). Thus, a more conservative value of 7.0 for both the normalized slab length and the normalized slab width (W/l) was selected to ensure an infinite slab condition. The following factorial finite-element runs were performed:

a/l: 0.05, 0.10, 0.20, and 0.30 and

L/l: 2.0, 2.5, 3.0, 3.5, 4.0, 4.5, 5.0, 6.0, and 7.0.

Note that W/l was kept at a constant value of 7.0 for all runs. The pertinent input parameters of these factorial runs regarding load size, total wheel load, slab thickness, concrete modulus, and subgrade reaction are given in Table 3. The resulting ILLI-SLAB edge stresses when L/l was equal to 7.0 and W/l was equal to 7.0 were used to approximate Westergaard's solution in calculating adjustment factors. A three-dimensional perspective plot providing a very clear picture of the relationship among R_L, a/l, and L/l is shown in Figure 1(*a*).

By using the aforementioned predictive modeling approach, the following one-term projection model was developed:

$$R_L = 0.9399 + 0.07986\Phi_1(ATX1) \quad (17)$$

$$\Phi_1(ATX1) = -4.0308 + \frac{1}{0.2029 + 0.0345ATX1^{-3.3043}} \quad (18)$$

$$ATX1 = -0.9436\frac{a}{l} + 0.3310\frac{L}{l} \quad (19)$$

Statistics: N = 36, R^2 = 0.994, SEE = 0.0063, CV = 0.67 percent
Limits: $2 \le L/l \le 7$, $0.05 \le a/l \le 0.3$
(note that N is the number of datum points, R^2 is the coefficient of determination, SEE is the standard error of estimates, and CV is the coefficient of variation.)

Effect of Finite Slab Width

The effect of finite slab width was often neglected in practice, since it is not as significant as the slab length effect. However, this effect as represented by the following adjustment factor (R_W) was considered in the present study to have a more complete coverage on this topic:

$$R_W = \frac{\sigma_i}{\sigma_w} = f\left(\frac{a}{l}, \frac{W}{l}\right) \quad (20)$$

TABLE 3 Pertinent Input Parameters for Loading and Loading Plus Curling

a/l	c	*a*	E	k	h	*l*	P	DG	DP
	in.	in.	Mpsi	pci	in.	in.	lbs		
0.05	2.5*	1.995	5	200	10.59	39.89	1250	3.07	2.61
0.10	5.0	2.821	4	300	8.23	28.21	2500	2.47	10.82
0.20	10.0	5.642	3	400	9.97	28.21	10000	2.72	39.34
0.30	10.0	5.642	2	500	7.16	18.81	10000	2.52	114.40

Note:

1. Load dimensions are c x c, except those starred cases use 2c x c. α = 5.5E-06 /°F, μ = 0.15, γ = 0.087 pci, p = 100 psi, DG = D_γ x 10^5, DP = D_p x 10^5.
2. 1 °F = (F - 32) / 1.8 °C, 1 lb = 4.45 N, 1 inch = 2.54 cm, 1 psi = 6.89 kPa, 1 pci = 0.27 MN/m^3.

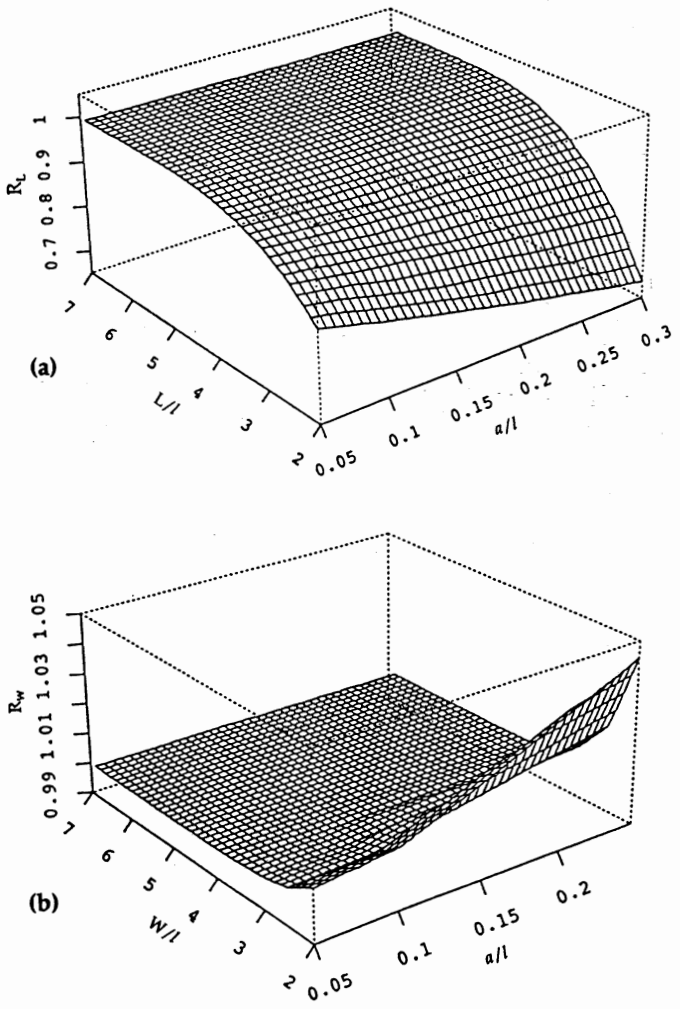

FIGURE 1 Finite slab size effects: (*a*) length and (*b*) width.

Thus, the following factorial ILLI-SLAB runs were performed:

a/l: 0.05, 0.10, 0.20, and 0.30 and

W/l: 2.0, 2.5, 3.0, 3.5, 4.0, 4.5, 5.0, 6.0, and 7.0.

Note that *L/l* was kept at a constant value of 7.0 for all runs. The pertinent input parameters were the same as before. A three-dimensional perspective plot for the relationship of R_w, *a/l*, and *W/l* is shown in Figure 1(*b*). As expected the slab width effect is not very significant. In fact this effect is negligible when *W/l* is greater than 3 or 4. Besides, this effect is more pronounced for a pavement slab with a smaller *W/l* but a larger *a/l*.

Similarly, the following one-term projection model was developed:

$$R_w = 1.00477 + 0.01214\Phi_1(ATX1) \quad (21)$$

$$\Phi_1(ATX1) = -0.5344 + 1.6540(1 - ATX1)^{-10.7412} \quad (22)$$

$$ATX1 = 0.9951\,\frac{a}{l} - 0.09856\,\frac{W}{l} \quad (23)$$

Statistics: $N = 36$, $R^2 = 0.947$, SEE = 0.00299, CV = 0.30 percent

Limits: $2.0 \leq W/l \leq 7.0$, $0.05 \leq a/l \leq 0.3$

Because of the limited number of runs performed and the narrow range of the adjustment factors obtained, this projection model was not as accurate as expected. However, it is relatively adequate for practical pavement design. With finer grids and more finite-element runs performed, the above equations can easily be improved by using the same modeling approach to achieve a higher degree of accuracy if necessary.

EFFECT OF THERMAL CURLING ONLY

The effect of a linear temperature differential and the finite extent of slab sizes must be considered together, since the principles of superposition cannot be applied here. To account for the theoretical difference between Westergaard's solution and the finite-element model, an adjustment factor (R_c) for curling may be defined as:

$$R_c = \frac{\sigma_i}{\sigma_c} = f\left(\alpha\Delta T, \frac{L}{l}, \frac{W}{l}, \frac{\gamma h^2}{kl^2}\right) \quad (24)$$

where σ_c is Westergaard's and Bradbury's edge stress solution given in Equation 9 (FL^{-2}).

Note that the adjustment factor introduced here is undefined when there is no temperature differential across the slab thickness. If temperature differentials are small, the ILLI-SLAB results caused by daytime curling are approximately equal to those caused by nighttime curling. The difference between them becomes substantial because of the combination effects of the self-weight of the concrete slab and the different extent of the loss of subgrade support caused by higher temperature differentials. Therefore, predictive models were separately developed for each daytime (positive ΔT) and nighttime (negative ΔT) curling condition.

Preliminary Analysis

To investigate the combination effects of a linear temperature differential, a finite slab length, and a finite slab width, the following full factorial ILLI-SLAB runs were performed:

L/l: 3, 5, 7, 9, 11, 13, and 15;

W/l: 3, 5, 7, 9, 11, 13, and 15; and

ΔT: ±10, ±20, ±30, and ±40°F.

The symmetry option of the program was used to allow finer grids generated for the ILLI-SLAB runs. A constant slab thickness of 10.59 in. with an elastic concrete modulus of 5×10^6 psi over a subgrade with a *k*-value of 200 pci was also chosen for these runs. The coefficient of thermal expansion α was 5.5×10^{-6}/°F, and the slab Poisson's ratio was 0.15. The unit weight of concrete slab (γ) was set to 0.087 pci because it is approximately constant in practice. [Note that 1°F = (°F − 32)/1.8°C, 1 in. = 2.54 cm, 1 lb/in.^{2} = 6.89 kPa, 1 pci = 0.27 MN/m^3.]

The relationships among these variables and adjustment factors for the daytime curling condition are displayed in Figure 2. Through the assistance of graphical displays the overall trend and the individual adjustment factor can be easily identified. In this manner any extraordinary behavior of the data may be located as well. As expected, the *L/l* requirement for an infinite slab condition is higher for higher temperature differentials. The theoretical discrepancy is higher for a shorter slab with a large negative temperature differential. On the basis of this investigation, those shorter slabs having both *L/l* and *W/l* equal to 3.0 were decided to be excluded from later predictive model development. It is mainly because numerical difficulties might arise while taking the ratio of small ILLI-SLAB results and small theoretical Westergaard solutions. Any approximation that resulted from the ILLI-SLAB program might adversely affect the accuracy of the adjustment factors.

Attempts to develop predictive models with only these three important variables were not very successful. This was also the main reason that prompted the authors to search for an additional mechanistic variable, as previously discussed.

Predictive Models for Thermal Curling Only

Additional ILLI-SLAB runs were apparently necessary since D_γ was unintentionally kept at a constant value in the previous factorial runs, that is, D_γ was equal to 3.07E-05. Thus, the following full factorial finite-element runs were performed:

W/l: 3, 7, and 11;

L/l: 3, 5, 7, 9, 11, 13, and 15;

ΔT: ±20 and ±40°F; and

D_γ: 0.78E-05, 6.13E-05, and 11.03E-05.

This was done by simply changing the unit weight of the concrete slab from the previous 0.087 pci to 0.022, 0.174, and 0.313 pci (1 pci = 0.27 MN/m^3) while keeping all the rest of the input parameters the same as before. Together with those 392 cases previously analyzed, a total of 644 ILLI-SLAB runs that repre-

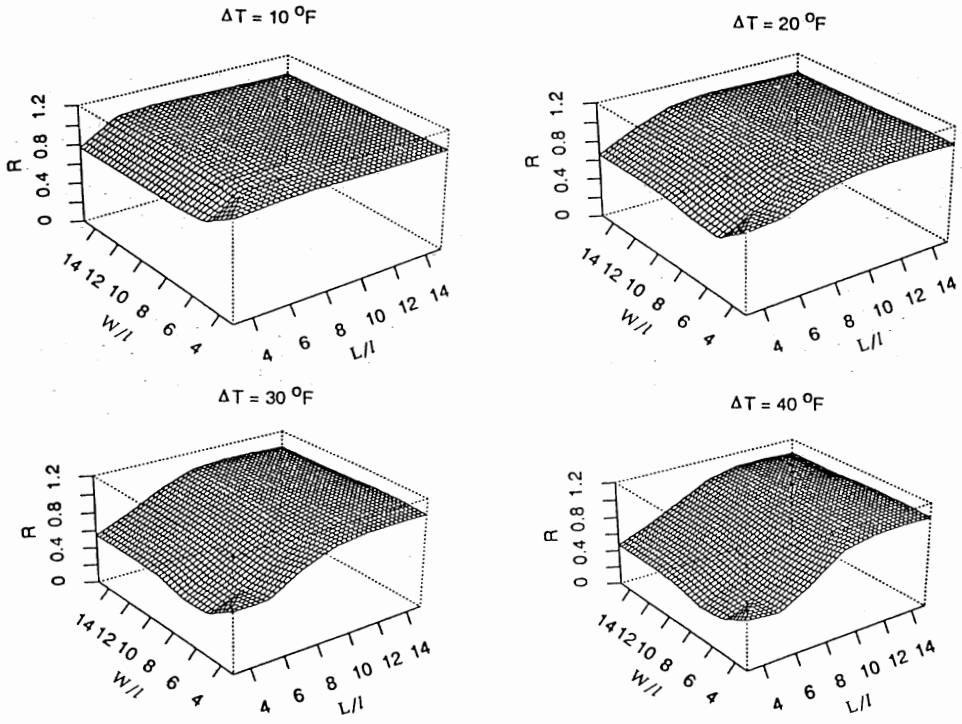

FIGURE 2 Effects of a positive temperature differential and finite slab size.

sented a partial factorial of these four dimensionless parameters were obtained to develop the following predictive models.

In general, the adjustment factor may be adequately defined by the sum of a series of projected curves by using only these dimensionless parameters as independent variables. However, it was decided not to rely only on the projection algorithm for modeling variable interactions to obtain the least number of projected curves for this high dimensional response surface (five dimensions). Some highly probable interaction terms were tested and included during the modeling process as well. By doing so, only a limited number of projected curves, which are more comprehensible to the user and which can be easily formulated, are necessary for the model.

For the daytime curling condition the following two-term projection model was developed (note that a piecewise linear model was chosen to represent these projected curves):

$$R_c = 0.88369 + 0.22005\Phi_1(ATX1) + 0.02383\Phi_2(ATX2) \quad (25)$$

$$\Phi_1(ATX1) = \begin{cases} -2.8903 + 2.7825ATX1 + 1.2565ATX1^2, \\ \qquad \text{if } ATX1 \le 0.85 \\ -2.4275 + 4.9285ATX1 - 1.9459ATX1^2, \\ \qquad \text{if } 0.85 < ATX1 \le 1.5 \\ 0.8111 - 0.1409ATX1, \text{ if } ATX1 > 1.5 \end{cases} \quad (26)$$

$$\Phi_2(ATX2) = \begin{cases} 2.3228 - 3.8187ATX2 - 52.8964ATX2^2, \\ \qquad \text{if } ATX2 \le -0.2 \\ -0.1891 - 0.2237ATX2 + 6.3312ATX2^2, \\ \qquad \text{if } -0.2 < ATX2 \le 0.6 \\ 25.7909 - 58.8336ATX2 + 32.4322ATX2^2, \\ \qquad \text{if } ATX2 > 10.6 \end{cases} \quad (27)$$

$$ATX1 = 0.00656\frac{W}{l} + 0.09886\frac{L}{l} - 0.02621ADT - 0.01857DG + 0.99456\log_{10}DG + 0.00129DG\frac{L}{l} \quad (28)$$

$$ATX2 = -0.00306\frac{W}{l} + 0.01649\frac{L}{l} + 0.02163ADT + 0.01336DG - 0.99953\log_{10}DG + 0.00413DG\frac{L}{l} \quad (29)$$

Statistics: $N = 312$, $R^2 = 0.987$, SEE = 0.0248, CV = 2.81 percent

Similarly, the following two-term projection model was developed for the nighttime curling condition:

$$R_c = 0.69811 + 0.36425\Phi_1(ATX1) + 0.03841\Phi_2(ATX2) \quad (30)$$

$$\Phi_1(ATX1) = \begin{cases} -1.5663 + 1.3093ATX1 + 0.7435ATX1^2, \\ \qquad \text{if } ATX1 \le 0.5 \\ -2.3037 + 3.6569ATX1 - 1.0298ATX1^2, \\ \qquad \text{if } 0.5 < ATX1 \le 2 \\ 1.0017 - 0.0272ATX1, \text{ if } ATX1 > 2 \end{cases} \quad (31)$$

$$\Phi_2(ATX2) = \begin{cases} -0.5836 + 1.0057ATX2 + 0.9323ATX2^2, \\ \qquad \text{if } ATX2 \le 1 \\ -0.9296 + 2.2040ATX2, \text{ if } ATX2 > 1 \end{cases} \quad (32)$$

$$ATX1 = -0.02688\frac{W}{l} + 0.13185\frac{L}{l} + 0.04738ADT - 0.02553DG + 0.98938\log_{10}DG + 0.01089DG\frac{L}{l} \quad (33)$$

$$ATX2 = -0.14612\frac{W}{l} + 0.01252\frac{L}{l} - 0.10378ADT - 0.01890DG - 0.98355\log_{10}DG + 0.00053DG\frac{L}{l} \quad (34)$$

Statistics: N = 312, R^2 = 0.986, SEE = 0.0431, CV = 6.17 percent
Where: $ADT = \alpha\Delta T \times 10^5$, $DG = D_\gamma \times 10^5$.
Limits: $3 \le L/l \le 15$, $3 \le W/l \le 15$, $5.5 \le ADT \le 22$, $0.78 \le DG \le 11.03$

EFFECT OF LOADING PLUS THERMAL CURLING

The combination effects of loading and thermal curling cannot be adequately described by simply superimposing the individual effects of loading and thermal curling alone, since the assumption of a condition of full contact between the slab and subgrade is often violated. Thus, the following adjustment factor (R_T) was introduced to quantify this difference (*20*):

$$\sigma_i = \sigma_L + R_T\sigma_c \quad (35)$$

Together with knowledge of the dominating mechanistic variables involved, the adjustment factor can be determined by the following expression:

$$R_T = \frac{\sigma_i - \sigma_L}{\sigma_c} = f\left(\frac{a}{l}, \alpha\Delta T, \frac{L}{l}, \frac{W}{l}, \frac{\gamma h^2}{kl^2}, \frac{Ph}{kl^4}\right) \quad (36)$$

where σ_L is the edge stress determined by the finite-element model because of loading alone, which may be estimated by $(R_L \cdot R_W \cdot \sigma_w)$ (FL^{-2}).

Preliminary Analysis

A preliminary analysis was conducted by using the following four parameters: a/l, L/l, W/l, and $\alpha\Delta T$. The following full factorial ILLI-SLAB runs were performed:

a/l: 0.05, 0.1, 0.2, and 0.3;

L/l: 3, 5, 7, 9, 11, 13, and 15;

W/l: 3, 5, 7, 9, and 11; and

ΔT: 0, ±20, and ±40°F.

The pertinent input parameters are given in Table 3. Extreme difficulties were encountered while using only these four dimensionless parameters to develop a predictive model for the adjustment factor. The addition of more interaction terms and more projected curves did not resolve this model inadequacy either. This problem also prompted us to search for the additional dimensionless mechanistic variables as discussed previously.

Predictive Models for Loading Plus Thermal Curling

To assess the effect of all six parameters on edge stress it was necessary to perform additional ILLI-SLAB runs. However, a complete full factorial of these six parameters, which requires a tremendous amount of computer time, is not feasible. Thus, it was decided to generate a smaller supplemental factorial that could be added to the previous data base to form a partial factorial for later model development. The data previously presented gave four D_γ values (3.07E-05, 2.47E-05, 2.72E-05, and 2.52E-05) and four D_P values (2.61E-05, 10.82E-05, 39.34E-05, and 114.40E-05) corresponding to four a/l values of 0.05, 0.1, 0.2, and 0.3. In other words, a/l and D_P were correlated with each other. To randomize the relationship among a/l, D_γ, and D_P, a smaller full factorial on the basis of the following parameters was performed:

a/l: 0.05, 0.1, 0.2, and 0.3;

L/l: 3, 5, 7, 9, 11, 13, and 15;

W/l: 3, 7, and 11; and

ΔT: 0, ±10, and ±30°F

This was done by changing the unit weight of the concrete slab and the total wheel load (or tire pressure) while keeping the other input parameters the same as before for different a/l values. The pertinent input parameters are given in Table 4.

For the case of daytime curling plus loading the following three-term projection model was developed:

$$R_T = 0.94825 + 0.15054\Phi_1(ATX1) + 0.03724\Phi_2(ATX2) + 0.03395\Phi_3(ATX3) \quad (37)$$

$$\Phi_1(ATX1) = \begin{cases} -2.5575 + 0.8003ATX1, & \text{if } ATX1 \le 3 \\ -2.6338 + 1.1038ATX1 - 0.0914ATX1^2, & \text{if } 3 < ATX1 \le 7 \\ 0.7564 - 0.0155ATX1, & \text{if } ATX1 > 7 \end{cases} \quad (38)$$

$$\Phi_2(ATX2) = \begin{cases} -0.6788 + 0.0107ATX2, & \text{if } ATX2 \le 3 \\ 3.7674 - 2.2970ATX2 + 0.2963ATX2^2, & \text{if } 3 < ATX2 \le 7 \\ -7.0337 + 1.2945ATX2, & \text{if } ATX2 > 7 \end{cases} \quad (39)$$

$$\Phi_3(ATX3) = \begin{cases} 4.0843 + 4.8241ATX3, & \text{if } ATX3 \le -1 \\ 0.1815 + 0.0541ATX3 - 1.0899ATX3^2, & \text{if } -1 < ATX3 \le 0.5 \\ 0.0453 + 0.0383ATX3, & \text{if } ATX3 > 0.5 \end{cases} \quad (40)$$

$$ATX1 = -0.04724\frac{W}{l} + 0.56954\frac{L}{l} - 0.08408ADT + 0.20033\frac{a}{l} - 0.26647DG + 0.00375DP + 0.73881\frac{a}{l}\frac{L}{l} - 0.01142ADT\frac{L}{l} + 0.09530DG\frac{L}{l} + 0.01121DG\frac{W}{l} \quad (41)$$

TABLE 4 Pertinent Input Parameters for Loading Plus Curling (Additional Runs)

a/l	c	a	E	k	h	l	γ	p	P	DG	DP
	in.	in.	Mpsi	pci	in.	in.	pci	psi	lbs		
0.05	2.5*	1.995	5	200	10.59	39.89	0.030	5000	62500	1.06	130.74
0.10	5.0	2.821	4	300	8.23	28.21	0.350	600	15000	9.93	64.94
0.20	10.0	5.642	3	400	9.97	28.21	0.170	250	25000	5.31	98.34
0.30	10.0	5.642	2	500	7.16	18.81	0.300	10	1000	8.69	11.44

Note:

1. Load dimensions are c x c, except those starred cases use 2c x c. α = 5.5E-06 /°F, μ = 0.15, DG = D_γ x 10^5, DP = D_P x 10^5.
2. 1 °F = (F - 32) / 1.8 °C, 1 lb = 4.45 N, 1 inch = 2.54 cm, 1 psi = 6.89 kPa, 1 pci = 0.27 MN/m^3.

$$ATX2 = 0.03869\frac{W}{l} + 0.35781\frac{L}{l} + 0.09078ADT - 0.04054\frac{a}{l} + 0.86388DG + 0.01635DP - 0.31246\frac{a}{l}\frac{L}{l} + 0.00552ADT\frac{L}{l} - 0.12677DG\frac{L}{l} - 0.01765DG\frac{W}{l} \quad (42)$$

$$ATX3 = 0.58567\frac{W}{l} + 0.25804\frac{L}{l} + 0.14784ADT + 0.14984\frac{a}{l} + 0.12743DG - 0.05012DP + 0.72295\frac{a}{l}\frac{L}{l} - 0.01310ADT\frac{L}{l} - 0.01304DG\frac{L}{l} - 0.06591DG\frac{W}{l} \quad (43)$$

Statistics: N = 432, R^2 = 0.970, SEE = 0.0280, CV = 2.95 percent

Similarly, the following three-term projection model was developed for the case of nighttime curling plus loading:

$$R_T = 0.76068 + 0.28490\Phi_1(ATX1) + 0.10707\Phi_2(ATX2) + 0.10048\Phi_3(ATX3) \quad (44)$$

$$\Phi_1(ATX1) = \begin{cases} -2.5301 + 0.3866ATX1, \text{ if } ATX1 \le 6 \\ -4.0938 + 0.8799ATX1 - 0.0395ATX1^2, \text{ if } 6 < ATX1 \le 12 \\ 0.3181 + 0.0435ATX1, \text{ if } ATX1 > 12 \end{cases} \quad (45)$$

$$\Phi_2(ATX2) = \begin{cases} -1.4980 - 1.1359ATX2, \text{ if } ATX2 \le -1 \\ -0.4956 - 0.0892ATX2 + 0.0174ATX2^2, \text{ if } -1 < ATX2 \le 5 \\ -1.1278 + 0.1075ATX2, \text{ if } ATX2 > 5 \end{cases} \quad (46)$$

$$\Phi_3(ATX3) = \begin{cases} 3.6341 + 0.6512ATX3, \text{ if } ATX3 \le -7 \\ -0.2683 - 0.6808ATX3 - 0.1116ATX3^2, \text{ if } -7 < ATX3 \le -1 \\ 0.1966 - 0.2061ATX3, \text{ if } ATX3 > -1 \end{cases} \quad (47)$$

$$ATX1 = -0.13971\frac{W}{l} + 0.85779\frac{L}{l} + 0.07003ADT + 0.19562\frac{a}{l} + 0.36589DG + 0.05950DP - 0.24211\frac{a}{l}\frac{L}{l} + 0.07242DG\frac{L}{l} - 0.00482DP\frac{L}{l} + 0.00797ADT\frac{L}{l} + 0.01220ADT\frac{W}{l} \quad (48)$$

$$ATX2 = -0.15106\frac{W}{l} + 0.08443\frac{L}{l} + 0.28234ADT - 0.48812\frac{a}{l} + 0.17449DG - 0.03194DP - 0.78445\frac{a}{l}\frac{L}{l} - 0.01999DG\frac{L}{l} + 0.00206DP\frac{L}{l} - 0.06949ADT\frac{L}{l} - 0.00419ADT\frac{W}{l} \quad (49)$$

$$ATX3 = 0.10960\frac{W}{l} - 0.60315\frac{L}{l} - 0.26836ADT + 0.06965\frac{a}{l} - 0.71547DG - 0.12704DP + 0.02846\frac{a}{l}\frac{L}{l} + 0.13364DG\frac{L}{l} + 0.01088DP\frac{L}{l} + 0.02248ADT\frac{L}{l} + 0.00260ADT\frac{W}{l} \quad (50)$$

Statistics: N = 432, R^2 = 0.961, SEE = 0.0546, CV = 7.17 percent

Where: $ADT = \alpha\Delta T \times 10^5$, $DG = D_\gamma \times 10^5$, $DP = D_P \times 10^5$
Limits: $0.05 \leq a/l \leq 0.30$, $3 \leq L/l \leq 15$, $3 \leq W/l \leq 11$, $5.5 \leq ADT \leq 22$, $1.06 \leq DG \leq 9.93$, $2.61 \leq DP \leq 140.74$

VALIDATION OF PROPOSED PREDICTIVE MODELS

To further validate the applicability of the developed predictive models, a series of ILLI-SLAB factorial runs were performed on the basis of a wide range of input parameters. These factorial runs were totally independent of the previous modeling process. The following input parameters covering most of the practical cases found in the field were selected:

Elastic modulus of the concrete, E = 3.0, 5.5, and 8.0 Mpsi;
Modulus of subgrade reaction, k = 50, 250, and 500 pci;
Slab length, L = 10, 20, and 30 ft;
Slab thickness, h = 8, 12, and 16 in.; and
Temperature differential, $\Delta T = \pm 20$ and ± 40°F.
[Note: 1 psi = 6.89 kPa, 1 pci = 0.27 MN/m^3, 1 ft = 30.48 cm, 1°F = (F − 32)/1.8°C.]

The above factorial runs (324 runs) were performed for the case of curling only without an external wheel load being applied. The width of the slab was 12 ft, the slab Poisson's ratio was 0.15, the coefficient of thermal expansion was 5.5×10^{-6}/°F, and the unit weight of concrete slab was set to 0.087 pci.

For the case of loading only, a wheel load of 9,000 lb (40 KN) was applied to the 10-ft slabs, whereas an 18,000-lb (80-KN) load was applied to the other 20- and 30-ft slabs. The tire pressure was set to 90 psi. Thus, a single loaded rectangle of the size of 10 × 10 or 20 × 10 in.^{2} was used for the 10-ft slabs or the 20- and 30-ft slabs, respectively. Therefore, only 81 ILLI-SLAB runs were performed. As for the case of loading and curling, a total of 324 runs similar to the case of curling only but with the wheel loads were performed.

Thus, the above factorials essentially result in a group of pavement slabs whose data ranges are a/l = 0.07 to 0.35, L/l = 1.4 to 15.9, W/l = 1.7 to 6.4, $\alpha\Delta T = -0.00022$ to 0.00022, D_γ = 1.3E-05 to 9.7E-05, and D_P = 5.2E-05 to 110.0E-05. To examine the applicability of the predictive models to pavement slabs with any other input parameters, some of the datum points that are outside the specified limits of the proposed predictive models were not considered.

The adequacy of the proposed predictive models for the effects of loading alone, thermal curling alone, and loading plus curling were further validated by using the above factorial data. The predicted edge stresses are plotted against the actual values as shown in Figure 3(*a*), (*b*), and (*c*), respectively. Clearly, these predictive models were able to make fairly good predictions for these data. Thus, it further reconfirmed the applicability of the proposed predictive models.

CALCULATED VERSUS MEASURED STRESSES

The edge stresses computed by the proposed predictive models were compared with the actual measured stress from the AASHO Road Test (*21*) and the Arlington Road Test (*8*). Favorable agreements (*19*) have also been achieved for the three cases analyzed.

NUMERICAL EXAMPLES

Consider a pavement slab with the following characteristics: E = 5.5 Mpsi, k = 250 pci, L = 10 ft, W = 12 ft, h = 12 in., γ = 0.087 pci, μ = 0.15, and $\alpha = 5.5 \times 10^{-6}$/°F. A single wheel load of 9,000 lb with a loaded rectangle of the size of 10 × 10 in.^{2} is applied. A linear temperature differential of +20°F (daytime condition) exists through the slab thickness. Determine the critical edge stresses due to loading alone, curling alone, and loading plus curling. [Note: 1 psi = 6.89 kPa, 1 pci = 0.27 MN/m^3, 1 ft = 30.48 cm, 1 in. = 2.54 cm, 1°F = (F − 32)/1.8°C, 1 lb = 4.45 N.]

The equivalent radius of the loaded area is a = 5.64 in., and the radius of relative stiffness of the slab-subgrade system is l = 31.20 in. Therefore, the actual dominating mechanistic variables are a/l = 0.18, L/l = 3.83, W/l = 4.60, $\alpha\Delta T$ = +11.0E-05, D_γ = 2.27E-05, and D_P = 29.99E-05. The theoretical Westergaard's solutions on the basis of Equations 1 and 9 are σ_w = 345.75 psi and σ_c = 118.25 psi for loading only and curling only, respectively.

For the case of loading only the adjustment factors for finite slab length and width are R_L = 0.968 and R_W = 1.000 by using Equations 17 and 21, respectively. Thus, the edge stress determined by the proposed models is 0.968 × 1.000 × 345.75 = 334.7 psi. (Note that the actual ILLI-SLAB edge stress was 344.36 psi.)

For the case of curling only, the adjustment factor is R_c = 0.570, which is determined by Equation 25. This gives a predicted edge stress of 118.25 × 0.570 = 67.40 psi. (Note that the actual ILLI-SLAB edge stress was 68.4 psi.)

For the case of loading plus curling the adjustment factor is R_T = 0.732 based on Equation 37. Thus, the predicted total edge stress determined by the proposed model is 334.7 + 0.732 × 118.25 = 421.3 psi by using Equation 35. (Note that the actual ILLI-SLAB edge stress was 436.42 psi for this case.)

CONCLUSIONS

The edge stress of a concrete pavement due to the individual and combination effects of a single wheel load and a linear temperature differential across the slab thickness was conducted in the present study. The subgrade was assumed to act as a dense liquid foundation.

On the basis of previous research using dimensional analysis, the major independent variables were normalized load radius (a/l), normalized slab length (L/l), normalized slab width (W/l), and a dimensionless product ($\alpha\Delta T$) of a temperature differential and thermal expansion coefficient. However, by using only these four parameters the actual structural response to a temperature influence could not be described adequately. Fortunately, two additional dimensionless parameters (D_γ and D_P) representing the relative deflection stiffness due to the self-weight of the concrete slab, the applied load, and the possible loss of support were recently identified. With this discovery the problems encountered in previous investigations (*12*) in which dimensional analysis was used for thermal-related curling problems are now resolved.

A new predictive modeling procedure proposed by Lee (*19*), which makes use of the projection pursuit regression (PPR or projection) algorithm and traditional linear and nonlinear regression techniques, was used to develop the proposed models. The new models use only the dominating mechanistic variables, as opposed to earlier attempts, which used an arbitrary linear combination of input parameters with few insights into the actual re-

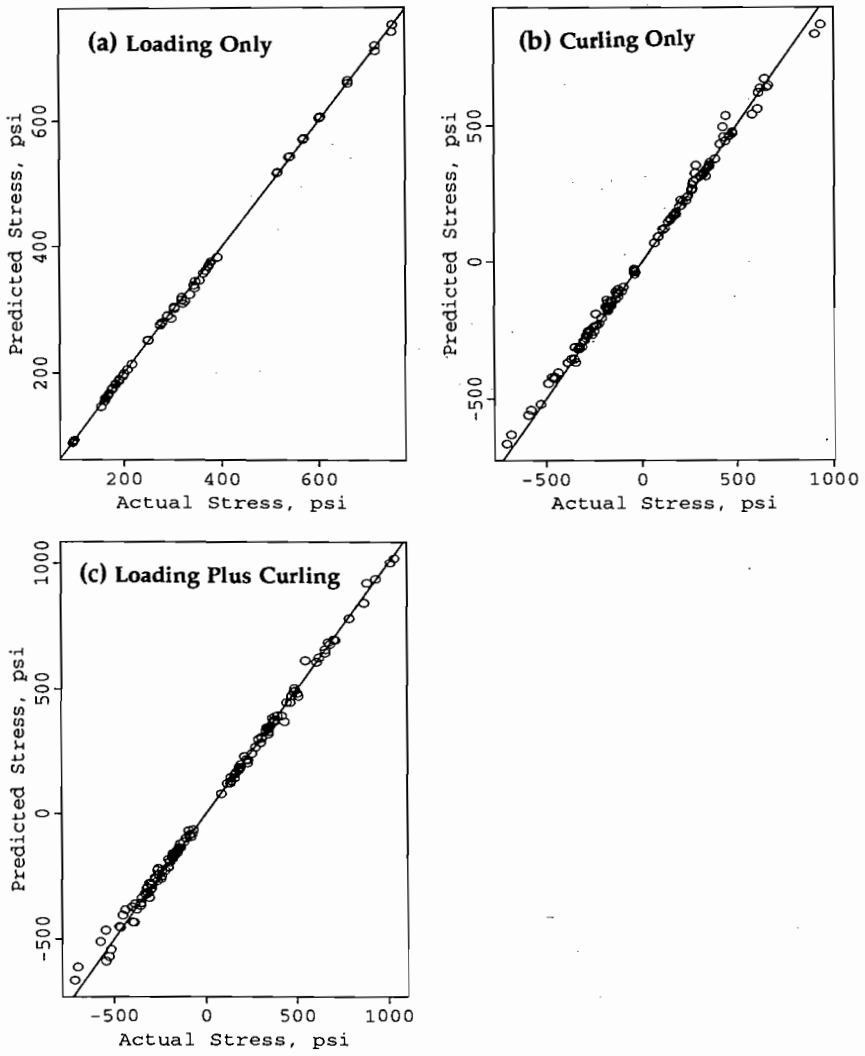

FIGURE 3 Validation of the proposed models for: (*a*) loading only, (*b*) curling only, and (*c*) loading plus curling.

lationships among the variables. Consequently, three closed-form mechanistic design models that have been carefully validated and that are ready for implementation on a spreadsheet or computer program were presented. These stress models turned out to be very accurate representations of the finite-element model.

The new models were also properly formulated to satisfy applicable engineering boundary conditions. They are also simple, easy to comprehend, and dimensionally correct and may be extrapolated to wider ranges of other input parameters. Practical numerical examples showing the use of the new models are also provided.

The predictive models cover almost all practical ranges of pavement designs. Because they are dimensionally correct they can be used in any other unit systems as well. However, extrapolation outside the specified ranges of these dominating parameters is not recommended. Practical pavement design guidelines for edge stress analysis may be easily developed on the basis of these predictive models, together with the use of some reliability concepts. Besides, the predictive modeling procedures and the deflection ratio concept can be used in other pavement-related modeling problems as well.

ACKNOWLEDGMENTS

This research work was sponsored by the Illinois Department of Transportation. The authors are grateful to James Hall for assistance in this project.

REFERENCES

1. Westergaard, H. M. Computation of Stresses in Concrete Roads. In *HRB Proc.*, Vol. 5, Part I, HRB, National Research Council, Washington, D.C., 1926, pp. 90–112. Also in "Stresses in Concrete Pavements Computed by Theoretical Analysis." *Public Roads*, Vol. 7, No. 2, April 1926, pp. 25–35.
2. Westergaard, H. M. Stress Concentrations in Plates Loaded over Small Areas. *Transactions*, Vol. 108, 1943, pp. 831–886. Also in *ASCE Proc.*, Vol. 68, No. 4, April 1942.

3. Westergaard, H. M. New Formulas for Stresses in Concrete Pavements
of Airfields. *Transactions*, Vol. 113, 1948, pp. 425–444. Also in *ASCE Proceedings*, Vol. 73, No. 5, May 1947.
4. Ioannides, A. M., and R. A. Salsilli-Murua. Temperature Curling in Rigid Pavements: An Application of Dimensional Analysis. In *Transportation Research Record 1227*, TRB, National Research Council, Washington, D.C., 1989.
5. Ioannides, A. M., M. R. Thompson, and E. J. Barenberg. The Westergaard Solutions Reconsidered. In *Transportation Research Record 1043*, TRB, National Research Council, Washington, D.C., 1985.
6. Westergaard, H. M. Analysis of Stresses in Concrete Pavements due to Variations of Temperature. *HRB Proc.*, Vol. 6, HRB, National Council, Washington, D.C., 1926, pp. 201–217. Also in *Public Roads*, Vol. 8, No. 3, May 1927.
7. Bradbury, R. D. *Reinforced Concrete Pavements*. Wire Reinforcement Institute, Washington, D.C., 1938.
8. Teller, L. W., and E. C. Sutherland. The Structural Design of Concrete Pavements, Part 2. *Public Roads*, Vol. 16, No. 9, Nov. 1935.
9. Tabatabaie-Raissi, A. M. *Structural Analysis of Concrete Pavement Joints*. Ph.D. thesis. University of Illinois, Urbana, 1978.
10. Ioannides, A. M. *Analysis of Slabs-on-Grade for a Variety of Loading and Support Conditions*. Ph.D. thesis. University of Illinois, Urbana, 1984.
11. Korovesis, G. T. *Analysis of Slab-on-Grade Pavement Systems Subjected to Wheel and Temperature Loadings*. Ph.D. thesis. University of Illinois, Urbana, 1990.
12. Salsilli-Murua, R. A. *Calibrated Mechanistic Design Procedure for Jointed Plain Concrete Pavements*. Ph.D. thesis. University of Illinois, Urbana, 1991.
13. Hastie, T. J., and R. J. Tibshirani. *Generalized Additive Models. Monographs on Statistics and Applied Progability* 43. Chapman & Hall, 1990.
14. Friedman, J. H., and W. Stuetzle. Projection Pursuit Regression. *Journal of the American Statistical Association*, Vol. 76, 1981, pp. 817–823.
15. Becker, R. A., J. M. Chambers, and A. R. Wilks. *The New S Language—A Programming Environment for Data Analysis and Graphics*. The Wadsworth & Brooks/Cole Computer Science Series, AT&T Bell Laboratories, 1988.
16. *S-PLUS for DOS: Reference Manual*, Version 2.0. Statistical Sciences, Inc., Seattle, Wash., Nov. 1991.
17. *S-PLUS for DOS: User's Manual*, Version 2.0. Vol. 1 and 2, Statistical Sciences, Inc., Seattle, Wash., Nov. 1991.
18. Chambers, J. M., and T. J. Hastie. *Statistical Models in S*. Wadsworth & Brooks/Cole Computer Science Series, AT&T Bell Laboratories, 1992.
19. Lee, Y. H. *Development of Pavement Prediction Models*. Ph.D. thesis. University of Illinois, Urbana, 1993.
20. Darter, M. I. Design of Zero-Maintenance Plain Jointed Concrete Pavement, Vol. I. Development of Design Procedures. Report FHWA-RD-77-111. FHWA, U.S. Department of Transportation, 1977.
21. *Special Report 61E: The AASHO Road Test, Report 5: Pavement Research*. Publication 954. HRB, National Research Council, Washington, D.C., 1962.

Publication of this paper sponsored by Committee on Rigid Pavement Design.

New Predictive Modeling Techniques for Pavements

YING-HAUR LEE AND MICHAEL I. DARTER

Statistical regression algorithms have been utilized extensively in pavement engineering for more than three decades. Multiple linear regression, stepwise regression, and nonlinear regression techniques are the most popular ones for pavement predictive modeling. The advantages, the deficiencies, and the limitations of these regression techniques are reviewed. To minimize these problems, the projection pursuit regression (PPR) introduced by Friedman and Stuetzle (1981) was selected to assist in the proper selection of functional forms. Through the use of local smoothing techniques, the PPR attempts to model the response surface as a sum of nonparametric functions of projections of the explanatory variables. The projected terms are essentially two-dimensional curves that can be graphically represented, easily visualized, and properly formulated. As a result a two-step predictive modeling approach is proposed and demonstrated in a case study for the prediction of the edge stress of a pavement slab. It is also demonstrated that statistical regression techniques should not be used alone to obtain a more reliable and comprehensive predictive model. The importance of subject-related engineering knowledge, the principles of dimensional analysis, the proper selecton of functional forms, and applicable engineering boundary conditions are considered essential and are also demonstrated. A comparison of the predictive models previously developed and the proposed approach to "prediction" and "extrapolation" clearly shows the preference of the proposed approach and the promising features of the PPR algorithm.

Statistical regression techniques have been utilized extensively in predicting complicated pavement performance indicators for more than three decades. Multiple linear regression, stepwise regression, and nonlinear regression techniques are the most popular ones among transportation engineers. Undoubtedly, regression analysis is a very important statistical tool for many sciences. This paper starts with a review of the advantages and the limitations of these currently used regression techniques. Some specific problems in the selection of proper functional forms and the violation of some embedded statistical assumptions by use of these techniques are discussed.

Traditional parametric regression techniques such as linear and nonlinear regressions require the imposition of a parametric form on the functions and then obtaining the parameter estimates afterward. In situations in which little knowledge about the shape and the form of a function exists, several new nonparametric regression techniques developed over the past 10 years have gradually gained popularity. Without imposing an unjustified parametric assumption, nonparametric regression techniques strive to estimate the actual functional form that best fits the data through the use of scatter plot smoothers (*1*).

The alternating conditional expectation (ACE) algorithm developed by Breiman and Friedman (*2*) for optimal transformation of multiple regression and correlation does an excellent job in maximizing the squared multiple correlation, R^2 (*1–3*). By using the same alternative backfitting procedures for variable transformations as used in the ACE algorithm, Tibshirani (*4*) introduced the additivity and variance stabilization (AVAS) algorithm, which tries to achieve the constant error variance assumption of regression (*1,4*). Both techniques provide an invaluable tool in suggesting proper transformations of variables. However, neither the ACE nor the AVAS algorithm is capable of modeling interactions between the explanatory variables. The variable interactions must be explicitly specified in the assumed model form.

Consequently, the projection pursuit regression (PPR) introduced by Friedman and Stuetzle (*5*) and Friedman (*6*) is selected because of its ability to handle variable interactions. As a result a two-step predictive modeling approach is proposed and demonstrated in a case study for the prediction of concrete pavement edge stress owing to the finite slab length effect.

The demonstration is based on a comparison between the previous modeling approaches from the zero-maintenance study (*7*), a stress analysis procedure (*8*), and the proposed methodology. The importance of incorporating subject-related engineering knowledge such as the use of the principles of dimensional analysis and the proper selection of functional forms is demonstrated. The proposed modeling procedure illustrates how to select a proper functional form through the use of the PPR as well as the aid of graphical representation and visual inspection. Nonlinear regression is used to obtain the parameter estimates for the specified functional forms. The proper selection of initial parameter estimates is also discussed to guarantee convergence of the iterative nonlinear regression routines. The applications of the resulting predictive models to "prediction" and "extrapolation" are also discussed.

MULTIPLE REGRESSION

Multiple regression is one of the most time-honored and widely used regression techniques for the study of linear relationships among a group of measurable variables. Suppose there exists a true model to describe the relationship between response variables (y's) and explanatory variables (or predictors, x's) (*9–11*):

$$y_i = x_i^T\beta + \epsilon_i \qquad (i = 1, \ldots, n) \tag{1}$$

where x_i^T is the ith row of the $(n \times p)$ matrix X of the column of 1's if an intercept and the explanatory variables are included. The superscript T denotes the transpose of the column vector x_i. β is a $p \times 1$ vector of unknown regression coefficients, and p and n are the number of parameter estimates in the model and the total number of observations, respectively.

Y.-H. Lee, Department of Civil Engineering, Tamkang University, E725, #151, Ying-Chuan Road, Tamsui, Taipei, Taiwan 25137, Republic of China. M. I. Darter, Department of Civil Engineering, University of Illinois, NCEL #1212, 205 North Mathews Avenue, Urbana, Ill. 61801.

The basic assumptions are usually that the random errors (ϵ's) are mutually uncorrelated and normally distributed with zero mean and constant variance and are additive and independent of the expectation function. For any arbitrary β value of $\hat{\beta}$, the residuals $r_i(\hat{\beta})$ can be determined by the following expression:

$$r_i(\hat{\beta}) = y_i - x_i^T\hat{\beta} \quad (i = 1, \ldots, n) \tag{2}$$

On the basis of the above assumptions multiple regression tries to find a set of parameters $\hat{\beta}$ such that the sum of the squared residuals given in Equation 3 is minimized, which is also best known as the least-squares (LS) method.

$$RSS(\hat{\beta}) = \sum_{i=1}^{n} [r_i^2(\hat{\beta})] = r_1^2(\hat{\beta}) + r_2^2(\hat{\beta}) + \cdots + r_n^2(\hat{\beta}) \tag{3}$$

The LS method is best known and most frequently adopted because of its simple structure, elegant LS theory, fast computation time, as well as its estimators, which can be obtained explicitly from the data and are interpretable to its user.

As far as variable selection is concerned, all-subset regression and stepwise regression techniques are often utilized for automatic variable selection for preliminary and exploratory analyses of linear relationships among a group of important variables.

ALL-SUBSET REGRESSION AND STEPWISE REGRESSION

All-subset regression procedure finds all possible combinations of variables in the model when the set of candidate variables is not too large. To select the "best" subset of variables, different measurements including the coefficient of determination (R^2), adjusted R^2 (adj-R^2), and the C_p statistics due to Mallows have been proposed (*11,12*). The Mallows C_p statistic can be defined as follows:

$$C_p = \frac{RSS}{s^2} + 2p - n \tag{4}$$

where RSS represents the residual sum of squares of the regression, p is the number of parameters, and s^2 is the estimate of the residual variance from the full regression model. According to Draper and Smith (*12*), a regression model with "a low C_p value about equal to p" is preferred such that the model fits the actual data better with the least number of parameters (*11,12*).

Stepwise regression uses a forward selection or a backward elimination procedure that iteratively adds or deletes one explanatory variable at a time to find the "best" subset of significant independent variables in the model (*13*). However, this procedure does not necessarily produce the "best" subset among a group of candidate variables. The first variable added or deleted may not necessarily be the best or the worst overall. It is quite possible that the first variable selected by forward selection becomes unnecessary in the presence of the other variables entered afterward or vice versa. In other words, forward selection and backward elimination techniques may result in totally different subsets of variables with similar summary statistics. "It is unlikely that there is a single best subset, but rather several equally good ones," as observed by Gorman and Toman (*14*).

In comparison with the high computational cost of all-subset regression, stepwise regression is one of the most popular techniques used in transportation research because of its fast computation, simplicity of use, and capability in progressively adding or dropping variables in a regression model. It is expected that some latent or lurking variables may be included in a regression model.

Because of the ease of use and the efficiency of computation, stepwise regression may be easily abused in some respects if one fails to recognize possible physical interpretations on the parameter estimates and the embedded basic assumptions. A very long regression model with dozens of parameter estimates may be the typical result of a stepwise regression that fits the data very well but with no comprehensive engineering insight into the data analyzed. Often, some applicable engineering boundary conditions are violated as well.

NONLINEAR REGRESSION

Practical real-world problems are often found to be nonlinear in nature. Because of its favorable feature of handling a complicated nonlinear model, nonlinear regression has been widely used as a modeling technique for pavement research. In addition, some applicable boundary conditions may be incorporated into the specified nonlinear model form and the parameter estimates may have their own physical meanings as well. However, nonlinear models are more difficult to specify and develop than linear models.

Suppose there exists a true model that best describes the relationship between response variables (y's) and explanatory variables (x's) (*10,15*):

$$y_i = F(\beta, x_i) + \epsilon_i \quad (i = 1, \ldots, n) \tag{5}$$

where $F(\beta, x_i)$ is a nonlinear function based on the predictors x_i. β is a $p \times 1$ vector of unknown regression coefficients to be estimated, and n is the total number of observations. Similar to linear regressions, the disturbance (or error) term is usually assumed to be additive, mutually uncorrelated, and normally distributed with zero mean and constant variance. For any arbitrary β value of $\hat{\beta}$, the residuals $r_i(\hat{\beta})$ are

$$r_i(\hat{\beta}) = y_i - F(\hat{\beta}, x_i) \quad (i = 1, \ldots, n) \tag{6}$$

Unlike linear regressions whose parameters can be explicitly estimated by a closed-form expression, nonlinear regressions must use an iterative routine to find the best parameter estimates ($\hat{\beta}$) such that the sum of the squared residuals as given in Equation 3 is minimized.

Before carrying out a nonlinear regression, engineers must first assume a feasible descriptive (or conceptual) model form with the most important parameters prespecified on the basis of previous experience and engineering knowledge. In a two-dimensional factor space the model form can be determined as easily as it can be visualized in a scatter plot. Subsequently, reliable parameter estimates may be obtained.

The situation is quite different for the case of multidimensional (three or higher) factor space, where the data trend and the possible interactions among candidate variables cannot be easily identified. Unfortunately, real engineering problems most likely belong to the latter case, in which higher dimensions are concerned and

the true functional forms are rarely known to engineers. Thus, the proper selection of a plausible functional form from a multidimensional factor space provides a real challenge for pavement engineers.

Guessing initial parameter estimates for a multidimensional model is also a very time-consuming process. It is not uncommon that the resulting model does not converge or contains insignificant parameter estimates, with poor initial parameter estimates and an improper model form. In addition, parameter estimates are sometimes toward the wrong direction of their physical interpretations, and they may depend heavily on the initial starting values as well. Specifying bounds for some parameters is not uncommon, although the final resulting model may eventually reach the assumed bounds but without achieving the specified convergence criterion. Thus, "some models are difficult to fit, and there is no guarantee that the procedure will be able to fit the model successfully" (*10*,p.576).

Furthermore, even when parameter estimates are successfully obtained, the assumption of constant error variance is frequently violated, as indicated by residual analyses. This problem, which is probably due to improper selection of the model form, is often unrecognized, and there is no quick remedy for this situation.

Thus, it is very dangerous to develop such a nonlinear model without acquiring more knowledge of the complicated relationships between the predictors and the dependent variable. The prediction based on an inadequate model specification is also very questionable.

PROJECTION PURSUIT REGRESSION

Unlike the ACE and the AVAS algorithms previously discussed, the projection pursuit regression introduced by Friedman and Stuetzle (*5*) and Friedman (*6*) is capable of modeling interactions between predictor variables when suggesting nonparametric transformations to improve the fit. This algorithm is an exploratory nonlinear regression technique that tries to model the response surface (y's) as a sum of nonparametric functions of projections of the predictor variables (x's) through the use of super smoothers (*5,6*). Assume there exists a true model given as follows (*16*, Vol. 2):

$$y = \bar{y} + \sum_{m=1}^{M_0} \beta_m \Phi_m(a_m^T x) + \epsilon \tag{7}$$

where x is equal to $(x_1, x_2, \ldots, x_p)^T$ and denotes the vector of predictor variables and $\bar{y}$ is the expected value (or mean) of the response variable. The "projection" part of the "projection pursuit regression" indicates that the vector of predictors, x, is projected onto the direction vectors, a_m, to get the lengths of the projection $a_m^T x$, where $m = 1, \ldots, M_0$. The "pursuit" part indicates that an optimization technique is used to find the best direction vectors, a_m. $\Phi_m(a_m^T x)$ stands for the unknown nonparametric transformation functions of the projected lengths $a_m^T x$ to be estimated. ϵ is the random error. Notice that Φ_m has been standardized to have zero mean and the unity variance given in the following expression:

$$E[\Phi_m(a_m^T x)] = 0 \qquad E[\Phi_m^2(a_m^T x)] = 1$$

$$(m = 1, \ldots, M_0) \tag{8}$$

The PPR algorithm strives to minimize the mean squared residuals, $E[r^2]$, over all possible combinations of β_m, Φ_m, and a_m values. This algorithm first performs a forward stepwise fitting procedure starting with a single term and ending up with M_{max} terms. Supersmoother is used to estimate the conditional expectation functions. After having fitted the M_{max} term model in a forward stepwise manner, a backward stepwise procedure is followed and stopped with an M_{min} term model. Notice that M_{max} and M_{min} are the user-specified maximum and minimum number of terms in the model, respectively. The relative importance of each term can be measured by the absolute value of β_m as well. The expectation function of the squared residuals is given as follows:

$$E[r^2] = E\left[y - \bar{y} - \sum_{m=1}^{M_0} \beta_m \Phi_m(a_m^T x)\right]^2 \tag{9}$$

Conceptually, the explanatory variables x's are projected onto the direction vectors $a_1, a_2, \ldots, a_m$, to find good nonlinear transformations $\Phi_1, \Phi_2, \ldots, \Phi_m$ for the multidimensional response surface. In other words, the response surface is broken down into a series of smooth projected terms adding all together. Thus, the largest trend in the factor space is captured as the first projected term Φ_1, and the residuals become the sources for additional projections afterward. More technical details about the development process, the application, and the demonstration on modeling interactions of the PPR algorithm can be found elsewhere (*5,6,16*).

PROPOSED TWO-STEP MODELING APPROACH

The proper selection of regression techniques is one of the most important factors in the success of prediction modeling. Since most of the regression algorithms currently available do not directly consider interaction effects during the modeling process, the interaction terms must be subjectively determined prior to performing a regression analysis. With the multidimensional pavement engineering problems in mind, several unresolved deficiencies are frequently identified in the use of stepwise regression and nonlinear regression. These include problems in the selection of correct functional form, violations of the embedded statistical assumptions, and failure to satisfy some engineering boundary conditions as previously discussed.

The projection pursuit regression, however, appears to have the most favorable features in handling these problems. As a result a two-step regression analysis procedure is proposed herein to better find the correct functional form and to better fit the response surface as well.

1. With the help of the PPR a multidimensional response surface is broken down into the sum of several smooth projected curves that are graphically representable in two dimensions. Plausible functional forms and applicable boundary conditions may then be easily identified and specified through visual inspection or engineering knowledge of the physical relationships to model these individual projected curves separately.
2. Traditional parametric regression techniques such as linear and nonlinear regressions are then utilized for these purposes with higher confidence in the parameter estimates.

The overall regression statistics and the goodness of fit often clearly show the advantages of the proposed two-step modeling

approach over the traditional counterparts. The S-PLUS statistical package (*16–19*), which has been widely used by statisticians, was selected for the analysis due because of the availability of this new regression technique.

EDGE STRESS DUE TO LOADING AND FINITE SLAB LENGTH EFFECTS: CASE STUDY

Since transverse cracking is one of the major structural distresses in jointed concrete pavements, the determination of the maximum bending stress at the longitudinal edge (midway between the transverse joints) is very crucial in any mechanistic or mechanistic-empirical design procedures.

However, the theoretical Westergaard edge stress solution (*20*) based on an infinite slab assumption may not be well suited for the actual finite slab size conditions. To assess the effect of a finite slab length, a series of finite-element (FE) runs are often performed. Unfortunately, the FE model cannot be easily implemented as a part of a design procedure because of the required running time.

Several attempts in edge stress prediction that proved to be very successful in the past are reviewed and discussed below. The basic concepts behind those analysis procedures were to design and perform a full factorial of FE runs under various combinations of different conditions. Statistical regression techniques were utilized to develop predictive models for different situations. The predictive equations were then used as alternatives for design purposes with sufficient accuracy in estimating stresses.

To demonstrate the proposed two-step predictive modeling procedures, the following case study was performed. The purpose of this case study was to demonstrate the advantages of incorporating dimensional analysis and selecting proper functional forms for the predictive models analyzed. Three different approaches are discussed in the following sections:

1. Use arbitrary but "best" linear combinations of individual variables with interaction terms for regression;
2. Introduce as many mechanistic variables as possible on the basis of engineering knowledge, and also find the "best" linear combinations of these variables with interaction terms for regression; and
3. Introduce as many mechanistic variables (or clusters of variables) as before, and also try to find the best functional forms on the basis of the proposed two-step predictive modeling procedures.

Principles of Dimensional Analysis

According to Westergaard (*20,21*), the closed-form stress solution due to a circular edge loading on a semi-infinite slab over a dense liquid foundation on the basis of medium-thick plate theory is given as follows:

$$\sigma = \frac{3(1+\mu)P}{\pi(3+\mu)h^2}\left[\log_e \frac{Eh^3}{100ka^4} + 1.84 - \frac{4\mu}{3} + \frac{1-\mu}{2} + 1.18(1+2\mu)\frac{a}{l}\right] \quad (10)$$

where

σ = theoretical Westergaard edge stress (FL^{-2}),
P = total applied wheel load (F),
a = radius of the applied circular load (L),
E = elastic modulus of the concrete slab (FL^{-2}),
h = slab thickness (L),
μ = slab Poisson's ratio,
k = modulus of subgrade reaction (FL^{-3}), and
l = radius of relative stiffness of the slab subgrade system (L) given by

$$l = \sqrt[4]{\frac{Eh^3}{12(1-\mu^2)k}} \quad (11)$$

[Note that the basic dimensions are abbreviated as length (L) and force (F).]

Through the use of the principles of dimensional analysis, the above stress equation may be reduced to the following equation form in which both sides of the equation are dimensionless (*22,23*).

$$\frac{\sigma h^2}{P} = f\left(\frac{a}{l}\right) \quad (12)$$

Therefore, the above normalized stress equation ($\sigma h^2/P$) is simply a function of the dominating variable, a/l, representing the combination effect of the input parameters, namely E, h, k, and a, for constant μ (usually $\mu \approx 0.15$).

To account for the finite slab length effect, Ioannides et al. (*21*) introduced a normalized length term, L/l, when comparing FE results with the theoretical Westergaard solution. Similarly, a normalized width term, W/l, was introduced to account for the effect of finite slab width. Note that L and W represent slab length and slab width, respectively. However, it is also recognized that the finite slab width effect (W/l) is not as significant as the other two dimensionless parameters (i.e., a/l and L/l), as suggested by earlier investigators (*8,23*).

An adjustment (or multiplication) factor may be introduced to account for the theoretical difference between the Westergaard solution (σ) and the results from the FE model by using only these two dimensionless factors (a/l and L/l). The adjustment factor (R) is defined by the following expression:

$$R = \frac{\sigma_i}{\sigma} = f\left(\frac{a}{l}, \frac{L}{l}\right) \quad (13)$$

where σ_i is the edge stress determined by the FE model.

The advantages of using the principles of dimensional analysis to derive the above formulation are evident. They can be very helpful in identifying the governing dependent and independent variables (or clustered variables) of a given relationship. In addition, they may also help to reduce the number of factorial FE runs needed for the analysis. The above formulation is not only easy to comprehend but is also dimensionally correct. Thus, the resulting edge stress from FE studies (σ_i) can be determined by multiplying the theoretical Westergaard solution and the adjustment factor (R) together, if it is properly formulated.

Use of Arbitrary Linear Combination of Variables

The analysis of edge stress due to different axle loads, slab lengths, slab thicknesses, foundation supports, thermal gradients, and edge supports was initially studied by Darter (*7*). A large full factorial of FE runs was performed to determine the edge stresses for different conditions, and subsequently separate predictive models were developed. For the case of loading only, an 18-kip single axle loading was applied on the following factorial pavement sections:

1. Slab length L = 15, 20, 25, and 30 ft;
2. Slab thickness h = 8, 10, and 14 in.;
3. Foundation support k = 50, 200, and 500 pci; and
4. Edge support ES = 0, 12, 36, and 60 in.

where other pertinent input parameters are

$E = 5 \times 10^6$ psi lb/in^2,
W = 12 ft,
μ = 0.15, and
loaded area per wheel = 12 × 15 in.^{2}.

The results of these FE runs were directly used to derive a regression model for edge stress (σ_L) prediction.

Stepwise regression procedure was utilized to pick the "best" linear combinations of individual variables including interaction terms during the modeling process. The slab length (L) was not proved to affect the edge stress prediction significantly and thus was excluded from the model. The proposed predictive model for single axle load without the loss of edge support (ES = 0) is given as follows:

$$\sigma_L = \frac{\text{load}}{18 \cdot h^2} \cdot \left(17.35783 - 0.05388 \cdot \frac{h^3}{k} + 7.41722 \cdot \log_{10}\frac{h^3}{k}\right) \quad (14)$$

Using Equation 14 to predict the actual calculated edge stresses from the above FE runs, a fairly good agreement is observed.

However, this model does not contain the elastic modulus of the concrete slab (E) and the finite slab length (L) because of the limitations of the factorial runs conducted. The variables included in this model are numerically significant, but they are not the actual dominating factors with correct dimensions. Thus, the applicability of using this equation beyond the ranges of the data for which the model was originally developed such as different E values and other shorter slabs is very questionable.

Introducing Mechanistic Variables (Clustered Variables)

The analysis of edge stress was further studied by Salsilli-Murua (*8*). The concept of equivalent single axle radius (ESAR) was utilized for analyzing different load configurations including dual wheels, tandem gears, and tridem gears. The effects of slab sizes, widened outer lanes or tied shoulders, subbase and subgrade layers, and thermal curling were also analyzed separately. Through the use of the principles of dimensional analysis, a series of small factorial FE runs covering most practical engineering conditions were performed and separate predictive models were developed.

As previously discussed, the effects of wheel loading and finite slab length can be best represented by two dimensionless factors: a/l and L/l. Thus, only a minimum number of factorial FE runs on the basis of these two factors were performed. The adjustment (or multiplication) factor (R) as defined in Equation 13 was also introduced for edge stress prediction. Note that the Westergaard solution (σ) for infinite slab condition is approximated by the resulting ILLI-SLAB edge stress (σ_∞) for L/l = 7.0 herein when calculating the adjustment factor ($R = \sigma_i/\sigma_\infty$).

A multiple stepwise regression procedure was utilized again because of its favorable feature of progressively adding and dropping variables in a regression model. The proposed predictive model is given as follows:

$$R = 0.582282 - 0.533078\left(\frac{a}{l}\right) + 0.181706\left(\frac{L}{l}\right) - 0.019824\left(\frac{L}{l}\right)^2 + 0.109051\left(\frac{a}{l}\right)\left(\frac{L}{l}\right) \quad (15)$$

Statistics: $N = 12$, $R^2 = 0.996$, SEE = 0.0028, CV = 0.29 percent
Limits: $3 \le L/l \le 5$, $0.05 \le a/l \le 0.3$

N is number of datum points, R^2 is the coefficient of determination, SEE is the standard error of estimates, and CV is the coefficient of variation).

His work has repeatedly demonstrated the advantages of using dimensional analysis to discover the underlying dominating factors for the analysis. In addition, the proposed predictive model not only has fairly good agreement with the data analyzed, but it may also be applied to a wide range of input parameters (i.e., E, h, k, and a). This model is also dimensionally correct. The prediction of edge stress is simply a matter of multiplying the theoretical Westergaard solution by the predicted R value on the basis of this model.

Nevertheless, the conclusions should be restricted to the ranges of the data for which the model was originally developed. This is also true for any regression technique chosen to develop such a predictive model. Besides, a reasonable doubt is raised as to the adequacy of the functional form, especially when an asymptotic trend of the relationship between R and L/l is observed. This asymptotic trend could not be captured simply because of the multiple stepwise regression technique chosen. Thus, the usefulness of the model beyond the specified limits is highly questionable.

Selecting Proper Functional Forms

The importance of incorporating subject-related engineering knowledge into the modeling process, as has been done in the previous example in identifying dominating clustered variables, cannot be overemphasized. In addition, the selection of proper functional forms to satisfy some applicable engineering boundary conditions is a crucial component of a successful predictive model. The proposed two-step modeling approach was adopted herein to illustrate this point. The following factorial ILLI-SLAB runs were performed:

a/l: 0.05, 0.1, 0.2, and 0.3 and
L/l: 2.0, 2.5, 3.0, 3.5, 4.0, 4.5, 5.0, 6.0, and 7.0.

Note that *W/l* was set to 7.0 for all runs. The FE grids were generated according to the recommendations of Ioannides (*24*, pp. 187–188) to provide sufficient accuracy. The pertinent input parameters and the results of these factorial runs are presented in Table 1. A three-dimensional perspective plot providing a very clear picture of the relationship among *R*, *a/l*, and *L/l* is shown in Figure 1.

Because the relationship is a nonlinear three-dimensional surface, a nonlinear regression model may be better suited for this prediction purpose than an arbitrarily selected linear or polynomial model form. But, what kinds of functional forms to be used in the model and how to choose a proper one remain unanswered.

The proposed two-step modeling approach is aimed at search-

TABLE 1 ILLI-SLAB Runs on Slab Size Effects

a/l	L/*l*	c	*a*	P	*l*	L	W	E	k	h	σ
0.05	2.0	2.5	1.995	1250	39.89	79.79	279.26	5	200	10.59	40.868
0.05	2.5	2.5	1.995	1250	39.89	99.74	279.26	5	200	10.59	43.559
0.05	3.0	2.5	1.995	1250	39.89	119.68	279.26	5	200	10.59	45.458
0.05	3.5	2.5	1.995	1250	39.89	139.63	279.26	5	200	10.59	46.744
0.05	4.0	2.5	1.995	1250	39.89	159.58	279.26	5	200	10.59	47.536
0.05	4.5	2.5	1.995	1250	39.89	179.52	279.26	5	200	10.59	47.973
0.05	5.0	2.5	1.995	1250	39.89	199.47	279.26	5	200	10.59	48.180
0.05	6.0	2.5	1.995	1250	39.89	239.37	279.26	5	200	10.59	48.287
0.05	7.0	2.5	1.995	1250	39.89	279.26	279.26	5	200	10.59	48.293
0.10	2.0	5.0	2.821	2500	28.21	56.42	197.47	4	300	8.23	100.494
0.10	2.5	5.0	2.821	2500	28.21	70.52	197.47	4	300	8.23	109.154
0.10	3.0	5.0	2.821	2500	28.21	84.63	197.47	4	300	8.23	115.240
0.10	3.5	5.0	2.821	2500	28.21	98.73	197.47	4	300	8.23	119.399
0.10	4.0	5.0	2.821	2500	28.21	112.84	197.47	4	300	8.23	121.952
0.10	4.5	5.0	2.821	2500	28.21	126.94	197.47	4	300	8.23	123.347
0.10	5.0	5.0	2.821	2500	28.21	141.05	197.47	4	300	8.23	123.999
0.10	6.0	5.0	2.821	2500	28.21	169.26	197.47	4	300	8.23	124.304
0.10	7.0	5.0	2.821	2500	28.21	197.47	197.47	4	300	8.23	124.311
0.20	2.0	10.0	5.642	10000	28.21	56.42	197.47	3	400	9.97	178.536
0.20	2.5	10.0	5.642	10000	28.21	70.52	197.47	3	400	9.97	201.014
0.20	3.0	10.0	5.642	10000	28.21	84.63	197.47	3	400	9.97	216.928
0.20	3.5	10.0	5.642	10000	28.21	98.73	197.47	3	400	9.97	227.837
0.20	4.0	10.0	5.642	10000	28.21	112.84	197.47	3	400	9.97	234.529
0.20	4.5	10.0	5.642	10000	28.21	126.94	197.47	3	400	9.97	238.158
0.20	5.0	10.0	5.642	10000	28.21	141.05	197.47	3	400	9.97	239.822
0.20	6.0	10.0	5.642	10000	28.21	169.26	197.47	3	400	9.97	240.510
0.20	7.0	10.0	5.642	10000	28.21	197.47	197.47	3	400	9.97	240.443
0.30	2.0	10.0	5.642	10000	18.81	37.61	131.64	2	500	7.16	251.011
0.30	2.5	10.0	5.642	10000	18.81	47.02	131.64	2	500	7.16	292.598
0.30	3.0	10.0	5.642	10000	18.81	56.42	131.64	2	500	7.16	322.461
0.30	3.5	10.0	5.642	10000	18.81	65.82	131.64	2	500	7.16	342.758
0.30	4.0	10.0	5.642	10000	18.81	75.23	131.64	2	500	7.16	355.316
0.30	4.5	10.0	5.642	10000	18.81	84.63	131.64	2	500	7.16	362.178
0.30	5.0	10.0	5.642	10000	18.81	94.03	131.64	2	500	7.16	365.327
0.30	6.0	10.0	5.642	10000	18.81	112.84	131.64	2	500	7.16	366.408
0.30	7.0	10.0	5.642	10000	18.81	131.64	131.64	2	500	7.16	365.845

a = radius of loaded area, in.
c = load dimensions are c x c, except those cases with c = 2.5 use 2c x c instead, in.
l = radius of relative stiffness, in.
h = slab thickness, in.
E = elastic modulus of concrete, $*10^6$ psi
k = modulus of subgrade reaction, pci
L = slab length, in.
W = slab width, in.
P = total applied load, lb
σ = edge bending stress, psi

The tire pressure was held constant at 100 psi for all the runs.
Note: 1 inch = 2.54 cm, 1 psi = 6.89 kPa, 1 pci = 0.27 MN/m^3, 1 lb = 0.454 kg.

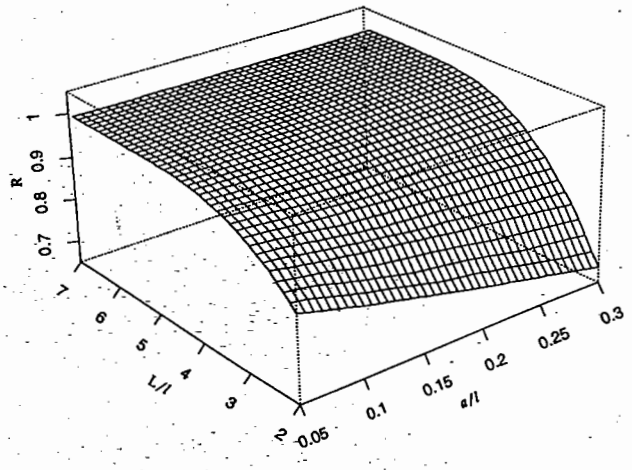

FIGURE 1 Slab size effect: three-dimensional plot.

ing for a series of two-dimensional projected curves first to ease these important modeling decisions. First, the PPR technique was utilized to determine the direction vectors for a/l and L/l and the suggested single-term nonlinear transformation $\Phi_1(a_1^T x)$ by using only those datum points within the specified limits of Equation 15. The results of this PPR trial are given in the following equations:

$$R = 0.9667 + 0.0330\Phi_1(\text{ATX1}) \tag{16}$$

$$\text{ATX1} = -0.8945\frac{a}{l} + 0.4471\frac{L}{l} \tag{17}$$

A graphical representation of this PPR trial is shown in Figure 2. The first two plots are the scatter plots of the one-to-one relationships of R versus a/l and L/l. The next plot shows the resulting first PPR projected term versus the length of the projection, that is, $\Phi_1(a_1^T x)$ versus $a_1^T x$. Notice that $a_1^T x$ is represented by the axis label ATX1, whereas $\Phi_1(\text{ATX1})$ is represented by the axis label "1st Projected Term" in this plot. The goodness-of-fit of this PPR model including a plot of the predicted versus actual values and a plot of the residual versus predicted values is displayed in the last two plots. If this curve is properly modeled and the above two equations are used, fairly good predictions with a relatively high R^2 of 0.995 may be obtained.

Thus, the task was reduced to simply finding a feasible model for this projected curve. An asymptotic trend was clearly identified through visual inspection. Therefore, an asymptotic nonlinear model with two to three (or at most four) parameters may describe this curve adequately. The following four-parameter equation form was selected to offer the maximum flexibility in the modeling process:

$$\Phi_1(\text{ATX1}) = a_1 + \frac{1}{a_2 + a_3\text{ATX1}^{a_4}} \tag{18}$$

The nonlinear regression technique was then used to obtain the parameter estimates. The first derivative of this equation form with respect to each parameter was also provided to help the iterative regression routine converge faster. The starting value of each parameter was carefully chosen so that a_1 and a_4 were large negative values, for example, -4.0, and a_1 was the minimum possible value of Φ_1. Since a_2 and a_3 were still undecided, two small positive values, for example, 0.01, were chosen as their starting points. The following equation satisfies the convergence criteria even with many other different starting values:

$$\Phi_1(\text{ATX1}) = -5.5869 + \frac{1}{0.1473 + 0.2627\text{ATX1}^{-5.1659}} \tag{19}$$

The overall statistics for the prediction of R (or σ_s/σ_∞) because of the slab length effect by using Equations 16, 17, and 19 are summarized as follows:

Statistics: $N = 20$; $R^2 = 0.994$; SEE = 0.0027, CV = 0.28 percent
Limits: $3 \leq L/l \leq 5$, $0.05 \leq a/l \leq 0.3$

To illustrate how the three-dimensional response surface (Figure 1) might be broken down into the sum of a series of two-dimensional curves, the PPR algorithm was utilized again to obtain a two-term model and a three-term model as shown in Figures 3 and 4, respectively. By analogy, the axis labels "ATX2" and "ATX3" represent $a_2^T x$ and $a_3^T x$, respectively, whereas the axis labels "2nd Projected Term" and "3rd Projected Term" represent $\Phi_2(\text{ATX2})$ and $\Phi_3(\text{ATX3})$ in Equation 7, respectively. The other plots are similar to the plots defined in Figure 2.

As an example, the results of the two-term PPR model are given in the following equations:

$$R = 0.9667 + 0.0330\Phi_1(\text{ATX1}) + 0.00210\Phi_2(\text{ATX2}) \tag{20}$$

$$\text{ATX1} = -0.8945\frac{a}{l} + 0.4471\frac{L}{l} \tag{21}$$

$$\text{ATX2} = 0.9970\frac{a}{l} + 0.07787\frac{L}{l} \tag{22}$$

The second projected term contributes little to the prediction of R, since its coefficient is very small when compared with the coefficient of the first projected term (i.e., $\beta_2 = 0.0021$, whereas $\beta_1 = 0.0330$). The third projected term also contributes very little to the accuracy of the prediction when compared with the first one and the second one, and thus the associated equations for the three-term model are not presented herein. In fact, the use of only one or two projected curves can adequately describe this three-dimensional response surface, as suggested by these figures.

The plausible model forms suggested by these PPR trials are an asymptotic nonlinear model for the first projected curve, a second-degree polynomial for the second projected curve, and a third-degree polynomial for the third projected curve if necessary. Of course, some piecewise linear and nonlinear curves may also be formulated for these purposes without much loss of generality.

Prediction and Extrapolation

From the above demonstration, it is evident that using different regression procedures may result in totally different predictive models, but with excellent agreement with the same set of data.

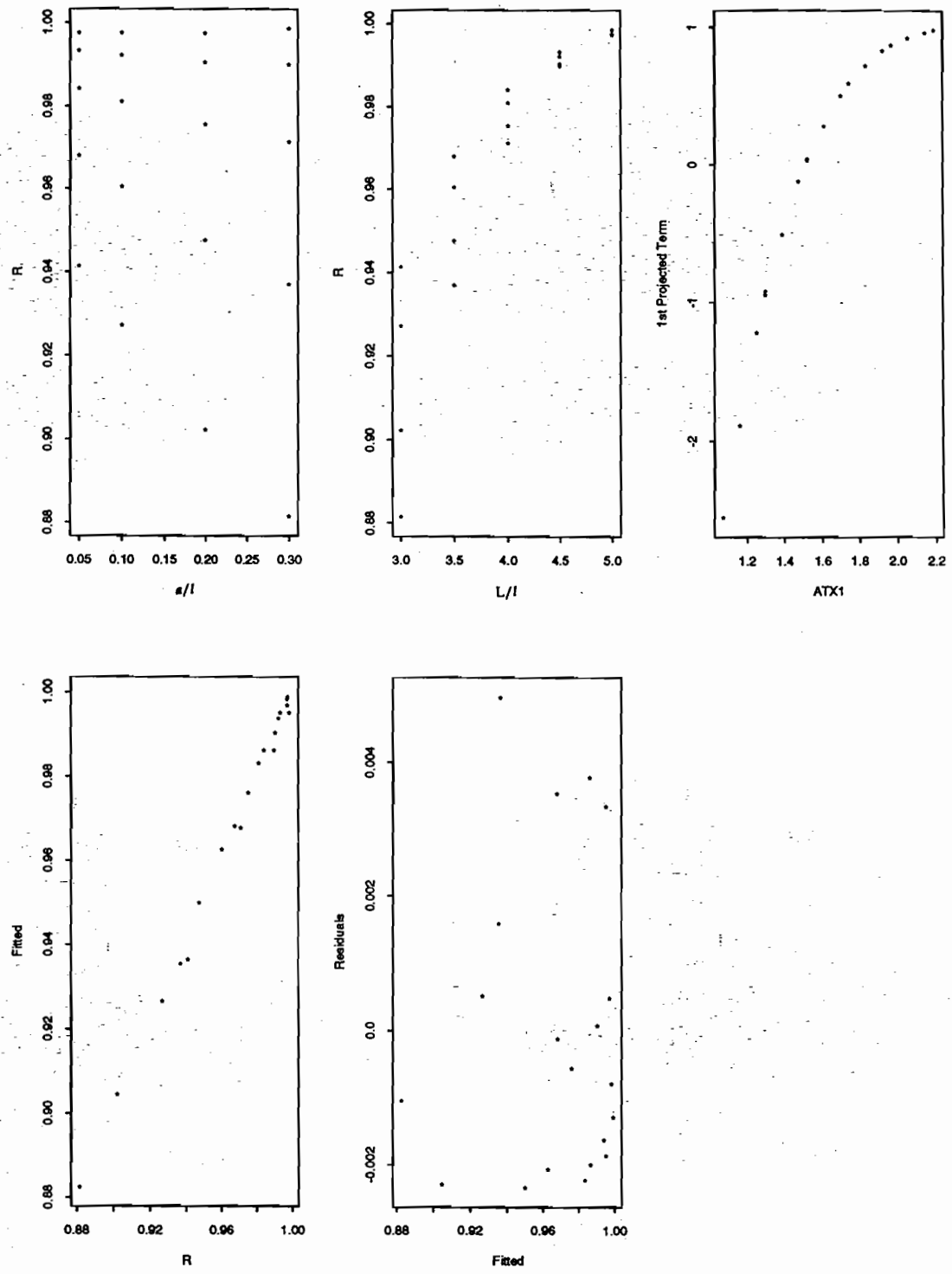

FIGURE 2 Slab size effect: one-term PPR model.

Under the umbrella of statistical regression analysis, they are all feasible solutions of the targeted problem as long as the conclusions are restricted to the range of the data. In other words "extrapolation beyond the range of the data" is never considered feasible with statistical regression analysis procedures.

However, it is also recognized that "extrapolation" is often necessary in actual engineering practice because of the limited resources available and technical limitations. To judge which equation is preferable, both Equations 15 and 16 were checked by plotting the predicted versus the actual R values within the specified data ranges as displayed by the symbol "o" in Figures 5(a) and 5(b), respectively. It is clearly shown that both equations result in very good predictions within the range of the data from which they were originally developed. In addition, Figures 5(a)

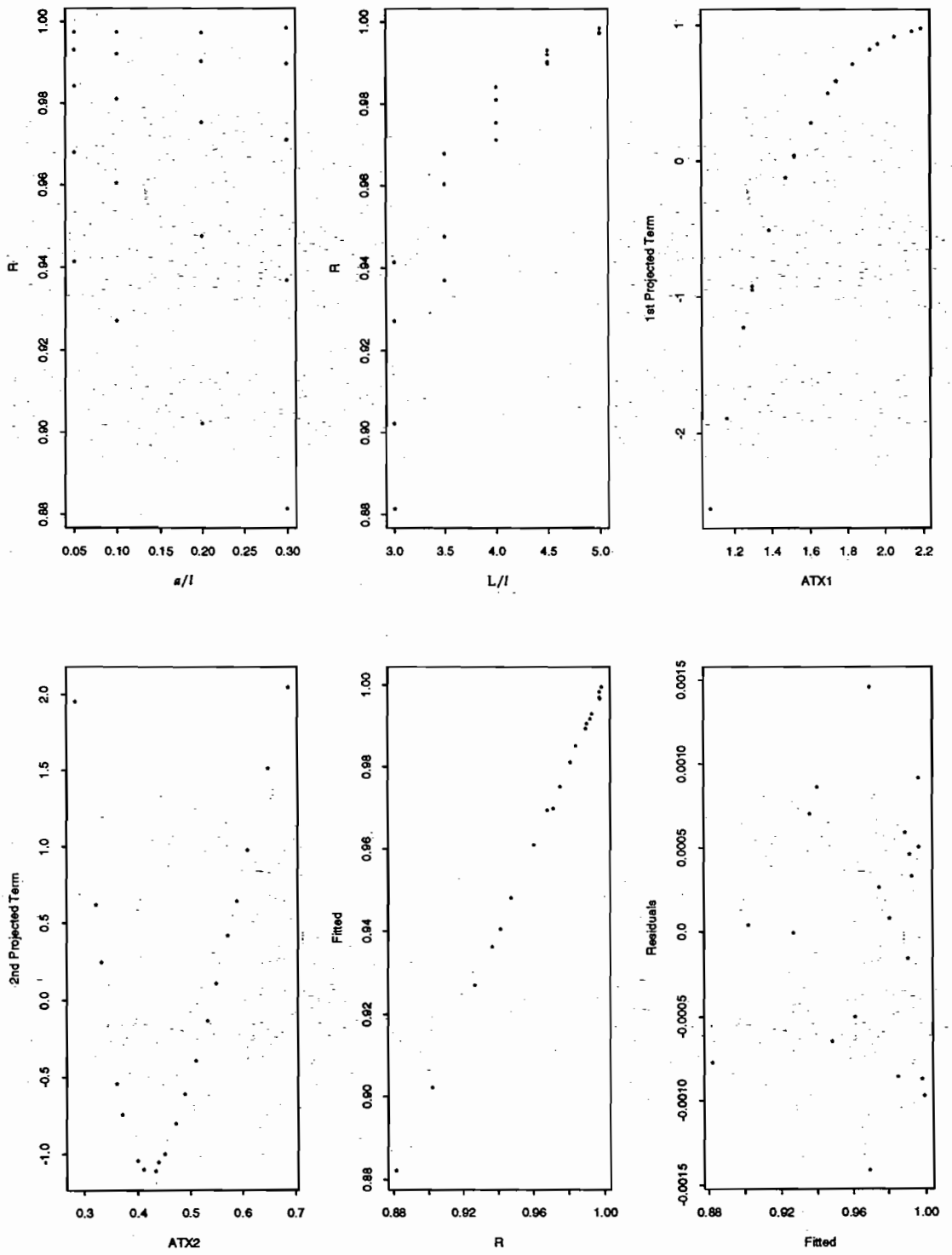

FIGURE 3 Slab size effect: two-term PPR model.

and 5(*b*) present the results when extrapolating beyond the specified limits by using these two models and the data from all of the 36 FE runs, respectively. These datum points, as displayed by the symbol "*" in the graphs, clearly show the difference.

Extrapolation by using Equation 15 results in totally unacceptable predictions outside the specified limits as shown in Figure 5(*a*). However, this problem is less pronounced as shown in Figure 5(*b*) when using Equation 16. In fact, the extrapolation of L/l greater than 5.0 provides excellent agreements with the actual data, since the functional form was properly selected to be asymptotic such that the predicted R values are very close to unity, as they should be. Nevertheless, some discrepancies still exist when extrapolating Equation 16 to smaller L/l values, that is, $L/l < 3.0$, which generally result in smaller R values.

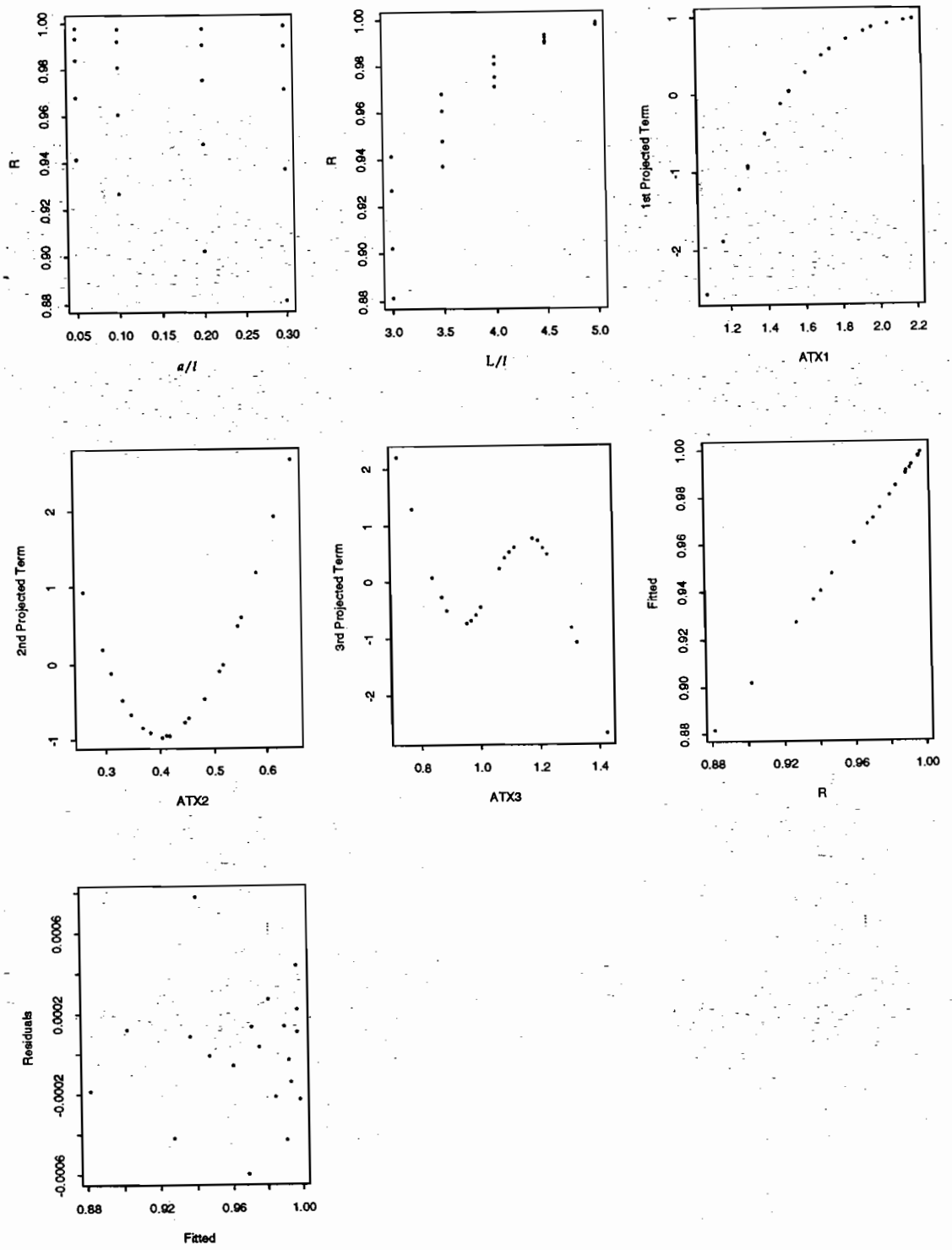

FIGURE 4 Slab size effect: three-term PPR model.

This result may be explained by the fact that the first parameter [a_1, or the minimum possible value of Φ_1(ATX1)] of Equation 19 was estimated to be -5.5869, such that Equation 16 will never result in a value below 0.7823. This approximation is acceptable for the ranges of data that were used to develop Equations 16, 17, and 19. However, it may not be as accurate when extrapolating too far away from this specified range. If the minimum possible value of R is known, this boundary condition may also be imposed on the predictive model. Thus, better agreement with the data can be obtained even in the case of extrapolation.

In summary, this case study not only demonstrates the benefits of using mechanistic variables through the use of the principles of dimensional analysis but it also emphasizes the importance of selecting proper functional forms. Correct functional forms pro-

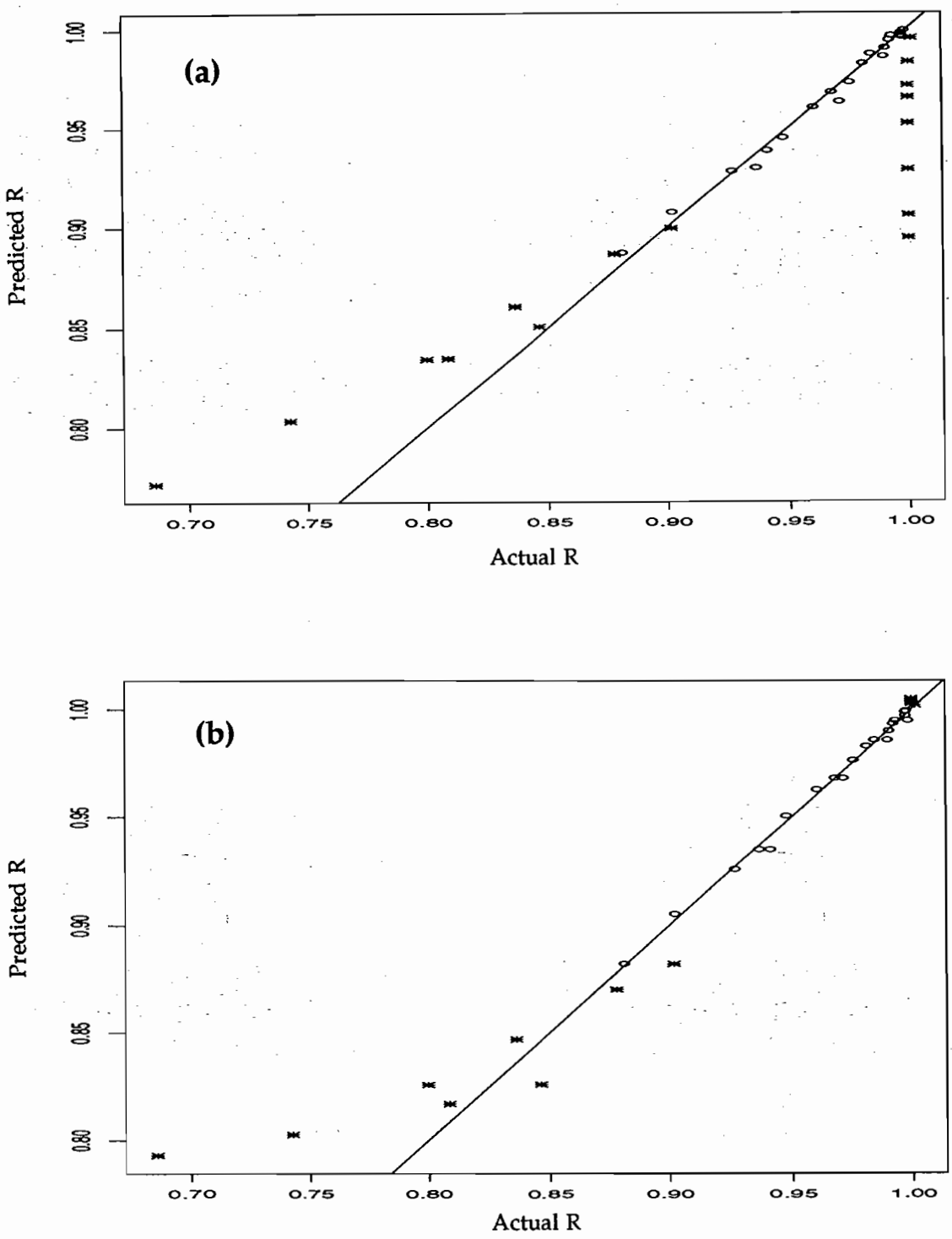

FIGURE 5 Extrapolated prediction plots using (*a*) existing model; (*b*) new model.

vide more comprehensive insights into the performance of the predictive model and may also lead to reasonable results even when extrapolation beyond the range of the data is required. It can be concluded that proper functional form is also a very crucial component in the success of a modeling process. The proper selection of functional forms to satisfy some applicable physical boundary conditions and subject-related engineering knowledge are the best supplements to statistical regression algorithms.

CONCLUSIONS

Several traditional linear and nonlinear regression techniques that have been widely adopted in pavement research were reviewed. Their advantages and limitations were discussed. Application of these regression techniques to practical engineering problems often shows the deficiencies in the selection of proper functional forms, the violation of some embedded statistical assumptions,

and failures to satisfy some applicable engineering boundary conditions.

Through the use of projection pursuit regression technique, a two-step predictive modeling approach was proposed in an attempt to minimize these problems. The proposed modeling approach was demonstrated in a case study for edge stress prediction owing to the finite slab length effect. Without imposing an unjustified parametric assumption, the PPR provides a unique routine for breaking down higher-dimensional engineering problems into a series of sensible projected curves. By doing so the individual projected curves may be formulated separately with better choices of feasible functional forms as well as possible boundary conditions. Not only did the demonstration reemphasize the advantages of using the principles of dimensional analysis but it also illustrated the importance of the proper selection of functional forms. Correct functional form provides more comprehensive insights into the performance of the predictive equation and may also lead to reasonable results even when extrapolation beyond the range of the data is required.

The demonstration was based on the data from the theoretical FE solutions in which no erroneous data are expected. As for applying the PPR to field or laboratory data with some possible errors, the promising features of the PPR algorithm are also helpful for identifying any extremely strange behavior because of data errors. Engineering knowledge of the physical mechanism of the problem may be applied in identifying the possible bad datum points as well.

It is also believed that only through the application of both engineering and statistical knowledge and techniques will a more theoretically correct predictive equation be developed. If properly developed it may also be applied beyond the range of the data. Nevertheless, the conclusions should be restricted to the range of the data.

ACKNOWLEDGMENTS

This research work was partially sponsored by the Illinois Department of Transportation under the project titled Implementation of Illinois Pavement Feedback System, for which different modern regression techniques were utilized for predictive model development. The authors would like to express much appreciation to James Hall, Illinois Department of Transportation, for valuable assistance in this project.

REFERENCES

1. Hastie, T. J., and R. J. Tibshirani. *Generalized Additive Models.* Monographs on Statistics and Applied Probability 43. Chapman & Hall, 1990.
2. Breiman, L., and J. H. Friedman. Estimating Optimal Transformations for Multiple Regression and Correlation (with Discussion). *Journal of the American Statistical Association,* Vol. 80, 1985, pp. 580–619.
3. Buja, A. Remarks on Functional Canonical Variates, Alternating Least Squares Methods and ACE. *Annals of Statistics,* Vol. 18, No. 3, 1990, pp. 1032–1069.
4. Tibshirani, R. Estimating Transformations for Regression via Additivity and Variance Stabilization. *Journal of the American Statistical Association,* Vol. 83, 1987, pp. 394–405.
5. Friedman, J. H., and W. Stuetzle. Projection Pursuit Regression. *Journal of the American Statistical Association.* Vol. 76, 1981, pp. 817–823.
6. Friedman, J. H. *SMART User's Guide.* Technical Report No. 1. LCS, Department of Statistics, Stanford University, Stanford, Calif., 1984.
7. Darter, M. I. *Design of Zero-Maintenance Plain Jointed Concrete Pavement, Vol. I. Development of Design Procedures.* FHWA Report FHWA-RD-77-111. FHWA, U.S. Department of Transportation, June 1977.
8. Salsilli-Murua, R. A. *Calibrated Mechanistic Design Procedure for Jointed Plain Concrete Pavements.* Ph.D. thesis. University of Illinois, Urbana, 1991.
9. *SAS User's Guide: Basics,* Version 5 edition. SAS Institute, Inc., 1985.
10. *SAS User's Guide: Statistics,* Version 5 edition. SAS Institute, Inc., 1985.
11. Weisberg, S. *Applied Linear Regression,* 2nd ed. Wiley Series in Probability and Mathematical Statistics. John Wiley & Sons, Inc., New York, 1985.
12. Draper, N. R., and H. Smith. *Applied Regression Analysis,* 2nd ed. Wiley Series in Probability and Mathematical Statistics. John Wiley & Sons, Inc., New York, 1981.
13. Rousseeuw, P. J., and A. M. Leroy. *Robust Regression and Outlier Detection.* Wiley Series in Probability and Mathematical Statistics. John Wiley & Sons, Inc., New York, 1987.
14. Gorman, J. W., and R. J. Toman. Selection of Variables for Fitting Equations to Data. *Technometrics,* Vol. 8, 1966, pp. 27–51.
15. Bates, D. M., and D. G. Watts. *Nonlinear Regression Analysis and Its Applications.* Wiley Series in Probability and Mathematical Statistics. John Wiley & Sons, Inc., New York, 1988.
16. *S-PLUS User's Manual,* Vol. 1 and Vol. 2. Statistical Sciences, Inc., Seattle, Wash., Nov. 1991.
17. *S-PLUS Reference Manual.* Statistical Sciences, Inc., Seattle, Wash., Nov. 1991.
18. Chambers, J. M., and T. J. Hastie. *Statistical Models in S.* Wadsworth & Brooks/Cole Computer Science Series. AT&T Bell Laboratories, 1992.
19. Becker, R. A., J. M. Chambers, and A. R. Wilks. *The New S Language—A Programming Environment for Data Analysis and Graphics.* The Wadsworth & Brooks/Cold Computer Science Series. AT&T Bell Laboratories, 1988.
20. Westergaard, H. M. New Formulas for Stresses in Concrete Pavements of Airfields. *Transactions, ASCE,* Vol. 113, pp. 425–444, 1948. Also in *Proceedings, ASCE,* Vol. 73, No. 5, May 1947.
21. Ioannides, A. M., M. R. Thompson, and E. J. Barenberg. The Westergaard Solutions Reconsidered. In *Transportation Research Record* 1043, TRB, National Research Council, Washington, D.C., 1985.
22. Tayabji, S. D., and D. J. Halpenny. Thickness Design of Roller-Compacted Concrete Pavements. In *Transportation Research Record 1136,* TRB, National Research Council, Washington, D.C., 1987.
23. Ioannides, A. M., and R. A. Salsilli-Murua. Temperature Curling in Rigid Pavements: An Application of Dimensional Analysis. In *Transportation Research Record 1227,* TRB, National Research Council, Washington, D.C., 1989.
24. Ioannides, A. M. *Analysis of Slabs-on-Grade for a Variety of Loading and Support Conditions.* Ph.D. thesis. University of Illinois, Urbana, 1984.

Publication of this paper sponsored by Task Force on Statistical Methods in Transportation.

E 剛性鋪面之厚度設計法之建立

E.1 PCA厚度設計法之發展過程

資料來源：

Portland Cement Association, "Thickness Design for Concrete Highway and Street Pavements," Skokie, Illinois, 1984.

E.2 FAA厚度設計法之簡介

資料來源：

周義華，運殊工程，鼎漢國際工程顧問股份有限公司，第二版，中華民國八十二年八月。

Federal Aviation Administration, "Airport Pavement Design and Evaluation," FAA Advisory Circular AC 150/5320-6C, 1978.

E.3 FAA厚度設計法之發展過程

資料來源：

Federal Aviation Administration, "Airport Pavement Design and Evaluation," FAA Advisory Circular AC 150/5320-6C, 1978.

E.4 Modified PCA Stress Analysis and Thickness Design Procedures

資料來源：

Lee, Y. H., J.. H. Bair, C. T. Lee, S. T. Yen, Y. M. Lee, "Modified PCA Stress Analysis and Thickness Design Procedures," Presented at the 76th Annual Meeting of the Transportation Research Board and Accepted for Publication in the Future Transportation Research Record, 1997.

E.1 PCA厚度設計法之發展過程

APPENDIX A

Development of Design Procedure

The thickness design procedure presented here was prepared to recognize current practices in concrete pavement construction and performance experience with concrete pavements that previous design procedures have not addressed. These include:

- Pavements with different types of load transfer at transverse joints or cracks
- Lean concrete subbases under concrete pavements
- Concrete shoulders
- Modes of distress, primarily due to erosion of pavement foundations, that are unrelated to the traditional criteria used in previous design procedures

A new aspect of the procedure is the erosion criterion that is applied in addition to the stress-fatigue criterion. The erosion criterion recognizes that pavements can fail from excessive pumping, erosion of foundation, and joint faulting. The stress criterion recognizes that pavements can crack in fatigue from excessive load repetitions.

This appendix explains the basis for these criteria and the development of the design procedure. Reference 30 gives a more detailed account of the topic.

Analysis of Concrete Pavements

The design procedure is based on a comprehensive analysis of concrete stresses and deflections at pavement joints, corners, and edges by a finite-element computer program.[8] It allows considerations of slabs with finite dimensions, variable axle-load placement, and the modeling of load transfer at transverse joints or cracks and load transfer at the joint between pavement and concrete shoulder. For doweled joints, dowel properties such as diameter and modulus of elasticity are used directly. For aggregate interlock, keyway joints, and cracks in continuously reinforced pavements, a spring stiffness value is used to represent the load-deflection characteristics of such joints based on field and laboratory tests.

Jointed Pavements

After analysis of different axle-load positions on the slab, the critical placements shown in Fig. A1 were established with the following conclusions:

1. The most critical pavement stresses occur when the truck wheels are placed at or near the pavement edge and midway between the joints, Fig. A1(*a*). Since the joints are at some distance from this location, transverse joint spacing and type of load transfer have very little effect on the magnitude of stress. In the design procedure, therefore, the analysis based on flexural stresses and fatigue yield the same values for different joint spacings and different types of load transfer mechanisms (dowels or aggregate interlock) at transverse joints. When a concrete shoulder is tied

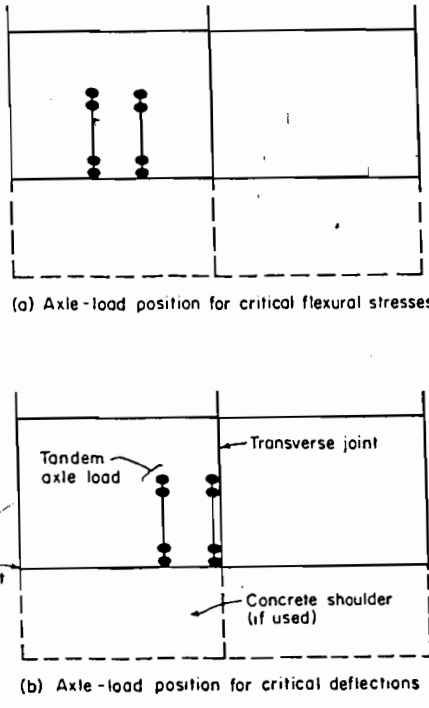

Fig. A1. Critical axle-load positions.

on to the mainline pavement, the magnitude of the critical stresses is considerably reduced.

2. The most critical pavement deflections occur at the slab corner when an axle load is placed at the joint with the wheels at or near the corner, Fig. A1(*b*).* In this situation, transverse joint spacing has no effect on the magnitude of corner deflections but the type of load transfer mechanism has a substantial effect. This means that design results based on the erosion criteria (deflections) may be substantially affected by the type of load transfer selected, especially when large numbers of trucks are being designed for. A concrete shoulder reduces corner deflections considerably.

Continuously Reinforced Pavements

A continuously reinforced concrete pavement (CRCP) is one with no transverse joints and, due to the heavy, continuous steel reinforcement in the longitudinal direction, the pavement develops cracks at close intervals. These crack spacings on a given project are variable, running generally from 3 to 10 ft with averages of 4 to 5 ft.

In the finite-element computer analysis, a high degree of load transfer was assigned at the cracks of CRCP and the crack spacing was varied. The critical load positions established were the same as those for jointed pavements.

For the longer crack spacings, edge stresses for loads placed midway between cracks are of about the same magnitude as those for jointed pavements. For the average and shorter crack spacings, the edge stresses are less than those for jointed pavements, because there is not enough length of uncracked pavement to develop as much bending moment.

For the longer crack spacings, corner deflections are somewhat less than those for jointed pavements with doweled transverse joints. For average to long crack spacings, corner deflections are about the same as those for jointed, doweled pavements. For short crack spacings of 3 or 4 ft, corner deflections are somewhat greater than those for jointed, doweled pavements, especially for tandem-axle loads.

Considering natural variations in crack spacing that occur in one stretch of pavement, the following comparison of continuously reinforced pavements with jointed, doweled pavements is made. Edge stresses will sometimes be the same and sometimes less, while corner deflections will sometimes be less, the same, and greater at different areas of the pavement depending on crack spacing.

The average of these pavement responses is neither substantially better nor worse than those for jointed, doweled pavements. As a result, in this design procedure, the same pavement responses and criteria are applied to continuously reinforced pavements as those used with jointed, doweled pavements. This recommendation is consistent with pavement performance experience. Most design agencies suggest that the thickness of continuously reinforced pavements should be about the same as the thickness of doweled-jointed pavements.

*The greatest deflections for tridems occur when two axles are placed at one side of the joint and one axle at the other side.

Truck Load Placement

Truck wheel loads placed at the outside pavement edge create more severe conditions than any other load position. As the truck placement moves inward a few inches from the edge, the effects decrease substantially.[39]

Only a small fraction of all the trucks run with their outside wheels placed at the edge. Most of the trucks traveling the pavement are driven with their outside wheel placed about 2 ft from the edge. Taragin's[40] studies reported in 1958, showed very little truck encroachment at pavement edge for 12-ft lanes for pavements with unpaved shoulders. More recent studies by Emery[41] showed more trucks at edge. Other recent studies[42] showed fewer trucks at edge than Emery. For this design procedure, the most severe condition, 6% of trucks at edge,* is assumed so as to be on the safe side and to take account of recent changes in United States law permitting wider trucks.

At increasing distances inward from the pavement edge, the frequency of load applications increases while the magnitudes of stress and deflection decrease. Data on truck placement distribution and distribution of stress and deflection due to loads placed at and near the pavement edge are difficult to use directly in a design procedure. As a result, the distributions were analyzed and more easily applied techniques were prepared for design purposes.

For stress-fatigue analysis, fatigue was computed incrementally at fractions of inches inward from the slab edge for different truck-placement distributions; this gave the equivalent edge-stress factors shown in Fig. A2. (This factor, when multiplied by edge-load stress, gives the same degree of fatigue consumption that would result from a given truck placement distribution.) The most severe condition, 6% truck encroachment, has been incorporated in the design tables.

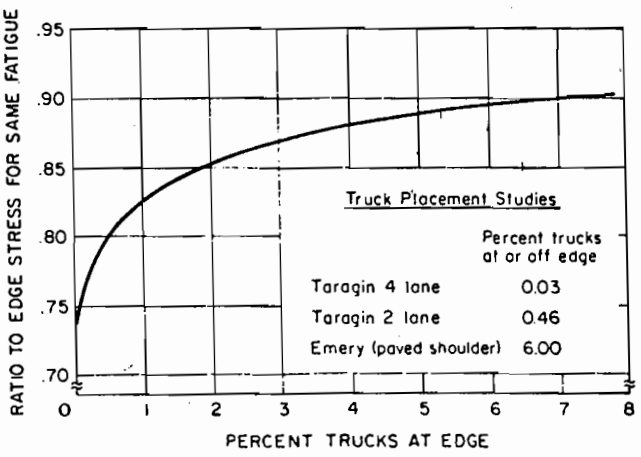

Fig. A2. Equivalent edge stress factor depends on percent of trucks at edge.

*As used here, the term "percent trucks at edge" is defined as the percent of total trucks that are traveling with the outside of the contact area of the outside tire at or beyond the pavement edge.

For erosion analysis, which involves deflection at the slab corner, the most severe case (6% of trucks at edge) is again assumed. Where there is no concrete shoulder, corner loadings (6% of trucks) are critical; and where there is a concrete shoulder, the greater number of loadings inward from the pavement corner (94% of trucks) are critical. These factors are incorporated into the design charts as follows:

Percent erosion damage = $100\ \Sigma n_i\ (C/Ni)$

where: n_i = expected number of axle-load repetitions for axle-group i

Ni = allowable number of repetitions for axle-group i

C = 0.06 for pavements without shoulder, and
0.94 for pavements with shoulder

To save a design calculation step, the effects of (C/Ni) are incorporated in Figs. 6*a* and 6*b* of Chapter 3 and Tables 11 through 14 of Chapter 4.

Variation in Concrete Strength

Recognition of the variations in concrete strength is considered a realistic addition to the design procedure. Expected ranges of variations in the concrete's modulus of rupture have far greater effect than the usual variations in the properties of other materials, such as subgrade and subbase strength, and layer thicknesses. Variation in concrete strength is introduced by reducing the modulus of rupture by one coefficient of variation.

For design purposes, a coefficient of variation of 15% is assumed and is incorporated into the design charts and tables. The user does not directly apply this effect. The value of 15% represents fair-to-good quality control, and, combined with other effects discussed elsewhere in this appendix, was selected as being realistic and giving reasonable design results.

Concrete Strength Gain With Age

The 28-day flexural strength (modulus of rupture) is used as the design strength. This design procedure, however, incorporates the effect of concrete strength gain after 28 days. This modification is based on an analysis that incremented strength gain and load repetitions month by month for 20-year and 40-year design periods. The effect is included in the design charts and tables so the user simply inputs the 28-day value as the design strength.

Warping and Curling of Concrete

In addition to traffic loading, concrete slabs are also subjected to warping and curling. Warping is the upward concave deformation of the slab due to variations in moisture content with slab depth. The effect of warping is twofold: It results in loss of support along the slab edges and also in compressive restraint stresses in the slab bottom. Since warping is a long-term phenomenon, its resultant effect is influenced greatly by creep.

Curling refers to slab behavior due to variations of temperature. During the day, when the top surface is warmer than the bottom, tensile-restraint stresses develop at the slab bottom. During the night, the temperature distribution is reversed and tensile restraint stresses develop at the slab surface. Temperature distribution is usually nonlinear and constantly changing. Also, maximum daytime and nighttime temperature differentials exist for short durations.

Usually the combined effect of curling and warping stresses are subtractive from load stresses because the moisture content and temperature at the bottom of the slab exceed that at the top more than the reverse.

The complex situation of differential conditions at a slab's top and bottom plus the uncertainty of the zero-stress position make it difficult to compute or measure the restraint stresses with any degree of confidence or verification. At present, the information available on actual magnitudes of restraint stresses does not warrant incorporation of the items in this design procedure.

As for the loss of support, this is considered indirectly in the erodibility criterion, which is derived from actual field performance and therefore incorporates normal loss of support conditions.

Calculated stress increase due to loss of support varies from about 5% to 15%. This theoretical stress increase is counteracted in the real case because a portion of the load is dissipated in bringing the slab edges back in contact with the support. Thus, the incremental load stress due to a warping-type loss of support is not incorporated in this design procedure.

Fatigue

The flexural fatigue criterion used in the procedure presented here is shown in Fig. A3. It is similar to that used in the previous PCA method[44] based conservatively on

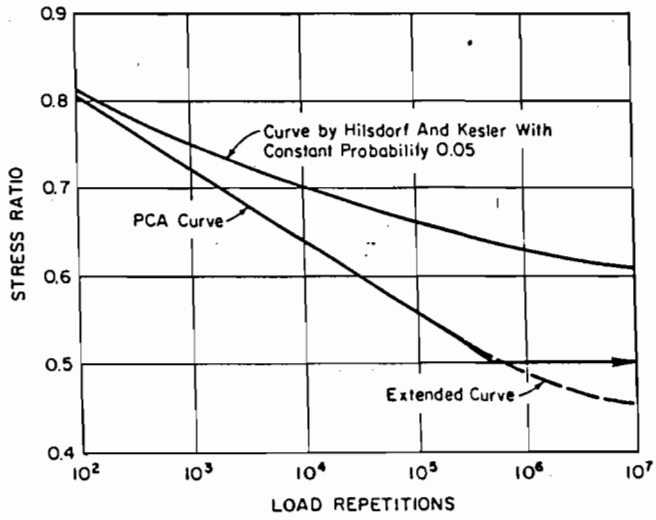

Fig. A3. Fatigue relationships.

studies of fatigue research[45-49] except that it is applied to edge-load stresses that are of higher magnitude. A modification in the high-load-repetition range has been made to eliminate the discontinuity in the previous curve that sometimes causes unrealistic effects.

The allowable number of load repetitions for a given axle load is determined based on the stress ratio (flexural stress divided by the 28-day modulus of rupture). The fatigue curve is incorporated into the design charts for use by the designer.

Use of the fatigue criterion is made on the Miner hypothesis[48] that fatigue resistance not consumed by repetitions of one load is available for repetitions of other loads. In a design problem, the total fatigue consumed should not exceed 100%.

Combined with the effect of reducing the design modulus of rupture by one coefficient of variation, the fatigue criterion is considered to be conservative for thickness design purposes.

Erosion

Previous mechanistic design procedures for concrete pavements are based on the principle of limiting the flexural stresses in a slab to safe values. This is done to avoid flexural fatigue cracks due to load repetitions.

It has been apparent that there is an important mode of distress in addition to fatigue cracking that needs to be addressed in the design process. This is the erosion of material beneath and beside the slab.

Many repetitions of heavy axle loads at slab corners and edges cause pumping; erosion of subgrade, subbase, and shoulder materials; voids under and adjacent to the slab; and faulting of pavement joints, especially in pavements with undoweled joints.

These particular pavement distresses are considered to be more closely related to pavement deflections than to flexural stresses.

Correlations of deflections computed from the finite-element analysis[8] with AASHO Road Test[24] performance data were not completely satisfactory for design purposes. (The principal mode of failure of concrete pavements at the AASHO Road Test was pumping or erosion of the granular subbase from under the slabs.) It was found that to be able to predict the AASHO Road Test performance, different values of deflection criteria would have to be applied to different slab thicknesses, and to a small extent, different foundation moduli (k values).

More useful correlation was obtained by multiplying the computed corner deflection values (w) by computed pressure values (p) at the slab-foundation interface. Power, or rate of work, with which an axle load deflects the slab is the parameter used for the erosion criterion—for a unit area, the product of pressure and deflection divided by a measure of the length of the deflection basin (ℓ — radius of relative stiffness, in inches). The concept is that a thin pavement with its shorter deflection basin receives a faster load punch than a thicker slab. That is, at equal pw's and equal truck speed, the thinner slab is subjected to a faster rate of work or power (inch-pound per second). A successful correlation with road test performance was obtained with this parameter.

The development of the erosion criterion was also generally related to studies on joint faulting.[28 29] These studies included pavements in Wisconsin, Minnesota, North Dakota, Georgia, and California, and included a range of variables not found at the AASHO Road Test, such as a greater number of trucks, undoweled pavements, a wide range of years of pavement service, and stabilized subbases.

Brokaw's studies[28] of undoweled pavements suggest that climate or drainage is a significant factor in pavement performance. So far, this aspect of design has not been included in the design procedure, but it deserves further study. Investigations of the effects of climate on design and performance of concrete pavements have also been reported by Darter.[43]

The erosion criterion is suggested for use as a guideline. It can be modified according to local experience since climate, drainage, local factors, and design innovations may have an influence. Accordingly, the 100% erosion-damage criterion, an index number correlated with general performance experience, can be increased or decreased based on specific performance data gathered in the future for more favorable or more adverse conditions.

E.2 FAA厚度設計法之簡介

23.5.2 鋪面厚度設計

1.柔性鋪面之厚度設計

FAA 發展出一套機場柔性鋪面之設計方法，此方法建議對路基土壤之物理特性作徹底的調查，並依統一土壤分類法(Unified Soil Classification System)判定路基土壤之類別。

統一土壤分類法係由美國的陸軍工兵團 (Army Corps of Engineers)所發展，此分類法根據土壤顆粒之粗細、級配、塑性及壓縮性等，將土壤分成粗粒土壤、細粒土壤、高度有機質土壤三大類。另再分爲十五細目，每一細目以兩個字母作代號；第一個字母表示影響土壤性能最大的主要成分，計分六種：礫 (G)、砂 (S)、沉泥 (M) 、黏土 (C)、有機質沉泥或黏土 (O)、泥炭 (Pt)；第二個字母表示其顆粒級配性質、塑性以及次要成分，計分四種：優良級配 (W)、不良級配 (P)、低塑性 (L)、高塑性 (H)。

粗粒土壤係指未通過#200篩的分量在50%以上者。凡粗粒土壤留於#4篩的分量在50%以上者稱爲礫石 (Gravel) ，一共分成四個細目計：GW、GP、GM、GC；留於#4篩少於50%者稱爲砂 (Sand) ，亦分成四個細目計：SW、SP、SM、SC。

細粒土壤係指通過#200篩的分量在50%以上者。凡細粒土壤的液性限度 (Liquid Limit) 小於50者，一共分成三個細目計：ML、CL及OL；液性限度大於50者，亦分成三個細目計：MH、CH及OH。

高度有機質土壤包括泥炭、砂質泥炭與黏質泥炭，以Pt 表示。

統一土壤分類法可列如表23-4。

在此須說明的是，統一土壤分類法僅能概略地表示路基土壤的特性，因此FAA 建議應作CBR 試驗。此試驗係由美國加州公路局研究成功之一種測定路基土壤抗剪力試驗方法，CBR 之涵義則爲夯實土壤的貫入抗力與標準土壤貫入抗力的比值，以百分率表示。所謂標準土壤之貫入抗力，則爲用一定級配之碎石，納入規定之模筒，受規定之夯實能量，再浸入水內若干規定時間，再根據標準試驗方法，測定貫入深度在0.25cm時之所施壓力而言。由CBR 值即可準確表明路基土壤之強度，各類土壤之相對CBR 值列於表23-4中。

FAA 的設計方法主要係依據路基土壤的CBR 值、飛機之全重 (Gross Aircraft Weight)及每年離地的飛機數量三項因素設計鋪面之厚度，並依降落裝置 (Landing Gear) 分爲單輪、雙輪及雙輪縱排 (Dual-tandem)等繪製設計曲線圖。此外，並對B-747、DC-10及L-1011等廣體客機個別製作設計曲線圖。

圖23-3爲雙輪降落裝置之柔性鋪面設計曲線圖。由於落地飛機之全重平均約爲離地飛機之75%，因此圖中之飛機全重係以最大的離地飛機全重爲準；在每年離地的飛機數量一項，則須考慮各型飛機輪重之累加效應 (Cumulative Effect)，而爲了設計方便，可將各型飛機之輪重換算爲設計機型，其當量 (Equivalence)之換算式如下：

表 23-4　統一土壤分類及相對應之CBR 值與k 值表

主要分類		簡號	土壤說明	CBR 值	路基係數k(kg / cm³)
粗粒土壤，留存在#200篩的份量佔全重50%以上	礫石土（留存在#4號篩的佔全重的50%以上）	GW	級配優良的礫石與砂質礫。	60～80	Ⅳ 8.3
		GP	跳越級配或均勻的礫石、砂質礫	35～60	Ⅳ Ⅳ 8
		GM	沉泥質礫、黏土質砂礫。	40～80	Ⅳ 8
		GC	黏土質礫、黏土質砂礫。	20～40	6～8
	砂質土（通過#4號篩的佔全重的50%以上）	SW	級配優良的砂、礫質砂。	20～40	6～8
		SP	跳越級配或均勻砂、礫質砂。	15～25	6～8
		SM	沉泥質砂、沉泥質礫砂。	20～40	6～8
		SC	黏土質沉泥、黏土質礫砂。	10～20	6～8
細粒土壤，通過#200篩的佔全重50%以上	可壓縮性低，液性限度小於50。	ML	沉泥、極細砂、沉泥質或黏土質砂、雲母質沉泥。	5～15	3～6
		CL	低塑性黏土、砂質或沉泥質黏土	5～15	3～6
		OL	有機質沉泥與黏土具低塑性者。	4～8	3～6
	可壓縮性高，液性限度大於50。	MH	雲母質沉泥、矽藻土、火山灰。	4～8	3～6
		CH	高塑性黏土、與砂質黏土。	3～5	1.5～3
		OH	有機質沉泥與黏土具高塑性者。	3～5	1.5～3
土內含有纖維狀有機質		Pt	泥炭、砂質泥炭與黏質泥炭。	—	—

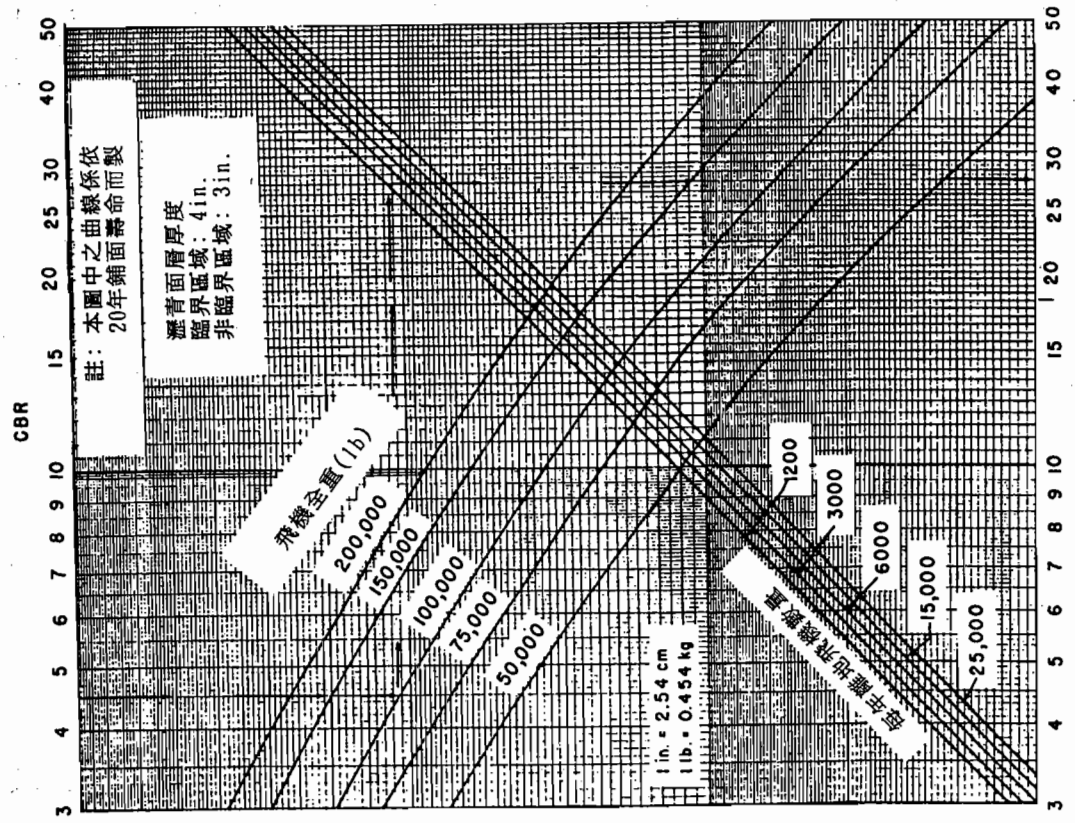

圖 23-3　柔性鋪面臨界區域之厚度設計曲線圖，雙輪降落裝置（資料來源：[9]）

$$\log R_i = \log\left[R_d \right] \left(\frac{W_d}{W_i}\right)^{1/2}$$

$$E_i = \frac{R_i}{R_d}$$

式中，

R_d 爲設計機型離地之全重 等效起飛架次數當量 (Equivalent Annual Departures)

R_i 爲i 型飛機離地之全重 年起飛次數

W_d 爲設計機型離地之輪重

W_i 爲i 型飛機離地之輪重

~~E_i 爲i 型飛機換算爲設計機型之當量~~

圖23-3係用以設計機場臨界區域之鋪面厚度。所謂臨界區域 (Critical Area)，係指跑道- 滑行道系統中承受最大密集壓力之區域，包括跑道端部、所有滑行道及停機坪，如圖23-4所示。此區域之鋪面厚度須較大，其他非臨界區域之鋪面厚度可減少20%。

圖23-3之使用方法爲：依據路基土壤之CBR 值在圖中上面之座標找到一點，再往下作垂直線與對應之飛機全重曲線相交，再由此交點作水平線與對應之全年離地飛機數量線相交，由此交點作垂直線即可在下面之座標求得臨界區域之鋪面厚度。

圖23-5爲全重在13,600kg (30,000 lb)以下輕型飛機之鋪面厚度設計圖，由此圖所得出之厚度同時適用於臨界區域與非臨界區域，而不須作任何折減。

2.剛性鋪面之厚度設計

FAA 針對剛性鋪面所發展之厚度設計方法與柔性鋪面之設計方法相類似。其設計曲線圖所包含之設計要素爲混凝土之撓曲強度 (

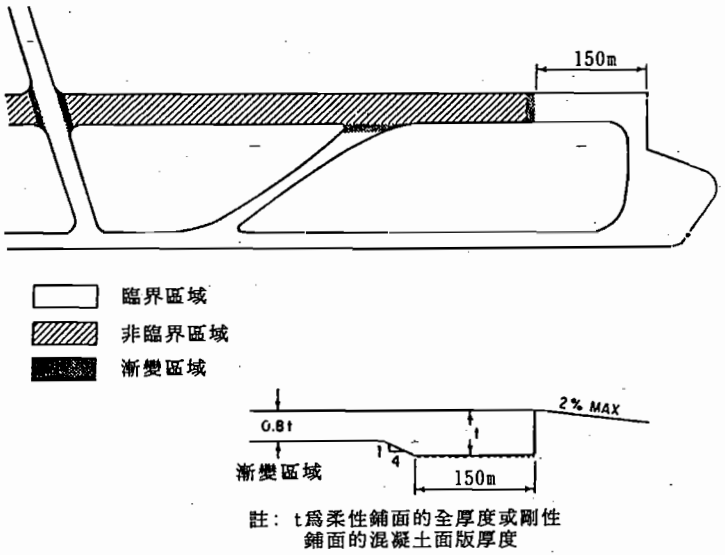

註：t爲柔性鋪面的全厚度或剛性鋪面的混凝土面版厚度

圖 23-4 機場鋪面之臨界區域圖 (資料來源：[10])

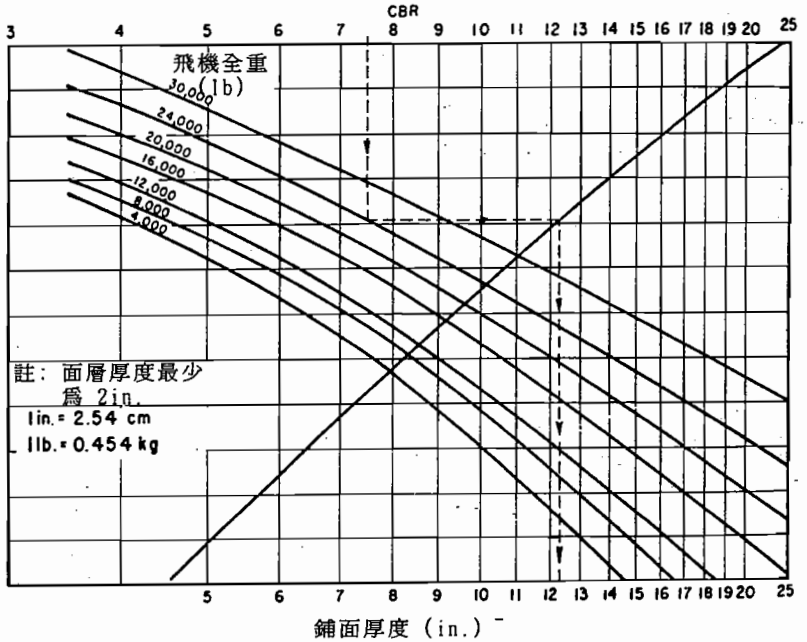

圖 23-5 輕型飛機之柔性鋪面厚度設計曲線圖

(資料來源：[9])

Flexural Stength）、路基係數（Subgrade Modulus）、飛機全重及每年離地飛機數量。

路基係數係產生單位沉陷所需之壓力，亦稱爲路基抗力係數（Coefficient of Subgrade Reaction），以k 表示，其定義爲單位壓力（kg / cm²)除以單位沉陷量（cm），因此其單位爲kg / cm³ 。k 值之測定乃以 75 cm直徑之圓鈑載重試驗依AASHTO所訂之T-222試驗程序測得。若圓鈑載重試驗不易實施，則可採用表23-4中之k值。

圖23-6爲雙輪降落裝置之剛性鋪面設計曲線圖，此圖之使用方法與圖23-3相同。由圖中所得之厚度爲臨界區域之厚度，在非臨界區域則可減少20％之厚度，但總厚度不可少於15cm。

FAA 又規定，除了表23-5中所列之地區外，剛性鋪面至少應有10cm之基層。若基層之厚度再增加，則有提高路基係數及減少混凝土面版厚度之效益，其取捨主要依經濟的觀點而定。

機場剛性鋪面之接縫及鋼筋設計與公路鋪面相似，但因機場鋪面之厚度較大，其所需路面版之寬度較寬，合釘亦較大。縱向接縫（Longitudinal Joint）之間距在面版厚度爲25cm以下時爲 3.8 m，面版厚度在25cm以上時，間距可爲3.8～7.6 m。

表 23-5　機場鋪面構造不需基層之地區表

土壤分類	排水良好		排水不良	
	無冰凍	冰凍	無冰凍	冰凍
GW	v	v	v	v
GP	v	v	v	
GM	v			
GC	v			
SW	v			

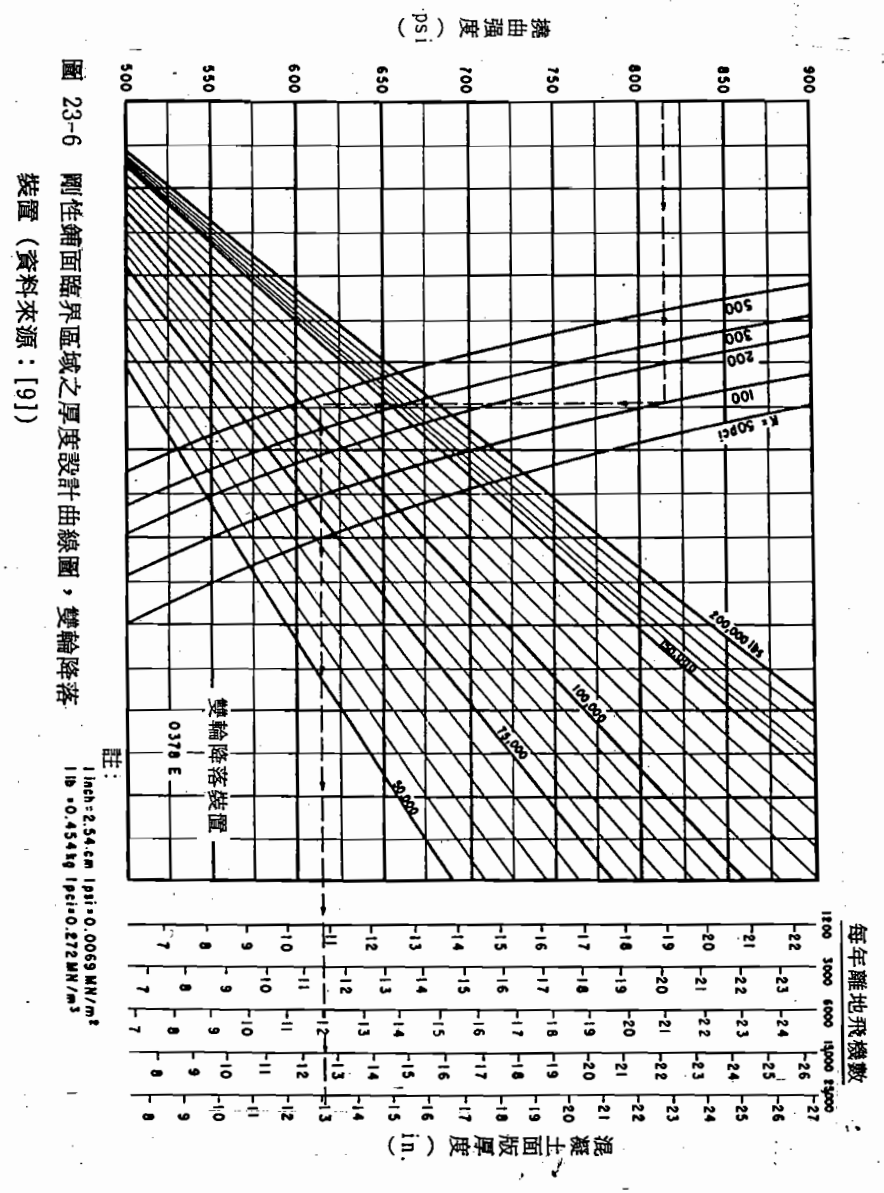

圖 23-6　剛性鋪面臨界區域之厚度設計曲線圖，雙輪降落裝置（資料來源：[9]）

CHAPTER 3. PAVEMENT DESIGN.

SECTION 1. DESIGN CONSIDERATIONS

15. SCOPE. This chapter covers pavement design for airports serving aircraft with gross weights of 30,000 pounds (13 000 kg) or more. Chapter 5 is devoted to the design of pavements serving lighter aircraft with gross weights under 30,000 pounds (13 000 kg).

16. DESIGN PHILOSOPHY. The FAA policy of treating the design of aircraft landing gear and the design and evaluation of airport pavements as three separate entities is described in the Foreword to this advisory circular. The design of airport pavements is a complex engineering problem which involves a large number of interacting variables. The design curves presented in this chapter are based on the CBR method of design for flexible pavements and a jointed edge stress analysis for rigid pavements. These procedures represent a change from prior FAA design methods and will result in slightly different pavement thicknesses. The design curves in this chapter will satisfy the standards required by Section 16(a) of the Airport and Airway Development Act of 1970, as amended. Other design procedures such as those based on layered elastic analysis and those developed by The Asphalt Institute and the Portland Cement Association may be utilized to determine pavement thicknesses when approved by the FAA. These procedures will yield slightly different design thicknesses due to different basic assumptions. All pavement designs should be summarized on FAA Form 5100-1, Airport Pavement Design, (see AC 150/5100-3A) which is considered to be part of the Engineer's Report. Because of thickness variations, the evaluation of existing pavements should be performed using the same method as was employed in the design. Procedures to be used in evaluating pavements are described in detail in Chapter 6 of this advisory circular. Details on how the new FAA methods of design were developed are as follows:

a. Flexible Pavements. The flexible pavement design curves presented in this chapter are based on the California Bearing Ratio (CBR) method of design. The CBR design method is basically empirical; however, a great deal of research has been done with the method and reliable correlations have been developed. Gear configurations are related using theoretical concepts as well as empirically developed data. The design curves provide the required total thickness of flexible pavement (surface, base, and subbase) needed to support a given weight of aircraft over a particular subgrade. The curves also show the required surface thickness. Minimum base course thicknesses are shown on a separate curve. A more detailed discussion of CBR design is presented in Appendix 2.

b. Rigid Pavements. The rigid pavement design curves in this chapter are based on the Westergaard analysis of edge loading. The edge loading analysis has been modified to simulate a jointed edge condition. Design curves are furnished for areas where traffic will predominantly follow parallel to the joints and for areas where traffic is likely to cross joints at some acute angle. Previous FAA rigid pavement criteria were based on an interior loading assumption. Pavement stresses are higher at the jointed edge than at the slab interior. Test validations and field performance show practically all load induced cracks develop at the jointed edge and migrate toward the slab interior. For these reasons the basis of design was changed from interior to jointed edge, as recommended by the U. S. Army Corps of Engineers, under a pavement research contract for the FAA. The design curves contain lines for five different annual traffic volumes. The thickness of pavement determined from the curves is for slab thickness only. Subbase thicknesses are determined separately. A more detailed discussion of the basis for rigid pavement design is presented in Appendix 2.

17. BACKGROUND. An airfield pavement and the operating aircraft represent an interactive system which must be recognized in the pavement design process. Design considerations associated with both the aircraft and the pavement must be satisfied in order to produce a satisfactory design. Careful construction control and some degree of maintenance will be required to produce a pavement which will achieve the intended design life. Pavements are designed to provide a finite life and fatigue failures are anticipated. Poor construction and lack of preventative maintenance will usually result in disappointing performance of even the best designed pavement.

a. The determination of pavement thickness requirements is a complex engineering problem. Pavements are subject to a wide variety of loadings and climatic effects. The design process involves a large number of interacting variables which are often difficult to quantify. Although a great deal of research work has been completed and more is underway, it has been impossible to arrive at a direct mathematical solution of thickness requirements. For this reason the determination of pavement thickness must be based on the theoretical analysis of load distribution through pavements and soils, the analysis of experimental pavement data, and a study of the performance of pavements under actual service conditions. Pavement thickness curves presented in this chapter have been developed through correlation of the data obtained from these sources. Pavements designed in accordance with these standards are intended to provide a structural life of 20 years that is free of major maintenance if no major changes in forecast traffic are

encountered. It is likely that rehabilitation of surface grades and renewal of skid resistant properties will be needed before 20 years due to destructive climatic effects and deteriorating effects of normal usage.

b. The structural design of airport pavements consists of determining both the overall pavement thickness and the thickness of the component parts of the pavement. There are a number of factors which influence the thickness of pavement required to provide satisfactory service. These include the magnitude and character of the aircraft loads to be supported, the volume of traffic, the concentration of traffic in certain areas, and the quality of the subgrade soil and materials comprising the pavement structure.

18. AIRCRAFT CONSIDERATIONS.

a. Load. The pavement design method is based on the gross weight of the aircraft. For design purposes the pavement should be designed for the maximum takeoff weight of the aircraft. The design procedure assumes 95 percent of the gross weight is carried by the main landing gears and 5 percent is carried by the nose gear. AC 150/5325-5, Aircraft Data, lists the weight of nearly all civil aircraft. The maximum takeoff weight should be used in calculating the pavement thickness required. Use of the maximum takeoff weight is recommended to provide some degree of conservatism in the design and is justified by the fact that changes in operational use can often occur and recognition of the fact that forecast traffic is approximate at best. By ignoring arriving traffic some of the conservatism is offset.

b. Landing Gear Type and Geometry.

(1) The gear type and configuration dictate how the aircraft weight is distributed to the pavement and determine pavement response to aircraft loadings. It would have been impractical to develop design curves for each type of aircraft. However, since the thickness of both rigid and flexible pavements is dependent upon the gear dimensions and the type of gear, separate design curves would be necessary unless some valid assumptions could be made to reduce the number of variables. Examination of gear configuration, tire contact areas, and tire pressure in common use indicated that these follow a definite trend related to aircraft gross weight. Reasonable assumptions could therefore be made and design curves constructed from the assumed data. These assumed data are as follows:

(a) Single Gear Aircraft. No special assumptions needed.

(b) Dual Gear Aircraft. A study of the spacing between dual wheels for these aircraft indicated that a dimension of 20 inches (0.51 m) between the centerline of the tires appeared reasonable for the lighter aircraft and a dimension of 34 inches (0.86 m) between the centerline of the tires appeared reasonable for the heavier aircraft.

(c) Dual Tandem Gear Aircraft. The study indicated a dual wheel spacing of 20 inches (0.51 m) and a tandem spacing of 45 inches (1.14 m) for lighter aircraft, and a dual wheel spacing of 30 inches (0.76 m) and a tandem spacing of 55 inches (1.40 m) for the heavier aircraft are appropriate design values.

(d) Wide Body Aircraft. Wide body aircraft; i.e., B-747, DC-10, and L-1011 represent a radical departure from the geometry assumed for dual tandem aircraft described in paragraph (c) above. Due to the large differences in gross weights and gear geometries, separate design curves have been prepared for the wide body aircraft.

(2) Tire pressure varies between 75 and 200 psi (516 to 1 380 kPa) depending on gear configuration and gross weight. It should be noted that tire pressure asserts less influence on pavement stresses as gross weight increases, and the assumed maximum of 200 psi (1 380 kPa) may be safely exceeded if other parameters are not exceeded.

c. Traffic Volume. Forecasts of annual departures by aircraft type are needed for pavement design. Information on aircraft operations is available from Airport Master Plans, Terminal Area Forecasts, the National Airport System Plan, Airport Activity Statistics and FAA Air Traffic Activity. These publications should be consulted in the development of forecasts of annual departures by aircraft type.

19. DETERMINATION OF DESIGN AIRCRAFT. The forecast of annual departures by aircraft type will result in a list of a number of different aircraft. The design aircraft should be selected on the basis of the one requiring the greatest pavement thickness. Each aircraft type in the forecast should be checked to determine the pavement thickness required by using the appropriate design curve with the forecast number of annual departures for that aircraft. The aircraft type which produces the greatest pavement thickness is the design aircraft. The design aircraft is not necessarily the heaviest aircraft in the forecast.

20. DETERMINATION OF EQUIVALENT ANNUAL DEPARTURES BY THE DESIGN AIRCRAFT.

a. Since the traffic forecast is a mixture of a variety of aircraft having different landing gear types and different weights, the effects of all traffic must be accounted for in terms of the design aircraft. First, all aircraft must be converted to the same landing gear type as the design aircraft. The following conversion factors should be used to convert from one landing gear type to another:

To Convert From	To	Multiply Departures By
single wheel	dual wheel	0.8
single wheel	dual tandem	0.5
dual wheel	dual tandem	0.6
double dual tandem	dual tandem	1.0
dual tandem	single wheel	2.0
dual tandem	dual wheel	1.7
dual wheel	single wheel	1.3
double dual tandem	dual wheel	1.7

Secondly, after the aircraft have been grouped into the same landing gear configuration, the conversion to equivalent annual departures of the design aircraft should be determined by the following formula:

$$\log R_1 = \log R_2 \times \left(\frac{W_2}{W_1}\right)^{\frac{1}{2}}$$

where R_1 = equivalent annual departures by the design aircraft

R_2 = annual departures expressed in design aircraft landing gear

W_1 = wheel load of the design aircraft

W_2 = wheel load of the aircraft in question

For this computation 95 percent of the gross weight of the aircraft is assumed to be carried by the main landing gears. Wide body aircraft require special attention in this calculation. The procedure discussed above is a relative rating which compares different aircraft to a common design aircraft. Since wide body aircraft have radically different landing gear assemblies than other aircraft, special considerations are needed to maintain the relative effects. This is done by treating each wide body as a 300,000-pound (136 100 kg) dual tandem aircraft when computing equivalent annual departures. This should be done in every instance even when the design aircraft is a wide body. After the equivalent annual departures are determined, the design should proceed using the appropriate design curve for the design aircraft. For example if a wide body is the design aircraft, all equivalent departures should be calculated as described above; then the design curve for the wide body should be used with the calculated equivalent annual departures.

b. Example: Assume an airport pavement is to be designed for the following forecast traffic:

Aircraft	Gear Type	Forecast Annual Departures	Maximum Takeoff Weight lbs.	(kg)
727-100	dual	3,760	160,000	(72 600)
727-200	dual	9,080	190,500	(86 500)
707-320B	dual tandem	3,050	327,000	(148 500)
DC-9-30	dual	5,800	108,000	(49 000)
CV-880	dual tandem	400	184,500	(83 948)
737-200	dual	2,650	115,500	(52 440)
L-1011-100	dual tandem	1,710	450,000	(204 120)
747-100	double dual tandem	85	700,000	(317 800)

(1) Determine Design Aircraft. A pavement thickness is determined for each aircraft in the forecast using the appropriate design curves. The pavement input data, CBR, K value, flexural strength, etc., should be the same for all aircraft. Aircraft weights and departure levels must correspond to the particular aircraft in the forecast. In this example the 727-200 requires the greatest pavement thickness and is thus the design aircraft.

(2) Group Forecast Traffic into Landing Gear of Design Aircraft. In this example the design aircraft is equipped with a dual wheel landing gear so all traffic must be grouped into the dual wheel configuration.

(3) Convert Aircraft to Equivalent Annual Departures of the Design Aircraft. After the aircraft mixture has been grouped into a common landing gear configuration, the equivalent annual departures of the design aircraft can be calculated.

Aircraft	Dual Gear Departures	Wheel Load lbs.	Wheel Load (kg)	Wheel Load of Design Aircraft lbs.	Wheel Load of Design Aircraft (kg)	Equivalent Annual Departures Design Aircraft
727-100	3,760	38,000	(17 240)	45,240	(20 520)	1,891
727-200	9,080	45,240	(20 520)	45,240	(20 520)	9,080
707-320B	5,185	38,830	(17 610)	45,240	(20 520)	2,764
DC-9-30	5,800	25,650	(11 630)	45,240	(20 520)	682
CV-880	680	21,910	(9 940)	45,240	(20 520)	94
737-200	2,650	27,430	(12 440)	45,240	(20 520)	463
747-100	145	35,625 1/	(16 160)	45,240	(20 520)	83
L-1011-100	2,907	35,625 1/	(16 160)	45,240	(20 520)	1,184
					Total	16,241

1/ Wheel loads for wide body aircraft will be taken as the wheel load for a 300,000-pound (136 100 kg) aircraft for equivalent annual departure calculations.

(4) For this example the pavement would be designed for 16,000 annual departures of a dual wheel aircraft weighing 190,500 pounds (86 500 kg). The design should, however, provide for the heaviest aircraft in the traffic mixture when considering depth of compaction, thickness of asphalt surface, drainage structures, etc.

21. TRAFFIC DISTRIBUTION.

a. Research studies have shown that aircraft traffic is distributed laterally across runways and taxiways according to statistically normal (bell shaped) distribution. FAA Report No. FAA-RD-36, Field Survey and Analysis of Aircraft Distribution on Airport Pavements, dated February 1975, contains the latest research information on traffic distribution. The design procedures presented in this circular incorporate the statistically normal distribution in the departure levels.

b. In addition to the lateral distribution of traffic across pavements, traffic distribution and nature of loadings are considered at runway ends, aprons, and high speed turnoffs.

22. TYPICAL SECTIONS. Typical plan and cross section drawings for runway pavements are shown in Figure 3-1. These typical sections are intended for runways to serve jet powered aircraft. Deviations from these typical sections will be common due to the change inherent in staged construction projects where runways are extended and the location of taxiways is uncertain. As a general rule-of-thumb the designer should specify full pavement thickness T where departing traffic will be using the pavement; pavement thickness of 0.9T will be specified where traffic will be arrivals such as high speed turnoffs; and pavement thickness of 0.7T will be specified where pavement is required but traffic is unlikely such as along the extreme outer edges of the runway. Note that the full-strength keel section has been reduced to 50 feet (15 m) on the basis of the research study discussed in paragraph 21.

23. CLIMATIC CONSIDERATIONS.

a. General. The design of an airport pavement must consider the climatic conditions which will act on the pavement during its construction and life. Most climatic effects such as protection of the pavement during curing, laydown temperatures, etc., are handled by construction specifications and local construction experience.

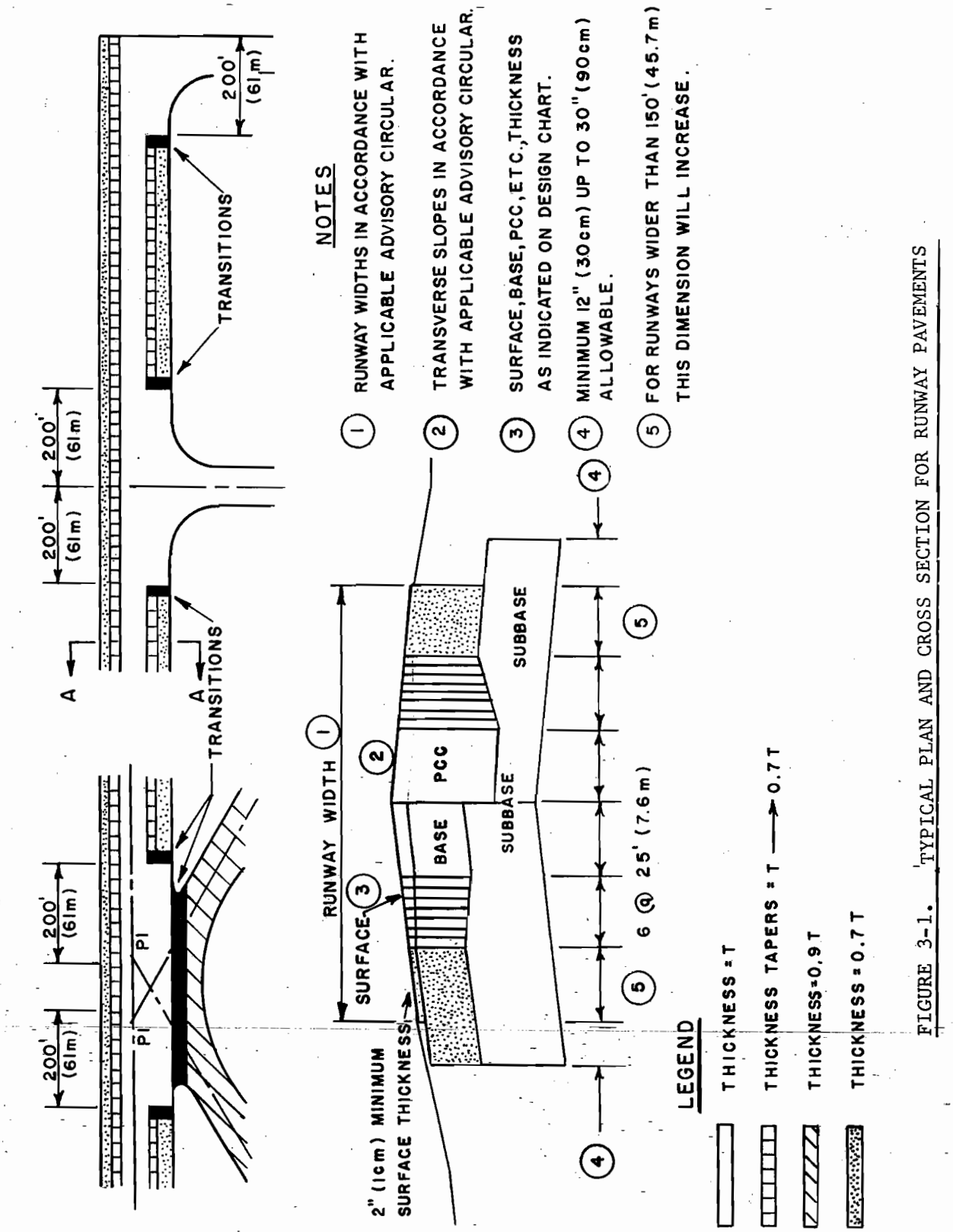

FIGURE 3-1. TYPICAL PLAN AND CROSS SECTION FOR RUNWAY PAVEMENTS

E.3 FAA厚度設計法之發展過程

APPENDIX 2. DEVELOPMENT OF PAVEMENT DESIGN CURVES.

1. BACKGROUND.

a. The pavement design curves presented in this circular were developed using the California Bearing Ratio (CBR) method for flexible pavements and the Westergaard edge loading analysis for rigid pavements. The curves are constructed for the gross weight of the aircraft assuming 95% of the gross weight is carried on the main landing gear assembly and 5% of the gross weight is carried on the nose gear assembly. Aircraft traffic is assumed to be normally distributed across the pavement in the transverse direction. See FAA Research Report No. FAA-RD-74-36, Field Survey and Analysis of Aircraft Distribution on Airport Pavement. Pavements are designed on the basis of static load analysis. Impact loads are not considered to increase the pavement thickness requirements. See FAA Research Report No. FAA-RD-74-39, Pavement Response to Aircraft Dynamic Loads.

b. Generalized design curves are presented in Chapter 3 for single, dual, and dual tandem main landing gear assemblies. These generalized curves do not represent specific aircraft but are prepared for a range of aircraft characteristics which are representative of all civil aircraft except wide body. The aircraft characteristics assumed for each landing gear assembly are shown in Tables 1, 2, and 3.

2. RIGID PAVEMENTS.

a. The design of rigid airport pavements is based on the Westergaard analysis of an edge loaded slab resting on a dense liquid foundation. The edge loading stresses are reduced by 25 percent to account for load transfer across joints. Two different cases of edge loading are covered by the design curves. Figures 3-14 through 3-22 assume the landing gear assembly is either tangent to a longitudinal joint or perpendicular to a transverse joint, whichever produces the largest stress. Figures 3-23 through 3-29 are for dual tandem assemblies and have been rotated through an angle to produce the maximum edge stress. Computer analyses were performed for angles from 0 to 90 degrees in 10-degree increments. Single and dual wheel assemblies were analyzed for loadings tangent to the edge only as the stress is maximum in that position. Sketches of the various assembly positions are shown in Figure 1.

TABLE 1. SINGLE WHEEL ASSEMBLY

Gross Weight lbs.	(kg)	Tire Pressure psi	(MN/m^3)
30,000	(13 600)	75	(0.52)
45,000	(20 400)	90	(0.62)
60,000	(27 200)	105	(0.72)
75,000	(34 000)	120	(0.83)

TABLE 2. DUAL WHEEL ASSEMBLY

Gross Weight lbs.	(kg)	Tire Pressure psi	(MN/m^2)	Dual Spacing in.	(cm)
50,000	(22 700)	80	(0.55)	20	(51)
75,000	(34 000)	110	(0.76)	21	(53)
100,000	(45 400)	140	(0.97)	23	(58)
150,000	(68 000)	160	(1.10)	30	(76)
200,000	(90 700)	200	(1.38)	34	(86)

TABLE 3. DUAL TANDEM ASSEMBLY

Gross Weight lbs.	(kg)	Tire Pressure psi	(MN/m^2)	Dual Spacing in.	(cm)	Tandem Spacing in.	(cm)
100,000	(45 400)	120	(0.83)	20	(51)	45	(114)
150,000	(68 000)	140	(0.97)	20	(51)	45	(114)
200,000	(90 700)	160	(1.10)	21	(53)	46	(117)
300,000	(136 100)	180	(1.24)	26	(66)	51	(130)
400,000	(181 400)	200	(1.38	30	(76)	55	(140)

Specific design curves are presented for wide body aircraft. The aircraft characteristics are shown on the design curves.

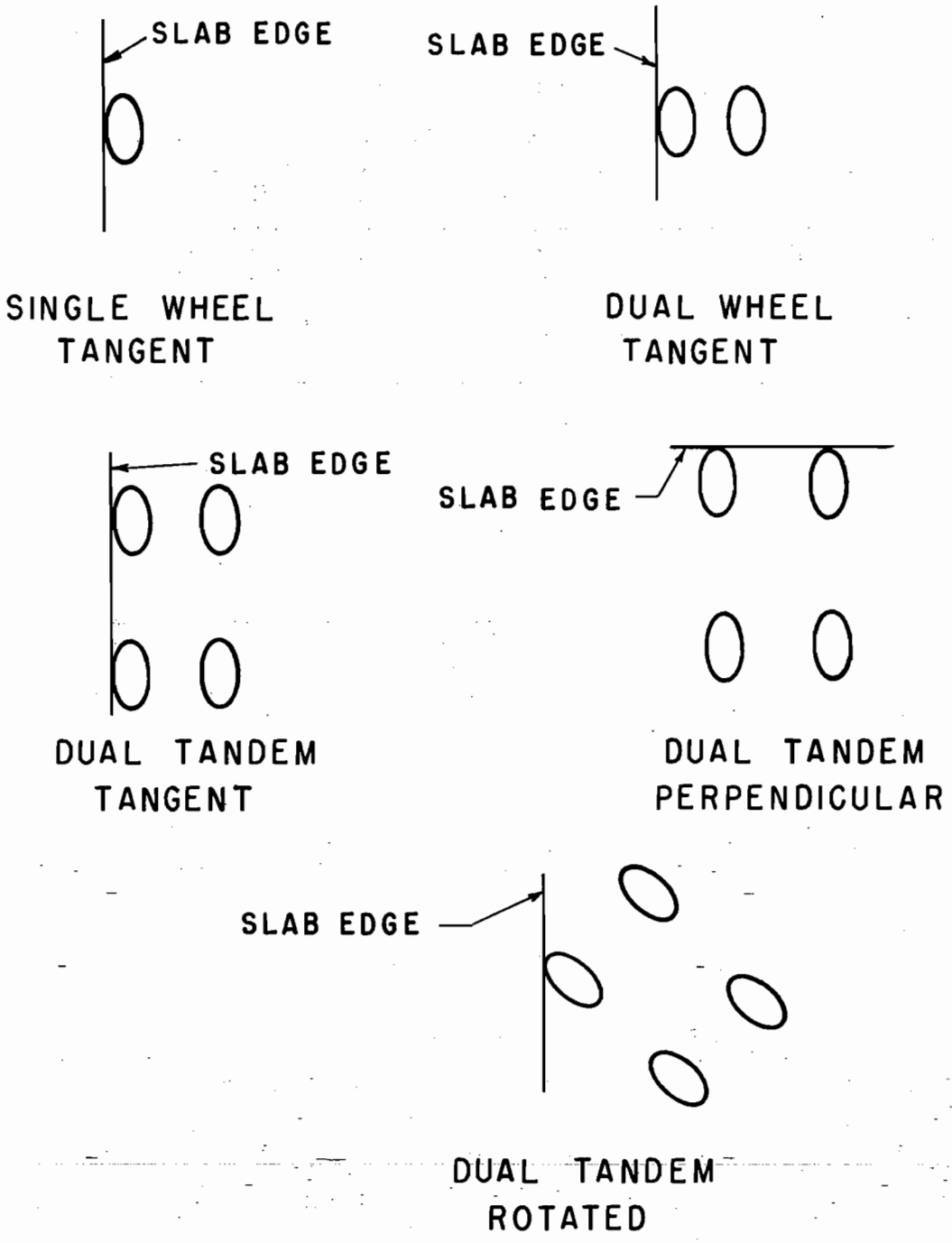

FIGURE 1. ASSEMBLY POSITIONS FOR RIGID PAVEMENT ANALYSIS

b. Fatigue effects are taken into consideration by converting traffic to coverages. The coverage concept provides a means of normalizing pavement performance data which can consist of a variety of wheel sizes, spacings and loads for pavements of different cross sections. For rigid pavements, coverage is a measure of the number of maximum stress applications occurring within the pavement slab due to the applied traffic. One coverage occurs when each point in the pavement within the limits of the traffic lane has experienced a maximum stress, assuming the stress is equal under the full tire print. Each pass (departure) of an aircraft can be converted to coverages using a single pass-to-coverage ratio which is developed assuming a normal distribution and applying standard statistical techniques. The pass-to-coverage ratios used in developing the rigid pavement design curves in Chapter 3 are given in Table 4. Annual departures are converted to coverages assuming a 20-year design life. Coverages are determined by multiplying annual departures by 20 and dividing that product by the pass-to-coverage ratio shown in Table 4.

TABLE 4. PASS-TO-COVERAGE RATIOS FOR RIGID PAVEMENTS

Design Curve	Pass-to-Coverage Ratio
Single Wheel	5.18
Dual Wheel	3.48
Dual Tandem	3.68
B-747	3.70
DC 10-10	3.64
DC 10-30	3.38
L-1011	3.62

c. After the conversion of departures to coverages, the slab thickness is adjusted in accordance with the fatigue curve developed by the Corps of Engineers from test track data and observation of in-service pavements. The fatigue relationship is applicable to the pavement structure; i.e., the slab and foundation are both included in the relationship. The thickness of pavement required to sustain 5,000 coverages of the design loading is considered to be 100 percent thickness. Any coverage level could have been selected as the 100 percent thickness level as long as the relative thicknesses for other coverage levels shown in Figure 2 is maintained.

d. Pavement thickness requirements for 5,000 coverages were computed for various concrete strengths and subgrade moduli. Allowable concrete stress for 5,000 coverages was computed by dividing the concrete flexural strength by 1.3 (analogous to a safety factor). The pavement thickness necessary to produce the allowable concrete stress for 5,000 coverages is then multiplied by the percent thickness shown in Figure 2 for other coverage levels.

3. FLEXIBLE PAVEMENTS.

a. The design curves for flexible pavements in Chapter 3 of this circular are based on the CBR method of design. The CBR is the ratio of the load required to produce a specified penetration of a standard piston into the material in question to the load required to produce the same penetration in a standard well-graded, crushed limestone. Pavement thicknesses necessary to protect various CBR values from shear failure have been developed through test track studies and observations of in-service pavements. These thicknesses have been developed for single wheel loadings. Assemblies other than single wheel are designed by computing the equivalent single wheel load for the assembly based on deflection. Once the equivalent single wheel is established, the pavement section thickness can be determined from the relationships discussed above.

b. Load repetitions are indicated on the design curves in terms of annual departures. The annual departures are assumed to occur over a 20-year life. In the development of the design curves, departures are converted to coverages. For flexible pavements, coverage is a measure of the number of maximum stress applications that occur on the surface of the pavement due to the applied traffic. One coverage occurs when all points on the pavement surface within the traffic lane have been subjected to one application of maximum stress, assuming the stress is equal under

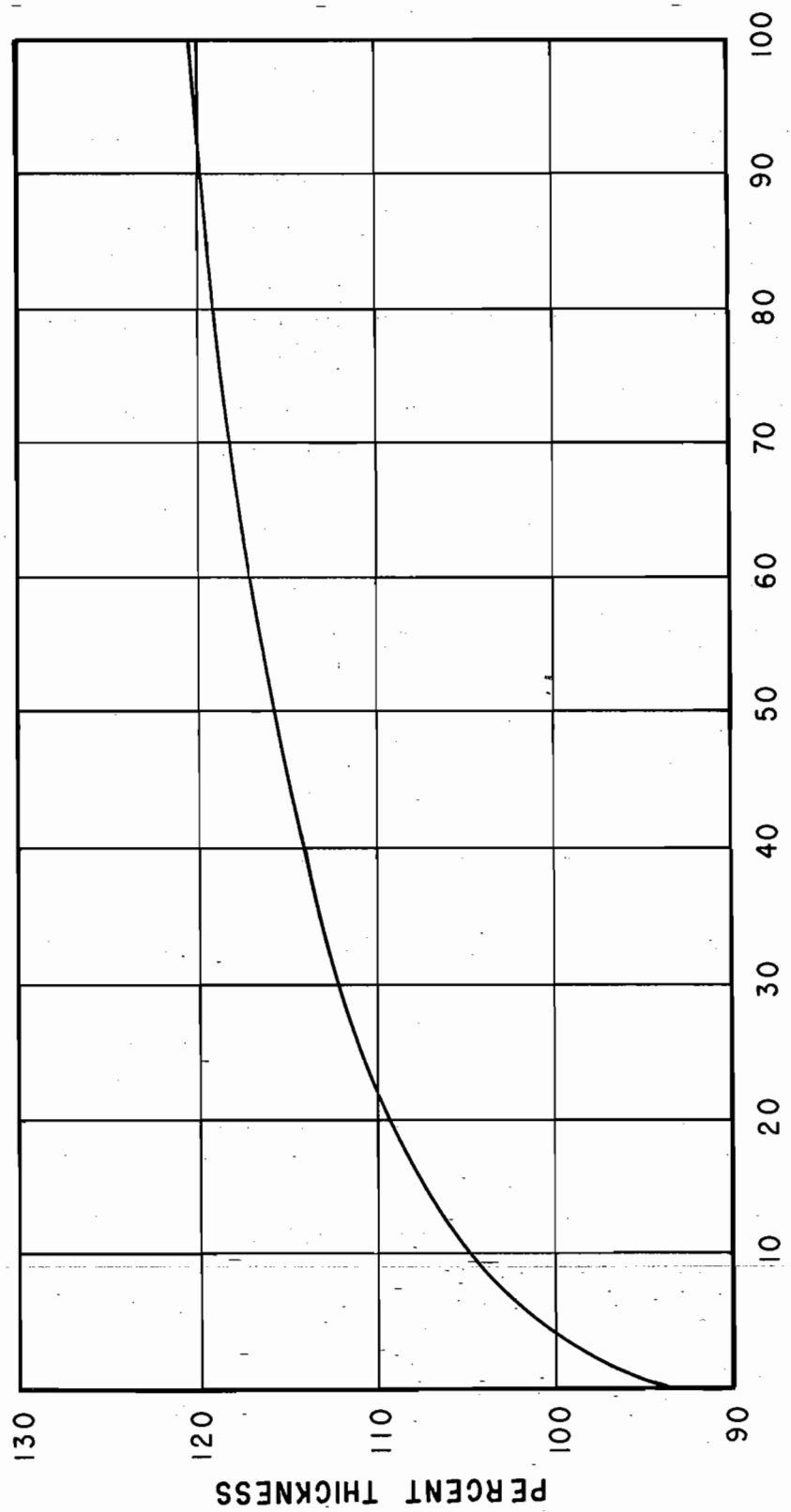

FIGURE 2. PERCENT THICKNESS VS. COVERAGES

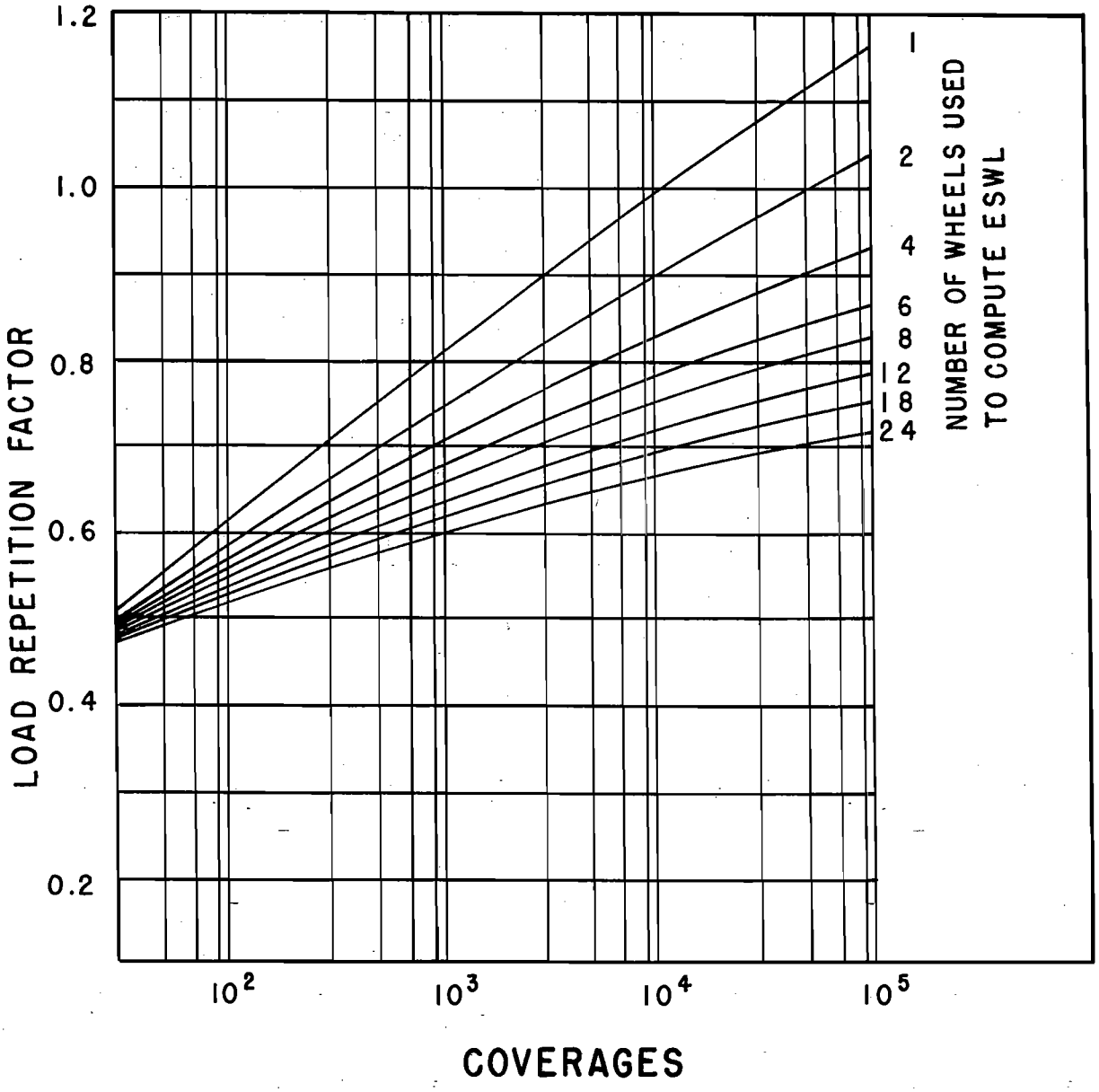

FIGURE 3. LOAD REPETITION FACTOR VS. COVERAGES

the full tire print. Each pass (departure) of an aircraft can be converted to coverages using a single pass-to-coverage ratio which is developed assuming a normal distribution and applying standard statistical techniques. The pass-to-coverage ratios used in developing the flexible pavement design curves in Chapter 3 are given in Table 5. Annual departures are converted to coverages by multiplying by 20 and dividing that product by the pass-to-coverage ratio given in Table 5. Figure 3 shows the relationship between load repetition factor and coverages. The pavement section thickness determined in accordance with paragraph a above is multiplied by the appropriate load repetition factor (Figure 3) to give the final pavement thickness required for various traffic levels.

TABLE 5. PASS-TO-COVERAGE RATIOS FOR FLEXIBLE PAVEMENTS

Design Curve	Pass-to-Coverage Ratio
Single Wheel	5.18
Dual Wheel	3.48
Dual Tandem	1.84
B-747	1.85
DC 10-10	1.82
DC 10-30	1.69
L-1011	1.81

MODIFIED PCA STRESS ANALYSIS AND THICKNESS DESIGN PROCEDURES

Ying-Haur Lee[1], Jean-Hwa Bair, Chao-Tsung Lee, Shao-Tang Yen, and Ying-Ming Lee

ABSTRACT

This study focused on the development of a new stress analysis and thickness design procedure for jointed concrete pavements. Based on Westergaard's edge stress solution and several prediction models for stress adjustments for a variety of loading and environmental (i.e., thermal curling) conditions, a modified PCA equivalent stress analysis and thickness design procedure was proposed and implemented in a highly user-friendly, window-based TKUPAV program for practical trial applications. The proposed approach has been further verified by reproducing very close results to the PCA's equivalent stresses and fatigue damages using a spreadsheet program and the TKUPAV program. The possible detrimental effect of loading plus day-time curling has also been illustrated in a case study, which also indicated that the effect of thermal curling should be considered in the thickness design of concrete pavements.

INTRODUCTION

The Portland Cement Association's thickness design procedure (or PCA method) is the most well-known, widely-adopted, and mechanically-based procedure for the thickness design of jointed concrete pavements [*1*]. Since PCA's equivalent stress was determined based on a fixed slab modulus, a fixed slab length and width, a constant contact area, wheel spacing, axle spacing, and aggregate interlock factor in order to simplify the calculations, the required minimum slab thickness will be the same using the PCA method despite the fact that a shorter or longer joint spacing, a better or worse load transfer mechanism, different wheel spacing and axle spacing, and environmental effects are often considered in reality. Therefore, the main objective of this study was to develop a new stress analysis and thickness design procedure for jointed concrete pavements through proposed modifications to the PCA's equivalent stress calculations and fatigue analysis [*2*].

REVIEW OF PCA THICKNESS DESIGN PROCEDURE

The PCA method is the most widely-adopted thickness design procedure for jointed concrete pavements based on mechanical principles. Based on the results of J-SLAB [*3*] finite element (F.E.) analysis, the PCA method uses design tables and charts and a PCAPAV personal

[1] **Ying-Haur Lee, Associate Professor; Jean-Hwa Bair, Chao-Tsung Lee, Shao-Tang Yen, and Ying-Ming Lee, Graduate Research Assistants, Department of Civil Engineering, Tamkang University, E725, #151 Ying-Chuan Rd., Tamsui, Taipei, Taiwan 251, R.O.C., TEL: (886-2) 623-2408, FAX: (886-2) 620-9747, E-mail: yinghaur@tedns.te.tku.edu.tw.**

computer program to determine the minimum slab thickness required to satisfy the following design factors: design period, the flexural strength of concrete (or the concrete modulus of rupture), the modulus of subbase-subgrade reaction, design traffic (including load safety factor, axle load distribution), with or without doweled joints and a tied concrete shoulder [*4*].

The PCA thickness design criteria are to limit the number of load repetitions based on both fatigue analysis and erosion analysis. Cumulative damage concept is used for the fatigue analysis to prevent the first crack initiation due to critical edge stresses, whereas the principal consideration of erosion analysis is to prevent pavement failures such as pumping, erosion of foundation, and joint faulting due to critical corner deflections during the design period. Since the main focus of his study was to develop alternative stress analysis procedures for thickness design of concrete pavements, the erosion analysis was not within the scope of this study.

Equivalent Stress Calculations

In the PCA thickness design procedure, the determination of equivalent stress is based on the resulting maximum edge bending stress of J-SLAB F.E. analysis under a single axle (SA) load and a tandem axle (TA) load for different levels of slab thickness and modulus of subgrade reaction. The basic input parameters were assumed as: slab modulus E = 4E+06 psi (2.8E+5 kg/cm^2), Poisson's ratio μ = 0.15, finite slab length L = 180 in. (4.57 m), finite slab width W = 144 in. (3.66 m). A standard 18-kip (8,165 kg) single axle load (dual wheels) with each wheel load equal to 4,500 pounds (2,041 kg), wheel contact area = 7*10 in.^{2} (17.8*25.4 cm^2) or an equivalent load radius a = 4.72 in. (12.0 cm), wheel spacing s = 12 in. (30.5 cm), axle width (distance between the center of dual wheels) D = 72 in. (183 cm) was used for the analysis, whereas a standard 36-kip (16,330 kg) tandem axle load (dual wheels) with axle spacing t = 50 in. (127 cm) and remaining gear configurations same as the standard single axle was also used. If a tied concrete shoulder (WS) was present, the aggregate interlock factor was assumed as AGG = 25000 psi (1,750 kg/cm^2). PCA also incorporated "the results of computer program MATS [*5*], developed for analysis and design of mat foundations, combined footings and slabs-on-grade" to account for the support provided by the subgrade extending beyond the slab edges for a slab with no concrete shoulder (NS). Together with several other adjustment factors, the equivalent stress was defined as follows: [*6*]

$$\sigma_{eq} = \frac{6 * M_e}{h^2} * f_1 * f_2 * f_3 * f_4 \qquad \text{(E.1)}$$

$$M_e = \begin{cases} -1600 + 2525 * \log(\ell) + 24.42 * \ell + 0.204 * \ell^2 & \text{for SA / NS} \\ 3029 - 2966.8 * \log(\ell) + 133.69 * \ell - 0.0632 * \ell^2 & \text{for TA / NS} \\ (-970.4 + 1202.6 * \log(\ell) + 53.587 * \ell) * (0.8742 + 0.01088 * k^{0.447}) & \text{for SA / WS} \\ (2005.4 - 1980.9 * \log(\ell) + 99.008 * \ell) * (0.8742 + 0.01088 * k^{0.447}) & \text{for TA / WS} \end{cases}$$

$$f_1 = \begin{cases} (24 / SAL)^{0.06} * (SAL / 18) & \text{for SA} \\ (48 / TAL)^{0.06} * (TAL / 36) & \text{for TA} \end{cases}$$

$$f_2 = \begin{cases} 0.892 + h / 85.71 - h^2 / 3000 & \text{for NS} \\ 1 & \text{for WS} \end{cases}$$

$f_3 = 0.894$ for 6% Truck at the Slab Edge

$f_4 = 1/[1.235*(1-CV)]$

where:

σ_{eq} = equivalent stress, psi;
h = thickness of the slab, in.;
$\ell = [Eh^3/(12*(1-\mu^2)*k)]^{0.25}$, radius of relative stiffness of the slab-subgrade system, in.;
k = modulus of subgrade reaction, pci;
f_1 = adjustment factor for the effect of axle loads and contact areas;
f_2 = adjustment factor for a slab with no concrete shoulder based on the results of MATS computer program;
f_3 = adjustment factor to account for the effect of truck placement on the edge stress (PCA recommended a 6% truck encroachment, f_3=0.894);

edge truck placement, %	1	2	3	4	5	6	7
adjustment factor, f_3	0.825	0.855	0.870	0.880	0.890	0.894	0.901

f_4 = adjustment factor to account for the increase in concrete strength with age after the 28*th* day, along with a reduction in concrete strength by one coefficient of variation (CV); (PCA used CV=15%, f_4=0.953); and
SAL, TAL = actual single axle or tandem axle load, kips.

It was also noted that the above equivalent stress equation (E.1) is only applicable to U.S. customary system (English system). Until proper adjustments to the coefficients in the equation, it cannot be directly used with pertinent input variables in metric unit (SI system).

Fatigue Analysis

PCA's fatigue analysis concept was to avoid pavement failures (or first initiation of crack) by fatigue of concrete due to critical stress repetitions. Based on Miner's cumulative fatigue damage assumption, the PCA thickness design procedures first let the users select a trial slab thickness, calculate the ratio of equivalent stress (σ_{eq}) versus the concrete modulus of rupture (S_c) for each axle load and axle type, then determine the maximum allowable load repetitions (N_f) based on the following σ_{eq}/S_c - N_f relationship : [*4*]

$$\begin{cases} \log N_f = 11.737 - 12.077*(\sigma_{eq}/S_c) & \text{for } \sigma_{eq}/S_c \geq 0.55 \\ N_f = \left(\dfrac{4.2577}{\sigma_{eq}/S_C - 0.4325}\right)^{3.268} & \text{for } 0.45 < \sigma_{eq}/S_c < 0.55 \\ N_f = \text{Unlimited} & \text{for } \sigma_{eq}/S_c \leq 0.45 \end{cases} \quad \text{(E.2)}$$

The PCA thickness design procedures then use the expected number of load repetitions dividing by N_f to calculate the percentage of fatigue damage for each axle load and axle type. The total cumulative fatigue damage has to be within the specified 100% limiting design criterion, or a different trial slab thickness has to be used and repeat previous calculations again. Thus, in the

PCAPAV program, an iterative process was utilized to help the users automatically determine the minimum required slab thickness.

Identical equivalent stresses and fatigue damages were obtained, after comparing the results of a spreadsheet using the aforementioned equations (E.1) and (E.2) with the PCAPAV program outputs. A more detailed example was described later in a case study.

EFFECTS OF THERMAL CURLING AND MOISTURE WARPING

Whether curling and warping stresses should be considered in concrete pavement thickness design is quite controversial. The temperature differential through the slab thickness and the self-weight of the slab induces additional thermal curling stresses. For day-time curling condition, compressive curling stresses are induced at the top of the slab whereas tensile stresses occur at the bottom; or vice versa for night-time curling condition. The moisture gradient in concrete slabs also results in additional warping stresses. Since higher moisture content is generally at the bottom of the slab, compressive and tensile stresses will occur at the bottom and at the top of the slab, respectively. A totally different situation will happen if the moisture content at the top of the slab is higher than that at the bottom right after raining.

Even though the effects of thermal curling and moisture warping have been discussed in the PCA design guide, curling stresses were not considered in the fatigue analysis due to the possible beneficial effect of most heavy trucks driving at night and only quite limited number of day-time curling combined with load repetitions. Furthermore, since moisture gradient highly depends on a variety of factors such as the ambient relative humidity at the slab surface, free water in the slab, and the moisture content of the subbase or subgrade, which are very difficult to measure accurately, thus it was also ignored in the PCA's fatigue analysis [*4*].

On the other hand, many others have repetitively indicated that curling stress should be considered in pavement thickness design, because curling stress may be quite large and cause the slab to crack when combined with only very few number of load repetitions. Darter and Barenberg [*7*] surveyed the non-traffic loop of the AASHO Road Test and have found after 16 years most of the long slabs (40 ft or 12.2 m) had cracks, but not in the 15-foot (4.57 m) slabs, probably because longer slabs have much greater curling stress than shorter slabs. In consideration of zero-maintenance design, Darter and Barenberg have suggested the inclusion of curling stress for pavement thickness design. More detailed descriptions and similar suggestions to include curling stress in the fatigue analysis may also be found in the NCHRP 1-26 report [*8*].

MODIFIED PCA STRESS ANALYSIS AND THICKNESS DESIGN PROCEDURES

PCA's equivalent stress was determined based on the assumptions of a fixed slab modulus, a fixed slab length and width, a constant contact area, wheel spacing, axle spacing, and aggregate interlock factor, which may influence the stress occurrence, in order to simplify the calculations. Thus, the required minimum slab thickness will be the same based on the PCA thickness design

procedure disregard the fact that a shorter or longer joint spacing, a better or worse load transfer mechanism, different wheel spacing and axle spacing, and environmental effects are considered.

Therefore, this study strives to revise PCA's equivalent stress calculation process and to develop a new thickness design procedure by including the effect of thermal curling. A well-known slab-on-grade finite element program (ILLI-SLAB) was used for the analysis. Based on Westergaard's closed-form edge stress solution and several prediction models for stress adjustments for a variety of loading and environmental conditions, a modified PCA equivalent stress calculation procedure was developed. Thus, the required minimum slab thickness may be determined using the original PCA's fatigue analysis concept.

ILLI-SLAB Finite Element Solutions

The basic tool for this analysis is the ILLI-SLAB F.E. computer program which was originally developed in 1977 and has been continuously revised and expanded at the University of Illinois over the years. The ILLI-SLAB model is based on classical medium-thick plate theory, and employs the 4-noded 12-degree-of-freedom plate bending elements. The Winkler foundation assumed by Westergaard is modeled as a uniform, distributed subgrade through an equivalent mass foundation. Curling analysis was not implemented until versions after June 15, 1987. The present version (March 15, 1989) [*9*] was successfully compiled on available Unix-based workstations of the Civil Engineering Department at Tamkang University. With some modifications to the original codes, a micro-computer version of the program was also developed using Microsoft FORTRAN PowerStation [*10*].

Identification of Mechanistic Variables (Dimensionless)

To account for the effects of a finite slab, dual-wheel, tandem axle, or tridem axle, a widened outer lane, a tied concrete shoulder, a second bonded or unbonded layer under loading only condition, the following relationship has been identified through many intensive F.E. studies for a constant Poisson's ratio (usually $\mu \approx 0.15$) [*2, 11*]:

$$\frac{\sigma h^2}{P}, \frac{\delta k \ell^2}{P}, \frac{q\ell^2}{P} = f\left(\frac{a}{\ell}, \frac{L}{\ell}, \frac{W}{\ell}, \frac{s}{\ell}, \frac{t}{\ell}, \frac{D_0}{\ell}, \frac{AGG}{k\ell}, \left(\frac{h_{eff}}{h_1}\right)^2\right) \tag{E.3}$$

Where σ, q are slab bending stress and vertical subgrade stress, respectively, $[FL^{-2}]$; δ is the slab deflection, [L]; P = wheel load, [F]; a = the radius of the applied load, [L]; $\ell=(E*h^3/(12*(1-\mu^2)*K))^{0.25}$ is the radius of relative stiffness of the slab-subgrade system [L]; k = modulus of subgrade reaction, $[FL^{-3}]$; L, W = length and width of the finite slab, [L]; s = transverse wheel spacing, [L]; t = longitudinal axle spacing, [L]; D_0 = offset distance between the outer face of the wheel and the slab edge, [L]; AGG = aggregate interlock factor, $[FL^{-2}]$; $h_{eff} = (h_1^2 + h_2^2 * (E_2*h_2)/(E_1*h_1))^{0.5}$ is the effective thickness of two unbonded layers, [L]; h_1, h_2 = thickness of the top slab, and the bottom slab, [L]; and E_1, E_2 = concrete modulus of the top slab, and the bottom slab, $[FL^{-2}]$. Note that variables in both sides of the expression are all dimensionless and primary dimensions are represented by [F] for force and [L] for length.

Furthermore, the following concise relationship has been identified by Lee and Darter [*12*] for the effects of loading plus thermal curling:

$$\frac{\sigma}{E}, \frac{\delta h}{\ell^2}, \frac{qh}{k\ell^2} = f\left(\frac{a}{\ell}, \alpha\Delta T, \frac{L}{\ell}, \frac{W}{\ell}, \frac{\gamma h^2}{k\ell^2}, \frac{ph}{k\ell^4}\right) \qquad \text{(E.4)}$$

Where α is the thermal expansion coefficient, $[T^{-1}]$; ΔT is the temperature differential through the slab thickness, [T]; γ is the unit weight of the concrete slab, $[FL^{-3}]$; $D_\gamma=\gamma*h^2/(k*\ell^2)$; and $D_P=P*h/(k*\ell^4)$. Also note that D_γ was defined as the relative deflection stiffness due to self-weight of the concrete slab and the possible loss of subgrade support, whereas D_P was the relative deflection stiffness due to the external wheel load and the loss of subgrade support. The primary dimension for temperature is represented by [T].

Development of Stress Prediction Models

A series of F. E. factorial runs were performed based on the dominating mechanistic variables identified. Several BASIC programs were written to automatically generate the F. E. input files and summarize the desired outputs. The F. E. mesh was generated according to the guidelines established in earlier studies [*13*]. As proposed by Lee and Darter [*14*], a two-step modeling approach using the projection pursuit regression (PPR) technique introduced by Friedman and Stuetzle [*15*] was utilized for the development of prediction models. Through the use of local smoothing techniques, the PPR attempts to model a multi-dimensional response surface as a sum of several nonparametric functions of projections of the explanatory variables. The projected terms are essentially two-dimensional curves which can be graphically represented, easily visualized, and properly formulated. Piece-wise linear or nonlinear regression techniques were then used to obtain the parameter estimates for the specified functional forms of the predictive models. This algorithm is available in the S-PLUS statistical package [*16*]. The proposed prediction models for the stress adjustments are given in Table 1. More detailed descriptions of the development process can be found in Reference [*2*].

Modified Equivalent Stress Calculations

To expand the applicability of the PCA's equivalent stress for different material properties, finite slab sizes, gear configurations, and environmental effects (e.g., temperature differentials), the following equation was proposed [*2, 17, 18*]:

$$\sigma_{eq} = \left(\sigma_w * R_1 * R_2 * R_3 * R_4 * R_5 + R_T * \sigma_c\right) * f_3 * f_4 \qquad \text{(E.5)}$$

$$\sigma_w = \frac{3(1+\mu)P}{\pi(3+\mu)h^2}\left[\log_e \frac{Eh^3}{100ka^4} + 1.84 - \frac{4}{3}\mu + \frac{1-\mu}{2} + 1.18(1+2\mu)\frac{a}{\ell}\right]$$

$$\sigma_c = \frac{CE\alpha\Delta T}{2} = \frac{E\alpha\Delta T}{2}\left\{1 - \frac{2\cos\lambda\cosh\lambda}{\sin 2\lambda \sinh 2\lambda}\left(\tan\lambda + \tanh\lambda\right)\right\}$$

where:

σ_{eq} = modified equivalent stress, [FL^{-2}];
σ_w = Westergaard's closed-form edge stress solution, [FL^{-2}];
σ_c = Westergaard/Bradbury's curling stress, [FL^{-2}];
E = elastic modulus of the slab, [FL^{-2}];
h = slab thickness, [L];
λ = $W/((8^{0.5})*\ell)$;
C = the curling stress coefficient;
R_1 = adjustment factor for different gear configurations including dual-wheel, tandem axle, and tridem axle;
R_2 = adjustment factor for finite slab length and width;
R_3 = adjustment factor for a tied concrete shoulder;
R_4 = adjustment factor for a widened outer lane;
R_5 = adjustment factor for a bonded/unbonded second layer; and
R_T = adjustment factor for the combined effect of loading plus day-time curling.

Based on the principles of superposition, the effects of other different variations of gear configurations such as dual wheel / tridem axle, and dual wheel / tandem axle may also be obtained by a simple matter of multiplication. Also note that the last column of Table 1 indicates the applicable ranges of the predictive model; the upper or the lower bound may be used if the input data exceeds these limits.

For the case of a bonded or unbonded second layer, the pertinent variables are defined as: h_{eff} = effective thickness of two unbonded layers converted to a single slab, [L]; α = a distance from the middle surface of the bottom layer to the location of the neutral axis of an equivalent system, [L]; β = a distance from the neutral axis to the middle surface of the top layer, [L]; h_{1f}, h_{2f} = the equivalent thickness of top layer and bottom layer when converting a bonded layer to an unbonded layer, [L] ◦

Modified Thickness Design Procedure

A new thickness design procedure was developed based on the above "modified equivalent stresses," and the PCA's cumulative fatigue damage concept. The NCHRP 1–26 report [*8*] has suggested the inclusion of thermal curling by separating traffic repetitions into three parts: loading with no curling, loading combined with day-time curling, and loading combined with night-time curling. Nevertheless, based on practical considerations of the difficulty and variability in determining temperature differentials, a more conservative design approach was proposed by neglecting possible beneficial effects due to night-time curling. Thus, only the conditions of loading with no curling, and loading combined with day-time curling were considered under this study. Separated fatigue damages are then calculated and accumulated. The 100% limiting criterion of the cumulative fatigue damage is also applied to determine the minimum required slab thickness. A brief description of the proposed thickness design procedures is as follows:

1. Data input: assume a trial slab thickness; input other pertinent design factors, material properties, load distributions, and environmental factors (i.e., temperature differentials).
2. Expected repetitions (n_i): calculate the expected repetitions for the case of loading with

no curling and for the case of loading with day-time curling during the design period.

3. Modified equivalent stress (σ_{eq}): calculate the "modified equivalent stresses" using equation (E.5) for each case.
4. Stress Ratio(σ_{eq} /S_C): calculate the ratio of the modified equivalent stress versus the concrete modulus of rupture (S_C) for each case.
5. Maximum allowable load repetitions (N_i): determine the maximum allowable load repetitions for different stress ratios based on the fatigue equation (E.2).
6. Calculate the percentage of each individual fatigue damage (n_i/N_i).
7. Check if the cumulative fatigue damage $\Sigma (n_i/N_i)<100\%$.
8. If not, assume a different slab thickness and repeat steps (1) - (7) again to obtain the minimum required slab thickness.

DEVELOPMENT OF THE TKUPAV PROGRAM

To facilitate practical trial applications of the proposed stress analysis and thickness design procedures, a window-based computer program (TKUPAV) was developed using the Microsoft Visual Basic software package [*19*]. The TKUPAV program was designed to be highly user-friendly and thus came with many well-organized graphical interfaces, selection menus, and command buttons for easy use. Both English version and Chinese version of the program are available. Furthermore, since all the mechanistic variables used in the proposed models are dimensionally correct, both English and metric (SI) systems can be used by the program. Several example input screens of the TKUPAV program are shown in Figure 1.

VERIFICATION OF THE TKUPAV PROGRAM

The proposed stress analysis and thickness design procedures have been further verified by reproducing very close results to the PCA's equivalent stresses and fatigue damages in the following case study using a spreadsheet program and the TKUPAV program. Furthermore, the possible detrimental effect of loading plus day-time curling has been clearly observed even when a very small percentage of loading plus curling repetitions was considered in the case study. Thus, it also illustrated the importance of incorporating the effect of thermal curling in the thickness design of concrete pavements.

Suppose a four-lane divided highway with the following design factors: design period = 20 years, load safety factor LSF = 1.2, average daily traffic ADT = 12,900, lane distribution LD = 81%, directional distribution = 50%, percentage of heavy trucks = 19%, annual traffic growth rate = 4% (compounded), the modulus of subbase/subgrade reaction k = 130 pci (3.64 kg/cm^3), the concrete modulus of rupture S_C = 650 psi (45.5 kg/cm^2), and the coefficient of variation = 15%. The expected axle load distributions are listed in the following table [*1, 4*]: (Note: 1 in. = 2.54 cm, 1 psi = 0.07 kg/cm^2, 1 pci = 0.028 kg/cm^3, 1 kip = 454 kg)

Single Axle		Tandem Axle	
Load, kips	Axles / 1000 Trucks	Load, kips	Axles / 1000 Trucks
30	0.58	52	1.96
28	1.35	48	3.94
26	2.77	44	11.48
24	5.92	40	34.27
22	9.83	36	81.42
20	21.67	32	85.54
18	28.24	28	152.23
16	38.83	24	90.52
14	53.94	20	112.81
12	168.85	16	124.69

(1) Comparison of Equivalent Stress Calculations (TKUPAV / PCA):

Note that many important factors were implicitly selected by the PCA method: t = 50 in. (127 cm), s = 12 in. (30.5 cm), D = 72 in. (183 cm), a = 4.72 in. (12.0 cm), L = 180 in. (4.57 m), W=144 in. (3.66 m), AGG = 25000 psi (1,750 kg/cm^2), E = 4E+06 psi (2.8E+5 kg/cm^2), μ = 0.15. The results of this comparison are summarized in Table 2 (a) - (b) for the case with no concrete shoulder, and Table 2 (c) - (d) when a concrete shoulder was considered. The effect of the four PCA adjustments (f_i) may be excluded in such a comparison. The last column (Column (B) / Column (A)) represent the ratio of equivalent stresses determined by the proposed approach (TKUPAV) and by the PCA method. Apparently, adequate precision to the PCA method can be obtained if the proposed stress analysis procedures are adopted.

(2) Fatigue Analysis Example for Loading Only (TKUPAV / PCAPAV):

Assume a trial slab thickness h = 9.5 in. (24.1 cm) with no concrete shoulder, the results of this fatigue analysis example for loading only are summarized in Table 3. In the PCAPAV analysis, ℓ = 38.73 in. (98.37 cm), f_2 = 0.973, f_3 = 0.894, and f_4 = 0.953. The detailed calculations of stress adjustment factors are given in Table 4; thus,

(a) For a single axle (dual wheels): R_1 = 0.754 * 0.528 = 0.398; and

(b) For a tandem axle (dual wheels): R_1 = 0.754 * 0.528 * 0.452 = 0.180.

Note that the adjustment factor for "axle width" was to account for the effect of other wheels in the far side of the axle using the prediction equation for dual wheels. And the effect of finite slab length and width is R_2 = 0.992 * 1.000 = 0.992.

Apparently, the resulting 71.4% of cumulative fatigue damage calculated by the TKUPAV program is very close to that determined by the PCAPAV program (63.4%). Very good agreement to the equivalent stress calculations was also observed.

(3) TKUPAV Fatigue Analysis Example (with Curling):

Assume a trial slab thickness h = 9.5 in. (24.1 cm) with no concrete shoulder and only a very small portion (10%) of load repetitions was combined with day-time curling. Other pertinent variables are: γ = 0.087 pci (2,436 kg/m^3), α = 5.5E-06 /°F (9.9E-06 /°C), ΔT= 20 °F (11.1°C).

Thus, $\alpha\Delta T = 0.00011$, $W/\ell = 3.873$, $L/\ell = 4.648$, $a/\ell = 0.1219$, $DG = 4.0274$, $\lambda = 1.370$, and σ_c= 88.5 psi (6.20 kg/cm^2). More detailed calculations of the adjustment factors for loading plus curling are given in Table 5.

The results of this TKUPAV fatigue analysis example are summarized in Table 6. Thus, a total of 64.2% fatigue damage was caused by 90% of load repetitions, whereas a total 138.84% of fatigue damage could be induced by only 10% of load repetitions plus day-time curling. In this case, an additional 1/2 inch (1.27 cm) of slab thickness which may reduce the total cumulative fatigue damage from 203.0% to an acceptable level of 41.3% is required.

CONCLUSIONS AND RECOMMENDATIONS

This study focused on the development of a new stress analysis and thickness design procedure for jointed concrete pavements through proposed modifications to the PCA's equivalent stress calculations and fatigue analysis. The proposed approach has been further verified by reproducing very close results to the PCA's equivalent stresses and fatigue damages using Microsoft Excel spreadsheets and the window-based TKUPAV program.

Furthermore, this study also enhanced the applicability of the PCA method by the fact that any different material properties, finite slab sizes, gear configurations (such as additional effects of a single axle / single wheel, and a tridem axle / dual wheels), and environmental effects (e.g., temperature differentials) could be analyzed by the proposed approach. In addition, the proposed approach and prediction models are all applicable to the U. S. customary system or SI unit system because all the mechanistic variables involved are dimensionally correct.

The possible detrimental effect of loading plus day-time curling has also been illustrated in a case study, which also indicated that the effect of thermal curling should be considered in the thickness design of concrete pavements. In addition, a relatively small increase in slab thickness (e.g., 1/2 in.) will result in a very significant reduction in cumulative fatigue damage. The possible beneficial effect of night-time curling was ignored in the proposed approach, however it may be easily incorporated into the proposed approach using an additional prediction model for night-time curling developed by Lee and Darter [*12*]. With some proper adjustments to the TKUPAV program, it may also be applicable to the stress analysis and thickness design of airport concrete pavements.

ACKNOWLEDGMENTS

This research work was sponsored by the National Science Council, Taiwan, Republic of China, under the grant No. NSC85-2211-E032-010. Professor A. M. Ioannides and Professor M. I. Darter are greatly acknowledged for providing many fruitful ideas to the successful accomplishment of this project.

REFERENCES

1. Portland Cement Association, "The Design for Concrete Highway and Street Pavements," PCA, Skokie, Illinois, 1984.
2. Lee, Y. H., Y. M. Lee, S. T. Yen, J. H. Bair, and C. T. Lee, "Development of New Stress Analysis and Thickness Design Procedures for Jointed Concrete Pavements," Final Report - Second Phase (In Chinese), National Science Council, Grant No. NSC85-2211-E032-010, Taiwan, August 1996.
3. Tayabji, S. D., and B. E. Colley, "Analysis of Jointed Concrete Pavement," Report No. FHWA-RD-86-041, Federal Highway Administration, 1986.
4. Huang, Y. H., Pavement Analysis and Design, Prentice-Hall, Inc., 1993.
5. Portland Cement Association, "MATS -User's Manual," Computer Software MC012, PCA, Skokie, Illinois, 1990.
6. Ioannides, A. M., R. A. Salsilli, I. Vinding, and R. G. Packard, "Super-Singles: Implications for Design," Proceedings of the Third International Symposium on Heavy Vehicle Weights and Dimensions, "Heavy Vehicles and Roads - Technology, Safety and Policy," Edited by D. Cebon and C. G. B. Mitchell, University of Cambridge, UK, 1992.
7. Darter, M. I., and E. J. Barenberg, "Design of Zero-Maintenance Plain Jointed Concrete Pavement," Report No. FHWA-RD-77-111, Vol. 1, Federal Highway Administration, 1977.
8. NCHRP, "Calibrated Mechanistic Structural Analysis Procedures for Pavement," NCHRP 1-26, Vol. 1, Final Report; Vol. 2, Appendices, University of Illinois, 1990.
9. Korovesis, G. T., "Analysis of Slab-on-Grade Pavement Systems Subjected to Wheel and Temperature Loadings," Ph.D. Thesis, University of Illinois, Urbana, 1990.
10. Microsoft, "Microsoft FORTRAN PowerStation Professional Development System," User's and Reference Manuals, Microsoft Taiwan Corp., 1994.
11. Salsilli-Murua, R. A., "Calibrated Mechanistic Design Procedure for Jointed Plain Concrete Pavements," Ph.D. Thesis, University of Illinois, Urbana, 1991.
12. Lee, Y. H., and M. I. Darter, "Loading and Curling Stress Models for Concrete Pavement Design," Transportation Research Record 1449, Transportation Research Board, National Research Council, Washington, D. C., 1994, pp. 101-113.
13. Ioannides, A. M., "Analysis of Slabs-on-Grade for a Variety of Loading and Support Conditions," Ph.D. Thesis, University of Illinois, Urbana, 1984.
14. Lee, Y. H., and M. I. Darter, "New Predictive Modeling Techniques for Pavements," Transportation Research Record 1449, Transportation Research Board, National Research Council, Washington, D. C., 1994, pp. 234-245.
15. Friedman, J. H. and W. Stuetzle, "Projection Pursuit Regression," Journal of the American Statistical Association, Vol. 76, 1981, pp. 817-823.
16. Statistical Sciences, Inc., S-PLUS for Windows: User's and Reference Manuals, Ver. 3.3, Seattle, Washington, 1995.
17. Westergaard, H. M., "New Formulas for Stresses in Concrete Pavements of Airfields," American Society of Civil Engineering (ASCE), Transactions, Vol. 113, 1948, pp. 425-444,
18. Bradbury, R. D., Reinforced Concrete Pavements, Wire Reinforcement Institute, Washington, D. C., 1938.
19. Microsoft, "Microsoft Visual Basic," Programmer's Guide and Language Reference, Ver. 3.0, Microsoft Taiwan Corp., 1993.

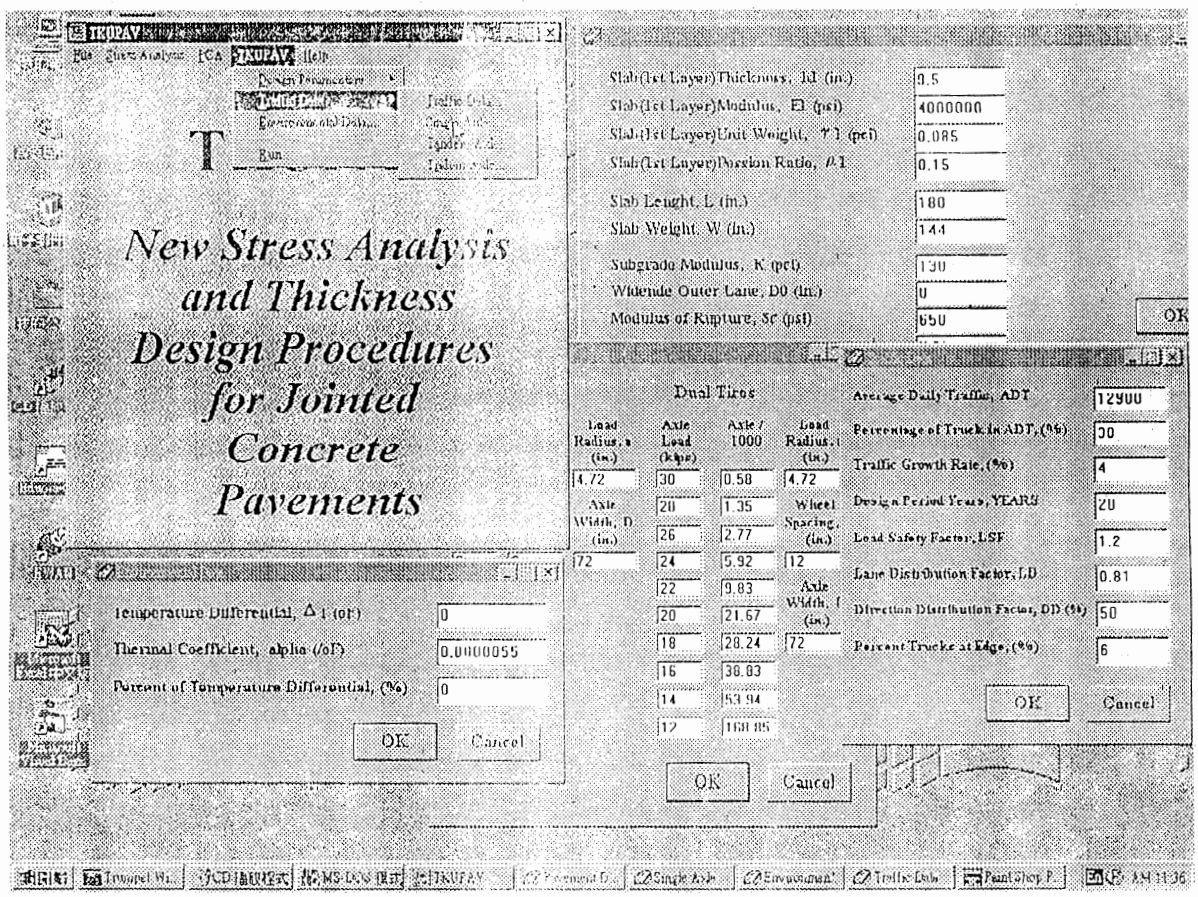

Figure 1 - Sample Input Screens of the TKUPAV Program

Table 1 -- Proposed Prediction Models for Stress Adjustments

Dual Wheel (Single Axle)	R_1=0.56197+0.09313Φ_1+0.0065Φ_2 $\Phi_1 = \begin{cases} -0.043+0.452(A1)+0.075(A1)^2 & if\ A1 \le -2 \\ 2.997+6.278(A1)+4.122(A1)^2+0.964(A1)^3 & if\ A1>-2 \end{cases}$ $\Phi_2 = \begin{cases} -1.461-4.460(A2)+392.524(A2)^2+2955.995(A2)^3+4914.455(A2)^4 & if\ A2 \le 0 \\ -1.425+45.240(A2)-309.329(A2)^2+832.054(A2)^3-765.888(A2)^4 & if\ A2 > 0 \end{cases}$ $A1 = -0.7919x1+0.60762x2+0.06072x3$ $A2=0.01799x1-0.88168x2+0.4715x3$ $X=[x1, x2, x3]=\left[\frac{s}{\ell}, \frac{a}{\ell}, \frac{s \times a}{\ell^2}\right]$	$0.05 \le \frac{a}{\ell} \le 0.4$ $0 \le \frac{s}{\ell} \le 4.0$
Tandem Axle (Single Wheel)	$R_1 = 0.58306 + 0.19316\Phi_1 + 0.06236\ \Phi_2$ $\Phi_1 = \begin{cases} 0.159 + 1.604(A1) + 0.820(A1)^2 + 0.135(A1)^3 & if\ A1 \le -1 \\ 1.319 + 4.509(A1) + 1.760(A1)^2 - 0.914(A1)^3 & if\ A1 > -1 \end{cases}$ $\Phi_2 = \begin{cases} 2.151 + 11.020(A2) - 2.894(A2)^2 & if\ A2 \le -0.2 \\ 2.210 + 11.770(A2) - 16.209(A2)^2 - 70.589(A2) & if\ A2 > -0.2 \end{cases}$ $A1 = -0.51308x1 + 0.85264x2 + 0.08604x3 - 0.04849x4$ $A2 = -0.07313x1 - 0.93937x2 + 0.33502x3 + 0.00055x4$ $X = [x1, x2, x3, x4] = \left[\frac{t}{\ell}, \frac{a}{\ell}, \frac{t \times a}{\ell^2}, \frac{t}{a}\right]$	$0.1 \le \frac{a}{\ell} \le 0.4$ $0 \le \frac{t}{\ell} \le 1.6$
Tridem Axle (Single Wheel)	$R_1 = 0.44485 + 0.17726\Phi_1 + 0.02072\Phi_2$ $\Phi_1 = \begin{cases} 0.230 + 1.078(A1) + 0.177(A1)^2 & if\ A1 \le -1 \\ 2.480 + 6.329(A1) + 3.363(A1)^2 & if\ A1 > -1 \end{cases}$ $\Phi_2 = \begin{cases} -1.754 + 11.049(A2) + 8.611(A2)^2 & if\ A2 \le 0.12 \\ -2.398 + 20.152(A2) - 15.813(A2)^2 & if\ A2 > 0.12 \end{cases}$ $A1 = -0.54456x1 + 0.83346x2 - 0.09349x3 - 0.00724x4$ $A2 = 0.05007x1 + 0.87037x2 - 0.48983x3 + 0.00362x4$ $X = [x1, x2, x3, x4] = \left[\frac{t}{\ell}, \frac{a}{\ell}, \frac{t \times a}{\ell^2}, \frac{t}{a}\right]$	$0.05 \le \frac{a}{\ell} \le 0.4$ $0 \le \frac{t}{\ell} \le 3$
Finite Slab Length	$R_2 = 0.9399 + 0.07986\Phi_1$ $\Phi_1 = -4.0308 + \frac{1}{0.2029 + 0.0345(A1)^{-3.3043}}$ $A1 = -0.9436\frac{a}{\ell} + 0.3310\frac{L}{\ell}$	$2 \le \frac{L}{\ell} \le 7$ $0.05 \le \frac{a}{\ell} \le 0.3$
Finite Slab Width	$R_2 = 1.00477 + 0.01214\Phi_1$ $\Phi_1 = -0.5344 + 1.654(1 - A1)^{-10.7412}$ $A1 = 0.9951\frac{a}{\ell} - 0.09856\frac{W}{\ell}$	$2 \le \frac{W}{\ell} \le 7$ $0.05 \le \frac{a}{\ell} \le 0.3$
Tied Concrete Shoulder [6]	$R_3 = \begin{cases} 0.99864 - 0.51237(x1) - 0.0672 * \ln(x2) + 0.00315 * \ln^2(x2) \\ +0.015936(x1)^2 * \ln^2(x2) & if\ x1 \le 5 \\ 1.04284 - 0.84692(x1) - 0.0009299 * \ln(x2) + 0.06837(x1) * \ln(x2) \\ +0.63417(x1)^2 + 0.0042 * \ln^2(x2) - 0.000629(x1) * \ln(x2)^3 & if\ x1 > 5 \end{cases}$ $X = [x1, x2] = \left[\frac{a}{\ell}, \frac{AGG}{k\ell}\right]$	$0.05 \le \frac{a}{\ell} \le 0.3$ $5 \le \frac{AGG}{k\ell}$

Table 1 -- Proposed Prediction Models for Stress Adjustments (Continue ...)

Widened Outer Lane	$R_4 = 0.61711 + 0.15373\Phi_1 + 0.02504\Phi_2$ $\Phi_1 = \begin{cases} 0.693 + 1.279(A1) + 0.369(A1)^2 + 0.037(A1)^3 & if\ A1 \le -2.5 \\ 2.839 + 8.234(A1) + 8.158(A1)^2 + 3.608(A1)^3 + 0.576(A1)^4 & if\ A1 > -2.5 \end{cases}$ $\Phi_2 = \begin{cases} -2.285 + 5.921(A2) - 6.001(A2)^2 + 7.743(A2)^3 & if\ A2 \le 0.5 \\ -3.008 + 4.693(A2) + 4.334(A2)^2 - 2.167(A2)^3 & if\ A2 > 0.5 \end{cases}$ $A1 = -0.98868x1 - 0.12214x2 - 0.08717x3$ $A2 = 0.19802x1 + 0.98019x2 + 0.00305x3$ $X = [x1, x2, x3] = \left[\frac{D_0}{\ell}, \frac{a}{\ell}, \frac{D_0}{a}\right]$	$0.1 \le \frac{a}{\ell} \le 0.4$ $0 \le \frac{D_0}{\ell} \le 2$
Unbonded Second Layer	$R_5 = 0.72692 + 0.14272\Phi_1 + 0.00933\Phi_2$ $\Phi_1 = \begin{cases} 3.31765 + 2.4036(A1) & if\ A1 \le -1.4 \\ 5.72684 + 4.10244(A1) & if\ A1 > -1.4 \end{cases}$ $\Phi_2 = \begin{cases} 14.535 - 20.351(A2) + 5.986(A2)^2 & if\ A2 \le 1.2 \\ 1.619 - 8.367(A2) + 4.877(A2)^2 & if\ A2 > 1.2 \end{cases}$ $A1 = 0.11914x1 - 0.99288x2$ $A2 = 0.65518x1 + 0.75547x2$ $h_{effl} = \sqrt{h_1^2 + \frac{E_2 h_2}{E_1 h_1} h_2^2}$, $X = [x1, x2] = \left[\frac{a}{\ell}, \left(\frac{h_{effl}}{h1}\right)^2\right]$	$0.05 \le \frac{a}{\ell} \le 0.4$ $1 \le \left(\frac{h_{effl}}{h_1}\right)^2 \le 2$
Bonded Second Layer	$\alpha = \frac{(1/2)h_1(h_1 + h_2)}{h_1 + h_2(E_1/E_2)}$, $\beta = (1/2)(h_1 + h_2) - \alpha$ $h_{1f} = \sqrt[3]{h_1^3 + 12h_1\beta^2}$, $h_{2f} = \sqrt[3]{h_2^3 + 12h_2\beta^2}$ $h_{effl} = \sqrt{h_{1f}^2 + \left(\frac{h_{2f}}{h_{1f}}\right)h_{2f}^2}$, $X = [x1, x2] = \left[\frac{a}{\ell}, \left(\frac{h_{effl}}{h_{1f}}\right)^2\right]$ Use the above unbonded prediction model to calculate R_5	(same as above)
Load plus Day-time Curling	$R_T = 0.94825 + 0.15054\Phi_1 + 0.03724\Phi_2 + 0.03395\Phi_3$ $\Phi_1 = \begin{cases} -2.5575 + 0.8003(A1) - 0.8003(A1)^2 & if\ A1 \le 3 \\ -2.6338 + 1.1038(A1) - 0.0914(A1)^2 & if\ 3 < A1 \le 7 \\ 0.7564 - 0.0155(A1) & if\ A1 > 7 \end{cases}$ $\Phi_2 = \begin{cases} -0.6788 + 0.0.8003(A2) - 0.8003(A2)^2 & if\ A2 \le 3 \\ 3.7674 - 2.297(A2) + 0.2963(A2)^2 & if\ 3 < A2 \le 7 \\ -7.0337 + 1.2945(A2) & if\ A2 > 7 \end{cases}$ $\Phi_3 = \begin{cases} 4.0843 + 4.8241(A3) & if\ A3 \le 3 \\ 0.1815 + 0.0541(A3) - 1.0899(A3)^2 & if\ -1 < A3 \le 0.5 \\ 0.0453 + 0.0383(A3) & if\ A3 > 0.5 \end{cases}$ $A1 = -0.04724X1 + 0.56954X2 - 0.08408X3 + 0.20033X4 - 0.26647X5 + 0.00375X6 + 0.73881X7 - 0.01142X8 + 0.0953X9 + 0.01121X10$ $A2 = 0.03869X1 + 0.35781X2 + 0.09078X3 - 0.04054X4 + 0.86388X5 + 0.01635X6 - 0.31246X7 + 0.00552X8 - 0.12677X9 - 0.01765X10$ $A3 = 0.58567X1 + 0.25804X2 + 0.14784X3 + 0.14984X4 + 0.12743X5 - 0.05012X6 + 0.72295X7 - 0.0131X8 - 0.01304X9 - 0.06591X10$ $X = [x1, x2, x3, \ldots, x10]$ $= \left[\frac{W}{\ell}, \frac{L}{\ell}, AT, \frac{a}{\ell}, DG, DP, \frac{L}{\ell} * \frac{a}{\ell}, \frac{L}{\ell} * AT, DG * \frac{L}{\ell}, DG * \frac{W}{\ell}\right]$	$0.05 \le \frac{a}{\ell} \le 0.3$ $3 \le \frac{W}{\ell} \le 11$ $\frac{W}{\ell} = \frac{L}{\ell}$ $1.06 \le DG \le 9.93$ $2.61 \le DP \le 140.74$ $5.5 \le AT \le 22$ $DG = d\gamma \times 10^5$ $DP = dp \times 10^5$ $AT = \alpha \times \Delta T \times 10^5$

Table 2 -- Comparison of Equivalent Stress Calculations (TKUPAV / PCA)

(A) Equivalent Stress Calculations for Single Axle Load (No Shoulder)

h	k	ℓ	6*Me/h^2	σ_w	Dual	D	R_1	R_2	$\sigma_w*R_1*R_2$	B/A
in.	pci	in.	psi (A)	psi					psi (B)	Ratio
4	100	21.6	897.5	2489.0	0.702	0.501	0.352	1.007	881.8	0.98
6	100	29.3	499.0	1303.1	0.732	0.511	0.374	1.003	489.2	0.98
8	100	36.4	327.9	812.9	0.749	0.526	0.394	0.995	318.8	0.97
10	100	43.0	237.0	560.4	0.761	0.531	0.404	0.985	222.7	0.94
12	100	49.3	182.2	412.1	0.769	0.536	0.412	0.971	165.1	0.91
4	300	16.4	721.9	2099.5	0.670	0.500	0.335	1.009	709.2	0.98
6	300	22.3	407.9	1125.1	0.705	0.502	0.354	1.007	401.0	0.98
8	300	27.6	269.0	711.3	0.727	0.502	0.365	1.004	260.6	0.97
10	300	32.7	194.2	494.7	0.741	0.521	0.386	0.999	191.1	0.98
12	300	37.4	148.9	366.2	0.752	0.527	0.396	0.994	144.0	0.97
4	500	14.5	646.7	1922.6	0.654	0.500	0.327	1.009	634.0	0.98
6	500	19.6	369.9	1043.7	0.691	0.499	0.345	1.008	362.6	0.98
8	500	24.3	245.0	664.7	0.715	0.505	0.361	1.006	241.1	0.98
10	500	28.7	177.2	464.6	0.730	0.509	0.372	1.003	173.2	0.98
12	500	32.9	135.8	345.1	0.742	0.522	0.387	0.999	133.5	0.98

(B) Equivalent Stress Calculations for Tandem Axle Load (No Shoulder)

h	k	ℓ	6*Me/h^2	σ_w	Dual	D	Tandem	R_1	R_2	$\sigma_w*R_1*R_2$	B/A
in.	pci	in.	psi, (A)	psi						psi, (B)	Ratio
4	100	21.6	723.4	4978.1	0.702	0.501	0.404	0.142	1.007	712.5	0.98
6	100	29.3	423.3	2606.1	0.732	0.511	0.424	0.159	1.003	414.6	0.98
8	100	36.4	297.7	1625.9	0.749	0.526	0.445	0.175	0.995	283.8	0.95
10	100	43.0	228.7	1120.8	0.761	0.531	0.463	0.187	0.985	206.5	0.90
12	100	49.3	185.0	824.1	0.769	0.536	0.505	0.208	0.971	166.9	0.90
4	300	16.4	600.6	4199.0	0.670	0.500	0.407	0.136	1.009	576.8	0.96
6	300	22.3	329.3	2250.2	0.705	0.502	0.405	0.143	1.007	324.9	0.99
8	300	27.6	224.8	1422.7	0.727	0.502	0.419	0.153	1.004	218.2	0.97
10	300	32.7	170.1	989.5	0.741	0.521	0.434	0.168	0.999	165.8	0.97
12	300	37.4	136.6	732.4	0.752	0.527	0.448	0.177	0.994	129.1	0.95
4	500	14.5	565.0	3845.2	0.654	0.500	0.420	0.137	1.009	532.4	0.94
6	500	19.6	298.4	2087.5	0.691	0.499	0.405	0.140	1.008	294.1	0.99
8	500	24.3	199.7	1329.5	0.715	0.505	0.410	0.148	1.006	197.5	0.99
10	500	28.7	149.5	929.1	0.730	0.509	0.422	0.157	1.003	146.2	0.98
12	500	32.9	119.3	690.1	0.742	0.522	0.435	0.168	0.999	116.1	0.97

(Note: 1 in. = 2.54 cm, 1 psi = 0.07 kg/cm^2, 1 pci = 0.028 kg/cm^3, 1 kip = 454 kg)

Table 2 -- Comparison of Equivalent Stress Calculations (TKUPAV / PCA) (Continue ...)

(C) Equivalent Stress Calculations for Single Axle Load (With Shoulder)

h	k	ℓ	6*Me/h^2	σ_w	Dual	D	R_1	R_2	R3	$\sigma_w*R_1*R_2*R_3$	B/A
in.	pci	in.	psi (A)	psi						psi (B)	Ratio
4	100	21.6	897.5	2489.0	0.702	0.501	0.352	1.007	0.764	638.101	0.989
6	100	29.3	499.0	1303.1	0.732	0.511	0.374	1.003	0.769	376.296	0.996
8	100	36.4	327.9	812.9	0.749	0.526	0.394	0.995	0.798	254.361	0.991
10	100	43.0	237.0	560.4	0.761	0.531	0.404	0.985	0.819	182.325	0.961
12	100	49.3	182.2	412.1	0.769	0.536	0.412	0.971	0.834	137.761	0.930
4	300	16.4	721.9	2099.5	0.670	0.500	0.335	1.009	0.739	524.445	1.006
6	300	22.3	407.9	1125.1	0.705	0.502	0.354	1.007	0.796	319.262	1.026
8	300	27.6	269.0	711.3	0.727	0.502	0.365	1.004	0.831	216.621	1.016
10	300	32.7	194.2	494.7	0.741	0.521	0.386	0.999	0.856	163.608	1.035
12	300	37.4	148.9	366.2	0.752	0.527	0.396	0.994	0.875	126.060	1.020
4	500	14.5	646.7	1922.6	0.654	0.500	0.327	1.009	0.744	471.896	1.000
6	500	19.6	369.9	1043.7	0.691	0.499	0.345	1.008	0.807	292.767	1.025
8	500	24.3	245.0	664.7	0.715	0.505	0.361	1.006	0.846	204.007	1.038
10	500	28.7	177.2	464.6	0.730	0.509	0.372	1.003	0.873	151.263	1.034
12	500	32.9	135.8	345.1	0.742	0.522	0.387	0.999	0.894	119.347	1.042

(D) Equivalent Stress Calculations for Tandem Axle Load (With Shoulder)

h	k	ℓ	6*Me/h^2	σ_w	Dual	D	Tandem	R_1	R_2	R_3	$\sigma_w*R_1*R_2*R_3$	B/A
in.	pci	in.	psi, (A)	psi							psi, (B)	Ratio
4	100	21.6	723.4	4978.1	0.702	0.501	0.404	0.142	1.007	0.724	515.605	0.955
6	100	29.3	423.3	2606.1	0.732	0.511	0.424	0.159	1.003	0.769	318.857	0.997
8	100	36.4	297.7	1625.9	0.749	0.526	0.445	0.175	0.995	0.798	226.409	1.002
10	100	43.0	228.7	1120.8	0.761	0.531	0.463	0.187	0.985	0.819	168.995	0.971
12	100	49.3	185.0	824.1	0.769	0.536	0.505	0.208	0.971	0.834	139.260	0.987
4	300	16.4	600.6	4199.0	0.670	0.500	0.407	0.136	1.009	0.739	426.540	0.917
6	300	22.3	329.3	2250.2	0.705	0.502	0.405	0.143	1.007	0.796	258.680	0.994
8	300	27.6	224.8	1422.7	0.727	0.502	0.419	0.153	1.004	0.831	181.385	1.013
10	300	32.7	170.1	989.5	0.741	0.521	0.434	0.168	0.999	0.856	141.992	1.043
12	300	37.4	136.6	732.4	0.752	0.527	0.448	0.177	0.994	0.875	113.006	1.031
4	500	14.5	565.0	3845.2	0.654	0.500	0.420	0.137	1.009	0.744	396.251	0.884
6	500	19.6	298.4	2087.5	0.691	0.499	0.405	0.140	1.008	0.807	237.428	0.980
8	500	24.3	199.7	1329.5	0.715	0.505	0.410	0.148	1.006	0.846	167.120	1.019
10	500	28.7	149.5	929.1	0.730	0.509	0.422	0.157	1.003	0.873	127.664	1.034
12	500	32.9	119.3	690.1	0.742	0.522	0.435	0.168	0.999	0.894	103.794	1.050

(Note: 1 in. = 2.54 cm, 1 psi = 0.07 kg/cm^2, 1 pci = 0.028 kg/cm^3, 1 kip = 454 kg)

Table 3 -- Fatigue Analysis Example for Loading Only (PCAPAV and TKUPAV)

(A)Single Axle (kips)			PCAPAV (f2=0.973, f3=0.894, f4=0.953)						TKUPAV (R1=0.398, R2=0.992, f3=0.894, f4=0.953)					σ_{eq} Ratio
Load	Load*1.2	n_i	6*Me/h^2	f1	σ_{eq}, psi (A)	σ_{eq}/S_c	N_i	n_i/N_i, (%)	σ_w, psi	σ_{eq}, psi (B)	σ_{eq}/S_c	N_i	n_i/N_i, (%)	(B/A)
30	36.0	6310	243.4	1.952	393.6	0.606	26536	23.8	1186.5	398.6	0.613	21414	29.5	1.01
28	33.6	14690	243.4	1.829	368.9	0.568	76395	19.2	1107.4	372.0	0.572	66751	22.0	1.01
26	31.2	30140	243.4	1.706	344.1	0.529	234343	12.9	1028.3	345.5	0.531	218058	13.8	1.00
24	28.8	64410	243.4	1.583	319.1	0.491	1218769	5.3	949.2	318.9	0.491	1243647	5.2	1.00
22	26.4	106900	243.4	1.458	294.1	0.452	41207557	0.3	870.1	292.3	0.450	Unlimited	0.0	0.99
20	24.0	235800	243.4	1.333	268.9	0.414	Unlimited	0.0	791.0	265.7	0.409	Unlimited	0.0	0.99
18	21.6	307200	243.4	1.208	243.5	0.375	Unlimited	0.0	711.9	239.2	0.368	Unlimited	0.0	0.98
16	19.2	422500	243.4	1.081	218.0	0.335	Unlimited	0.0	632.8	212.6	0.327	Unlimited	0.0	0.98
14	16.8	586900	243.4	0.954	192.3	0.296	Unlimited	0.0	553.7	186.0	0.286	Unlimited	0.0	0.97
12	14.4	1837000	243.4	0.825	166.3	0.256	Unlimited	0.0	474.6	159.4	0.245	Unlimited	0.0	0.96
							Subtotal =	61.4%				Subtotal =	70.5%	
(B)Tandem Axle (kips)			PCAPAV (f2=0.973, f3=0.894, f4=0.953)						TKUPAV (R1=0.180, R2=0.992, f3=0.894, f4=0.953)					
52	62.4	21320	226.0	1.706	319.5	0.492	1177998	0.018	2056.6	312.2	0.480	2342697	0.9	0.98
48	57.6	42870	226.0	1.583	296.4	0.456	24134471	0.002	1898.4	288.2	0.443	Unlimited	0.0	0.97
44	52.8	124900	226.0	1.458	273.1	0.42	Unlimited	0.000	1740.2	264.2	0.406	Unlimited	0.0	0.97
40	48.0	372900	226.0	1.333	249.7	0.384	Unlimited	0.000	1582.0	240.2	0.370	Unlimited	0.0	0.96
36	43.2	885800	226.0	1.208	226.1	0.348	Unlimited	0.000	1423.8	216.2	0.333	Unlimited	0.0	0.96
32	38.4	930200	226.0	1.081	202.4	0.311	Unlimited	0.000	1265.6	192.1	0.296	Unlimited	0.0	0.95
28	33.6	1656000	226.0	0.954	178.6	0.275	Unlimited	0.000	1107.4	168.1	0.259	Unlimited	0.0	0.94
24	28.8	984900	226.0	0.825	154.5	0.238	Unlimited	0.000	949.2	144.1	0.222	Unlimited	0.0	0.93
20	24.0	1227000	226.0	0.695	130.1	0.2	Unlimited	0.000	791.0	120.1	0.185	Unlimited	0.0	0.92
16	19.2	1356000	226.0	0.563	105.5	0.162	Unlimited	0.000	632.8	96.1	0.148	Unlimited	0.0	0.91
							Subtotal =	2.0%				Subtotal =	0.9%	
(Note: 1 psi = 0.07 kg/cm^2, 1 kip = 454 kg)							$\Sigma n_i/N_i$ =	63.4%				$\Sigma n_i/N_i$ =	71.4%	

Table 4 -- Adjustment Factors for Loading Only

Dual		Tandem		Axle Width		Slab Length		Slab Width	
s/ℓ=	0.310	t/ℓ=	1.291	s/ℓ =	1.859	a/ℓ=	0.122	a/ℓ=	0.122
a/ℓ=	0.122	a/ℓ=	0.122	a/ℓ=	0.122	L/ℓ=	4.648	W/ℓ=	3.873
s*a/ℓ^2=	0.038	t*a/ℓ^2=	0.157	s*a/ℓ^2=	0.227	A1=	1.424	A1=	-0.260
A1=	-0.169	t/a=	10.593	A1=	-1.385	Φ1=	0.650	Φ1=	-0.397
A2=	-0.084	A1=	-1.059	A2=	0.033	R2=	0.992	R2=	1.000
Φ1=	2.049	A2=	-0.150	Φ1=	-0.352				
Φ2=	0.177	Φ1=	-0.780	Φ2=	-0.245				
R1=	0.754	Φ2=	0.314	R1=	0.528				
		R1=	0.452						

Table 5 - Adjustment Factor (R_T) for Loading Plus Curling

(A) Single Axle									
1.2 *Axle Load	P, lb.	DP	A1	A2	A3	Φ1	Φ2	Φ3	R_T
36000	18000	58.49	2.504	4.699	1.162	-0.554	-0.484	0.090	0.850
33600	16800	54.59	2.489	4.635	1.356	-0.565	-0.514	0.097	0.847
31200	15600	50.69	2.475	4.571	1.551	-0.577	-0.541	0.105	0.845
28800	14400	46.79	2.460	4.508	1.747	-0.589	-0.566	0.112	0.842
26400	13200	42.89	2.446	4.444	1.942	-0.600	-0.589	0.120	0.840
24000	12000	38.99	2.431	4.380	2.138	-0.612	-0.609	0.127	0.838
21600	10800	35.09	2.416	4.316	2.333	-0.624	-0.627	0.135	0.836
19200	9600	31.19	2.402	4.253	2.529	-0.635	-0.642	0.142	0.833
16800	8400	27.29	2.387	4.189	2.724	-0.647	-0.655	0.150	0.831
14400	7200	23.40	2.372	4.125	2.919	-0.659	-0.666	0.157	0.830
18000	9000	29.24	2.394	4.221	2.626	-0.641	-0.649	0.146	0.832
(B) Tandem Axle									
62400	31200	101.38	2.665	5.400	-0.989	-0.425	0.004	-0.938	0.853
57600	28800	93.58	2.636	5.273	-0.598	-0.448	-0.106	-0.241	0.869
52800	26400	85.78	2.606	5.145	-0.207	-0.472	-0.207	0.123	0.874
48000	24000	77.98	2.577	5.018	0.183	-0.495	-0.298	0.155	0.868
43200	21600	70.19	2.548	4.890	0.574	-0.518	-0.380	0.067	0.858
38400	19200	62.39	2.519	4.763	0.965	-0.542	-0.451	0.082	0.853
33600	16800	54.59	2.489	4.635	1.356	-0.565	-0.514	0.097	0.847
28800	14400	46.79	2.460	4.508	1.747	-0.589	-0.566	0.112	0.842
24000	12000	38.99	2.431	4.380	2.138	-0.612	-0.609	0.127	0.838
19200	9600	31.19	2.402	4.253	2.529	-0.635	-0.642	0.142	0.833
36000	18000	58.49	2.504	4.699	1.161	-0.554	-0.484	0.090	0.850

(Note: Axle loads are in pounds (lb.), 1 lb. = 0.454 kg)

Table 6 -- TKUPAV Fatigue Analysis Example (with Curling)

(A)Single Axle (kips)			90% Load Only				10% Load plus Curling (σ_c = 88.5 psi)						Total
Load	Load*1.2	n_i	σ_{eq}, psi (A)	ni*90%	N_i	Damage (%)	RT	σ_{eq}, psi	σ_{eq}/S_c	ni*10%	N_i	Damage (%)	Damage (%)
30	36.0	6310	398.6	5679	21414	26.5	0.850	462.7	0.712	631	1382	45.7	72.2
28	33.6	14690	372.0	13221	66751	19.8	0.847	435.9	0.671	1469	4345	33.8	53.6
26	31.2	30140	345.5	27126	218058	12.4	0.845	409.1	0.629	3014	13654	22.1	34.5
24	28.8	64410	318.9	57969	1243647	4.7	0.842	382.4	0.588	6441	42899	15.0	19.7
22	26.4	106900	292.3	96210	Unlimited	0.0	0.840	355.6	0.547	10690	135064	7.9	7.9
20	24.0	235800	265.7	212220	Unlimited	0.0	0.838	328.9	0.506	23580	577713	4.1	4.1
18	21.6	307200	239.2	276480	Unlimited	0.0	0.836	302.1	0.465	30720	8444924	0.4	0.4
16	19.2	422500	212.6	380250	Unlimited	0.0	0.833	275.4	0.424	42250	Unlimited	0.0	0.0
14	16.8	586900	186.0	528210	Unlimited	0.0	0.831	248.7	0.383	58690	Unlimited	0.0	0.0
12	14.4	1837000	159.4	1653300	Unlimited	0.0	0.830	222.0	0.341	183700	Unlimited	0.0	0.0
					Subtotal =	63.4%					Subtotal =	128.9%	192.3%
(B)Tandem Axle (kips)													
52	62.4	21320	312.2	19188	2342697	0.8	0.853	376.5	0.579	2132	55171	3.9	4.7
48	57.6	42870	288.2	38583	Unlimited	0.0	0.869	353.7	0.544	4287	147221	2.9	2.9
44	52.8	124900	264.2	112410	Unlimited	0.0	0.874	330.1	0.508	12490	533733	2.3	2.3
40	48.0	372900	240.2	335610	Unlimited	0.0	0.868	305.6	0.470	37290	5139145	0.7	0.7
36	43.2	885800	216.2	797220	Unlimited	0.0	0.858	280.9	0.432	88580	Unlimited	0.0	0.0
32	38.4	930200	192.1	837180	Unlimited	0.0	0.853	256.4	0.394	93020	Unlimited	0.0	0.0
28	33.6	1656000	168.1	1490400	Unlimited	0.0	0.847	232.0	0.357	165600	Unlimited	0.0	0.0
24	28.8	984900	144.1	886410	Unlimited	0.0	0.842	207.6	0.319	98490	Unlimited	0.0	0.0
20	24.0	1227000	120.1	1104300	Unlimited	0.0	0.838	183.2	0.282	122700	Unlimited	0.0	0.0
16	19.2	1356000	96.1	1220400	Unlimited	0.0	0.833	158.9	0.244	135600	Unlimited	0.0	0.0
					Subtotal =	0.8%					Subtotal =	9.8%	10.7%
(Note: 1 psi = 0.07 kg/cm^2, 1 kip = 454 kg)					Σ n_i/N_i =	64.2%					Σ n_i/N_i =	138.84%	203.0%

F 鋪面厚度設計個人電腦程式之簡介

F.1 AASHTO 厚度設計法(1993 年版) - (PAVEMENT ANALYSIS SOFTWARE, PAS)

F.2 PCA 厚度設計法(1990 年版) - (PCAPAV)

(資料來源：

1. American Concrete Pavement Association, "Pavement Analysis Software" (PAS), Arlington Heights, Illinois, U.S.A., 1993.
2. Portland Cement Association, "PCAPAV -Thickness Design of Highway and Street Pavements," Skokie, Illinois, U.S.A., 1990.

F.1 AASHTO 厚度設計法(1993 年版) - (PAVEMENT ANALYSIS SOFTWARE, PAS)

PAVEMENT DESIGN AND EVALUATION

You can design new pavements or analyze old pavements with PAS's pavement design and evaluation module. Depending on your problem, you can work with both rigid and flexible pavements either separately or in a side-by-side format.

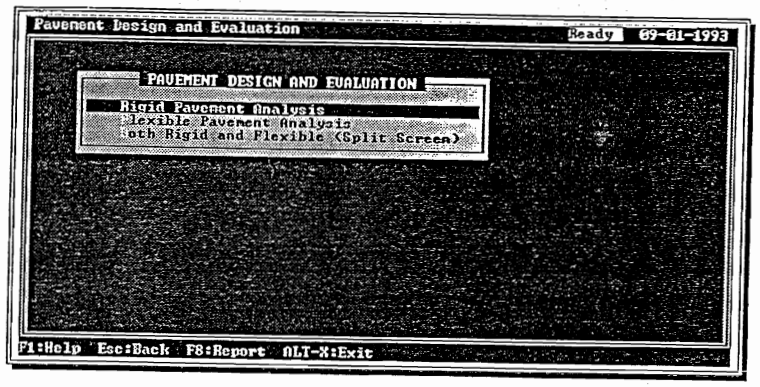

RIGID PAVEMENT DESIGN AND EVALUATION

The 'Rigid Pavement Analysis' section uses the methodology of Part II of the 1993 Guide. However, correlation equation from compressive strengths, modulus of rupture, and concrete modulus of elasticity from the American Concrete Institute are also included on the 'HELP' screens to aid the user in determining appropriate values. Similarly, 'HELP' screens and correlation equation between modulus of subgrade reaction (k), soil resilient modulus (M_r), California bearing ratio (CBR), and resistance value (R) from the Army Corps of Engineers and NCHRP Project 128 are also included.

Note: The correlation equation for CBR and R-value on the 'HELP' screens are for estimating the soil resilient modulus and should not to be used to relate each other.

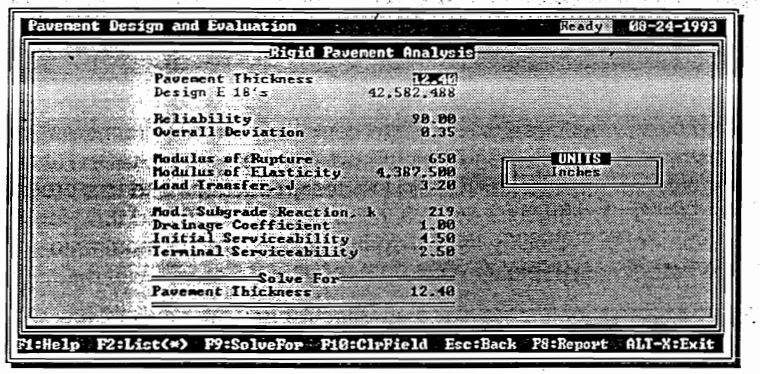

Inputs for the 'Rigid Pavement Analysis' screen are pavement thickness, design E-18s, reliability, overall standard deviation, modulus of rupture, modulus of elasticity, load transfer (J), modulus of subgrade reaction (k), drainage coefficient, and initial and terminal serviceability. By using the 'F9 SolveFor' function key, you can solve for any of these variables, except modulus of elasticity, terminal serviceability, and overall deviation.

Although the AASHO Road test included concrete pavements from 2.5 to 12.5 inches, we recommend that the minimum new pavement thickness for streets be 5.0 inches and for parking lots 4.0 inches. Therefore, PAS uses 4.0 and 20.0 inches, respectively, as the minimum and maximum allowable inputs for thickness. Of course, overlays can be less than 4.0 inches.

The input variable for design E-18's does not include boundary values. The design E-18's are either the allowable or predicted traffic expressed in E-18s. For more information, see 'Traffic Conversion' in the user's guide, 'Traffic' in the 'Simplified Guide,' or Section 2.1.2 of Part II of the 1993 AASHTO Guide.

As discussed in the 'Simplified Guide,' reliability is essentially a factor of safety for a given design. reliability input ranges from 50 to 100 percent. The 'HELP' screen for reliability provides recommendations for an appropriate value depending on roadway functional classification:

FUNCTIONAL CLASSIFICATION	RECOMMENDED LEVEL OF RELIABILITY Urban	Rural
Interstate/Freeways	85 - 99.9	80 - 99.9
Principal Arterials	80 - 99	75 - 95
Collectors	80 - 95	75 - 95
Local	50 - 80	50 - 80

The overall deviation, or standard deviation, is a coefficient that describes how well the AASHO Road Test data fit the AASHTO design equations. It also is an input in the design equation and this program. AASHTO recommends using a value between 0.30 and 0.40 for rigid pavements. Typically, 0.35 is an adequate value for most rigid pavement design problems.

The modulus of rupture is the average 28-day third-point flexural strength of the concrete. AASHTO recommends you increase the minimum specified flexural strength (S_c) by a 'z' factor multiplied by the standard deviation (SD) of the flexural strength to determine the design flexural strength (S'_c).

$$S'_c(\text{design}) = S_c + z(SD)$$

The 'z' factor is a function of the percentage of tests allowed below the minimum specified value. For more information on this, see the 'Simplified Guide,' or section 2.3.4 of Part II of the 1993 Guide.

Modulus of elasticity describes the stress-strain properties of a material. Since this value can be difficult to determine for concrete, it is usually correlated to the compressive or flexural strength by the use of ACI equations. By using the 'HELP' screen, PAS will calculate the modulus of elasticity based on the flexural strength. The value PAS calculates on the help screen will be transferred to the main input screen.

The load transfer coefficient, or J-factor describes the slab interaction across a joint. A lower J-factor indicates better load transfer across the joint. Edge support and load transfer devices also increase slab

E 18's Millions	Doweled & Mesh Reinforced Edge Support No	Yes	Aggregate Interlock Edge Support No	Yes	Continuously Reinforced Edge Support No	Yes	Pavement Class
Up to 0.3	3.2	2.7	3.2	2.8			Local
0.3 to 1	3.2	2.7	3.4	3.0			Streets &
1 to 3	3.2	2.7	3.6	3.1			Roads
3 to 10	3.2	2.7	3.8	3.2	2.9	2.5	Arterials
10 to 30	3.2	2.7	4.1	3.4	3.0	2.6	and
over 30	3.2	2.7	4.3	3.6	3.1	2.6	Highways

Load Transfer, J: 3.20

interaction and decrease the J-factor. The J-factor 'HELP' screen displays J-factor recommendations depending on the pavement type and edge support. We have adopted these recommendations which were originated by the Portland Cement Association. They fall within the guideline values that AASHTO recommends.

The modulus of subgrade reaction, or k-value describes the support strength for rigid pavements. Typical values range from about 50 psi/in for soft, marshy soils to about 500 psi/in for cement-treated and lean concrete bases. The modulus of subgrade reaction 'HELP' screen provides a correlation between the resilient modulus of the subgrade and base course to the k-value for different subbase materials.

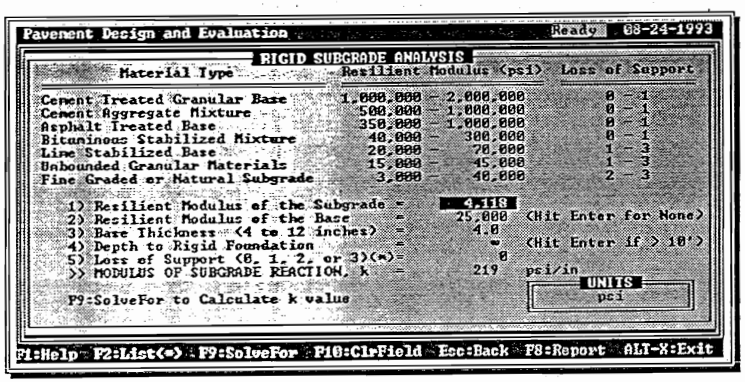

The drainage coefficient (C_d) is available to quantify the drainage capabilities of the pavement structure. Pavement structures with poor drainage have a low C_d while good draining pavement structures have higher C_d values. The 'HELP' screen which is found within the subgrade 'HELP' screen, recommends the following values:

Quality of Drainage	Percent of Time Pavement Structure is Exposed to Moisture Levels Approaching Saturation: Less than 1%	1 - 5 %	5 - 25 %	Greater than 25%
Excellent	1.25 - 1.20	1.20 - 1.15	1.15 - 1.10	1.10
Good	1.20 - 1.15	1.15 - 1.10	1.10 - 1.00	1.00
Fair	1.15 - 1.10	1.10 - 1.00	1.00 - 0.90	0.90
Poor	1.10 - 1.00	1.00 - 0.90	0.90 - 0.80	0.80
Very Poor	1.00 - 0.90	0.90 - 0.80	0.80 - 0.70	0.70

Note: The drainage coefficient (C_d) values are based on the poor soil conditions found at the AASHO Road Test. Therefore, we do not

recommend assigning C_d values less than 1.0, except in extremely poor soil locations.

The 'Rigid Pavement Analysis' screen provides an input for initial and terminal serviceability. The serviceability scale ranges from 0 to 5 with a '5' being a perfect pavement and a '0' being a pavement that is impassable. The initial serviceability (p_i) was 4.5 for rigid pavement and 4.2 for flexible pavements at the road test. These are good starting values for a design problem if no other information is available. The terminal serviceability (p_t) is the serviceability at which a pavement is considered to require major rehabilitation. The 'HELP' screen for terminal serviceability (p_t) provides the following recommendations for selecting the terminal serviceability depending on roadway functional classification:

Typical Minimum Terminal Serviceability (pt) values for various road and street classifications.

pt	Street or Highway Classification
2.50	Interstate and Major Highways or Arterials
2.25	Prime Secondary Routes, Industrial & Commercial Streets
2.00	Secondary Routes, Residential Streets & Parking Lots

FLEXIBLE PAVEMENT DESIGN AND EVALUATION

The 'Flexible Pavement Analysis' section is based on Part II of the 1993 Guide. Correlation equations between the soil resilient modulus (M_r), and the California bearing ratio (CBR), and resistance value (R) developed by the Army Corps of Engineers and NCHRP Project 128 are found on the 'HELP' screens. The relationships for CBR and R-value are for estimating the soil resilient modulus and cannot be used to relate CBR and R-values.

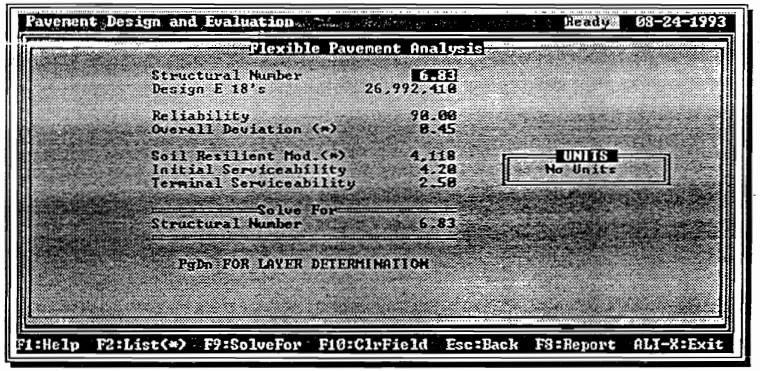

Inputs for the 'Flexible Pavement Analysis' screen are structural number (SN), design E-18s, reliability, overall standard deviation, soil resilient modulus, and initial and terminal serviceability. Like the 'Rigid Pavement Analysis' screen, you can use the 'F9 SolveFor' function key on any input variable to determine its result based on the other input values.

The structural number (SN) of a flexible pavement system indicates the required total pavement section. The first input field on the 'Flexible Pavement Analysis' screen is for the SN. In most ordinary flexible pavement design problems, the user will solve for this value.

The input variable for design E-18's does not include boundary values. The design E-18's are either the allowable or predicted traffic expressed in E-18s. For more information, see 'Traffic Conversion' in the user's guide, 'Traffic' in the 'Simplified Guide,' or Section 2.1.2 of Part II of the 1993 AASHTO Guide.

Reliability in flexible pavement design is similar to reliability for rigid pavement design. The 'HELP' screen for reliability provides the same recommendations based on roadway functional classification.

The overall deviation, or standard deviation, is a coefficient that describes how well the AASHO Road Test data fits the AASHTO design equations. It also is an input in the design equation and this program. AASHTO recommends using a value between 0.40 and 0.50 for flexible pavements. Typically, 0.45 is an adequate value for most flexible pavement design problems.

The soil resilient modulus describes the subgrade strength for flexible pavements. Typical values range from about 1000 psi for soft, marshy soils to about 40,000 psi for stable coarse grained soils. The 'HELP' screen for soil resilient modulus includes correlation equations between for soil resilient modulus and the CBR and R-value.

The 'Flexible Pavement Analysis' input screen provides an input for both initial and terminal serviceability. Remember, the serviceability scale ranges from 0 to 5 with a '5' being a perfect pavement and a '0' being a pavement that is impassable. The initial serviceability (p_i) was 4.2 for flexible pavements at the road test. This is a good starting value for a flexible pavement design problem if no other information is available. The terminal serviceability (p_t) is the serviceability at which a pavement is considered to require major rehabilitation. The 'HELP' screen for terminal serviceability (p_t) provides the same recommendations for selecting the terminal serviceability as are shown for rigid pavements.

Flexible Layer Determination

An additional step is necessary to complete a flexible pavement design. This is because the AASHTO flexible design equation only provides a structural number to characterize the pavement thickness,. After determining the SN, it is necessary to determine layer thicknesses which when combined will provide the required structural number. This is accomplished by pressing the 'PgDn' key to access the 'Layer Determination' screen:

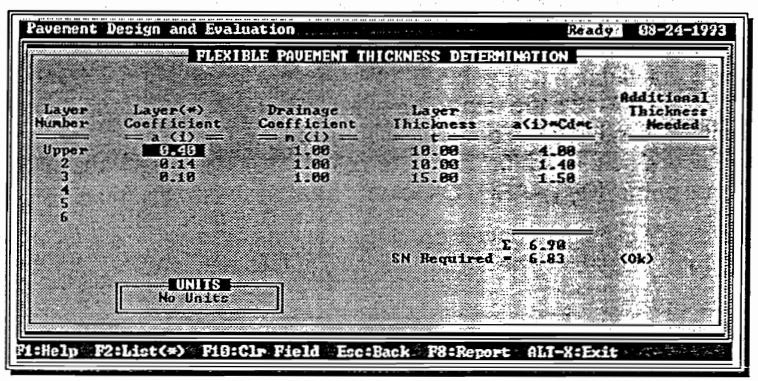

The flexible pavement 'Layer Determination' screen provides a simple spreadsheet format for trying different combinations of layers and materials. In a flexible pavement design, a coefficient is assigned to each flexible pavement layer that converts the actual layer thickness to a layer structural number. The coefficients are indicative of the relative strengths of the materials. The sum of all the layer structural numbers must equal or exceed the required structural number (SN) from the AASHTO equation.

The SN is converted to layer thickness by using the following formula:

$$SN = a_1t_1 + a_2t_2m_2 + a_3t_3m_3 + ...$$

where

a_1,a_2,a_3 = layer coefficients representative of the surface, base, subbase, etc. These are based on the ability of a material to function as a structural component of the pavement. Typical values for several materials can be found in the 'HELP' screen. For more information, see section 2.3.5 of the 1993 Guide.

t_1,t_2,t_3 = actual thickness of the surface, base, subbase, etc. in inches.

m_2,m_3 = drainage coefficients for the base, subbase, etc. Values for the drainage coefficient can be found in the 'HELP' screen. For more information, see section 2.4.2 of the 1993 Guide.

The pavement thickness is found by iterating layer thickness until the sum of the $a_i*t_i*m_i$ of each layer is equal or greater than the required SN.

The Additional Thickness Needed column on the right-hand side of the 'Layer Determination' screen provides a check to ease layer thickness design. The column displays how much additional thickness is needed to meet the total SN for the layer/material on which the cursor rests. You may use the value PAS displays to adjust your layer thicknesses and optimize your design.

BOTH RIGID AND FLEXIBLE PAVEMENT DESIGN AND EVALUATION

This split screen performs the same functions as both the Rigid Pavement Analysis' and 'Flexible Pavement Analysis' screens. However, it allows you to perform both designs in a side-by-side format, so that you can easily make direct comparisons between the two pavement types. All inputs, variables and 'HELP' screens are identical. You are still required to press the 'PgDn' key for the flexible pavement 'Layer Determination' screen.

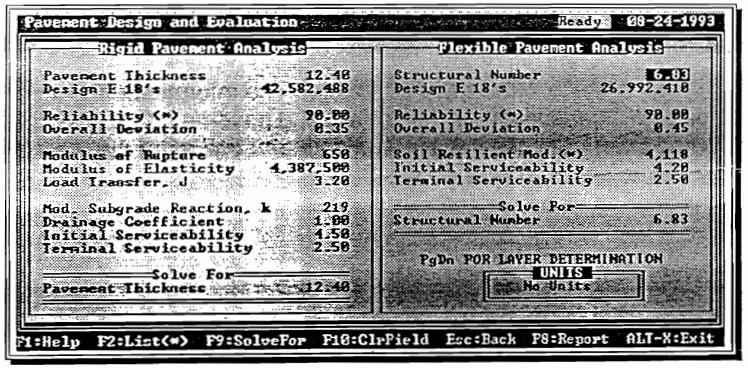

NOTE: When using the split screen for design and evaluation, you must press 'F9 SolveFor' twice: once to solve for the rigid unknown and once for the flexible unknown.

Running PCAPAV

Boot your system. Insert the PCAPAV disk into drive A:, and type:

PCAPAV

(Note: Starting PCAPAV from a fixed-disk system is done by setting the default drive to C:. At the C> prompt, type PCAPAV.)

PCAPAV is loaded into memory and screen page 1 looks like:

```
14:05:23                    PCAPAV(TM) 1.10                          Page 1
02-06-86   Proprietary Software of PORTLAND CEMENT ASSOCIATION
                          Pavement Design
                      PPPPP      ccccc      aaaaa
                      P    P     c     c    a    a
                      P    P     c     c         a
                      P    P     c          aaaaa
                      PPPPP      c     c    a    a
                      P          c     c    a    a
                      P          ccccc     aaaaa
            (C) Copyright Portland Cement Association 1985
                          All Rights Reserved
    This program is to be used as a design aid by experienced qualified
    ENGINEERS.   This program is not intended for use as a final design
    or a substitute for  sound  engineering  judgement.   The purchaser
    assumes all responsibilty for the use of this program in connection
    with any project.

  Input File: PAVEMENT.EX1              Output File: PAVEMENT.EX1
  Project ID. example 1
  Engineer:   Everyman, USA
  Solution Options: Normal

  Esc-QUIT F8-Print Data F9-Save F10-compute   move cursor  PgDn-Next Page
```

Fig. 1 shows the input format that will appear on the screen. The input items (menu items) are listed in the order that input data is entered.

```
14:07:47                    PCAPAV(TM) 1.10                          Page 2
02-06-86    Proprietary Software of PORTLAND CEMENT ASSOCIATION
                        Pavement  Design  Data
Modulus of Subg/Subb K  150.0 PCI       Axle Load Cat.  1.Light
Modulus of Rupture  MR  600.0 PSI                       2.Medium
                                                        3.Heavy
A D T T  290.00                                         4.Very Heavy
                                                        5.Input Axles
Design Life  20 Years

Load Transfer
  At Joint        1.Dowel
                  2.Agg. Interlock

  At Shoulder     1.Conc. Shoulder
                  2.No Conc. Shoulder

 Load Safety Factor    1. 1.0
                       2. 1.1
                       3. 1.2

 Estimated Pavement Thickness 7.0  IN

  Esc-QUIT F8-Print Data F9-Save F10-compute   move cursor  PgDn-Next Page
```

Fig. 1 - Input Format

Identification Screen

Input File

Data already stored in the file may be recalled onto the input screen for running a design problem. The data at this point may be altered if desired before executing the problem without changing the data on file. The disk is issued with six design examples which may be recalled or deleted as the user desires.

Output File

Input data may be stored in the file under the name typed into the output file by the user. The input data is stored in the file by typing the F9 SAVE key after the data has been entered onto the input screen.

Solution Options

The user may choose the normal mode or single thickness mode of operation by typing any character or using the space bar to select a design solution for either an optimum thickness or a desired trial thickness.

Average Daily Truck Traffic

The average daily truck traffic (ADTT) in both directions is selected as any number between 0.01 and 200,000. This includes only trucks with six tires or more and does not include panel and pickup trucks and other four-tire vehicles. For facilities of four lanes or more, the ADTT is adjusted by the use of Fig. 2.

Axle-Load Categories

Several axle-load data sets are stored in the computer program. These are shown in Table 1 (reproduced from Table 15 of Reference 1). The specific category is selected by the user when typing any character or using the space bar to select the desired axle-load category. In the case of Categories 1 through 4, no additional input is required on this menu item.

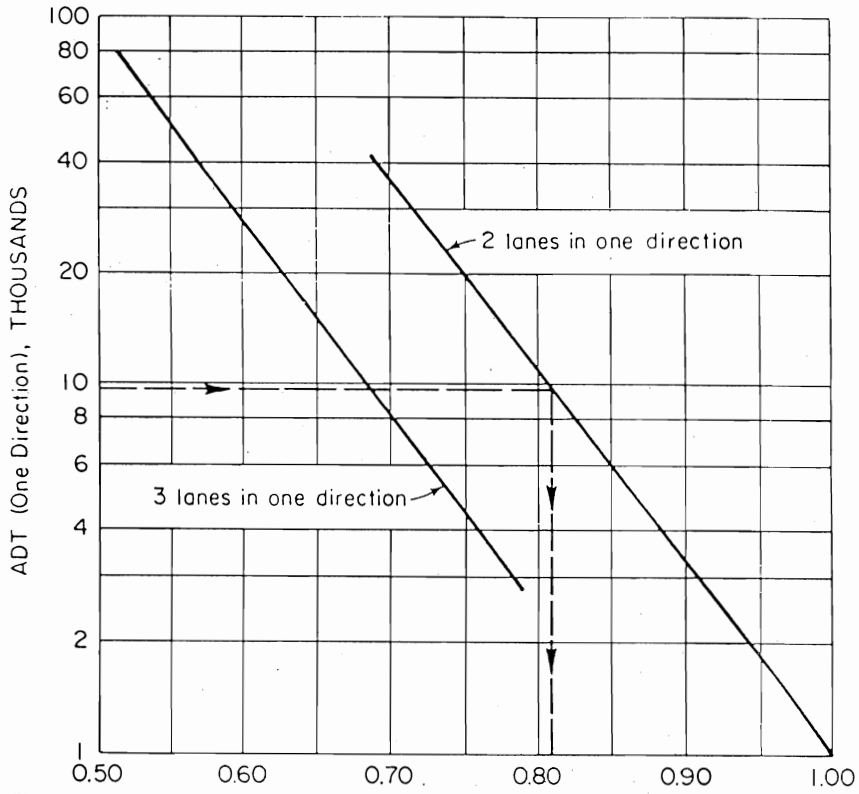

Fig. 2 - Proportion of Trucks in Right Lane of a Multilane Divided Highway

Axle-Load, kips	Axles per 1000 Trucks (excluding all two-axle, four-tire trucks)			
	Category 1	Category 2	Category 3	Category 4
Single Axles				
4	1693.31			
6	732.28			
8	483.10	233.60		
10	204.96	142.70		
12	124.00	116.76	182.02	
14	56.11	47.76	47.73	
16	38.02	23.88	31.82	57.07
18	15.81	16.61	25.15	68.27
20	4.23	6.63	16.33	41.82
22	0.96	2.60	7.85	9.69
24		1.60	5.21	4.16
26		0.07	1.78	3.52
28			0.85	1.78
30			0.45	0.63
32				0.54
34				0.19
Tandem Axles				
4	31.90			
8	85.59	47.01		
12	139.30	91.15		
16	75.02	59.25	99.34	
20	57.10	45.00	85.94	
24	39.18	30.74	72.54	71.16
28	68.48	44.43	121.22	95.79
32	69.59	54.76	103.63	109.54
36	4.19	38.79	56.25	78.19
40		7.76	21.31	20.31
44		1.16	8.01	3.52
48			2.91	3.03
52			1.19	1.79
56				1.07
60				0.57

Table 1 - Four Axle-Load Categories Stored in Program

If the user elects to input his own axle-load data, he selects Category 5 under Axle-Load Category. In this case, additional input data is required (refer to Fig. 3 for a description of the appropriate input). The user can input any value (integer only) to a maximum of 998 kips for the maximum single-axle load or 996 kips for the maximum tandem-axle load. For both single- and tandem-axle loads, the user inputs 10 values of the expected number of load repetitions expressed as axles per 1000 trucks starting with the maximum load, decremented by 2 kips for single axles and 4 kips for tandem axles. The number of load repetitions must be a number between 0.01 and 9999.99. The user may move the cursor up or down while in this category by using the cursor left [←] or cursor right [→] keys, respectively. (See, for example, Column 3 of Table 5 in Reference 1.)

```
 14:17:03                    PCAPAV(TM) 1.10                          Page 2
 02-06-86    Proprietary Software of PORTLAND CEMENT ASSOCIATION
                        Pavement  Design  Data
Modulus of Subg/Subb K  150.0 PCI        Axle Load Cat.  1.Light
Modulus of Rupture  MR  600.0 PSI                        2.Medium
                                                         3.Heavy
A D T T    0.25                                          4.Very Heavy
                                                         5.Input Axles
Design Life  20 Years                      Maximum Single axle load   22  KIPS
                                           Maximum Tandem axle load   36  KIPS
Load Transfer                                    A X L E   L O A D S
  At Joint        1.Dowel                  SAL     Axles     TAL     Axles
                  2.Agg. Interlock         KIPS    /1000     KIPS    /1000
                                             22      0.96      36      4.19
  At Shoulder     1.Conc. Shoulder           20      4.23      32     69.59
                  2.No Conc. Shoulder        18     15.81      28     68.48
                                             16     38.02      24     39.18
 Load Safety Factor   1. 1.0                 14     56.11      20     57.10
                      2. 1.1                 12    124.00      16     75.02
                      3. 1.2                 10    204.96      12    139.30
                                              8    483.10       8     85.59
 Estimated Pavement Thickness 5.5  IN         6    732.28       4     31.90
                                              4   1693.31       0      0.00
  Esc-QUIT F8-Print Data F9-Save F10-compute   move cursor  PgDn-Next Page
```

Fig. 3 - Example of Input Using Axle-Load Category 5 & User Data

Note: For the maximum axle loads, the program will not accept values less than 22 kips for single axles and 36 kips for tandem axles. If the user's values are not this high for "Axles per 1000 trucks," he can assign values of zero to the highest loads that are not wanted.

Load-Safety Factors

In the design manual[1], appropriate load-safety factors of 1.0, 1.1, 1.2, and 1.2, respectively, have been incorporated into design tables for axle-load categories 1, 2, 3, and 4. However, in the computer program, these values are not automatically assigned to axle-load categories. It is generally intended that the program user should input the appropriate value specified above depending on the axle-load category selected. Once the load safety factor item is selected for input, the user can choose the desired factor by typing any character or using the space bar to move the cursor down.

Load Transfer—At Joint and Shoulder

When the load transfer item has been selected, the user may select the type of load transfer provided at the joint. By typing any character or using the space bar, the cursor is moved down and the selection is made between a doweled joint or aggregate interlock (undoweled) joint. When the load transfer is selected, the carriage return key is pressed, giving the user the next choice of either a concrete shoulder (curb and gutter) or no concrete shoulder. This selection is made by moving the cursor down by typing any character or using the space bar. The carriage return key is then pressed to enter the shoulder type selected.

14:19:29 PCAPAV(TM) 1.10 Page 1
02-06-86 Proprietary Software of PORTLAND CEMENT ASSOCIATION

Project: example 3
Engineer: Everyman, USA
Input Data: Axle Load Category 2.Medium
Subgrade / Subbase K 150.0 PCI
Modulus of Rupture MR 600.0 PSI
Avg. Daily Truck Traffic (2 way) ADTT 2100.00
Design Life 20 years
Doweled Joints
No Concrete Shoulders
Load Safety Factor 1.1
Estimated Pavement Thickness 6.0 IN
Design Thickness =8.0 Inches

		Load Repetitions		---Fatigue Analysis-----			----Erosion Analysis---		
SAL	*LSF	Axle/ 1000	Expected Reps	Stress Ratio	Allowable Reps	Fatigue Consump	Power	Allowable Reps	Erosion
26	28.6	0.07	537.	0.656	6577.	8.16	39.411	1300473.	0.04
24	26.4	1.60	12264.	0.608	24661.	49.73	33.581	2103953.	0.58
22	24.2	2.60	19929.	0.560	93087.	21.41	28.217	3623011.	0.55
20	22.0	6.63	50819.	0.512	438472.	11.59	23.320	6814367.	0.75
18	19.8	16.61	127316.	0.464	9082815.	1.40	18.889	14696439.	0.87
16	17.6	23.88	183040.	0.415	**********	0.00	14.925	40629368.	0.45
14	15.4	47.76	366080.	0.366	**********	0.00	11.427	211779898.	0.17
12	13.2	116.76	894965.	0.317	**********	0.00	8.395	**********	0.00
10	11.0	142.70	1093796.	0.267	**********	0.00	5.830	**********	0.00
8	8.8	233.60	1790544.	0.217	**********	0.00	3.731	**********	0.00

TAL	*LSF	Axle/ 1000	Expected Reps	Stress Ratio	Allowable Reps	Fatigue Consump	Power	Allowable Reps	Erosion
44	48.4	1.16	8891.	0.492	1163597.	0.76	39.369	1304593.	0.68
40	44.0	7.76	59480.	0.450	**********	0.00	32.536	2317990.	2.57
36	39.6	38.79	297325.	0.407	**********	0.00	26.354	4519721.	6.58
32	35.2	54.76	419735.	0.365	**********	0.00	20.823	10179958.	4.12
28	30.8	44.43	340556.	0.322	**********	0.00	15.943	29826993.	1.14
24	26.4	30.74	235622.	0.278	**********	0.00	11.713	173686912.	0.14
20	22.0	45.00	344925.	0.234	**********	0.00	8.134	**********	0.00
16	17.6	59.25	454151.	0.190	**********	0.00	5.206	**********	0.00
12	13.2	91.15	698665.	0.145	**********	0.00	2.928	**********	0.00
8	8.8	47.01	360332.	0.099	**********	0.00	1.301	**********	0.00

Total Fatigue Used = 93.05 Erosion Damage = 18.64

7.5 Inch Thickness Inadequate, Fatigue Used= 477.20 Erosion Damage = 33.46

Fig. 5 - Example of Output

Most of the output is self-explanatory. Additional information concerning specific output items is explained below:

MR The input 28-day concrete flexural strength (modulus of rupture). The computer program automatically decreases this by a 15% coefficient of variation.

SAL Single-Axle Loads in kips.

TAL Tandem-Axle Loads in kips (a Tandem-Axle Load is the total load on two axles).

LSF Load-Safety Factor. It is multiplied by the axle loads. (See page 10 of Reference 1.)

Axle/1000 Axles per thousand trucks inputted for each axle load.

<u>Expected Reps</u> - the computed number of these axles in the design period (Axle/1000 x ADTT/2 x 365 days x Age) in one direction only.

Stress Ratio (Fatigue Analysis) - The stress due to load divided by concrete strength.

<u>Allowable Reps</u> - the allowable number of axle-load repetitions based on the fatigue criteria.

<u>Fatigue Consump</u> - the fatigue consumption (expected repetitions divided by allowable repetitions).

Power (Erosion Analysis) - The rate of work (magnitude and speed of deflection) applied to a slab corner by the axle load.

<u>Allowable Reps</u> - the allowable number of axle-load repetitions based on the erosion criteria.

<u>Erosion</u> - erosion damage (expected repetitions divided by allowable repetitions).

G 加鋪厚度設計

G.1 REHABILITATION METHODS WITH OVERLAYS (AASHTO, 1993 年版, CHAPTER 5)

資料來源：

AASHTO, "AASHTO Guide for Design of Pavement Structures," Volume I, 1993.

G.2 1993 年 AASHTO 加鋪設計法 (張記恩期末報告)

G.1 REHABILITATION METHODS WITH OVERLAYS (AASHTO, 1993 年版, CHAPTER 5)

CHAPTER 5
REHABILITATION METHODS WITH OVERLAYS

Overlays are used to remedy functional or structural deficiencies of existing pavements. It is important that the designer consider the type of deterioration present in determining whether the pavement has a functional or structural deficiency, so that an appropriate overlay type and design can be developed.

Functional deficiency arises from any conditions that adversely affect the highway user. These include poor surface friction and texture, hydroplaning and splash from wheel path rutting, and excess surface distortion (e.g., potholes, corrugation, faulting, blow-ups, settlements, heaves). The overlay design procedures in this chapter address structural deficiencies. If a pavement has only a functional deficiency, procedures in Part III, Chapter 4 and Section 5.3.2 should be used.

Structural deficiency arises from any conditions that adversely affect the load-carrying capability of the pavement structure. These include inadequate thickness as well as cracking, distortion, and disintegration. It should be noted that several types of distress (e.g., distresses caused by poor construction techniques, low-temperature cracking) are not initially caused by traffic loads but do become more severe under traffic to the point that they also detract from the load-carrying capability of the pavement. Part III, Section 4.1.2 provides descriptions of various structural conditions.

Maintenance overlays and surface treatments are sometimes placed as preventive measures to slow the rate of deterioration of pavements. This type of treatment includes thin AC overlays and various surface treatments which help keep out moisture.

The following abbreviations for pavement and overlay types are used in this chapter:

AC:	Asphalt concrete
PCC:	Portland cement concrete
JPCP:	Jointed plain concrete pavement
JRCP:	Jointed reinforced concrete pavement
CRCP:	Continuously reinforced concrete pavement
AC/PCC:	AC-overlaid Portland cement concrete (JPCP, JRCP, or CRCP)

The procedures described in this chapter address the following types of overlays and existing pavements:

Section	Overlay	Existing Pavement
5.4	AC	AC
5.5	AC	Break/crack and seat and rubblized PCC
5.6	AC	JPCP, JRCP, and CRCP
5.7	AC	AC/JPCP, AC/JRCP, and AC/CRCP
5.8	Bonded PCC	JPCP, JRCP, and CRCP
5.9	Unbonded PCC	JPCP, JRCP, and CRCP
5.10	PCC	AC

5.1 OVERLAY TYPE FEASIBILITY

The feasibility of any type of overlay depends on the following major considerations.

(1) Availability of adequate funds for construction of the overlay. This is basically a constraint, as illustrated in Part III, Figure 2.1.

(2) Construction feasibility of the overlay. This includes several aspects.
   (a) Traffic control
   (b) Materials and equipment availability
   (c) Climatic conditions
   (d) Construction problems such as noise, pollution, subsurface utilities, overhead bridge clearance, shoulder thickness and side slope extensions in the case of limited right-of-way, etc.
   (e) Traffic disruptions and user delay costs

(3) Required future design life of the overlay. Many factors will affect the life of an overlay, such as the following.
   (a) Existing pavement deterioration (specific distress types, severities, and quantities)

(b) Existing pavement design, condition of pavement materials (especially durability problems), and subgrade soil
(c) Future traffic loadings
(d) Local climate
(e) Existing subdrainage situation

All of these factors and others specific to the site need to be considered to determine the suitability of an overlay.

5.2 IMPORTANT CONSIDERATIONS IN OVERLAY DESIGN

Overlay design requires consideration of many different items, including: preoverlay repair, reflection crack control, traffic loadings, subdrainage, milling an existing AC surface, recycling portions of an existing pavement, structural versus functional overlay needs, overlay materials, shoulders, rutting in an existing AC pavement and overlay, durability of PCC slabs, design of joints, reinforcement, and bonding/separation layers for PCC overlays, overlay design reliability level and overall standard deviation, and pavement widening.

These considerations must not be overlooked by the designer. Each of these is briefly described in this section, especially those that are common for all overlay types. They are described in more detail in the sections for each overlay type.

5.2.1 Pre-overlay Repair

Deterioration in the existing pavement includes visible distress as well as damage which is not visible at the surface but which may be detected by other means. How much of this distress should be repaired before an overlay is placed? The amount of pre-overlay repair needed is related to the type of overlay selected. If distress in the existing pavement is likely to affect the performance of the overlay within a few years, it should be repaired prior to placement of the overlay. Much of the deterioration that occurs in overlays results from deterioration that was not repaired in the existing pavements. The designer should also consider the cost tradeoffs of preoverlay repair and overlay type. If the existing pavement is severely deteriorated, selecting an overlay type which is less sensitive to existing pavement condition may be more cost-effective than doing extensive preoverlay repair. Excellent guidelines are available on preoverlay repair techniques (*1, 2, 3, 4*).

5.2.2 Reflection Crack Control

Reflection cracks are a frequent cause of overlay deterioration. The thickness design procedures in this chapter do not consider reflection cracking. Additional steps must be taken to reduce the occurrence and severity of reflection cracking. Some overlays are less susceptible to reflection cracking than others because of their materials and design. Similarly, some reflection crack control measures are more effective with some pavement and overlay types than with others. Reflection crack control is discussed in more detail in the sections for each overlay type.

5.2.3 Traffic Loadings

The overlay design procedures require the 18-kip equivalent single-axle loads (ESALs) expected over the design life of the overlay in the design lane. The estimated ESALs must be calculated using the appropriate flexible pavement or rigid pavement equivalency factors from Part II of this Guide. The appropriate type of equivalency factors for each overlay type and existing pavement type are given in the following table.

Existing Pavement	Overlay Type	Equivalency Factors to Use
Flexible	AC	Flexible
Rubblized PCC	AC	Flexible
Break/Crack/Seat JRCP, JRCP	AC	Flexible
Jointed PCC	AC or PCC	Rigid
CRCP	AC or PCC	Rigid
Flexible	PCC	Rigid
Composite (AC/PCC)	AC or PCC	Rigid

An approximate correlation exists between ESALs computed using flexible pavement and rigid pavement equivalency factors. Converting from rigid pavement ESALs to flexible pavement ESALs requires multiplying the rigid pavement ESALs by 0.67. For example, 15 million rigid pavement ESALs equal 10 million flexible pavement ESALs. Five million flexible pave-

ment ESALs equal 7.5 million rigid pavement ESALs. Failure to utilize the correct type of ESALs will result in significant errors in the overlay designs. Conversions must be made, for example, when designing an AC overlay of a flexible pavement (flexible ESALs required) and when designing an alternative PCC overlay of the same flexible pavement (rigid ESALs required). Throughout this chapter, ESALs are designated as rigid ESALs or flexible ESALs as appropriate.

The type of ESALs used in the overlay design depends on the pavement performance model (flexible or rigid) being used. In the overlay design procedures presented in this chapter, the flexible pavement model is used in designing AC overlays of AC pavements and fractured slab PCC pavements. The rigid pavement model is used in designing AC and PCC overlays of PCC and ACC/PCC pavements and PCC overlays of AC pavements.

5.2.4 Subdrainage

The subdrainage condition of an existing pavement usually has a great influence on how well the overlay performs. A subdrainage evaluation of the existing pavement should be conducted as described in Part III, Section 3.3. Further guidance is provided in Reference 5. Improving poor subdrainage conditions will have a beneficial effect on the performance of an overlay. Removal of excess water from the pavement cross-section will reduce erosion and increase the strength of the base and subgrade, which in turn will reduce deflections. In addition, stripping in AC pavement and "D" cracking in PCC pavement may be slowed by improved subdrainage.

5.2.5 Rutting in AC Pavements

The cause of rutting in an existing AC pavement must be determined before an AC overlay is designed. An overlay may not be appropriate if severe rutting is occurring due to instability in any of the existing pavement layers. Milling can be used to remove the rutted surface and any underlying rutted asphalt layers.

5.2.6 Milling AC Surface

The removal of a portion of an existing AC surface frequently improves the performance of an AC overlay due to the removal of cracked and hardened AC material. Significant rutting or other major distortion of any layer should be removed by milling before another overlay is placed; otherwise, it may contribute significantly to rutting of the overlay.

5.2.7 Recycling the Existing Pavement

Recycling a portion of an existing AC layer may be considered as an option in the design of an overlay. This has become a very common practice. Complete recycling of the AC layer may also be done (sometimes in conjunction with the removal of a deteriorated base course).

5.2.8 Structural versus Functional Overlays

The overlay design procedures in this chapter provide an overlay thickness to correct a structural deficiency. If no structural deficiency exists, an overlay thickness less than or equal to zero will be obtained. This does not mean, however, that the pavement does not need an overlay to correct a functional deficiency. If the deficiency is primarily functional, then the overlay thickness should be only that which is needed to remedy the functional problem (*6*). If the pavement has a structural deficiency as well, a structural overlay thickness which is adequate to carry future traffic over the design period is needed.

5.2.9 Overlay Materials

The overlay materials must be selected and designed to function within the specific loading, climatic conditions, and underlying pavement deficiencies present.

5.2.10 Shoulders

Overlaying traffic lanes generally requires that the shoulders be overlaid to match the grade line of the traffic lanes. In selecting an overlay material and thickness for the shoulder, the designer should consider the extent to which the existing shoulder is deteriorated and the amount of traffic that will use the shoulder. For example, if trucks tend to park on the shoulder at certain locations, this should be considered in the shoulder overlay design.

If an existing shoulder is in good condition, any deteriorated areas should be patched. An overlay may

then be placed to match the shoulder grade to that of the traffic lanes. If an existing shoulder is in such poor condition that it cannot be patched economically, it should be removed and replaced.

5.2.11 Existing PCC Slab Durability

The durability of an existing PCC slab greatly influences the performance of AC and bonded PCC overlays. If "D" cracking or reactive aggregate exists, the deterioration of the existing slab can be expected to continue after overlay. The overlay must be designed with this progressive deterioration of the underlying slab in mind (*7*).

5.2.12 PCC Overlay Joints

Bonded or unbonded jointed concrete overlays require special joint design that considers the characteristics (e.g., stiffness) of the underlying pavement. Factors to be considered include joint spacing, depth of saw cut, sealant reservoir shape, and load transfer requirements.

5.2.13 PCC Overlay Reinforcement

Jointed reinforced and continuously reinforced concrete overlays require an adequate amount of reinforcement to hold cracks together. Friction between the overlay slab and the base slab should be considered in the reinforcement design.

5.2.14 PCC Overlay Bonding/Separation Layers

The bonding or separation of concrete overlays must be fully considered. Bonded overlays must be constructed to insure that the overlay remains bonded to the existing slab. Unbonded overlays must be constructed to insure that the separation layer prevents any reflection cracks in the overlay.

5.2.15 Overlay Design Reliability Level and Overall Standard Deviation

An overlay may be designed for different levels of reliability using the procedures described in Part I, Chapter 4 for new pavements. This is accomplished through determination of the structural capacity (SN_f or D_f) required to carry traffic over the design period at the desired level of reliability.

Reliability level has a large effect on overlay thickness. Varying the reliability level used to determine SN_f or D_f between 50 and 99 percent may produce overlay thicknesses varying by 6 inches or more (*8*). Based on field testing, it appears that a design reliability level of approximately 95 percent gives overlay thicknesses consistent with those recommended for most projects by State highway agencies, when the overall standard deviations recommended in Part I and II are used (*8*). There are, of course, many situations for which it is desirable to design at a higher or lower level of reliability, depending on the consequences of failure of the overlay. The level of reliability to be used for different types of overlays may vary, and should be evaluated by each agency for different highway functional classifications (or traffic volumes).

The designer should be aware that some sources of uncertainty are different for overlay design than for new pavement design. Therefore, the overall standard deviations recommended for new pavement design may not be appropriate for overlay design. The appropriate value for overall standard deviation may vary by overlay type as well. An additional source of variation is the uncertainty associated with establishing the effective existing structural capacity (SN_{eff} or D_{eff}). However, some sources of variation may be smaller for overlay design than for new pavement design (e.g., estimation of future traffic). Additional research is needed to better establish the standard deviations for overlay design. At the present time it is recommended to use 0.39 for any type of concrete overlay and 0.49 for any type of AC overlay, which is consistent with Part I, Section 4.3.

5.2.16 Pavement Widening

Many AC overlays are placed over PCC pavements in conjunction with pavement widening (either adding lanes or adding width to a narrow lane). If multiple lane widening is to be designed, refer to Part II for guidance. Widening requires coordination between the design of the widened pavement section and the overlay, not only so that the surface will be functionally adequate, but also so that both the existing and widening sections will be structurally adequate. Many lane widening projects have developed serious deterioration along the longitudinal joint due to improper design. The key design recommendations are as follows:

(1) The design "lives" of both the overlay and the new widening construction should be the same to avoid the need for future rehabilitation at significantly different ages.
(2) The widened cross section should generally closely match the existing pavement or cross section in material type, thickness, reinforcement, and joint spacing. However, a shorter joint spacing may be used.
(3) A widened PCC slab section must be tied with deformed bars to the existing PCC slab face. The tie bars should be securely anchored and consistent with ties used in new pavement construction (e.g., No. 5 bars, 30 inches long, grouted and spaced no more than 30 inches apart).
(4) A reflection crack relief fabric may be placed along the longitudinal widening joint.
(5) The overlay should generally be the same thickness over the widening section as over the rest of the traffic lane.
(6) Longitudinal subdrainage should be placed if needed.

5.2.17 Potential Errors and Possible Adjustments to Thickness Design Procedure

The overlay thicknesses obtained using these procedures should be reasonable when the pavement has a structural deficiency. If the overlay thickness appears to be unreasonable, one or more of the following causes may be responsible.

(1) The pavement deterioration may be caused primarily by nonload-associated factors. A computed overlay thickness less than zero or close to zero suggests that the pavement does not need a structural improvement. If a functional deficiency exists, a minimum constructible overlay thickness that addresses the problem could be placed.
(2) Modifications may be needed in the overlay design inputs to customize the procedures to the agency's specific conditions. Each agency should test the overlay design procedures on actual projects to investigate the need for modifications. Reference 8 contains many example overlay designs that illustrate typical inputs and outputs.
    (a) Overlay reliability design level, R. The recommended design reliability levels should be reviewed for overlay designs by each agency, since the recommendations given in Part I are intended for new pavement designs. See Section 5.2.15 for discussion of overlay design reliability.
    (b) Overall standard deviation, S_o. The values recommended for new pavement design may be either too low or too high for overlay design. See Section 5.2.15 for discussion of overall standard deviation.
    (c) Effective slab thickness and structural number adjustment factors. There are many aspects to these that may need agency adjustment.
    (d) Design subgrade resilient modulus and effective k-value. Specifically, a resilient modulus which is consistent with that incorporated into the flexible pavement design equation in Part II, Section 5.4.5 must be used.
    (e) Other design inputs may be in error. Ranges of typical values for inputs are given in the worksheets for overlay design.

5.2.18 Example Designs and Documentation

Reference 8 provides many examples of overlay designs for pavements in different regions of the United States. These may provide the designer with valuable insight into results obtained for actual projects. Reference 9 contains documentation for the concepts involved in the overlay design procedures.

5.3 PAVEMENT EVALUATION FOR OVERLAY DESIGN

It is important that an evaluation of the existing pavement be conducted to identify any functional and structural deficiencies, and to select appropriate preoverlay repair, reflection crack treatments and overlay designs to correct these deficiencies. This section provides guidance in pavement evaluation for overlay design.

The following sections of Part III of this Guide provide information on pavement evaluation for rehabilitation:

Section 2.3: Selection of Alternative Rehabilitation Methods

Chapter 3: Guides for Field Data Collection
Chapter 4: Rehabilitation Methods Other Than Overlay (portions of this chapter are applicable to preoverlay pavement evaluation and preoverlay repair)

The guidelines and procedures in these chapters are not repeated in this section, but are referenced as needed. This section provides guidelines for pavement evaluation specifically for overlay design purposes. Further details are provided in the sections for design of each overlay type.

5.3.1 Design of Overlay Along Project

Pavement rehabilitation projects involve lengths of pavement that range from a few hundred feet to several miles. There are two approaches to designing an overlay thickness for a project, and both have advantages and disadvantages. The design engineer should select the approach that best fits the specific design situation.

(1) *Uniform Section Approach.* The project is divided into sections of relatively uniform design and condition. Each uniform section is considered independently and overlay design inputs are obtained from each section that represents its average condition (e.g., mean thicknesses, mean number of transverse cracks per mile, mean resilient modulus). Identification of uniform sections is described in Part III, Section 3.2.2. The mean inputs for the section are used to obtain a single overlay thickness for the entire length of the section. The mean inputs must be used in the AASHTO design procedure because design reliability is applied later to give the appropriate safety factor.

(2) *Point-By-Point Approach.* Overlay thicknesses are determined for specific points along the uniform design section (e.g., every 300 feet). All required inputs are determined for each point so that the overlay thickness can be designed. Factors that may change from point to point include deflection, thickness, and condition; other inputs are usually fairly constant along the project. This approach may appear to require much more work; however, in reality it does not require much additional field work, only more runs through the design procedure. This can be done efficiently using a computer.

The point-by-point approach produces a required overlay design thickness for each analysis point along the entire project for a given reliability level. In selecting one thickness for the uniform section, be aware that each overlay thickness has already been increased to account for the design reliability level. Selection of a thickness that is greater than the mean of these values would be designing for a higher level of reliability. The point by point overlay thicknesses can be used to divide the project into different overlay design thickness sections if systematic variation exists along the project, or one design thickness can be selected for the entire project. Areas having unusually high thickness requirements may be targeted for additional field investigation, and may warrant extensive repair or reconstruction.

5.3.2 Functional Evaluation of Existing Pavement

Functional deterioration is defined as any condition that adversely affects the highway user. Some recommended overlay solutions to functional problems are provided (also see table on next page).

(1) Surface Friction and Hydroplaning

All pavement types. Poor wet-weather friction due to polishing of the surface (inadequate macrotexture and/or microtexture). A thin overlay that is adequate for the traffic level may be used to remedy this problem. Guidelines for use of asphalt concrete friction courses are provided in Reference 10.

AC-surfaced pavement. Poor friction due to bleeding of the surface. Milling the AC surface may be required to remove the material that is bleeding to prevent further bleeding through the overlay, and to prevent rutting due to instability. After milling, an open-graded friction course or an overlay thickness adequate for the traffic level may be used to remedy this problem.

AC-surfaced pavement. Hydroplaning and splashing due to wheel path rutting. Determining which layer or layers are rutting and taking appropriate corrective action are important.

(2) Surface Roughness

All pavement types. Long wavelength surface distortion, including heaves and swells. A

Cause of Rutting	Layer(s) Causing Rut	Solution
Total pavement thickness inadequate	Subgrade	Thick overlay
Unstable granular layer due to saturation	Base or subbase	Remove unstable layer or thick overlay
Unstable layer due to low shear strength	Base	Remove unstable layer or thick overlay
Unstable AC mix (including stripping)	Surface	Remove unstable layer
Compaction by traffic	Surface, base, subbase	Surface milling and/or leveling overlay
Studded tire wear	Surface	Surface milling and/or leveling overlay

level-up overlay with varying thickness (adequate thickness on crests) usually corrects these problems.

AC-surfaced pavement. Roughness from deteriorated transverse cracks, longitudinal cracks, and potholes. A conventional overlay will correct the roughness only temporarily, until the cracks reflect through the overlay. Full-depth repair of deteriorated areas and a thicker AC overlay incorporating a reflection crack control treatment may remedy this problem.

AC-surfaced pavement. Roughness from ravelling of surface. A thin AC overlay could be used to remedy this problem. Milling the existing surface may be required to remove deteriorated material to prevent debonding. If the ravelling is due to stripping, the entire layer should be removed because the stripping will continue and may accelerate under an overlay.

PCC-surfaced pavement. Roughness from spalling (including potholes) and faulting of transverse and longitudinal joints and cracks. Spalling can be repaired by full- or partial-depth repairs consisting of rigid materials. Faulting can be alleviated by an overlay of adequate thickness; however, faulting indicates poor load transfer and poor subdrainage. Poor load transfer will lead to spalling of reflected cracks in an AC overlay. Subdrainage improvement may be needed.

Some agencies apply what are called "preventive overlays" that are intended to slow the rate of deterioration. This type of overlay includes thin AC and various surface treatments. These may be applied to pavements which do not present any immediate functional or structural deficiency, but whose condition is expected to deteriorate rapidly in the future.

Overlay designs (including thickness, preoverlay repairs and reflection crack treatments) must address the causes of functional problems and prevent their recurrence. This can only be done through sound engineering, and requires experience in solving the specific problems involved. The overlay design required to correct functional problems should be coordinated with that required to correct any structural deficiencies.

5.3.3 Structural Evaluation of Existing Pavement

Structural deterioration is defined as any condition that reduces the load-carrying capacity of the pavement. The overlay design procedures presented here are based on the concept that time and traffic loadings reduce a pavement's ability to carry loads and an overlay can be designed to increase the pavement's ability to carry loads over a future design period.

Figure 5.1 illustrates the general concepts of structural deficiency and effective structural capacity. The structural capacity of a pavement when new is denoted as SC_o. For flexible pavements, structural capacity is the structural number, SN. For rigid pavements, structural capacity is the slab thickness, D. For existing composite pavements (AC/PCC) the structural capacity is expressed as an equivalent slab thickness.

The structural capacity of the pavement declines with time and traffic, and by the time an evaluation for overlay design is conducted, the structural capacity has decreased to SC_{eff}. The effective structural capacity for each pavement type is expressed as follows:

Flexible pavements: SN_{eff}
Rigid and composite pavements: D_{eff}

If a structural capacity of SC_f is required for the future traffic expected during the overlay design period, an overlay having a structural capacity of SC_{ol} (i.e., $SC_f - SC_{eff}$) must be added to the existing structure. This approach to overlay design is commonly called the structural deficiency approach. Obviously, the required overlay structural capacity can be correct only if the evaluation of existing structural capacity is correct. The primary objective of the structural evalua-

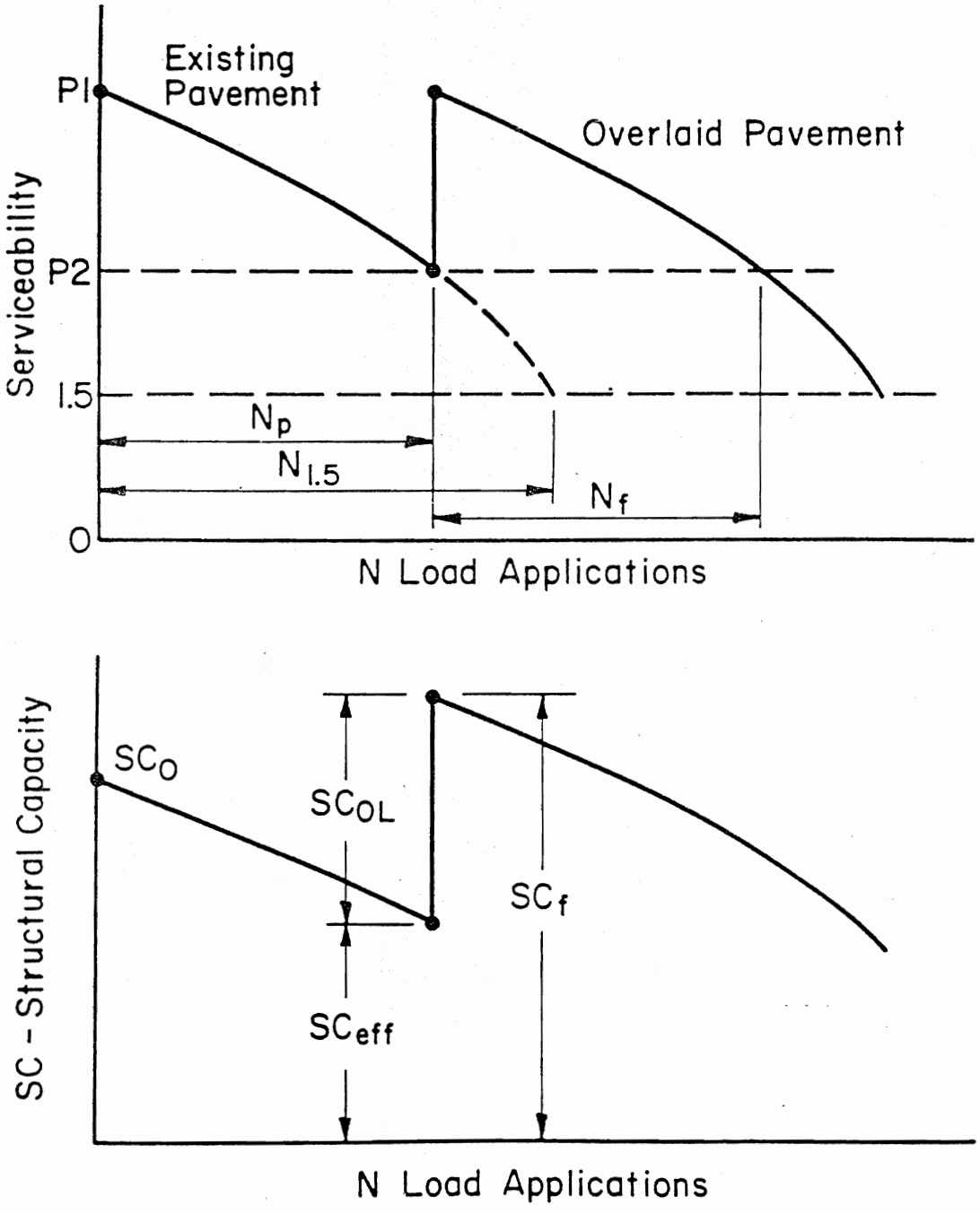

Figure 5.1. Illustration of Structural Capacity Loss Over Time and with Traffic

tion is to determine the effective structural capacity of the existing pavement.

If the declining relationship depicted in Figure 5.1 were well defined, the evaluation of effective structural capacity would be quite easy. This, however, is not the case. No single, specific method exists for evaluating structural capacity. The evaluation of effective structural capacity must consider the current condition of the existing pavement materials, and also consider how those materials will behave in the future. Three alternative evaluation methods are recommended to determine effective structural capacity.

(1) *Structural capacity based on visual survey and materials testing.* This involves the assessment of current conditions based on distress and drainage surveys, and usually some coring and testing of materials.

(2) *Structural capacity based on nondestructive deflection testing (NDT).* This is a direct evaluation of in situ subgrade and pavement stiffness along the project.

(3) *Structural capacity based on fatigue damage from traffic.* Knowledge of past traffic is used to assess the existing fatigue damage in the pavement. The pavement's future remaining fatigue life can then be estimated. The remaining life procedure is most applicable to pavements which have very little visible deterioration.

Because of the uncertainties associated with the determination of effective structural capacity, the three methods cannot be expected to provide equivalent estimates. The designer should use all three methods whenever possible and select the "best" estimate based on his or her judgement. There is no substitute for solid experience and judgment in this selection.

(1) Structural Capacity Based on Visual Survey and Materials Testing

Visual Survey. A key component in the determination of effective structural capacity is the observation of existing pavement conditions. The observation should begin with a review of all information available regarding the design, construction, and maintenance history of the pavement. This should be followed by a detailed survey to identify the type, amount, severity, and location of surface distresses.

Some of the key distress types that are indicators of structural deficiencies are listed below. Some of these are not initially caused by loading, but their severity is increased by loading and thus load-carrying capacity is reduced.

(a) AC-surfaced pavements

Fatigue or alligator cracking in the wheel paths. Patching and a structural overlay are required to prevent this distress from recurring.

Rutting in the wheel paths.

Transverse or longitudinal cracks that develop into potholes.

Localized failing areas where the underlying layers are disintegrating and causing a collapse of the AC surface (e.g., underlying PCC slab with severe "D" cracking, CRCP punchouts, major shear failure of base course/subgrade, stripping of AC base course). This is a very difficult problem to repair and an investigation should be carried out to determine its extent. If it is not extensive, full-depth PCC repair (when a PCC slab exists), and a structural overlay should remedy the problem. If the problem is too extensive for full-depth repair, reconstruction or a structural overlay designed for the weakest area is required.

(b) PCC-surfaced pavements

Deteriorating (spalling or faulting) transverse or longitudinal cracks. These cracks usually must be full-depth repaired, or they will reflect through the overlay. This does not apply to unbonded JPCP or JRCP overlays.

Corner breaks at transverse joints or cracks. Must be full-depth repaired with a full-lane-width repair (this is not required for unbonded JPCP or JRCP overlays).

Localized failing areas where the PCC slab is disintegrating and causing spalls and potholes (e.g., caused by severe "D" cracking, reactive aggregate, or other durability problems). Overlay thickness and preoverlay repair requirements may be prohibitive for some types of overlays.

Localized punchouts, primarily in CRCP. Full-depth repair of existing punchouts and placement of a structural overlay will greatly reduce the likelihood of future punchouts.

Subdrainage Survey. A drainage survey should be coupled with the distress survey. The

objective of the drainage survey is to identify moisture-related pavement problems and locations where drainage improvements might be effective in improve the existing structure or reducing the influence of moisture on the performance of the pavement following the overlay.

Coring and Materials Testing Program. In addition to a survey of the surface distress, a coring and testing program is recommended to verify or identify the cause of the observed surface distress. The locations for coring should be selected following the distress survey to assure that all significant pavement conditions are represented. If NDT is used, the data from that testing should also be used to help select the appropriate sites for coring.

The objective of the coring is to determine material thicknesses and conditions. A great deal of information will be gained simply by a visual inspection of the cored material. However, it should be kept in mind that the coring operation causes a disturbance of the material especially along the cut face of AC material.

For example, in some cases coring has been known to disguise the presence of stripping. Consequently, at least some of the asphalt cores should be split apart to check for stripping.

The testing program should be directed toward determining how the existing materials compare with similar materials that would be used in a new pavement, how the materials may have changed since the pavement was constructed, and whether or not the materials are functioning as expected. The types of tests to be performed will depend on the material types and the types of distress observed. A typical testing program might include strength tests for AC and PCC cores, gradation tests to look for evidence of degradation and/or contamination of granular materials, and extraction tests to determine binder contents and gradations of AC mixes. PCC cores exhibiting durability problems may be examined by a petrographer to identify the cause of the problem.

Specific recommendations on estimating the effective structural capacity from the distress survey information are given in the sections for each overlay type.

(2) Structural Capacity Based on Nondestructive Deflection Testing

Nondestructive deflection testing is an extremely valuable and rapidly developing technology. When properly applied, NDT can provide a vast amount of information and analysis at a very reasonable expenditure of time, money, and effort. The analyses, however, can be quite sensitive to unknown conditions and must be performed by knowledgeable, experienced personnel.

Within the scope of these overlay design procedures, NDT structural evaluation differs depending on the type of pavement. For rigid pavement evaluation, NDT serves three analysis functions: (1) to examine load transfer efficiency at joints and cracks, (2) to estimate the effective modulus of subgrade reaction (effective k-value), and (3) to estimate the modulus of elasticity of the concrete (which provides an estimate of strength). For flexible pavement evaluation, NDT serves two functions: (1) to estimate the roadbed soil resilient modulus, and (2) to provide a direct estimate of SN_{eff} of the pavement structure. Some agencies use NDT to backcalculate the moduli of the individual layers of a flexible pavement, and then use these moduli to estimate SN_{eff}. This approach is not recommended for use with these overlay design procedures because it implies and requires a level of sophistication that does not exist with the structural number approach to design.

In addition to structural evaluation, NDT can provide other data useful to the design process. Deflection data can be used to quantify variability along the project and to subdivide the project into segments of similar structural strength. The NDT data may also be used in a backcalculation scheme to estimate resilient modulus values for the various pavement layers. Although this procedure does not include the use of these values as a part of the structural condition determination, backcalculation of an unusually low value for any layer should be viewed as a strong indication that a detailed study of the condition of that layer is needed.

The specific methods for estimating effective structural capacity by NDT analysis are discussed within the sections pertaining to the specific overlay types.

(3) Structural Capacity Based on Remaining Life

The remaining life approach to structural evaluation relies directly on the concepts illus-

trated in Figure 5.1. This follows a fatigue damage concept that repeated loads gradually damage the pavement and reduce the number of additional loads the pavement can carry to failure. At any given time, there may be no directly observable indication of damage, but there is a reduction in structural capacity in terms of the future load-carrying capacity (the number of future loads that the pavement can carry).

To determine the remaining life, the designer must determine the actual amount of traffic the pavement has carried to date and the total amount of traffic the pavement could be expected to carry to "failure" (when serviceability equals 1.5, to be consistent with the AASHO Road Test equations). Both traffic amounts must be expressed in 18-kip ESAL. The difference between these values, expressed as a percentage of the total traffic to "failure," is defined as the remaining life:

$$RL = 100\left[1 - \left(\frac{N_p}{N_{1.5}}\right)\right]$$

where

RL = remaining life, percent
N_p = total traffic to date, 18-kip ESAL
$N_{1.5}$ = total traffic to pavement "failure" (P2 = 1.5), 18-kip ESAL

With RL determined, the designer may obtain a condition factor (CF) from Figure 5.2. CF is defined by the equation:

$$CF = \frac{SC_n}{SC_o}$$

where

SC_n = pavement structural capacity after N_p ESAL
SC_o = original pavement structural capacity

The existing structural capacity may be estimated by multiplying the original structural capacity of the pavement by CF. For example, the original structural number (SN_o) of a flexible pavement may be calculated from material thicknesses and the structural coefficients for those materials in a new pavement. SN_{eff} of the pavement based on a remaining life analysis would be:

$$SN_{eff} = CF * SN_o$$

The structural capacity determined by this relationship does not account for any preoverlay repair. The calculated structural capacity should be viewed as a lower limit value and may require adjustment to reflect the benefits of preoverlay repair.

For the remaining life determination, $N_{1.5}$ can be roughly estimated using the new pavement design equations or nomographs, or other equations based on local agency information. To be consistent with the AASHO Road Test and the development of these equations, a failure PSI equal to 1.5 and a reliability of 50 percent is recommended.

When using this approach, the designer need not be alarmed if the traffic to date (N_p) is found to exceed the expected traffic to failure ($N_{1.5}$) resulting in a calculated negative remaining life. When this happens, the designer could use the minimum value for CF (0.50), or not use the remaining life approach.

The remaining life approach to determine SN_{eff} or D_{eff} has some serious deficiencies associated with it. There are four major sources of error:

(1) The predictive capability of the AASHO Road Test equations,
(2) The large variation in performance typically observed even among pavements of seemingly identical designs,
(3) Estimation of past 18-kip ESALs, and
(4) Inability to account for the amount of preoverlay repair to the pavement. For pavements with considerable deterioration, the SN_{eff} or D_{eff} value obtained from the remaining life method may be much lower than values obtained from other methods that adjust for preoverlay repairs. Thus, the remaining life procedure is most applicable to pavements which have very little visible deterioration.

As a result, this method of determining the remaining life of the pavement can in some cases produce very erroneous results. The following two extreme errors may occur with this approach:

(1) The remaining life estimate may be extremely low even though very little load-associated distress is present. While some fatigue damage

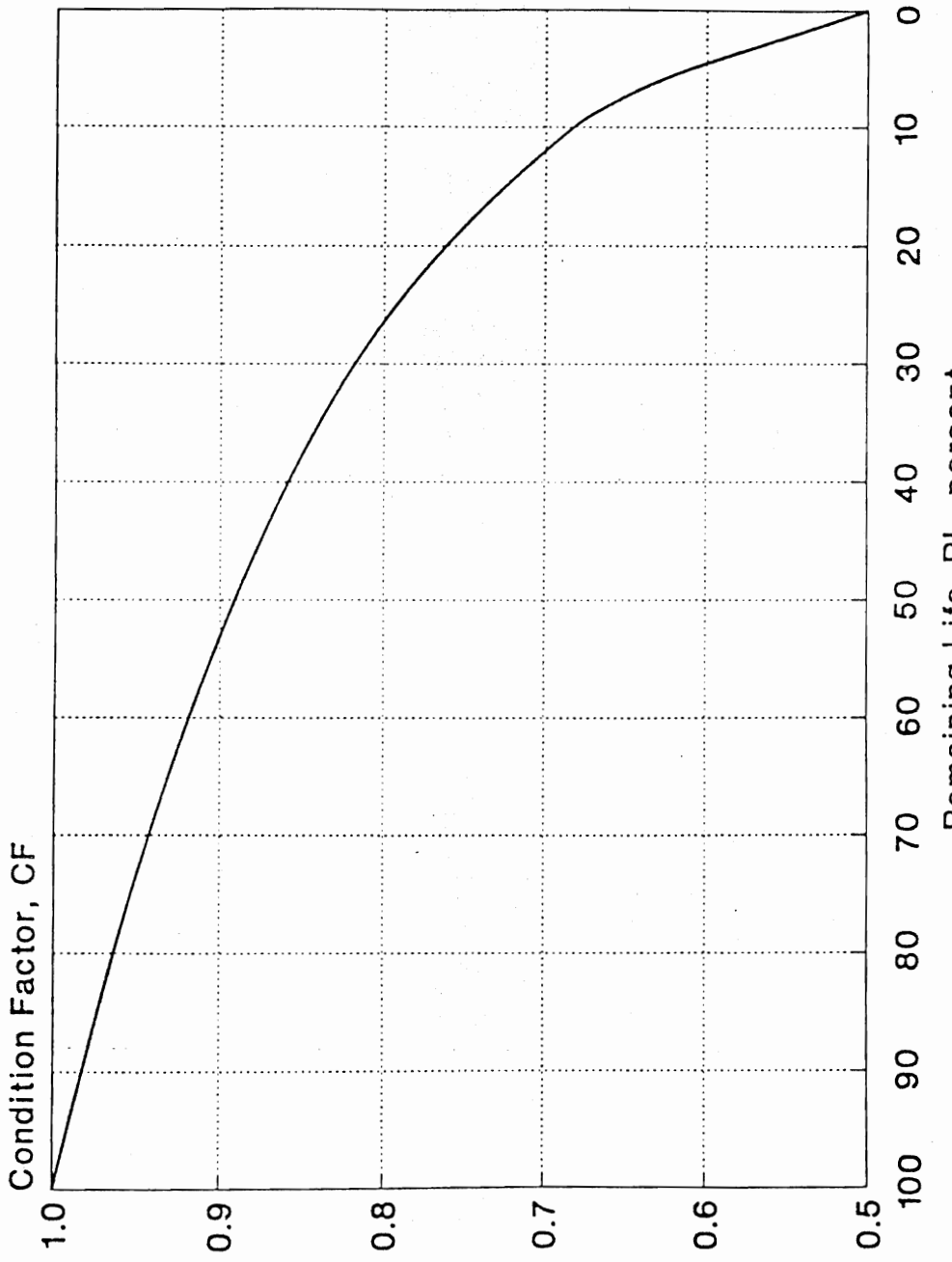

Figure 5.2. Relationship Between Condition Factor and Remaining Life

can exist in a pavement structure before a significant amount of cracking appears, it cannot be a large amount of damage, or it would certainly be evidenced by a significant amount of cracking. If load-related cracking is present in very small amounts and at a low severity level, the pavement has considerable remaining life, regardless of what the traffic-based remaining life calculation suggests.

(2) The remaining life estimate may be extremely high even though a substantial amount of medium- and high-severity load-related cracking is present. In this case, the pavement really has little remaining life.

At any point between these two extremes, the remaining life computed from past traffic may not reflect the amount of fatigue damage in the pavement, but discerning this from observed distress may be more difficult. If the computed remaining life appears to be clearly at odds with the amount and severity of load-associated distress present, do not use the remaining life method to compute the structural capacity of the existing pavement.

The remaining life approach to determining structural capacity is not directly applicable, without modification, to pavements which have already received one or more overlays.

5.3.4 Determination of Design M_R

The design subgrade M_R may be determined by: (1) laboratory testing, (2) NDT backcalculation, (3) estimation from resilient modulus correlation studies, or (4) original design and construction data. Regardless of the method used, the design M_R value must be consistent with the value used in the design performance equation for the AASHO Road Test subgrade. This is especially important when M_R is determined by NDT backcalculation. The backcalculated value is typically too high to be consistent and must be adjusted. If M_R is not adjusted, the SN_f value will be unconservative and poor overlay performance can be expected.

A subgrade M_R may be backcalculated from NDT data using the following equation:

$$M_R = \frac{0.24P}{d_r r}$$

where

M_R = backcalculated subgrade resilient modulus, psi
P = applied load, pounds
d_r = measured deflection at radial distance r, inches
r = radial distance at which the deflection is measured, inches

This equation for backcalculating M_R is based on the fact that, at points sufficiently distant from the center of loading, the measured surface deflection is almost entirely due to deformation in the subgrade, and is also independent of the load radius. For practical purposes, the deflection used should be as close as possible to the loading plate, but must also be sufficiently far from the loading plate to satisfy the assumptions inherent in the above equation. Guidance is provided later in this chapter for selecting the minimum radial distance for determination of M_R.

The recommended method for determination of the design M_R from NDT backcalculation requires an adjustment factor (C) to make the value calculated consistent with the value used to represent the AASHO subgrade. A value for C of no more than 0.33 is recommended for adjustment of backcalculated M_R values to design M_R values. The resulting equation is:

$$\text{Design } M_R = C\left(\frac{0.24P}{d_r r}\right)$$

A subgrade M_R value of 3,000 psi was used for the AASHO Road Test soil in the development of the flexible pavement performance model. This value is consistent with some laboratory tests of soil samples from the AASHO Road Test site, as Figure 5.3 illustrates (*11*). However, these data also show that the resilient modulus of the AASHO Road Test soil is quite stress-dependent, increasing rapidly for deviator stresses less than 6 psi. The subgrade deviator stress at a radial distance appropriate for use in the equation given above for backcalculated M_R will almost always be far less than 6 psi. Thus, the subgrade modulus determined by backcalculation can be expected to be too high to be consistent with the 3,000 psi assumed for the AASHO subgrade.

This was confirmed by two methods. In the first analysis, M_R values backcalculated from deflection data were compared with M_R values obtained from laboratory tests, for the AASHO Road Test and other sites (*12, 13*). The results, which are shown in Figure 5.4, indicate that backcalculated M_R values exceed laboratory M_R values by a factor of three or more. In

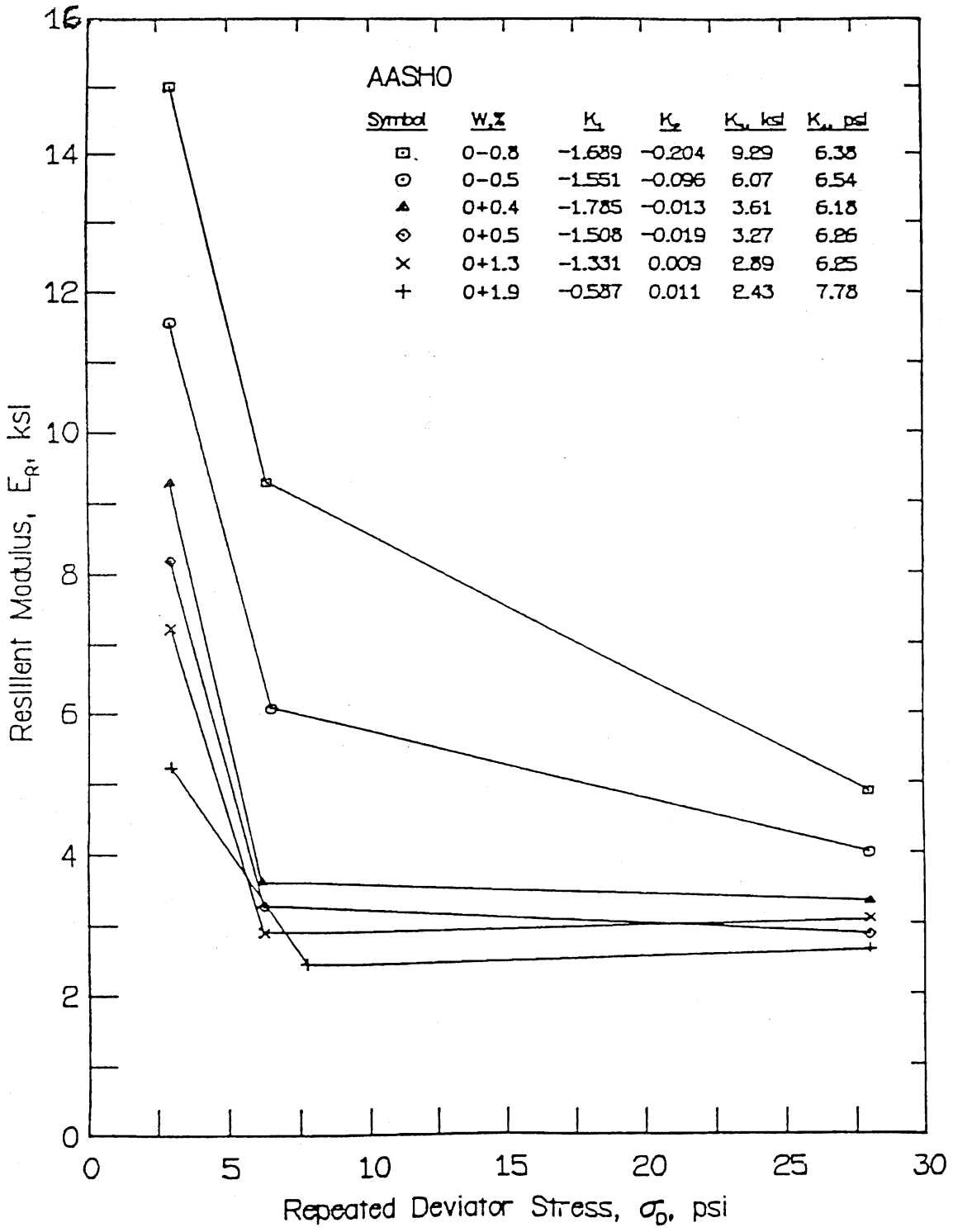

Figure 5.3. AASHO Road Test Subgrade Resilient Modulus Test Results (*11*)

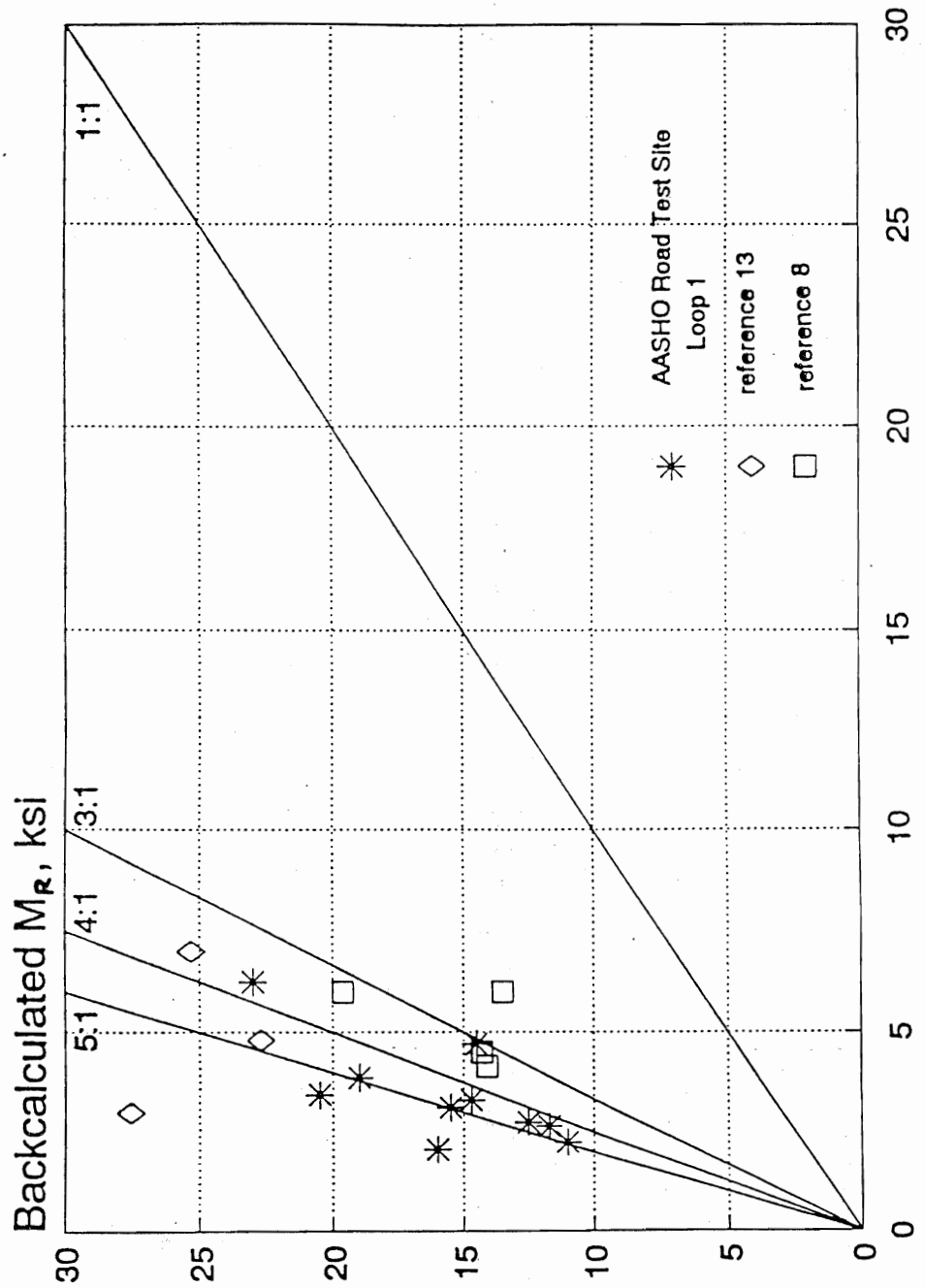

Figure 5.4. Backcalculated Resilient Modulus Versus Laboratory Results on Shelby Tube Samples from the AASHO Road Test Site Plus Data from Two Additional States

the second analysis, the ILLI-PAVE finite element program (*14, 15*) was used to compute M_R values for a variety of pavement structures and subgrade characteristics representative of the AASHO Road Test soil. At radial distances appropriate for backcalculation of M_R, the computed M_R values also exceeded the value of 3,000 psi assumed in development of the AASHO flexible pavement model by a factor of at least three. Similarly, pavement surface deflections computed by ILLI-PAVE produced backcalculated M_R values three or more times greater than 3,000 psi.

All of these analyses suggest that for the soils examined, backcalculated M_R values should be multiplied by an adjustment factor C of no more than 0.33 in order to obtain M_R values appropriate for use in design with the AASHTO flexible pavement model.

The analyses described here pertain to the fine-grained, stress-sensitive soil at the AASHO Road Test site plus fine-grained soil from seven other projects. No attempt has been made in this study to investigate the relationship between backcalculated and laboratory M_R values for granular subgrades. It may be that backcalculated M_R values for granular subgrades would not require a correction factor as large as is required for cohesive subgrades. However, this subject requires further research.

Users are cautioned that the resilient modulus value selected has a very significant effect on the resulting structural number determined. Therefore, users should be very cautious about using high resilient modulus values, or their overlay thickness values will be too thin.

5.4 AC OVERLAY OF AC PAVEMENT

This section covers the design of AC overlays of AC pavements. The following construction tasks are involved in the placement of an AC overlay on an existing AC pavement:

(1) Repairing deteriorated areas and making subdrainage improvements (if needed).
(2) Correcting surface rutting by milling or placing a leveling course.
(3) Constructing widening (if needed).
(4) Applying a tack coat.
(5) Placing the AC overlay (including a reflective crack control treatment if needed).

5.4.1 Feasibility

An AC overlay is a feasible rehabilitation alternative for an AC pavement except when the condition of the existing pavement dictates substantial removal and replacement. Conditions under which an AC overlay would not be feasible include the following.

(1) The amount of high-severity alligator cracking is so great that complete removal and replacement of the existing surface is dictated.
(2) Excessive surface rutting indicates that the existing materials lack sufficient stability to prevent recurrence of severe rutting.
(3) An existing stabilized base shows signs of serious deterioration and would require an inordinate amount of repair to provide uniform support for the overlay.
(4) An existing granular base must be removed and replaced due to infiltration of and contamination by a soft subgrade.
(5) Stripping in the existing AC surface dictates that it should be removed and replaced.

5.4.2 Pre-overlay Repair

The following types of distress should be repaired prior to overlay of AC pavements. If they are not repaired, the service life of the overlay will be greatly reduced.

Distress Type	Required Repair
Alligator Cracking	All areas of high-severity alligator cracking must be repaired. Localized areas of medium-severity alligator cracking should be repaired unless a paving fabric or other means of reflective crack control is used. The repair must include removal of any soft subsurface material.
Linear Cracks	High-severity linear cracks should be patched. Linear cracks that are open greater than 0.25 inch should be filled with a sand-asphalt mixture or other suitable crack filler. Some method of reflective crack control is recommended for transverse cracks that experience significant opening and closing.

Rutting	Remove ruts by milling or placement of a leveling course. If rutting is severe, an investigation into which layer is causing the rutting should be conducted to determine whether or not an overlay is feasible.
Surface Irregularities	Depressions, humps, and corrugations require investigation and treatment of their cause. In most cases, removal and replacement will be required.

5.4.3 Reflection Crack Control

The basic mechanism of reflection cracking is strain concentration in the overlay due to movement in the vicinity of cracks in the existing surface. This movement may be bending or shear induced by loads, or may be horizontal contraction induced by temperature changes. Load-induced movements are influenced by the thickness of the overlay and the thickness and stiffness of the existing pavement. Temperature-induced movements are influenced by daily and seasonal temperature variations, the coefficient of thermal expansion of the existing pavement, and the spacing of cracks.

Pre-overlay repair (patching and crack filling) may help delay the occurrence and deterioration of reflection cracks. Additional reflection crack control measures which have been beneficial in some cases include the following:

(1) Synthetic fabrics and stress-absorbing interlayers (SAMIs) have been effective in controlling reflection of low- and medium-severity alligator cracking. They may also be useful for controlling reflection of temperature cracks, particularly when used in combination with crack filling. They generally do little, however, to retard reflection of cracks subject to significant horizontal or vertical movements.

(2) Crack relief layers greater than 3 inches thick have been effective in controlling reflection of cracks subject to larger movements. These crack relief layers are composed of open-graded coarse aggregate and a small percentage of asphalt cement.

(3) Sawing and sealing joints in the AC overlay at locations coinciding with straight cracks in the underlying AC may be effective in controlling the deterioration of reflection cracks. This technique has been very effective when applied to AC overlays of jointed PCC pavements when the sawcut matches the joint or straight crack within an inch.

(4) Increased AC overlay thickness reduces bending and vertical shear under loads and also reduces temperature variation in the existing pavement. Thus, thicker AC overlays are more effective in delaying the occurrence and deterioration of reflection cracks than are thinner overlays. However, increasing the AC overlay thickness is a costly approach to reflection crack control.

Reflection cracking can have a considerable (often controlling) influence on the life of an AC overlay. Deteriorated reflection cracks detract from a pavement's serviceability and also require frequent maintenance, such as sealing and patching. Reflection cracks also permit water to enter the pavement structure, which may result in loss of bond between the AC overlay and existing AC surface, stripping in either layer, and softening of the granular layers and subgrade. For this reason, reflection cracks should be sealed as soon as they appear and resealed periodically throughout the life of the overlay. Sealing low-severity reflection cracks may also be effective in retarding their progression to medium and high severity levels.

5.4.4 Subdrainage

See Section 5.2.4 for guidelines.

5.4.5 Thickness Design

If the overlay is being placed for the purpose of structural improvement, the required thickness of the overlay is a function of the structural capacity required to meet future traffic demands and the structural capacity of the existing pavement. The required thickness to increase structural capacity to carry future traffic is determined by the following equation.

$$SN_{ol} = a_{ol} * D_{ol} = SN_f - SN_{eff}$$

where

SN_{ol} = Required overlay structural number
a_{ol} = Structural coefficient for the AC overlay
D_{ol} = Required overlay thickness, inches

SN_f = Structural number required to carry future traffic
SN_{eff} = Effective structural number of the existing pavement

The required overlay thickness may be determined through the following design steps. These steps provide a comprehensive design approach that recommends testing the pavement to obtain valid design inputs. If it is not possible to conduct testing (e.g., for a low-volume road), an approximate overlay design may be developed based upon visible distress observation, by skipping Steps 4 and 5 and by estimating other inputs.

Step 1: Existing pavement design and construction.

(1) Thickness and material type of each pavement layer.
(2) Available subgrade soil information (from construction records, soil surveys, county agricultural soils reports, etc.)

Step 2: Traffic analysis.

(1) Past cumulative 18-kip ESALs in the design lane (N_p), for use in the remaining life method of SN_{eff} determination only.
(2) Predicted future 18-kip ESALs in the design lane over the design period (N_f).

Step 3: Condition survey.

Distress types and severities are defined in reference 11. The following distresses are measured during the condition survey and are used in the determination of the structural coefficients. Sampling along the project in the heaviest trafficked lane can be used to estimate these quantities.

(1) Percent of surface area with alligator cracking (class 1, 2, and 3 corresponding to low, medium, and high severities).
(2) Number of transverse cracks per mile (low, medium, and high severities).
(3) Mean rut depth.
(4) Evidence of pumping at cracks and at pavement edges.

Step 4: Deflection testing (strongly recommended).

Measure deflections in the outer wheel path at an interval sufficient to adequately assess conditions. Intervals of 100 to 1,000 feet are typical. Areas that are deteriorated and will be repaired should not be tested. A heavy-load deflection device (e.g., Falling Weight Deflectometer) and a load magnitude of approximately 9,000 pounds are recommended. ASTM D 4694 and D 4695 provide additional guidance on deflection testing. Deflections should be measured at the center of the load and at least one other distance from the load, as described below.

(1) Subgrade resilient modulus (M_R). At sufficiently large distances from the load, deflections measured at the pavement surface are due to subgrade deformation only, and are also independent of the size of the load plate. This permits the backcalculation of the subgrade resilient modulus from a single deflection measurement and the load magnitude, using the following equation:

$$M_R = \frac{0.24P}{d_r r}$$

where

M_R = backcalculated subgrade resilient modulus, psi
P = applied load, pounds
d_r = deflection at a distance r from the center of the load, inches
r = distance from center of load, inches

It should be noted that no temperature adjustment is needed in determining M_R since the deflection used is due only to subgrade deformation.

The deflection used to backcalculate the subgrade modulus must be measured far enough away that it provides a good estimate of the subgrade modulus, independent of the effects of any layers above, but also close enough that it is not too small to measure accurately. The minimum distance may be determined from the following relationship:

$$r \geq 0.7a_e$$

where

$$a_e = \sqrt{\left[a^2 + \left(D \sqrt[3]{\frac{E_p}{M_R}}\right)^2\right]}$$

a_e = radius of the stress bulb at the subgrade-pavement interface, inches
a = NDT load plate radius, inches
D = total thickness of pavement layers above the subgrade, inches
E_p = effective modulus of all pavement layers above the subgrade, psi (described below)

Before the backcalculated M_R value is used in design, it must be adjusted to make it consistent with the value used in the AASHTO flexible pavement design equation. An adjustment may also be needed to account for seasonal effects. These adjustments are described in Step 6.

(2) Temperature of AC mix. The temperature of the AC mix during deflection testing must be determined. The AC mix temperature may be measured directly, or may be estimated from surface or air temperatures.

(3) Effective modulus of the pavement (E_p). If the subgrade resilient modulus and total thickness of all layers above the subgrade are known or assumed, the effective modulus of the entire pavement structure (all pavement layers above the subgrade) may be determined from the deflection measured at the center of the load plate using the following equation:

$$d_0 = 1.5pa \left\{ \frac{1}{M_R \sqrt{1 + \left(\frac{D}{a} \sqrt[3]{\frac{E_p}{M_R}}\right)^2}} + \frac{\left[1 - \frac{1}{\sqrt{1 + \left(\frac{D}{a}\right)^2}}\right]}{E_p} \right\}$$

where

d_0 = deflection measured at the center of the load plate (and adjusted to a standard temperature of 68°F), inches
p = NDT load plate pressure, psi
a = NDT load plate radius, inches
D = total thickness of pavement layers above the subgrade, inches
M_R = subgrade resilient modulus, psi
E_p = effective modulus of all pavement layers above the subgrade, psi

For a load plate radius of 5.9 inches, Figure 5.5 may be used to determine the ratio E_p/M_R, and E_p may then be determined for a known or assumed value of M_R.

For purposes of comparison of E_p along the length of a project, the d_0 values used to determine E_p should be adjusted to a single reference temperature. Furthermore, if the effective structural number of the existing pavement is to be determined in Step 7 using the values of E_p backcalculated from deflection data, the reference temperature for adjustment of d_0 should be 68°F, to be consistent with the procedure for new AC pavement design described in Part II. Figure 5.6 may be used to adjust d_0 for AC pavements with granular and asphalt-stabilized bases. Figure 5.7 may be used to adjust d_0 for AC pavements with cement- and pozzolanic-stabilized bases.

Step 5: Coring and materials testing (strongly recommended).

(1) *Resilient modulus of subgrade.* If deflection testing is not performed, laboratory testing of samples of the subgrade may be conducted to determine its resilient modulus using AASHTO T 292-91 I with a deviator stress of 6 psi to match the deviator stress used in establishing the 3,000 psi for the AASHO Road Test soil that is incorporated into the flexible design equation. Alternatively, other tests such as R value, CBR or soil classification tests could be conducted and approximate correlations used to estimate resilient modulus. Use of the estimating equation $M_R = 1500 * CBR$ may produce a value that is too large for use in this design procedure. The relationships found in Appendix FF, Figure FF-6 may be more reasonable.

(2) *Samples of AC layers and stabilized base* should be visually examined to assess asphalt stripping, degradation, and erosion.

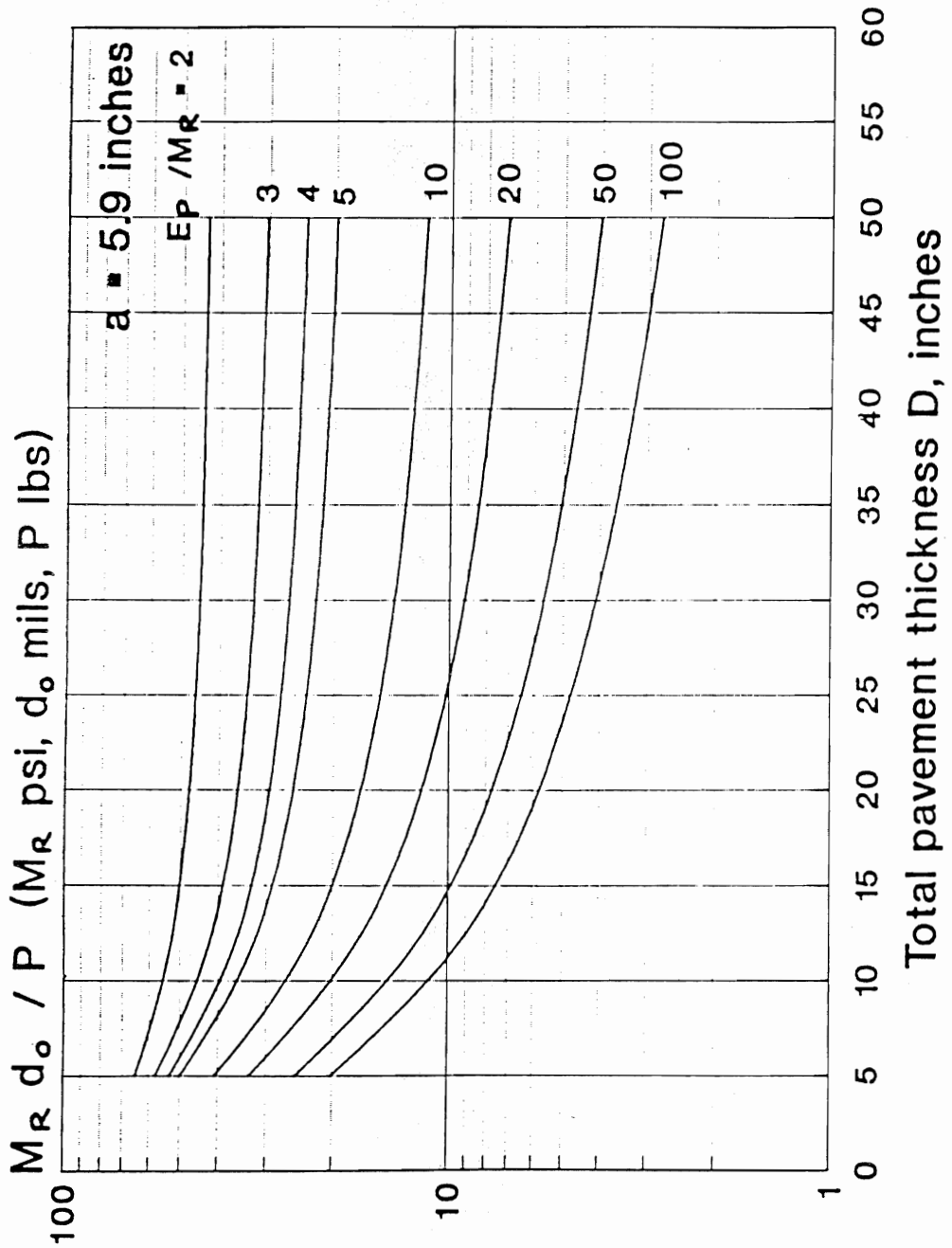

Figure 5.5. Determination of E_p/M_R

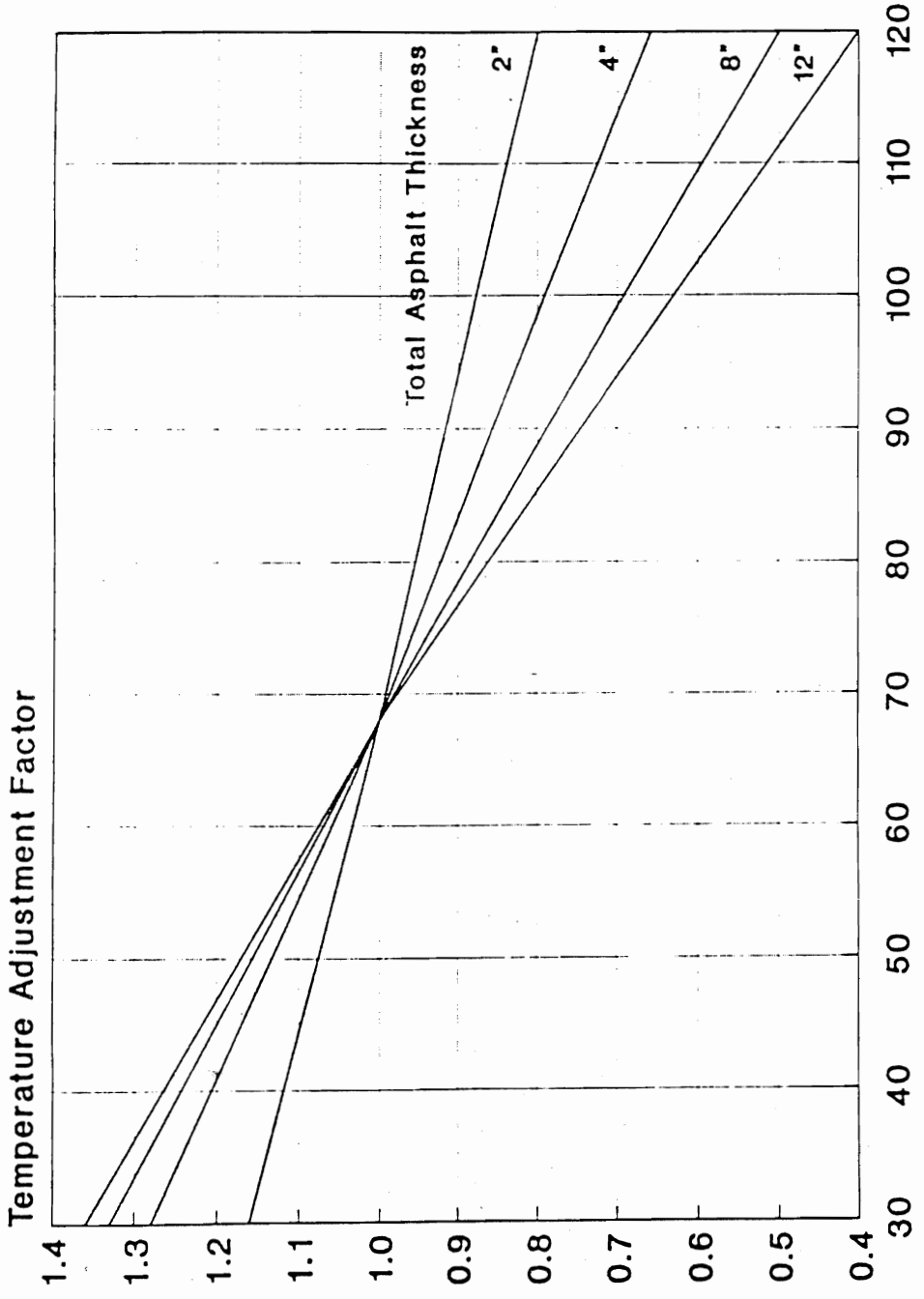

Figure 5.6. Adjustment to d_0 for AC Mix Temperature for Pavement with Granular or Asphalt-Treated Base

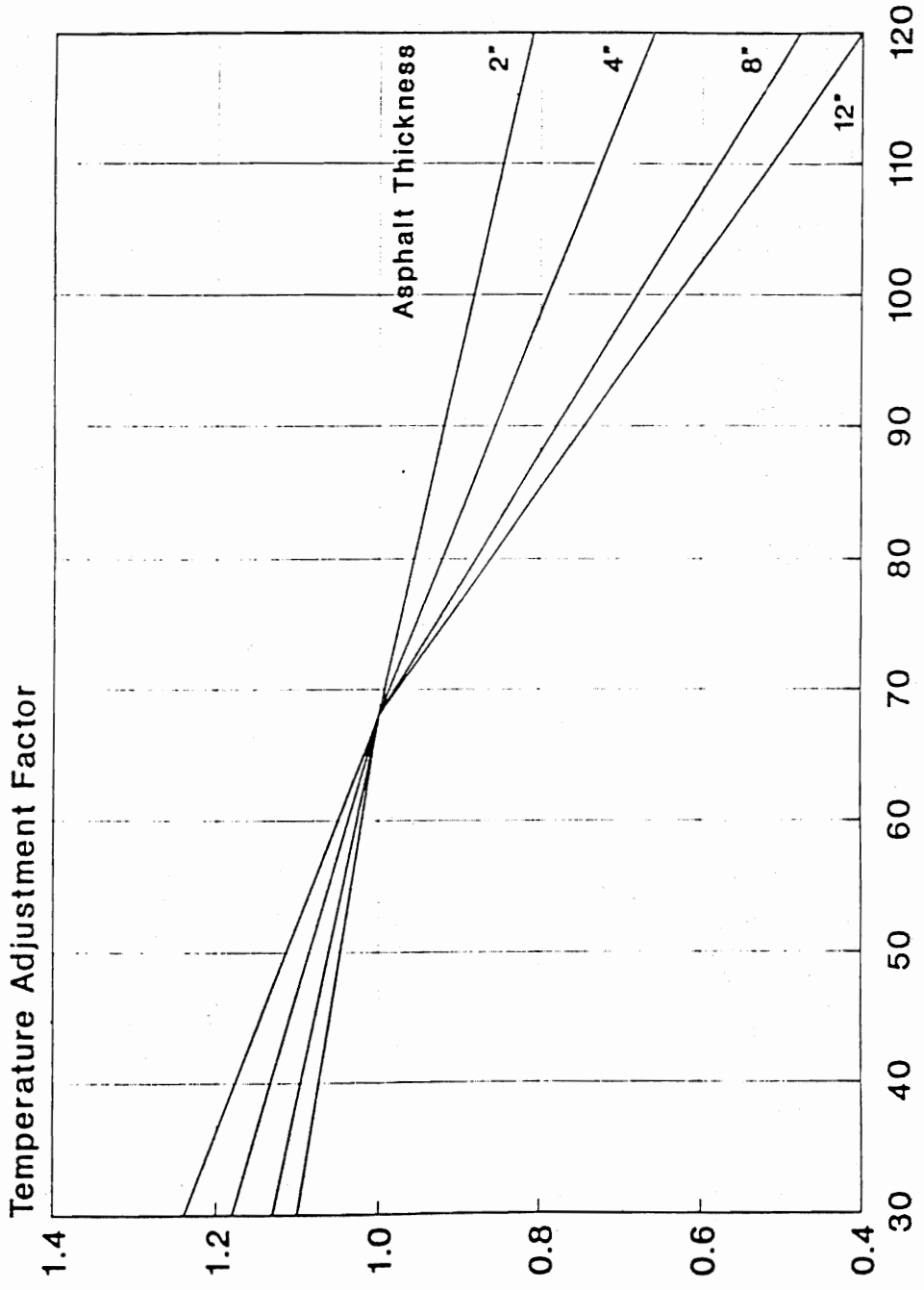

Figure 5.7. Adjustment to d_0 for AC mix Temperature for Pavement with Cement- or Pozzolanic-Treated Base

(3) *Samples of granular base and subbase* should be visually examined and a gradation run to assess degradation and contamination by fines.
(4) *The thickness of all layers* should be measured.

Step 6: Determination of required structural number for future traffic (SN_f).

(1) *Effective design subgrade resilient modulus.* Determine by one of the following methods:
  (a) Laboratory testing described in Step 5.
  (b) Backcalculation from deflection data. (NOTE: this value must be adjusted to be consistent with the value used in the AASHTO flexible pavement design equation as described below.)
  (c) A very approximate estimate can be made using available soil information and relationships developed from resilient modulus studies. However, if as-constructed soil data are used, the resilient modulus may have changed since construction due to changes in moisture content or other factors.

Regardless of the method used, the effective design subgrade resilient modulus must be (1) representative of the effects of seasonal variation and (2) consistent with the resilient modulus value used to represent the AASHO Road Test soil. A seasonal adjustment, when needed, may be made in accordance with the procedures described in Part II, Section 2.3.1. M_R values backcalculated from deflections must be adjusted to be consistent with the laboratory-measured value used for the AASHO Road Test soil in the development of the flexible pavement design equation. It is recommended that backcalculated M_R values be multiplied by a correction factor C = 0.33 for use in determination of SN_f for design purposes when an FWD load of approximately 9,000 pounds is used (*9*). This value should be evaluated and adjusted if needed by user agencies for their soil and deflection measurement equipment. Therefore, the following design M_R should be used to determine SN_f:

$$\text{Design } M_R = C\left(\frac{0.24P}{d_r r}\right)$$

where recommended C = 0.33

Note also that the presence of a very stiff layer (e.g., bedrock) within about 15 feet of the top of the subgrade may cause the backcalculated M_R to be high. When such a condition exists, a value less than 0.33 for C may be warranted (*9*).

The designer is cautioned against using a value of M_R that is too large. The value of M_R selected for design is extremely critical to the overlay thickness. The use of a value greater than 3,000 psi is an indication that the soil is stiffer than the silty-clay A-6 soil at the Road Test site, and consequently will provide increased support and extended pavement life.

(2) *Design PSI loss.* PSI immediately after overlay (P1) minus PSI at time of next rehabilitation (P2).
(3) *Overlay design reliability R (percent).* See Part I, Section 4.2, Part II, Table 2.2, and Part III, Section 5.2.15.
(4) *Overall standard deviation S_o for flexible pavement.* See Part I, Section 4.3.

Compute SN_f for the above design inputs using the flexible pavement design equation or nomograph in Part II, Figure 3.1. When designing an overlay thickness for a uniform pavement section, mean input values must be used. When designing an overlay thickness for specific points along the project, the data for that point must be used. A worksheet for determining SN_f is provided in Table 5.1.

Step 7: Determination of effective structural number (SN_{eff}) of the existing pavement.

Three methods are presented for determining the effective structural number of a conventional AC pavement: an NDT method, a condition survey method, and a remaining fatigue life method. It is suggested that the designer use all three of these to evaluate the pavement, and then select a value for SN_{eff} based on the results, using engineering judgment and the past experience of the agency.

SN_{eff} from NDT for AC Pavements

The NDT method of SN_{eff} determination follows an assumption that the structural capacity of the pavement is a function of its total thickness and overall stiffness. The relationship between SN_{eff}, thickness, and stiffness is:

Table 5.1. Worksheet for Determination of SN_f for AC Pavements

TRAFFIC:

Future 18-kip ESALs in design lane over design period, N_f = _____

EFFECTIVE ROAD-BED SOIL RESILIENT MODULUS:

Design resilient modulus, M_R = _____ psi

(Adjusted for consistency with flexible pavement model and for seasonal variations. Typical design M_R is 2,000 to 10,000 psi for fine-grained soils, 10,000 to 20,000 for coarse-grained soils. The AASHO Road Test soil value used in the flexible pavement design equation was 3,000 psi.)

SERVICEABILITY LOSS:

Design PSI loss (P1 − P2) (1.2 to 2.5) = _____

DESIGN RELIABILITY:

Overlay design reliability, R (80 to 99 percent) = _____ percent

Overall standard deviation, S_o (typically 0.49) = _____

FUTURE STRUCTURAL CAPACITY:

Required structural number for future traffic is determined from flexible pavement design equation or nomograph in Part II, Figure 3.1.

SN_f = _____

$$SN_{eff} = 0.0045D\sqrt[3]{E_p}$$

$$SN_{eff} = a_1D_1 + a_2D_2m_2 + a_3D_3m_3$$

where

- D = total thickness of all pavement layers above the subgrade, inches
- E_p = effective modulus of pavement layers above the subgrade, psi

E_p may be backcalculated from deflection data as described in Step 4. Figure 5.8 may be used to determine SN_{eff} according to the above equation.

SN_{eff} from Condition Survey for AC Pavements

The condition survey method of SN_{eff} determination involves a component analysis using the structural number equation:

where

- D_1, D_2, D_3 = thicknesses of existing pavement surface, base, and subbase layers
- a_1, a_2, a_3 = corresponding structural layer coefficients
- m_2, m_3 = drainage coefficients for granular base and subbase

See Part II, Table 2.4, for guidance in determining the drainage coefficients. In selecting values for m_2 and m_3, note that the poor drainage situation for the base and subbase at the AASHO Road Test would be given drainage coefficient values of 1.0.

Depending on the types and amounts of deterioration present, the layer coefficient values assigned to materials in in-service pavement should in most cases be less than the values that would be assigned to the same materials for new construction. An exception to

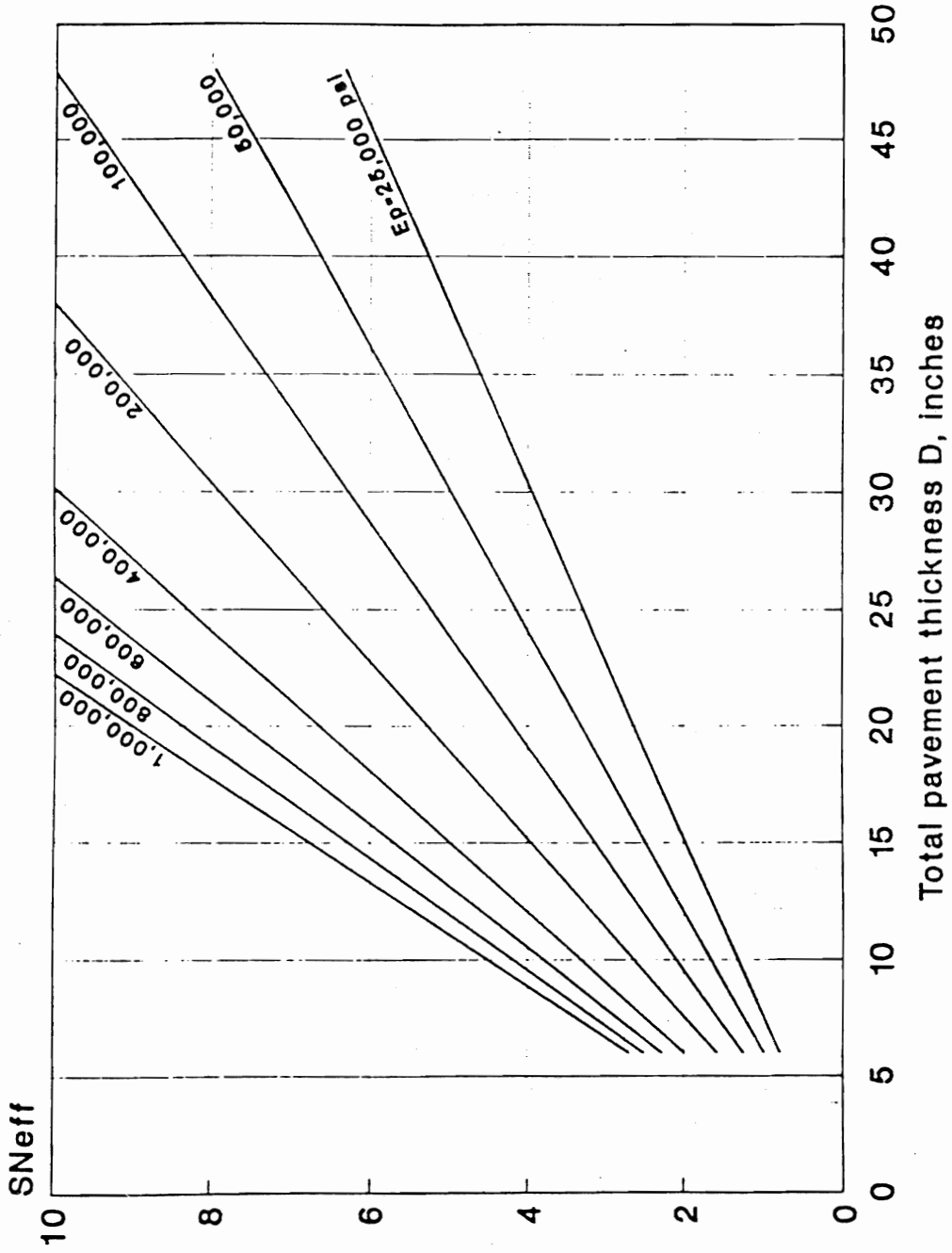

Figure 5.8. SN_{eff} from NDT Method

this general rule might be for unbound granular materials that show no sign of degradation or contamination.

For example, one State uses 0.44 for its new high-quality AC surface, but for overlay design purposes uses a reduced coefficient for the same material in an existing pavement. A value of 0.34 is assigned if the AC layer is in good condition, 0.25 if its condition is fair, and 0.15 if its condition is poor. The condition ratings are made on the basis of the amount of cracking present.

Limited guidance is presently available for the selection of layer coefficients for in-service pavement materials. Each agency must adopt its own set of values. Some suggested layer coefficients for existing materials are provided in Table 5.2.

The following notes apply to Table 5.2:

(1) All of the distress is as observed at the pavement surface.
(2) Patching all high-severity alligator cracking is recommended. The AC surface and stabilized base layer coefficients selected should reflect the amount of high-severity cracking remaining after patching.
(3) In addition to evidence of pumping noted during condition survey, samples of base material should be obtained and examined for evidence of erosion, degradation and contamination by fines, as well as evaluated for drainability, and layer coefficients reduced accordingly.
(4) The percentage of transverse cracking is determined as (linear feet of cracking/square feet of pavement) * 100.
(5) Coring and testing are recommended for evaluation of all materials and are strongly recommended for evaluation of stabilized layers.
(6) There may be other types of distress that, in the opinion of the engineer, would detract from the performance of an overlay. These should be considered through an appropriate decrease of the structural coefficient of the layer exhibiting the distress (e.g., surface raveling of the AC, stripping of an AC layer, freeze-thaw damage to a cement-treated base).

SN_{eff} from Remaining Life for AC Pavements

The remaining life of the pavement is given by the following equation:

$$RL = 100\left[1 - \left(\frac{N_p}{N_{1.5}}\right)\right]$$

where

RL = remaining life, percent
N_p = total traffic to date, ESALs
$N_{1.5}$ = total traffic to pavement "failure," ESALs

$N_{1.5}$ may be estimated using the new pavement design equations or nomographs in Part II. To be consistent with the AASHO Road Test and the development of these equations, a "failure" PSI equal to 1.5 and a reliability of 50 percent is recommended.

SN_{eff} is determined from the following equation:

$$SN_{eff} = CF * SN_o$$

where

CF = condition factor determined from Figure 5.2
SN_o = structural number of the pavement if it were newly constructed

The designer should recognize that SN_{eff} determined by this method does not reflect any benefit for pre-overlay repair. The estimate of SN_{eff} obtained should thus be considered a lower limit value. The SN_{eff} of the pavement will be higher if pre-overlay repair of load-associated distress (alligator cracking) is done. This method for determining SN_{eff} is not applicable, without modification, to AC pavements which have already received one or more AC overlays.

A worksheet for determination of SN_{eff} is provided in Table 5.3.

Step 8: Determination of overlay thickness.

The thickness of AC overlay is computed as follows:

$$D_{ol} = \frac{SN_{ol}}{a_{ol}} = \frac{(SN_f - SN_{eff})}{a_{ol}}$$

where

SN_{ol} = Required overlay structural number
a_{ol} = Structural coefficient for the AC overlay
D_{ol} = Required overlay thickness, inches
SN_f = Structural number determined in Step 6

Table 5.2. Suggested Layer Coefficients for Existing AC Pavement Layer Materials

MATERIAL	SURFACE CONDITION	COEFFICIENT
AC Surface	Little or no alligator cracking and/or only low-severity transverse cracking	0.35 to 0.40
	< 10 percent low-severity alligator cracking and/or < 5 percent medium- and high-severity transverse cracking	0.25 to 0.35
	> 10 percent low-severity alligator cracking and/or < 10 percent medium-severity alligator cracking and/or > 5–10 percent medium- and high-severity transverse cracking	0.20 to 0.30
	> 10 percent medium-severity alligator cracking and/or < 10 percent high-severity alligator cracking and/or > 10 percent medium- and high-severity transverse cracking	0.14 to 0.20
	> 10 percent high-severity alligator cracking and/or > 10 percent high-severity transverse cracking	0.08 to 0.15
Stabilized Base	Little or no alligator cracking and/or only low-severity transverse cracking	0.20 to 0.35
	< 10 percent low-severity alligator cracking and/or < 5 percent medium- and high-severity transverse cracking	0.15 to 0.25
	> 10 percent low-severity alligator cracking and/or < 10 percent medium-severity alligator cracking and/or > 5–10 percent medium- and high-severity transverse cracking	0.15 to 0.20
	> 10 percent medium-severity alligator cracking and/or < 10 percent high-severity alligator cracking and/or > 10 percent medium- and high-severity transverse cracking	0.10 to 0.20
	> 10 percent high-severity alligator cracking and/or > 10 percent high-severity transverse cracking	0.08 to 0.15
Granular Base or Subbase	No evidence of pumping, degradation, or contamination by fines	0.10 to 0.14
	Some evidence of pumping, degradation, or contamination by fines	0.00 to 0.10

SN_{eff} = Effective structural number of the existing pavement, from Step 7

The thickness of overlay determined from the above relationship should be reasonable when the overlay is required to correct a structural deficiency. See Section 5.2.17 for discussion of factors which may result in unreasonable overlay thicknesses.

5.4.6 Surface Milling

If the AC pavement is to be milled prior to overlay, the depth of milling must be reflected in the SN_{eff} analyses. No adjustment need be made to SN_{eff} values determined by NDT if the depth of milling does not exceed the minimum necessary to remove surface ruts. If a greater depth is milled, the NDT-determined SN_{eff} may be reduced by an amount equal to the depth milled times a structural coefficient for the AC surface based on the condition survey.

5.4.7 Shoulders

See Section 5.2.10 for guidelines.

Table 5.3. Worksheet for Determination of SN_{eff} for AC Pavement

(1) NDT Method For SN_{eff} For AC Pavement:

Total thickness of all pavement layers above subgrade, D	= _____	inches
Backcalculated subgrade resilient modulus, M_R	= _____	psi
Backcalculated effective pavement modulus, E_p	= _____	psi

$$SN_{eff} = 0.0045D\sqrt[3]{E_p} = \_\_\_\_\_$$

(2) Condition Survey Method For SN_{eff} For AC Pavement:

Thickness of AC surface, D_1	= _____	inches
Structural coefficient of AC surface, a_1, based on condition survey and coring data	= _____	
Thickness of base, D_2	= _____	inches
Structural coefficient of base, a_2, based on condition survey, matcrial inspection, and testing	= _____	
Drainage coefficient of base, m_2	= _____	
Thickness of subbase, D_3, if present	= _____	inches
Structural coefficient of subbase, a_3, based on condition survey, material inspection, and testing	= _____	
Drainage coefficient of subbase, m_3	= _____	

$$SN_{eff} = a_1D_1 + a_2D_2m_2 + a_3D_3m_3 = \_\_\_\_\_$$

5.4.8 Widening

See Section 5.2.16 for guidelines.

5.5 AC OVERLAY OF FRACTURED PCC SLAB PAVEMENT

This section covers the design of AC overlays placed on PCC pavements after they have been fractured by any of the following techniques: break/seat, crack/seat or rubblize/compact.

Break/seat consists of breaking a JRCP into pieces larger than about one foot, rupturing the reinforcement or breaking its bond with the concrete, and seating the pieces firmly into the foundation.

Crack/seat consists of cracking a JPCP into pieces typically one to three feet in size and seating the pieces firmly into the foundation.

Seating typically consists of several passes of a 35- to 50-ton rubber-tired roller over a cracked or broken slab.

Rubblize/compact consists of completely fracturing any type of PCC slab (JRCP, JPCP, or CRCP) into pieces smaller than one foot and then compacting the layer, typically with two or more passes of a 10-ton vibratory roller.

The following construction tasks are involved in the placement of an AC overlay on a fractured PCC slab pavement:

(1) Removing and replacing areas that will result in uneven support after fracturing
(2) Making subdrainage improvements if needed

Table 5.3. Worksheet for Determination of SN_{eff} for AC Pavement (continued)

(3) **Remaining Life Method For SN_{eff} for AC Pavement:**

Past 18-kip ESALs in design lane since construction, N_p = _____

18-kip ESALs to failure of existing design, $N_{1.5}$ = _____

$$RL = 100\left[1 - \left(\frac{N_p}{N_{1.5}}\right)\right] = \_\_\_\_\_$$

Condition factor, CF (Figure 5.2) = _____

Thickness of AC surface, D_1 = _____ inches

Structural coefficient of AC surface, a_1, if newly constructed = _____

Thickness of base, D_2 = _____ inches

Structural coefficient of base, a_2, if newly constructed = _____

Thickness of subbase, D_3, if present = _____ inches

Structural coefficient of subbase, a_3, if newly constructed = _____

$$SN_o = a_1D_1 + a_2D_2m_2 + a_3D_3m_3 = \_\_\_\_\_$$

$$SN_{eff} = CF * SN_o = \_\_\_\_\_$$

(3) Breaking and seating, crack and seating or rubblizing the PCC slab and rolling to seat or compact
(4) Constructing widening if needed
(5) Applying a tack or prime coat
(6) Placing the AC overlay (including a reflection crack control treatment if needed)

5.5.1 Feasibility

Break/seat, crack/seat and rubblizing techniques are used to reduce the size of PCC pieces to minimize the differential movements at existing cracks and joints, thereby minimizing the occurrence and severity of reflection cracks. The feasibility of each technique is described below.

Rubblizing can be used on all types of PCC pavements in any condition. It is particularly recommended for reinforced pavements. Fracturing the slab into pieces less than 12 inches reduces the slab to a high-strength granular base. Recent field testing of several rubblized projects showed a wide range in backcalculated modulus values among different projects, from less than 100,000 psi to several hundred thousand psi (*16, 17, 18*), and within-project coefficients of variation of as much as 40 percent (*16, 18*).

Crack and seat is used only with JPCP and involves cracking the slab into pieces typically one to three feet in size. Recent field testing of several cracked and seated JPCP projects showed a wide range in backcalculated modulus values among different projects, from a few hundred thousand psi to a few million psi (*16, 19, 20, 21, 22*), and within-project coefficients of variation of 40 percent or more (*16*). Reference 16 recommends that to avoid reflection cracking no more than 5 percent of the fractured slab have a modulus greater than 1 million psi. Effective slab cracking techniques are necessary in order to satisfy this criterion for crack/seat of JPCP.

Break/seat is used only with JRCP and includes the requirement to rupture the reinforcement steel across each crack, or break its bond with the concrete. If the reinforcement is not ruptured and its bond with the concrete is not broken, the differential movements at working joints and cracks will not be reduced and reflection cracks will occur. Recent field testing of

several break/seat projects showed a wide range in backcalculated modulus values ranging from a few hundred thousand psi to several million psi (*16, 18, 19, 22*), and within-project coefficients of variation of 40 percent or more (*16, 18*). The wide range in backcalculated moduli reported for break and seat projects suggests a lack of consistency in the technique as performed with past construction equipment. Even though cracks are observed, the JRCP frequently retains a substantial degree of slab action because of failure to either rupture the reinforcing steel or break its bond with the concrete. This may also be responsible for the inconsistency of this technique in reducing reflection cracking. More effective breaking equipment may overcome this problem. This design procedure assumes that the steel will be ruptured or that its bond to the concrete will be broken through an aggressive break/seat process, and that this will be verified in the field through deflection testing before the overlay is placed. The use of rubblization is recommended for JRCP due to its ability to break slab continuity.

These slab fracturing techniques are generally more cost-effective on more deteriorated concrete pavements than on less deteriorated concrete pavements. This is due to the trade-off between the reduction in the amount of pre-overlay repair required for working cracks and deteriorated joints, and the cost of slab fracturing and increased overlay thickness required (*1, 22*).

5.5.2 Pre-overlay Repair

The amount of preoverlay repair needed for break/seat, crack/seat and rubblized projects is not clear. Most projects done prior to 1991 have not included a significant amount of repair. However, the recommended approach is to repair any condition that may provide nonuniform support after the fracturing process so that it will not rapidly reflect through the AC overlay. Also, some AC leveling may be needed for settled areas before the overlay is placed.

5.5.3 Reflection Crack Control

Slab fracturing techniques were developed as methods of reflection crack control. When properly constructed, the crack/seat and rubblizing methods are reasonably effective and should require no additional crack control treatment. However, care must be exercised to assure uniform cracking or rubblizing across the slab width and to firmly seat the cracked slab or compact the rubble. At least one agency that has used crack/seat of JPCP successfully for several years specifies that a fabric be placed in the overlay to aid in controlling reflection cracking. For break/seat of JRCP, reflective cracks will develop if the steel reinforcement is not ruptured and its bond to the concrete is not broken, and if this cannot be guaranteed, it is recommended that JRCP be rubblized.

5.5.4 Subdrainage

See Section 5.2.4 for guidelines. Rubblizing PCC pavement produces fines which may clog the filter materials placed in edge drains. This should be considered in the design of the filter materials. If longitudinal subdrains are to be installed, this should be done prior to fracturing the slab.

5.5.5 Thickness Design

The required thickness of the overlay is a function of the structural capacity required to meet future traffic demands and the structural capacity of the existing slab after fracturing. The required thickness is determined by the following equation:

$$SN_{ol} = a_{ol} * D_{ol} = SN_f - SN_{eff}$$

where

SN_{ol} = Required overlay structural number
a_{ol} = Structural coefficient for the AC overlay
D_{ol} = Required overlay thickness, inches
SN_f = Structural number required to carry future traffic
SN_{eff} = Effective structural number of the existing pavement after fracturing

The required overlay thickness is determined through the following design steps.

Step 1: Existing pavement design and construction.

(1) Thickness and material type of each pavement layer
(2) Available subgrade soil information (from construction records, soil surveys, county agricultural soils reports, etc.)

Step 2: Traffic analysis.

(1) Predicted future 18-kip ESALs in the design lane over the design period (N_f)

Use flexible pavement equivalency factors. If available future traffic estimates are in terms of rigid pavement ESALs, they must be converted to flexible pavement ESALs by dividing by 1.5 (e.g., 15 million rigid pavement ESALs approximately equal 10 million flexible pavement ESALs).

Step 3: Condition survey.

Condition survey data are not used in the determination of overlay thickness. However, condition survey data should be used to determine whether or not fracturing is cost-effective compared to other types of rehabilitation.

Step 4: Deflection testing (recommended).

Deflection measurements are used only for the determination of the design subgrade resilient modulus. Deflections should be measured on the bare PCC slab surface (prior to fracturing) at midslab locations that are not cracked. A heavy-load deflection device (e.g., Falling Weight Deflectometer) and a load magnitude of approximately 9,000 pounds are recommended. ASTM D 4694 and D 4695 provide additional guidance on deflection testing. A deflection measurement at a distance of approximately 4 feet from the center of load is needed.

(1) Subgrade resilient modulus (M_R). At sufficiently large distances from the load, deflections measured at the pavement surface are due to subgrade deformation only, and are also independent of the size of the load plate. This permits the backcalculation of the subgrade resilient modulus from a single deflection measurement and load magnitude, using the following equation.

$$M_R = \frac{0.24P}{d_r r}$$

where

M_R = backcalculated subgrade resilient modulus, psi
P = applied load, pounds
d_r = deflection at a distance r from the center of the load, inches
r = distance from center of load, inches

The deflection used to backcalculate the subgrade modulus must be measured far enough away that it provides a good estimate of the subgrade modulus, independent of the effects of any layers above, but also close enough that it is not too small to measure accurately. The minimum distance may be determined from the following relationship:

$$r \geq 0.7a_e$$

where

$$a_e = \sqrt{\left[a^2 + \left(D\sqrt[3]{\frac{E_p}{M_R}}\right)^2\right]}$$

a_e = radius of the stress bulb at the subgrade-pavement interface, inches
a = NDT load plate radius, inches
D = total thickness of pavement layers above the subgrade, inches
E_p = effective modulus of all pavement layers above the subgrade, psi (described below)

Before the backcalculated M_R value is used in design, it must be adjusted to make it consistent with the value used in the AASHTO flexible pavement design equation. An adjustment may also be needed to account for seasonal effects. These adjustments are described in Step 6.

(2) Effective modulus of the pavement (E_p). If the subgrade resilient modulus and total thickness of all layers above the subgrade are known or assumed, the effective modulus of the entire pavement structure (all pavement layers above the subgrade) may be determined from the deflection measured at the center of the load plate using the following equation:

$$d_0 = 1.5pa\left\{\frac{1}{M_R\sqrt{1 + \left(\frac{D}{a}\sqrt[3]{\frac{E_p}{M_R}}\right)^2}} + \frac{\left[1 - \frac{1}{\sqrt{1 + \left(\frac{D}{a}\right)^2}}\right]}{E_p}\right\}$$

where

d_0 = deflection measured at the center of the load plate, inches
p = NDT load plate pressure, psi
a = NDT load plate radius, inches
D = total thickness of pavement layers above the subgrade, inches
M_R = subgrade resilient modulus, psi
E_p = effective modulus of all pavement layers above the subgrade, psi

For a load plate radius of 5.9 inches, Figure 5.5 may be used to determine the ratio E_p/M_R, and E_p may then be determined for a known or assumed value of M_R.

Deflection measurements are also useful after the break/seat or crack/seat operations to insure that the slab has been sufficiently fractured (*16*).

Step 5: Coring and material testing.

(1) *Resilient modulus of subgrade.* If deflection testing is not performed, laboratory testing of samples of the subgrade may be conducted to determine its resilient modulus using AASHTO T 292-91 I with a deviator stress of 6 psi to match the deviator stress used in establishing the 3,000 psi for the AASHO Road Test soil that is incorporated into the flexible design equation. Alternatively, other tests such as R value, CBR or soil classification tests could be conducted and approximate correlations used to estimate resilient modulus. Use of the estimating equation $M_R = 1500 * CBR$ may produce a value that is too large for use in this design procedure. The relationships found in Appendix FF, Figure FF-6 may be more reasonable.

(2) *Samples of base layers* should be examined to assess degradation and contamination by fines.

Step 6: Determination of required structural number for future traffic (SN_f).

(1) Effective design subgrade resilient modulus. Determine by one of the following methods:

(a) Laboratory testing as described in Step 5.
(b) Backcalculation from deflection data. (NOTE: this value must be adjusted to be consistent with the value used in the AASHTO flexible pavement design equation as described below.)
(c) A very approximate estimate can be made using available soil information and relationships developed from resilient modulus studies. However, if as-built records are used, it should be noted that the resilient modulus may have changed since construction due to changes in moisture content or other factors.

Regardless of the method used, the effective design subgrade resilient modulus must be (1) representative of the effects of seasonal variation and (2) consistent with the resilient modulus value used to represent the AASHO Road Test soil. A seasonal adjustment, when needed, may be made in accordance with the procedures described in Part II, Section 2.3.1. M_R values backcalculated from deflections must be adjusted to make the values consistent with the laboratory-measured value used for the AASHO Road Test soil in the development of the flexible pavement design equation. For conventional AC pavements, it was recommended that backcalculated M_R values be multiplied by a correction factor C = 0.33 for use in determination of SN_f for design purposes when a FWD load of approximately 9,000 pounds is used (*9*). However, because subgrade stresses are much lower under a PCC slab than under a flexible pavement, it is recommended that a smaller correction factor, C = 0.25, be used to provide a better estimate of the subgrade M_R. This value should be evaluated and adjusted if needed by user agencies for their soil and deflection measurement equipment. The following design M_R is recommended for use in determining the SN_f for fractured slabs when deflection testing is done on top of the PCC slab:

$$\text{Design } M_R = C\left(\frac{0.24P}{d_r r}\right)$$

where recommended C = 0.25.

NOTE also that the presence of a very stiff layer (e.g., bedrock) within about 15 feet of the top of the subgrade may cause the back-calculated M_R to be high. When such a condition exists, a value less than 0.25 for C may be warranted (*8, 9*).

The designer is cautioned against using a value of M_R that is too large. The value of M_R selected for design is extremely critical to the overlay thickness. The use of a value greater than 3,000 psi is an indication that the soil is stiffer than the silty-clay A-6 soil at the Road Test site, and consequently will provide increased support and extended pavement life.

(2) *Design PSI loss.* PSI immediately after overlay (P1) minus PSI at time of next rehabilitation (P2).

(3) *Overlay design reliability R (percent).* See Part I, Section 4.2, Part II, Table 2.2, and Part III, Section 5.2.15.

(4) *Overall standard deviation S_o for flexible pavement.* See Part I, Section 4.3.

Compute SN_f for the above design inputs using the flexible pavement design equation or nomograph in Part II, Figure 3.1. When designing an overlay thickness for a uniform pavement section, mean input values must be used. When designing an overlay thickness for specific points along the project, the data for that point must be used. A worksheet for determining SN_f is provided in Table 5.4.

Step 7: Determination of effective structural number (SN_{eff}) of the existing fractured slab pavement.

SN_{eff} is determined by component analysis using the structural number equation:

$$SN_{eff} = a_2D_2m_2 + a_3D_3m_3$$

where

D_2, D_3 = thicknesses of fractured slab and base layers
a_2, a_3 = corresponding structural layer coefficients
m_2, m_3 = drainage coefficients for fractured PCC and granular subbase

See Part II, Table 2.4, for guidance in determining the drainage coefficients. Due to lack of information on drainage characteristics of fractured PCC, a default value of 1.0 for m_2 is recommended. In selecting values for m_3, note that the poor drainage situation for the base and subbase at the AASHO Road Test would be given drainage coefficient values of 1.0.

Suggested layer coefficients for fractured slab pavements are provided in Table 5.5. Each agency should adopt its own set of layer coefficient values for fractured slabs keyed to its construction results on its pavements.

Since the layer coefficient represents the overall performance contribution of that layer, it is likely that it is not related solely to the modulus of that layer, but to other properties as well, such as the load transfer capability of the pieces. The large variability of layer moduli within a project is also of concern. This extra variability should ideally be expressed in an increased overall standard deviation in designing for a given reliability level.

A worksheet for determination of SN_{eff} is provided in Table 5.6.

Step 8: Determination of overlay thickness.

The thickness of AC overlay is computed as follows:

$$D_{ol} = \frac{SN_{ol}}{a_{ol}} = \frac{(SN_f - SN_{eff})}{a_{ol}}$$

where

SN_{ol} = Required overlay structural number
a_{ol} = Structural coefficient for the AC overlay
D_{ol} = Required AC overlay thickness, inches
SN_f = Structural number determined in Step 6
SN_{eff} = Effective structural number of the existing pavement, from Step 7

The thickness of overlay determined from the above relationship should be reasonable when the overlay is required to correct a structural deficiency. See Section 5.2.17 for discussion of factors which may result in unreasonable overlay thicknesses.

5.5.6 Shoulders

See Section 5.2.10 for guidelines.

5.5.7 Widening

See Section 5.2.16 for guidelines.

Table 5.4. Worksheet for Determination of SN_f for Fractured Slab Pavements

TRAFFIC:

Future 18-kip ESALs in design lane over design period, N_f = _____

EFFECTIVE ROADBED SOIL RESILIENT MODULUS:

Design resilient modulus, M_R = _____ psi

(Adjusted for consistency with flexible pavement model and for seasonal variations. Typical design M_R is 2,000 to 10,000 psi for fine-grained soils, 10,000 to 20,000 for coarse-grained soils. The AASHO Road Test soil value used in the flexible pavement design equation was 3,000 psi.)

SERVICEABILITY LOSS:

Design PSI loss (P1 − P2) (1.2 to 2.5) = _____

DESIGN RELIABILITY:

Overlay design reliability, R (80 to 99 percent) = _____ percent

Overall standard deviation, S_o (typically 0.49) = _____

FUTURE STRUCTURAL CAPACITY:

Required structural number for future traffic is determined from flexible pavement design equation or nomograph in Part II, Figure 3.1.

SN_f = _____

Table 5.5. Suggested Layer Coefficients for Fractured Slab Pavements

MATERIAL	SLAB CONDITION	COEFFICIENT
Break/Seat JRCP	Pieces greater than one foot with ruptured reinforcement or steel/concrete bond broken	0.20 to 0.35
Crack/Seat JPCP	Pieces one to three feet	0.20 to 0.35
Rubblized PCC (any pavement type)	Completely fractured slab with pieces less than one foot	0.14 to 0.30
Base/subbase granular and stabilized	No evidence of degradation or intrusion of fines	0.10 to 0.14
	Some evidence of degradation or intrusion of fines	0.00 to 0.10

Table 5.6. Worksheet for Determination of SN_{eff} for Break/Seat, Crack/Seat and Rubblized Pavements

Thickness of break/crack or rubblized PCC, D_2	= _____	inches
Structural coefficient of break/crack/seat or rubblized PCC, a_2	= _____	
Drainage coefficient of fractured slab, m_2 (1.0 recommended)	= _____	
Thickness of subbase, D_3, if present	= _____	inches
Structural coefficient of subbase, a_3	= _____	
Drainage coefficient of subbase, m_3	= _____	
$SN_{eff} = a_2D_2m_2 + a_3D_3m_3$	= _____	

5.6 AC OVERLAY OF JPCP, JRCP, AND CRCP

This section covers the design of AC overlays of existing JPCP, JRCP, or CRCP. This section may also be used to design an AC overlay if a previous AC overlay is completely removed.

Construction of an AC overlay over JPCP, JRCP, or CRCP consists of the following major activities:

(1) Repairing deteriorated areas and making subdrainage improvements (if needed).
(2) Constructing widening (if needed).
(3) Applying a tack coat.
(4) Placing the AC overlay, including a reflection crack control treatment (if needed).

5.6.1 Feasibility

An AC overlay is a feasible rehabilitation alternative for PCC pavements except when the condition of the existing pavement dictates substantial removal and replacement. Conditions under which an AC overlay would not be feasible include:

(1) The amount of deteriorated slab cracking and joint spalling is so great that complete removal and replacement of the existing surface is dictated.
(2) Significant deterioration of the PCC slab has occurred due to severe durability problems (e.g., "D" cracking or reactive aggregates).
(3) Vertical clearance at bridges is inadequate for required overlay thickness. This may be addressed by reducing the overlay thickness under the bridges (although this may result in early failure at these locations), by raising the bridges, or by reconstructing the pavement under the bridges. Thicker AC overlays may also necessitate raising signs and guardrails, as well as increasing side slopes and extending culverts. Sufficient right-of-way must be available or obtainable to permit these activities.

5.6.2 Preoverlay Repair

The following types of distress in JPCP, JRCP, and CRCP should be repaired prior to placement of an AC overlay.

Distress Type	Repair Type
Working cracks	Full-depth repair or slab replacement
Punchouts	Full-depth PCC repair
Spalled joints	Full-depth or partial-depth repair
Deteriorated repairs	Full-depth repair
Pumping/faulting	Edge drains
Settlements/heaves	AC level-up, slab jacking, or localized reconstruction

Full-depth repairs and slab replacements in JPCP and JRCP should be PCC, dowelled or tied to provide load transfer across repair joints. Some agencies have placed full-depth AC repairs in JPCP and JRCP prior

to an AC overlay. However, this has often resulted in rough spots in the overlay, opening of nearby joints and cracks, and rapid deterioration of reflection cracks at AC patch boundaries. (See Part III, Section 4.3.1 and References 1 and 3.)

Full-depth repairs in CRCP should be PCC and should be continuously reinforced with steel which is tied or welded to reinforcing steel in the existing slab to provide load transfer across joints and slab continuity. Full-depth AC repairs should not be used in CRCP prior to placement of an AC overlay, and any existing AC patches in CRCP should be removed and replaced with continuously reinforced PCC. Guidelines on repairs are provided in References 1 and 3.

Installation of edge drains, maintenance of existing edge drains, or other subdrainage improvement should be done prior to placement of the overlay if a subdrainage evaluation indicates a need for such an improvement.

Pressure relief joints should be placed only at fixed structures, and not at regular intervals along the pavement. The only exception to this is where reactive aggregate has caused expansion of the slab. On heavily trafficked routes, pressure relief joints should be of heavy-duty design with dowels (*3*). If joints contain significant incompressibles, they should be cleaned and resealed prior to placement of the overlay.

5.6.3 Reflection Crack Control

The basic mechanism of reflection cracking is strain concentration in the overlay due to movement in the vicinity of joints and cracks in the existing pavement. This movement may be bending or shear induced by loads, or may be horizontal contraction induced by temperature changes. Load-induced movements are influenced by the thickness of the overlay and the thickness and stiffness of the existing pavement. Temperature-induced movements are influenced by daily and seasonal temperature variations, the coefficient of thermal expansion of the existing pavement, and the spacing of joints and cracks.

In an AC overlay of JPCP or JRCP, reflection cracks typically develop relatively soon after the overlay is placed (often in less than a year). The rate at which they deteriorate depends on the factors listed above as well as the traffic level. Thorough repair of deteriorated joints and working cracks with full-depth dowelled or tied PCC repairs reduces the rate of reflection crack occurrence and deterioration, so long as good load transfer is obtained at the full-depth repair joints. Other preoverlay repair efforts which will discourage reflection crack occurrence and subsequent deterioration include subdrainage improvement, subsealing slabs which have lost support, and restoring load transfer at joints and cracks with dowels grouted in slots.

A variety of reflection crack control measures have been used in attempts to control the rates of reflection crack occurrence and deterioration. Any one of the following treatments may be employed in an effort to control reflection cracking in an AC overlay of JPCP or JRCP:

(1) *Sawing and sealing joints in the AC overlay* at locations coinciding with joints in the underlying JPCP or JRCP. This technique has been very successful when applied to AC overlays of jointed PCC pavements when the sawcut matches the joint or straight crack within an inch.

(2) *Increasing AC overlay thickness.* Reflection cracks will take more time to propagate through a thicker overlay and deteriorate more slowly.

(3) *Placing a bituminous-stabilized granular interlayer (large-sized large stone), prior to or in combination with placement of the AC overlay* has been effective.

(4) *Placing a synthetic fabric or a stress-absorbing interlayer prior to or within the AC overlay.* The effectiveness of this technique is questionable.

(5) *Rubblizing and compacting JPCP, JRCP, or CRCP* prior to placement of the AC overlay. This technique reduces the size of PCC pieces to a maximum of about 12 inches and essentially reduces the slab to a high-strength granular base course. See Section 5.5 for the design procedure for AC overlays of rubblized PCC pavement.

(6) *Cracking and seating JPCP or breaking and seating JRCP* prior to placement of the AC overlay. This technique reduces the size of PCC pieces and seats them in the underlying base, which reduces horizontal (and possibly vertical) movements at cracks. See Section 5.5 for the design procedure for AC overlays of crack/seat JPCP and break/seat JRCP.

Reflection cracking can have a considerable (often controlling) influence on the life of an AC overlay of JPCP or JRCP. Deteriorated reflection cracks detract from a pavement's serviceability and also require frequent maintenance, such as sealing, milling, and

patching. Reflection cracks also permit water to enter the pavement structure, which may result in loss of bond between the AC and PCC, stripping in the AC, progression of "D" cracking or reactive aggregate distress in PCC slabs with these durability problems, and softening of the base and subgrade. For this reason, reflection cracks should be sealed as soon as they appear and resealed periodically throughout the life of the overlay. Sealing low-severity reflection cracks may also be effective in retarding their progression to medium and high severity levels.

With an AC overlay of CRCP, permanent repair of punchouts and working cracks with tied or welded reinforced PCC full-depth repairs will delay the occurrence and deterioration of reflection cracks. Improving subdrainage conditions and subsealing in areas where the slab has lost support will also discourage reflection crack occurrence and deterioration. Reflection crack control treatments are not necessary for AC overlays of CRCP, except for longitudinal joints, as long as continuously reinforced PCC repairs are used to repair deteriorated areas and cracks.

5.6.4 Subdrainage

See Section 5.2.4 for guidelines.

5.6.5 Thickness Design

If the overlay is being placed for some functional purpose such as roughness or friction, a minimum thickness overlay that solves the functional problem should be placed. If the overlay is being placed for the purpose of structural improvement, the required thickness of the overlay is a function of the structural capacity required to meet future traffic demands and the structural capacity of the existing pavement. The required overlay thickness to increase structural capacity to carry future traffic is determined by the following equation.

$$D_{ol} = A(D_f - D_{eff})$$

where

D_{ol} = Required thickness of AC overlay, inches
A = Factor to convert PCC thickness deficiency to AC overlay thickness
D_f = Slab thickness to carry future traffic, inches
D_{eff} = Effective thickness of existing slab, inches

The A factor, which is a function of the PCC thickness deficiency, is given by the following equation, and is illustrated in Figure 5.9.

$$A = 2.2233 + 0.0099(D_f - D_{eff})^2 - 0.1534(D_f - D_{eff})$$

AC overlays of conventional JPCP, JRCP, and CRCP have been constructed as thin as 2 inches and as thick as 10 inches. The most typical thicknesses that have been constructed for highways are 3 to 6 inches.

The required overlay thickness may be determined through the following design steps. These design steps provide a comprehensive design approach that recommends testing the pavement to obtain valid design inputs. If it is not possible to conduct this testing (e.g., for a low-volume road), an approximate overlay design may be developed based upon visible distress observations by skipping Steps 4 and 5, and by estimating other inputs.

The overlay design can be done for a uniform section or on a point-by-point basis as described in Section 5.3.1.

Step 1: Existing pavement design.

(1) Existing slab thickness
(2) Type of load transfer (mechanical devices, aggregate interlock, CRCP)
(3) Type of shoulder (tied PCC, other)

Step 2: Traffic analysis.

(1) Past cumulative 18-kip ESALs in the design lane (N_p), for use in the remaining life method of D_{eff} determination only
(2) Predicted future 18-kip ESALs in the design lane over the design period (N_f)
Use ESALs computed from rigid pavement load equivalency factors

Step 3: Condition survey.

The following distresses are measured during the condition survey for JPCP, JRCP, and CRCP. Sampling along the most heavily trafficked lane of the project may be used to estimate these quantities. Distress types and severities are defined in Reference 23. Deteriorated means medium or higher severity.

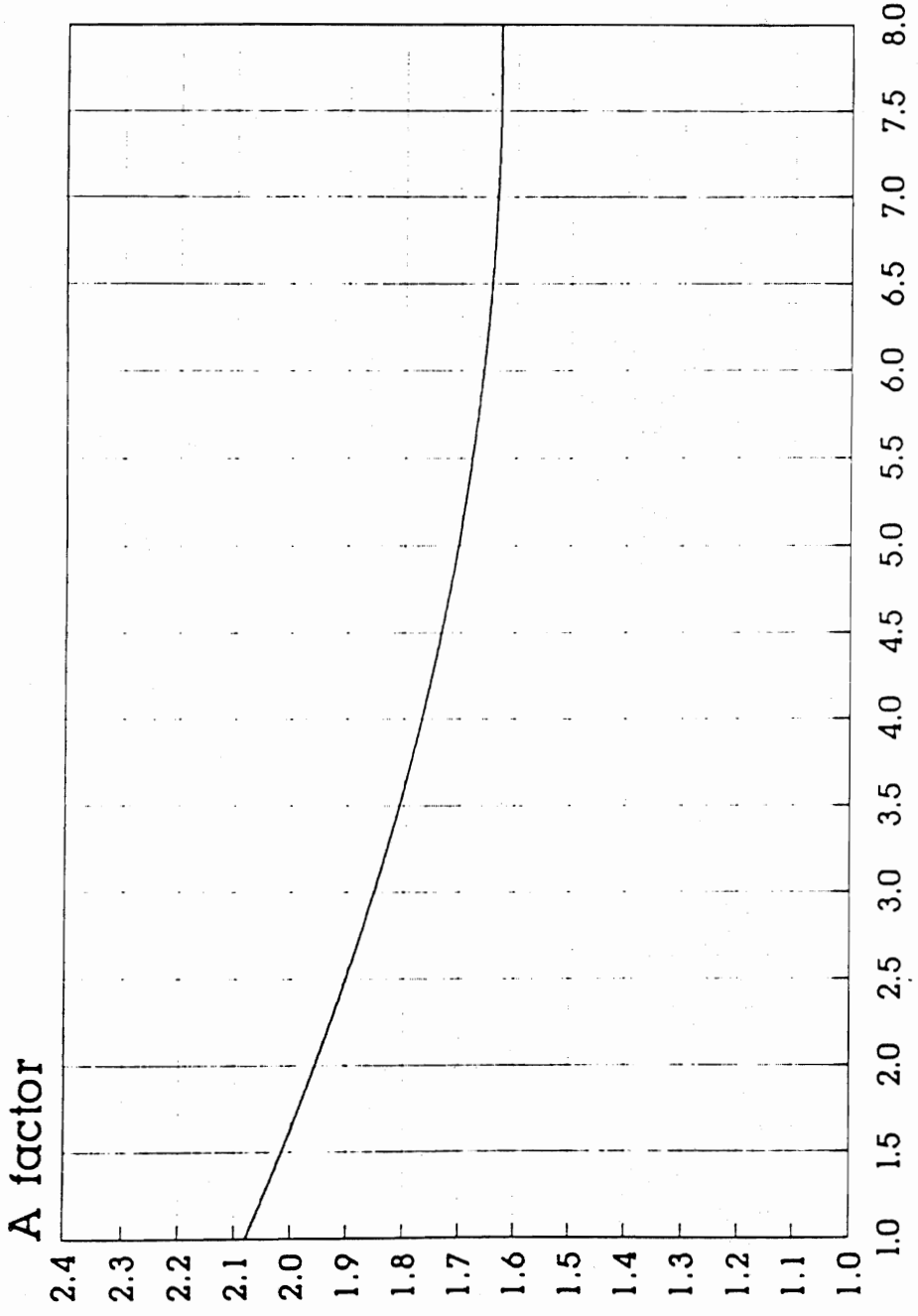

Figure 5.9. A Factor for Conversion of PCC Thickness Deficiency to AC Overlay Thickness

JPCP/JRCP:

(1) Number of deteriorated transverse joints per mile
(2) Number of deteriorated transverse cracks per mile
(3) Number of full-depth AC patches, exceptionally wide joints (greater than 1 inch), and expansion joints per mile (except at bridges)
(4) Presence and overall severity of PCC durability problems
  (a) "D" cracking: low severity (cracks only), medium severity (some spalling), high severity (severe spalling)
  (b) Reactive aggregate cracking: low, medium, high severity
(5) Evidence of faulting, or pumping of fines or water at joints, cracks, and pavement edge

CRCP:

(1) Number of punchouts per mile
(2) Number of deteriorated transverse cracks per mile
(3) Number of full-depth AC patches, exceptionally wide joints (greater than 1 inch) and expansion joints per mile (except at bridges)
(4) Number of existing and new repairs prior to overlay per mile
(5) Presence and general severity of PCC durability problems (NOTE: surface spalling of tight cracks where the underlying CRCP is sound should not be considered a durability problem.)
  (a) "D" cracking: low severity (cracks only), medium severity (some spalling), high severity (severe spalling)
  (b) Reactive aggregate cracking: low, medium, high severity
(6) Evidence of pumping of fines or water

Step 4: Deflection testing (strongly recommended).

Measure slab deflection basins along the project at an interval sufficient to adequately assess conditions. Intervals of 100 to 1,000 feet are typical. Measure deflections with sensors located at 0, 12, 24, and 36 inches from the center of load. Measure deflections in the outer wheel path. A heavy-load deflection device (e.g., Falling Weight Deflectometer) and a load magnitude of 9,000 pounds are recommended. ASTM D 4694 and D 4695 provide additional guidance on deflection testing. For each slab tested, backcalculate the effective k-value and the slab's elastic modulus using Figures 5.10 and 5.11 or a backcalculation program.

The AREA of each deflection basin is computed by the following equation. AREA will typically range from 29 to 32 for sound concrete.

$$\text{AREA} = 6 * \left[1 + 2\left(\frac{d_{12}}{d_0}\right) + 2\left(\frac{d_{24}}{d_0}\right) + \left(\frac{d_{36}}{d_0}\right)\right]$$

where

d_0 = deflection in center of loading plate, inches
d_i = deflections at 12, 24, and 36 inches from plate center, inches

(1) *Effective dynamic k-value.* Enter Figure 5.10 with d_0 and AREA to determine the effective dynamic k-value beneath each slab for a circular load radius of 5.9 inches and magnitude of 9,000 pounds. For loads within 2,000 pounds more or less, deflections may be scaled linearly to 9,000-pound deflections.

If a single overlay thickness is being designed for a uniform section, compute the mean effective dynamic k-value of the slabs tested in the uniform section.

(2) *Effective static k-value.*

Effective static k-value = Effective dynamic k-value/2

The effective static k-value may need to be adjusted for seasonal effects using the approach presented in Part II, Section 3.2.1. However, the k-value can change substantially and have only a small effect on overlay thickness.

(3) *Elastic modulus of PCC slab (E).* Enter Figure 5.11 with AREA, proceed to the effective dynamic k-value curves, and determine a value for ED^3, where D is the slab thickness. Solve for E knowing the slab thickness, D. Typical slab E values range from 3 to 8 million psi. If a slab E value is obtained that is out of this range, an error may exist in the assumed slab thickness, the deflection basin may have been measured over a crack, or the PCC may be significantly deteriorated.

If a single overlay thickness is being designed for a uniform section, compute the mean E value of the slabs tested in the uniform section.

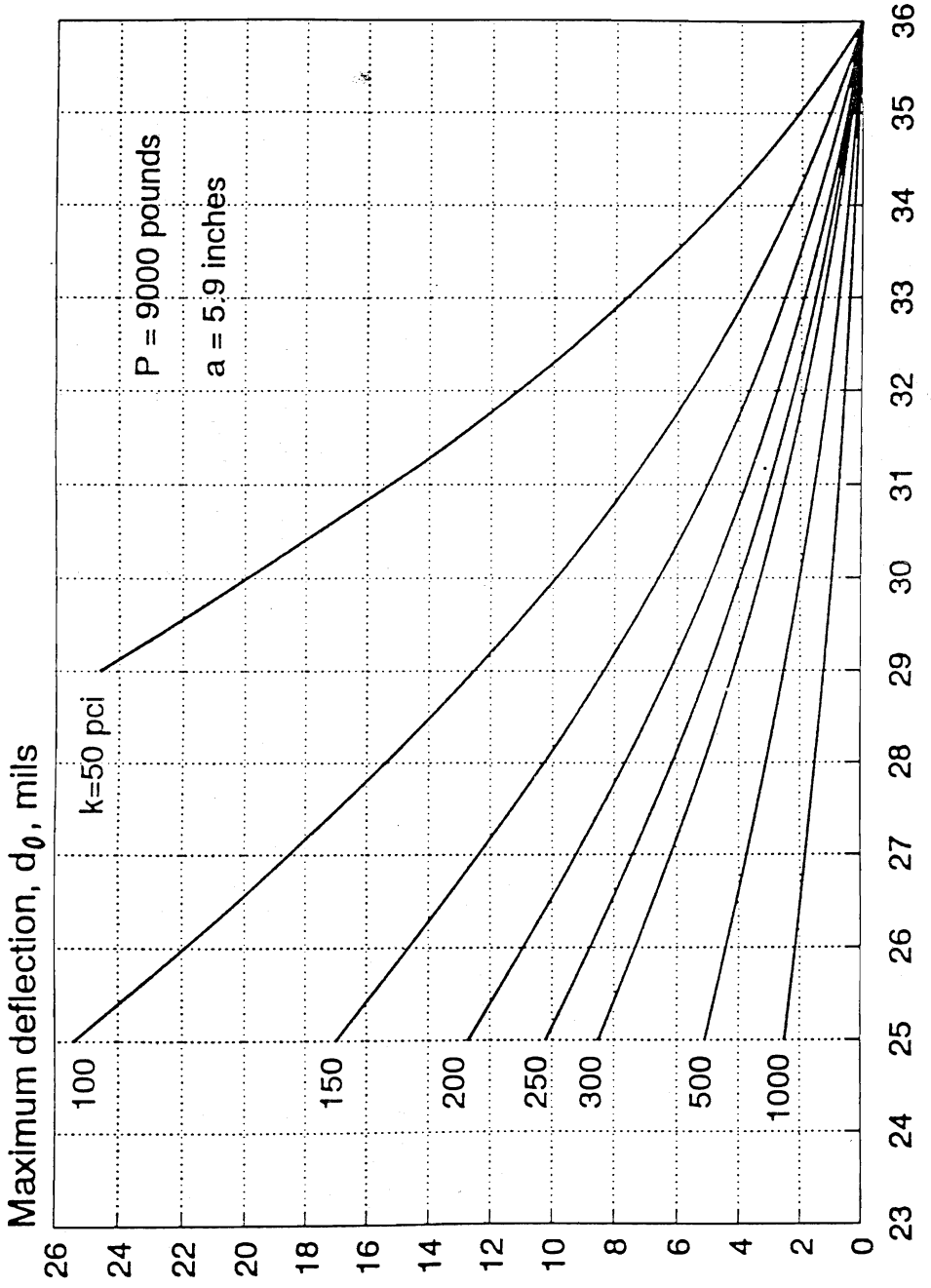

Figure 5.10. Effective Dynamic k-Value Determination from d_0 and AREA

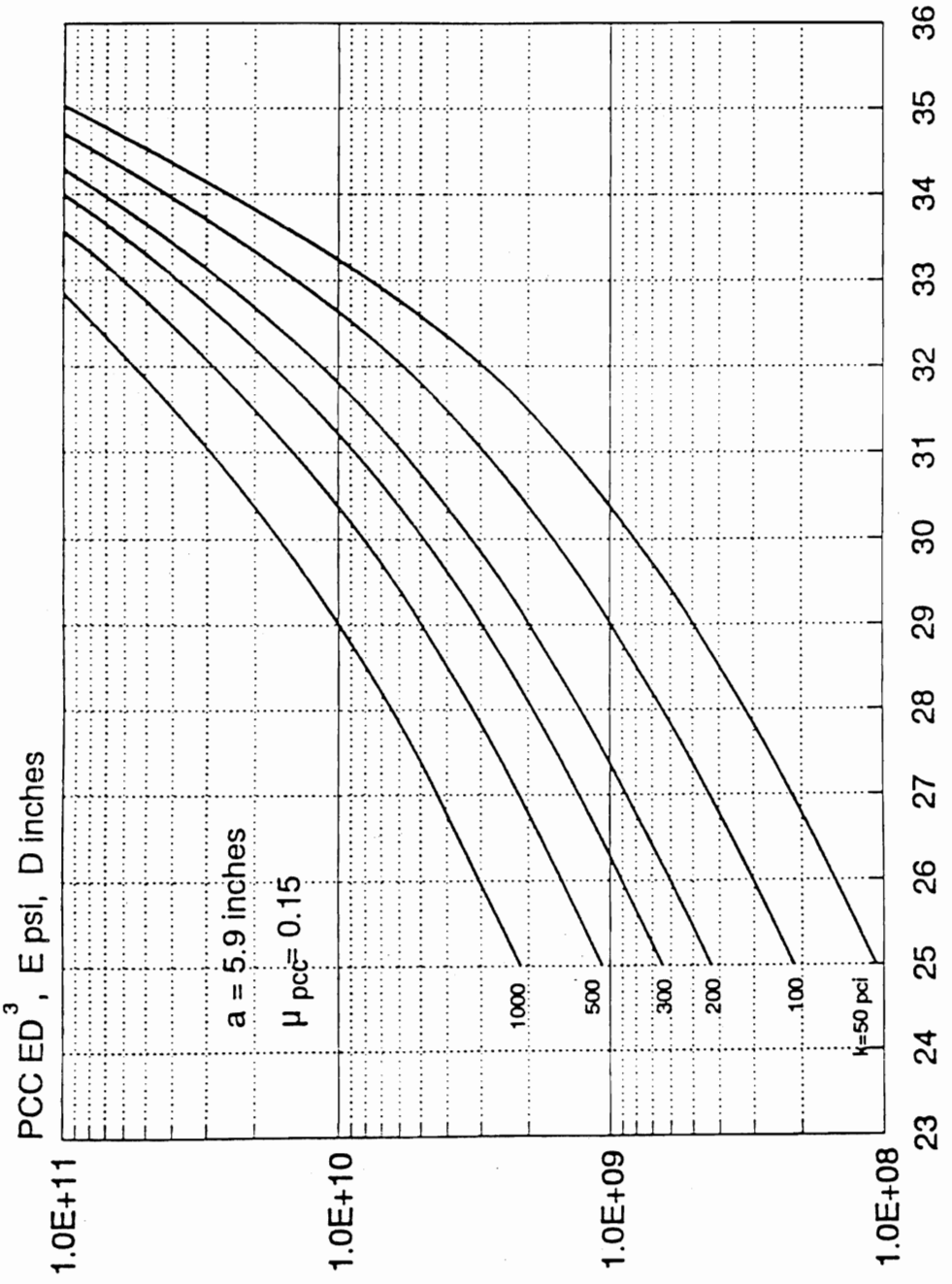

Figure 5.11. PCC Elastic Modulus Determination from k-Value, AREA, and Slab Thickness

Do not use any k-values or E values that appear to be significantly out of line with the rest of the data.

(4) *Joint load transfer.* For JPCP and JRCP, measure joint load transfer in the outer wheelpath at representative transverse joints. Do not measure load transfer when the ambient temperature is greater than 80°F. Place the load plate on one side of the joint with the edge of the plate touching the joint. Measure the deflection at the center of the load plate and at 12 inches from the center. Compute the deflection load transfer from the following equation.

$$\Delta LT = 100 * \left(\frac{\Delta_{ul}}{\Delta_l}\right) * B$$

where

ΔLT = deflection load transfer, percent
Δ_{ul} = unloaded side deflection, inches
Δ_l = loaded side deflection, inches
B = slab bending correction factor

The slab bending correction factor, B, is necessary because the deflections d_0 and d_{12}, measured 12 inches apart, would not be equal even if measured in the interior of a slab. An appropriate value for the correction factor may be determined from the ratio of d_0 to d_{12} for typical center slab deflection basin measurements, as shown in the equation below. Typical values for B are between 1.05 and 1.15.

$$B = \frac{d_{0\ center}}{d_{12\ center}}$$

If a single overlay thickness is being designed for a uniform section, compute the mean deflection load transfer value of the joints tested in the uniform section.

For JPCP and JRCP, determine the J load transfer coefficient using the following guidelines:

Percent Load Transfer	J
>70	3.2
50–70	3.5
<50	4.0

If the rehabilitation will include the addition of a tied concrete shoulder, a lower J factor may be appropriate. See Part II, Table 2.6.

For CRCP, use J = 2.2 to 2.6 for overlay design, assuming that working cracks are repaired with continuously reinforced PCC.

Step 5: Coring and materials testing (strongly recommended).

(1) *PCC modulus of rupture (S'_c).* Cut several 6-inch-diameter cores at midslab and test in indirect tension (ASTM C 496). Compute the indirect tensile strength (psi) of the cores. Estimate the modulus of rupture with the following equation.

$$S'_c = 210 + 1.02IT$$

where

S'_c = modulus of rupture, psi
IT = indirect tensile strength of 6-inch-diameter cores, psi

Step 6: Determination of required slab thickness for future traffic (D_f).

The inputs to determine D_f for AC overlays of PCC pavements are representative of the existing slab and foundation properties. This is emphasized because it is the properties of the existing slab (i.e., elastic modulus, modulus of rupture, and load transfer) which will control the performance of the AC overlay.

(1) *Effective static k-value beneath existing PCC slab.* Determine from one of the following methods.
   (a) Backcalculate the effective dynamic k-value from deflection basins. Divide the effective dynamic k-value by 2 to obtain the effective static k-value. The effective static k-value may need to be adjusted for seasonal effects using the approach presented in Part II, Section 3.2.1.
   (b) Conduct plate load tests (ASTM D 1196) after slab removal at a few sites. This alternative is very costly and time-consuming and not often used. The static k-value obtained may need to be adjusted for seasonal effects (see Part II, Section 3.2.1).
   (c) Estimate from soils data and base type and thickness, using Figure 3.3 in Part

II, Section 3.2. This alternative is simple, but the static k-value obtained must be recognized as a rough estimate. The static k-value may need to be adjusted for seasonal effects (see Part II, Section 3.2.1).

(2) *Design PSI loss.* PSI immediately after overlay (P1) minus PSI at time of next rehabilitation (P2).

(3) *J, load transfer factor of existing PCC slab.* See Step 4.

(4) *PCC modulus of rupture of existing slab* determined by one of the following methods:
   (a) Estimated from indirect tensile strength measured from 6-inch-diameter cores as described in Step 5.
   (b) Estimated from the backcalculated E of slab using the following equation.

$$S_c' = 43.5 \left(\frac{E}{10^6}\right) + 488.5$$

where

S_c' = modulus of rupture, psi
E = backcalculated elastic modulus of PCC slab, psi

For CRCP, S_c' may be determined from the backcalculated E values only at points which have no cracks within the deflection basins.

(5) *Elastic modulus of existing PCC slab*, determined by one of the following methods:
   (a) Backcalculated from deflection measurements as described in Step 4.
   (b) Estimated from indirect tensile strength.

(6) *Loss of support of existing slab.* Joint corners that have loss of support may be identified using FWD deflection testing as described in Reference 2. CRCP loss of support may be determined by plotting a slab edge or wheelpath deflection profile and identifying locations with significantly high deflections. Existing loss of support can be corrected with slab stabilization. For overlay thickness design assume a fully supported slab, LS = 0.

(7) *Overlay design reliability, R (percent).* See Part I, Section 4.2, Part II, Table 2.2, and Part III, Section 5.2.15.

(8) *Overall standard deviation (S_o) for rigid pavement.* See Part I, Section 4.3.

(9) *Subdrainage capability of existing slab,* after subdrainage improvements, if any. See Part II, Table 2.5, as well as reference 5, for guidance in determining C_d. Pumping or faulting at joints and cracks determined in Step 3 is evidence that a subdrainage problem exists. In selecting this value, note that the poor subdrainage situation at the AASHO Road Test would be given a C_d of 1.0.

Compute D_f for the above design inputs using the rigid pavement design equation or nomograph in Part II, Figure 3.7. When designing an overlay thickness for a uniform pavement section, mean input values must be used. When designing an overlay thickness for specific points along the project, the data for that point must be used. A worksheet for determining D_f is provided in Table 5.7. Typical values of inputs are provided for guidance. Values outside these ranges should be used with caution.

Step 7: Determination of effective slab thickness (D_{eff}) of existing pavement.

Condition survey and remaining life procedures are presented.

D_{eff} From Condition Survey For PCC Pavements

The effective thickness of the existing slab (D_{eff}) is computed from the following equation:

$$D_{eff} = F_{jc} * F_{dur} * F_{fat} * D$$

where

D = existing PCC slab thickness, inches

(1) *Joints and cracks adjustment factor (F_{jc}).* This factor adjusts for the extra loss in PSI caused by deteriorated reflection cracks in the overlay that will result from any unrepaired deteriorated joints, cracks, and other discontinuities in the existing slab prior to overlay. A deteriorated joint or crack in the existing slab will rapidly reflect through an AC overlay and contribute to loss of serviceability. Therefore, it is recommended that all deteriorated joints and cracks (for non-"D" cracked or reactive aggregate related distressed pavements) and any other major discontinuities in the existing slab be full-depth repaired with dowelled or tied PCC repairs prior to overlay, so that F_{jc} = 1.00.

Table 5.7. Worksheet for Determination of D_f for JPCP, JRCP, and CRCP

SLAB:

Existing PCC slab thickness = _____ inches

Type of load transfer system: mechanical device, aggregate interlock, CRCP

Type of shoulder = tied PCC, other

PCC modulus of rupture (typically 600 to 800 psi) = _____ psi

PCC E modulus (3 to 8 million psi for sound PCC, <3 million for unsound PCC) = _____ psi

J load transfer factor (3.2 to 4.0 for JPCP, JRCP 2.2 to 2.6 for CRCP) = _____

TRAFFIC:

Future 18-kip ESALs in design lane over the design period (N_f) = _____

SUPPORT AND DRAINAGE:

Effective dynamic k-value = _____ psi/inch

Effective static k-value = Effective dynamic k-value/2 (typically 50 to 500 psi/inch) = _____ psi/inch

Subdrainage coefficient, C_d (typically 1.0 for poor subdrainage conditions) = _____

SERVICEABILITY LOSS:

Design PSI loss (P1 – P2) = _____

RELIABILITY:

Design reliability, R (80 to 99 percent) = _____ percent

Overall standard deviation, S_o (typically 0.39) = _____

FUTURE STRUCTURAL CAPACITY:

Required slab thickness for future traffic is determined from rigid pavement design equation or nomograph in Part II, Figure 3.7.

D_f = _____ inches

If it is not possible to repair all deteriorated areas, the following information is needed to determine F_{jc}, to increase the overlay thickness to account for the extra loss in PSI from deteriorated reflection cracks in the design lane:

Pavements with no "D" cracking or reactive aggregate distress:

Number of unrepaired deteriorated joints/mile

Number of unrepaired deteriorated cracks/mile

Number of unrepaired punchouts/mile

Number of expansion joints, exceptionally wide joints (greater than 1 inch), and

full-depth, full-lane-width AC patches/mile

Note that tight cracks held together by reinforcement in JRCP or CRCP are not included. However, if a crack in JRCP or CRCP is spalled and faulted the steel has probably ruptured, and the crack should be considered as working. Surface spalling of CRCP cracks is not an indication that the crack is working.

The total number of unrepaired deteriorated joints, cracks, punchouts, and other discontinuities per mile in the design lane is used to determine the F_{jc} from Figure 5.12.

Pavements with "D" cracking or reactive aggregate deterioration:

These types of pavements often have deterioration at the joints and cracks from durability problems. The F_{dur} factor is used to adjust the overlay thickness for this problem. Therefore, when this is the case, the F_{jc} should be determined from Figure 5.12 only using those unrepaired deteriorated joints and cracks that are not caused by durability problems. If all of the deteriorated joints and cracks are spalling due to "D" cracking or reactive aggregate, then F_{jc} = 1.0. This will avoid adjusting twice with F_{jc} and F_{dur} factors.

(2) *Durability adjustment factor (F_{dur}).* This factor adjusts for an extra loss in PSI of the overlay when the existing slab has durability problems such as "D" cracking or reactive aggregate distress. Using condition survey data from Step 3, F_{dur} is determined as follows.

1.00:	No sign of PCC durability problems
0.96–0.99:	Durability cracking exists, but no spalling
0.88–0.95:	Substantial cracking and some spalling exists
0.80–0.88:	Extensive cracking and severe spalling exists

(3) *Fatigue damage adjustment factor (F_{fat}).* This factor adjusts for past fatigue damage that may exist in the slab. It is determined by observing the extent of transverse cracking (JPCP, JRCP) or punchouts (CRCP) that may be caused primarily by repeated loading. Use condition survey data from Step 3 and the following guidelines to estimate F_{fat} in the design lane.

0.97–1.00:	Few transverse cracks/punchouts exist (none caused by "D" cracking or reactive aggregate distress)
JPCP:	<5 percent slabs are cracked
JRCP:	<25 working cracks per mile
CRCP:	<4 punchouts per mile
0.94–0.96:	A significant number of transverse cracks/punchouts exist (none caused by "D" cracking or reactive aggregate distress)
JPCP:	5–15 percent slabs are cracked
JRCP:	25–75 working cracks per mile
CRCP:	4–12 punchouts per mile
0.90–0.93:	A large number of transverse cracks/punchouts exist (none caused by "D" cracking or reactive aggregate distress)
JPCP:	>15 percent slabs are cracked
JRCP:	>75 working cracks per mile
CRCP:	>12 punchouts per mile

D_{eff} From Remaining Life For PCC Pavements

The remaining life of the pavement is given by the following equation:

$$RL = 100\left[1 - \left(\frac{N_p}{N_{1.5}}\right)\right]$$

where

RL = remaining life, percent
N_p = total traffic to date, ESALs
$N_{1.5}$ = total traffic to pavement "failure," ESALs

$N_{1.5}$ may be estimated using the new pavement design equations or nomographs in Part II. To be consistent with the AASHO Road Test and the development of these equations, a "failure" PSI equal to 1.5 and a reliability of 50 percent are recommended.

D_{eff} is determined from the following equation:

$$D_{eff} = CF * D$$

where

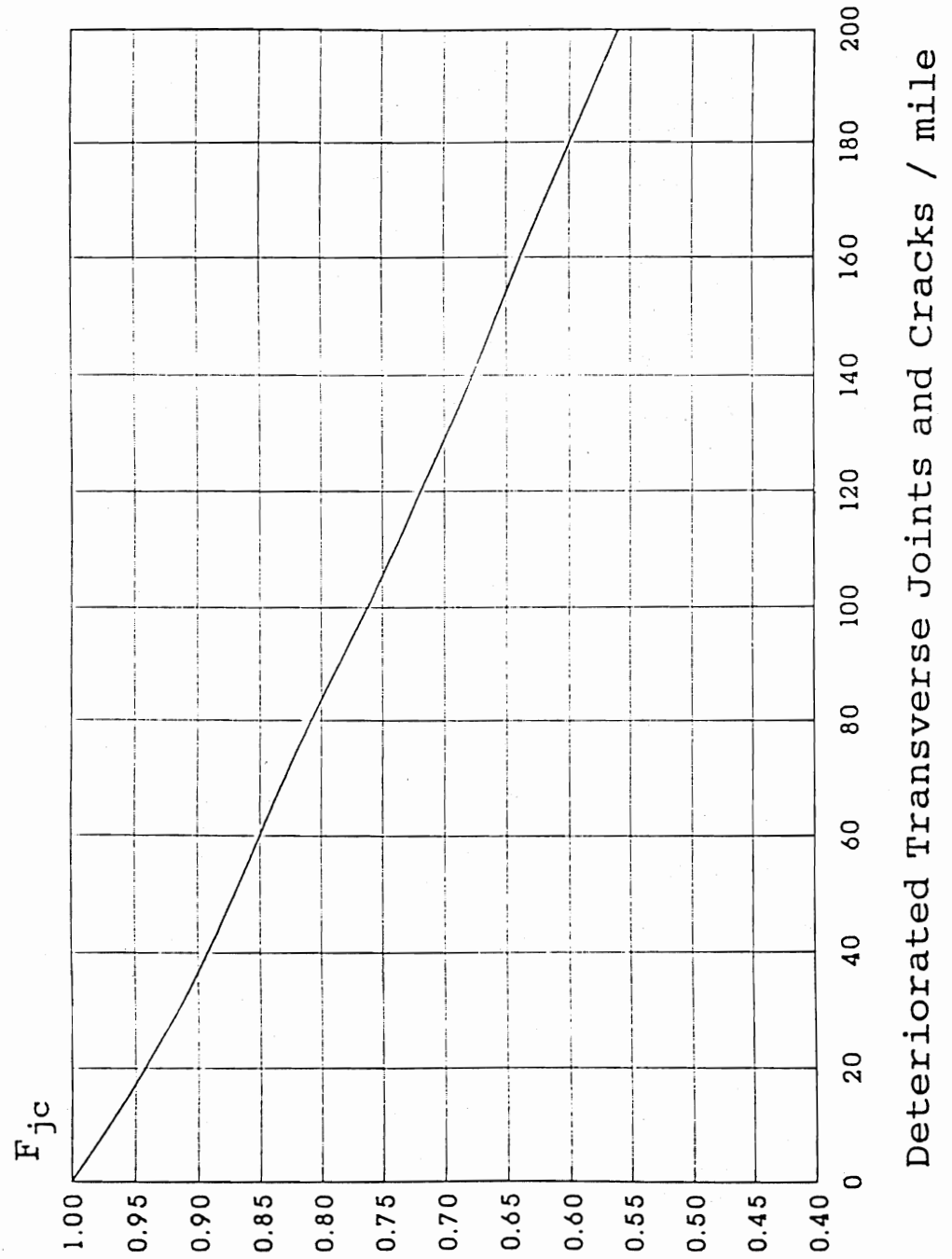

Figure 5.12. F_{jc} Adjustment Factor

CF = condition factor determined from Figure 5.2
D = thickness of the existing slab

The designer should recognize that D_{eff} determined by this method does not reflect any benefit for preoverlay repair. The estimate of D_{eff} obtained should thus be considered a lower limit value. The D_{eff} of the pavement will be higher if preoverlay repair of load-associated distress is done. This method for determining D_{eff} is not applicable without modification to pavements which have already received one or more overlays, even if the overlay has been or will be completely milled off.

A worksheet for determination of D_{eff} for JPCP, JRCP, and CRCP is provided in Table 5.8.

Step 8: Determination of Overlay Thickness.

The thickness of AC overlay is computed as follows:

$$D_{ol} = A(D_f - D_{eff})$$

where

D_{ol} = Required thickness of AC overlay, inches
A = Factor to convert PCC thickness deficiency to AC overlay thickness
D_f = Slab thickness determined in Step 6, inches
D_{eff} = Effective thickness of existing slab determined in Step 7, inches

The A factor, which is a function of the PCC thickness deficiency, is given by the following equation and is illustrated in Figure 5.9.

$$A = 2.2233 + 0.0099(D_f - D_{eff})^2 - 0.1534(D_f - D_{eff})$$

The thickness of overlay determined from the above relationship should be reasonable when the overlay is required to correct a structural deficiency. See Section 5.2.17 for discussion of factors which may result in unreasonable overlay thicknesses.

5.6.6 Shoulders

See Section 5.2.10 for guidelines.

5.6.7 Widening

See Section 5.2.16 for guidelines.

5.7 AC OVERLAY OF AC/JPCP, AC/JRCP, AND AC/CRCP

This section covers the design of AC overlays of existing AC/JPCP, AC/JRCP, or AC/CRCP. Although some pavements are newly constructed as AC/PCC, the vast majority of existing AC/PCC pavements are PCC pavements which have been overlaid with AC at least once.

Construction of an AC overlay of AC/JPCP, AC/JRCP, or AC/CRCP consists of the following major activities:

(1) Repairing deteriorated areas and making subdrainage improvements (if needed)
(2) Milling a portion of the existing AC surface
(3) Constructing widening (if needed)
(4) Applying a tack coat
(5) Placing the AC overlay, including a reflection crack control treatment (if needed)

5.7.1 Feasibility

An AC overlay is a feasible rehabilitation alternative for an AC/PCC pavement except when the condition of the existing pavement dictates substantial removal and replacement. Conditions under which another AC overlay would not be feasible include the following.

(1) The amount of deteriorated slab cracking and joint spalling is so great that complete removal and replacement of the existing surface is dictated.
(2) Significant deterioration of the PCC slab has occurred due to severe durability problems (e.g., "D" cracking or reactive aggregates).
(3) Vertical clearance at bridges is inadequate for required overlay thickness. This may be addressed by reducing the overlay thickness under the bridges (although this may result in early failure at these locations), by raising the bridges, or by reconstructing the pavement under the bridges. Thicker AC overlays may also necessitate raising signs and guardrails, as well as increasing side slopes and extending culverts. Sufficient right-of-way must be available or obtainable to permit these activities.

Table 5.8. Calculation of D_{eff} for AC Overlay of JPCP, JRCP, and CRCP in the Design Lane

Condition Survey Method:

F_{jc} Number of unrepaired deteriorated joints/mile = _____

Number of unrepaired deteriorated cracks/mile = _____

Number of unrepaired punchouts/mile = _____

Number of expansion joints, exceptionally wide joints (>1 inch) or AC full-depth patches/mile = _____

Total/mile = _____

F_{jc} = _____ (Figure 5.12)

(Recommended value 1.0, repair all deteriorated areas)

F_{dur}

1.00: No sign of PCC durability problems

0.96–0.99: Some durability cracking exists, but no spalling exists

0.88–0.95: Substantial cracking and some spalling exists

0.80–0.88: Extensive cracking and severe spalling exists

F_{dur} = _____

F_{fat}

0.97–1.00: Very few transverse cracks/punchouts exist

0.94–0.96: A significant number of transverse cracks/punchouts exist

0.90–0.93: A large number of transverse cracks/punchouts exist

F_{fat} = _____

$$D_{eff} = F_{jc} * F_{dur} * F_{fat} * D = \_\_\_\_\_$$

Remaining Life Method:

N_p = Past design lane ESALs = _____

$N_{1.5}$ = Design lane ESALs to P2 of 1.5 = _____

$$RL = 100\left[1 - \left(\frac{N_p}{N_{1.5}}\right)\right] = \_\_\_\_\_$$

CF = _____ (Figure 5.2)

$$D_{eff} = CF * D = \_\_\_\_\_$$

When another AC overlay of an existing AC/JPCP, AC/JRCP, or AC/CRCP is being considered, the causes of the deterioration in the existing pavement should be carefully investigated. If the PCC slab is sound and in good condition but the existing AC layer is badly rutted or otherwise deteriorated, the AC should be thoroughly repaired or milled off. If, however, distress visible at the AC surface is predominantly a reflection of deterioration in the underlying PCC, the pavement must be repaired through the full depth of the AC and PCC. Otherwise, the distress will reflect rapidly through the new AC overlay. It is strongly recommended that coring and deflection testing be conducted to thoroughly investigate the causes and extent of deterioration in the existing pavement.

5.7.2 Pre-overlay Repair

The following types of distress in AC/JPCP, AC/JRCP, and AC/CRCP should be repaired prior to placement of an AC overlay.

Distress Type	Repair Type
Rutting	Milling
Deteriorated reflection cracks	Full-depth repair or slab replacement
Deteriorated repairs	Full-depth repair
Punchouts	Full-depth repair
Localized distress in AC only	AC patching
Localized distress in PCC	Full-depth repair
Pumping	Edge drains
Settlements/heaves	AC level-up, slab jacking, or localized reconstruction

In AC/JPCP and AC/JRCP, medium- and high-severity reflection cracks in the AC surface are evidence of working cracks, deteriorated joints, or failed repairs in the PCC slab, all of which should be full-depth repaired. Low-severity reflection cracks may exist at regular joints and full-depth repair joints. If these cracks are sealed and do not appear to be deteriorating at a significant rate, they might not warrant pre-overlay repair other than sealing.

In AC/CRCP, reflection cracks of all severities suggest the presence of working cracks, deteriorated construction joints, or failed repairs in the PCC slab, all of which should be repaired. Coring through selected reflection cracks should be conducted to assess the condition of the underlying pavement.

Coring should be conducted at areas of localized distress to determine whether they are caused by a problem in the AC mix or deterioration in the PCC (e.g., "D" cracking). In the latter case, the PCC may be deteriorated to a much greater extent than is evident at the AC surface. Additional coring or removal of portions of the AC may be necessary to select appropriate repair boundaries.

Full-depth repairs to AC/PCC pavements should match the existing cross-section, i.e., the PCC slab should be full-depth repaired with the same thickness of PCC, and then capped with AC to the same thickness as the existing AC. Full-depth repairs and slab replacements in AC/JPCP or AC/JRCP should be AC/PCC, dowelled or tied to provide load transfer across repair joints. Some agencies have placed full-depth AC repairs in AC/JPCP and AC/JRCP prior to an AC overlay. However, this has often resulted in rough spots in the new overlay, opening of nearby joints and cracks, and rapid deterioration of reflection cracks at AC patch boundaries.

AC/CRCP full-depth repairs should be AC/PCC and should be continuously reinforced with steel which is tied or welded to reinforcing steel in the existing slab, to provide load transfer across joints and slab continuity. Full-depth AC repairs should not be used in AC/CRCP prior to placement of an AC overlay, and any existing AC patches in AC/CRCP should be removed and replaced with AC over continuously reinforced PCC. Guidelines on repair are provided in References 1 and 3.

Installation of edge drains, maintenance of existing edge drains, or other subdrainage improvement should be done prior to placement of the overlay if a subdrainage evaluation indicates a need for such an improvement.

Pressure relief joints should be placed only at fixed structures, and not at regular intervals along the pavement. The only exception to this is where reactive aggregate has caused expansion of the slab. On heavily trafficked routes, pressure relief joints should be of heavy-duty design with dowels (*3*).

5.7.3 Reflection Crack Control

Reflection cracking in an AC overlay of AC/JPCP, AC/JRCP, or AC/CRCP occurs over reflection cracks in the first AC overlay, and may also occur over new repairs. The basic mechanism of reflection cracking is strain concentration in the overlay due to movement in

the vicinity of joints and cracks in the existing pavement. This movement may be bending or shear induced by loads, or may be horizontal contraction induced by temperature changes. Load-induced movements are influenced by the thickness and stiffness of the AC layers, the thickness of the PCC, the degree of load transfer at the joints and cracks, and the extent of loss of support under the PCC slab. Temperature-induced movements are influenced by daily and seasonal temperature variations, the coefficients of thermal expansion of the existing pavement layers, and the spacing of joints and cracks.

Pre-overlay repair, including full-depth repair, subdrainage improvement, and subsealing, is the most effective means of controlling reflection crack occurrence and deterioration in a second AC overlay of an AC/JPCP or AC/JRCP pavement. Additional reflection crack control treatments may be used as well, including:

(1) *Placing a synthetic fabric, stress-absorbing interlayer, or bituminous-stabilized granular layer prior to or in combination with the AC overlay.*
(2) *Sawing and sealing joints in the AC overlay* at locations coinciding with reflection cracks and repair boundaries in the AC/JPCP or AC/JRCP. This technique has been very successful when applied to AC overlays of jointed PCC pavements when the sawcut matches the joint or straight crack within an inch.
(3) *Increasing the AC overlay thickness.* Reflection cracks will take more time to propagate through a thicker overlay and may deteriorate more slowly.

Reflection cracking can have a considerable (often controlling) influence on the life of an AC overlay of AC/JPCP or AC/JRCP. Deteriorated reflection cracks detract from a pavement's serviceability and also require frequent maintenance, such as sealing, milling, and patching. Reflection cracks also permit water to enter the pavement structure, which may result in loss of bond between the AC and PCC, stripping in the AC layers, progression of "D" cracking or reactive aggregate distress in PCC slabs with these durability problems, and softening of the base and subgrade. For this reason, reflection cracks should be sealed as soon as they appear and resealed periodically throughout the life of the overlay. Sealing low-severity reflection cracks may also be effective in retarding their progression to medium and high severity levels.

Repairing reflection cracks in existing AC/CRCP prior to placement of an AC overlay will delay the occurrence and deterioration of new reflection cracks. Improving subdrainage conditions and subsealing in areas where the slab has lost support will also discourage reflection crack occurrence and deterioration. Reflection crack control treatments are not necessary for AC overlays of AC/CRCP, except for longitudinal joints, as long as continuously reinforced AC/PCC repairs are used to repair deteriorated areas and cracks.

5.7.4 Subdrainage

See Section 5.2.4 for guidelines.

5.7.5 Thickness Design

If the overlay is being placed for some functional purpose such as roughness or friction, a minimum thickness overlay that solves the functional problem should be placed. If the overlay is being placed for the purpose of structural improvement, the required thickness of the overlay is a function of the structural capacity required to meet future traffic demands and the structural capacity of the existing pavement. The required overlay thickness to increase structural capacity to carry future traffic is determined by the following equation.

$$D_{ol} = A(D_f - D_{eff})$$

where

D_{ol} = Required thickness of AC overlay, inches
A = Factor to convert PCC thickness deficiency to AC overlay thickness
D_f = Slab thickness to carry future traffic, inches
D_{eff} = Effective equivalent PCC slab thickness of existing AC/PCC, inches

The A factor, which is a function of the PCC thickness deficiency, is given by the following equation and is illustrated in Figure 5.9.

$$A = 2.2233 + 0.0099(D_f - D_{eff})^2 - 0.1534(D_f - D_{eff})$$

The required overlay thickness may be determined through the following design steps. These design steps

provide a comprehensive design approach that recommends testing the pavement to obtain valid design inputs. If it is not possible to conduct this testing (e.g., for a low-volume road), an approximate overlay design may be developed based upon visible distress observations by skipping Steps 4 and 5, and by estimating other inputs.

The overlay design can be done for a uniform section or on a point-by-point basis as described in Section 5.3.1.

Step 1: Existing pavement design.

(1) Existing AC surface thickness
(2) Existing PCC slab thickness
(3) Type of load transfer (mechanical devices, aggregate interlock, CRCP)
(4) Type of shoulder (tied PCC, other)

Step 2: Traffic analysis.

(1) Predicted future 18-kip ESALs in the design lane over the design period (N_f)
Use ESALs computed from rigid pavement load equivalency factors

Step 3: Condition survey.

The following distresses are measured during the condition survey. Sampling along the most heavily trafficked lane of the project may be used to estimate these quantities. Distress types and severities are defined in Reference 23. Deteriorated means medium or higher severity.

AC/JPCP OR AC/JRCP:

(1) Number of deteriorated reflection cracks per mile
(2) Number of full-depth AC patches and expansion joints per mile (except at bridges)
(3) Evidence of pumping of fines or water at cracks and pavement edge
(4) Mean rut depth
(5) Number of localized failures

The following distresses are measured during the condition survey for AC/CRCP. Sampling may be used to estimate these quantities.

AC/CRCP:

(1) Number of unrepaired punchouts per mile
(2) Number of unrepaired reflection cracks per mile
(3) Number of unrepaired existing deteriorated repairs and full-depth AC repairs per mile
(4) Evidence of pumping of fines or water
(5) Mean rut depth

Step 4: Deflection testing (strongly recommended).

Measure slab deflection basins along the project at an interval sufficient to adequately assess conditions. Intervals of 100 to 1,000 feet are typical. Measure deflections with sensors located at 0, 12, 24, and 36 inches from the center of the load. Measure deflections in the outer wheel path, unless rutting of the AC surface interferes with proper seating of the load plate, in which case deflections should be measured between the wheelpaths. A heavy-load deflection device (e.g., Falling Weight Deflectometer) and a load magnitude of 9,000 pounds are recommended. ASTM D 4694 and D 4695 provide additional guidance on deflection testing.

(1) *Temperature of AC mix.* The temperature of the AC mix during deflection testing must be determined. This may be measured directly by drilling a hole into the AC surface, inserting a liquid and a temperature probe, and reading the AC mix temperature when it has stabilized. This should be done at least three times during each day's testing, so that a curve of AC mix temperature versus time may be developed and used to assign a mix temperature to each basin.

If measured AC mix temperatures are not available, they may be approximated from correlations with pavement surface and air temperatures (*24, 25, 26, 27*). Pavement surface temperature may be monitored during deflection testing using a hand-held infrared sensing device which is aimed at the pavement. The mean air temperature for the five days prior to deflection testing, which is an input to some of the referenced methods for estimating mix temperature, may be obtained from a local weather station or other local sources.

(2) *Elastic modulus of AC.* The modulus of the AC layer should be determined for each deflection basin. Two methods are available for determining the AC modulus, E_{ac}.
(a) *Estimate E_{ac} from AC mix temperature.* The elastic modulus of the AC layer may be estimated from AC mix properties and the AC mix temperature assigned to a deflection basin using the following equation (*26*):

$$\log E_{ac} = 5.553833 + 0.028829\left(\frac{P_{200}}{F^{0.17033}}\right) - 0.03476V_v + 0.070377\eta_{70°F,10^6} + 0.000005t_p^{(1.3+0.49825\log F)}P_{ac}^{0.5} - \frac{0.00189}{F^{1.1}}t_p^{(1.3+0.49825\log F)}P_{ac}^{0.5} + 0.931757\left(\frac{1}{F^{0.02774}}\right)$$

where

E_{ac} = elastic modulus of AC, psi
P_{200} = percent aggregate passing the No. 200 sieve
F = loading frequency, Hz
V_v = air voids, percent
$\eta_{70°F,10^6}$ = absolute viscosity at 70°F, 10^6 poise (e.g., 1 for AC-10, 2 for AC-20)
P_{ac} = asphalt content, percent by weight of mix
t_p = AC mix temperature, °F

This may be reduced to a relationship between AC modulus and AC mix temperature for a particular loading frequency (i.e., approximately 18 Hz for the FWD load duration of 25 to 30 milliseconds) by assuming typical values for the AC mix parameters P_{ac}, V_v, P_{200}, and η. For example, the AC mix design used by one State has the following typical values:

P_{200} = 4 percent
V_v = 5 percent
$\eta_{70°F,10^6}$ = 2 for AC-20
P_{ac} = 5 percent

For these values and an FWD loading frequency of 18 Hz, the following equation for AC elastic modulus versus AC mix temperature is obtained:

$$\log E_{ac} = 6.451235 - 0.000164671t_p^{1.92544}$$

Each agency should establish its own relationship for AC modulus versus temperature which is representative of the properties of its AC mixes.

It should be noted that the equation for AC modulus as a function of mix parameters and temperature applies to new mixes. AC which has been in service for some years may have either a higher modulus (due to hardening of the asphalt) or lower modulus (due to deterioration of the AC, from stripping or other causes) at any given temperature.

(b) Diametral resilient modulus testing of AC cores taken from the in-service AC/PCC pavement, as described in Step 5, may be used to establish a relationship between AC modulus and temperature. This relationship may be used to determine the AC modulus of each deflection basin at the time and temperature at which it was measured.

(3) *Effective dynamic k-value beneath PCC slab.* Compute the compression which occurs in the AC overlay beneath the load plate using the following equations.

AC, PCC LAYERS BONDED:

$$d_{0\,compress} = -0.0000328 + 121.5006 * \left(\frac{D_{ac}}{E_{ac}}\right)^{1.0798}$$

AC, PCC LAYERS UNBONDED:

$$d_{0\,compress} = -0.00002133 + 38.6872 * \left(\frac{D_{ac}}{E_{ac}}\right)^{0.94551}$$

where

$d_{0\,compress}$ = AC compression at center of load, inches
D_{ac} = AC thickness, inches
E_{ac} = AC elastic modulus, psi

The interface condition is a significant unknown in backcalculation. The AC/PCC interface is fully bonded when the AC layer is first placed, but how well that bond is retained is

not known. Examination of cores taken at a later time may show that bond has been reduced or completely lost. This is particularly likely if stripping occurs at the AC/PCC interface. If the current interface bonding condition is not determined by coring, the bonding condition which is considered more representative of the project may be assumed.

Using the above equations, the d_0 of the PCC slab in the AC/PCC pavement may be determined by subtracting the compression which occurs in the AC surface from the d_0 measured at the AC surface.

Compute the AREA of the PCC slab for each deflection basin from the following equation.

$$AREA_{pcc} = 6 * \left[1 + 2\left(\frac{d_{12}}{d_{0\,pcc}}\right) + 2\left(\frac{d_{24}}{d_{0\,pcc}}\right) + \left(\frac{d_{36}}{d_{0\,pcc}}\right)\right]$$

where

$d_{0\,pcc}$ = PCC deflection in center of loading plate, inches (surface deflection d_0 minus AC compression $d_{0_{compress}}$)
d_i = deflections at 12, 24, and 36 inches from plate center, inches

Enter Figure 5.10 with the $d_{0\,pcc}$ and $AREA_{pcc}$ of the PCC slab to determine the effective dynamic k-value beneath the slab for a circular load radius of 5.9 inches and magnitude of 9,000 pounds. Note that for loads within 2,000 pounds more or less, deflections may be scaled linearly to 9,000-pound deflections.

If a single overlay thickness is being designed for a uniform section, compute the mean effective dynamic k-value of the slabs tested in the uniform section.

(4) *Effective static k-value.*

Effective static k-value

= Effective dynamic k-value/2

The effective static k-value may need to be adjusted for seasonal effects using the approach presented in Part II, Section 3.2.1. However, the k-value can change substantially and have only a small effect on overlay thickness.

(5) *Elastic modulus of PCC slab (E).* Enter Figure 5.11 with the $AREA_{pcc}$ of the top of the PCC slab, proceed to the effective dynamic k-value curves, and determine a value for ED^3, where D is the PCC slab thickness. Solve for E knowing the slab thickness, D. Typical slab E values range from 3 to 8 million psi. If a slab E value is obtained out of this range, an error may exist in the assumed slab thickness, the deflection basin may have been measured over a crack, or the PCC may be significantly deteriorated.

If a single overlay thickness is being designed for a uniform section, compute the mean E value of the slabs tested in the uniform section.

Do not use any k-values or E values that appear to be significantly out of line with the rest of the data.

(6) *Joint load transfer.* For AC/JPCP and AC/JRCP, measure joint load transfer in the outer wheelpath (or between the wheelpaths if the AC is badly rutted) at representative reflection cracks above transverse joints in the PCC slab. Do not measure load transfer when the ambient temperature is greater than 80°F. Place the load plate on one side of the reflection crack with the edge of the plate touching the joint. Measure the deflection at the center of the load plate and at 12 inches from the center. Compute the deflection load transfer from the following equation.

$$\Delta LT = 100 * \left(\frac{\Delta_{ul}}{\Delta_l}\right) * B$$

where

ΔLT = deflection load transfer, percent
Δ_{ul} = unloaded side deflection, inches
Δ_l = loaded side deflection, inches
B = slab bending and AC compression correction factor

The slab bending and AC compression correction factor, B, is necessary because the deflections d_0 and d_{12}, measured 12 inches apart, would not be equal even if measured in the interior of a slab. An appropriate value for the correction factor may be determined from the

ratio of d_0 to d_{12} for typical center slab deflection basin measurements, as shown in the equation below.

$$B = \frac{d_{0\,center}}{d_{12\,center}}$$

If a single overlay thickness is being designed for a uniform section, compute the mean deflection load transfer value of the joints tested in the uniform section.

For AC/JPCP and AC/JRCP, determine the J load transfer coefficient using the following guidelines:

Percent Load Transfer	J
>70	3.2
50–70	3.5
<50	4.0

If the rehabilitation will include the addition of a tied concrete shoulder, a lower J factor may be appropriate. See Part II, Table 2.6.

For AC/CRCP, use J = 2.2 to 2.6 for overlay design, assuming that working cracks are repaired with continuously reinforced PCC overlaid with AC.

Step 5: Coring and materials testing (strongly recommended).

(1) *Modulus of AC surface.* Laboratory testing of cores taken from the AC surface in uncracked areas may be used to determine the elastic modulus of the AC surface. This may be done using a repeated-load indirect tension test (ASTM D 4123). The tests should be run at two or more temperatures (e.g., 40, 70, and 90°F) to establish points for a curve of log E_{ac} versus temperature. AC modulus values at any temperature may be interpolated from the laboratory values obtained at any two temperatures. For example, E_{ac} values at 70° and 90°F may be used in the following equation to interpolate E_{ac} at any temperature t°F:

$$\log E_{act°F} = \left(\frac{\log E_{ac\,70°F} - \log E_{ac\,90°F}}{70 - 90}\right) * (t°F - 70°F) + \log E_{ac\,70°F}$$

For purposes of interpreting NDT data, AC modulus values obtained from laboratory testing of cores must be adjusted to account for the difference between the loading frequency of the test apparatus (typically 1 to 2 Hz) and the loading frequency of the deflection testing device (18 Hz for the FWD). This adjustment is made by multiplying the laboratory-determined E_{ac} by a constant value which may be determined for each laboratory testing temperature using the equation given in Step 4 for AC modulus as a function of mix parameters and temperature. Field-frequency E_{ac} values will typically be 2 to 2.5 times higher than lab-frequency values.

Agencies may also wish to establish correlations between resilient modulus and indirect tensile strength for specific AC mixes.

(2) *PCC modulus of rupture (S'_c).* Cut several 6-inch-diameter cores at midslab and test in indirect tension (ASTM C 496). Compute the indirect tensile strength (psi) of the cores. Estimate the modulus of rupture with the following equation.

$$S'_c = 210 + 1.02IT$$

where

S'_c = modulus of rupture, psi
IT = indirect tensile strength of 6-inch-diameter cores, psi

Step 6: Determination of required slab thickness for future traffic (D_f).

The inputs to determine D_f for AC overlays of AC/PCC pavements are representative of the existing slab and foundation properties. This is emphasized because it is the properties of the existing slab (i.e., elastic modulus, modulus of rupture, and load transfer) which will control the performance of the AC overlay.

(1) *Effective static k-value beneath existing PCC slab.* Determine from one of the following methods.

(a) Backcalculate effective dynamic k-value from deflection basins as described in Step 4. Divide the effective dynamic k-value by 2 to obtain the effective static k-value. The effective static k-value may

need to be adjusted for seasonal effects using the approach presented in Part II, Section 3.2.1.

(b) Conduct plate load tests (ASTM D 1196) after slab removal at a few sites. This alternative is very costly and time-consuming and not often used. The static k-value obtained may need to be adjusted for seasonal effects (see Part II, Section 3.2.1).

(c) Estimate from soils data and base type and thickness, using Figure 3.3 in Part II, Section 3.2. This alternative is simple, but the static k-value obtained must be recognized as a rough estimate. The static k-value obtained may need to be adjusted for seasonal effects (see Part II, Section 3.2.1).

(2) *Design PSI loss.* PSI immediately after overlay (P1) minus PSI at time of next rehabilitation (P2).

(3) *J, load transfer of existing PCC slab.* See Step 4.

(4) *PCC modulus of rupture,* determined by one of the following methods:

(a) Estimate from indirect tensile strength measured from 6-inch-diameter cores, as described in Step 5.

(b) For AC/JPCP and AC/JRCP, estimate from the E of the slab, backcalculated as described in Step 4. Use the following equation:

$$S_c' = 43.5 \left(\frac{E}{10^6}\right) + 488.5$$

where

S_c' = modulus of rupture, psi
E = backcalculated elastic modulus of PCC slab, psi

For AC/CRCP, estimating S_c' from backcalculated E values is not recommended since cracks which are not reflected in the existing AC overlay may exist in the CRCP within the deflection basins.

(5) *Elastic modulus of existing PCC slab,* determined by one of the following methods:

(a) Backcalculated from deflection measurements, as described in Step 4.

(b) Estimated from indirect tensile strength.

(6) *Loss of support of existing slab* that might exist after rehabilitation. Procedures for use of deflection testing to investigate loss of support beneath AC/PCC pavements have not yet been established. For overlay thickness design assume the slab is fully supported, LS = 0.

(7) *Overlay design reliability, R (percent).* See Part I, Section 4.2, Part II, Table 2.2, and Part III, Section 5.2.15.

(8) *Overall standard deviation, S_o, for PCC pavement.* See Part I, Section 4.3.

(9) *Subdrainage capability of existing slab, after subdrainage improvements, if any.* See Part II Table 2.5, as well as reference 5, for guidance in determining C_d. Pumping or faulting at reflection cracks is evidence that a subdrainage problem exists. In selecting this value, note that the poor drainage situation at the AASHO Road Test would be given a C_d of 1.0.

Compute D_f for the above design inputs using the rigid pavement design equation or nomograph in Part II, Figure 3.7. When designing an overlay thickness for a uniform pavement section, mean input values must be used. When designing an overlay thickness for specific points along the project, the data for that point must be used. A worksheet for determining D_f is provided in Table 5.9. Typical values of inputs are provided for guidance. Values outside these ranges should be used with caution.

Step 7: Determination of effective slab thickness (D_{eff}) of existing pavement.

A condition survey method for determination of D_{eff} is presented for AC/PCC pavements. The effective thickness of the existing slab (D_{eff}) is computed from the following equation:

$$D_{eff} = (D_{pcc} * F_{jc} * F_{dur}) + \left[\left(\frac{D_{ac}}{2.0}\right) * F_{ac}\right]$$

where

D_{pcc} = thickness of existing PCC slab, inches
D_{ac} = thickness of existing AC surface, inches

(1) *Joints and cracks adjustment factor (F_{jc}).* This factor adjusts for the extra loss in PSI caused by deteriorated reflection cracks that will occur in a second overlay due to unrepaired deteriorated reflection cracks and other d

Table 5.9. Worksheet for Determination of D_f for AC/JPCP, AC/JRCP, and AC/CRCP

SLAB:

Existing AC surface thickness = _____ inches

Existing PCC slab thickness = _____ inches

Type of load transfer system: mechanical device, aggregate interlock, CRCP

Type of shoulder = tied PCC, other

PCC modulus of rupture (typically 600 to 800 psi) = _____ psi

PCC E modulus (3 to 8 million psi for sound PCC, <3 million for unsound PCC) = _____ psi

J load transfer factor (3.2 to 4.0 for AC/JPCP, AC/JRCP 2.2 to 2.6 for AC/CRCP) = _____

TRAFFIC:

Future 18-kip ESALs in design lane over the design period (N_f) = _____

SUPPORT AND DRAINAGE:

Effective dynamic k-value = _____ psi/inch

Effective static k-value = Effective dynamic k-value/2 (typically 50 to 500 psi/inch) = _____ psi/inch

Subdrainage coefficient, C_d (typically 1.0 for poor subdrainage conditions) = _____

SERVICEABILITY LOSS:

Design PSI loss (P1 – P2) = _____

RELIABILITY:

Design reliability, R (80 to 99 percent) = _____ percent

Overall standard deviation, S_o (typically 0.39) = _____

FUTURE STRUCTURAL CAPACITY:

Required slab thickness for future traffic is determined from rigid pavement design equation or nomograph in Part II, Figure 3.7.

D_f = _____ inches

continuities in the existing AC/PCC pavement prior to overlay. A deteriorated reflection crack in the existing AC/PCC pavement will rapidly reflect through a second overlay and contribute to loss of serviceability. Therefore, it is recommended that all deteriorated reflection cracks and any other major discontinuities in the existing pavement be full-depth repaired with dowelled or tied PCC repairs prior to overlay, so that $F_{jc} = 1.00$.

If it is not possible to repair all deteriorated areas, the following information is needed to

determine F_{jc}, to increase the overlay thickness to account for the extra loss in PSI from deteriorated reflection cracks:

Number of unrepaired deteriorated reflection cracks/mile
Number of unrepaired punchouts/mile
Number of expansion joints, exceptionally wide joints (greater than 1 inch), and full-depth, full-lane-width AC patches/mile

The total number of unrepaired deteriorated reflection cracks, punchouts, and other discontinuities per mile is used to determine the F_{jc} from Figure 5.12.

(2) *Durability adjustment factor (F_{dur}).* This factor adjusts for an extra loss in PSI of the overlay when the existing slab has durability problems such as "D" cracking or reactive aggregate distress. Using historical records and condition survey data from Step 3, F_{dur} is determined as follows.

1.00:	No evidence or history of PCC durability problems
0.96–0.99:	Pavement is known to have PCC durability problems, but no localized failures or related distresses are visible
0.88–0.95:	Some durability distress (localized failures, etc.) is visible at pavement surface
0.80–0.88:	Extensive durability distress (localized failures, etc.) is visible at pavement surface

(3) AC quality adjustment factor (F_{ac}). This factor adjusts the existing AC layer's contribution to D_{eff} based on the quality of the AC material. The value selected should depend only on distresses related to the AC layer (i.e., not reflection cracking) which are not eliminated by surface milling: rutting, stripping, shoving, and also weathering and ravelling if the surface is not milled. Consideration should be given to complete removal of a poor-quality AC layer.

1.00:	No AC material distress
0.96–0.99:	Minor AC material distress (weathering, ravelling) not corrected by surface milling
0.88–0.95:	Significant AC material distress (rutting, stripping, shoving)
0.80–0.88:	Severe AC material distress (rutting, stripping, shoving)

A worksheet for calculation of D_{eff} is provided in Table 5.10.

Step 8: Determination of Overlay Thickness.

The thickness of AC overlay is computed as follows:

$$D_{ol} = A(D_f - D_{eff})$$

where

D_{ol} = Required thickness of AC overlay, inches
A = Factor to convert PCC thickness deficiency to AC overlay thickness
D_f = Slab thickness determined in Step 6, inches
D_{eff} = Effective thickness of existing slab determined in Step 7, inches

The A factor, which is a function of the PCC thickness deficiency, is given by the following equation and is illustrated in Figure 5.9.

$$A = 2.2233 + 0.0099(D_f - D_{eff})^2 - 0.1534(D_f - D_{eff})$$

The thickness of overlay determined from the above relationship should be reasonable when the overlay is required to correct a structural deficiency. See Section 5.2 for discussion of factors which may result in unreasonable overlay thicknesses.

5.7.6 Surface Milling

If the AC surface is to be milled prior to overlay, the depth of milling should be considered in the determination of D_{eff}. No adjustment need be made to D_{eff} values if the depth of milling does not exceed the minimum necessary to remove surface ruts. If a greater depth is milled, the AC thickness remaining after milling should be used in determining D_{eff}.

5.7.7 Shoulders

See Section 5.2.10 for guidelines.

Table 5.10. Calculation of D_{eff} for AC Overlay of AC/JPCP, AC/JRCP, and AC/CRCP

Condition Survey Method:

F_{jc} Number of unrepaired deteriorated reflection cracks/mile = _____

Number of punchouts/mile = _____

Number of expansion joints, exceptionally wide joints (>1 inch) or full-depth patches/mile = _____

Total/mile = _____

F_{jc} = _____ (Figure 5.12)

(Recommended value 1.0, repair all deteriorated areas)

F_{dur}

1.00: No sign or knowledge of PCC durability problems

0.96–0.99: Pavement is known to have PCC durability problems, but no localized failures or related distresses

0.88–0.95: Some durability distress (localized failures, etc.) is visible at pavement surface

0.80–0.88: Extensive durability distress (localized failures, etc.)

F_{dur} = _____

F_{ac}

1.00: No AC material distress

0.96–0.99: Minor AC material distress (weathering, ravelling) not corrected by surface milling

0.88–0.95: Significant AC material distress (rutting, stripping, shoving)

0.80–0.88: Severe AC material distress (rutting, stripping, shoving)

F_{ac} = _____

$$D_{eff} = (D_{pcc} * F_{jc} * F_{dur}) + \left[\left(\frac{D_{ac}}{2.0}\right) * F_{ac}\right] = \_\_\_\_\_$$

5.7.8 Widening

See Section 5.2.16 for guidelines.

5.8 BONDED CONCRETE OVERLAY OF JPCP, JRCP, AND CRCP

Bonded concrete overlays have been placed on jointed plain, jointed reinforced and continuously reinforced concrete pavements to improve both structural capacity and functional condition. A bonded concrete overlay consists of the following construction tasks:

(1) Repairing deteriorated areas and making subdrainage improvements (if needed)
(2) Constructing widening (if needed)
(3) Preparing the existing surface to ensure a reliable bond
(4) Placing the concrete overlay
(5) Sawing and sealing the joints

5.8.1 Feasibility

A bonded overlay of JPCP, JRCP, or CRCP is a feasible rehabilitation alternative for PCC pavements except when the conditions of the existing pavement dictate substantial removal and replacement or when

durability problems exist (*28*). Conditions under which a PCC bonded overlay would not be feasible include:

(1) The amount of deteriorated slab cracking and joint spalling is so great that a substantial amount of removal and replacement of the existing surface is dictated.
(2) Significant deterioration of the PCC slab has occurred due to durability problems (e.g., "D" cracking or reactive aggregates). This will affect performance of the overlay.
(3) Vertical clearance at bridges is inadequate for required overlay thickness. This is not usually a problem because bonded overlays are usually fairly thin.

If construction duration is critical, PCC overlays may utilize high-early-strength PCC mixes. PCC overlays have been opened within 6 to 24 hours after placement using these mixtures.

5.8.2 Pre-overlay Repair

The following types of distress should be repaired prior to placement of the bonded PCC overlay.

Distress Type	Repair Type
Working cracks	Full-depth repair or slab replacement
Punchouts	Full-depth repair
Spalled joints	Full- or partial-depth repair
Deteriorated patches	Full-depth repair
Pumping/faulting	Edge drains
Settlements/heaves	Slab jack or reconstruct area

Full-depth repairs and slab replacements in JPCP and JRCP should be PCC, dowelled or tied to provide load transfer across repair joints. Full-depth repairs in CRCP should be PCC and should be continuously reinforced with steel which is tied or welded to reinforcing steel in the existing slab, to provide load transfer across joints and slab continuity. Full-depth AC repairs should not be used prior to placement of a bonded PCC overlay, and any existing AC patches should be removed and replaced with PCC. Guidelines on repairs are provided in References 1 and 3.

Installation of edge drains, maintenance of existing edge drains, or other subdrainage improvement should be done prior to placement of the overlay if a subdrainage evaluation indicates a need for such an improvement.

Pressure relief joints should be done only at fixed structures, and not at regular intervals along the pavement. The only exception to this is where a reactive aggregate has caused expansion of the slab. On heavily trafficked routes, expansion joints should be of the heavy-duty type with dowels (*3*). If joints contain significant incompressibles, they should be cleaned and resealed prior to overlay placement.

5.8.3 Reflection Crack Control

Any working (spalled) cracks in the existing JPCP, JRCP, or CRCP slab may reflect through the bonded concrete overlay within one year. Reflection cracks can be controlled in bonded overlays by full-depth repair of working cracks in the existing pavement, and for JPCP or JRCP, sawing and sealing joints through the overlay directly over the repair joints. Tight nonworking cracks do not need to be repaired because not all will reflect through the overlay and those that do will usually remain tight. Tight cracks in CRCP will take several years to reflect through, and even then will remain tight.

5.8.4 Subdrainage

See Section 5.2.4 for guidelines.

5.8.5 Thickness Design

If the overlay is being placed for some functional purpose such as roughness or friction, a minimum thickness overlay that solves the functional problem should be placed.

If the overlay is being placed for the purpose of structural improvement, the required thickness of the overlay is a function of the structural capacity required to meet future traffic demands and the structural capacity of the existing pavement. The required overlay thickness to increase structural capacity to carry future traffic is determined by the following equation.

$$D_{ol} = D_f - D_{eff}$$

where

D_{ol} = Required thickness of bonded PCC overlay, inches
D_f = Slab thickness to carry future traffic, inches
D_{eff} = Effective thickness of existing slab, inches

Bonded concrete overlays have been successfully constructed as thin as 2 inches and as thick as 6 inches or more. Three to 4 inches has been typical for most highway pavement overlays (*28*). If the bonded overlay is being placed only for a functional purpose such as roughness or friction, a thickness of 3 inches should be adequate.

The required overlay thickness may be determined through the following design steps. These design steps provide a comprehensive design approach that recommends testing the pavement to obtain valid design inputs. If it is not possible to conduct this testing, an approximate overlay design may be developed based upon visible distress observations by skipping Steps 4 and 5, and by estimating other inputs.

The overlay design can be done for a uniform section or on a point-by-point basis as described in Section 5.3.1.

Step 1: Existing pavement design.

(1) Existing slab thickness
(2) Type of load transfer (mechanical devices, aggregate interlock, CRCP)
(3) Type of shoulder (tied, PCC, other)

Step 2: Traffic analysis.

(1) Past cumulative 18-kip ESALs in the design lane (N_p), for use in the remaining life method of D_{eff} determination only
(2) Predicted future 18-kip ESALs in the design lane over the design period (N_f)

Step 3: Condition survey.

The following distresses are measured during the condition survey for JPCP, JRCP, and CRCP. Sampling along the project may be used to estimate these quantities in the most heavily trafficked lane. Distress types and severities are defined in Reference 23. Deteriorated means medium or higher severity.

JPCP/JRCP:

(1) Number of deteriorated transverse joints per mile
(2) Number of deteriorated transverse cracks per mile
(3) Number of existing expansion joints, exceptionally wide joints (>1 inch) or AC full-depth patches
(4) Presence and general severity of PCC durability problems
  (a) "D" cracking: low severity (cracks only), medium severity (some spalling), high severity (severe spalling)
  (b) Reactive aggregate cracking: low, medium, high severity
(5) Evidence of faulting, pumping of fines or water at joints, cracks and pavement edge

CRCP:

(1) Number of punchouts per mile
(2) Number of deteriorated transverse cracks per mile
(3) Number of existing expansion joints, exceptionally wide joints (>1 inch) or AC full-depth patches
(4) Number of existing and new repairs prior to overlay per mile
(5) Presence and general severity of PCC durability problems (NOTE: surface spalling of tight cracks where the underlying CRCP is sound should not be considered a durability problem)
  (a) "D" cracking: low severity (cracks only), medium severity (some spalling), high severity (severe spalling)
  (b) Reactive aggregate cracking: low, medium, high severity
(6) Evidence of pumping of fines or water

Step 4: Deflection testing (strongly recommended).

Measure slab deflection basins in the outer wheel path along the project at an interval sufficient to adequately assess conditions. Intervals of 100 to 1,000 feet are typical. Measure deflections with sensors located at 0, 12, 24, and 36 inches from the center of load. A heavy-load deflection device (e.g., Falling Weight Deflectometer) and a load magnitude of 9,000 pounds are recommended. ASTM D 4694 and D 4695 provide additional guidance on deflection testing.

For each slab tested, backcalculate the effective k-value and the slab's elastic modulus using Figures 5.10 and 5.11 or a backcalculation procedure. The AREA of each deflection basin is computed as follows:

$$AREA = 6 * \left[1 + 2\left(\frac{d_{12}}{d_0}\right) + 2\left(\frac{d_{24}}{d_0}\right) + \left(\frac{d_{36}}{d_0}\right)\right]$$

where

d_0 = deflection in center of loading plate, inches
d_i = deflections at 12, 24, and 36 inches from plate center, inches

AREA will typically range from 29 to 32 for sound concrete.

(1) *Effective dynamic k-value.* Enter Figure 5.10 with d_0 and AREA to determine the effective dynamic k-value beneath each slab for a circular load radius of 5.9 inches and magnitude of 9,000 pounds. Note that for loads within 2,000 pounds more or less, deflections may be scaled linearly to 9,000-pound deflections.

If a single overlay thickness is being designed for a uniform section, compute the mean effective dynamic k-value of the slabs tested in the uniform section.

(2) *Effective static k-value.*

Effective static k-value

= Effective dynamic k-value/2

The effective k-value may need to be adjusted for seasonal effects using the approach presented in Part II, Section 3.2.1. However, the k-value can change substantially and have only a small effect on overlay thickness.

(3) *Elastic modulus of PCC slab (E).* Enter Figure 5.11 with AREA, proceed to the effective dynamic k-value curves, and determine a value for ED^3, where D is the slab thickness. Solve for E knowing the slab thickness, D. Typical slab E values range from 3 to 8 million psi. If a slab E value is obtained that is out of this range, an error may exist in the assumed slab thickness, the deflection basin may have been measured over a crack, or the PCC may be significantly deteriorated.

If a single overlay thickness is being designed for a uniform section, compute the mean E value of the slabs tested in the uniform section.

Do not use any k-values or E values that appear to be significantly out of line with the rest of the data.

(4) *Joint load transfer.* For JPCP and JRCP, measure joint load transfer in the outer wheelpath at representative transverse joints. Do not measure load transfer when the ambient temperature is greater than 80°F. Place the load plate on one side of the joint with the edge of the plate touching the joint. Measure the deflection at the center of the load plate and at 12 inches from the center. Compute the deflection load transfer from the following equation.

$$\Delta LT = 100 * \left(\frac{\Delta_{ul}}{\Delta_l}\right) * B$$

where

ΔLT = deflection load transfer, percent
Δ_{ul} = unloaded side deflection, inches
Δ_l = loaded side deflection, inches
B = slab bending correction factor

The slab bending correction factor, B, is necessary because the deflections d_0 and d_{12}, measured 12 inches apart, would not be equal even if measured in the interior of a slab. An appropriate value for the correction factor may be determined from the ratio of d_0 to d_{12} for typical center slab deflection basin measurements, as shown in the equation below. Typical values for B are between 1.05 and 1.15.

$$B = \frac{d_{0\,center}}{d_{12\,center}}$$

If a single overlay thickness is being designed for a uniform section, compute the mean deflection load transfer value of the joints tested in the uniform section.

For JPCP and JRCP, determine the J load transfer coefficient using the following guidelines:

Percent Load Transfer	J
>70	3.2
50–70	3.5
<50	4.0

If the rehabilitation will include the addition of a tied concrete shoulder, a lower J factor may be appropriate. See Part II, Table 2.6.

For CRCP, use J = 2.2 to 2.6 for overlay design, assuming that working cracks and punchouts are repaired with continuously reinforced PCC.

Step 5: Coring and materials testing (strongly recommended).

(1) *PCC modulus of rupture (S_c').* Cut several 6-inch-diameter cores at mid-slab and test in indirect tension (ASTM C 496). Compute the indirect tensile strength (psi) of the cores. Estimate the modulus of rupture with the following equation:

$$S_c' = 210 + 1.02IT$$

where

S_c' = modulus of rupture, psi
IT = indirect tensile strength of 6-inch diameter cores, psi

Step 6: Determination of required slab thickness for future traffic (D_f).

The inputs to determine D_f for bonded PCC overlays of PCC pavements are representative of the existing slab and foundation properties. This is emphasized because it is the properties of the existing slab (i.e., elastic modulus, modulus of rupture, and load transfer) which will control the performance of the bonded overlay.

(1) *Effective static k-value.* Determine from one of the following methods.
   (a) Backcalculate the effective dynamic k-value from deflection basins as described in Step 4. Divide the effective dynamic k-value by 2 to obtain the effective static k-value.
   (b) Conduct plate load tests (ASTM D 1196) after slab removal at a few sites. This alternative is very costly and time-consuming and not often used. The static k-value obtained may need to be adjusted for seasonal effects using the approach presented in Part II, Section 3.2.1.
   (c) Estimate from soils data and base type and thickness, using Figure 3.3 in Part II, Section 3.2. This alternative is simple, but the static k-value obtained must be recognized as a rough estimate. The static k-value obtained may need to be adjusted for seasonal effects using the approach presented in Part II, Section 3.2.1.

(2) *Design PSI loss.* PSI immediately after overlay (P1) minus PSI at time of next rehabilitation (P2).

(3) *J, load transfer factor.* See Step 4.

(4) *PCC modulus of rupture* determined by one of the following methods:
   (a) Estimated from indirect tensile strength measured from 6-inch diameter cores as described in Step 5.
   (b) Estimated from the backcalculated E of slab using the following equation:

$$S_c' = 43.5\left(\frac{E}{10^6}\right) + 488.5$$

where

S_c' = modulus of rupture, psi
E = backcalculated elastic modulus of PCC slab, psi

For CRCP, S_c' may be determined from the backcalculated E values only at points which have no cracks within the deflection basins.

(5) *Elastic modulus of existing PCC slab,* determined by one of the following methods:
   (a) Backcalculate from deflection measurements as described in Step 4.
   (b) Estimate from indirect tensile strength.

(6) *Loss of support of existing slab.* Joint corners that have loss of support may be identified using FWD deflection testing as described in Reference 2. CRCP loss of support can be determined by plotting a slab edge or wheel path deflection profile and identifying locations with significantly high deflections. Existing loss of support can be improved with slab stabilization. For thickness design, assume a fully supported slab, LS = 0.

(7) *Overlay design reliability, R (percent).* See Part I, Section 4.2, Part II, Table 2.2, and Part III, Section 5.2.15.

(8) *Overall standard deviation (S_o) for rigid pavement.* See Part I, Section 4.3.

(9) *Subdrainage capability of existing slab, after subdrainage improvements, if any.* See Part II,

Table 2.5, as well as Reference 5, for guidance in determining C_d. Pumping or faulting at joints and cracks determined in Step 3 is evidence that a subdrainage problem exists. In selecting this value, note that the poor subdrainage situation at the AASHO Road Test would be given a C_d of 1.0.

Compute D_f for the above design inputs using the rigid pavement design equation or nomograph in Part II, Figure 3.7. When designing an overlay thickness for a uniform pavement section, mean input values must be used. When designing an overlay thickness for specific points along the project, the data for that point must be used. A worksheet for determining D_f is provided in Table 5.11. Typical values of inputs are provided for guidance. Values outside these ranges should be used with caution.

Step 7: Determination of effective slab thickness (D_{eff}) of existing pavement.

The condition survey and remaining life procedures are presented.

D_{eff} From Condition Survey For PCC Pavements

The effective thickness of the existing slab (D_{eff}) is computed from the following equation:

$$D_{eff} = F_{jc} * F_{dur} * F_{fat} * D$$

where

D = existing PCC slab thickness, inches

(1) *Joints and cracks adjustment factor (F_{jc}).* This factor adjusts for the extra loss in PSI caused by deteriorated reflection cracks in the overlay that will result from any unrepaired deteriorated joints, cracks, and other discontinuities in the existing slab prior to overlay. A deteriorated joint or crack in the existing slab will rapidly reflect through an AC overlay and contribute to loss of serviceability. Therefore, it is recommended that all deteriorated joints and cracks (for non-"D" cracked or reactive aggregate related distressed pavements) and any other major discontinuities in the existing slab be full-depth repaired with dowelled or tied PCC repairs prior to overlay, so that F_{jc} = 1.00.

If it is not possible to repair all deteriorated areas, the following information is needed to determine F_{jc}, to increase the overlay thickness to account for the extra loss in PSI from deteriorated reflection cracks (per design lane):

Pavements with no "D" cracking or reactive aggregate distress:

Number of unrepaired deteriorated joints/mile

Number of unrepaired deteriorated cracks/mile

Number of unrepaired punchouts/mile

Number of expansion joints, exceptionally wide joints (greater than 1 inch), and full-depth, full-lane-width AC patches/mile

NOTE that tight cracks held together by reinforcement in JRCP or CRCP are not included. However, if a crack in JRCP or CRCP is spalled and faulted the steel has probably ruptured, and the crack should be considered as working. Surface spalling of CRCP cracks is not an indication that the crack is working.

The total number of unrepaired deteriorated joints, cracks, punchouts, and other discontinuities per mile is used to determine the F_{jc} from Figure 5.12.

Pavements with "D" cracking or reactive aggregate deterioration:

These types of pavements often have deterioration at the joints and cracks from durability problems. The F_{dur} factor is used to adjust the overlay thickness for this problem. Therefore, when this is the case, the F_{jc} should be determined from Figure 5.12 only using those unrepaired deteriorated joints and cracks that are not caused by durability problems. If all of the deteriorated joints and cracks are spalling due to "D" cracking or reactive aggregate, then F_{jc} = 1.0. This will avoid adjusting twice with the F_{jc} and F_{dur} factors.

(2) *Durability adjustment factor (F_{dur}).* This factor adjusts for an extra loss in PSI of the overlay when the existing slab has durability problems such as "D" cracking or reactive aggregate distress. Using condition survey data from Step 3, F_{dur} is determined as follows.

1.00: No sign of PCC durability problems

0.96–0.99: Durability cracking exists, but no spalling

Table 5.11. Worksheet for Determination of D_f for JPCP, JRCP, and CRCP

SLAB:

Existing PCC slab thickness = _____ inches

Type of load transfer system: mechanical device, aggregate interlock, CRCP

Type of shoulder = tied PCC, other

PCC modulus of rupture (typically 600 to 800 psi) = _____ psi

PCC E modulus (3 to 8 million psi for sound PCC, <3 million for unsound PCC) = _____ psi

J load transfer factor (3.2 to 4.0 for JPCP, JRCP 2.2 to 2.6 for CRCP) = _____

TRAFFIC:

Future 18-kip ESALs in design lane over the design period (N_f) = _____

SUPPORT AND DRAINAGE:

Effective dynamic k-value = _____ psi/inch

Effective static k-value = effective dynamic k-value/2 (typically 50 to 500 psi/inch) = _____ psi/inch

Subdrainage coefficient, C_d (typically 1.0 for poor subdrainage conditions) = _____

SERVICEABILITY LOSS:

Design PSI loss (P1 − P2) = _____

RELIABILITY:

Design reliability, R (80 to 99 percent) = _____ percent

Overall standard deviation, S_o (typically 0.39) = _____

FUTURE STRUCTURAL CAPACITY:

Required slab thickness for future traffic is determined from rigid pavement design equation or nomograph in Part II, Figure 3.7.

D_f = _____ inches

0.80–0.95: Cracking and spalling exist (normally a bonded PCC overlay is not recommended under these conditions)

(3) *Fatigue damage adjustment factor (F_{fat}).* This factor adjusts for past fatigue damage that may exist in the slab. It is determined by observing the extent of transverse cracking (JPCP, JRCP) or punchouts (CRCP) that may be caused primarily by repeated loading. Use condition survey data from Step 3 and the following guidelines to estimate F_{fat} for the design lane.

0.97–1.00: Few transverse cracks/punchouts exist (none caused by "D" cracking or reactive aggregate distress)

JPCP: <5 percent slabs are cracked
JRCP: <25 working crack per mile
CRCP: <4 punchouts per mile

0.94–0.96: A significant number of transverse cracks/punchouts exist (none caused by "D" cracking or reactive aggregate distress)
JPCP: 5–15 percent slabs are cracked
JRCP: 25–75 working cracks per mile
CRCP: 4–12 punchouts per mile

0.90–0.93: A large number of transverse cracks/punchouts exist (none caused by "D" cracking or reactive aggregate distress)
JPCP: >15 percent slabs are cracked
JRCP: >75 working cracks per mile
CRCP: >2 punchouts per mile

D_{eff} From Remaining Life For PCC Pavements

The remaining life of the pavement is given by the following equation:

$$RL = 100\left[1 - \left(\frac{N_p}{N_{1.5}}\right)\right]$$

where

RL = remaining life, percent
N_p = total traffic to date, ESALs
$N_{1.5}$ = total traffic to pavement "failure," ESALs

$N_{1.5}$ may be estimated using the new pavement design equations or nomographs in Part II. To be consistent with the AASHO Road Test and the development of these equations, a "failure" PSI equal to 1.5 and a reliability of 50 percent is recommended.

D_{eff} is determined from the following equation:

$$D_{eff} = CF * D$$

where

CF = condition factor determined from Figure 5.2
D = thickness of the existing slab, inches

The designer should recognize that D_{eff} determined by this method does not reflect any benefit for pre-overlay repair. The estimate of D_{eff} obtained should thus be considered a lower limit value. The D_{eff} of the pavement will be higher if pre-overlay repair of load-associated distress is done.

A worksheet for determination of D_{eff} for JPCP, JRCP, and CRCP is provided in Table 5.12.

Step 8: Determination of Overlay Thickness.

The thickness of bonded PCC overlay is computed as follows:

$$D_{ol} = D_f - D_{eff}$$

where

D_{ol} = Required thickness of bonded PCC overlay, inches
D_f = Slab thickness determined in Step 6, inches
D_{eff} = Effective thickness of existing slab determined in Step 7, inches

The thickness of overlay determined from the above relationship should be reasonable when the overlay is required to correct a structural deficiency. See Section 5.2.17 for discussion of factors which may result in unreasonable overlay thicknesses.

5.8.6 Shoulders

See Section 5.2.10 for guidelines.

5.8.7 Joints

Existing JPCP and JRCP. Transverse and longitudinal joints should be saw cut completely through the overlay thickness (plus 0.5-inch depth) as soon as curing allows after overlay placement. Failure to saw joints soon after placement may result in debonding and cracking at the joints. No dowels or reinforcing steel should be placed in these joints. An appropriate sealant reservoir should be sawed and sealant should be placed as soon as possible.

Existing CRCP. Transverse joints must not be cut in the bonded overlay, as they are not needed. Transverse joints are also not needed for the end joints for full-

Table 5.12. Calculation of D_{eff} for Bonded PCC Overlay of JPCP, JRCP, and CRCP

Condition Survey Method:

F_{jc} Number of unrepaired deteriorated joints/mile = _____

Number of unrepaired deteriorated cracks/mile = _____

Number of unrepaired punchouts/mile = _____

Number of expansion joints, exceptionally wide joints (>1 inch) or AC full-depth patches/mile = _____

Total/mile = _____

F_{jc} = _____ (Figure 5.12)

(Recommended value 1.0, repair all deteriorated areas)

F_{dur}

1.00: No sign of PCC durability problems

0.96–0.99: Some durability cracking exists, but no spalling exists

0.88–0.95: Cracking and spalling exist

F_{dur} = _____

F_{fat}

0.97–1.00: Very few transverse cracks/punchouts exist

0.94–0.96: A significant number of transverse cracking/punchouts exist

0.90–0.93: A large amount of transverse cracking/punchouts exist

F_{fat} = _____

$$D_{eff} = F_{jc} * F_{dur} * F_{fat} * D = \_\_\_\_\_$$

Remaining Life Method:

N_p = Past design lane ESALs = _____

$N_{1.5}$ = Design lane ESALs to P2 of 1.5 = _____

$$RL = 100\left[1 - \left(\frac{N_p}{N_{1.5}}\right)\right] = \_\_\_\_\_$$

CF = _____ (Figure 5.2)

$$D_{eff} = CF * D = \_\_\_\_\_$$

depth reinforced tied concrete patches. Longitudinal joints should be sawed in the same manner as for JPCP and JRCP.

5.8.8 Bonding Procedures and Material

The successful performance of the bonded overlay depends on a reliable bond with the existing surface (*28*). The following guidelines are provided:

(1) The existing surface must be cleaned and roughened, through a mechanical process that removes a thin layer of concrete, but does not damage (crack) the surface. Shot blasting is the most used system. Cold milling has been used, but may cause damage to the surface and thus requires sand blasting afterward to remove any loose particles.
(2) A bonding agent is recommended to help achieve a more reliable bond. Water, cement, and sand mortar; water and cement slurry; and low-viscosity epoxy have been used for this purpose. Bonded overlays constructed without a bonding agent have performed well in some instances.

5.8.9 Widening

See Section 5.2.16 for guidelines.

5.9 UNBONDED JPCP, JRCP, AND CRCP OVERLAY OF JPCP, JRCP,CRCP, AND AC/PCC

An unbonded JPCP, JRCP, or CRCP overlay of an existing JPCP, JRCP, CRCP, or composite (AC/PCC) pavement can be placed to improve both structural capacity and functional condition. An unbonded concrete overlay consists of the following construction tasks:

(1) Repairing only badly deteriorated areas and making subdrainage improvements (if needed)
(2) Constructing widening (if needed)
(3) Placing a separation layer (this layer may also serve as a leveling course)
(4) Placing the concrete overlay
(5) Sawing and sealing the joints

5.9.1 Feasibility

An unbonded overlay is a feasible rehabilitation alternative for PCC pavements for practically all conditions. They are most cost-effective when the existing pavement is badly deteriorated because of reduced need for pre-overlay repair. Conditions under which a PCC unbonded overlay would not be feasible include:

(1) The amount of deteriorated slab cracking and joint spalling is not large and other alternatives would be much more economical.
(2) Vertical clearance at bridges is inadequate for required overlay thickness. This may be addressed by reconstructing the pavement under the overhead bridges or by raising the bridges. Thicker unbonded overlays may also necessitate raising signs and guardrails, as well as increasing side slopes and extending culverts. Sufficient right-of-way must be available or obtainable to permit these activities.
(3) The existing pavement is susceptible to large heaves or settlements.

If construction duration is critical, PCC overlays may utilize high-early-strength PCC mixes. PCC overlays have been opened within 6 to 24 hours after placement using these mixtures.

5.9.2 Pre-overlay Repair

One major advantage of an unbonded overlay is that the amount of repairs to the existing pavement are greatly reduced. However, unbonded overlays are not intended to bridge localized areas of nonuniform support. The following types of distress (on the next page) should be repaired prior to placement of the overlay to prevent reflection cracks that may reduce its service life.

Guidelines on repairs are provided in References 1 and 3. Other forms of pre-overlay treatment for badly deteriorated pavements include slab fracturing (break/seat, crack/seat, or rubblizing) the existing PCC slab prior to placement of the separation layer. Fracturing and seating the existing slab may provide more uniform support for the overlay.

5.9.3 Reflection Crack Control

When an AC separation layer of 1 to 2 inches is used, there should be no problem with reflection of cracks through unbonded overlays. However, this sep-

Distress Type	Overlay Type	Repair
Working crack	JPCP or JRCP	No repair needed
	CRCP	Full-depth dowelled repair if differential deflection is significant
Punchout	JPCP, JRCP, CRCP	Full-depth repair
Spalled joint	JPCP or JRCP	No repair needed
	CRCP	Full-depth repair of severely deteriorated joints
Pumping	JPCP, JRCP, CRCP	Edge drains (if needed)
Settlement	JPCP, JRCP, CRCP	Level-up with AC
Poor joint/crack load transfer	JPCP, JRCP, CRCP	No repair needed; if pavement has many joints or cracks with poor load transfer, consider a thicker AC separation layer

aration layer thickness may not be adequate for an unbonded overlay when the existing pavement has poor load transfer and high differential deflections across transverse cracks or joints.

5.9.4 Subdrainage

See Section 5.2.4 for guidelines.

5.9.5 Thickness Design

The required thickness of the unbonded overlay is a function of the structural capacity required to meet future traffic demands and the structural capacity of the existing pavement. The required overlay thickness to increase structural capacity to carry future traffic is determined by the following equation.

$$D_{ol} = \sqrt{D_f^2 - D_{eff}^2}$$

where

D_{ol} = Required thickness of unbonded PCC overlay, inches
D_f = Slab thickness to carry future traffic, inches
D_{eff} = Effective thickness of existing slab, inches

Unbonded concrete overlays have been successfully constructed as thin as 5 inches and as thick as 12 inches or more. Thicknesses of seven to 10 inches have been typical for most highway pavement unbonded overlays.

The required overlay thickness may be determined through the following design steps. These design steps provide a comprehensive design approach that recommends testing the pavement to obtain valid design inputs. If it is not possible to conduct this testing, an approximate overlay design may be developed based upon visible distress observations by skipping Steps 4 and 5, and by estimating other inputs.

The overlay design can be done for a uniform section or on a point-by-point basis as described in Section 5.3.1.

Step 1: Existing pavement design.

(1) Existing slab thickness
(2) Type of load transfer (mechanical devices, aggregate interlock, CRCP)
(3) Type of shoulder (tied, PCC, other)

Step 2: Traffic analysis.

(1) Past cumulative 18-kip ESALs in the design lane (N_p), for use in the remaining life method of D_{eff} determination only
(2) Predicted future 18-kip ESALs in the design lane over the design period (N_f)

Step 3: Condition survey.

The following distresses are measured during the condition survey for JPCP, JRCP, and CRCP. Sampling along the project may be used to estimate these quantities in the most heavily trafficked lane. Distress types and severities are defined in Reference 23. Deteriorated means medium or higher severity.

JPCP/JRCP:

(1) Number of deteriorated transverse joints per mile

(2) Number of deteriorated transverse cracks per mile
(3) Number of existing expansion joints, exceptionally wide joints (more than 1 inch) or full-depth, full-lane-width AC patches
(4) Presence and general severity of PCC durability problems
  (a) "D" cracking: low severity (cracks only), medium severity (some spalling), high severity (severe spalling)
  (b) Reactive aggregate cracking: low, medium, high severity
(5) Evidence of faulting, pumping of fines or water at joints, cracks and pavement edge

CRCP:

(1) Number of punchouts per mile
(2) Number of deteriorated transverse cracks per mile
(3) Number of existing expansion joints, exceptionally wide joints (>1 inch) or full-depth, full-lane-width AC patches
(4) Number of existing and new repairs prior to overlay per mile
(5) Presence and general severity of PCC durability problems (NOTE: surface spalling of tight cracks where the underlying CRCP is sound should not be considered a durability problem)
  (a) "D" cracking: low severity (cracks only), medium severity (some spalling), high severity (severe spalling)
  (b) Reactive aggregate cracking: low, medium, high severity
(6) Evidence of pumping of fines or water

*Step 4: **Deflection testing (strongly recommended).***

When designing an unbonded overlay for existing JPCP, JRCP, or CRCP, follow the guidelines given below for deflection testing and determination of the effective static k-value. When designing an unbonded overlay for existing AC/PCC, follow the guidelines given in Section 5.7, Step 4, for deflection testing and determination of the effective static k-value.

Measure slab deflection basins in the outer wheel path along the project at an interval sufficient to adequately assess conditions. Intervals of 100 to 1,000 feet are typical. Measure deflections with sensors located at 0, 12, 24, and 36 inches from the center of load. A heavy-load deflection device (e.g., Falling Weight Deflectometer) and a load magnitude of 9,000 pounds are recommended. ASTM D 4694 and D 4695 provide additional guidance on deflection testing.

For each slab tested, backcalculate the effective k-value using Figure 5.10 or a backcalculation procedure. The AREA of each deflection basin is computed from the following equation.

$$\text{AREA} = 6 * \left[1 + 2\left(\frac{d_{12}}{d_0}\right) + 2\left(\frac{d_{24}}{d_0}\right) + \left(\frac{d_{36}}{d_0}\right)\right]$$

where

d_0 = deflection in center of loading plate, inches
d_i = deflections at 12, 24, and 36 inches from plate center, inches

AREA will typically range from 29 to 32 for sound concrete.

(1) *Effective dynamic k-value.* Enter Figure 5.10 with d_0 and AREA to determine the effective dynamic k-value beneath each slab for a circular load radius of 5.9 inches and magnitude of 9,000 pounds. NOTE that for loads within 2,000 pounds more or less, deflections may be scaled linearly to 9,000-pound deflections.

If a single overlay thickness is being designed for a uniform section, compute the mean effective dynamic k-value of the slabs tested in the uniform section.

(2) *Effective static k-value.*

Effective static k-value

= Effective dynamic k-value/2

The effective static k-value may need to be adjusted for seasonal effects using the approach presented in Part II, Section 3.2.1. However, the k-value can change substantially and have only a small effect on overlay thickness.

*Step 5: **Coring and materials testing.***

When designing an unbonded overlay for existing JPCP, JRCP, or CRCP, coring and materials testing of the existing PCC slab are not needed for overlay thickness design. When designing an unbonded overlay for existing AC/PCC, follow the guidelines given in Section 5.7, Step 5, for determination of the AC modulus by coring and materials testing.

Step 6: Determination of required slab thickness for future traffic (D_f).

The elastic modulus, modulus of rupture, and load transfer inputs to determine D_f for unbonded PCC overlays of PCC and AC/PCC pavements are representative of the new PCC overlay to be placed rather than of the existing slab. This is emphasized because it is the properties of the overlay slab (i.e., elastic modulus, modulus of rupture, and load transfer), which will control the performance of the unbonded overlay.

(1) *Effective static k-value beneath the existing pavement.* Determine from one of the following methods.
   (a) Backcalculate the effective dynamic k-value from deflection basins as described in Step 4. Divide the effective dynamic k-value by 2 to obtain the effective static k-value. The static k-value obtained may need to be adjusted for seasonal effects (see Part II, Section 3.2.1).
   (b) Conduct plate load tests (ASTM D 1196) after slab removal at a few sites. This alternative is very costly and time-consuming and not often used. The static k-value obtained may need to be adjusted for seasonal effects (see Part II, Section 3.2.1).
   (c) Estimate from soils data and base type and thickness, using Figure 3.3 in Part II, Section 3.2. This alternative is simple, but the static k-value obtained must be recognized as a rough estimate. The static k-value obtained may need to be adjusted for seasonal effects (see Part II, Section 3.2.1).

(2) *Design PSI loss.* PSI immediately after overlay (P1) minus PSI at time of next rehabilitation (P2).

(3) *J, load transfer factor for joint design of the unbonded PCC overlay.* See Part II, Section 2.4.2, Table 2.6.

(4) *PCC modulus of rupture of unbonded PCC overlay.*

(5) *Elastic modulus of unbonded PCC overlay.*

(6) *Loss of support.* Use LS = 0 for unbonded PCC overlay.

(7) *Overlay design reliability, R (percent).* See Part I, Section 4.2, Part II, Table 2.2, and Part III, Section 5.2.15.

(8) *Overall standard deviation (S_o) for rigid pavement.* See Part I, Section 4.3.

(9) *Subdrainage capability of existing slab,* after subdrainage improvements, if any. See Part II, Table 2.5, as well as Reference 5, for guidance in determining C_d. Pumping or faulting at joints and cracks determined in Step 3 is evidence that a subdrainage problem exists. In selecting this value, note that the poor drainage situation at the AASHO Road Test would be given a C_d of 1.0.

Compute D_f for the above design inputs using the rigid pavement design equation or nomograph in Part II, Figure 3.7. A worksheet for determining D_f is provided in Table 5.13.

Step 7: Determination of effective slab thickness (D_{eff}) of existing pavement.

The condition survey and remaining life procedures are presented.

D_{eff} From Condition Survey

The effective thickness (D_{eff}) of an existing PCC or AC/PCC pavement is computed from the following equation:

$$D_{eff} = F_{jcu} * D$$

where

D = existing PCC slab thickness, inches (NOTE: maximum D for use in unbonded concrete overlay design is 10 inches even if the existing D is greater than 10 inches)
F_{jcu} = joints and cracks adjustment factor for unbonded concrete overlays

NOTE that the existing AC surface is neglected in determining the effective slab thickness of an existing AC/PCC pavement.

Field surveys of unbonded jointed concrete overlays have shown very little evidence of reflection cracking or other problems caused by the existing slab. Therefore, the F_{dur} and F_{fat} are not used for unbonded concrete overlays. The F_{jcu} factor is modified to show a reduced effect of deteriorated cracks and joints in the existing slab, and is given in Figure 5.13.

(1) *Joints and cracks adjustment factor (F_{jcu}).* This factor adjusts for the extra loss in PSI caused by deteriorated reflection cracks or punchouts in the overlay that result from any unrepaired

Table 5.13. Worksheet for Determination of D_f for Unbonded PCC Overlay

SLAB:

Type of load transfer system: mechanical device, aggregate interlock, CRCP

Type of shoulder = tied PCC, other

PCC modulus of rupture of unbonded overlay (typically 600 to 800 psi) = _____ psi

PCC E modulus of unbonded overlay (3 to 5 million psi) = _____ psi

J load transfer factor of unbonded overlay (2.5 to 4.4 for jointed PCC, 2.3 to 3.2 for CRCP) = _____

TRAFFIC:

Future 18-kip ESALs in design lane over the design period (N_f) = _____

SUPPORT AND DRAINAGE:

Effective dynamic k-value = _____ psi/inch

Effective static k-value = Effective dynamic k-value/2 (typically 50 to 500 psi/inch) = _____ psi/inch

Subdrainage coefficient, C_d (typically 1.0 for poor subdrainage conditions) = _____

SERVICEABILITY LOSS:

Design PSI loss (P1 − P2) = _____

RELIABILITY:

Design reliability, R (80 to 99 percent) = _____ percent

Overall standard deviation, S_o (typically 0.39) = _____

FUTURE STRUCTURAL CAPACITY:

Required slab thickness for future traffic is determined from rigid pavement design equation or nomograph in Part II, Figure 3.7.

D_f = _____ inches

deteriorated joints, cracks and other discontinuities in the existing slab prior to overlay. Very little such loss in PSI has been observed for JPCP or JRCP unbonded overlays.

The following information is needed to determine F_{jcu} to adjust overlay thickness for the extra loss in PSI from deteriorated reflection cracks that are not repaired:

Number of unrepaired deteriorated joints/mile

Number of unrepaired deteriorated cracks/mile

Number of expansion joints, exceptionally wide joints (greater than 1 inch) or full-depth, full-lane-width AC patches/mile

The total number of unrepaired deteriorated joints/cracks and other discontinuities per mile

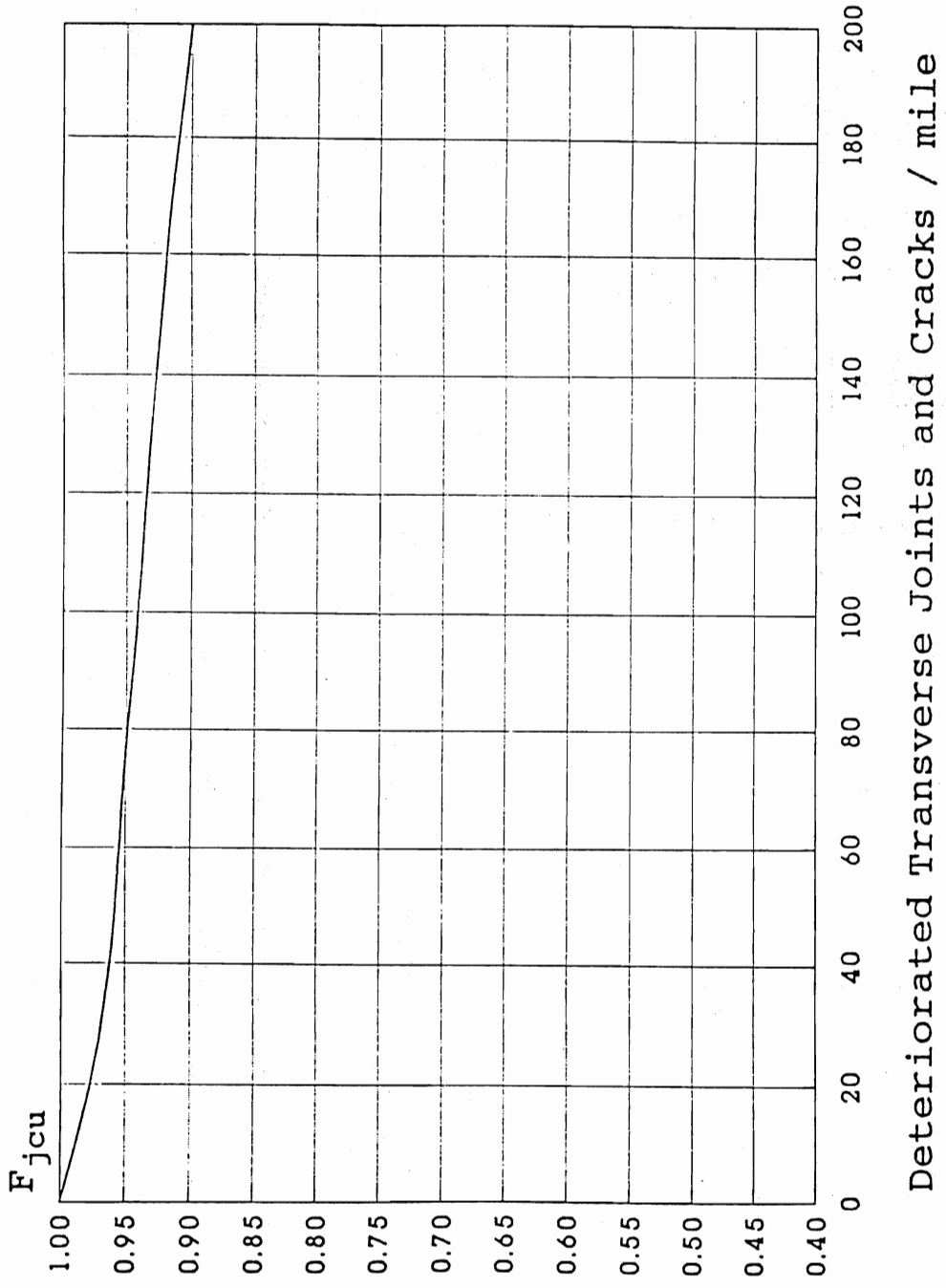

Figure 5.13. F_{jcu} Adjustment Factor for Unbonded JPCP, JRCP, and CRCP Overlays

prior to overlay is used to determine the F_{jcu} from Figure 5.13 for the appropriate type of PCC overlay. As an alternative to extensive full-depth repair for an unbonded overlay to be placed on a badly deteriorated pavement, a thicker AC interlayer should eliminate any reflection cracking problem, so that $F_{jcu} = 1.0$.

D_{eff} From Remaining Life For PCC Pavements

The remaining life of the pavement is given by the following equation:

$$RL = 100\left[1 - \left(\frac{N_p}{N_{1.5}}\right)\right]$$

where

RL = remaining life, percent
N_p = total traffic to date, ESALs
$N_{1.5}$ = total traffic to pavement "failure," ESALs

$N_{1.5}$ may be estimated using the new pavement design equations or nomographs in Part II. To be consistent with the AASHO Road Test and the development of these equations, a "failure" PSI equal to 1.5 and a reliability of 50 percent are recommended.

D_{eff} is determined from the following equation:

$$D_{eff} = CF * D$$

where

CF = condition factor determined from Figure 5.2
D = thickness of the existing slab, inches (NOTE: maximum D for use in unbonded concrete overlay design is 10 inches even if the existing D is greater than 10 inches)

The designer should recognize that D_{eff} determined by this method does not reflect any benefit for preoverlay repair. The estimate of D_{eff} obtained should thus be considered a lower limit value. The D_{eff} of the pavement will be higher if preoverlay repair of load-associated distress is done. It is also emphasized that this method of determining D_{eff} is not applicable to AC/PCC pavements.

A worksheet for determination of D_{eff} is provided in Table 5.14.

Step 8: Determination of Overlay Thickness.

The thickness of unbonded PCC overlay is computed as follows:

$$D_{ol} = \sqrt{D_f^2 - D_{eff}^2}$$

where

D_{ol} = Required thickness of unbonded PCC overlay, inches
D_f = Slab thickness determined in Step 6, inches
D_{eff} = Effective thickness of existing slab determined in Step 7, inches

The thickness of overlay determined from the above relationship should be reasonable when the overlay is required to correct a structural deficiency. See Section 5.2.17 for discussion of factors which may result in unreasonable overlay thicknesses.

5.9.6 Shoulders

See Section 5.2.10 for guidelines.

5.9.7 Joints

Transverse and longitudinal joints must be provided in the same manner as for new pavement construction, except for the following joint spacing guidelines for JPCP overlays. Due to the unusually stiff support beneath the slab, it is advisable to limit joint spacing to the following to control thermal gradient curling stress:

Maximum joint spacing (feet)

= 1.75 * Slab thickness (inches)

Example: slab thickness = 8 inches

joint spacing = 8 * 1.75 = 14 feet

Table 5.14. Calculation of D_{eff} for Unbonded PCC Overlay of JPCP, JRCP, CRCP, and AC/PCC

Condition Survey Method:

JPCP, JRCP, or CRCP Overlay:

F_{jcu} Number of unrepaired deteriorated joints/mile = _____

Number of unrepaired deteriorated cracks/mile = _____

Number of unrepaired deteriorated punchouts/mile = _____

Number of expansion joints, exceptionally wide joints (>1 inch) or full-depth, full-lane-width AC patches/mile = _____

Total/mile = _____

F_{jcu} = _____ (Figure 5.13)

Effective Slab Thickness:

$$D_{eff} = F_{jcu} * D = \_\_\_\_\_$$

NOTES: Maximum D allowed is 10 inches for use in calculating D_{eff} for unbonded overlays. Existing AC surface is neglected in calculating D_{eff} for existing AC/PCC pavement when designing an unbonded PCC overlay.

Remaining Life Method:

N_p = Past design lane ESALs = _____

$N_{1.5}$ = Design lane ESALs to P2 of 1.5 = _____

$$RL = 100\left[1 - \left(\frac{N_p}{N_{1.5}}\right)\right] = \_\_\_\_\_$$

CF = _____

$$D_{eff} = CF * D = \_\_\_\_\_$$

NOTE: Maximum D allowed is 10 inches for use in calculating D_{eff} for unbonded overlays.

5.9.8 Reinforcement

Unbonded JRCP and CRCP overlays must contain reinforcement to hold cracks tightly together. The design of the reinforcement would follow the guidelines given for new pavement construction, except that the friction factor would be high (e.g., 2 to 4) due to bonding between the AC separation layer and the new PCC overlay (see Part II, Section 3.4).

5.9.9 Separation Interlayer

A separation interlayer is needed between the unbonded PCC overlay and the existing slab to isolate the overlay from the cracks and other deterioration in the existing slab. The most common and successfully used separation interlayer material is an AC mixture placed one inch thick. If a level-up is needed the AC interlayer may also be used for that purpose (*29, 30*).

Some thin materials that have been used as bondbreakers have not performed well. Other thin layers have been used successfully, including surface treatments, slurry seals, and asphalt with sand cover for existing pavements without a large amount of faulting or slab breakup. For heavily trafficked highways, the potential problem of erosion of the interlayer must be considered. A thin surface treatment may erode faster than an AC material. There is no reason that a permeable open-graded interlayer cannot be used, provided a drainage system is designed to collect the water from this layer. This type of interlayer would provide excellent reflective crack control as well as preventing pumping and erosion of the interlayer.

5.9.10 Widening

See Section 5.2.16 for guidelines.

5.10 JPCP, JRCP, AND CRCP OVERLAY OF AC PAVEMENT

JPCP, JRCP, and CRCP overlays of AC pavement can be placed to improve both structural capacity and functional conditions. This type of overlay consists of the following major construction tasks:

(1) Repairing deteriorated areas and making subdrainage improvements (if needed)
(2) Constructing widening (if needed)
(3) Milling the existing surface if major distortion or inadequate cross-slope exists
(4) Placing an AC leveling course (if needed)
(5) Placing the concrete overlay
(6) Sawing and sealing the joints

5.10.1 Feasibility

A PCC overlay is a feasible rehabilitation alternative for AC pavements for practically all conditions. They are most cost-effective when the existing pavement is badly deteriorated. Conditions under which a PCC overlay would not be feasible include:

(1) The amount of deterioration is not large and other alternatives would be much more economical.
(2) Vertical clearance at bridges is inadequate for required overlay thickness. This may be addressed by reconstructing the pavement under the overhead bridges or by raising the bridges. Thicker PCC overlays may also necessitate raising signs and guardrails, as well as increasing side slopes and extending culverts. Sufficient right-of-way must be available or obtainable to permit these activities.
(3) The existing pavement is susceptible to large heaves or settlements.

If construction duration is critical, PCC overlays may utilize high-early-strength PCC mixes. PCC overlays have been opened within 6 to 24 hours after placement using these mixtures.

5.10.2 Pre-overlay Repair

One major advantage of a JPCP, JRCP, or CRCP overlay over AC pavement is that the amount of repair required for the existing pavement is greatly reduced. However, the following types of distress (on the next page) should be repaired prior to placement of the overlay to prevent reflection cracks that may reduce its service life. Guidelines on repairs are provided in References 1 and 3.

5.10.3 Reflection Crack Control

Reflection cracking is generally not a problem for JPCP, JRCP, or CRCP overlays of AC pavement. However, if the existing AC pavement has severe transverse thermal cracks, it may be desirable to place some type of separation layer over the transverse cracks to reduce the potential for reflection cracking.

Distress Type	Overlay Type	Repair Type
Alligator cracking	JPCP or JRCP	No repair needed
	CRCP	Patch areas with high deflections
Transverse cracks	JPCP, JRCP, CRCP	No repair needed
Pumping, stripping	JPCP, JRCP, CRCP	Edge drains (if needed)
		Remove stripping layer if severe
Settlement/heave	JPCP, JRCP, CRCP	Level-up with AC

5.10.4 Subdrainage

See Section 5.2.4 for guidelines.

5.10.5 Thickness Design

The required thickness of the PCC overlay is a function of the structural capacity required to meet future traffic demands and the support provided by the underlying AC pavement. The required overlay thickness to increase structural capacity to carry future traffic is determined by the following equation.

$$D_{ol} = D_f$$

where

D_{ol} = Required thickness of PCC overlay, inches
D_f = Slab thickness to carry future traffic, inches

PCC overlays of AC pavement have been successfully constructed as thin as 5 inches and as thick as 12 inches or more. Seven to 10 inches has been typical for most highway pavement overlays.

The required overlay thickness may be determined through the following design steps. These design steps provide a comprehensive design approach that recommends testing the pavement to obtain valid design inputs. If it is not possible to conduct this testing, an approximate overlay design may be developed based upon visible distress observations by skipping Steps 4 and 5, and by estimating other inputs.

The overlay design can be done for a uniform section or on a point-by-point basis as described in Section 5.3.1.

Step 1: Existing pavement design.

(1) Existing material types and layer thicknesses.

Step 2: Traffic analysis.

(1) Predicted future 18-kip ESALs in the design lane over the design period (N_f).

Step 3: Condition survey.

A detailed survey of distress conditions is not required. Only a general survey that identifies any of the following distresses that may affect the performance of a PCC overlay is needed:

(1) Heaves and swells.
(2) Signs of stripping of the AC. This could become even more serious under a PCC overlay.
(3) Large transverse cracks that, without a new separation layer, may reflect through the PCC overlay.

Step 4: Deflection testing (strongly recommended).

Measure deflection basins in the outer wheel path along the project at an interval sufficient to adequately assess conditions. Intervals of 100 to 1,000 feet are typical. A heavy-load deflection device (e.g., Falling Weight Deflectometer) and a load magnitude of 9,000 pounds are recommended. ASTM D 4694 and D 4695 provide additional guidance on deflection testing. Deflections should be measured at the center of the load and at least one other distance from the load, as described in Section 5.4.5, Step 4.

For each point tested, backcalculate the subgrade modulus (M_R) and the effective pavement modulus (E_p) according to the procedures described in Section 5.4 for AC pavements.

(1) *Effective dynamic k-value.* Estimate the effective dynamic k-value from Figure 3.3 in Part II, Section 3.2, using the backcalculated subgrade resilient modulus (M_R), the effective modulus of the pavement layers above the subgrade (E_p), and the total thickness of the pavement layers above the subgrade (D). It is emphasized that the backcalculated subgrade

resilient modulus value used to estimate the effective dynamic k-value should *not* be adjusted by the C factor (e.g., 0.33) which pertains to establishing the design M_R for AC overlays of AC pavements.

If a single overlay thickness is being designed for a uniform section, compute the mean effective dynamic k-value of the uniform section.

Step 5: Coring and materials testing.

Unless some unusual distress condition exists, coring and materials testing are not required.

Step 6: Determination of required slab thickness for future traffic (D_f).

(1) *Effective static k-value (at bottom of PCC overlay over an existing AC pavement).* Determine from one of the following methods.
   (a) Determine the effective dynamic k-value from the backcalculated subgrade modulus M_R, pavement modulus E_p, and pavement thickness D as described in Step 4. Divide the effective dynamic k-value by 2 to obtain the static k-value. The static k-value may need to be adjusted for seasonal effects (see Part II, Section 3.2.1).
   (b) Estimate from soils data and pavement layer types and thicknesses, using Figure 3.3 in Part II, Section 3.2. The static k-value obtained may need to be adjusted for seasonal effects (see Part II, Section 3.2.1).

(2) *Design PSI loss.* PSI immediately after overlay (P1) minus PSI at time of next rehabilitation (P2).

(3) *J, load transfer factor for joint design of the PCC overlay.* See Part II, Section 2.4.2, Table 2.6.

(4) *Modulus of rupture of PCC overlay.* Use mean 28-day, third-point-loading modulus of rupture of the overlay PCC.

(5) *Elastic modulus of PCC overlay.* Use mean 28-day modulus of elasticity of overlay PCC.

(6) *Loss of support.* See Part II.

(7) *Overlay design reliability, R (percent).* See Part I, Section 4.2, Part II, Table 2.2, and Part III, Section 5.2.15.

(8) *Overall standard deviation (S_o) for rigid pavement.* See Part I, Section 4.3.

(9) *Subdrainage capability of existing AC pavement,* after subdrainage improvements, if any. See Part II, Table 2.5, as well as Reference 5, for guidance in determining C_d. In selecting this value, note that the poor drainage situation at the AASHO Road Test would be given a C_d of 1.0.

Compute D_f for the above design inputs using the rigid pavement design equation or nomograph in Part II, Figure 3.7. When designing an overlay thickness for a uniform pavement section, mean input values must be used. When designing an overlay thickness for specific points along the project, the data for that point must be used. A worksheet for determining D_f is provided in Table 5.15.

Step 7: Determination of Overlay Thickness.

The PCC overlay thickness is computed as follows:

$$D_{ol} = D_f$$

The thickness of overlay determined from the above relationship should be reasonable when the overlay is required to correct a structural deficiency. See Section 5.2.17 for discussion of factors which may result in unreasonable overlay thicknesses.

5.10.6 Shoulders

See Section 5.2.10 for guidelines.

5.10.7 Joints

See Section 5.8.7 for guidelines.

5.10.8 Reinforcement

See Section 5.8.8 for guidelines.

5.10.10 Widening

See Section 5.2.16 for guidelines.

Table 5.15. Worksheet for Determination of D_f for PCC Overlay of AC Pavement

SLAB:

Type of load transfer system: mechanical device, aggregate interlock, CRCP

Type of shoulder = tied PCC, other

PCC modulus of rupture of unbonded overlay (typically 600 to 800 psi) = _____ psi

PCC E modulus of unbonded overlay (3 to 5 million psi) = _____ psi

J load transfer factor of unbonded overlay (2.5 to 4.4 for jointed PCC, 2.3 to 3.2 for CRCP) = _____

TRAFFIC:

Future 18-kip ESALs in design lane over the design period (N_f) = _____

SUPPORT AND DRAINAGE:

Effective dynamic k-value = _____ psi/inch

Effective static k-value = Effective dynamic k-value/2 (typically 50 to 500 psi/inch) = _____ psi/inch

Subdrainage coefficient, C_d (typically 1.0 for poor subdrainage conditions) = _____

SERVICEABILITY LOSS:

Design PSI loss (P1 − P2) = _____

RELIABILITY:

Design reliability, R (80 to 99 percent) = _____ percent

Overall standard deviation, S_o (typically 0.39) = _____

FUTURE STRUCTURAL CAPACITY:

Required slab thickness for future traffic is determined from rigid pavement design equation or nomograph in Part II, Figure 3.7.

D_f = _____ inches

REFERENCES FOR CHAPTER 5

1. Federal Highway Administration, "Pavement Rehabilitation Manual," Pavement Division, Office of Highway Operations, Washington, D.C. (current edition).
2. Darter, M.I., Barenberg, E.J., and Yrjanson, W.A., "Joint Repair Methods For Portland Cement Concrete Pavements," NCHRP Report No. 281, Transportation Research Board, 1985.
3. "Techniques for Pavement Rehabilitation," Training Course Participants Notes, National Highway Institute, Federal Highway Administration, 3d Edition, 1987.
4. Snyder, M.B., Reiter, M.J., Hall, K.T., and Darter, M.I., "Rehabilitation of Concrete Pavements, Volume I—Repair Rehabilitation Techniques," Report No. FHWA-RD-88-071, Federal Highway Administration, 1989.
5. Smith, K.D., Peshkin, D.G., Darter, M.I., Mueller, A.L., and Carpenter, S.H., "Performance of Jointed Concrete Pavements, Phase I, Volume 5, Data Collection and Analysis Procedures," Federal Highway Administration Report No. FHWA/RD/89/140, March 1990.
6. Finn, F.N., and Monismith, C.L., "Asphalt Overlay Design Procedures," NCHRP Synthesis No. 116, Transportation Research Board, 1984.
7. Vespa, J.W., Hall, K.T., Darter, M.I., and Hall, J.P., "Performance of Resurfacing of JRCP and CRCP on the Illinois Interstate Highway System," Illinois Highway Research Report No. 517-5, Federal Highway Administration Report No. FHWA-IL-UI-229, 1990.
8. Darter, M.I., Elliott, R.P., and Hall, K.T., "Revision of AASHTO Pavement Overlay Design Procedures, Appendix: Overlay Design Examples," NCHRP Project 20-7/Task 39, Final Report, April 1992.
9. Darter, M.I., Elliott, R.P., and Hall, K.T., "Revision of AASHTO Pavement Overlay Design Procedures, Appendix: Documentation of Design Procedures," NCHRP Project 20-7/Task 39, April 1992.
10. Halstead, W.J., "Criteria For Use of Asphalt Friction Surfaces," NCHRP Synthesis No. 104, Transportation Research Board, 1983.
11. Thompson, M.R. and Robnett, Q.L., "Resilient Properties of Subgrade Soils," Final Report—Data Summary, Transportation Engineering Series No. 14, Illinois Cooperative Highway Research and Transportation Program Series No. 160, University of Illinois at Urbana-Champaign, 1976.
12. Taylor, M.L., "Characterization of Flexible Pavements by Nondestructive Testing," Ph.D. thesis, University of Illinois at Urbana-Champaign, 1979.
13. Carpenter, S.H., "Layer Coefficients for Flexible Pavements," ERES Consultants, Inc., report for Wisconsin DOT, August 1990.
14. Figueroa, J.L., "Resilient-Based Flexible Pavement Design Procedure for Secondary Roads," Ph.D. thesis, University of Illinois at Urbana-Champaign, 1979.
15. Raad, L. and Figueroa, J.L., "Load Response of Transportation Support Systems," *Transportation Engineering Journal*, American Society of Civil Engineers, Volume 106, No. TE1, 1980.
16. Pavement Consultancy Services/Law Engineering, "Guidelines and Methodologies for the Rehabilitation of Rigid Highway Pavements Using Asphalt Concrete Overlays," for National Asphalt Paving Association, June 1991.
17. Pavement Consultancy Services/Law Engineering, "FWD Analysis of PA I-81 Rubblization Project," for Pennsylvania Department of Transportation, February 1992.
18. Hall, K.T., "Performance, Evaluation, and Rehabilitation of Asphalt Overlaid Concrete Pavements," Ph.D. thesis, University of Illinois at Urbana-Champaign, 1991.
19. Schutzbach, A.M., "Crack and Seat Method of Pavement Rehabilitation," *Transportation Research Record* No. 1215, 1989.
20. Kilareski, W.P. and Bionda, R.A., "Performance/Rehabilitation of Rigid Pavements, Phase II, Volume 2—Crack and Seat and AC Overlay

of Rigid Pavements," Federal Highway Administration Report No. FHWA-RD-89-143, 1989.
21. Ahlrich, R.C., "Performance and Structural Evaluation of Cracked and Seated Concrete," *Transportation Research Record* No. 1215, 1989.
22. Thompson, M.R., "Breaking/Cracking and Seating Concrete Pavements," NCHRP Synthesis No. 144, 1989.
23. Smith, K.D., Darter, M.I., Rauhut, J.B., and Hall, K.T., "Distress Identification Manual for the Long-Term Pavement Performance (LTPP) Studies," Strategic Highway Research Program, 1988.
24. Southgate, H.F., "An Evaluation of Temperature Distribution Within Asphalt Pavements and its Relationship to Pavement Deflection," Kentucky Department of Highways, Research Report KYHPR-64-20, 1968.
25. Shell International Petroleum Company, "Pavement Design Manual," London, England, 1978.
26. Asphalt Institute, "Research and Development of the Asphalt Institute's Thickness Design Manual (MS-1) Ninth Edition," Research Report 82-2, 1982.
27. Hoffman, M.S. and Thompson, M.R., "Mechanistic Interpretation of Nondestructive Pavement Testing Deflections," Transportation Engineering Series No. 32, Illinois Cooperative Highway and Transportation Research Series No. 190, University of Illinois at Urbana-Champaign, 1981.
28. Peshkin, D.G., Mueller, A.L., Smith, K.D., and Darter, M.I., "Structural Overlay Strategies for Jointed Concrete Pavements, Vol. 3: Performance Evaluation and Analysis of Thin Bonded Concrete Overlays," Report No. FHWA-RD-89-144, Federal Highway Administration, 1990.
29. Hutchinson, R.L., "Resurfacing With Portland Cement Concrete," NCHRP Synthesis No. 99, Transportation Research Board, 1982.
30. Voigt, G.F., Carpenter, S.H., and Darter, M.I., "Rehabilitation of Concrete Pavements, Volume II—Overlay Rehabilitation Techniques," Report No. FHWA-RD-88-072, Federal Highway Administration, 1989.

G.2 1993 年 AASHTO 加鋪設計法 (張記恩期末報告)

鋪面評估與維修期末報告

1993年AASHTO加鋪設計法

授課先生：李英豪　老師

學生姓名：張記恩

學　　號：684310260

繳交日期：1996/06/27

1993 年 *AASHTO* 加鋪設計法

前言

隨著社會的進步與發展，道路使用者對於鋪面所提供之舒適程度要求日益增高，道路管理者爲保持行車介面的舒適、平坦及安全，相關鋪面維修技術因此孕育而生，而加鋪(*Overlay*)即爲其中的一項重要維修方法。

加鋪作業簡單而言乃是利用適當的方法對欲施行加鋪之道路進行結構性的評估，配合相關設計法則及恰當的施工方式，在原路面上方鋪上一層新的鋪面材料，如此一來不但改善舊有道路的行車品質，更增加了鋪面的結構強度，阻隔舊有鋪面的壞機制及提昇鋪面服務之年限，因此加鋪成爲維持鋪面能力的重要工作，而加鋪設計法的重要性自然也不亞於新建鋪面之設計。

第一節 研究動機與目的

由於國內公路養護單位長期以來對於加鋪作業均採取固定之模式，設計準則也多經由工程師的判斷與經驗而得，故不經濟的加鋪設計則經常發生，而因加鋪設計與施工時考慮的不周全，造成加鋪後不平整或反射裂縫(*reflection cracking*)等缺失，導致加鋪的失敗，更無形中浪費了許多社會成本。

本研究擬對 *1993* 年改版的 *AASHTO* 加鋪設計法爲主幹，進行相關設計觀念的闡述及設計流程與步驟的說明，予以中文化並製成講義，提供對鋪面加鋪設計學習的方便性，期望藉此一拋磚引玉動作，能引起各界對加鋪設計之重視，進而提昇國內加鋪設計之水準。

第二節 基本觀念介紹

2-1 設計理念

1993 年 *AASHTO* 加鋪設計法基本上仍是承襲有效厚度法則(*effective thickness approach*)爲設計基礎，參考圖一所示，其觀念乃假設鋪面新建時之有效結構承載力 SC_0 與鋪面服務績效 P_1 會隨交通荷重負載的增加而逐年減退爲 SC_{eff} 與 P_{eff}，若決定鋪面服務績效下降至 P_2 時進行加鋪作業，則考量未來預期承受交通量與現存鋪面狀況，以新建路面設計法求得需求結構承載力 SC_f，並運用適當方法評估現存鋪面有效結構承載力 SC_{eff}，兩者相減所得之差即爲加鋪需提供之結構承載力 SC_{OL}，表示式如下：

$$SC_{OL} = SC_f - SC_{eff}$$

根據此原則，將鋪面有效結構承載力 *SC* 視爲 *AASHTO* 規範定義之柔性路面結構數 *SN*，與剛性路面厚度 *D*，即可方便求得加鋪需求厚度。

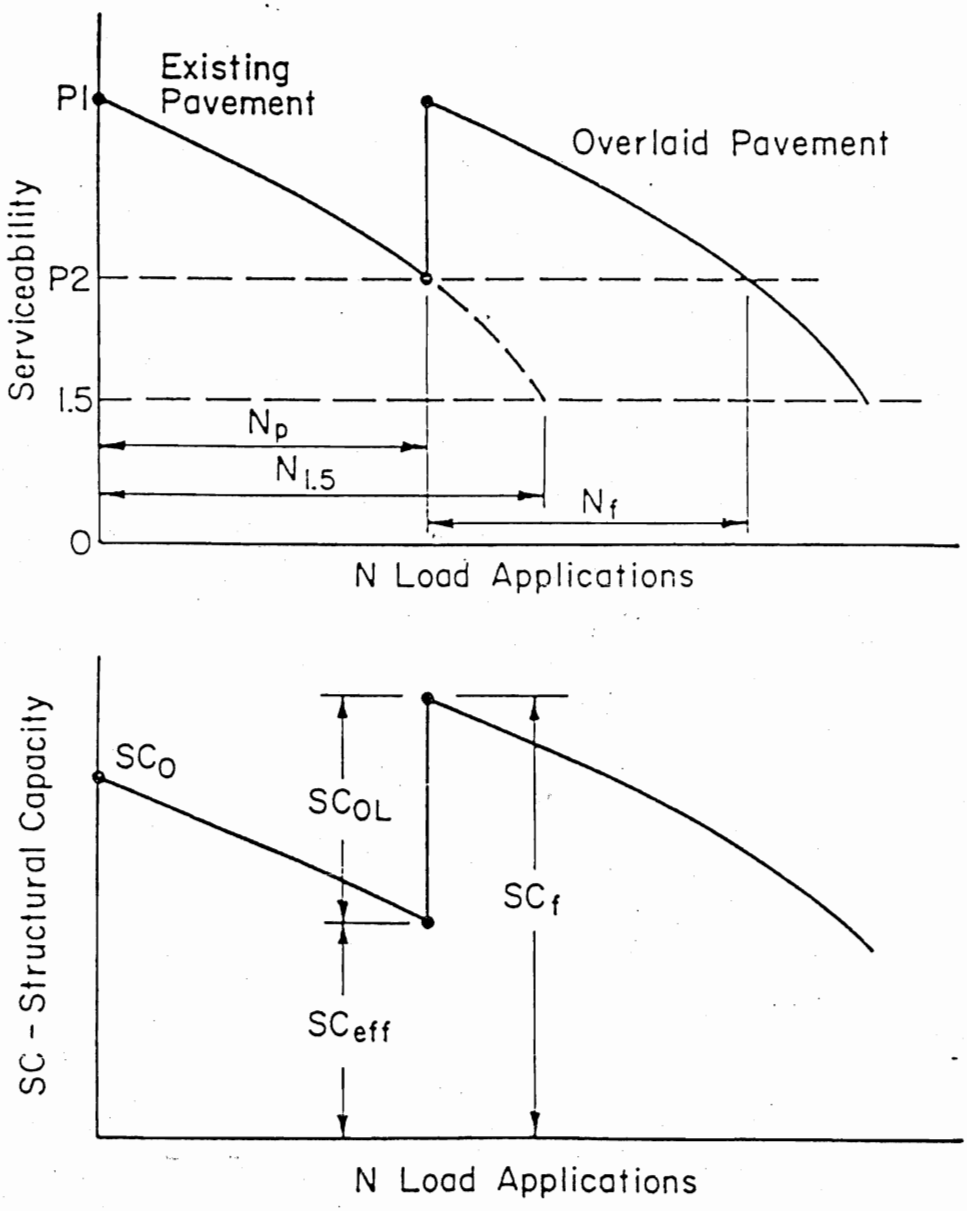

圖一 鋪面服務能力、結構數與交通荷重次數關係圖

2-2 各類加鋪組合基本公式

爲適用於各種不同材質組合的加鋪狀況，規範針對各類加鋪組合，建議運用柔性路面設計法 SN 或剛性路面設計法 D ，將新建、現存及欲加鋪之鋪面材料轉換成等值厚度，待求得加鋪等值厚度後，經材料性質轉換即可得加鋪厚度需求值。各類加鋪組合之加鋪厚度計算公式如表一所示：

表一 加鋪厚度計算公式

加鋪材料	現存鋪面	加鋪設計公式	備註
AC	AC	$h_{ol}= SN_{ol}/a$ $=(Snf- SN_{eff})/a$	$SN=SC$
AC	Break/PCC	$h_{ol}= SN_{ol}/a$ $=(Snf- SN_{eff})/a$	$SN=SC$
AC	PCC	$D_{ol}=A(Df-Deff)$	$D=D_{ol}$;A 爲材料轉換因子。
AC	AC/PCC	$D_{ol}=A(Df-Deff)$	$D=D_{ol}$;A 爲材料轉換因子。
Bound PCC	PCC	$D_{ol}= Df-Deff$	$D= D_{ol}$
Unbound PCC	PCC	$D^2_{ol}= D^2f-D^2_{eff}$	$D= D_{ol}$
PCC	AC	$D_{ol}= Df$	視 AC 爲路基重新設計。

第三節 加鋪前準備工作

3-1 各類破壞形式修復方法

爲確保舊有之破壞在加鋪後數年內不會影響加鋪路面的結構完整性，加鋪前應勘查現有路面之破壞類型與狀況，確實調查產生原因並加以改善。以下將就不同加鋪材料與現有鋪面類型組合，分析各種形式的鋪面就其不同類型破壞的建議處置方法。

3-1-1 AC 材料加鋪於 AC 路面

此種加鋪組合因兩者材料特性相同故考量較爲單純，不同類型破壞的建議處置方法如表二所主要目的除避免反射裂縫之外，亦重視加鋪前表面之平整，避免日後因加鋪層厚度不同而造成不均勻沈陷狀況發生。

表二 AC 材料加鋪於 AC 路面不同類型破壞的建議處置方法

破壞形式	破壞狀況	修護方法
1.鱷魚皮裂縫	輕、中度	加鋪前使用纖維、開放級配等材料處理以阻止反射裂縫發生。
	重度	去除面層及下方之鬆軟土層。
2.線型裂縫	寬度< 0.25 in	修補(patch)。
	寬度> 0.25 in	壓入填縫料並加以修補。
	經常發生嚴重裂縫地點	加鋪前施以阻止反射裂縫材料處理。
3.車轍	輕度	刨除或以適當材料填平。
	重度	同輕度，並於加鋪前確實調查車轍原因，並加以改善。
4.表面不平整	凹洞、隆起、波浪狀等	調查發生原因，並去除及復原破壞層。

3-1-2 AC 材料加鋪於經破碎處理之 PCC 路面

此狀況爲舊有 PCC 路面板經 *break/seat* 、 *crack/seat* 與 *rubblized/compact* 等處理，其主要目的乃希望經由降低原鋪面板尺寸，減少因溫度造成過量水平變位而產生反射裂縫。此處理方式對反射裂縫的防止成效目前尚不明確，但值得注意的是除水平變位外，因交通荷重造成之垂直變位亦爲反射裂縫的發生主因，故除破碎處理之外，利用適當填充料加於經破碎處理路面，以確保均勻的荷重承載，亦爲加鋪前的處理重點。

3-1-3 AC 材料加鋪於 JPCP 、JRCP 與 CRCP 路面

不同類型破壞的建議處置方法如表三所述：

表三 AC 加鋪於 PCC 路面不同類型破壞建議處置方法

破壞形式	修護方法
1.工作裂縫	全厚度修復及鋪面板替換。
2.貫穿(punchouts)	全厚度修復。
3.嚴重破壞區的修補	全厚度修復。
4.接縫處破裂(spalling joints)	全厚度或部份厚度修復。
5.斷裂與唧水(pumping/faulting)	排水處理。
6.沈陷	板塊提昇或部分重建。

表中敘述的全厚度修復(*full-depth repair*)及鋪面板替換(*slab replacement*)等加鋪前處理工作所用之材料均應爲波特蘭水泥混凝土，於 *CRCP* 上舊有的修補 *AC* 材料亦須完全去除，且於修復 *JPCP* 、*JRCP* 配合繫筋與縱縫筋、*CRCP* 配置連續鋼筋與原鋪面結構接合，以確保荷重確實傳遞。過去曾有使用 *AC* 進行全厚度修復，但其結果則易於 *AC* 修復部份產生坑洞及反射裂縫等不良結果。

3-1-4 AC 材料加鋪於 *AC/JPCP* 、*AC/JRCP* 與 *AC/CRCP* 路面

對於 *AC* 材料加鋪於 *AC/JPCP* 、*AC/JRCP* 與 *AC/CRCP* 路面，不同類型破壞的建議處置方法如表四所述：

表四 *AC* 加鋪於 *AC/PCC* 路面不同類型破壞建議處置方法

破壞形式	破壞狀況	修護方法
1.車轍	重度	刨除
2.反射裂縫	輕度	*AC/JPCP* 、*AC/JRCP* 壓入填縫料修補，但 *AC/CRCP* 則需調查再在給予適當處理。
	中、重度	全厚度修復及鋪面板替換。
3.貫穿(punchouts)	——	全厚度修復。
4.嚴重破壞區的修補	——	全厚度修復。
5.局部 *PCC* 破壞	——	全厚度修復。
6.局部 *AC* 破壞	——	*AC* 材料修補(patch)。
7.唧水(pumping)	——	排水處理。
8.沈陷	——	板塊提昇或部分重建。

當任何程度的反射裂縫發生於 *AC/CRCP* 或中、重度反射裂縫發生於 *AC/JPCP* 、*AC/JRCP* 路面時，經驗顯示下方之剛性路面極可能有工作裂縫、接縫破壞及修復失敗等情況發生，且嚴重程度將大於表面所見，故建議配合鑽心取樣評估鋪面狀況。而表中敘述的全厚度修復及鋪面板替換，除利用 *PCC* 材料配合繫筋、縮縫筋與連續鋼筋修復之外，更要在加鋪前填上與舊有路面相等厚度之 *AC* 材料。

3-1-5 PCC 材料(*Bounded*)加鋪於 *JPCP* 、*JRCP* 與 *CRCP* 路面

各種破壞的修復方式完全與 *2-1-3* 節中所提 *AC* 材料加鋪於 *JPCP* 、*JRCP* 與 *CRCP* 路面之修復方式相同。

3-1-6 PCC 材料(*Unbounded*)加鋪於 *JPCP* 、*JRCP* 、*CRCP* 與 *AC/PCC* 路面

由於 *Unbounded PCC* 材料加鋪方式可避免舊有路面水平位移的傳遞，因此加鋪前的處理工作只需專注於舊有鋪面是否能提供加鋪層均勻的承載力，表五將敘述不同類型破壞的建議處置方法。

表五 *Unbounded PCC* 加鋪於 PCC 路面不同類型破壞建議處置方法

破壞形式	加鋪材料	舊有鋪面修護方法
1.工作裂縫	CRCP	若程度相當嚴重，則進行修補(patch)。
	JPCP 、JRCP	不需處理。
2.貫穿(punchouts)	JPCP 、JRCP 及 CRCP	全厚度修復。
3.接縫處破裂 (spalling joints)	JPCP 、JRCP	不需處理，若傳遞荷重情況太差則可考慮利用 AC 材料填充。
	CRCP	對嚴重破壞接縫處進行全厚度修復。
4.沈陷	JPCP 、JRCP 及 CRCP	利用 AC 材料填平
5.唧水(pumping)	JPCP 、JRCP 及 CRCP	排水處理。

另針對經破碎處理之 *PCC* 路面，則建議在加鋪前鋪上一隔離層(sparation layer)，以確保原鋪面能提供均勻的承載力。

3-1-7 JPCP 、*JRCP* 與 *CRCP* 加鋪於 *AC* 路面

此種加鋪狀況前之修復工作，主要爲避免反射裂縫的發生，因此根據不同破壞類型與欲加鋪之剛性鋪面形式，有不同的修復方式如表六：

表六 PCC 加鋪於 AC 路面不同類型破壞建議處置方法

破壞形式	加鋪材料	舊有鋪面修護方法
1.鱷魚皮裂縫	CRCP	若程度相當嚴重，則進行全厚度修復及鋪面板替換。
	JPCP 、JRCP	不需處理。
2.橫向裂縫	JPCP 、JRCP 及 CRCP	不需處理。
3.嚴重沈陷	JPCP 、JRCP 及 CRCP	利用 AC 材料填平
4.唧水與剝脫 (pumping/stripping)	JPCP 、JRCP 及 CRCP	排水處理或去除剝脫層。

3-2 反射裂縫的控制

反射裂縫發生的原因，爲原有路面上之接縫與裂縫因溫度、濕度改變造成之水平方向位移，或交通荷重所造成之垂直位移傳遞到加鋪層，造成加鋪層的裂縫破壞而嚴重折減加鋪層之服務績效與結構強度，因此加鋪設計時必須考慮現有鋪面的接縫類型、損害形式與程度，於施工時選取適當避免反射裂縫發生的措施，包括增加 HMA 加鋪厚度、在兩介質間鋪上開放級配的隔離材、加勁格網，或在加鋪後立即在原有接縫(*joint*)與裂縫處鋸開，甚有將原路面經破壞處理

(*fractured*)成小塊狀等，藉由減少位移傳遞狀況達到避免反射裂縫的發生。

第四節 現存鋪面有效厚度求取

4-1 柔性鋪面 SN_{eff} 求取

AASHTO 建議三種柔性路面現存有效結構數 SN_{eff} 評估法則，分別爲非破壞性撓度檢測法、現地目測調查評估法與現存鋪面殘餘壽年法三種，由於三種評估法理念各不相同，結果差異甚大，因此建議三種方法均進行評估，再視需要取較保守值爲設計之用。

4-1-1 非破壞性撓度檢測法

規範建議使用落重撓度儀(*FWD*)，參考 *ASTM D4694* 與 *D4695* 之非破壞性撓度檢測相關規定，配合下述步驟評估現存有效結構數 SN_{eff}。

*1.*求取路床回彈模數值 M_R

鋪面受荷重時表面撓度盤(*deflection basin*)外側撓度值大小通常反應路床回彈模數值之高低，故規範建議使用下式概估路床回彈模數值 M_R：

$$M_R = \left(\frac{0.24\,P}{d_r\,r} \right)$$

其中 M_R 爲路床回彈模數值(*psi*)， P 爲施加荷重(*lbs* ；規範建議使用 *9000 lb*)，d_r 爲離荷重中心距離所量得之撓度值(*in*)，r 爲離荷重中心距離(*in*)，距離 r 的選取則建議 $r \geq 0.7a_e$，求取公式如下。

$$a_e = \sqrt{\left[a^2 + \left(D * \sqrt[3]{\left(E_p / M_R \right)} \right)^2 \right]}$$

公式中 a_e 爲路床與鋪面之間應力分佈半徑(*in* ； *stress bulb*)， a 爲荷重盤半徑(*in* ；建議取 *5.9 in*)， D 爲鋪面各層總厚度(*in*)， E_p 爲路床以上鋪面有效回彈模數值(*psi*)， M_R 爲路床回彈模數值(*psi*)。

根據上述公式，取離荷重中心距離 r 所量得之撓度值，得路床回彈模數值 M_R，並已知鋪面各層總厚度 D，施加荷重 P 及荷重中心之撓度值 d_0，其中撓度值 d_0，需根據施測當時材料溫度(*F*)及其路面形式參考圖二(瀝青面層及波特蘭水泥處裡底層路面)、圖三(瀝青面層及瀝青處裡底層底層路面)之修正係數，將撓度值 d_0 修正至標準溫度 70 F，以去除溫度對撓度值的影響。故可查圖四得路床以上鋪面有效回彈模數值 E_p，並帶回 a_e 公式中檢查 r 是否恰當，若符合 $r \geq 0.7a_e$ 之規定，則 SN_{eff} 可由下式求得。

$$SN_{eff} = 0.0045D \sqrt[3]{E_p}$$

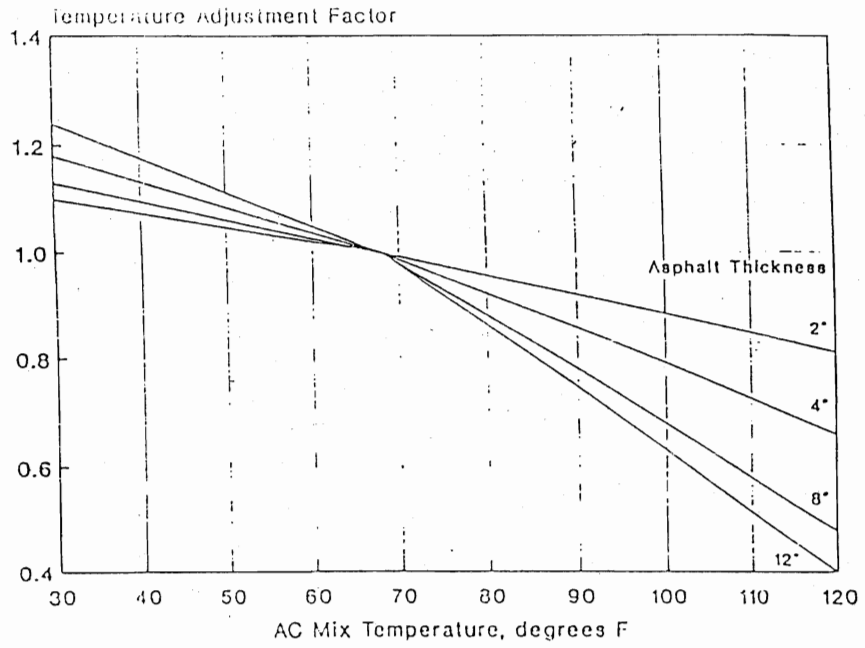

圖二 瀝青面層及波特蘭水泥處裡底層路面溫度修正係數圖

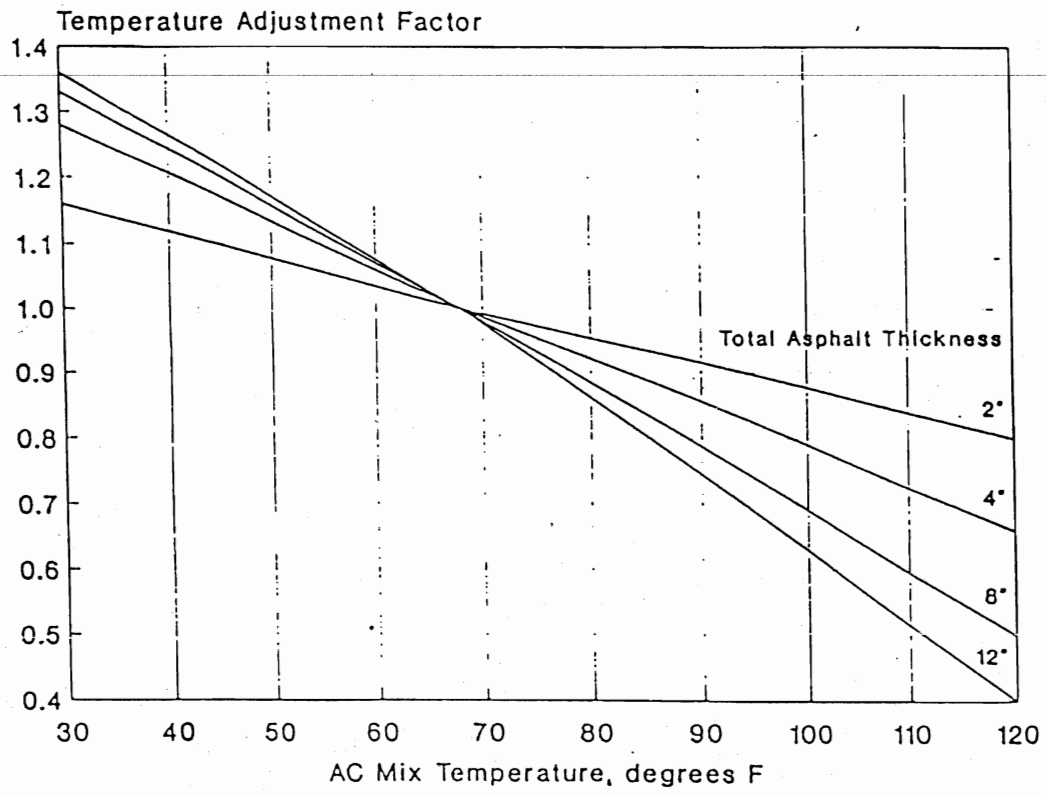

圖三 瀝青面層及瀝青處裡底層底層路面溫度修正係數圖

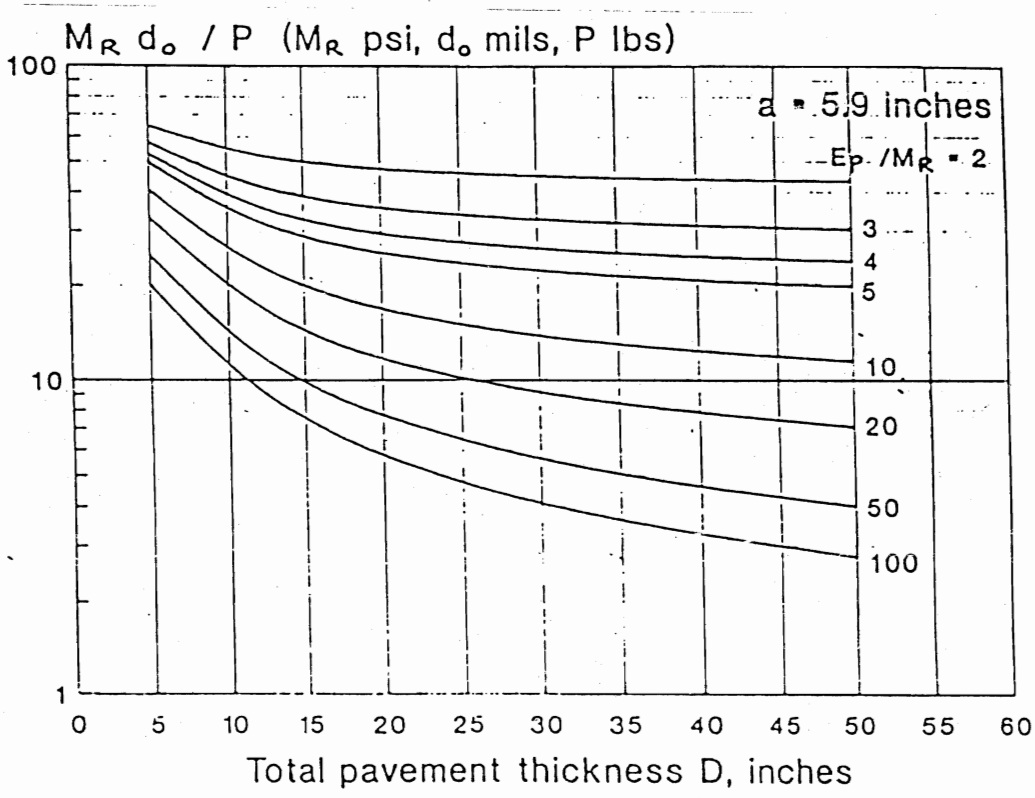

圖四 路床以上柔性鋪面撓度、厚度與回彈模數值 E_P 關係圖

4-1-2 現地目測調查評估法

鋪面材料由於交通荷重與氣候的影響，導致材料發生破壞進而影響其回彈模數值，因此現地目測調查評估法根據各類型破壞的程度及水分對基、底層之影響，適當降低層係數 a_1~a_3，並配合鋪面結構數公式 $SN_{eff}=a_1D_1+a_2D_2m_2+a_3D_3m_3$，即可評估路面現存有結構數。

表七提出各類型破壞對基、底層層係數的折減建議表，其中裂縫的破壞百分比爲(線性裂縫(*feet*)/平方英尺)*100，若機底層有唧水現象發生，則建議經由鑽心評估對基、底層的層係數 a_2、a_3 及排水係數 m_2、m_3 進行折減。令若基、底層爲碎石級配料，並無明顯破壞且排水狀況良好，則不需折減其層係數。

4-1-3 現存鋪面殘餘壽年法

現存鋪面殘餘壽年法主要觀念乃依據鋪面已承受之交通量及預估能承受交通量的比值，評估鋪面殘餘壽年，表示式如下：

$$RL = 100\left[1-\left(\frac{N_x}{N_f}\right)\right]$$

公式中 *RL* 爲鋪面殘餘壽年百分比，N_x 爲加鋪前鋪面已承受之交通量(*ESAL*)，N_f 爲預估當鋪面服務能力達破壞程度時所能承受之交通量(*ESAL*)。

另就評估鋪面結構強度方面，*AASHTO* 建立評估鋪面狀況因子 *CF*(*condirion factor*)，表式如下：

$$CF = \frac{SN_n}{SN_o}$$

其中 SN_n 爲加鋪前鋪面有效結構數，SN_o 爲鋪面新建之鋪面結構數。將上述鋪面殘餘壽年百分比 *RL* 與鋪面狀況因子 *CF*，分析其數值關

係式並考量眞實結構數遞減狀況(appendix cc)，訂定殘餘壽年百分比與鋪面狀況因子關係式。

$$CF = 1 - 0.7 \times e^{-(RL+0.85)^2}$$

故評估鋪面現存有效結構數步驟如下：

1.計算殘餘壽年百分比 RL 。

2.將 RL 帶入殘餘壽年百分比與鋪面狀況因子關係式求取 CF 。

3.計算鋪面現存有效結構數 $SN_{eff} = CF \times SN_o$ 。

表七 各類型破壞對基、底層層係數的折減建議表

MATERIAL	SURFACE CONDITION	COEFFICIENT
AC Surface	Little or no alligator cracking and/or only low-severity transverse cracking	0.35 to 0.40
	< 10 percent low-severity alligator cracking and/or < 5 percent medium- and high-severity transverse cracking	0.25 to 0.35
	> 10 percent low-severity alligator cracking and/or < 10 percent medium-severity alligator cracking and/or > 5–10 percent medium- and high-severity transverse cracking	0.20 to 0.30
	> 10 percent medium-severity alligator cracking and/or < 10 percent high-severity alligator cracking and/or > 10 percent medium- and high-severity transverse cracking	0.14 to 0.20
	> 10 percent high-severity alligator cracking and/or > 10 percent high-severity transverse cracking	0.08 to 0.15
Stabilized Base	Little or no alligator cracking and/or only low-severity transverse cracking	0.20 to 0.35
	< 10 percent low-severity alligator cracking and/or < 5 percent medium- and high-severity transverse cracking	0.15 to 0.25
	> 10 percent low-severity alligator cracking and/or < 10 percent medium-severity alligator cracking and/or > 5–10 percent medium- and high-severity transverse cracking	0.15 to 0.20
	> 10 percent medium-severity alligator cracking and/or < 10 percent high-severity alligator cracking and/or > 10 percent medium- and high-severity transverse cracking	0.10 to 0.20
	> 10 percent high-severity alligator cracking and/or > 10 percent high-severity transverse cracking	0.08 to 0.15
Granular Base or Subbase	No evidence of pumping, degradation, or contamination by fines	0.10 to 0.14
	Some evidence of pumping, degradation, or contamination by fines	0.00 to 0.10

4-2 剛性鋪面 D_{eff} 求取

AASHTO 建議兩種剛性路面現存有效厚度 D_{eff} 評估法則，分別爲現地目測調查評估法與現存鋪面殘餘壽年法兩種，分述如下：

4-2-1 現地目測調查評估法

由於加鋪前的修復工作會因各種主、客關因素而無法完全修復，此法乃將經加鋪前修復之剛性路面上仍殘餘的破壞型態，依據其破壞程度與將來對加鋪層服務能力所產生的影響，設定對現存路面厚度適當折減值，進而求取剛性路面現存有效厚度 D_{eff}，其計算式如下。

$$D_{eff} = F_{jc} \times F_{dur} \times F_{fat} \times D$$

計算式中 D_{eff} 爲剛性路面現存有效厚度(*in*)， D 爲現存剛性路面厚度(*in*)，而折減係數 F_{jc}、F_{dur} 與 F_{fat} 之選取規定如下：

1.接縫與裂縫折減係數 F_{jc}

考慮損壞的接縫與鋪面裂縫對未來加鋪層會造成反射裂縫，圖五提供每一英里內所包含之損壞的接縫與鋪面裂縫長度所對應之接縫與裂縫折減係數 F_{jc} 值。

2.耐久性折減係數 F_{dur}

若現存剛性路面存有影響加鋪層耐久性之破壞，如：裂縫以及裂縫、角隅處破碎(*spall*)，則耐久性折減係數 F_{dur} 建議如表八：

表八 耐久性折減係數 F_{dur}

F_{dur}	破壞狀況
1.00	現存剛性路面無明顯耐久性破壞。
0.99~0.96	有耐久性裂縫存在但無裂縫及角隅處破碎。
0.95~0.88	有耐久性裂縫存與部份裂縫及角隅處破碎。
0.88~0.80	有明顯裂縫存與嚴重裂縫及角隅處破碎。

3.疲勞破壞折減係數 F_{fat}

觀察現有路面之疲勞破壞，如 *JPCP* 與 *JRCP* 出現之橫向裂縫及 *CRCP* 之貫穿破壞，並參照表九評估現存剛性鋪面板之疲勞破壞。

表九 疲勞破壞折減係數 F_{fat}

F_{fat}	鋪面形式	破壞程度
1.00~0.97	JPCP	<5 %之路面板有裂縫產生。
	JRCP	每英里之工作裂縫(working crack)小於 25 個。
	CRCP	每英里之貫穿破壞(punchout)小於 4 個。
0.96~0.94	JPCP	5~15 %之路面板有裂縫產生。
	JRCP	每英里之工作裂縫(working crack)介於 25~75 個。
	CRCP	每英里之貫穿破壞(punchout)介於 4~12 個。
0.93~0.90	JPCP	<15 %之路面板有裂縫產生。
	JRCP	每英里之工作裂縫(working crack)大於 75 個。
	CRCP	每英里之貫穿破壞(punchout)大於 12 個。

另外，對於 *UNBONDED PCC* 加鋪型態而言，經驗顯示原先鋪面之耐久性破壞與疲勞破壞對加鋪層並不造成影響，因此，於評估剛性路面現存有效厚度 D_{eff} 則不考慮折減值 F_{dur} 與 F_{fat} ，而是利用 F_{jcu} 值作爲折減係數值，計算式表示如下。

$$D_{eff} = F_{jcu} \times D$$

計算式中 D_{eff} 爲剛性路面現存有效厚度(in)， D 爲現存剛性路面厚度(in)， F_{jcu} 值參考圖六所示。

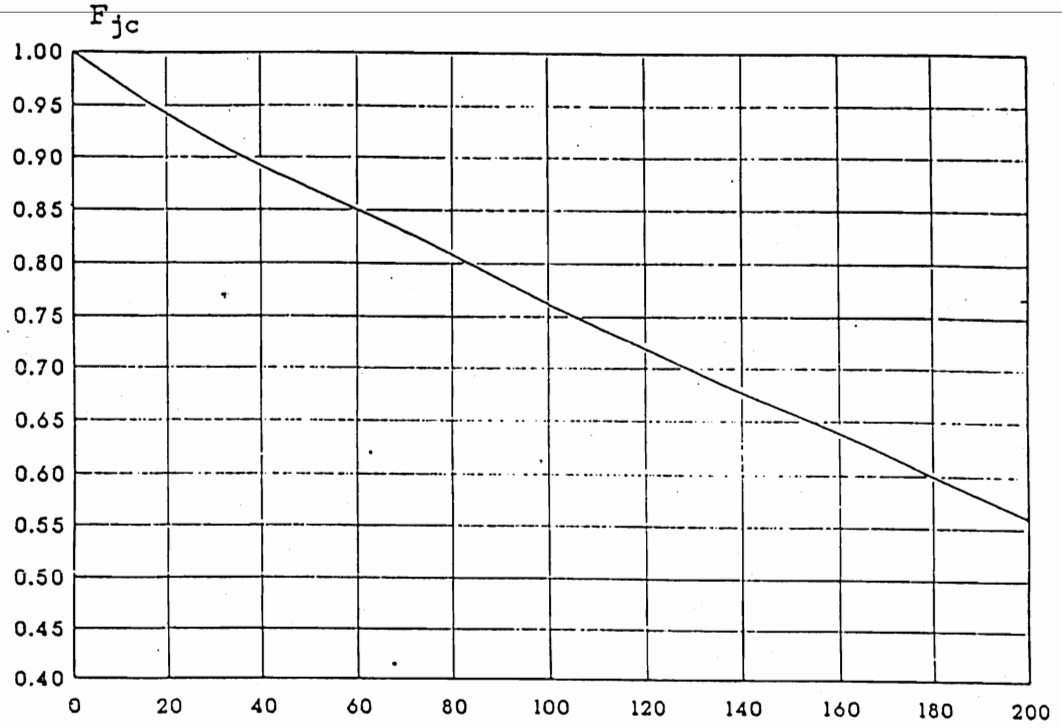

圖五 每一英里內損壞接縫、鋪面裂縫長度與裂縫折減係數 F_{jc} 關係圖

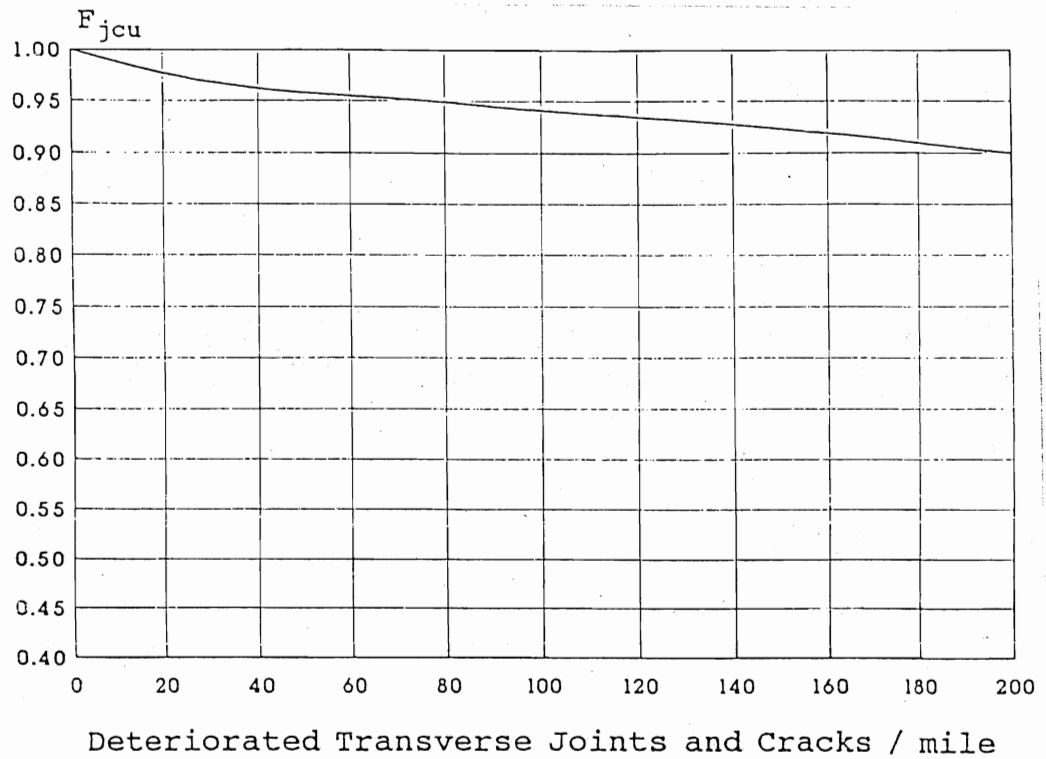

圖六 *UNBOUND PCC* 加鋪型態之 F_{jcu} 折減係數值

4-2-2 現存鋪面殘餘壽年法

1.評估鋪面殘餘壽年

$$RL = 100\left[1 - \left(\frac{N_x}{N_f}\right)\right]$$

2.將 *RL* 帶入殘餘壽年百分比與鋪面狀況因子關係式求取 *CF*

剛性鋪面狀況因子 *CF*(*condirion factor*)，表式如下：

$$CF = \frac{D_n}{D_o}$$

其中 D_n 爲加鋪前鋪面有效厚度，D_o 爲鋪面新建之鋪面厚度。而殘餘壽年百分比與鋪面狀況因子關係式如下

$$CF = 1 - 0.7 \times e^{-(RL+0.85)^2}$$

3.計算鋪面現存有效厚度 $D_{eff} = CF \times D_o$ 。

4-3 AC/PCC 鋪面 *Deff* 求取

因 *AC/PCC* 於評估現存路面有效厚度 *Deff* 時，需考量兩種材料個別之特性，故 *AASHTO* 建議採用現地目測調查評估法，評估殘餘的破壞型態與其破壞程度對將來對加鋪層服務能力所產生的影響，以避免繁雜之評估步驟，其評估式如下：

$$D_{eff} = \left(D_{pcc} * F_{jc} * F_{dur}\right) + \left[\left(\frac{D_{ac}}{2.0}\right) * F_{ac}\right]$$

計算式中 D_{pcc} 爲剛性路面現存厚度(*in*)， D_{ac} 爲現存柔性路面厚度(*in*)，而折減係數 F_{jc} 與 F_{dur} 之選取規定與 *4-2-1* 節所述相同，而 *AC* 破壞折減係數 F_{ac} 必須針對 *AC* 材料所發生之破壞形式給予適當折減值，故破壞形式應不包含反射裂縫，而應是部份刨除亦無法避

免之車轍、剝脫、風化等破壞，表十即根據不同 *AC* 材料破壞形式給予建議折減值。

表十 破壞折減係數 F_{ac}

F_{ac}	破壞程度
1.00	無明顯 *AC* 材料之破壞形式。
0.99~0.96	無法以刨除避免之輕微材料風化。
0.95~0.88	明顯 *AC* 材料之破壞，如：車轍、剝脫、風化等。
0.88~0.80	嚴重的車轍、剝脫、風化等 *AC* 材料破壞。

4-4 經破碎處理之 *PCC* 鋪面 SN_{eff} 求取

經破碎處理 *PCC* 路面現存有效結構數 SN_{eff} 的求取，規範建議使用鋪面結構數公式 $SN_{eff}=a_2D_2m_2+a_3D_3m_3$ 評估之，公式中 D_2 、D_3 為經破碎處理 *PCC* 路面板及處理底層厚度，a_2 、a_3 為經破碎處理路面之層係數，m_2 、m_3 為經破碎處理路面之排水係數。

工程師於評估經破碎處理路面之排水係數 m_2 、m_3 時，若排水情況不明，則建議求取保守值 m_2 、$m_3=1.0$ 。表十一則提供經破碎處理路面之 a_2 、a_3 層係數建議值，工程師可依現地破碎路面傳遞荷重、殘餘強度等狀況較保守之層係數值。

表十一 經破碎處理路面之 a_2 、a_3 層係數建議值

材料形式	破壞處理狀況	層係數
Break/Seat JRCP	破片大於一英尺，且鋼筋與混凝土仍接合。	0.35 ~ 0.25
Crack/Seat JPCP	破片介於 2 ~3 英尺。	0.35 ~0.20
any pavement type	破片均小於一英尺。	0.30~0.14
Base/subbase granular	無明顯侵蝕破壞。	0.14 ~0.10
Base/subbase stabilized	部份侵蝕破壞。	0.10 ~0.00

第五節 加鋪需求結構強度求取

5-1 柔性鋪面設計法

柔性鋪面設計法適用於求取 *AC* 加鋪於 *AC* 路面以及 *AC* 加鋪於 *Break PCC* 路面之加鋪類型，鋪面所需結構強度設計步驟與新建柔性路面設計步驟完全相同，唯設計者於估計未來預期交通量時，應根據選擇柔性鋪面等值軸重因子(*EALF*)，作爲估計 *18-kip* 等值單軸重(*EASL*)交通量之用，此外，路基土壤模數值 M_r 應將現地經 *NDT* 施測所得之模數值乘上 *0.33* 之模數折減值，表示式如下：

$$M_R = C * \left(\frac{0.24P}{d_r r} \right)$$

公式中 *C* 爲應力修正因子(規範建議使用 *C=0.33*)，而基底層排水係數可經由非破壞性撓度檢測法或根據現地狀況，選擇足以反應加鋪時現存鋪面之狀況值，以求得加鋪需求鋪面結構數 SN_f 值。

5-2 剛性鋪面設計法(*Bound*)

剛性鋪面設計法(*Bound*)適用於 *AC* 加鋪於 *PCC* 路面、 *AC* 加鋪於 *AC /PCC* 路面以及 *PCC* 加鋪於 *Bound PCC* 路面等加鋪類型之鋪面所需結構強度的求取，唯前兩種加鋪類形於求得加鋪需求厚度後，在經由轉換因子 *A*(見圖七)將需求之剛性加鋪厚度轉換成 AC 所需加鋪厚度。

剛性鋪面設計法(*Bound*)之設計步驟與新建剛性路面設計步驟完全相同，但設計時相關設計參數必須根據現有路面狀況進行評估而

得，，以充分表示現地之狀況，各參數之求取敘述如下：

*1.*加鋪後預期交通量

估計預期交通量時，應選擇剛性路面之等值軸重因子(*EALF*)，作為估計 *18-kip* 等值單軸重(*EASL*)交通量。

*2.*路床有效反力模數值 *k*

路床有效反力模數值 *k* 之求取建議使用非破壞性撓度檢測法，利用半徑 *a=5.9in* 荷重盤施予 *9000 lb* 荷重，並於施測時讀取距荷重中心 *0* 、*12* 、*24* 及 *36 in* 處之撓度值，帶入下式求取 *AREA* 值

$$AREA = 6 * \left[1 + 2\left(\frac{d_{12}}{d_0}\right) + 2\left(\frac{d_{24}}{d_0}\right) - \left(\frac{d_{36}}{d_0}\right) \right]$$

公式中 d_0 、d_{12} 、d_{24} 、d_{36} 分別為距荷重中心 *0* 、*12* 、*24* 及 *36 in* 處之撓度值。由 *AREA* 值配合荷重中心 *0 in* 處之撓度值 d_0 ，查圖八即可求得動態路床有效反力模數值 $k_{dynamic}$，則路床有效反力模數值 $k = k_{dynamic}/2$ 即可得。

若為 *AC* 加鋪於 *AC /PCC* 路面，則上式之 d_0 必須以 $d_{0\,PCC}$ 代替之，$d_{0\,PCC}$ 即為面層量得之 d_0 扣除 *AC* 材料所佔之 $d_{0\,compress}$ 之值($d_{0\,PCC} = d_0 - d_{0\,compress}$)求取如下：

i. 若原 *AC /PCC* 路面為 *BONDED*

$$d_{0\,compress} = -0.0000328 + 121.5006 * \left(\frac{D_{ac}}{E_{ac}}\right)^{1.0798}$$

ii. 若原 *AC /PCC* 路面為 *UNBONDED*

$$d_{0\,compress} = -0.00002133 + 38.6872 * \left(\frac{D_{ac}}{E_{ac}}\right)^{0.94551}$$

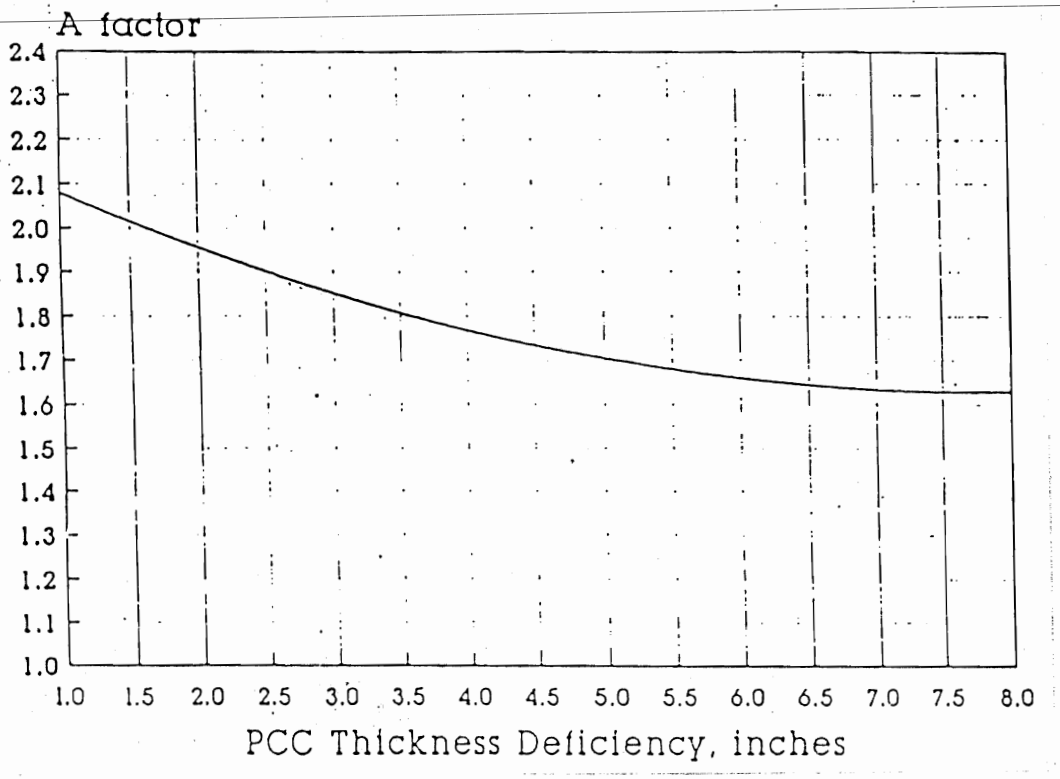

圖七 剛性路面厚度轉換柔性路面厚度之轉換係數 A 圖

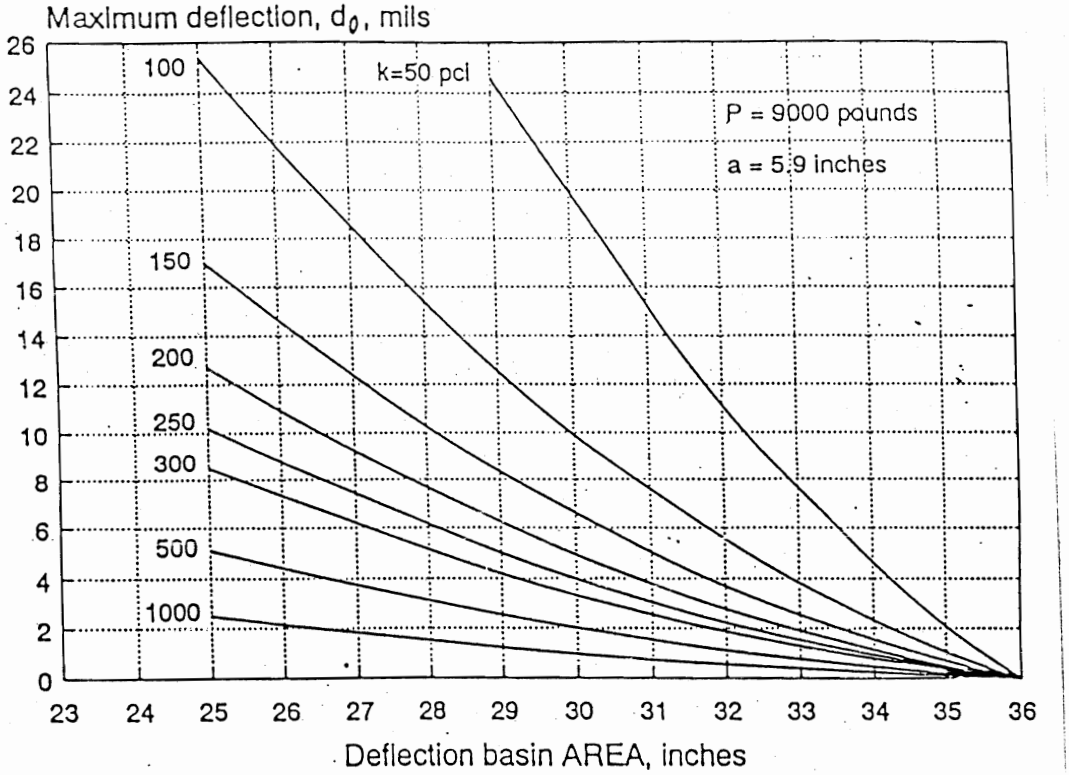

圖八 撓度盤面積與動態路床反力模數 $k_{dynamic}$ 關係圖

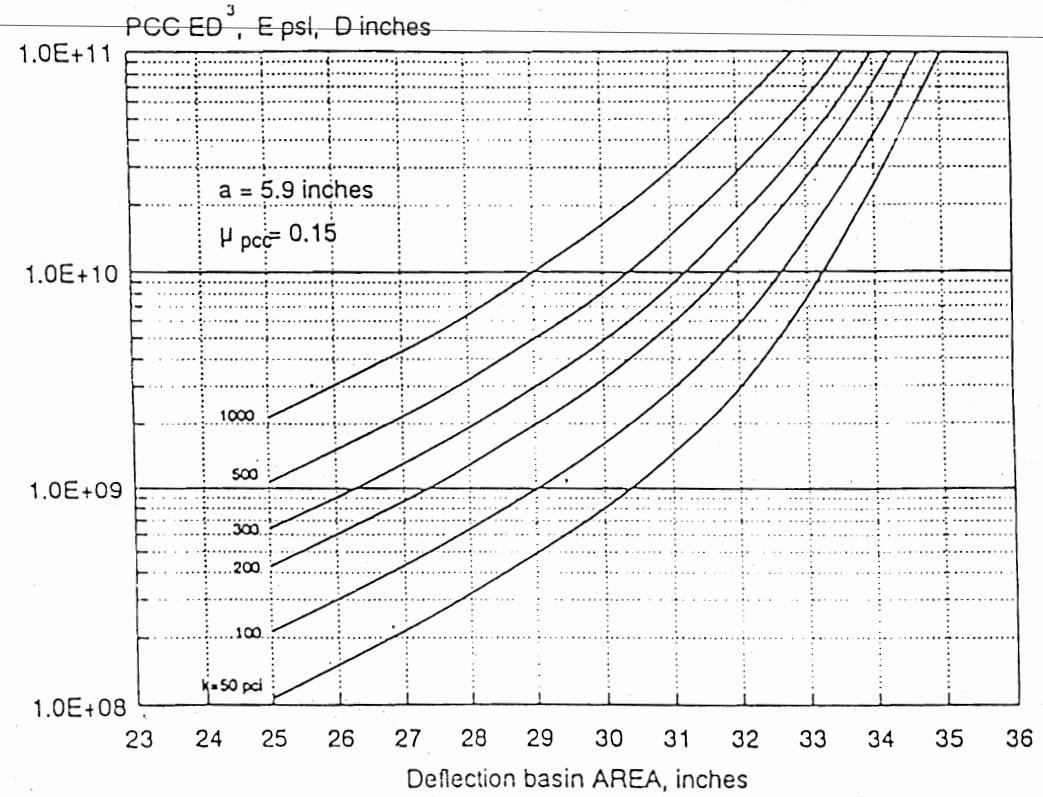

圖九 撓度盤面積與剛性路面模數值 E 關係圖

3.混凝土楊氏模數 E

混凝土楊氏模數的求取除可利用鑽心取得之圓柱試體進行間接拉力試驗，進而推演混凝土楊氏模數外，亦可使用非破壞性撓度檢測法，將求得之 $AREA$ 值配合路床有效反力模數值 k，查圖九即可得柏松比 $\nu=0.15$ 之混凝土 $E \times D^3$ 值，再將現有路面厚度 D 帶入，即可得混凝土楊氏模數 E 值。

4.混凝土破裂模數 S_c'

混凝土破裂模數 S_c' 之求取可分下列兩種

(1)取鑽心取得之 $6\ in$ 直徑圓柱試體進行間接拉力試驗，求得間接拉力強度 IT 後，帶入下式即可得混凝土破裂模數 S_c'。

$$S_c' = 210 + 1.021(IT)$$

(2)利用非破壞性撓度檢測法回算所得混凝土楊氏模數 E 值，帶入下式即可得混凝土破裂模數 S_c'。

$$S_c' = 43.5\left(\frac{E}{10^6}\right) + 488.5$$

5.荷重傳遞係數 J

為評估現有路面荷重傳遞係數 J 作為需求厚度設計之用，針對 *JPCP* 與 *JRCP* 路面時，建議在鋪面板接縫處利用落重撓度儀於接縫一邊施壓，量測施加荷重版接縫邊緣處下陷 Δ_{load} 與未施加荷重版接縫邊緣處下陷 Δ_{unload}，如圖十所示，並同時計算施壓側撓度 d_0 與未施壓側撓度 d_{12} 之比值 $B(B= d_0/ d_{12})$，帶入下式求取撓度荷重傳遞百分比(*deflection load transfer*)

$$\Delta LT = 100 * \left(\frac{\Delta_{unload}}{\Delta_{load}}\right) * B$$

其中 ΔLT 為撓度荷重傳遞百分比，d_0 為施壓側之撓度值，d_{12} 為未施壓側之撓度值，B 為於該版中央施測時荷重中心撓度值 d_0 /距荷重中心 *12 in* 之撓度值 d_{12} 之比值，一般約在 *1.05~1.15* 之間。

再求得為撓度荷重傳遞百分比後，參考表十二選擇適當之荷重傳遞係數 J。

表十二 荷重傳遞係數 J

撓度荷重傳遞百分比 ΔLT	荷重傳遞係數 J
＞70	3.2
50~70	3.5
＜50	4.0

對於 *CRCP* 路面，規範則建議於加鋪厚度設計時，荷重傳遞係數 J 應介於 *2.2~2.6* 之間。

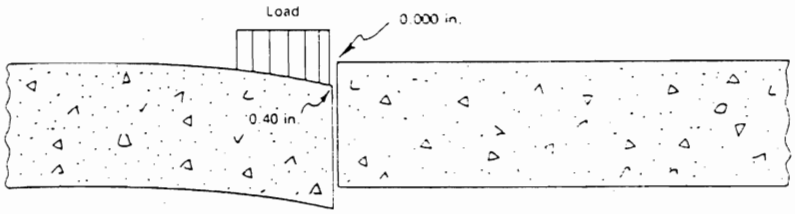

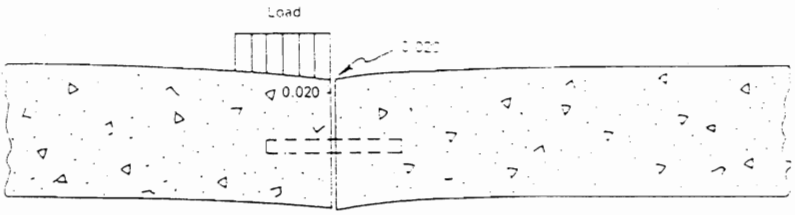

圖十 荷重傳遞施測示意圖

Example:

D_{SB} = 6 inches

E_{SB} = 20,000 psi

M_R = 7,000 psi

Solution: k_∞ = 400 pci

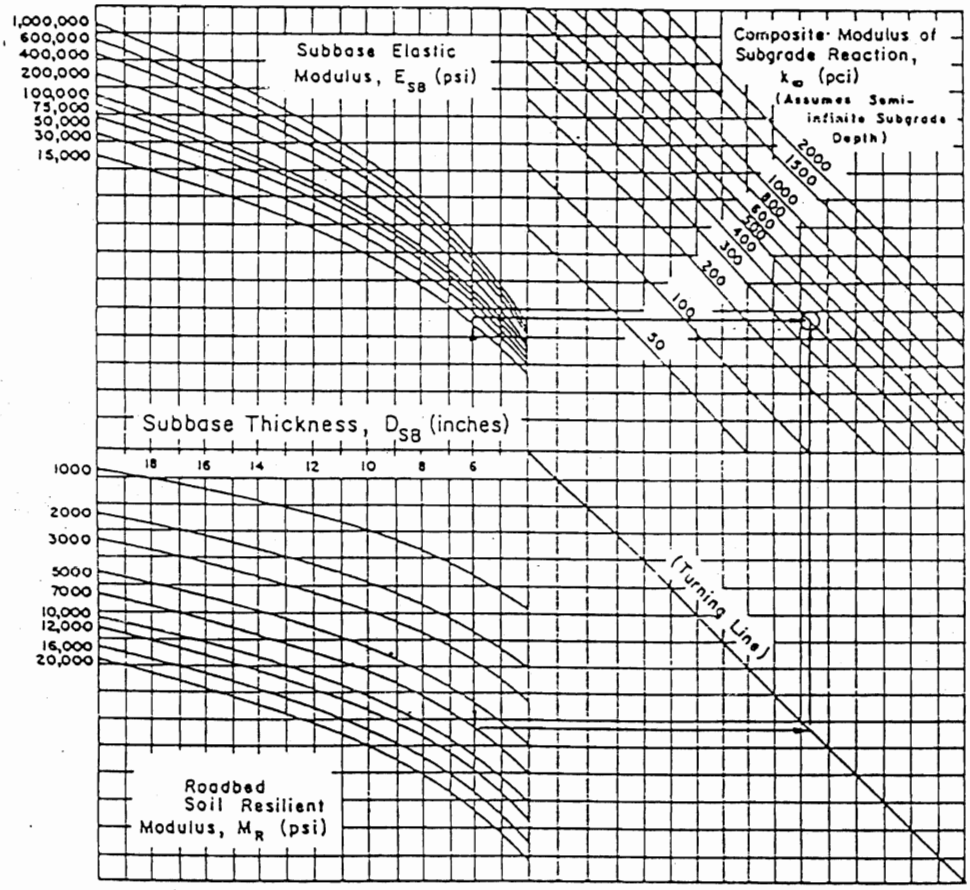

圖十一 路床反力模數與路床回彈模數值、基層楊氏模數值關係圖

5-3 剛性鋪面設計法(*UnBound*)

PCC 加鋪於 *Unbound PCC* 路面與 *PCC* 加鋪於 *AC* 路面，均屬於視原路面爲路基承載層因此於設計加鋪需求結構時，除應考慮現有鋪面所提供之路基承載力外，其餘設計步驟與相關參數之使用均比照全新路面厚度設計。

對於 *PCC* 加鋪於 *AC* 路面，路基承載力評估除可利用鑽心試驗而得，亦可參考 *3-1-1* 節所述，利用非破壞性撓度檢測法，求得 *AC* 路面楊氏模數值與路床土壤值後，查圖十一求取路床反力模數值 *k*。而 *PCC* 加鋪於 *Unbound PCC* 路面可參照 *4-2* 節所述，運用非破壞性撓度檢測法求取路床反力模數值 *k*。

第六節 實例應用

公路主管機關之鋪面維修程序，乃於例行性的鋪面調查資料中確認現有鋪面有不符需求時，經相關資料的蒐集配合成本分析與非經濟因素分析等最佳化(*Optimization*)分析技術訂定出維修方案，並開始著手細部設計。

本節即以 *AC* 加鋪於 *AC* 路面與 *PCC* 加鋪於 *PCC* 路面爲例，進行加鋪厚度設計演算，並對於加鋪設計給予適當建議。

6-1 *AC* 加鋪於 *AC* 路面

某路段 *AC* 路面之相關資訊與現存結構強度、*NDT* 檢測資料、目測調查資料等，如表十三所示，今考慮於加鋪後提供 *2,400,000*(*Flexible ESAL*)交通量，請依據 *1993* 年 *AASHTO* 加鋪設計

法設計加鋪厚度。

表十三 現存*AC*路面之相關資訊

現存現存*AC*路面結構與交通資料

鋪面層材料	新建時層係數	鋪面厚度(in)
AC SURFACE	0.44	4.25
GRAN BASE	0.14	8.00

SN_0=2.99　　總鋪面厚度： 12.25 in

$N_{1.5}$ = 1,140,161 ESAL　　N_P = 400,000 ESAL

*NDT*檢測資料

荷重(lbs)	荷重半徑 *a* (in)	溫度校正 d_0 (mils)	溫度校正 d_r (mils)
9000	5.9	12.80	3.55

r = 36 inches

目測調查資料

鋪面層材料	評估層係數(考參表七)	排水係數 m	SN_{eff}
AC SURFACE	0.35	1.00	1.49
GRAN BASE	0.14	1.00	1.12

總 SN_{eff} = 2.61

6-1-1 非破壞性撓度檢測法

*1.*求取路床回彈模數值 M_R

$$M_R = \left(\frac{0.24 * 9000}{0.00355 * 36}\right) = 16{,}901\,psi$$

*2.*求取路床以上鋪面有效回彈模數值 E_p

已知得路床回彈模數值 M_R =16901 *psi* 並已知鋪面各層總厚度 D=12.25 *in* ，施加荷重 P=9000 *lb* 及荷重中心之撓度值 d_o=12.80 *mils*，撓度值 d_r=3.55 *mils*，查圖四可得 E_p / M_R =8.45，則求得路床以上鋪面有效回彈模數值 E_p =142,817 *psi*

*3.*檢查 *r* 是否≥0.7a_e

$$a_e = \sqrt{\left[5.9^2 + \left(12.25 * \sqrt[3]{(142817/16901)}\right)^2\right]} = 17.95\ in$$

=36 *in* ≥0.7(17.95)=12.565　　*OK!*

4.求取 SN_{eff} 值

$$SN_{eff} = 0.0045(12.25)\sqrt[3]{142817}$$
$$= 2.88$$

6-1-1 現地目測調查評估法

由先前目測調查所得資料配合鋪面結構數公式 $SN_{eff}=0.35*4.25+0.14*8.00*1$，即可評估路面現存有結構數 $SN_{eff}=2.61$。

6-1-3 現存鋪面殘餘壽年法

根據資料已知新建路面的設計交通量 $N_{1.5}=1,140,161$ ESAL，現有累計交通量 $N_p=400,000$ ESAL，則

1.求爲鋪面殘餘壽年百分比 RL

$$RL = 100\left[1-\left(\frac{400,000}{1,140,161}\right)\right] = 0.65\%$$

2.求取鋪面狀況因子 CF

$$CF = 1 - 0.7 \times e^{-(0.65+0.85)^2} = 0.93$$

3.計算鋪面現存有效結構數 $SN_{eff} = CF \times SN_o$。

$SN_{eff} = CF \times SN_o = 0.93*2.99 = 2.78$

6-1-4 求取加鋪需求結構數 SN_f

依據現地 NDT 所得之路床回彈模數值 M_R，乘上 0.33 折減值，得設計路床回彈模數值 $M_R=5577$ psi，配合 Flexible ESAL $=2,400,000$、信賴度 $R=95$、$S_0=0.45$、$m=1$ 與 $\Delta PSI=2.7$，等設計參數，依 AASHTO 新建路面設計步驟，求得 $SN_f=4.69$

完成上述 6-1-1~6-1-4 求取 SN_{eff} 與 SN_f 值，若加鋪 AC 材料層係數 $a=0.44$，則各分析方法所求得之加鋪厚度如表十三所示，根據

此原則，工程師可於分析路段中選取適當分析點，進行加鋪厚度評估與設計，選定最佳之加鋪厚度。

表十三 各類評估法求得之加鋪厚度表

評估方法	評估 SN_{eff}	需求 SN_{ol}	加鋪厚度(in)
非破壞性撓度檢測法	2.88	1.81	4.11
現地目測調查評估法	2.61	2.08	4.73
現存鋪面殘餘壽年法	2.78	1.91	4.34

at R=0.95

6-2 PCC 加鋪於 PCC 路面(Bound)

某路段 *PCC* 路面之現存結構資料與 *NDT* 檢測資料等，如表十四所示，今考慮於加鋪後提供 *11,000,000(REGID ESAL)*交通量，請依據 *1993* 年 *AASHTO* 加鋪設計法設計加鋪厚度。

表十四 *PCC* 路面之相關資訊

JPCP 路面之相關資訊

鋪面厚度=9 in

$N_{1.5}$ = 42,500,500 ESAL　　N_P = 2,500,000 ESAL

NDT 檢測資料

荷重(lbs)	d0(mils)	d12(mils)	d24(mils)	d36(mils)	AREA
9000	5.02	4.59	3.89	3.25	30.16

撓度荷重傳遞百分比 $\Delta LT=0.65$

目測調查資料

F_{jc}=1.0（經加鋪前修復）

F_{fat}=0.99

F_{dur}=1.00

6-2-1 現地目測調查評估法

*1.*接縫與裂縫折減係數 $F_{jc}=1.00$

*2.*耐久性折減係數 $F_{dur}=0.99$

3.疲勞破壞折減係數 $F_{fa}=1.00$

根據目測調查所得三項折減係數，可計算求取剛性路面現存有效厚度 D_{eff}。

$$D_{eff}=F_{jc}\times F_{dur}\times F_{fat}\times D$$

$$=1.00\times 0.99\times 1.00\times 9.0=8.91$$

6-2-2 現存鋪面殘餘壽年法

1.求爲鋪面殘餘壽年百分比 RL

$$RL=100\left[1-,\left(\frac{2,500,000}{4,250,000}\right)\right]=0.41\%$$

2.求取鋪面狀況因子 CF

$$CF=1-0.7\times e^{-(0.41+0.85)^2}=0.86$$

3.計算鋪面現存有效厚度 $D_{eff}=CF\times D_o$。

$$D_{eff}=CF\times D_o=9.00\times 0.86=7.71$$

6-2-3 求取加鋪需求厚度 D_f

1.加鋪後預期交通量

選擇剛性路面之等值軸重因子(*EALF*)，估計 *18-kip* 等值單軸重 *EASL=16,000,000*。

2.路床有效反力模數值 k

已知半徑 $a=5.9in$ 荷重盤施予 *9000 lb* 荷重，*AREA* 值可由 *NDT* 施測資料帶入下式求得。

$$AREA=6*\left[1+2\left(\frac{4.59}{5.02}\right)+2\left(\frac{3.89}{5.02}\right)+\left(\frac{3.25}{5.02}\right)\right]=30.16$$

由 *AREA* 值配合荷重中心 *0 in* 處之撓度值 $do=5.02mils$，查圖八即可求得動態路床有效反力模數值 $k_{dynamic}=260$，則路床有效反力模數值 $k=260/2=130psi/in$ 即可得。

3.混凝土楊氏模數 E

使用非破壞性撓度檢測法，將求得之 $AREA=30.16$ 值配合路床有效反力模數值 $k=130$ ，查圖九即可得柏松比 $\nu=0.15$ 之混凝土 $E \times D^3=4.4 \times 10^9$ ，又路面厚度 $D=9in$ ，即可得混凝土楊氏模數 $E \fallingdotseq 5900000\ psi$ 。

4.混凝土破裂模數 S_c'

混凝土破裂模數 S_c' 之求取可分取鑽心取得與利用非破壞性撓度檢測法回算兩種，非破壞性撓度檢測法主要將所得混凝土楊氏模數 E 值，帶入下式即可得混凝土破裂模數 S_c' 。

$$S_c' = 43.5\left(\frac{5900000}{10^5}\right) + 488.5 = 745\ psi$$

5.荷重傳遞係數 J

根據 NDT 施測得撓度荷重傳遞百分比 $\Delta LT=0.65$ ，參考表十二選擇適當之荷重傳遞係數 $J=3.5$ 。

依上述求得知設計參數，配合 $R=0.95$ 、$S_0=0.35$ 、$m=1$ 與 $\Delta PSI=2$ ，參考 $AASHTO$ 新建剛性路面路面設計步驟，即可求得加鋪需求厚度 $Df=10.80$ 。

求取 $Deff$ 與 Df 值，則各分析方法所求得之加鋪厚度如表十五所示，同樣的，工程師亦可於分析路段中選取適當分析點，進行加鋪厚度評估與設計，選定最佳之加鋪厚度。

表十五 各類評估法求得之加鋪厚度表

評估方法	評估 $Deff$	需求加鋪厚度 Dol(in)
現地目測調查評估法	8.91	$Dol= Df-Deff=10.68-8.91=1.77$
現存鋪面殘餘壽年法	7.71	$Dol= Df-Deff=10.68-7.71=2.97$
		$at\ R=0.95$

6-3 加鋪設計討論與建議

經由研讀 *1995* 年 *AASHTO* 加鋪設計規範，並參考附錄中的實例分析結果，列出下述事項，提供加鋪設計時之參考。

1.現況分析設計方法的選擇

面對一條欲進行加鋪維修區域，一般執行加鋪設計分析的方法可分爲路段平均分析設計法(*Uniform Section Approach*)與各點分析設計法(*Point-by-Point Approach*)兩種，兩種設計方式各有其優缺點，分述如下：

i.路段平均分析設計法(*Uniform Section Approach*)

將欲維修區域區分成若干路段，於各路段內分別求取或分析鋪面厚度、破壞狀況與路床模數值等加鋪設計所需之參數，再將區域所得之設計參數平均，作爲設計加鋪厚度之用。利用此設計法之優點爲只需計算加鋪厚度一次，但設計時信賴度的求取必須有適當的考量。

ii.各點分析設計法(*Point-by-Point Approach*)

此設計法爲將欲維修區域內每一固定距離取一分析點，針對各分析點取得之參數個別進行加鋪厚度設計，如此即可得到各分析點所需求的加鋪厚度，並取其中的最大需求加鋪厚度，作爲此維修區域的設計加鋪厚度。此方法取各分析點中的最大值爲設計加鋪厚度，因此信賴度高爲其優點，而其需要大量的個別運算的缺點，也經由電腦的輔助運算而迎刃而解。

經由上述比較，工程師面對加鋪計畫時需根據現地資料的完備性與當時之需要，選取最恰當且信賴度高的設計分析方式。

2.現有路面結構評估方法建議

1995 年 *AASHTO* 加鋪設計規範建議對於現有路面結構評估方式可分非破壞性撓度檢測法、現地目測調查評估法與現存鋪面殘餘壽年法三種，根據實例分析結果，三種分析方式所得加鋪設計厚度均有相近的趨勢，尤以非破壞性撓度檢測法爲佳，現地目測調查評估法與現存鋪面殘餘壽年法次之，因此，*AASHTO* 設計規範極力推薦使用非破壞性撓度檢測法進行加鋪設計，但若礙於現實環境考量而必須以現地目測調查評估法與現存鋪面殘餘壽年法進行評估時，規範則建議配合材料鑽心試驗，以確保分析的正確性與穩定性。

*3.*需求強度設計因子對加鋪厚度的影響

加鋪設計於計算 SN_f 與 D_f 時，除文中敘述應視現地狀況於以評估之設計因子應謹慎選擇之外，根據實例分析結果發現，信賴度的選擇對加鋪設計厚度結果的變動影響極大，因此建議工程師於同一路段設計時進行信賴度對加鋪厚度的敏感度分析，以選擇最適當且最經濟的加鋪厚度。另外，不分實例分析亦發現若未來設計需求 *ESAL* 值大於 *25 million*，則可能超越加鋪設計之極限，造成不恰當設計結果的發生。

*4.*環境因子與地理特性對加鋪設計之影響

由於規範的訂定主要以適用的普及性爲考量，因此，各個公路主管機構應在依循規範的準則下，考量當地環境因子與地理特性，適時調整相關設計因子，如信賴度、標準偏差、路床回彈模數值與材料特性等，並長期追蹤其服務績效，於以適當的調整，使加鋪設計結果處於最佳化狀態。

第七節 結論

鋪面的加鋪設計包含了因應未來交通量需求的需求強度設計與評估路面現存服務能力的分析技術，可說是一門工程藝術(state of art)，若有任何考量的疏失或不周全，均會造成未來加鋪路面的服務績效不如預期，甚至造成加鋪工程的失敗，因此，世界各大鋪面設計規範亦不斷採用不同的理念，試圖找出最有效的評估與設計準則，做爲工程師設計參考之用。

1995 年 *AASHTO* 加鋪設計規範大幅修正了舊版的設計評估理念，充分利用非破壞性檢測觀念作爲評估的準則，且經實例分析與現實情況均相當符合，可說提供了工程師一信賴度高的準則，故期待國內工程師亦能以此規範作爲加鋪設計之參考基準，並針對國內地理因素給於適當修正，使國內加鋪維修作業能以最適切的成本而發揮最高之績效。

H EXPEAR Program

H.1 EXPEAR User's Guide

資料來源：

Hall, K. T., and M. I. Darter, " Structural Overlay Strategies for Jointed Concrete Pavements," Volume VI, Appendix A - User's Manual for the EXPEAR Computer Program", ERES Consultants, Inc., Federal Highway Administration, 1990.

H.2 Case Studies in Rehabilitation Strategy Development

資料來源：

Darter, M. I., and K. T. Hall, "Case Studies in Rehabilitation Strategy Development," *Concrete International*, Magazine of the American Concrete Institute, December 1993.

H EXPEAR Program
H.1 EXPEAR User's Guide

1. INTRODUCTION

EXPEAR (EXpert system for Pavement Evaluation And Rehabilitation) is a practical and comprehensive computerized system to assist practicing engineers in evaluating concrete highway pavements, developing feasible rehabilitation alternatives, and predicting the performance and cost effectiveness of the alternatives. EXPEAR was originally developed for the Federal Highway Administration (FHWA) by the University of Illinois in 1985-1987.[1] It has been further developed with the support of the Illinois Department of Transportation (1988-1989). Additional work on EXPEAR has been supported by the FHWA under this research study.[2]

EXPEAR is intended for use by State highway engineers in project-level rehabilitation planning and design for high-volume (i.e., Interstate) conventional concrete pavements (jointed reinforced concrete pavement [JRCP], jointed plain concrete pavement [JPCP], and continuously reinforced concrete pavement [CRCP]). EXPEAR does not perform thickness or joint design; the engineer must use existing design procedures to determine these details.

EXPEAR has been developed in the form of a knowledge-based expert system, which simulates a consultation between an engineer and an expert in concrete pavements. EXPEAR uses information about the pavement to guide the engineer through evaluation of a pavement's present condition and development of one or more feasible rehabilitation strategies. The procedure was developed through extensive interviewing of authorities on concrete pavement performance. In addition, predictive models are included to show future pavement performance with and without rehabilitation.

Evaluation of a pavement and development of feasible rehabilitation alternatives is performed according to the following steps:

1. Project data collection.
2. Extrapolation of overall project condition.
3. Evaluation of present condition.
4. Prediction of future condition without rehabilitation.
5. Recommendations for physical testing.
6. Selection of main rehabilitation approach.
7. Development of detailed rehabilitation strategy.
8. Prediction of rehabilitation strategy performance.
9. Cost analysis of rehabilitation alternative.
10. Selection of preferred rehabilitation strategy.

A computer program has been developed for each of the three pavement types addressed. The programs operate on any IBM-compatible personal computer. The current version is EXPEAR 1.4, which possesses the capabilities to do life-cycle cost

analysis and delay rehabilitation up to 5 years. Many revisions were made in EXPEAR 1.4 to improve the user friendliness of the program.

2. PAVEMENT EVALUATION

Step 1. Data Collection and Entry

The engineer collects inventory and monitoring data for the project. Inventory data, which should be available from office records, includes design traffic, materials, soils, and climate. Monitoring data includes distress, drainage characteristics, rideability, and other items collected during a field visit to the project. Monitoring data is collected by sample unit; a sufficient number of sample units distributed throughout the project's length should be surveyed to obtain a reasonable representation of the project's condition.

It is recommended that a team of two engineers perform the project survey together. They should drive over the entire length of the project and rate the present serviceability in each lane. They should also note the number and location of settlements and heaves. They should then return to the start of the project and perform the distress survey by sample unit. It is convenient to start sample units at mileposts for easy reference.

Either the pavement distress identification manual provided in NCHRP Report No. 277 or the Strategic Highway Research Program (SHRP) Long-Term Pavement Performance (LTPP) distress identification manual should be used as a guide.[3,4] These manuals provide standard definitions for distresses by type, severity, and unit of measurement. They also provide photographs of distresses to assist the engineers in rating their severity. The engineers must also measure faulting at joints, cracks, and full-depth repair joints.

In the office, the data are entered into a personal computer using a full-screen editor. The format of the data entry screens is very similar to that of the field survey sheets. The editor provides function keys for moving forward and backward through the data items and screens. The editor will provide screens for the project inventory data and monitoring data (1 set for each sample unit, up to a maximum of 10).

Step 2. Extrapolation of Overall Project Condition

Using the project length and lengths of the sample units, EXPEAR extrapolates from the sample unit distress data to compute the overall average condition of the project. The project is then evaluated on the basis of this average condition.

Step 3. Evaluation of Present Condition

EXPEAR utilizes a set of decision trees to analyze all of the data and develop a specific detailed evaluation in the following major problem areas for JRCP and JPCP:

- Roughness.
- Structural adequacy.
- Drainage.
- Joint deterioration.
- Foundation movement.
- Skid resistance.
- Joint construction.
- Loss of support.
- Load transfer.
- Joint sealant condition.
- Concrete durability.
- Shoulders.

The same problem areas are examined for CRCP, with the exception of those related to transverse joints (construction, deterioration, load transfer, and loss of support), and with the addition of a decision tree for construction joints and terminal treatments.

From the decision trees, a set of evaluation conclusions is produced for each traffic lane and each shoulder.

Step 4. Prediction of Future Condition Without Rehabilitation

Based on the current traffic level, in terms of the annual 18-kip (80 kN) Equivalent Single-Axle Load (ESAL) applications, and the anticipated ESAL growth rate, the future condition of the pavement without rehabilitation is predicted. Faulting, cracking, joint deterioration, pumping, and present serviceability rating are projected for jointed pavements (and punchouts for CRCP) and the years in which they will become serious problems are identified. The predictive models used are calibrated to the existing condition of the pavement at the time of the survey.

Step 5. Physical Testing Recommendations

The initial data collection does not require physical testing. Based upon the available information, the program identifies types of physical testing suggested to verify the evaluation recommendations and to provide data needed for rehabilitation design. Testing may include nondestructive deflection testing, coring/material sampling and laboratory testing, and roughness and friction measurement. Types of deficiencies which may warrant physical testing include structural inadequacy, poor

rideability, poor surface friction, poor drainage conditions, poor concrete durability (D-cracking or reactive aggregate distress), foundation movement (due to swelling soil or frost heave), loss of load transfer at joints, loss of slab support, joint deterioration, and evidence of poor joint construction.

3. PAVEMENT REHABILITATION

Step 6. Selection of Main Rehabilitation Approach

Based upon the evaluation results, the system interacts with the engineer to select the most appropriate main rehabilitation approach for each traffic lane and shoulder. These include all 4R options: reconstruction (including recycling), resurfacing (with concrete or asphalt), or restoration. The major factors in determining whether a pavement needs reconstruction, resurfacing, or merely restoration are the extent of structural distress (e.g., cracking and corner breaks) and the extent of deterioration due to poor concrete durability (D-cracking or reactive aggregate distress).

Step 7. Development of Detailed Rehabilitation Strategy

Once an approach is selected for each traffic lane and shoulder, the engineer proceeds to develop the detailed rehabilitation alternative by selecting a feasible set of individual rehabilitation techniques to correct the deficiencies present. This may include such items as subdrainage, shoulder repair, full-depth repairs, joint resealing, etc. This is performed for each traffic lane and shoulder by interaction with the program. EXPEAR displays each of the evaluation conclusions reached earlier and recommends one or more appropriate rehabilitation techniques. A set of decision trees has been developed to guide the rehabilitation strategy development process for traffic lanes and for adjacent shoulders. Where more than one choice exists for an appropriate technique to repair a specific distress, the system presents the engineer with the choice to make.

EXPEAR computes needed quantities for the rehabilitation techniques selected based on the data in the project survey and additional information provided by the engineer. In general, the program assumes that 100 percent repair will be performed; that is, that the quantity of a certain type of distress to be repaired is equal to the quantity of that distress observed during the field survey.

If the rehabilitation work is being delayed, the quantities are increased where appropriate for each year of delay. Predictive models are used where available to increase the quantities. For distresses which do not have predictive models available, the quantities are increased by some constant amount (e.g., 5 percent per year).

When rehabilitation is delayed on a project which does not currently have any cracking or joint deterioration but which is predicted to develop some of either of these distresses between now and the time that the rehabilitation work will be done, appropriate quantities of full-depth repair are added to the rehabilitation strategy.

Step 8. Prediction of Rehabilitation Strategy Performance

The future performance of the developed rehabilitation strategy is predicted in terms of key distress types for 20 years into the future, based upon the traffic growth rate entered by the engineer. The JRCP and JPCP EXPEAR programs contain prediction models for the following key distresses for the various rehabilitation approaches:

• Reconstruction:	Faulting Cracking Pumping Joint deterioration PSR
• Bonded PCC overlay and Unbonded PCC overlay:	Faulting Cracking Joint deterioration
• AC structural overlay, AC nonstructural overlay, AC overlay/crack & seat, and AC overlay/saw & seal:	Reflective cracking Rutting
• Restoration:	Faulting: - with grinding - without grinding Full-depth repair faulting Cracking Pumping Joint deterioration PSR

The models are calibrated to the assumed condition of the pavement immediately after the rehabilitation is performed. If, for example, diamond grinding is not included in a restoration strategy, joint faulting after restoration is assumed to be the same value as was measured during the field survey, but if grinding is performed, joint faulting is assumed to be zero after the restoration.

EXPEAR evaluates the predicted performance of the rehabilitation strategy with respect to critical distress levels selected by the engineer, and determines in which years in the future these critical distress levels will be reached. From this information the predicted life of the rehabilitation strategy is determined as the earliest time when one of the distresses reaches a critical level (e.g., faulting exceeds 0.13 in [3.3 mm] for JPCP). The engineer may later override this life if desired.

Step 9. Cost Analysis of Rehabilitation Strategy

The first version of EXPEAR which was developed for the FHWA (EXPEAR 1.1) did not include the capability to perform a life-cycle cost analysis of the rehabilitation strategy developed. The most recent version of the program (EXPEAR 1.4) performs the cost analysis for the engineer. It uses the computed repair quantities and determines the rehabilitation alternative's life from the performance predictions. The engineer must specify the discount rate to be used in the analysis (values between 0 and 7 percent are permitted), and must also specify whether or not the rehabilitation will be delayed. Delays up to 5 years are permitted; considering the margin of error on some of the predictive models used by the program, it is not reasonable to assume the models can give meaningful predictions of the cost of rehabilitation postponed longer than that.

The engineer is given the opportunity to override the predicted life determined by the program. This may be desirable if the engineer has good reason to believe that the predicted life does not reflect the performance of that type of rehabilitation under the specific local conditions which apply to the pavement being considered. The cost analysis output indicates whether the life used in the computations was that predicted by the program or another value provided by the engineer.

EXPEAR also provides default unit costs for all of the rehabilitation techniques involved in the strategy being considered. The engineer may use these default costs or enter other values. Any number of sets of modified unit costs may be saved by the engineer and retrieved for future use.

EXPEAR computes the present cost and the equivalent annual cost of each technique over the entire project length, and summarizes the total present and annual costs of the strategy being examined. In the case of delayed rehabilitation, the program also computes the actual dollar cost of the rehabilitation in that year; that is, the "present cost" in the year the work is performed.

The cost analysis period is restricted to be the same as the first rehabilitation performance period. Therefore, it is not possible to include subsequent rehabilitation in the strategy to fill out a desired analysis period. This is largely due to the lack of predictive models for performance of such things as second overlays. It is also not possible to attach a salvage value to a strategy with a predicted life in excess of 20

years. When interpreting the results of the cost analyses for several strategies, the engineer must keep in mind that the analysis periods will in most cases be unequal. These limitations will be addressed in future improvements to EXPEAR.

The cost analysis in EXPEAR is a simple and approximate procedure, the primary purpose of which is to facilitate rapid generation and comparison of rehabilitation alternatives. It should help the engineer identify alternatives which are comparable in cost-effectiveness and deserve further investigation, and also eliminate alternatives which are clearly not cost-effective. It does not, however, take the place of the detailed evaluation and cost analysis which is required for preparation of plans, specifications, and bid estimates. It also does not consider cost items not directly related to improvement of the pavement (e.g., traffic control, bridge and guardrail work, etc.) though these costs may be incorporated into the engineer's unit costs if desired.

Step 10. Selection of Preferred Rehabilitation Strategy

EXPEAR can be used to develop several different rehabilitation strategies as described above. The costs and performance characteristics of each of these alternatives can be compared by the engineer. The one that fits the existing constraints and available funding the best can be identified.

4. EXPEAR OPERATION

System Requirements

Running EXPEAR requires an IBM DOS-compatible computer with approximately 350 Kbytes of free memory, and one of the following:

- Hard disk.
- Two 360 K, 5.25-in (133 mm) floppy disk drives.
- One 720 K, 3.5-in (89 mm) disk drive.

Hard disk operation is recommended both for speed of execution and storage of output files. EXPEAR will display on any type of monitor (monochrome, CGA, EGA, or VGA), and does not require a math coprocessor.

Each of the three EXPEAR versions (for the three pavement types: JPCP, JRCP, and CRCP) is distributed on a set of two 360 K, 5.25-in (133 mm) floppy disks. One disk contains the executable program (EXPEAR.EXE) and the second disk contains other files needed to run EXPEAR. The file names (EXPEAR.EXE, DISPLAYS.REC, STNDRD.DAT, etc.) are common to the programs for all three pavement types (JRCP, JPCP, and CRCP), so it is important that the programs for different pavement types be kept on separate floppy disks or separate hard disk directories.

Running EXPEAR

The program is started by typing "EXPEAR" from DOS. After the EXPEAR title screen and a few screens of introductory information, the system displays the main menu, which has four options:

MAIN MENU

1. ENTER OR EDIT PROJECT DATA
2. CONDUCT PROJECT EVALUATION
3. DEVELOP REHABILITATION STRATEGY
4. QUIT, RETURN TO DOS

Enter or Edit Project Data

When this option is selected, a menu will appear to ask whether you want to create a new data file or edit an existing file. A new data file is created by modifying the STNDRD.DAT file. If an existing data file is to be modified, the program will ask for the name of the data file without the .DAT extension.

A full-screen data editor is incorporated into the system for data entry and editing. Function keys for moving through the data items and screens are defined at the bottom of the screen. Some data items are defined as "toggle variables," meaning that available values (such as low, medium, high) can be selected using the tab key. After a file is edited, SHIFT-10 will exit the editor. This command does not however, save the file on disk. The program will prompt the user to save the file before continuing.

Conduct Project Evaluation

When this option is selected, the program asks for the name of the data file to be evaluated. It also asks whether the user wants to use the default critical distress levels incorporated in the program, or his or her own values. These may be selected each time the program is run, or may be saved to disk and retrieved when needed. The program will prompt the user for a file name under which to store critical distress values and save the file with a .CVL extension. Whether the default values or user-defined values are used, critical distress levels must be selected before proceeding with the evaluation.

The evaluation runs very quickly. When it is done, EXPEAR displays the results of the evaluation, which consists of evaluation conclusions for the traffic lanes and shoulders, predicted performance of each lane without rehabilitation, and physical testing recommendations. If the user desires, the data summary file and the project evaluation summary file may be printed from within the program. These files

are saved on disk (with .REP and .TXT extensions) and may also be printed from DOS at a later time. However, if the user exits the program at this point and enters it again, the evaluation process must be repeated in order to proceed, because EXPEAR must have a current evaluation in memory in order to develop a rehabilitation strategy.

When the evaluation is completed, a menu appears with the following options:

EVALUATION MENU

1. DISPLAY EVALUATION CONCLUSIONS
2. DISPLAY PHYSICAL TESTING RECOMMENDATIONS
3. DISPLAY FUTURE DISTRESS AND PSR PREDICTIONS
4. PRINT EVALUATION SUMMARY
5. RETURN TO MAIN MENU

This permits the user to examine any part of the evaluation results, print the evaluation results, or bypass viewing the evaluation results and proceed directly to developing a rehabilitation strategy.

Develop Rehabilitation Strategy

When this option is selected, EXPEAR interacts with the user to select the main rehabilitation approach (reconstruct, overlay, or restore) and the specific rehabilitation techniques needed to correct the deficiencies identified in the evaluation. EXPEAR recommends appropriate rehabilitation approaches and techniques and gives the user the option to choose whenever more than one appropriate technique exists. EXPEAR does not have the capability to permit the user to enter options other than the ones given. When the list of techniques making up the rehabilitation strategy has been developed, it will be displayed along with approximate quantities. For some quantity calculations, additional user input is required for which a prompt appears on the screen. The rehabilitation techniques and quantities may be printed from EXPEAR or from DOS; the output file has an .DTS extension.

After a strategy has been developed, the rehabilitation menu appears with the following options:

REHABILITATION MENU

1. REVISE REHABILITATION STRATEGY
2. PREDICT REHABILITATION PERFORMANCE
3. PERFORM LIFE-CYCLE COST ANALYSIS
4. RETURN TO MAIN MENU

The second option will predict the performance of the rehabilitation strategy developed, using predictive models for key distresses. EXPEAR prompts the user for any additional information needed, such as overlay thickness. The predictions are displayed for each lane and may be printed from EXPEAR or from DOS (the output file's extension is .DRH).

Only after a rehabilitation strategy has been developed and its performance predicted can a cost analysis of the strategy be performed. EXPEAR prompts the user for a discount rate and the number of years that the rehabilitation will be delayed, and also asks the user to select unit cost values for the rehabilitation techniques. Default unit costs are provided, or (in the same manner as for critical distress levels), user-defined unit costs can be saved to disk (the file extension will be .UCC), and retrieved when needed.

The program computes the present and equivalent annual costs over the project length for the rehabilitation strategy analyzed. The annual cost is computed on the basis of the predicted life of the strategy, which is computed by EXPEAR but which may be overridden by the user if desired. The cost analysis results are displayed on the screen and may be printed from EXPEAR or from DOS (the extension is .LCC).

5. EXAMPLE PROBLEM

On the following pages, an example output from EXPEAR is provided for the case study of NC 1-8, a section of JPCP on Interstate 95 near Rocky Mount, North Carolina. The outputs include the following files:

- NC1-8.REP — Project Survey Summary
- NC1-8.TXT — Evaluation Results:
  - Extrapolated (Per Mile) Values
  - Evaluation Conclusions
  - Physical Testing Recommendations
  - Predicted Condition Without Rehabilitation
  - Future Pavement Evaluation
- NC1-8.DTS — Rehabilitation Techniques and Quantities for Restoration Alternative
- NC1-8.DRH — Predicted Performance for Restoration Alternative
- NC1-8.LCC — Life-cycle Cost Analysis for Restoration Alternative

The example output for this project is shown in tables 1 through 15.

Table 1. Project design data for NC 1-8.

PROJECT SURVEY SUMMARY FOR: NC 1-8

Design engineer: KTH Date of survey: 08/22/87

PROJECT IDENTIFICATION
Highway designation: I-95
State: North Carolina
Direction of survey: north
Starting milepost: 0.00
Ending milepost: 1.00

Number of sample units: 1

CLIMATE
Climatic zone: wet nonfreeze
Estimated annual temperature range (F): 60.0
Mean annual precipitation (inches): 46.8
Corps of Engineers freezing index (Fahrenheit degree-days): 0
Average annual temperature (degrees Fahrenheit): 60.0

SLAB CONSTRUCTION.
Year constructed: 1967
Slab thickness (inches): 9.0
Width of traffic lanes (feet): 12.0
Concrete 28-day modulus of rupture (psi): 618

TRANSVERSE AND LONGITUDINAL JOINTS
Pattern of joint spacing: uniform
Average transverse joint spacing (feet): 30.00
Transverse joint sequence if random (feet):
Type of sealant: liquid
Average transverse joint reservoir dimensions:
width (inches): 0.50
depth (inches): 1.00
Method used to form transverse joints: sawing
Transverse joint sawed depth (inches): 1.00
Type of load transfer system: aggregate interlock
Dowel bar diameter (inches): 0.00
Method used to form longitudinal joints between lanes: sawing
Longitudinal joint sawed or formed depth (inches): 2.75

Table 1. Project design data for NC 1-8 (continued).

BASE
Base type: dense-graded untreated aggregate
Modulus of subgrade reaction (psi/inch): 513

SUBGRADE
Predominant subgrade soil AASHTO classification: A2
Are swelling soils a problem in area: no
Were steps taken to prevent the swelling soils problem: no

SHOULDER
Type of shoulder: AC
Width of shoulders (feet): inner: 6.0 outer: 10.2

Inner lane slope direction: toward inner shoulder

TRAFFIC
Estimated current through two-way ADT: 19100
Percent commercial trucks: 9.0
Total number of lanes in direction of survey: 2
Future 18-kip ESAL growth rate (percent per year): 4.0
Truck traffic volume growth rate: approximately same as in past

	Lane two	Lane one
Total accumulated 18-kip ESAL (millions):	1.88	9.14

RIDE QUALITY	Lane two	Lane one
PSR	3.7	3.3

1 in = 25.4 mm
1 ft = 0.3048 m
°F = 9/5(°C) + 32
1 psi = 0.00689 MPa

Case Studies in Rehabilitation Strategy Development

by Michael I. Darter and Kathleen T. Hall

Restoration is a rehabilitation strategy that involves a combination of methods for repairing distress, improving ride quality, and extending pavement life without a structural overlay. Restoration techniques for jointed concrete pavements include the following:

- Full-depth repair of joints, cracks, and corner breaks
- Partial-depth repair of spalls
- Grinding to remove faults and studded tire ruts and to improve surface friction
- Grooving to improve surface friction
- Subsealing to fill voids under slab corners
- Slabjacking to improve the pavement's longitudinal profile
- Load transfer restoration at joints and cracks
- Joint resealing
- Crack sealing
- Subdrainage improvement
- Shoulder improvement

Concrete pavement restoration typically involves a combination of several of these techniques. Over the past 25 years, many states have gained experience with restoration, and detailed information on design, construction, and performance of various restoration techniques is available from a variety of sources.[1,2,3,4]

Little guidance is available, however, to assist the practicing engineer in determining whether a particular pavement is a good candidate for restoration, or whether another rehabilitation strategy would be more appropriate. Restoration has been applied to many pavements that really were in need of structural improvement. The result, even if the restoration is a well designed and well constructed, is short rehabilitation life, high life-cycle costs, and diminished confidence in the effectiveness of restoration among engineers and highway users. Practicing engineers can be shown that it is possible to assess the appropriateness of restoration using information available about the design and condition of a particular pavement section, rehabilitation performance prediction models, and rehabilitation cost data. This is demonstrated using the EXPEAR computer program to compare rehabilitation strategies for 13 pavement projects from across the United States and representing a wide range of pavement conditions.

Pavement performance and rehabilitation needs

Maintenance versus restoration

The success of restoration depends on good design and construction, but it also depends on application of restoration at the appropriate time in the performance life of a pavement. The earliest time that restoration should be done is relatively easy to identify. Early in a pavement's life, its condition is excellent and its rate of deterioration is slow. For several years, routine or preventive maintenance is more cost-effective than any rehabilitation strategy. Restoration is generally not warranted until distresses such as cracking, faulting, and joint spalling have developed to the point that they detract from the pavement's serviceability. When annual maintenance costs equal or exceed the equivalent annual cost of restoration, the restoration work is justified.

Restoration versus resurfacing

It is more difficult to identify the latest point in the pavement's life at which restoration is likely to be cost-effective, i.e., the point at which the pavement has carried so much traffic and sustained so much structural damage that an overlay is needed. It is conceivable that resurfacing may be done before this point and be more cost-effective than restoration, primarily because of an overlay's ability to reduce deflections and slow deterioration in the slab. Early resurfacing seldom occurs however, due to funding limitations. More frequently, restoration is performed some years after the time when it has the greatest potential to cost-effectively extend the pavement's life, and in some cases, after the time when a structural improvement is warranted. The longer the delay, the less likely it is that restoration will be able to compete with resurfacing in performance and cost-effectiveness.

Indicators of structural deficiency

The following is a list of key distresses and levels that should be considered in assessing structural damage in

Table 1 — Case studies selected from the RPPR database

Section	Climate	Type	Condition	Cracking (no/mile)	Joint deterioration	Joint faulting (in.)	Pumping	PSR
AZ 1-6	DNF	JPCP	Good	0	5	0.01	None	3.5
FL 2	WNF	JPCP	Good	0	0	0.01	None	3.7
MI 3	WF	JRCP	Good	0	0	0.02	None	4.8
MN 3	DF	JRCP	Good	0	0	0.00	None	3.8
MN 2-3	DF	JRCP	Good	0	5	0.05	None	4.0
CA 6	DNF	JPCP	Fair	0	2	0.15	None	3.4
NC 1-8	WNF	JPCP	Fair	20	5	0.22	None	3.3
NC 2	WNF	JPCP	Fair	0	0	0.02	High	4.2
NJ 2	WF	JRCP	Fair	24	14	0.06	None	3.8
CA 1-3	DNF	JPCP	Poor	30	10	0.10	Medium	3.0
MI 4-1	WF	JRCP	Poor	222	0	0.12	None	2.4
MI 1-10b	WF	JPCP	Poor	0	219	0.19	Low	2.8
MN 1-8	DF	JRCP	Poor	102	141	0.09	None	3.4

Notes: Condition rating (good, fair or poor) is subjective assessment of overall pavement condition, based on vivible distress and PSR in outer traffic lane.
Sections CA 6 and CA 1-3 have low-severity reactive aggregate distress.

jointed concrete pavement. The critical values suggested are based upon observations of jointed reinforced concrete pavements (JPCP), and jointed plain concrete pavements (JRCP) performance in previous studies [4,5,6] and from use of EXPEAR[7] to predict the performance of restoration on pavements with varying levels of deterioration.

Transverse cracking provides direct evidence of fatigue damage. In JRCP, low-severity cracks are considered a normal consequence of drying shrinkage after construction, and are not considered structural distresses. In JPCP, unless the joint spacing is too long, transverse cracking of any severity is evidence of structural damage. Suggested critical levels for transverse cracking are 10 percent slabs cracked or 70 cracks per mile (all severities) for JPCP, and 70 cracks per mile (medium or high severity) for JRCP.

Longitudinal cracking in highway pavements is almost always caused initially by factors other than traffic (e.g., poor joint construction, foundation movement), but under traffic it can deteriorate to such an extent that it constitutes structural damage. More than 500 feet of longitudinal cracking per mile is suggested as a critical level for both JPCP and JRCP.

Joint faulting and pumping are not generally considered structural distresses, but they are caused by traffic loads and are visible indications of progressive loss of joint load transfer and erosion of slab support. Suggested critical levels of joint faulting are 0.10 in. for JPCP and 0.25 in. for JRCP.

Corner breaks, which occur as a result of substantial erosion of slab support and high corner deflections, are definite indications of structural damage. The suggested critical level for corner breaks is 25 per mile for both JPCP and JRCP.

Transverse joint spalling that reduces the thickness of the slab at the joints should be considered structural damage since it diminishes the structural integrity of the slab and is progressive in nature. This is often caused by poor joint construction, dowel bar corrosion, "D" cracking, or reactive aggregates. Suggested critical levels for joint spalling are 50 spalled joints per mile (medium or high severity) for JPCP and 25 spalled joints per mile (medium or high severity) for JRCP.

If JRCP or JPCP exhibits levels of structural damage beyond those given above, the pavement has probably reached or passed the point at which the rate of deterioration begins to accelerate rapidly. This is the stage at which a structural improvement is most appropriate. Restoration work performed on a pavement that has deteriorated past this point is likely to provide a relatively short performance life under medium to heavy traffic conditions. Attempting to delay a structural improvement by continued patching may result in annual maintenance costs so high that they completely offset any savings achieved by the delay.

Although visible distress is a good indicator of structural damage, it cannot give a complete picture of the extent of underlying deterioration. Coring and deflection testing are recommended on any project being considered for rehabilitation.

EXPEAR pavement evaluation, rehabilitation

EXPEAR is a computerized system to assist highway engineers in project-level evaluation of concrete highway pavements, development of feasible rehabilitation strategies, and prediction of rehabilitation performance and cost-effectiveness. EXPEAR is intended for use in rehabilitation planning and design for high-volume (e.g., Interstate) conventional concrete pavements (JRCP, JPCP, and continuous reinforced concrete pavement). EXPEAR was originally developed for the Federal Highway Administration (FHWA)[7] and was developed further with the support of the Illinois Department of Transportation.

Additional work on EXPEAR was supported by the FHWA under the "Performance and rehabilitation of rigid pavements" research study.[8] Additional information on the development of EXPEAR is available in References 9, 10, and 11. The current version is EXPEAR 1.4, which pos-

Table 2 — EXPEAR analysis results of AZ 1-6

Pavement design	
Highway:	Route 360 near Phoenix
Pavement type:	9 in. JPCP
Year constructed	1981
Joint spacing:	15-13-15-17
Dowels:	Undoweled
Base:	4 in. lean concrete
Subgrade:	A-6
Shoulders:	Tied PCC outer, AC inner
Drains	No drains
Traffic	
Current 2-way ADT:	97,770
Percent trucks:	3.8
Lanes each direction:	3
Accumulated Esal:	2.01 million (outer lane)
Existing pavement condition	
Year surveyed:	1987
PSR:	3.5
Deteriorated cracks:	0/ mile
Deteriorated joints:	5/ mile 20/ mile
Joint faulting:	0.01 in.
Longitudinal cracks:	0 ft/ mile
Pumping:	None
PCC surface:	Tined, not polished
Joint sealant damage:	Medium severity (resealed 1986)
"D" cracking:	None
Reactive aggregate:	None
Settlements/ heaves:	None
Shoulder condition:	Excellent
Lane/ shoulder joint:	Fair
Physical testing recommendations	
No physical testing warranted	

Future condition without rehabilitation		
Some joint deterioration is present, but no significant increase of any type of deterioration is predicted over the next 20 yr period.		
Consequence of delaying rehabilitation		
Rehabilitation may safely be delayed. Some joint resealing and joint spall repair is recommended.		
Predicted life of rehabilitation		
Alternative	Years	Unacceptable
Restoration	20+	
3 in. ACOL	7	Ref. cracking
5 in. crack/ seat AC OL	6	Rutting
3 in. saw/ seal AC OL	8	Rutting
3 in. bonded PCC OL	20+	
8 in. unbonded PCC OL	20+	
9 in. reconstruction	20+	
Results of life-cycle cost analysis		
Alternative	Initial cost	Annual cost
Restoration	59,200	3,800
3 in. AC OL	274,600	41,500
5 in. crack/ seat AC OL	273,200	47,500
3 in. saw/ seal AC OL	284,300	38,200
3 in. bonded PCC OL	368,800	23,400
8 in. unbonded PCC OL	514,200	32,600
9 in. reconstruction	506,000	32,000
Cost per 2-lane mile, based on predicted lives shown above (20 yr for bonded overlay, unbonded overlay, and reconstruction) and discount rate of 3 percent.		
Recommended rehabilitation (1989)		
Minor restoration work (spall repair and joint resealing) could be done to improve rideability and prevent water and incompressible infiltration.		
Rehabilitation techniques		Quantity
Full-depth repair of joints		200 sy
Reseal transverse joints		9450 ft
Reseal lane/ shoulder		10560 ft
Quantity per 2- lane mile and shoulders		

sesses the capabilities to do life-cycle cost analysis and delay rehabilitation up to five years.

EXPEAR was developed in the form of a knowledge-based expert system, that simulates a consultation between an engineer and an expert in concrete pavements. EXPEAR uses information about the pavement to guide the engineer through an evaluation of a pavement's present condition and development of one or more feasible rehabilitation strategies. The procedure was developed through extensive interviewing of authorities on concrete pavement performance. In addition, predictive models are used to estimate future pavement performance with and without rehabilitation.

Sections evaluated

The database developed for the RPPR study includes 95 sections of JPCP and JRCP in their first performance period.[6] Thirteen of these sections were selected for evaluation with the EXPEAR program. The sections, both JRCP and JPCP and located in all four major climatic zones, are listed in Table 1. The condition of each section was subjectively assessed as good, fair, or poor on the basis of observed distress and serviceability.

Pavements rated as "good" had little or no cracking or joint deterioration, minimal joint faulting, no pumping, and a Present Serviceability Rating (PSR) of 3.5 or more. "Fair" pavements had at least one of the following: moderate cracking and/or joint deterioration (due to "D" cracking or reactive aggregate distress), moderate to high faulting (exceeding the critical level), visible pumping, or serviceability less than 3.5.

Pavements rated as "poor" had at least two and in most cases three or four of the following: substantial cracking and/or joint deterioration (exceeding critical levels), high faulting (exceeding the critical level), visible pumping, and PSR less than 3.0.

Evaluation procedure

All EXPEAR input data required for each section were obtained from the database. The following steps were carried out for each of the 13 projects.

Table 3 — EXPEAR analysis results of NC 1-8

Pavement design	
Highway:	I-95 near Rocky Mount
Pavement type:	9 in. JPCP
Year constructed	1967
Joint spacing:	30 ft
Dowels:	Undoweled
Base:	4 in. untreated aggregate
Subgrade:	A-2
Shoulders:	AC
Drains	No drains
Traffic	
Current 2-way ADT:	19,100
Percent trucks:	9.0
Lanes each direction:	2
Accumulated Esal:	9.14 million (outer lane)
Existing pavement condition	
Year surveyed:	1987
PSR:	3.3
Deteriorated cracks:	20/ mile
Deteriorated joints:	5/ mile
Joint faulting:	0.22 in.
Longitudinal cracks:	0 ft/ mile
Pumping:	None
PCC surface:	Tined, not polished
Joint sealant damage:	Low severity
"D" cracking:	None
Reactive aggregate:	None
Settlements/ heaves:	None
Shoulder condition:	Good
Lane/ shoulder joint:	Poor
Overall: Excessive faulting indicates a load transfer deficiency. Some joint and crack deterioration present, reducing serviceability.	
Physical testing recommendations	
Deflection test for structure analysis and void detection. Core at center slab to obtain material samples. Core representative deteriorated joints. Test strength of PCC cores.	

Future condition without rehabilitation		
Serviceability:		PSR < 3.0 in 1994
Faulting:		> 0.10 in. in 1987
Joint deterioration:		5/ mile for 20 yr
Cracking:		24/ mile in 20 yr
Consequence of delaying rehabilitation		
Faulting is already high, but PSR is rated above 3.0. A few years of delay can be tolerated.		
Predicted life of rehabilitation		
Alternative	Years	Unacceptable
Restoration	14	Faulting
3 in. ACOL	10	Ref. cracking
5 in. crack/ seat AC OL	14	Ref. cracking
3 in. saw/ seal AC OL	15	Ref. cracking
7 in. unbonded PCC OL	20+	
11 in. reconstruction	20+	
Results of life-cycle cost analysis		
Alternative	Initial cost	Annual cost
Restoration	105,000	6,000
3 in. AC OL	303,000	28,900
5 in. crack/ seat AC OL	428,000	23,100
3 in. saw/ seal AC OL	313,000	21,400
7 in. unbonded PCC OL	635,000	30,200
11 in. reconstruction	506,000	29,300
Cost per 2-lane mile, based on predicted lives shown above (20 yr for unbonded overlay, unbonded overlay, and reconstruction) and discount rate of 3 percent.		
Recommended rehabilitation (1989)		
Technique		Quantity
Grinding		7040 sy
Full-depth repair of cracks		210 ft
Full-depth repair of joints		80 ft
Reseal transverse joints		4106 ft
Reseal lane/ shoulder joint		10560 ft
Quantity per 2-lane mile and shoulders.		

- Input data were verified by state employees and project team members familiar with the sections.
- A pavement evaluation was conducted and future performance was predicted without any rehabilitation.
- The following rehabilitation alternatives were considered:
  a. Restoration.
  b. Several resurfacing options (conventional AC overlay, crack and seat AC overlay, saw and seal AC overlay, bonded PCC overlay, and unbonded PCC overlay).
  c. Reconstruction with JPCP or JRCP.
- Rehabilitation performance was predicted using models contained in EXPEAR for distress after restoration (faulting, cracking, joint spalling, and PSR), resurfacing (rutting and reflective cracking for AC overlays; faulting, cracking, and joint spalling for PCC overlays) and reconstruction (faulting, cracking, joint spalling, and PSR).
- Life-cycle costs were estimated using Illinois statewide average costs. The costs include traffic control and other miscellaneous costs normally associated with the alternatives (guardrails, signs, etc.).

The cost analyses should be considered only as examples for comparison of the relative cost-effectiveness of various strategies, due to the highly variable nature of pavement rehabilitation costs throughout the United States.

It should be noted that all of the projects were surveyed in 1987 and analyzed using EXPEAR in 1989. This two-year delay is taken into account in the analyses: EXPEAR calibrated the performance prediction models to the 1987 distress and levels, predicted the distress levels in 1989, and used these levels to compute 1989 rehabilitation quantities and costs. For some projects in very good condition, the rehabilitation was delayed an additional few years in the analysis.

Good condition

Table 2 summarizes the results of the analysis of AZ 1-6, a section of 9 in. JPCP located on Rt. 360 near Phoenix, Ari-

Table 4 — EXPEAR analysis results of MI 4-1

Pavement design	
Highway:	I-69 near Charlotte
Pavement type:	9 in. JRCP
Year constructed	1973
Joint spacing:	71 ft
Joint sealant:	Preformed
Dowel diameter:	1.25 in.
Reinforcement:	0.162 in^2/ ft
Base:	4 in. untreated aggregate
Subgrade:	A-4
Shoulders:	Tied PCC
Drains	No drains
Traffic	
Current 2-way ADT:	13,700
Percent trucks:	11
Lanes each direction:	2
Accumulated ESAL:	4.37 million (outer lane)
Existing pavement condition	
Year surveyed:	1987
PSR:	2.4
Deteriorated cracks:	222/ mile
Crack faulting:	0.08 in.
Deteriorated joints:	0/ mile
Joint faulting:	0.12 in.
Longitudinal cracks:	0 ft/ mile
Long. joint spall:	0 ft
Pumping:	None
PCC surface:	Tined
Joint sealant damage:	Medium severity
"D" cracking:	Low
Settlements/ heaves:	None
Shoulder condition:	Good
Lane/ shoulder joint:	Good
Overall: Traffic lanes show extensive transversion crack deterioration; no joint deterioration. Some faulting exists at joints and cracks. Shoulders are in good condition. Subdrainage deficiency indicated by densegraded aggregate base, A-4 subgrade, inadequate ditch depth and heavy traffic.	

Physical testing recommendations		
Deflection testing needed for structural analysis and void detection. Coring and materials testing needed for assessing extent of deterioration from "D" cracking (bothy transverse and longitudinal joints). Materials testing for permeability.		
Future condition without rehabilitation		
Serviceability:	PSR < 3.0 in 1987	
Deteriorated joints:	> 27/ mile in 1997	
Deteriorated cracks	75/ mile in 1987	
Consequence of delaying rehabilitation		
Pavement already very rough and needs immediate rehabilitation. All types of deterioration are predicted to increase in future. Pavement is too deteriorated for restoration now. AC overlay may not be feasible due to deterioration of PCC slab.		
Predicted life of rehabilitation		
Alternative	Years	Unacceptable
Restoration	5	Jt. deterioration
3 in. ACOL	10	Ref. cracking
5 in. crack/ seat AC OL	15	Rutting
3 in. saw/ seal AC OL	13	Ref. cracking
3 in. bonded PCC OL	15	Ref. cracking
7 in. unbonded PCC OL	17	Jt. deterioration cracking
Results of life-cycle cost analysis		
Alternative	Initial cost	Annual cost
Restoration	718,200	143,500
3 in. AC OL	611,900 67,600	
5 in. crack/ seat AC OL	736,400	58,100
3 in. saw/ seal AC OL	621,600	55,100
3 in. bonded PCC OL	706,100	55,800
7 in. unbonded PCC OL	708,200	55,200
Cost per 2-lane mile, based on predicted lives shown above and discount rate of 3 percent.		
Recommended rehabilitation (1989)		
Three alternatives (3 in. saw/ seal AC OL, 3 in. bonded PCC OL, 7 in. unbonded PCC OL) are very similar in performance and cost. Further analysis is needed for selection		

zona, dry nonfreeze climatic zone. The pavement carried about 2 million 18 kip equivalent single-axle loads (ESALs) in the outer traffic lane since its construction in 1981 to 1987. When surveyed in 1987, its PSR was 3.5 and the only notable distress was some joint spalling. Joint resealing had been attempted unsuccessfully a year earlier.

Given the low truck traffic level on this pavement section, joint spalling on this pavement section was not predicted to increase significantly over the 20 year analysis period considered, and no other distresses were predicted to reach critical levels. As Table 2 shows, the strategy with the lowest annual cost was restoration. Restoration could probably also safely be delayed for several years.

Fair Condition

Table 3 summarizes the results of the analysis of NC 1-8, a section of 9 in. JPCP located on I-95 near Rocky Mount, North Carolina, wet nonfreeze climatic zone. The pavement carried about 9.1 million ESALs in the outer traffic lane from its construction in 1967 to 1987. When surveyed in 1987, its PSR was 3.3, it had some transverse cracking (20 per mile), some joint spalling (5 per mile), and faulting of 0.22 in. at transverse joints.

Although faulting was already high, the PSR was acceptable, and was predicted by EXPEAR to remain above the critical level of 3.0 for another 5 years. Rehabilitation could be delayed a few years. As Table 3 shows, restoration and overlay alternatives had comparable predicted lives, but restoration had the lowest annual cost.

Poor Condition

Table 4 summarizes the results of the analysis of MI 4-1, a section of 9 in. JRCP located on I-69 near Charlotte, Michigan, a wet freeze climatic zone. The pavement carried about 4.4 mil-

lion ESALs in the outer traffic lane its construction in 1973 to 1987. When surveyed in 1987, its PSR was 2.4, it had extensive transverse crack deterioration (222 per mile), moderate faulting (0.08 in. at cracks, 0.12 in. at joints), and medium-severity joint sealant damage.

The pavement needed immediate rehabilitation. As Table 4 shows, restoration was a poor rehabilitation choice, in terms of both performance life and annual cost. The crack and seat AC overlay, saw and seal AC overlay, and bonded and unbonded PCC overlay options were all very close in predicted life and annual cost.

Summary

The pavements examined here that were in "good" condition had minor faulting (average of 0.02 in.), little or no joint spalling or load-related cracking, and good ride quality (PSR greater than 3.5). For these pavements, restoration was consistently the most cost-effective rehabilitation strategy.

Pavements in "fair" condition had greater faulting (average of 0.11 in.), moderate joint spalling (average of 5 joints per mile) and load-related cracking (average of 11 cracks per mile), and fair ride quality (PSR greater than 3.0). Restoration was the most cost-effective rehabilitation strategy for four of the five case studies in fair condition. The exception was a pavement that had joint deterioration due to reactive aggregate.

The pavements in "poor" condition had high levels of faulting (average of 0.13 in.), a large number of spalled joints (average of 92 per mile) and load-related cracks (average of 88 per mile), and poor ride quality (PSR of 3.0 or less). In every case examined, overlay or reconstruction was more cost-effective than restoration.

The cost of rehabilitation is strongly tied to pavement condition, as shown below:

Condition	Average initial cost/ lane mile	Average annual cost/ lane mile
Good	$32,000	$2,000
Fair	163,000	16,000
Poor	605,000	45,000

It pays to maintain pavements in good condition and rehabilitate them before they exhibit substantial distress. In the case studies examined, an AC overlay with sawed and sealed joints was usually the most cost-effective AC overlay option.

The unbonded portland cement concrete overlay provided the longest life of all overlay alternatives and was determined cost-effective when the existing pavement was badly deteriorated. Reconstruction was cost-effective if the existing pavement exhibited extensive deterioration and the shoulders were in good enough condition that they did not need to be replaced.

Overall, the EXPEAR program provided realistic evaluations, future predictions, and selection of alternatives for the case studies.

Acknowledgments

The research reported in this paper was part of a study entitled "Performance/ Rehabilitation of Rigid Pavements" conducted for the Federal Highway Administration by ERES Consultants, Inc., Savoy, Illinois. The contract officer's technical representative for the study was Roger Larson. Kurt Smith and Sue James of ERES Consultants are gratefully acknowledged for their assistance.

References

1. Darter, M. I., Barenberg, E. J.; and Yrjanson, W. A. "Joint Repair Methods for Portland Cement Concrete Pavements," NCHRP Report No. 281, Transportation Research Board, 1985.

2. ERES Consultants, Inc., "Techniques for Pavement Rehabilitation," Participants' Notebook, National Highway Institute/Federal Highway Administration, 4th edition, 1987.

3. Federal Highway Administration, "Concrete Pavement Restoration -- Performance Review," Pavement Division and Demonstration Projects Division, 1987.

4. Snyder, M. B.; Reiter, M. J.; Hall, K. T.; and Darter, M. I. "Rehabilitation of Concrete Pavements, Volume I -- Repair Rehabilitation Techniques," Federal Highway Administration Report No. FHWA-RD-88-071, July 1989.

5. Darter, M. I.; Becker, J. M.; Snyder, M. B.; and Smith, R. E. "Concrete Pavement Evaluation System (COPES)," NCHRP Report No, 277, Transportation Research Board, 1985.

6. Smith, K. D.; Peshkin, D. G.; Darter, M. I.; Mueller, A. L.; and Carpenter, S. H. "Performance of Jointed Concrete Pavements, Volume I - Evaluation of Concrete Pavement Performance and Design Features," Federal Highway Administration, Report No. FHWA-RD-89-136, March 1990.

7. Hall, K. T.; Connor, J. M.; Darter, M. I.; Carpenter, S. H. "Rehabilitation of Concrete Pavements, Volume III - Concrete Pavement Evaluation and Rehabilitation System," Federal Highway Administration Report No. FHWA-RD-88-073, July 1989.

8. Darter, M. I. and Hall, K. T. "Structural Overlay Strategies for Jointed Concrete Pavements, Volume IV - Guidelines for the Selection of Rehabilitation Alternatives," Federal Highway Administration, Report No. FHWA-RD-89-145, June 1990.

9. Hall, K. T.; Darter, M. I.; Carpenter, S. H.; and Connor, J. M. "Development of a Demonstration Prototype Concrete Pavement Evaluation System," Transportation Research Record No. 1117, 1987.

10. Hall, K. T.; Connor, J. M.; Darter, M. I.; and Carpenter, S. H. "Development of an Expert System for Concrete Pavement Evaluation and Rehabilitation," *Proceedings*, Second North American Conference on Managing Pavements, Toronto, Ontario, Canada, November, 1987.

11. Hall, K. T.; Connor, J. M.; Darter, M. I.; and S. H. Carpenter, "Expert System for Concrete Pavement Evaluation and Rehabilitation," *Transportation Research Record* No. 1207, 1988.

Selected for reader interest by the editors.

ACI member **Michael I. Darter,** Ph.D., P.E. is a principal of ERES Consultants, Inc. and a professor of civil engineering at the University of Illinois at Urbana-Champaign.

Kathleen T. Hall, Ph.D., P.E., also is an ACI member and also is a post-doctoral research associate in civil engineering at the University at Urbana-Champaign.